UNIVERSITAT DE BARCELONA

Interacción molecular y funcional entre receptores involucrados en la ingesta de alimentos y el consumo de drogas de abuso

David Aguinaga Andrés

INTERACCIÓN MOLECULAR Y FUNCIONAL ENTRE RECEPTORES INVOLUCRADOS EN LA INGESTA DE ALIMENTOS Y EL CONSUMO DE DROGAS DE ABUSO

David Aguinaga Andrés

UNIVERSITAT DE BARCELONA
FACULTAT DE BIOLOGIA
DEPARTAMENT DE BIOQUÍMICA I BIOMEDICINA MOLECULAR

INTERACCIÓN MOLECULAR Y FUNCIONAL ENTRE RECEPTORES INVOLUCRADOS EN LA INGESTA DE ALIMENTOS Y EL CONSUMO DE DROGAS DE ABUSO

Memoria presentada por el Licenciado en Biología
DAVID AGUINAGA ANDRÉS
para optar al grado de Doctor por la Universidad de Barcelona

Esta tesis ha sido inscrita dentro del programa de doctorado de Biomedicina del Departamento de Bioquímica y Biomedicina molecular de la Universidad de Barcelona

El trabajo experimental y la redacción de la presente memoria han sido realizados por David Aguinaga Andrés bajo la dirección de la Dra. Gemma Navarro Brugal y el Dr. Enric Isidre Canela Campos

Dra. Gemma Navarro Brugal Dr. Enric Isidre Canela Campos

David Aguinaga Andrés

Barcelona, abril de 2017

L'essencial és
invisible als ulls

AGRAÏMENTS

Al llarg d'aquest temps de Tesi he planificat i realitzat molts experiments, alguns de senzills i d'altres de més sofisticats; he discutit amb experts en el camp tant en seminaris casolans com en congressos internacionals; he estat professor de pràctiques d'alumnes realment bons (amb la pressió que això comporta); he guiat un treball de final de grau i, finalment, he escrit una Tesi que sintetitza tota la feina feta després de quatre anys d'investigació en la qual he provat de donar-li sentit a peces que aparentment semblaven inconnexes… A priori, a aquestes alçades de la pel·lícula, res m'hauria d'espantar, oi?...

Doncs no és així. En realitat crec que en tot aquest temps no he fet res tan difícil en comparació amb el que em disposo a fer ara. Res em fa tanta por com seure davant d'aquest full en blanc, que porta per títol "agraïments" i mirar de fer-hi front. He estat molta estona (de debò, creu-me quan dic "molta estona"...) mirant el full completament en blanc i tinc pànic de deixar-me gent, deixar-me moments, o el que és pitjor, de no saber transmetre la gratitud que sento per tots vosaltres, per haver-me acompanyat en aquest viatge, tant en els bons moments com en els difícils. Sobretot en aquests darrers, en què és quan es demostra qui hi és de veritat. Al mateix temps, un altre element paralitzant que em ronda pel cap en encarar l'escriptura dels agraïments, és el factor "per sempre" que porta impregnat de forma implícita un treball com una Tesi doctoral; i és que el que quedi aquí plasmat, i malauradament també el que no hi quedi, hi serà "per sempre"... Et fas una idea del nivell de pressió al que estic sotmès ara mateix, oi?... Així que, per si les mosques, aquí va el primer GRÀCIES (serveix una mica de comodí, agafa'l ara i sent-lo teu, per si després se m'ha oblidat mencionar-te específicament. Davant de qualsevol tribunal, diré sempre que aquest gràcies era teu).

En primer lloc vull agrair als meus directors de Tesi, l'Enric Isidre Canela i la Gemma Navarro per haver-me guiat en aquest procés i haver fet arribar el vaixell a port; gràcies per estar sempre disposats a parar màquines quan us he necessitat i, sobretot, per confiar en mi. Al Rafa, gràcies per haver-me acollit sempre amb un somriure, però, per sobre de tot, per tenir les portes obertes del teu despatx sempre que ho he necessitat i per escoltar i valorar la meva opinió quan ens hem assegut davant d'uns resultats. A la Pepi, la tutora de la Tesi, gràcies per oferir-me sempre ajut quan l'he necessitat i per moure cel i terra quan alguna cosa no m'ha sigut favorable. Moltes gràcies. A la Carme, tot i no haver pogut gaudir dels teus consells i reunions científiques durant gaire temps, gràcies per les petites dosis que he tingut, han sigut increïbles. Tot un referent. A l'Antoni, gràcies per omplir els matins amb el teu "bon dia, nen!" tan necessari i ensenyar-me que la il·lusió no té edat. Al Vicent, per oferir-me, quan encara era un estudiant de carrera (sí... fa molts anys), la possibilitat d'entrar al grup i sembrar, així, la llavor del que esdevindria més tard un doctorat. Arribats a aquest punt, és bon moment per donar les gràcies, també, a tota la gent que em va acollir en aquells inicis al grup, quan només anava un dia al laboratori i ningú recordava que havia d'aparèixer per allà (la història que ha arribat a mi diu alguna cosa així com que sonava el timbre, us miràveu i la frase era "*ooh no! Avui venia el David, què fem? Amb qui el posem?*"). Gràcies, en tot cas, per superar la crisi de "*què fem? Amb qui el posem?*", obrir-me les portes i dedicar tantes hores a ensenyar-me a moure'm pel laboratori. Gràcies, Lucia, Jordi, Marc, Isaac i Victor. La vostra essència segueix present al laboratori.

Vull aprofitar aquestes línies, també, per donar les gràcies als meus companys d'aventura. Al Dani, amb qui, tot i no compartir gaire temps a nivell científic, si que ho he fet a nivell personal. Moltes gràcies pels consells i per les recomanacions literàries, per fer desaparèixer el mal rotllo quan entres pel laboratori de sorpresa i, sobretot, per mantenir els carrers segurs fent així que no tingui cap altra preocupació al cap a banda del que suposa tirar endavant la Tesi... A l'Estefa, per la paciència

inicial que vas tenir amb mi, quan no sabia caminar sol pel laboratori. A la Vero, estic segur que sóc capaç de guanyar-te en un 400 metres... tot i que les lesions m'han impedit demostrar-t'ho; queda pendent. A la Patri, per valorar-me en base a les teves pròpies experiències. Hem coincidit poc, però suficient com per saber amb certesa que seguirem coincidint. A l'Edgar, l'exterminador de *porex*, company de laboratori i company de pis; la gent posava en dubte que fos bona idea viure amb algú a qui veus tantes hores als dia, però tu ho fas fàcil. Passaran els anys i segur que guardaré la convivència amb tu com un encert. Gràcies per ensenyar-me a viure d'una forma més pausada. T'entregues al màxim en tot el que fas i ets una persona noble i transparent, no ho perdis mai, això. A la Mar, la persona més pacient del món, i segurament també una de les més fortes. En els moments difícils saps trobar ànims per un somriure i tirar endavant, no saps tot el que he arribat a aprendre de tu. Que mai et tallin les ales i "*que tu curiosidad no desaparezca*". Gràcies per mostrar sempre interès i estar disposada a donar un cop de mà pel que sigui i quan sigui. A la Mireia. Diu la llegenda que, en entrar al grup, ens comportàvem com rivals. Tots dos sabem que mai va ser veritat, això. No? O potser sí... Sempre t'he vist com un exemple a seguir, tant a nivell personal com a nivell científic. Gràcies per ser la meva còmplice cada cop que ens hem rigut en el moment més inoportú. No faré una enumeració de totes les situacions de riures continguts amb llàgrimes als ulls, ja que igual ocuparia set pàgines. Irene (Irenitas, piñita), la sonrisa constante y tu enorme corazón te hacen indispensable. Hay un antes y un después de tu llegada al grupo (¡y también hay un antes y un después del cuki-beso, eh!), le has dado forma a lo que somos dentro y fuera del laboratorio. Gracias por el asesoramiento lingüístico realizado en esta Tesis y gracias por estar siempre dispuesta a dejarlo todo por echar una mano a quien lo necesite. Y por encima de todo, gracias por abrirme las puertas de tus casas alrededor del mundo: Barcelona, Peñafiel, Estocolmo, Salamanca, ... A Iñigo, también gracias. Juntos hemos convertido nuestro laboratorio en la zona *nigga* más peligrosa de la ciudad y lo hemos evolucionado hasta llegar a convertirlo en Medellín. Ha sido un placer compartir laboratorio contigo teniendo así la posibilidad de tener tanto las discusiones más absurdas como las más apasionantes de la historia, así como ejercer de escriba oficial de tu lista negra. Me deja tranquilo saber que tengo cierta inmunidad diplomática al formar parte del régimen. Jas, moltes gràcies per tota l'ajuda, per estar sempre a punt quan he necessitat alguna cosa. Vam compartir poiata un temps i va ser una època difícil, el teu *síndrome de Diógenes* entrava en conflicte amb la meva obsessió pel minimalisme, però tots dos vam aprendre a conviure... Bé, en realitat no, no vam aprendre res... Jo segueixo tenint obsessió per no tenir res sobre la poiata i tu segueixes acumulant trastos per tot arreu. Per cert, suposo que a hores d'ara et dec molts milers d'euros. Ho sé. Tan bon punt els tingui, t'ho faré saber. Al David, per aparèixer sempre amb un somriure per la porta del laboratori i les converses de cada matí entre caixes de puntes i pots d'eppendorf.

A la Gemma. Tornes a aparèixer aquí, sí. Pensaves que ja t'ho havia dit tot? Doncs bé, no has estat "només" la directora de Tesi sinó que has estat també una companya de poiata i batalles al llarg de tot aquest temps. Potser necessito un gruix equiparable al d'aquesta Tesi per fer-te els agraïments que et mereixes. Se'm fa difícil intentar-ho plasmar en quatre línies i que no quedi pobre... En tot cas, una de les conclusions d'aquesta Tesi és que som les persones més oposades que existeixen al planeta Terra; crec que ha de quedar constància d'aquest fet i, ja que no puc posar-ho a l'apartat oficial de conclusions, ho poso aquí. No obstant, el fet de ser pols oposats, l'hem sabut convertir en una virtut, ja que ens ha permès saber en tot moment què necessitava o preferia l'altre. Moltes gràcies, Gemma. Gràcies per apostar per mi quan surava a la deriva, per estimar aquest projecte tant com jo, per entregar-te més enllà de les possibilitats humanes en cada experiment, en cada discussió i en cada línia inclosa en aquesta Tesi, gràcies per tot el que m'has ensenyat a nivell científic, però, sobretot, gràcies per ensenyar-me a veure i viure la vida amb el teu prisma de colors i gràcies per no desistir en la voluntat de tirar a terra els meus murs de línies grogues i vermelles i acostar-te, poc a poc, fins la verda. Per tot hi ha una primera vegada i al final ho hem tirat endavant, eh? Ets el meu principal referent. Ho saps, oi? Rellegint aquest fragment dels agraïments m'he

adonat que he començat el paràgraf dient "companys" de laboratori, però ben mirant, no em fa por referir-me a molts de vosaltres com a amics. Ens ha tocat remar junts contra corrent en més d'una ocasió, i això ens ha fet més forts. Hem viscut bé, al sol, però també hem descobert els avantatges de l'ombra. Vull que sapigueu que tinc la certesa que tot aquest camí no podria haver-lo fet rodejat de millors persones. Acaba una etapa, però en les que vinguin en un futur segur que seguirem ben a prop.

M'agradaria fer referència, també, a la gent més nova del laboratori amb qui malgrat haver compartit menys temps, també han format part de tot això, les TFM, Mireia 2.0, Cris, Laura, molta sort en l'aventura de la ciència, és un món apassionant, el que teniu davant; ja heu vist que no tot és idíl·lic, però que no us faci por encarar-lo, val la pena. Us ho dic de debò, *pinky-promise*. Y también a Antonio, nos has enseñado que la edad no es una barrera para luchar por lo que queremos. Mucha suerte!

Tampoc vull oblidar tota aquella gent que ha passat pel laboratori més o menys temporalment però que, d'alguna manera, han deixat algun record en aquest viatge. Així que, m'agradaria donar les gràcies pels moments compartits a la Berta; jugaves en una altra lliga. Vist en perspectiva, una crack! A la Júlia, amb qui espero tornar a coincidir en futurs congressos. I futures aventures. A la Marta, de qui vaig heretar la poiata i l'escriptori al laboratori; els he cuidat, eh? A tots els TFGs que heu passat per aquí i d'alguna manera m'heu estressat amb alguna liada o altra; en especial, al David Corón, amb qui vam fer possible l'impossible, un TFG en la meitat del temps establert. Ets un artista!

No seria just deixar aquí els agraïments, ja que tot aquesta aventura l'han patit també gent aliena al grup d'investigació. Començant per tots aquells que m'han acompanyat des dels inicis dels temps, donant forma al que sóc avui dia (per bé o per mal). A "*las gacelas*", per haver estat al peu del canó tot aquest temps; en especial al Joan. Ha sigut molt motivador que em recordessis pràcticament cada dia que el meu sou de becari l'estaves pagant tu amb els teus impostos... però que si els teus impostos havien d'invertir-se en alguna cosa, t'alegraves que fos en què jo tirés endavant els meus projectes. Gràcies, de debò.

Vull donar les gràcies també als amics que m'emporto dels anys a la facultat estudiant biologia i que sempre m'han animat a seguir fent ciència per difícil que pintava, sobretot vosaltres, Marc i Berron. Tinc la sensació que som inseparables, malgrat el pas del temps. A la Clara i la Mar, perquè presentar els resultats obtinguts en congressos internacionals és una experiència brutal, però més quan en fer-ho, a milers de quilòmetres d'aquí, heu estat al meu costat. Gràcies per les peixeres i per ser-hi sempre. A la Mire, per no perdre mai les ganes de compartir una estona de bar i arreglar el món. A la Cris, que no has deixat mai de preguntar com ho porto (i no deixis de fer-ho). Al Dr. Albert Vallejo, per se l'alegria de la casa i tenir una estona per xerrar malgrat tenir l'agenda més plena del món. A l'Olga Casulleras, per haver cregut sempre en les meves possibilitats i per haver-me fet costat en tants moments d'aquesta aventura. I a l'Olga Ruano, la Laura i la Sandra, i tants altres companys que heu estat a prop.

A la gent del Centre Montserrat-Xavier i als DesCentrats, per oxigenar el meu cervell quan necessitava una pausa. Sobretot a la Cristina, al Pepo i a la Clara, que sempre han cregut en mi i s'han interessat per l'estat de la Tesi, i pel meu estat, en tot moment. I en especial a l'Èlia, per apostar tan fort (i a cegues) per mi, per ser-hi sempre, en els bons moments i en els no tan bons, per alegrar-te quan un experiment funcionava i per fer-me veure que quan una cosa no funciona és només una excusa per seguir jugant i inventar una nova manera d'encarar una incògnita. I no voldria deixar-me d'agrair-te l'ajut bestial i impagable que has fet en la revisió ortogràfica d'aquest treball. Gràcies.

I per acabar, vull tancar els agraïments donant les gràcies a la meva família, perquè tot el que sóc és, en gran mesura, gràcies a vosaltres. A la meva àvia. Per animar-me sempre a seguir lluitant pels meus somnis. Ara quan vagis a classe a la universitat (sí, va a classe a la universitat!), ja podràs dir oficialment que el teu nét és doctor... que em temo que ja ho feies abans que ho fos, eh?. Als meus tiets i cosins, gràcies per creure en mi i estar sempre disposats a ajudar. Als meus pares, pel suport incondicional que sempre m'heu donat i per fer-me costat cada cop que he encarat un nou repte. També us vull donar les gràcies per fer cara d'entendre'm quan us parlava d'heteròmers de GPCR, agonistes i antagonistes, fent servir els gots que hi havia per sobre de la taula. I òbviament, moltes gràcies per l'esforç econòmic que heu fet per aplanar-me el camí fins aquí. I a ma germana, vals molt més del que creus, que mai t'ho facin dubtar. Sense vosaltres no hauria estat possible, res d'això.

I gràcies a tu, que has dedicat una estona del teu temps a llegir, o simplement fullejar, aquesta Tesi (tinc l'esperança que no t'hagis quedat només als agraïments ja que tot el que hi ha a les següents pàgines és apassionant).

Gràcies.

ABREVIATURAS

A

Aa	Aminoácido
AC	Adenilato ciclasa
ADA	Adenosina desaminasa
ADN	Ácido desoxirribonucleico
AK	Adenosina kinasa
AMPc	Adenosina monofosfato cíclico
AMY	Amígdala
A_nR	Receptor de adenosina
ARN	Ácido ribonucleico
ARNsi	Pequeño ARN de interferencia
ATP	Adenosina trifosfato

B

BiFC	*Bimolecular fluorescece complementation*
BiFCmc	*Multicolor bimolecular fluorescence complementation*
BiLC	*Bimolecular luminiscence complementation*
BiP/GPR-78	*Binding immunoglobulin protein/78 kDa glucose-regulated protein*
BNST	*Bed nucleus of the stria terminalis*
BRET	*Bioluminiscence resonance energy transfer*

C

Ca^{2+}	Calcio
Caln-n	Sensor de calcio calneurona-n
CaM	Calmodulina
Ca_vn	Canal de calcio dependiente de voltaje
CB_nR	Receptor de canabinoides
CeA	Núcleo central de la amígdala
CoH	*Coelenterazine H*
CRF	*Corticotropin-releasing factor*
CRF_nR	Receptor de *corticotropin-releasing factor*
CTX	Toxina colérica
cYFP	Fragmento c-terminal de la proteína fluorescente amarilla

D

DAG	Diacilglicerol
DAT	Transportador de dopamina
DMR	*Dynamic mass redistribution*
D_nR	Receptor de dopamina
DS	Estriado dorsal

E - F

ECn	Bucle extracelular
EGFR	*Epidermal growth factor receptor*

ERK	*Extracellular regulated kinases*
FRET	*Förster resonance energy transfer*

G

GABA	Ácido γ-aminobutírico
GDP	Guanosina difosfato
GEF	*Guanine nucleotide exchange factor*
GFP	Proteína fluorescente verde
GHS-1xR	Receptor de grelina
G_n	Subunidad de la proteína G
GPCR	*G-protein coupled receptor* (receptor acoplado a proteína G)
GPe	Globus pallidus externo
GPi	Segmento interno del globus pallidus
GRK	GPCR kinasa
GTP	Guanosina trifosfato

H - I - J

HEK-293T	Línea celular derivada de riñón de embrión humano
ICn	Bucle intracelular
IP_3	Inositol 1,4,5-trifosfato
JNKs	c-Jun N-terminal kinases

K

K^+	Potasio
Kd	Constante de disociación
kDa	KiloDalton
Kv1.2	Canal de potasio dependiente de voltaje

L

L-DOPA	Levodopa
LDTg	Tegmentum laterodorsal
LH	Hipotálamo lateral
LHb	Habénula lateral

M

M	Molar
MAPK	*Mitogen activated protein kinases*
MEK	*Mitogen activated protein kinase kinase*
Mg^{2+}	Magnesio
$mGlu_nR$	Receptor metabotrópico de glutamato
mM	miliMolar

N

NAc	Núcleo accumbens
NAD^+	*Nicotinamide adenine dinucleotide*
nCaBP	Proteínas neuronales de unión a calcio
NCS-1	Neuronal calcium sensor-1

NIDA	*National Institute on Drug Abuse*
nM	nanoMolar
NMDA	N-metil-D-aspartato
nYFP	Fragmento n-terminal de la proteína fluorescente amarilla

O - P

OX_nR	Receptor de orexina
PFC	Corteza prefrontal
PGRMC-1	*Progesterone receptor membrane component-1*
Pi	Fosfato
PKA	Proteína Kinasa A
PKC	Proteína Kinasa C
PLA	Fosfolipasa A
PLA	*Proximity ligation assay*
PLC	Fosfolipasa C
PTX	Toxina pertussis

R

R	Receptor
RE	Retículo endoplasmático
RGS	*Regulator of G-protein signaling protein*
Rluc	*Renilla luciferase*
RT-PCR	*Retro-transcriptase polymerase chain reaction*
RTK	Receptor tirosina kinasa

S - T

SN	Sustancia nigra
SNC	Sistema Nervioso Central
SNc	*Substantia nigra pars compacta*
SNr	*Substantia nigra pars reticulata*
SRET	*Sequential resonance energy transfer*
$SSTR_n$	Receptor de somatostatina
STN	Núcleo subtalámico
TMn	Dominio transmembrana

V - W - Y

VP	Ventral pallidum
VTA	Ventral tegmental área
WT	*Wild type*
YFP	Proteína fluorescente amarilla

CARACTERES ESPECIALES

$5\text{-}HT_nR$	Receptor de serotonina
μg	microgramo
μl	microlitro
μM	microMolar
σ_nR	Receptor sigma

INTRODUCCIÓN

1.1. RECEPTORES ACOPLADOS A PROTEÍNA G

1.1.1. Características generales

Los receptores acoplados a proteína G (GPCR) o de siete dominios transmembrana (7TM) constituyen el mayor y más versátil grupo de receptores de superficie celular implicados en la transducción de señal (*Gudermann, et al., 1997*). Cerca del 2% del genoma humano codifica para GPCR (*Jacoby, et al., 2006; Fredriksson, et al., 2003*) dando lugar a más de 1.000 proteínas de las cuales más del 90% se expresan en el Sistema Nervioso Central (SNC) (*George, et al., 2002*) conformando así la mayor superfamilia de proteínas del organismo (*Jones-Tabah, et al., 2016*). Los GPCR pueden encontrarse en prácticamente cualquier organismo eucariota, incluidos los insectos (Hill, et al., 2002) y plantas (*Josefsson, 1999*), indicando que son proteínas con un origen ancestral. Incluso ha sido encontrada en bacterias una proteína con siete dominios transmembrana sensible a la luz, nombrada rodopsina bacteriana. No obstante, no está claro que esta proteína bacteriana tenga un origen común con los GPCR de los organismos eucariotas debido a que no señaliza a través de una proteína G y a que sus secuencias carecen de homología (*Okada y Palczewski, 2001*).

Los GPCR son activados por una gran variedad de ligandos, tanto endógenos como exógenos, entre los que se incluyen hormonas, péptidos, aminoácidos, lípidos, nucleótidos, iones y fotones de luz. Estos receptores transducen la señal a través de un gran número de efectores como la adenilato ciclasa, las fosfolipasas o los canales iónicos entre otros, llevando a cabo multitud de funciones en el SNC y la periferia, donde controlan procesos biológicos como la proliferación, la supervivencia celular, el metabolismo, la secreción, la diferenciación, las respuestas inflamatorias e inmunes o la neurotransmisión (*Marinissen y Gutkind, 2001; Gether, et al., 2000*). Numerosas enfermedades y desórdenes están asociadas a mutaciones y polimorfismos de estos receptores (*Rana, et al., 2001*), por lo que son diana de un número creciente de agentes terapéuticos. Ha sido estimado que el 40% de los fármacos comercializados hoy en día (*Lu y Wu, 2016*) y casi un 25% de los 200 fármacos más vendidos en la actualidad modulan la actividad de los GPCR, actuando como activadores (agonistas) o bloquadores (antagonistas) (*Flower, et al., 1999; Howard, et al., 2001; Marinissen y Gutkind, 2001*) (**Figura 1**).

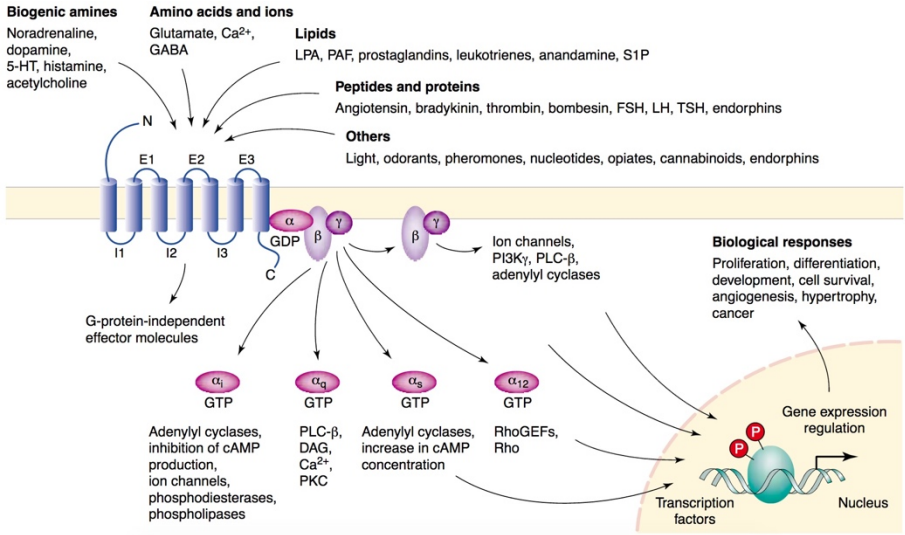

Figura 1. Ligandos endógenos y mecanismos de señalización celular responsables de las diversas funciones biológicas de los receptores acoplados a proteína G. Extraído de *Marinissen y Gukind, 2001*.

1.1.2. Arquitectura de los GPCR

Para que una proteína sea clasificada como GPCR debe cumplir dos características. En primer lugar, debe estar constituida por una única cadena proteica capaz de cruzar siete veces la membrana plasmática. Para ello, debe presentar una estructura con siete secuencias de 25-35 residuos aminoacídicos con alto grado de hidrofobicidad, dispuestos en una estructura de hélices α que atraviesan la membrana celular. Estas hélices están conectadas por tres bucles intracelulares y tres bucles extracelulares, quedando el dominio amino terminal (N-terminal) orientado hacia el medio extracelular y el dominio carboxilo terminal (C-terminal) hacia el intracelular, formando así una unidad que permite que un ligando extracelular ejerza su efecto específico dentro de la célula (**Figura 2A** y **2B**). La segunda característica es la capacidad de esta proteína para interactuar con una proteína G (**Figura 2C**).

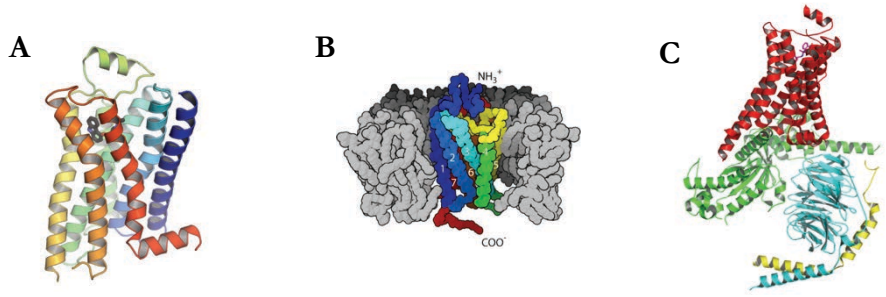

Figura 2. Representación esquemática del receptor adrenérgico β_2. A) Representación de las 7 hélices α del receptor adrenérgico β_2. **B)** Esquema de la disposición de un GPCR en la membrana plasmática. **C)** Representación de la interacción entre el receptor adrenérgico β_2 (rojo) y la proteína heterotrimérica G (Gα, verde; Gβ, azul y Gγ,amarillo). Extraído de *Cherezov, et al., 2007*.

La primera estructura cristalina de un GPCR fue descrita en el año 2000, cuando se determinó la estructura cristalina del receptor de rodopsina bovino (*Palczewski, et al., 2000*) (**Figura 3**). Desde entonces han sido cristalizados otros GPCR (*Weis y Kobilka, 2008; Rosenbaum, et al., 2009*) incluyendo el receptor A_{2A} de adenosina (*Jaakola, et al., 2008*) y el receptor β_2-adrenérgico (*Cherezov, et al., 2007*). Un año más tarde se publicó la estructura cristalina del receptor de opsina acoplado a la proteína G hecho que permitió una mejor interpretación de los cambios estructurales asociados a la transducción de señal (Scheerer, et al., 2008; Park, et al., 2008). En la actualidad, han sido descritas más de 100 estructuras tridimensionales de GPCR y el número de receptores que son cristalizados no deja de crecer (*Shonberg, et al., 2015*; *Yin, et al., 2016*). El nuevo enfoque en cuanto al estudio de GPCR es el diseño de agonistas y antagonistas en base a la estructura del receptor. Esto es posible a raíz del avance tecnológico de los últimos años; estas nuevas estructuras obtenidas mediante técnicas de rayos-X ofrecen a los investigadores una visión mucho más detallada acerca de la acción de estos receptores y como los fármacos interaccionan con ellos, además, sirve de guía para el diseño de nuevos compuestos (*Jacobson y Costanzi, 2012; Jacobson, 2015*). Estas nuevas perspectivas referentes al conocimiento estructural de los GPCR han hecho que el fenómeno conocido como agonismo parcial (*biased agonism*) haya evolucionado de un concepto teórico de interacción entre fármaco y receptor a un paradigma establecido que está teniendo un gran impacto en el descubrimiento de fármacos (Whalen, et al., 2011; Kenakin y Christopoulos, 2013). El agonismo parcial describe la habilidad de diferentes ligandos para estabilizar distintas conformaciones de un receptor determinado, de modo que solo una parte del posible repertorio de vías de señalización mediadas por dicho receptor son activadas en detrimento de otras vías (*Costa-Neto, et al., 2016; Klein Herenbrink, et al., 2016*). Este nuevo paradigma sugiere la posibilidad de diseñar nuevos fármacos capaces de activar específicamente unas vías de señalización y no otras, evitando así posibles efectos

secundarios no deseados (*Klein Herenbrink, et al., 2016*), motivo por el cual será imprescindible el conocimiento de la arquitectura de los GPCR y de cómo los distintos ligandos modifican la estructura del receptor.

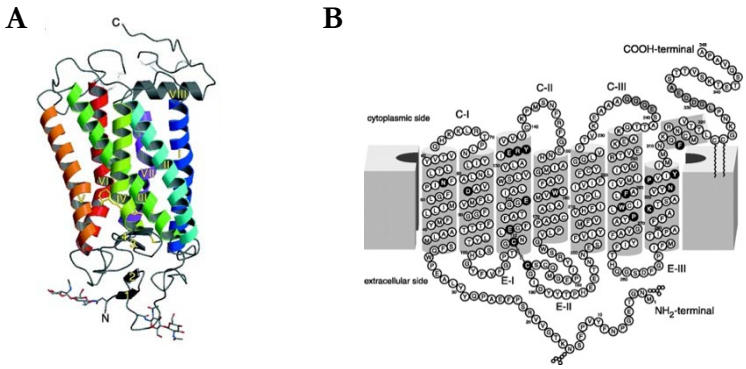

Figura 3. Estructura cristalina del receptor de rodopsina. **A)** Representación de las hélices α del receptor. **B)** Esquema de la disposición del receptor de rodopsina en la membrana. Extraído de *Palczewski, et al., 2000*.

1.1.3. Clasificación de los GPCR

Aunque los receptores acoplados a proteína G no comparten una gran homología en su secuencia aminoacídica (*Kolakowski, et al., 1994; Probst, et al., 1992*), han sido clasificados en diferentes familias según diferentes sistemas. Uno de los más clásicos es el sistema Kolakowski (*Kolakowski, et al., 1994*) donde los GPCR se clasifican en 6 familias (A-F) según su estructura y características genéticas. En la **Figura 4** se ilustran las 3 familias mayoritarias.

La familia A, también llamada *rhodopsin-like* contiene el 90% de todos los GPCR, siendo la más grande y la más estudiada, e incluye a receptores para una gran variedad de hormonas y neurotransmisores. La homología entre este tipo de receptores es baja y limitada a un número de residuos altamente conservados. Los receptores se caracterizan por tener un único residuo conservado en toda la familia que corresponde a la arginina del motivo Asp-Arg-Tyr (DRY) en el tercer segmento transmembrana (*Fraser, et al., 1988*) y por tener un puente disulfuro que conecta el primer bucle extracelular con el segundo. Además, muchos receptores tienen una cisteína palmitoilada en la cola C-terminal que sirve de anclaje a la membrana plasmática (**Figura 4A**, zigzag naranja). El estudio de la estructura cristalográfica de la rodopsina indica que los dominios transmembrana están inclinados y enroscados debido al aminoácido prolina que distorsiona los dominios helicoidales transmembrana. En esta familia, el ligando se une en una cavidad formada por los dominios transmembarna, aunque para alguna subfamilia de receptores activados por pequeños péptidos, el reconocimiento se produce a nivel de los bucles extracelulares y del dominio N-terminal (*George, et al., 2002; Jacaby, et al., 2006*).

La familia B incluye aproximadamente 50 receptores diferentes para una variedad de hormonas peptídicas y neuropéptidos como la calcitonina o el glucagón. Esta familia se caracteriza por tener un extremo N-terminal relativamente largo (aproximadamente 100 residuos) que contiene diversas cisteínas que forman una red de puentes disulfuro (*Ulric, et al., 1998*). Son de morfología similar a la familia A, pero no parecen palmitoilarse y los residuos y motivos conservados son diferentes (**Figura 4B**).

La familia C se caracteriza por tener un largo extremo carboxilo y amino terminal (500-600 aminoácidos). La estructura del lugar de unión (**Figura 4C**, en amarillo) ha sido deducida

mediante estudios de cristalografía del extremo N-terminal del receptor metabotrópico de glutamato solubilizado y unido a glutamato. Ha sido observado que este lugar de unión forma un dímero unido por puente disulfuro (*Pin, et al., 2003*) y que actúa como una planta carnívora, ya que puede abrirse o cerrarse en el proceso de unión de ligando. Excepto por las dos cisteínas conservadas en los bucles extracelulares 1 y 2 que forman un putativo puente disulfuro, esta familia no tiene ninguna característica común con las familias A y B. Una característica única de estos receptores es que poseen un tercer bucle intracelular corto y altamente conservado. Al igual que en la familia B, no se conoce la orientación de los dominios transmembrana (*George, et al., 2002; Jacoby, et al., 2006*).

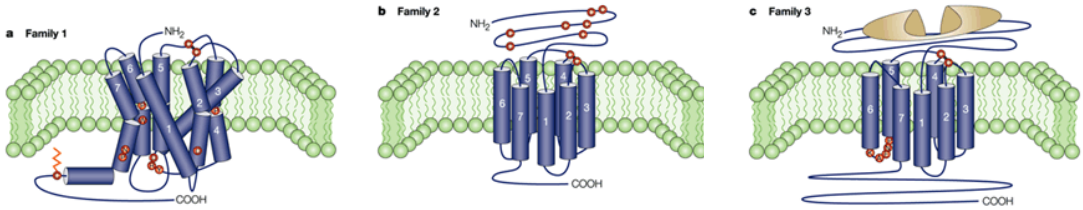

Figura 4. Representación esquemática de las tres principales familias de receptores acoplados a proteína G. A) Familia A, rhodopsin-like. **B)** Familia B. **C)** Familia C. Los residuos altamente conservados se indican en círculos rojos. Extraído de *George, et al., 2002*.

Las familias D y E son más pequeñas y están formadas por receptores de feromonas de levadura. Finalmente, cuatro receptores de AMP cíclico constituyen la familia F, que es muy pequeña pero única (*Kolakowski et al., 1994*).

Aunque la clasificación A-F se encuentra ampliamente aceptada, ha sido realizado un estudio filogenético de toda la superfamilia de GPCR en el genoma mamífero que ha dado lugar a una nueva clasificación más precisa (*Fredriksson, et al., 2003*). El análisis muestra que hay cinco familias principales para los GPCR humanos: *Glutamate, Rhodopsin, Adhesion, Frizzled/Tasted2* y *Secretin* (la clasificación GRAFS, basada en sus iniciales) y que dentro de cada familia los receptores comparten un origen evolutivo común. Las familias *Rhodopsin* (A), *Secretin* (B) y *Glutamate* (C) se corresponden con la clasificación A-F, mientras que las otras dos familias no están incluidas en este sistema. Los autores de este nuevo sistema de clasificación defienden la teoría de que los receptores acoplados a proteína G surgieron a partir de un único predecesor común, que evolucionó a través de duplicaciones génicas, desde la mayor simplicidad que presentaba en sus orígenes a la enorme complejidad que muestra esta superfamilia en la actualidad. La gran diversidad que alcanza esta superfamilia de proteínas de membrana da a entender el gran papel que juegan en la fisiología de cualquier organismo.

1.1.4. Vías de señalización

Los GPCR deben su nombre a su habilidad para reclutar, interaccionar y regular la función de la proteína G heterotrimérica, constituida por las subunidades α (39-46 kDa), β (37 kDa) y γ (8 kDa). La unión del ligando al receptor induce cambios conformacionales que se transmiten desde el receptor a la proteína G. El receptor actúa como un *guanine nucleotide exchange factor* (GEF), provocando que la subunidad α libere GDP y una GTP (*Syrovatkina, et al., 2016*). El mecanismo más comúnmente aceptado es que este intercambio de GDP por GTP desestabiliza el trímero y permite la disociación de la subunidad Gα-GTP del dímero βγ. Tanto la subunidad Gα como el dímero βγ son moléculas señalizadoras que,

interactuando y modulando diferentes moléculas efectoras, pueden activar o inhibir una gran variedad de segundos mensajeros. La señal termina cuando la actividad intrínseca GTPasa de Gα hidroliza el GTP a GDP y fosfato (*Bourne et al., 1991*). Las proteínas activadoras de la actividad GTPasa, como las proteínas RGS, pueden unirse a la subunidad Gα para acelerar la actividad GTPasa intrínsecamente lenta de esta subunidad (*Syrovatkina, et al., 2016*). La señalización mediada por Gβγ, por otro lado, finaliza por la reasociación con la subunidad Gα-GDP (**Figura 5**).

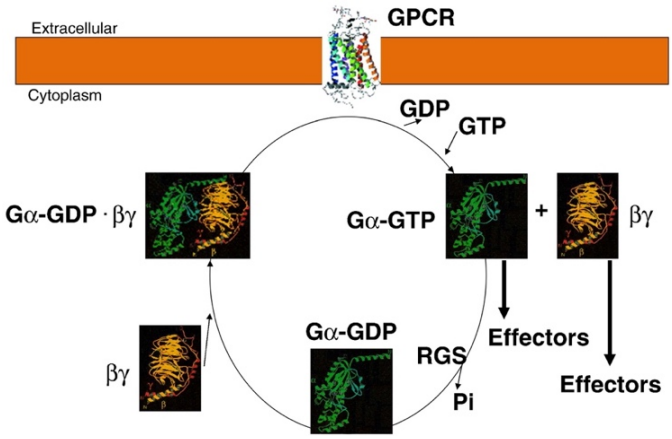

Figura 5. Ciclo de los GPCR. Extraído de *Syrovatkina, et al., 2016*

Existen cuatro grandes familias de subunidades Gα en mamíferos, que se caracterizan por su estructura primaria y por la cascada de señalización que activan (*Milligan y Kostenis, 2006*). En el caso de las subunidades $G\alpha_s$ o $G\alpha_i$, la proteína efectora es la adenilato ciclasa (AC). La familia $G\alpha_s$ estimula la adenilato ciclasa y la $G\alpha_{i/o}$ la inhibe. La adenilato ciclasa es una enzima que catalazia la conversión de ATP a AMPc, un importante segundo mensajero celular. El AMPc activa la PKA que, igual que la PKC, fosforila a múltiples y diversas proteínas (receptores, canales iónicos, enzimas o factores de transcripción) regulando así el funcionamiento celular. La $G\alpha_{q/11}$ activa la fosfolipasa Cβ (PLCβ), enzima que hidroliza fosfoinositoles de membrana generando IP_3 y DAG. El IP_3 aumenta la concentración de calcio intracelular vaciando los depósitos intracelulares, mientras que el DAG activa la PKC. La $G\alpha_{12/13}$ regula las proteínas Rho.

Muchas de las respuestas mediadas por estos receptores no consisten únicamente en la estimulación de segundos mensajeros convencionales, sino que son el resultado de la integración de diferentes redes de señalización, entre las que se incluyen la vía de las MAPK y las JNKs. La activación de la ruta de las MAPK por GPCR había sido poco estudiada hasta hace poco más de dos décadas, conociéndose sólo que el mecanismo involucraba una proteína G sensible a la toxina de la *Bordetella pertussis* ($G\alpha_{i/o}$) y que dependía fuertemente del complejo Gβγ de la proteína G y de tirosina quinasas no identificadas (*Faure, et al., 1994; Koch, et al., 1994; McKay y Morrison, 2007*). Entonces, se dedujo que, en ausencia de ligandos para receptores con actividad tirosina quinasas (RTK), la activación de receptores acoplados a proteína G podía inducir la estimulación de un RTK generando señales mitogénicas (*McKay y Morrison, 2007*). Este fenómeno se denominó transactivación. Una vez transactivado, el RTK inicia una cascada de señalización idéntica a la generada por su propio ligando; es decir, la activación de las MAPK se realiza por la vía Ras, Raf, MEK y ERK (**Figura 6**). El proceso es iniciado por las subunidades Gβγ, dando lugar al reclutamiento de Sos hacia la membrana, activando así el intercambio de GDP por GTP en la proteína Ras, siendo esta el intermediario

que conecta la cascada de señalización generada por la transactivación de un RTK con la fosforilación de ERK (*Marinissen y Gutkind, 2001; Paradis, et al., 2015*).
Existen otras vías independientes del fenómeno de transactivación que pueden inducir la activación de Ras, como por ejemplo vías dependientes de la concentración de calcio intracelular inducidas por receptores acoplados a $G\alpha_q$ (**Figura 6**). Una vez Ras está activada, inicia la cascada al unirse y activar a Raf, una serina/treonina quinasa que a su vez fosforila y activa a la quinasa de ERK/MAPK (denominada MEK), enzima que fosforila residuos de serina/treonina y de tirosina. La activación de ERK requiere la fosforilación de dos residuos (treonina y serina) separados por un solo aminoácido. Esta función sólo puede ser realizada por una enzima altamente especializada, por lo que se considera MEK una enzima limitante que hace altamente específico el proceso de activación de ERK. La activación de MEK también puede lograrse a través de B-Raf, quinasa que es activada por Rap, que a su vez es activada por la proteína quinasa A (PKA) dependiente de AMPc y por lo tanto bajo el control de receptores acoplados a $G\alpha_s$ (**Figura 6**). Según la magnitud de la activación de ERK, esta pasa del citoplasma al núcleo y regula, por fosforilación, a otras quinasas y factores de transcripción (*Davis, et al., 1995*).

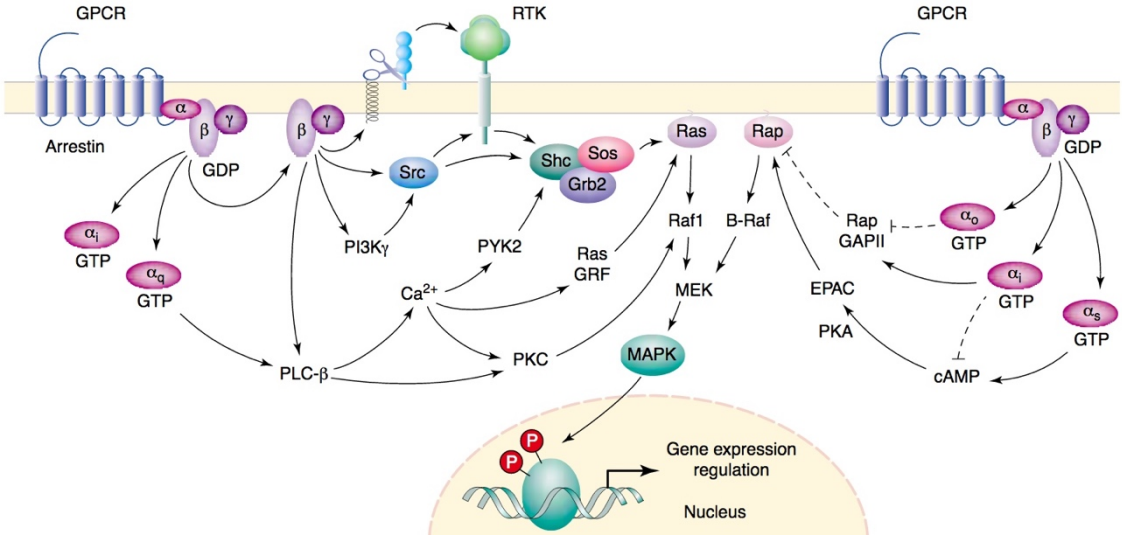

Figura 6. Representación de algunas de las vías que enlazan los GPCR con la vía de las MAPK. Extraído de *Marinissen y Gutkind, 2001.*

La complejidad de la señalización de los GPCR reside en el hecho de que estos receptores pueden actuar no sólo a través de la proteína heterotrimérica G, sino que también actúan por mecanismos independientes de la proteína G y de RTK y que probablemente implican la unión directa de Src y/o β-arrestina al receptor (*Lutrell y Lefkowitz, 2002; Ranjan, et al., 2016*). A lo largo de la última década, distintos autores han demostrado la habilidad de las β-arrestinas para transducir señales de forma independiente de proteína G (*DeWire, et al., 2007*), además, a las β-arrestinas se les ha atribuido la capacidad de actuar como proteínas *scaffolding* de distintos componentes de la cascada de señalización de las ERKs, aproximándolos así y facilitando la activación de esta vía (*Luttrell, 2005*).

1.1.5. Regulación de la actividad de los GPCR

Cuando un agonista interacciona con un GPCR a menudo resulta en una rápida atenuación de la respuesta del receptor, disminuyendo así la señalización del receptor y evitando los

posibles efectos adversos de una sobrestimulación celular. Este mecanismo de *feedback* se denomina desensibilización y puede manifestarse mediante diferentes procesos como el desacoplamiento del receptor de su proteína G en respuesta a la fosforilación del receptor (*Golan, et al., 2009; Ferguson, et al., 2001; Lohse, et al., 1990; Hausdorf, et al.f, 1989*), la internalización de los receptores de la superficie celular a compartimientos intracelulares (*Ferguson, et al., 2001; Moore, et al.,* 2007) y la disminución del número de receptores debido a la disminución del RNA mensajero y a la síntesis proteica, así como la degradación de los receptores preexistentes (*Jockers, et al., 1999; Pak, et al., 1999*). En el caso de las fosforilaciones, estos fenómenos tienen lugar en segundos, en minutos en el caso de las endocitosis y en horas cuando es regulada su expresión. La desensibilización del receptor puede ser completa, como ocurre en el sistema olfativo y visual o atenuada, disminuyendo la respuesta máxima, como ocurre con el receptor β_2 (*Thomsen, et al., 2016*).

La internalización de GPCR es un fenómeno común tras la estimulación por agonista. El tráfico de receptores desacoplados a compartimentos endosomales permite la desfosforilación y reciclaje del receptor a la superficie celular (*Krueger, et al., 1997; Boulay y Rabiet, 2005; Pavlos y Friedman, 2016*). Parte de los receptores internalizados pueden degradarse tras la exposición prolongada al agonista, lo que implica que el receptor sea marcado para entrar en la vía de degradación (*Böhm, et al., 1997*). El mecanismo de internalización de GPCR mejor caracterizado es el que sucede a través de la fosforilación del receptor mediada por las proteínas quinasas específicas de GPCR (GRK) y β-arrestinas (*Kelly, et al., 2008; Ranjan, et al., 2016*). La concepción clásica de este proceso explica que una vez el receptor es fosforilado por GRK, las β-arrestinas actúan como moléculas reguladoras que interactúan con componentes de la vía endocítica mediada por vesículas de clatrina (*Zhang, et al., 2016*). En respuesta a la activación de los GPCR, las proteínas β-arrestinas citosólicas translocan a la membrana plasmática, uniéndose a los receptores bloqueando así su capacidad para interaccionar con la proteína G heterotrímerica (*Kang, et al., 2015*), a la vez que se inicia el proceso de endocitosis mediado por clatrina (*Kang, et al., 2014*), reduciendo así la capacidad de señalización del receptor (**Figura 7**). Sin embargo, resultados muy recientes afirman la capacidad de los GPCR de clase B, pero no de los GPCR de clase A, para unir simultánemente la proteína G y la proteína β-arrestinas (*Wehbi, et al., 2013*), observándose también que esta unión de las proteínas β-arrestinas al receptor es capaz de promover una señalización sostenida del receptor una vez este ha sido internalizado (*Thomsen, et al., 2016*), poniendo en duda así el conocimiento clásico de este proceso de regulación de los GPCR.

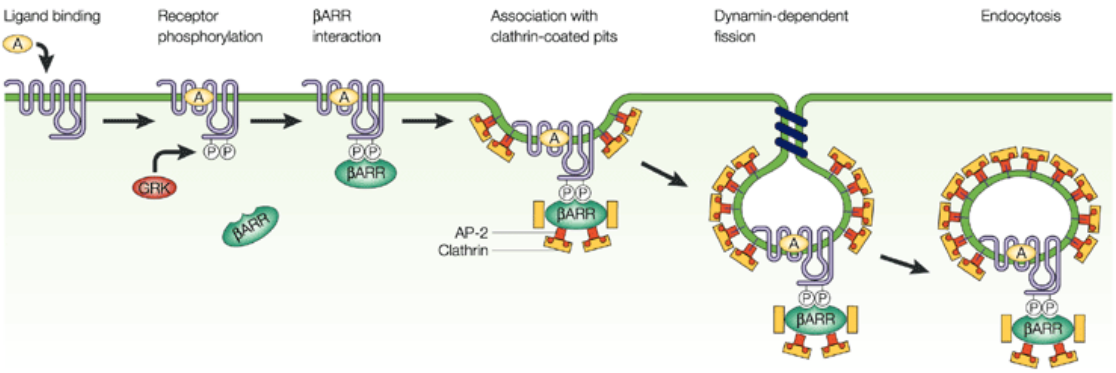

Figura 7. Mecanismo de desensibilización y reciclaje de los GPCR. Extraído de *Pierce y Lefkowitz, 2001.*

Algunos GPCR han sido encontrados en microdominios de membrana ricos en colesterol y caveolinas llamados caveolas (*Parton y del Pozo, 2013; Navarro, et al., 2014*). Estos dominios

son otro mecanismo para mediar la internalización de un receptor inducida por ligando (*Kong, et al., 2007; Wu, et al., 2008; Navarro, et al., 2014*). Las caveolas también son conocidas como dominios de señalización donde los GPCR pueden localizarse e interaccionar específicamente con proteínas de señalización (*Ostrom e Insel, 2004;* Villar, et al., 2016).
Finalmente, la desensibilización y endocitosis del GPCR desacoplado a los compartimentos endosomales permite la señalización del receptor por vías independientes de la proteína G (*Daaka, et al., 1998; Lefkowitz, et al., 1998*). Las β-arrestinas no solo participan en el secuestro de GPCR para la desensibilización e internalización, como ha sido mencionado anteriormente, sino que también actúan como proteínas para transducir y compartimentar las señales alternativas (*Golan, et al., 2009; Shukla, et al., 2014*), ya que estas proteínas tienen la habilidad de interaccionar con una gran variedad de proteínas endocíticas y de señalización como las c-Src (*Lutrel, et al., 1999*) MAPK y Raf (*DeFea, et al., 2000*). El proceso de endocitosis, además, facilita la desfosforilación del receptor por una proteína fosfatasa y el reciclaje hacia la superficie celular o la degradación (*Métayé, et al., 2005*) (**Figura 7**).

1.1.6. El fenómeno de la actividad constitutiva y ligandos de los GPCR

La activación de un GPCR se debe a un cambio conformacional que sufre el receptor una vez une al ligando agonista, pasando de un estado inactivo a uno activo, existiendo un equilibrio entre ambos estados. La actividad constitutiva que presentan estos receptores representa una isomerización del receptor al estado activo en ausencia de ligando (*Seifert y Wenzel-Seifert, 2002*). Como consecuencia de este cambio de GDP por GTP en las proteínas G acopladas a receptor se produce un aumento de la actividad basal de dicha proteína G y de los subsiguientes sistemas efectores (*Costa, et al., 1989*).

Los receptores acoplados a proteína G pueden encontrarse en múltiples conformaciones con distintas actividades biológicas. Estas conformaciones están estabilizadas por la unión del receptor a diferentes tipos de ligandos, siendo la más favorable para la señalización del receptor aquella estabilizada por un agonista total. Los agonistas parciales tienen una menor eficiencia para estabilizar al receptor en la conformación más activa y por lo tanto promueven un menor intercambio de GDP a GTP. Existen también los agonistas inversos parciales y los agonistas inversos totales, que estabilizan al receptor en su estado inactivo, en menor o mayor grado respectivamente, reduciendo la actividad basal o constitutiva del receptor. Por último, están los antagonistas neutros o simplemente antagonistas, que no alteran el equilibrio entre la forma activa y la inactiva, pero tienen la capacidad de bloquear el efecto de los agonistas (**Figura 8**).

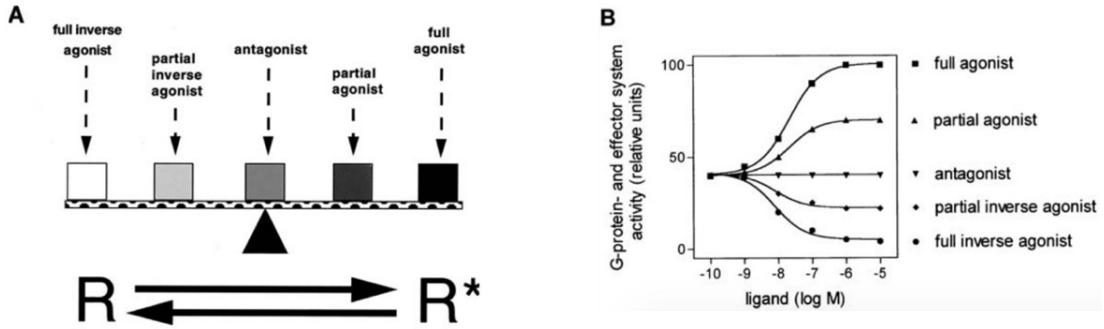

Figura 8. Activación de los receptores acoplados a proteína G según el modelo de dos estados. A) Modelo de dos estados que asume la isomerización del receptor de un estado inactivo R a uno activo R*. **B)** Acción de los diferentes tipos de ligandos sobre la actividad constitutiva del receptor. Extraído de *Seifert y Wenzel-Seifert, 2002*.

La mayoría de ligandos de los GPCR que actúan como agonistas, antagonistas o agonistas inversos se unen al mismo dominio del receptor reconocido por los agonistas propios del organismo, los agonistas endógenos, el lugar de unión ortostérico (*Neubig, et al., 2003*). En cambio, muchos GPCR poseen sitios alostéricos topográficamente distintos. Esto ha llevado a la identificación de ligandos que actúan como moduladores alostéricos, que pueden regular indirectamente la actividad de los ligandos ortostéricos y/o mediar directamente efectos agonista/agonista inverso (*May, et al., 2007; Bridges y Lindsley, 2008; Leach y Gregory, 2016*).

Tal y como ha sido comentado anteriormente, cada vez es más aceptado por la comunidad científica el fenómeno de *biased agonism*. Consecuentemente, la clasificación actual de los ligandos como agonistas totales, agonistas parciales, agonistas inversos o antagonistas deberá ser revisada y probablemente, reformulada. Hasta ahora no había sido tenido en cuenta que diferentes ligandos pueden estabilizar al receptor en distintas conformaciones promoviendo la activación de diferentes efectores o el acceso a distintas proteínas reguladoras (*Costa-Neto, et al., 2016*), de modo que, basándose en este nuevo paradigma, una molécula podría ser considerada agonista total al estudiar unas vías de señalización y antagonista al analizar otras vías (*van der Westhuizen, et al., 2014*). Del mismo modo, el modelo del *biased agonism* defiende que el transporte subcelular del receptor también puede depender del ligando que interaccione con este, promoviendo así señales distintas en el espacio. Por último, el modelo de *biased agonism* sugiere que cada ligando tiene una cinética de unión distinta y por lo tanto mantendrá al receptor en una conformación específica o condicionará su localización subcelular durante un periodo de tiempo diferente según la molécula que actúe como ligando (*Costa-Neto, et al., 2016*). Estos distintos aspectos en cuanto a la señalización promovida por un ligando específico deberán tenerse en cuenta para definir el perfil de señalización de cada molécula. Esta nueva visión de la señalización a través de los GPCR también plantea la cuestión de cómo debe ser cuantificada la eficacia relativa de cada ligando respecto cada vía de señalización, siendo el principal motivo de debate acerca del tema actualmente (*van der Westhuizen, et al., 2014; Kenakin, 2014*).

1.2. OLIGOMERIZACIÓN DE GPCR

Las características estructurales y la localización subcelular de los GPCR permiten a estos receptores interaccionar con otras proteínas tanto en el lado intracelular como extracelular de la membrana plasmática, así como también exhibir interacciones proteína-proteína con otros receptores o canales iónicos a nivel de membrana plasmática (*Franco, et al., 2003*).

Los GPCR tienen una topología que permite su interacción con una amplia variedad de proteínas. Estas interacciones determinan las propiedades del receptor, como la conformación, la compartimentación celular o la selección de una señal y pueden promover el ensamblaje en complejos que integran una función (*Kenakin y Miller, 2010; Gingell, et al., 2016*). Las proteínas que interactúan con los GPCR están involucradas principalmente en la organización de estructuras supramoleculares en las cuales se incluye todo tipo de receptores, proteínas implicadas en la transducción de señal e incluso proteínas citoesqueléticas (*Franco, et al., 2005*).

En el espacio extracelular, donde tiene lugar la unión a ligando, las regiones de los GPCR implicadas en la interacción con proteínas son, en la mayoría de casos, secuencias presentes en el extremo N-terminal, ya que los bucles extracelulares son muy cortos. Existen crecientes evidencias de que las interacciones receptor-proteína extracelulares pueden jugar un papel importante en la farmacología de los GPCR. Un ejemplo son las proteínas modificadoras de

la actividad de receptores (RAMPs*, receptor activity-modifying proteins*) (*Gingell, et al., 2016*). Actualmente se conoce la existencia de tres proteínas RAMP (*Sexton, et al., 2009*), las cuales, al interaccionar con ciertos GPCR como el receptor CRF_1R (*Wootten, et al., 2013*) o el receptor de glucagón (*Weston, et al., 2015*), afectan a la farmacología y señalización del receptor (*Gingell, et al., 2016*).

En la cara intracelular, tanto el extremo C-terminal como el tercer bucle intracelular de los GPCR pueden presentar un tamaño considerable. Por eso estas regiones son las que tienen mayor probabilidad de ser las responsables de interaccionar con las proteínas implicadas en la señalización o en la localización subcelular, mediadas por asociación a proteínas citoesqueléticas o relacionadas con el tráfico de receptores. Estas interacciones pueden ser transitorias o mucho más estables. Un ejemplo de proteína citosólica que interactúa con GPCR sería la calmodulina (CaM), un pequeño péptido con capacidad para unirse a distintos dominios citoplasmáticos de diferentes GPCR, entre los que se encuentra el extremo C-terminal del receptor A_{2A} de adenosina o el tercer bucle intracelular del receptor D_2 de dopamina, desarrollando una señal dependiente de calcio (*Bofill-Cardona, et al., 2000.; Navarro, et al., 2009*).

A nivel de la membrana plasmática, desde mediados de los años 90, diversos estudios han demostrado la oligomerización de numerosos GPCR (*George, et al., 2002; Navarro, et al., 2008, Navarro, et al., 2010; Moreno, et al., 2011; Herrick-Davis, et al., 2015; Franco, et al., 2016; Moreno, et al., 2016*). Hoy en día se acepta que la oligomeriazación es un hecho común en la biología de estos receptores y que pueden formar homodímeros, heterodímeros y/u oligómeros de orden superior (*Bouvier, et al., 2001; Franco, et al., 2003; Ferré, et al., 2009; Navarro, et al., 2013; Guitart, et al., 2014; Bonaventura, et al., 2015; Cordomí, et al., 2015; Franco, et al., 2016*). Cuando un GPCR participa en un oligómero pueden cambiar sus características funcionales, así la oligomerización confiere nuevas propiedades a los receptores, lo que establece un posible mecanismo para generar nuevas funciones en estos receptores. Este fenómeno ha dado lugar a un nuevo nivel de complejidad que gobierna la señalización y regulación de estas proteínas.

1.2.1. Interacción entre GPCR

Tradicionalmente los mecanismos de unión de ligando y de transducción de señal para los receptores acoplados a proteína G se basaban en el supuesto de que éstos actuaban como monómeros o proteínas independientes con estequiometria 1:1 respecto a su proteína G. Pero desde medidados de los años 90, diversos estudios han demostrado la oligomerización de numerosos GPCR y la relevancia que esto supone para su regulación.

Ciertas evidencias farmacológicas indirectas, como complejas curvas de unión, tanto de agonistas como de antagonistas de estos receptores, se interpretaron como la demostración de una cooperatividad que podía ser explicada mediante interacciones entre monómeros en complejos diméricos o multiméricos (*Franco, et al., 1996; Wreggett y Wells, 1995*). Maggio y colaboradores, utilizando quimeras de los receptores α_2-adrenérgicos y M_3 muscarínicos compuestas de los cinco primeros dominios transmembrana de uno de los receptores y los dos últimos dominios del otro receptor y viceversa, realizaron estudios de complementación y coinmunoprecipitación y sugirieron la formación de heterodímeros (*Maggio, et al., 1993*). Cuando cada quimera se expresaba independientemente no se observaba unión ni señalización tras la exposición a ligando, pero cuando ambas eran cotransfectadas se recuperaba la unión y la señalización tanto para ligandos adrenérgicos como muscarínicos.

La dimerización de los GPCR no está limitada a la homodimerización, entendida como la asociación física entre proteínas idénticas, sino que también incluye la asociación de un receptor con otro receptor o proteína distinta, lo que se conoce como heteromerización. Esta asociación puede darse entre dos monómeros para formar dímeros o entre múltiples monómeros para formar oligómeros. El término dímero ha sido tradicionalmente usado entendiendo que era la forma más simple de una unidad funcional oligomérica, debido a la dificultad que existía para la distinción entre dímeros u oligómeros con las técnicas de las que se disponía, sin embargo, actualmente gracias a los avances en la obtención de estructuras cristalográficas y la técnica *de single-particle imaging and tracking* (*Kasai y Kusumi, 2014*) ya es posible determinar la estequiometría del complejo oligomérico de forma más precesia, sugiriendo la existencia de nuevos modelos de heteromerización entre GPCRs en los que se destaca la importancia de los complejos tetraméricos (*Cordomí, et al., 2015*).

La oligomerización de receptores permite formular hipótesis sobre el alto grado de diversidad y plasticidad que es característico de una estructura altamente organizada y compleja como es el cerebro. Este fenómeno es importante para diversos aspectos en la funcionalidad de los GPCR como su biogénesis, la transducción de señales, su bloqueo (*Kim, et al., 2009; Ferré, et al., 2010*) o incluso, en algunos casos, esta dimerización es esencial para la funcionalidad del receptor, pues la formación del dímero induce una serie de cambios conformacionales en los receptores que posibilitan la unión de su ligando (*Zhang, et al., 2014*).

Ha sido descrito un nivel superior de organización por el que los receptores acoplados a proteína G forman estructuras compuestas no sólo por homo- o heterodímeros, sino por complejos supramoleculares formados por varios receptores y una variedad de proteínas que modifican la actividad del receptor. Estos complejos interaccionan tanto a lo largo de la membrana (interacciones horizontales), como a través de ella (interacciones verticales), y al ser activados por hormonas o neurotransmisores se redistribuyen en la membrana dando lugar a *clusters*. Los *clusters* supondrían un nivel superior de regulación de los receptores y enzimas asociadas y podrían ser regulados por otros receptores en estos complejos, además de por otras moléculas con las que no interaccionan físicamente, pero sí se comunican con ellos en el *cluster* (*Franco, et al., 2003; Thomsen, et al., 2016*).

El número creciente de publicaciones en este campo ha hecho necesario establecer nuevas definiciones y dotar de nomenclatura a los homómeros y heterómeros de GPCR, como han publicado Ferré y colaboradores (*Ferré, et al., 2009a*). Los nuevos desafíos pasan por entender cómo se forman y destruyen estos homo- o heterodímeros y cómo se regulan estos procesos, así como la identificación de nuevas parejas de heterómeros y la determinación exacta del papel de aquellas ya descritas.

Este concepto plantea una seria problemática, ya que prácticamente la totalidad de fármacos que tienen como diana un GPCR han sido diseñados partiendo de la base de que estos receptores funcionan de forma monomérica (*Franco, et al., 2013*). La constatación de que estos receptores pueden formar homo- o heterodímeros ha añadido una nueva dimensión al diseño de fármacos y ha planteado serias dudas acerca de la validez de muchos de ellos, siendo requerida en un futuro la reevaluación de muchos de estos fármacos, teniendo en cuenta las múltiples interacciones en las que puede estar implicado el receptor sujeto a estudio.

1.2.2. Arquitectura de los dímeros de GPCR

Para explicar el fenómeno de la dimerización de los receptores acoplados a proteína G se pueden considerar dos posibilidades: que estas interacciones sean directas, implicando contacto entre ambos receptores, o indirectas, cuando son necesarias otras proteínas que hagan de puente, como pueden ser las proteínas del citoesqueleto.

En las interacciones indirectas, los dominios intracelulares de los GPCR se unen a un gran número de proteínas citosólicas, algunas de las cuales han sido propuestas como posibles candidatas a participar en la dimerización de los receptores con los que interaccionan. Muchas de estas proteínas son proteínas andamio o *scaffolding proteins* que proporcionan una estructura compleja en la que diversos receptores pueden interaccionar entre ellos y con otras proteínas involucradas en la transducción de señal, controlando la velocidad y especificidad de dicha señalización (*Magalhaes, et al., 2012; Walther y Ferguson, 2015*).

En el caso de las interacciones directas hay distintas teorías. Por un lado, tradicionalmente ha sido considerado que los oligómeros se forman en el retículo endoplasmático, por lo que no son modulables por ligando, entendiendo la modulación como la formación o destrucción del oligómero (*Bouvier, et al., 2001; Van Craenenbroeck, et al, 2014*). Sin embargo, Bouvier y colaboradores ya sugerían que la gran complejidad estructural existente en esta superfamilia no permitía pensar en un único mecanismo de interacción directa (*Bouvier, et al., 2001*). Otras teorías acerca de la formación de los oligómeros defienden que los receptores se encuentran en equilibrio en la membrana plasmática, ya sea en forma monomérica o formando complejos, en función de las condiciones celulares, de la presencia de ligandos, de la región de la membrana donde se encuentran o de las modificaciones post-traduccionales del receptor (*Baltoumas, et al., 2016*). Baltoumas y colaboradores han sugerido la existencia de *hot spots* a nivel de membrana plasmática en los que los niveles de oligomerización de GPCR son más elevados, siendo una de las principales características de estas regiones la elevada presencia de colesterol, el cual facilitaría el proceso de interacción entre los receptores (*Baltoumas, et al., 2016*). En la misma línea, y basando también en las distintas características de algunas regiones de la membrana plasmática, algunos autores defienden que la formación de oligómeros se basa en el desajuste hidrofóbico que se establece entre el grosor de la membrana hidrofóbica y la longitud de la parte, también hidrofóbica, de la proteína que atraviesa la membrana. Si la parte hidrófoba de la proteína supera el grosor de la bicapa, la oligomerización puede reducir la zona hidrofóbica expuesta de la proteína (*Gahbauer y Böckmann, 2016*). Las interacciones directas pueden tener lugar mediante enlaces covalentes (puentes disulfuro) y/o no covalentes (fuerzas hidrofóbicas y/o electrostáticas) entre los dominios transmembrana y los dominios intracelulares de los receptores (**Figura 9**).

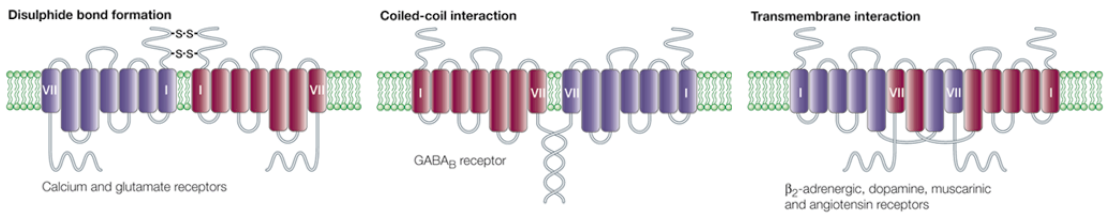

Figura 9. Determinantes moleculares de la dimerización de GPCR. Extraído de *Bouvier, et al., 2001.*

Han sido encontradas distintas interacciones intermoleculares involucradas en la formación de varios homómeros y heterómeros de GPCR. En la familia C de receptores acoplados a proteína G el gran dominio N-terminal extracelular contiene varios residuos de cisteína que

pueden contribuir a la dimerización mediante la formación de puentes disulfuro con el otro GPCR del complejo (*Romano, et al., 1996*; *Romano, et al., 2001; Miura, et al., 2005*). Este es el caso de los receptores sensibles a calcio y de los metabotrópicos de glutamato, así como de algunos receptores de la familia A como los receptores de angiotensina II (*Miura, et al., 2005*), el receptor de serotonina 5-HT_4R (*Berthouze, et al.,* 2007) o el receptor muscarínico de acetilcolina M_3 (Hu*, et al., 2012*), entre otros. También han sido descritas interacciones donde el dominio C-terminal de los receptores es fundamental, como la homodimerización del receptor β_2-adrenérgico (*Salahpour, et al., 2004*) o la interacción directa *coiled-coil* de la cola de los receptores $GABA_{B1}$ y $GABA_{B2}$ (*Margeta-Mitrovic, et al., 2000*). Finalmente, la dimerización directa entre GPCR también puede estar mediada por interacciones iónicas o hidrofóbicas entre los dominios extracelulares, intracelulares o transmembrana del receptor. Ha sido demostrada la existencia de interacciones iónicas entre péptidos presentes en los dominios intracelulares que contienen respectivamente dos o más cargas positivas adyacentes (RR, KK, o RKR) y dos o más cargas negativas (DD o EE) o residuos aminoacídicos fosforilados (*Woods y Huestis, 2001*). Un ejemplo de estas interacciones sería la participación de residuos cargados y/o fosforilados en la heteromerización de los receptores A_{2A} de adenosina y D_2 de dopamina (*Navarro, et al., 2010*). La idea de que las interacciones hidrofóbicas podrían tener un papel relevante en la formación de los dímeros se propuso por primera vez para el receptor β-adrenérgico. Mediante el uso de péptidos sintéticos y mutagénesis dirigida se propuso que residuos concretos de glicina y leucina situados en el sexto domino transmembrana del receptor estaban involucrados en su dimerización (*Hebert, et al., 1996*). También ha sido propuesto que las interacciones entre dominios transmembrana pueden estar implicadas en la homodimerización de receptores de dopamina (*Ng, et al., 1996; Guo, et al., 2008*), de los receptores μ-opiodes (*Manglik, et al., 2012*) o de los receptores β_1-adrenérgicos (*Huang, et al., 2013*) y β_2-adrenérgicos (*Parmar, et al., 2016*), entre otros. Sin embargo, todos estos mecanismos de interacción propuestos, más que reflejar diferentes estrategias utilizadas por diferentes clases de receptores, indican que múltiples sitios de interacción están implicados en el ensamblaje y la estabilización de los dímeros.

Actualmente, los avances en la resolución de estructuras cristalinas de GPCR y la combinación con modelos computacionales han revolucionado el estudio de la arquitectura de los oligómeros, proponiendo nuevos modelos tridimensionales que explican la dimerización de los receptores acoplados a proteína G. El análisis de las estructuras cristalinas disponibles de GPCR sugiere principalmente una interacción entre monómeros a través de los dominios transmembrana (TM), formando unas estructuras nombradas *head-to-head* entre los dos receptores. Estas interacciones pueden producirse potencialmente entre los TM1, TM4, TM4/5 o TM5/6 de cada receptor (*Gonzalez, et al., 2014*). Por un lado, los dímeros que más aparecen en los cristales son los correspondientes a los modelos de interacción entre TM1 y TM4/5, siendo por lo tanto los modelos diméricos más plausibles (*Gonzalez, et al., 2014*). Por otro lado, el modelo dimérico TM5/6 impediría los cambios conformacionales necesarios en los receptores para iniciar la señalización mediada por la proteína G, sugiriendo que los dímeros formados mediante esta interacción no formarían una unidad funcional (*Cordomí, et al., 2015*). Por lo que respecta al modelo TM4, en base al modelo estequimétrico actualmente aceptado, no sería compatible con la unión de la proteína G al dímero, ya que la subunidad Gα chocaría con el otro receptor del complejo (*Cordomí, et al., 2015*) (**Figura 10**). Del mismo modo que ha sucedido con los modelos diméricos de GPCR, nuevos datos han puesto en entredicho los conceptos establecidos respecto a la estequiometría de estos oligómeros. Hoy en día ya es aceptado por prácticamente la totalidad de la comunidad científica que la estequiometría de los dímeros es 2:1 (receptor:proteína G) (*Jastrzebska, et al., 2013*), además, muchos autores defienden que el tamaño mínimo a considerar como unidad

básica de un GPCR, correspondería precisamente a dos protómeros iguales y una proteína G (*Franco, et al., 2013*).

Estos modelos diméricos propuestos por Cordomí y colaboradores, además, explicarían cómo interaccionan los protómeros al formar complejos de orden mayor. La forma más sencilla para formar un tetrámero sería combinando dos dímeros en estructura *head-to-head* mediante otra de las cuatro posibles interacciones sugeridas (*Cordomí, et al., 2015*). Al tetrámero, en base a la estequiometría 2:1, podrían unirse, potencialmente, dos proteínas G, tanto en los protómeros internos como en los externos del complejo, dando lugar a distintas combinaciones "*in-in*", "*in-out*" u "*out-out*" (*Cordomí, et al., 2015*).

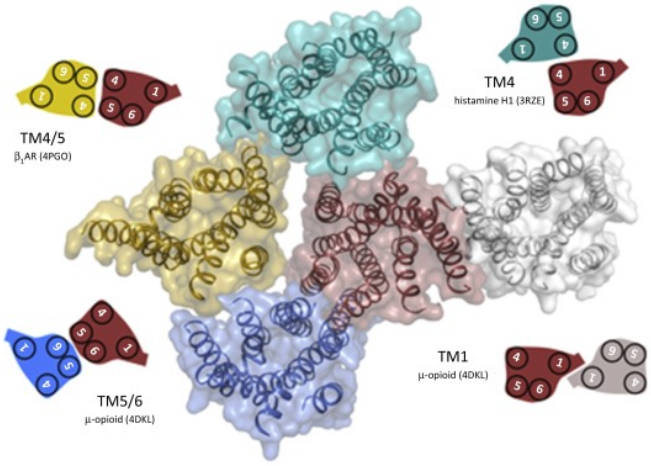

Figura 10. Modelo tridimensional de la dimerización de GPCR. Vista extracelular de la representación de parejas de receptores superpuestas en un protómero central (rojo). Las regiones de interacción que participarían en la formación del dímero son: TM1 (blanco), TM4 (gris), TM4/5 (amarillo) o TM5/6 (azul). Extraído de *Cordomí, et al., 2015*.

1.2.3. Técnicas para el estudio de la oligomerización de GPCR

Mediante estudios farmacológicos se obtuvieron las primeras evidencias de la existencia de homodímeros entre GPCR. Las complejas curvas de unión, tanto de agonistas como de antagonistas de estos receptores, se interpretaron considerando la existencia de una cooperatividad positiva o negativa, que se podía explicar mediante interacciones entre los sitios de unión de los receptores dentro de complejos diméricos u oligoméricos (*Wreggett y Wells, 1995*; *Limbird, et al., 1975*; *Mattera, et al., 1985*; *Hirschberg y Schimerlik, 1994*; *Franco, et al., 1996*). Una evidencia contundente de la existencia de hetero-oligómeros la constituyen los cambios cinéticos en la unión de radioligandos a un receptor provocados por la unión de ligandos no radioactivos al otro receptor del heterómero, utilizando membranas aisladas de células o de tejido que expresen los dos receptores. En preparaciones de membrana no existe ninguna maquinaria celular que pueda producir un *cross-talk* indirecto (por ejemplo, la producción de un segundo mensajero característico de la activación de uno de los GPCR del complejo, al estimular el otro receptor, es decir, un *cross-talk* a nivel de segundos mensajeros) y la explicación más sencilla de la existencia de una modulación a nivel de unión de radioligandos es la existencia de una interacción molecular entre ambos receptores. En estos casos la unión de un ligando a un receptor induce cambios conformacionales en el otro receptor que modulan su capacidad de unir a su ligando y estos cambios sólo se pueden producir si ambas proteínas interaccionan molecularmente directa o indirectamente (*Franco, et al., 2007*; *Franco, et al., 2008a*). En muchos casos esta clase de interacción ha sido encontrada

en tejido nativo, hecho que puede ser interpretado como un indicador de la existencia de receptores heteroméricos *in-vivo* (*González-Maeso, et al., 2008*; *Marcellino, et al., 2008*).

Una de las técnicas bioquímicas más utilizadas para investigar la dimerización de GPCR ha sido la coinmunoprecipitación. El primer estudio que utilizó esta técnica demostró la interacción específica entre los receptores β_2-adrenérgicos (*Hebert, et al., 1996*). Desde entonces, estrategias similares han sido usadas para documentar la homodimerización de los receptores metabotrópicos $mGlu_5R$ (*Romano, et al., 1996*), δ-opioides (*Cvejic y Devi, 1997*) y serotonina 5-HT_{2c} (*Herrick-Davis, et al., 2004*), entre otros. Los estudios de coinmunoprecipitación también han sido utilizados para demostrar la heterodimerización de receptores del mismo neurotransmisor, como $GABA_{B1}$ y $GABA_{B2}$ (*Jones, et al., 1998*; *Kaupmann, et al., 1998*; *White, et al., 1998*) o con los κ- y δ-opioides (*Jordan y Devi, 1999*), e incluso entre receptores menos relacionados como los receptores de adenosina A_1 y dopamina D_1 (*Ginés, et al., 2000*), los receptores A_{2A} de adenosina y metabotrópico $mGlu_5$ (*Ferré, et al., 2002*) o los receptores de cannabinoides CB_1 y de dopamina D_2 (*Kearn, et al., 2005*).

A pesar de haber tenido un papel importante en la detección de interacciones proteína-proteína, la coinmunoprecipitación de GPCR sufría de una gran desventaja: la formación de dímeros artefactuales por una solubilización incompleta de los receptores, que mayoritariamente son de naturaleza hidrofóbica. Actualmente, pese a todos los controles usados para descartar esta posibilidad, la aceptación generalizada de la dimerización de GPCR depende de una demostración directa de que estos complejos existen en células vivas. Esto ha sido posible con el desarrollo de métodos biofísicos basados en la transferencia de energía por resonancia (RET: *resonance energy transfer*).

En 1984 Theodor Förster formuló la teoría de transferencia de energía por resonancia (*Förster, et al., 1948*) que más tarde fue aplicada al estudio de interacciones entre GPCR. Esta aproximación biofísica está basada en la transferencia de energía no radiactiva (dipolo-dipolo) desde un cromóforo en estado excitado (dador) a una molécula cercana que absorbe (aceptor). En el caso de la transferencia de energía de resonancia fluorescente (FRET: *Fluorescence Resonance Energy Transfer*), tanto el dador como el aceptor son moléculas fluorescentes, mientras que en la transferencia de energía de resonancia bioluminiscente (BRET: *Bioluminiscence Resonance Energy Transfer*) el dador es bioluminiscente y el aceptor es fluorescente.

Para que la transferencia de energía tenga lugar es necesario que se cumplan dos requisitos. El primero consiste en que el espectro de emisión del dador y el espectro de excitación del aceptor se solapen, de forma que parte de la energía de emisión del dador se transfiera de forma directa al fluoróforo aceptor, el cual emite como si hubiera sido excitado directamente. El segundo requisito es que dador y aceptor estén muy próximos en el espacio (<100 Å o 10 nm). Además, la eficiencia de la transferencia va a disminuir con la sexta potencia de la distancia.

Hay que destacar que la mayor parte de complejos multiproteicos de una célula se encuentran entre 10 y 100 Å (*Stryer, et al., 1978*; *Sheng y Hoogenraad, 2007*). Así, las técnicas de transferencia de energía ofrecen una aproximación única que permite detectar la dimerización de proteínas en células vivas, sin perturbar el entorno donde este fenómeno ocurre.

Para la técnica de FRET se utilizan las diferentes variantes de la proteína fluorescente verde (GFP: *Green Fluorescent Protein*) obtenidas por mutación. Estas mutaciones confieren

diferentes propiedades espectrales, de forma que, dos proteínas mutadas diferentes con las características espectrales adecuadas, fusionadas a las proteínas de estudio, nos permiten determinar si estas están lo suficientemente cercanas como para que entre ellas se produzca una transferencia de energía. La pareja más ampliamente utilizada para los experimentos de FRET son la variante GFP^2, que se excita a 400 nm y emite a 510 nm, y la variante YFP (*Yellow Fluorescent Protein*), que se excita a 485 nm y emite a 530 nm. En la técnica de FRET, como se esquematiza en la **Figura 11**, cuando un haz de luz excita la proteína GFP^2, esta emite fluorescencia a 510 nm y si ambas proteínas están suficientemente próximas en el espacio, tendrá lugar una transferencia de energía y la proteína fusionada a YFP emitirá fluorescencia con un pico a 530 nm (*Pfleger y Eidne, 2005; Gandia, et al, 2008b; Navarro, et al., 2010*).

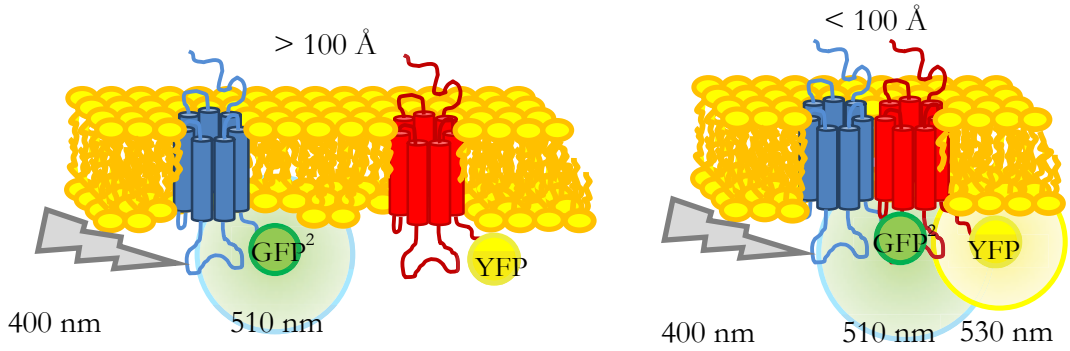

Figura 11. Representación esquemática de la técnica de FRET.

Similar al FRET y con los mismos requerimientos, cabe considerar la técnica de transferencia de energía por resonancia bioluminiscente, BRET. En esta técnica, la bioluminiscencia es el resultado de la degradación catalítica de cierto sustrato por la enzima luciferasa (*Rluc*) en presencia de oxígeno, generando luz. Esta luz es transferida a una variante de la proteína GFP, la cual a su vez emite fluorescencia a una longitud de onda característica si ambas proteínas están lo suficientemente cerca, indicando la dimerización de las proteínas fusionadas a *Rluc* y a GFP (*Gandia, et al., 2008b*; *Pfleger y Eidne, 2005*).

Han sido descritas dos variantes de esta técnica, el $BRET^1$ y el $BRET^2$. En el $BRET^1$ la enzima *Rluc* metaboliza el sustrato coelenterazine H generando luz con un pico de emisión de 480 nm, emisión que permite excitar a la proteína YFP, que emitiría a 530 nm. En el $BRET^2$ el sustrato DeepBlueC es oxidado por la *Rluc* emitiendo luz a 400 nm de forma que puede excitar a la proteína GFP^2, que emitiría a 510 nm (**Figura 12**).

Las ventajas de este fenómeno han sido utilizadas por los investigadores para el estudio de la dimerización de GPCR. Se generan proteínas de fusión que unen en el extremo carboxi terminal de un receptor la proteína luminiscente *Rluc* y en el otro receptor la proteína fluorescente GFP o una de sus variantes, y se co-expresan. Mediante estas técnicas de transferencia de energía ha sido demostrada la existencia de homodímeros de los receptores A_{2A} de adenosina (*Canals, et al., 2004*), δ-opioides (*Johnston, et al., 2011*) y β_2-adrenérgico (*Parmar, et al., 2016*), entre otros. También ha sido realizada una aproximación similar para el estudio de heterómeros de receptores acoplados a proteína G, como por ejemplo, los receptores A_1 y A_{2A} de adenosina (*Ciruela, et al., 2006*), los receptores D_1 y D_3 de dopamina (*Marcellino, et al., 2008*), los receptores D_1 y D_2 de dopamina (*Pei, et al., 2010*), los receptores D_1 o D_2 de dopamina y H_3 de histamina (*Moreno, et al., 2011*), los receptores CB_1 y CB_2

(*Callén, et al., 2012*), los receptores D_1 de dopamina y CRF_2 (*Fuenzalida, et al., 2014*) o los receptores A_{2A} de adenosina y D_2 de dopamina (*Bonaventura, et al., 2015*), entre otros.

En los últimos años, han sido desarrolladas variaciones de la técnica de FRET como el *photobleaching* o el *time-resolved* FRET (*Pfleger y Eidne, 2005*). Uno de los resultados más interesantes ha sido obtenido utilizando el microscopio de transferencia de energía por resonancia en milisegundos. Con esta técnica ha sido demostrada la existencia de un cross-talk conformacional entre el receptor α_2-adrenérgico y μ-opioide (*Vilardaga, et al., 2008*). La unión de morfina al receptor μ-opioide desencadena un cambio conformacional en el receptor α_2-adrenérgico ocupado por norepinefrina que inhibe su señalización.

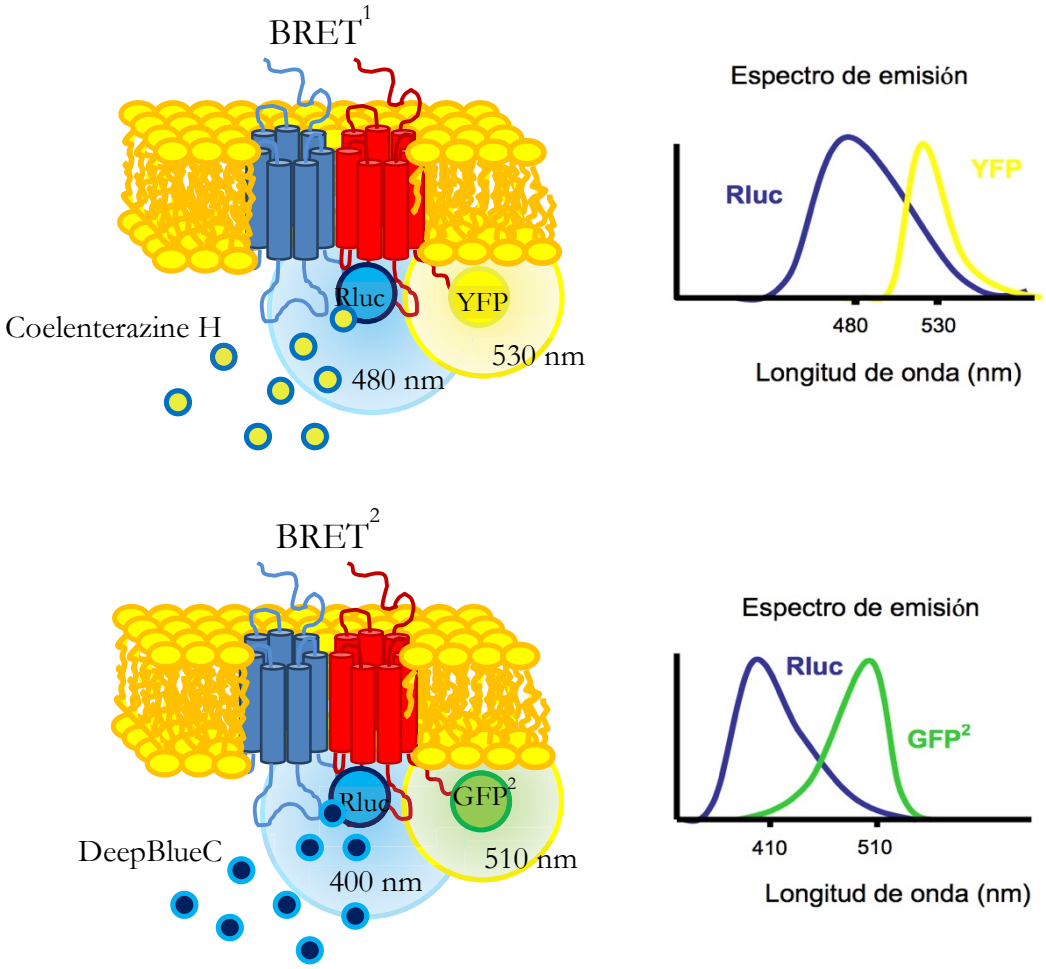

Figura 12. Representación esquemática de los fenómenos de BRET¹ y BRET² con sus correspondientes espectros de emisión.

En 2008 la experiencia y el buen funcionamiento de las técnicas RET plantearon su uso para la detección de complejos triméricos. Con este fin, de la combinación de la técnica de BRET y FRET se desarrolló la técnica de SRET, *sequential resonance energy transfer* (*Carriba, et al., 2008*).

El descubrimiento de las técnicas de Complementación Bimolecular (BiFC, *Bimolecular fluorescence complementation*) ha aportado un nuevo sistema muy eficaz para detectar interacciones proteína-proteína en células vivas. Esta técnica utiliza dos fragmentos no fluorescentes de la proteína sYFP o Venus (nYFP y cYFP). Cuando la proteína sYFP se reconstituye a partir de la interacción directa entre dos proteínas fusionadas con estos fragmentos, se genera una señal fluorescente (*Hu, et al., 2002*) (**Figura 13**). Esta señal sólo se

genera si las proteínas de fusión están muy próximas en el espacio (a una distancia inferior a 6 nm). Más adelante, en la misma línea de investigación, han sido desarrolladas técnicas que utilizan dos fragmentos de la proteína luminiscente *Rluc8* (BiLC *Bimolecular luminescence complementation*). Cuando las proteínas fusionadas a estos fragmentos interaccionan se reconstituye la proteína *Rluc8,* que resultará enzimáticamente activa (*Paulmurugan, et al., 2003*). La combinación de las técnicas de BiFC y BiLC, ha permitido el estudio de complejos tetraméricos (*Bonaventura, et al., 2015*). Finalmente, ha sido desarrollada también la técnica de multicolor BiFC (mcBiFC) que utiliza diferentes fragmentos de diferentes proteínas facilitando la investigación de redes de complejos de proteínas reguladoras (*Gehl, et al., 2009*).

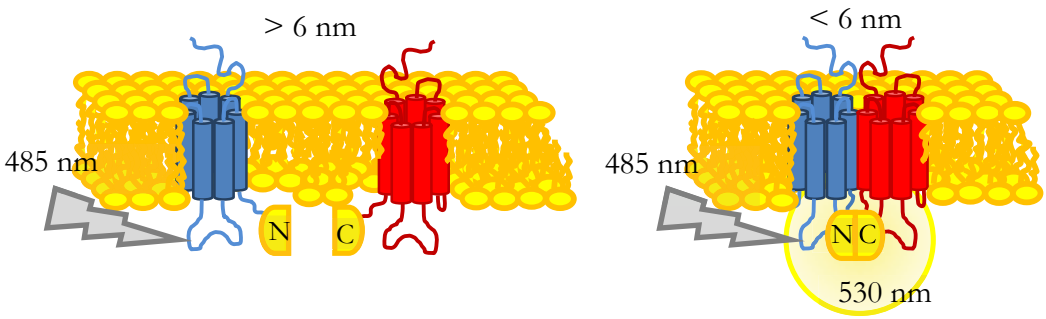

Figura 13. Representación esquemática de la técnica de BiFC (*Bimolecular Fluorescence Complementation*).

Debido a la gran repercusión del estudio de las interacciones entre proteínas se ha seguido trabajando en el diseño de nuevas técnicas para su detección. Una de las más novedosas es la conocida como *Proximity Ligation Assay* (PLA), desarrollada por Fredriksson y colaboradores (*Fredriksson, et al., 2002*) y la cual ha ido evolucionando para dar respuesta a múltiples necesidades científicas, como la detección de interacciones proteína-proteïna en muestras de tejido. Esta técnica requiere de dos anticuerpos primarios, generados en especies diferentes, específicos para las proteínas o antígenos a estudiar. Posteriormente, la muestra es incubada con los denominados *PLA probes*, dos anticuerpos secundarios específicos contra los anticuerpos primarios, los cuales llevan unidos un oligonucleótido. Mediante la acción de una enzima ligasa, los oligonucleótidos unidos al anticuerpo secundario formarán una cadena de ADN circular siempre y cuando las proteínas estudiadas se encuentren suficientemente próximas. Esta cadena de ADN circular actuará como molde para una posterior amplificación de círculo rodante por acción de una polimerasa y nucleótidos marcados (*Söderberg, et al., 2006*) (**Figura 14**). El producto final puede ser detectado posteriormente utilizando de un microscopio de fluorescencia.

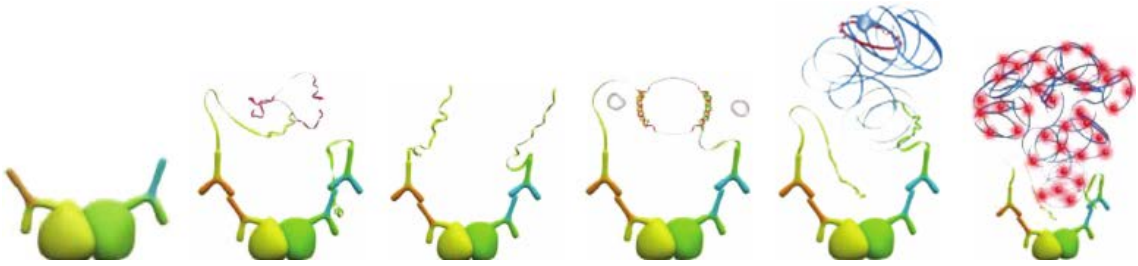

Figura 14. Esquema de la técnica de PLA. Extraído de *www.abnova.com*

1.2.4. Papel funcional de la dimerización

La disponibilidad de un gran número de técnicas para el estudio de la dimerización de GPCR ha facilitado enormemente la investigación del papel funcional de estos complejos de receptores. La dimerización se encuentra implicada en la regulación de la funcionalidad del receptor a diferentes niveles, desde la modulación de la expresión del receptor en la superficie celular hasta el hecho de conferir nuevas propiedades farmacológicas a los receptores expresados en el dímero (**Figura 15**). Esto ha proporcionado una nueva perspectiva para considerar cual es la unidad de señalización de los GPCR, además de una nueva vía para el diseño de drogas que actúen a través de estos receptores.

Aunque en muchos casos la relevancia fisiológica no se conoce completamente, diversos estudios llevados a cabo en sistemas de expresión heterólogos han sugerido distintos papeles funcionales para la oligomerización de GPCR. Por ejemplo, la oligomerización puede estar implicada en la ontogénesis de GPCR, es decir, en el control de calidad del plegamiento y de la destinación a la membrana de receptores sintetizados de *novo*. Asimismo, en algunos casos, ha sido observada una regulación de la formación/destrucción de oligómeros presentes en la membrana plasmática mediada por ligando. También ha sido constatado que la oligomerización confiere diversidad farmacológica, ya que la unión de un ligando a un receptor del dímero puede influir en la unión de otro ligando al segundo receptor dentro del dímero (*Ferré, et al., 2007*; *Franco, et al., 2008b*). La oligomerización también puede modificar las propiedades de señalización de un determinado ligando afectando a la selectividad de interacción entre el receptor correspondiente y su proteína G, resultando en una potenciación, atenuación o acoplamiento con otra proteína G. Finalmente también ha sido visto que la oligomerización puede alterar el patrón endocítico para un determinado receptor (*Terrillon y Bouvier, 2004*) (**Figura 15**).

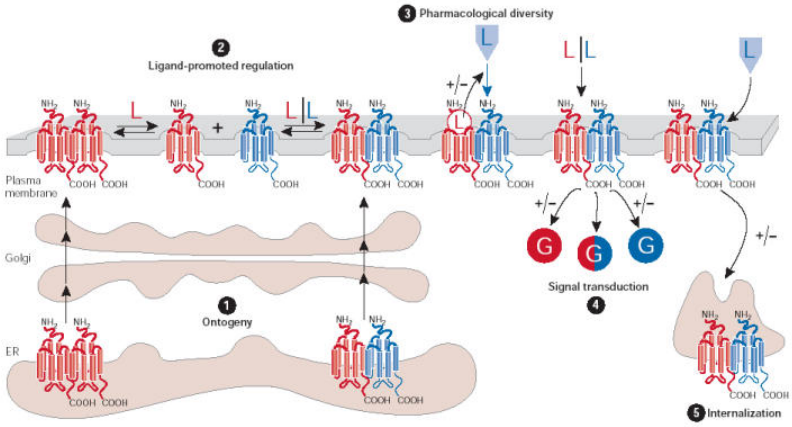

Figura 15. **Posibles papeles funcionales de la oligomerización de GPCR**. ER, retículo endoplasmático; L, ligando. Extraído de *Terrillon y Bouvier, et al., 2004*..

Hasta hace poco, un ejemplo claro de la funcionalidad de la dimerización entre receptores lo constituían los receptores metabotrópicos $GABA_B$, donde la heteromerización de los receptores $GABA_{B1}$ y $GABA_{B2}$ es necesaria para el correcto plegamiento del receptor y su transporte a la membrana plasmática, además de para su señalización. Tres estudios simultáneos aparecidos en 1998 demostraban que era necesaria la coexpresión de las dos isoformas del receptor $GABA_B$, $GABA_{B1}$ y $GABA_{B2}$ para la formación del receptor funcional en membrana (*Jones, et al., 1998*; *Kaupmann, et al., 1998*; *White et al., 1998*). Cuando se expresa individualmente la isoforma $GABA_{B1}$ del receptor, ésta queda retenida intracelularmente en

el retículo endoplasmático como glicoproteína inmadura. Por el contrario, cuando es la isoforma $GABA_{B2}$ la que se expresa, ésta sí es capaz de llegar a la membrana plasmática pero no puede unir GABA ni iniciar la transducción de señal. Cuando ambos receptores se coexpresan, las dos proteínas alcanzan la superficie celular y forman el receptor funcional (*White, et al., 1998*). En estudios posteriores ha sido demostrado que $GABA_{B2}$ sirve como una chaperona esencial para el apropiado plegamiento y transporte a la superficie celular de $GABA_{B1}$ (*Margeta-Mitrovic, et al., 2000*). Estas evidencias, junto al hecho de que un mutante de la isoforma $GABA_{B1}$ con capacidad de alcanzar la membrana plasmática tampoco es por sí solo capaz de iniciar la transducción de señal, sugirieron que el heterodímero es la unidad funcional (*Margeta-Mitrovic, et al., 2000*) (**Figura 16**). Sin embargo, teniendo en cuenta las definiciones sobre receptores aportadas por un grupo de expertos (*Ferré, et al., 2009a*), que definen a un receptor como una macromolécula o conjunto mínimo de macromoléculas capaces de inducir una señalización y teniendo en cuenta que los receptores pueden tener estructura cuaternaria, se debería considerar a la unidad funcional $GABA_{B1}$-$GABA_{B2}$ como un único receptor heteromérico. Es decir, como un receptor con una determinada estructura cuaternaria y no un heterómero de receptores GABA (*Ferré, et al., 2009a*).

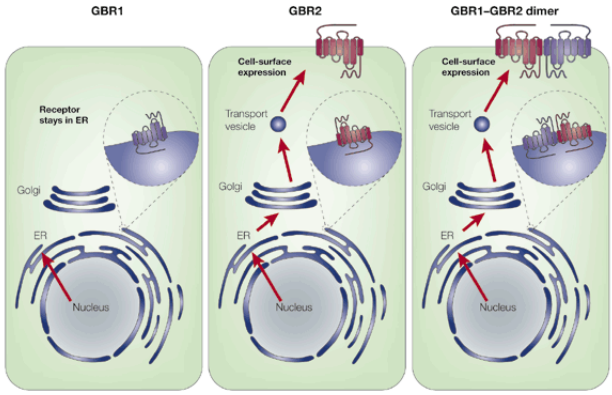

Figura 16. Papel de la heteromerización en los receptores $GABA_{B1}$-$GABA_{B2}$. Extraído de *Bouvier, 2001*.

El papel de la oligomerización como un evento temprano en la maduración y transporte del receptor ha sido demostrado claramente mediante la observación de que la expresión de formas truncadas de los receptores de vasopresina V_2 y quimiocina CCR5 provoca la retención intracelular de los homodímeros correspondientes, causando diabetes nefrogénica insípida y una lenta aparición de los efectos del SIDA, respectivamente (*Benkirane, et al., 1997*; *Zhy y Wess, 1998*).

En este mismo sentido cabe mencionar que la oligomerización también puede modular las propiedades de tráfico de GPCR mediadas por agonista. Este es el caso de los heterodímeros de los receptores de somatostatina $SSTR_1$ y $SSTR_5$, en el cual la internalización del heterodímero ocurre a pesar de la resistencia a la internalización que presenta el monómero $SSTR_1$ (*Rocheville, et al., 2000b*).

Existen evidencias que indican que, en un gran número de casos, la biogénesis de los dímeros u oligómeros de la familia A de los GPCR ocurre tempranamente durante la biosíntesis del receptor y el procesamiento en el RE y Golgi. Esto podría tener un importante papel en el control de calidad de los receptores recién sintetizados (*Herrick-Davis, et al., 2006*). Una vez se encuentran los receptores en la membrana plasmática, consideraciones teóricas y experimentales sugieren que el estado dimérico de los GPCR representa la unidad funcional básica del receptor, que se acopla a la proteína heterotrimérica G y exhibe características

funcionales y/o farmacológicas que difieren de la de los monómeros que los constituyen (*Bulenger, et al., 2005; Franco, et al., 2013*).

Los estudios de unión de ligando han dado alguna pista de la relevancia fisiológica de los oligómeros de GPCR, ya que la formación de estos complejos puede resultar en la generación de sitios de unión de ligando con nuevas propiedades. El primer oligómero descrito con distintas propiedades respecto de los receptores constituyentes fue el heterodímero formado por los receptores κ- y δ-opioide (*Jordan y Devi, 1999*). Este heterodímero no presenta alta afinidad por la unión de ligandos selectivos de los receptores κ- y δ-opioide, pero sí presenta alta afinidad por ligandos selectivos parciales. Los receptores en el heterodímero μ-δ-opioide también presentan propiedades funcionales propias, ya que el tratamiento con un antagonista específico de uno de los receptores del dímero provoca un incremento tanto en la potencia como en la eficiencia de la señalización del otro receptor del dímero, mientras que el tratamiento conjunto con agonistas de ambos receptores da lugar a una potenciación sinérgica de la señal mediada por el heterómero (*Gomes, et al., 2000*).

Ha sido demostrado que la unión de un ligando específico a un receptor en un dímero puede alterar la unión de un ligando específico para el receptor vecino, sugiriendo un posible mecanismo donde un ligando modula la eficacia y/o potencia de otro ligando. Un caso interesante es el de los receptores de dopamina y adenosina, entre los que ha sido descrita una cooperatividad negativa. Los agonistas del receptor A_1 inhiben la acción de los agonistas del receptor D_1 (Fuxe, et al., 2007) ya que inducen la desaparición del estado de alta afinidad del receptor de dopamina D_1 (*Ginés, et al., 2000*), y la estimulación del receptor de adenosina A_{2A} en el heterómero A_{2A}-D_2, reduce la afinidad de agonistas por el receptor de dopamina D_2, el acoplamiento a la proteína G y la señalización a través de este último receptor (*Fuxe, et al., 2007*). Del mismo modo sucede en el heterodímero entre los receptores A_{2A} y CB_1 (*Carriba, et al., 2007*), en el que, la activación del receptor A_{2A} disminuye la actividad del receptor CB_1 (*Ferreira, et al., 2015*). Otro caso de especial interés es el heterodímero formado por los receptores A_1 y A_{2A} de adenosina, en el que la estimulación del receptor A_{2A} disminuye enormemente la afinidad del receptor A_1 por su agonista e inhibe la señalización (*Ciruela, et al., 2006*). Teniendo en cuenta que la afinidad por la adenosina del receptor A_1 es más grande que la que muestra el receptor A_{2A} en este heterómero A_1/A_{2A}, cuando la concentración de adenosina es pequeña, el neuromodulador se une al receptor A_1 inhibiendo la liberación de glutamato en el estriado. Cuando la concentración de adenosina es elevada, por ejemplo, en casos de hipoxia, la adenosina se une también al receptor A_{2A} provocando en el heterómero la inhibición farmacológica y funcional del receptor A_1. En estas condiciones la adenosina estimula la liberación de glutamato en el estriado (*Ciruela, et al., 2006*). El heterómero A_1-A_{2A} actúa como un interruptor mediante el cual, dependiendo de cual sea la concentración de adenosina en el medio, se produce la inhibición o la estimulación de la liberación de glutamato en el estriado (*Ciruela, et al., 2006*).

Una de las primeras evidencias de que los dímeros forman una unidad compleja de señalización proviene de estudios que muestran que la disrupción del homodímero β_2-adrenérgico con un péptido derivado del sexto dominio transmembrana, implicado en la dimerización, inhibe la producción de AMPc inducida por el agonista (*Hebert, et al., 1996*), sugiriendo que el dímero es la especie activa del receptor. Frente a estos resultados algunos autores sugerían que no podía ser descartada la posibilidad de que el péptido estuviera modificando interacciones intramoleculares dentro del monómero, provocando así la falta de funcionalidad, siendo la pérdida de la unidad dimérica más bien una consecuencia y no una causa de la no señalización por parte del receptor. Sin embargo, ha sido demostrado recientemente que el uso de péptidos no imposibilita la funcionalidad del GPCR,

convirtiéndose así en una herramienta fundamental para el estudio de las interacciones entre receptores (*Jastrzebska, et al., 2015; Moreno, et al., 2016*).

Otra característica destacable derivada de la dimerización entre GPCR es la posibilidad de que se produzca un cambio de acoplamiento de proteína G. En 2004, se demostró que los receptores de dopamina D_1 y D_2 forman heterómeros en células transfectadas (*Lee, et al., 2004*). Los receptores D_1 están acoplados a proteína G_s mientras que los D_2 están acoplados a la proteína G_i, pero cuando los receptores D_1-D_2 forman el heterómero, se acoplan a una proteína G diferente, $G_{q/11}$. De hecho, la dopamina al activar a los receptores D_1 y D_2 en el heterómero no induce señalización vía PKA y AMPc sino que moviliza calcio y activa la calmodulin quinasa (*Hasbi, et al., 2014; Perreault, et al., 2016*).

Por lo que respecta a la estequiometría en los dímeros, el debate ha estado abierto durante más de veinte años. Ya en el año 2005, distintos estudios realizados con el receptor de glutamato demostraron que sólo uno de los protómero del receptor del dímero podía alcanzar un estado activo completo al mismo tiempo (*Goudet, et al., 2005*; *Hlavackova, et al., 2005*). No obstante, mediante el uso de ensayos realizados en nanodiscos, distintos investigadores pusieron en tela de juicio la estequiometría planteada en los estudios de Goudet y Hlavackova, ya que observaron que el receptor β_2-adrenérgico (*Whorton, et al., 2007*), el receptor rodopsina (*Bayburt, et al., 2007*) o los receptores μ-opioides (*Kuszak, et al., 2009*) podían funcionar como entidades monoméricas. Los estudios realizados en nanodiscos plantearon un debate paralelo en la comunidad científica, ya que muchos expertos en el campo consideraban que eran modelos artificiales muy alejados de la realidad al tener, en un espacio muy reducido, únicamente los elementos de estudio, sin considerar la multitud de posibles factores extra que podrían participan en las interacciones entre GPCR en una célula viva. Tras el paso del tiempo, con la aparición de nuevos resultados, la balanza se ha ido decantando a favor de los defensores de los dímeros. El Moustaine y colaboradores observaron que miembros de la familia C de GPCR aislados en forma monomérica eran capaces de unir proteína G, pero sin embargo, para la inducción de la señalización mediante la proteína G tras la exposición a ligandos se requería de la estructura dimérica de los GPCR (*El Moustaine, et al., 2012*). También ha sido relevante el hecho de que, para los tres GPCR citados anteriormente en los que se observó su posible funcionalidad como entidad monomérica, haya sido demostrado que puedan encontrarse en conformaciones de orden superior en células vivas. Por ejemplo, Fung y colaboradores demostraron la existencia de oligómeros estables del receptor β_2-adrenérgico en células vivas (*Fung, et al., 2009*). Además, gracias al avance en las técnicas cristalográficas ha sido posible determinar la estructura de muchos GPCR, incluidos algunos de los cuales se consideraba que funcionaban monoméricamente, obteniéndose cristales en forma de dímeros y/o tetrámeros, como por ejemplo, de los receptores μ-opioides (*Manglik, et al., 2012*) y κ-opioides (*Wu, et al., 2012*), o los β_1-adrenérgicos (*Huang, et al., 2013*). Actualmente pues, la comunidad científica ha aceptado que la organización física de los GPCR y proteínas G responde al modelo en el cual una proteína G interactúa con un receptor en un dímero (*Jastrzebska, et al., 2013; Franco, et al.,* 2013; *Cordomí, et al., 2015*).

1.3. RECEPTORES DE ADENOSINA Y DOPAMINA

Los receptores acoplados a proteína G que responden a señales endógenas se encuentran distribuidos en una gran variedad de tejidos, a diferencia de los receptores que reciben señales de origen externo, los cuales normalmente presentan una distribución más localizada en los

órganos sensoriales (*Vassilatis, et al., 2003*). A su vez, un determinado tejido expresa multitud de receptores diferentes. En el sistema nervioso central (SNC) se expresan un elevado número de receptores acoplados a proteínas G, más del 90% de los receptores de siete dominios transmembrana se expresan en el cerebro y para algunos de ellos su expresión está restringida a este tejido. La combinación de técnicas de inmunohistoquímica, RT-PCR e hibridación *in situ* en diferentes regiones del cerebro ha permitido descubrir que la expresión de estos receptores presenta patrones diferenciales, lo que sugiere que la expresión de un grupo de receptores concretos y no otros es clave en la regulación de diferentes procesos neurofisiológicos. El estudio de las asociaciones entre receptores acoplados a proteína G en determinados dominios de neuronas abre nuevas expectativas en el diseño racional de terapias para el tratamiento de desórdenes neurológicos como por ejemplo la adicción a las drogas de abuso o los trastornos motores. En esta tesis se hace énfasis en el estudio de los receptores de adenosina, dopamina y grelina localizados en el estriado.

1.3.1. Receptores de adenosina

La adenosina es un nucleósido endógeno formado por la base purínica adenina y un anillo de ribosa. Esta molécula es producida por prácticamente todas las células de nuestro organismo (*Liu y Xia, 2015*). Este nucleósido participa activamente en muchos procesos fisiológicos ampliamente descritos en la literatura, y en particular es muy abundante en el corazón y el cerebro (*Berne, et al., 1983*). Tanto la adenosina como sus derivados son constituyentes esenciales de toda célula viva, ya que conforman piezas claves para la formación de moléculas biológicas tan relevantes como los ácidos nucleicos, los nucleótidos ATP y AMP o cofactores como el NAD^+. Esta molécula juega por tanto un papel muy importante en procesos bioquímicos y de transferencia de energía, además de en la transducción de señales en su forma de AMPc (*Dunwiddie y Masino, 2001*). Es también un neuromodulador implicado en promover la fase de sueño y suprimir la vigilia. Además, la adenosina está implicada en la vasodilatación (*Ross, et al. 2013*). Esta capacidad vasodilatadora, junto a la acción estimuladora de la captación y oxidación de la glucosa, e inhibición de la lipólisis (*Lönnroth, et al., 1989; Johansson, et al., 2008*), incrementan la disponibilidad de sustratos metabólicos para el organismo. Por lo tanto, la adenosina juega un papel importante en el balance entre la energía subministrada y el gasto energético (*Dunwiddie y Masino, 2001*). En condiciones fisiológicas normales, tanto los niveles de adenosina intracelular como extracelular se encuentran en el rango nanoMolar, pero sin embargo, en una situación de estrés, daño celular o condiciones patológicas, las concentraciones de adenosina extracelular pueden alcanzar el rango miliMolar (*Phetarpekar, et al., 2010*). La adenosina extracelular está regulada por la enzima adenosina deaminasa (ADA), que es responsable de la degradación de la adenosina extracelular a ionosina (*Cristalli, et al., 2001*).

En el SNC la adenosina es secretada por la mayoría de células, incluyendo neuronas y células gliales, y actúa como neuromodulador de la actividad del SNC tanto a nivel presináptico como postsináptico y/o extrasináptico. Así, este nucleósido se ha visto implicado en procesos normales y patofisiológicos, como el control de la liberación de neurotransmisores excitadores (*Ciruela, et al., 2006*), la inhibición de la actividad motora espontánea, la diferenciación (*Canals, et al., 2005*) y migración neuronal (*Liu, et al. 2008; Young, et al., 2008*), el conocimiento y la memoria (*Florian, et al., 2011; Pagnussat, et al., 2015*), la regulación de la función respiratoria y en particular en aquellos procesos relacionados con el sueño (*Urry y Landolt, 2015*), la ansiedad y la depresión (*Johansson, et al., 2001; Yamada, et al., 2014*) y la excitación, además de la neuroprotección en episodios de hipoxia/isquemia o hipoglicemia

(*Duarte, et al., 2016*) y la plasticidad sináptica (*Cunha, 2016*). También ha sido relacionado con la enfermedad de Alzheimer (*Yan, et al. 2014*); en necropsias de pacientes de esta enfermedad ha sido detectado un cambio en la expresión y una redistribución de los receptores de adenosina comparado con cerebros control (*Angulo, et al., 2003*). También se ha relacionado la adenosina con la enfermedad de Parkinson (*Jenner, et al., 2009; Ramlackhansingh, et al., 2011*), la enfermedad de Huntington (*Chiu, et al., 2015*), la esquizofrenia (Wardas, 2008; *Turcin, et al., 2016*), la epilepsia (*Ribeiro, et al., 2003*), la adicción a drogas (Furlong, et al., 2015; *Pintsuk, et al., 2016*) y el cáncer. Cada vez más estudios sugieren la implicación de los diferentes receptores de adenosina en procesos relacionados con el cáncer, por ejemplo, ha sido observada una sobreexpresión del receptor A_3 de adenosina en células cancerosas en comparación con los niveles de este receptor en células sanas (*Gessi, et al., 2011; Montinaro, et al., 2013*). Ha sido demostrado también que existe una relación entre la adenosina y algunas enfermedades oculares como los ojos secos o el glaucoma (*Schlötzer-Schrehardt, et al., 2005*) así como en el dolor neuropático crónico (*Varani, et al., 2013*).

La adenosina lleva a cabo sus funciones a través de la interacción con diferentes receptores GPCR de la familia *rhodopsin-like* (*Martinelli y Ortore, 2013*). Estos receptores han sido clasificados en base a sus propiedades moleculares, bioquímicas y farmacológicas en cuatro subtipos: los receptores de alta afinidad A_1 y A_{2A} y los receptores de baja afinidad A_{2B} y A_3 (*Fredholm, et al., 2001; Fredholm, et al., 2011*) (**Figura 17**).

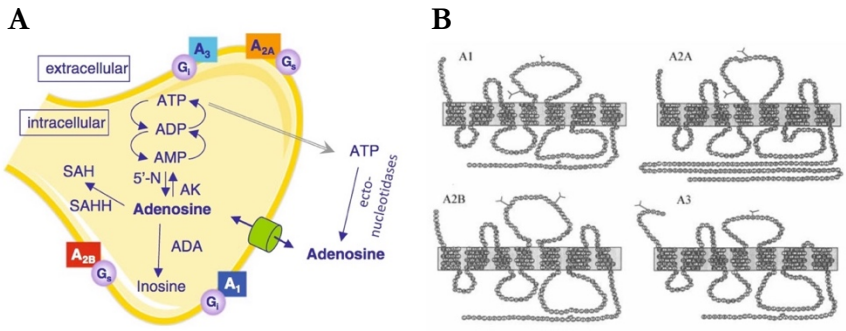

Figura 17. A) Representación esquemática de la formación, metabolismo y transporte de adenosina. Receptores de adenosina: A_1, A_{2A}, A_{2B}, A_3, acoplados a su proteína G correspondiente (representados en los rectangulos), transportadores de adenosina (cilindro verde). SAH, S-adenosil-homo-cisteina; 5'-N, 5'-nucleotidasa; AK, adenosina quinasa; ADA, adenosina deaminasa; SAHH, S-adenosil-homocisteina hidrolasa. Extraído de *Urry y Landolt, 2015*. **B)** Estructura de los receptores de adenosina humanos.

El grado de homología entre los receptores de adenosina es bajo, del orden del 45% (*Pierce, et al., 1992*), si bien existen diferencias entre especies como la que tiene lugar entre los receptores A_{2A} y A_{2B} que en rata presentan una homología del 46% y en humano del 61%. Al igual que para otros GPCR, la mayor homología tiene lugar en las regiones transmembrana, que se cree están próximas entre sí formando el centro de unión de ligando conjuntamente con la zona hipervariable correspondiente a la mitad N-terminal del segundo bucle extracelular (Rivkees, et al., 1999). Cabe destacar la larga cola C-terminal que presenta el receptor A_{2A}. La interacción con la proteína G tiene lugar básicamente a través del TM6, donde se inserta una pequeña cola de la proteína G, provocando así los cambios estructurales requeridos para la inducción de la señalización. Además, todos presentan secuencias consenso de fosforilación en los dominios intracelulares. Esta fosforilación está implicada en el mecanismo de desensibilización de los receptores de adenosina (*Saura, et al., 1998*). Todos los receptores de adenosina presentan también secuencias consenso de N-glicosilación en el EC2, las cuales se cree que están implicadas en el tránsito del receptor a la membrana (*Klotz*

y Lohse, 1986). Jaakola y colaboradores determinaron la estructura cristalina del receptor A_{2A} de adenosina humano (*Jaakola, et al., 2008*), siendo estudio de gran relevancia, pues hasta ese momento, de esta familia de GPCR, solo se había obtenido la estructura cristalográfica del receptor de rodopsina (*Palczewski, et al., 2000*) y del receptor β_2-adrenérgico (*Cherezov, et al., 2007*). Esto, por lo tanto, facilitó la comprensión de la estructura de los GPCR, así como el diseño de nuevos fármacos y ligandos más selectivos para estos receptores.

El interés por el estudio del papel de la adenosina en el cerebro recae en el hecho que, en mamíferos, los receptores de adenosina en este tejido son mucho más abundantes que en otros tejidos o tipos celulares (*Cunha, et al., 2008*). Mayoritariamente son los receptores de alta afinidad por la adenosina, A_1 y A_{2A}, los responsables de los efectos de este nucleósido en cerebro (*Fredholm, et al., 2005*), siendo el receptor A_1 de adenosina el más abundante, con una distribución más extensa. El receptor A_{2A} muestra altos niveles de expresión únicamente en zonas concretas del cerebro como los ganglios basales (*Fredholm, et al., 2005*). Los receptores de adenosina A_{2B} y A_3 son de baja afinidad por lo que su activación puede ser relevante en condiciones en las que la concentración de adenosina se ve incrementada de forma notoria. La adenosina es el agonista total de todos estos receptores, además, en los receptores A_1 y A_3 la ionosina puede actuar como agonista parcial (*Fredholm, et al., 2001*) (**Tabla 1**). Aunque la adenosina es el agonista endógeno, no es una buena herramienta para el estudio de estos receptores debido a su alta susceptibilidad para ser metabolizada por varios enzimas. Sin embargo, la adenosina es la base estructural de todos los agonistas conocidos. Por otro lado, las metilxantinas constituyen el prototipo de antagonista de estos receptores. Las modificaciones sobre esta molécula dan lugar a una elevada selección de derivados, muchos de los cuales presentan gran selectividad por distintos subtipos. En la **Tabla 1** se muestra la afinidad que presentan por la adenosina los diferentes subtipos y los agonistas y antagonistas más selectivos para cada miembro de la familia.

Los receptores de adenosina tradicionalmente participan en distintos procesos como el sueño/vigilia, atenuando la acción de neuronas implicadas en mantener al individuo en fase de vigilia, pero también participan en el aprendizaje, la memoria, el daño neuronal, la neurodegeneración y la maduración neuronal. Dada la gran variedad de funciones del SNC en las que la adenosina participa, es fácil suponer que los diversos subtipos de receptores estarán acoplados a diferentes señales intracelulares. Así, el receptor A_1 se acopla a proteínas $G_{i/o}$ provocando la inhibición de la adenilato ciclasa (*Londos, et al., 1980*) y, a través de las subunidades $G\beta\gamma$ de la proteína G, la activación de la PLC con el consiguiente incremento en los niveles de DAG e IP_3 en el interior celular (*Gerwins y Fredholm, 1992*), lo que aumenta los niveles de calcio intracelulares. El receptor A_1 también provoca la inactivación de los canales de calcio (*Macdonald, et al., 1986*) y la activación de varios tipos de canales de potasio, probablemente también vía las subunidades $G\beta\gamma$ de la proteína G (*Trussell y Jackson, 1985*). El receptor A_3 de adenosina también inhibe la adenilato ciclasa mediante el acoplamiento a G_i (*Zhou, et al., 1992; Borea, et al., 2015*), aunque también puede acoplarse a la proteína G_q (*Palmer, et al., 1995*) activando la PLC e incrementando los niveles de calcio intracelular (*Abbracchio, et al., 1995*). Por otro lado, la principal vía de señalización de los receptores A_{2A} y A_{2B} es la estimulación de la formación de AMPc a través del acoplamiento a una proteína G_s (*Jenner, et al., 2009*), lo que a su vez estimula la proteína quinasa dependiente de AMPc (PKA), regulando así el estado de fosforilación de diferentes sustratos intracelulares. Sin embargo, el receptor A_{2A} también puede acoplarse a proteínas G_{olf} y el receptor A_{2B} a proteínas G_q mediando la activación de la PLC y la movilización de calcio intracelular dependiente de DAG e IP_3 (*Feoktistov y Biaggioni, 1995*) (**Tabla 1**). Ha sido observado que todos los receptores de adenosina activan a las *Mitogen Activated Protein Kinases* (MAPK) y en concreto inducen la fosforilación de *Extracellular Signal-Regulated Kinase 1/2* (ERK1/2), pero

dependiendo del contexto celular, las vías de señalización implicadas pueden variar (*Schulte y Fredholm, 2003*).

Subtipo	A_1R	$A_{2A}R$	$A_{2B}R$	A_3R
Proteína G	$G_{i/o}$	$G_{s/olf}$	$G_{s/q}$	$G_{i/q}$
Mecanismo de transducción de señal	- AC + PLC - canales Ca^{2+} + canales K^+	+ AC - canales Ca^{2+}	+ AC + PLC	- AC + PLC
Moléculas efectoras	↓ AMPc ↑ IP_3 ↓ Ca^{2+} ↑ K^+	↑ AMPc ↑ IP_3 ↓ Ca^{2+}	↑ AMPc ↑ IP_3 ↑ Ca^{2+}	↓ AMPc ↑ IP_3 ↑ Ca^{2+}
Afinidad por la adenosina (K_D en nM)	70	150	5100	6500
Agonista selectivo	R-PIA	CGS 21680	-	IB-MECA
Antagonista selectivo	DPCPX	ZM 241385	MRS 1706	L-268605
Acción fisiológica	Inhibición transmisión sináptica y actividad motora. Hiperpolarización. Precondicionamiento isquémico	Facilita la liberación de neurotransmisores. Integración sensorial-motora	Modulación de canales de Ca^{2+}	Desacopla A_1R y mGluR. Precondicionamiento isquémico

Tabla 1. Receptores de adenosina.

En el cerebro, los dos principales subtipos de receptores de adenosina, el A_1 y el A_{2A}, se expresan tanto de forma pre- como postsináptica. El receptor A_1 se localiza abundantemente en todo el cerebro, en concreto su expresión es muy elevada en el estriado y el tálamo, aunque también es abundante en corteza, cerebelo, hipocampo y en la médula espinal. El receptor A_{2A}, como ha sido mencionado anteriormente, tiene una expresión más restringida, se encuentra altamente expresado en los ganglios basales, concretamente en el putamen y núcelo caudado, en las neuronas GABAérgicas estriatopalidales y en el bulbo olfatorio (*Brooks, et al., 2008*) (**Figura 18**).

Tradicionalmente a la adenosina se le ha conferido un papel inhibitorio. Sin embargo, a pesar de que a nivel sináptico esta molécula no es un neurotransmisor, a través de la activación de los receptores A_1 comparte muchas propiedades atribuidas al principal neurotransmisor inhibitorio, el ácido γ-aminobutírico (GABA). Así, el GABA y la adenosina constituyen las principales moléculas en el control de la transmisión sináptica glutamatérgica en el SNC. La adenosina, a través de los receptores A_1, inhibe la liberación de glutamato lo que permite desconectar fisiológicamente interneuronas GABAérgicas. Este proceso es importante en condiciones de intensa liberación de adenosina, como en los casos de hipoxia (*Sebastião, et al., 2001*). Además, está inhibición de la neurotransmisión excitadora ha hecho que se considere

este receptor como uno de los más importantes en la regulación del ciclo sueño-vigilia, promoviendo la fase de sueño. Esto explica por qué la cafeína, un antagonista de los receptores de adenosina, al contrarrestar el efecto de la adenosina sobre los receptores A_1 y A_{2A} del prosencèfalo, así como por sus efectos indirectos en los sistemas noradrenérgicos, sistemas histaminérgicos del hipotálamo y sistemas orexinérgicos, induce un estado de vigilia, entre otros efectos (*Ferré, 2010; McLellan, et al., 2016*). Respecto al receptor A_{2A}, parece ser uno de los principales neuromoduladores presinápticos (*Schiffmann, et al., 2007*) capaces de incrementar la liberación de GABA de terminales nerviosos del hipocampo (*Cunha y Ribeiro, 2000*).

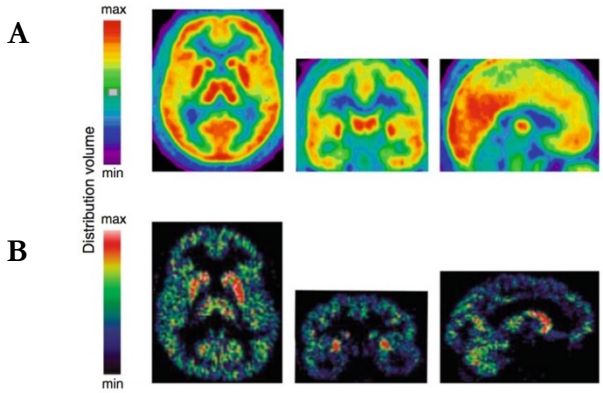

Figura 18. Distribución de los receptores de adenosina A_1 y A_{2A} en el SNC. A) Distribución colorimétrica del antagonista selectivo del receptor A_1, ^{18}C-CPFPX, en un individuo sano. De izquierda a derecha se muestran los planos axial, coronal y sagital. B) Distribución colorimétrica del antagonista selectivo del receptor A_{2A}, ^{11}C-KW6002, en un individuo sano. De izquierda a derecha se muestran los planos axial, coronal y sagital del cerebro obtenidos mediante la técnica de tomografía por emisión de positrones. Extraído de *Brooks, et al., 2008*.

1.3.2. Receptores de dopamina

La dopamina es la principal catecolamina que actúa como neurotransmisor en el sistema nervioso central (SNC), representando el 80% del contenido total de catecolaminas del cerebro, y controlando una gran variedad de funciones como la modulación de la actividad sensorial, la actividad motora, la actividad endocrina, el aprendizaje, la memoria, la emotividad, la afectividad, la recompensa y la motivación (*Missale, et al., 1998*). También desarrolla múltiples papeles en el sistema nervioso periférico como modulador de la función cardiovascular, secreción hormonal, tono vascular, función renal y motilidad gastrointestinal (*Missale, et al., 1998*).

La dopamina se sintetiza a partir del aminoácido L-tirosina y existen mecanismos que regulan de manera muy precisa su síntesis y liberación (*Bahena-Trujillo, et al., 2000*). Al no ser capaz de cruzar la barrera hematoencefálica, su biosíntesis tiene lugar en el citosol de los terminales nerviosos dopaminérgicos (*Elsworth y Roth, 1997*). Su liberación se realiza mediante canales de calcio dependientes de voltaje que promueven la fusión de vesículas llenas de dopamina con la membrana plasmática, que por difusión cruza el espacio de la hendidura sináptica hasta unirse a sus receptores localizados pre- y postsinápticamente. El resultado final es la activación o inhibición de la neurona postsináptica. La señal dopaminérgica finaliza por eliminación de la dopamina del espacio intersináptico. Este proceso se lleva a cabo mediante la catálisis de la dopamina por enzimas extraneuronales o por la recaptación por los propios terminales nerviosos mediante transportadores específicos (DAT: *Dopamine Transporters*) que juegan un papel importante en la función, inactivación y reciclaje de la dopamina liberada

(*Adell y Artigas, 2004*; *Sotnikova, et al., 2006*). Los receptores presinápticos son principalmente autoreceptores y constituyen uno de los mecanismos responsables de la regulación de la transmisión dopaminérgica (*Koeltzow, et al., 1998*). Estos son más sensibles a la dopamina que los receptores postsinápticos e inducen a una inhibición de la liberación continuada de dopamina.

La evolución de la investigación sobre la transimisión dopaminérgica puede remontarse a la década de los 50's, cuando la dopamina fue reconocida como un neurotransmisor, siendo detectada por primera vez en el SNC en 1958. En la década de los 60's se generaron las primeras evidencias del vínculo existente entre alteraciones en la transmisión dopaminérgica y la enfermedad de Parkinson y algunos desórdenes psiquiátricos, en particular la esquizofrenia (*Bahena-Trujillo, et al., 2000*). A lo largo de las últimas décadas el sistema dopaminérgico ha sido el foco de muchos estudios debido a su implicación en desórdenes psiquiátricos como el Parkinson y la esquizofrenia, pero también en desórdenes bipolares, la corea de Huntington, desórdenes de hiperactividad y déficit de atención y el síndrome de Tourette (*Beaulieu y Gainetdinov, 2011*), así como en la hiperprolactinémia y la adicción a drogas de abuso (*Missale, et al., 1998*; *Zack y Poulos, 2009*; *Dalley y Everitt, 2009*).

El 1978, en base a evidencias farmacológicas, bioquímicas y fisiológicas, los receptores de dopamina se clasificaron en dos grupos: receptores activadores de la adenilato ciclasa (AC) y receptores inhibidores de la AC (*Spano, et al., 1978*). Sin embargo, no fue hasta 1988 que se clonó el primer receptor dopaminérgico, el subtipo D_2 (*Bunzow, et al., 1988*). Posteriormente, usando la técnica de clonaje, fueron aislado 5 receptores distintos para la dopamina (*Gingrich y Caron, 1993*). Estos receptores han sido clasificados en dos subfamilias en función de sus propiedades bioquímicas y farmacológicas: los receptores D_1-*like*, que comprende los receptores D_1 y D_5 y los receptores D_2-*like* que comprende los receptores D_2, D_3 y D_4. La subfamilia D_1-*like* produce incrementos de AMPc a través de proteínas $G_{s/olf}$ que estimulan la AC (*Civelli, et al., 1993*) y se localizan en los terminales pre- y postsinápticos en función de la zona cerebral (*Wong, et al., 1999; Galvan, et al., 2014*). La D_2-*like* inhibe la AC por acoplamiento a proteínas $G_{i/o}$, además de activar canales de K^+ y disminuir la entrada de Ca^{+2} a través de canales dependientes de voltaje. Los receptores D_2-*like* pueden localizar-se en terminales presinápticos y postsinápticos (*Dal Toso, et al., 1989*; *De Mei, et al., 2009*).

La organización genómica de los receptores de dopamina sugiere que provienen de dos familias génicas que difieren principalmente en la presencia o no de intrones en su secuencia codificadora. Los receptores D_1-*like* no contienen intrones, característica que comparten con la mayoría de GPCR (*Dohlman, et al., 1987*). En cambio, y por analogía con el gen de rodopsina, los genes que codifican para los receptores D_2-*like* están interrumpidos por intrones (*Vallone, et al., 2000*). La presencia de intrones en la región codificadora de los receptores D_2-*like* permite la generación de variantes de estos receptores. De hecho, el receptor D_2 presenta dos isoformas, llamadas $D_{2s}R$ (*short*) y $D_{2l}R$ (*long*), que son generadas por *splicing* alternativo de 87 pares de bases entre los intrones 4 y 5. Esta diferencia de 29 aminoácidos les confiere ciertas características diferenciales, como su localización, expresándose principalmente el receptor D_{2S} a nivel presináptico mientras que el D_{2L} se expresa a nivel postsináptico. Pese a que tanto $D_{2s}R$ como $D_{2l}R$ tienen la misma capacidad de unir ligando, los niveles de expresión de la isoforma larga son diez veces mayores que los de la isoforma corta. También difieren en la capacidad de acoplarse a proteína G, $D_{2l}R$ sería más afín a G_i y $D_{2s}R$ tanto a G_i como a G_o, esto explicaría la regulación de diferentes respuestas biológicas por la diversidad de señal generada. Los dos subgrupos presentan, además peculiaridades estructurales diferenciales como se muestra en la **Figura 19**: los receptores D_1-*like* tienen un dominio carboxilo terminal unas siete veces más largo que el de

los D_2-*like*, mientras que estos últimos tienen el tercer bucle intracelular (IC3) muy largo, característica común en muchos receptores acoplados a proteína G_i (*Missale, et al., 1998*).

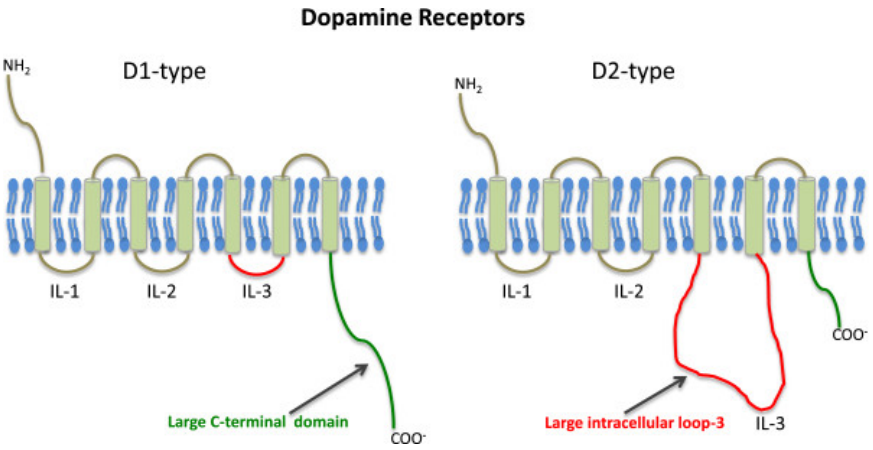

Figura 19. Representación esquemática de las dos familias de receptores de dopamina. Extraído de *Padey et al., 2013*.

Existe una alta homología de secuencia entre los dos miembros de la familia de receptores D_1-*like*, del orden del 80%. Entre los miembros del subgrupo D_2-*like* la homología es de un 75% entre los receptores D_2 y D_3 y de un 53% entre los receptores D_2 y D_4. Por el contrario, la homología entre los receptores D_1-*like* y D_2-*like* es solo del 42-46%. La homología más elevada se encuentra entre los dominios transmembrana y en aquellos residuos que son clave para la unión de catecolaminas. El extremo carboxi terminal, en ambas familias, contiene lugares de fosforilación y palmitoilación que se cree juegan un papel importante en la desensibilización del receptor y en la formación de un cuarto bucle intracelular, respectivamente. En cambio, los receptores de dopamina presentan diferencias en las modificaciones post-traduccionales, como diferentes lugares consenso de N-glicosilación (*Missale, et al., 1998*). Recientemente, mediante estudios filogenéticos ha sido demostrado que los receptores D_1-*like* y D_2-*like* no están filogenéticamente más relacionados entre ellos de lo que lo están con otros receptores de monoaminas (*Yamamoto, et al., 2013*). Este hecho sugiere que la habilidad para unir dopamina, compartida por los dos tipos de receptores, ha sido adquirida independientemente por convergencia a lo largo de la evolución.

Para el estudio de las propiedades farmacológicas de los receptores de dopamina se dispone de ligandos que fácilmente discriminan entra las dos subfamilias D_1-*like* y D_2-*like*, aunque no sean selectivos para los miembros de cada subfamilia. Puesto que los receptores D_1-*like* tienen alta homología dentro de los dominios transmembrana, regiones que se piensa forman el lugar de unión para ligando, no es sorprendente que estos receptores exhiban propiedades farmacológicas muy similares. Cada uno de los receptores D_1-*like* muestra alta afinidad por benzazepinas (agonistas) y baja afinidad por butiroferonas y benzamidas sustituidas (antagonistas). Una diferencia remarcable entre los receptores D_1-*like* es la afinidad que presentan sus miembros por la dopamina, ya que el receptor D_5 tiene una afinidad 10 veces superior a la que muestra el receptor D_1 (*Missale, et al., 1998*).

Las propiedades farmacológicas de los receptores D_2-*like* difieren entre sí más de lo que difieren entre sí las de los receptores de la subfamilia D_1-*like*. Así, las afinidades por muchos agonistas y antagonistas varían entre uno y dos órdenes de magnitud entre subtipos, incluyendo la dopamina por la que el receptor D_3 tiene una afinidad 20 veces más alta que el receptor D_2. Cada uno de estos receptores, sin embargo, tiene el sello característico de unión de ligando de los receptores D_2, es decir, alta afinidad por butirofenonas, como las

espiperonas y haloperidol, y baja afinidad por benzazepinas. Hay que especificar que el receptor D_4 se caracteriza por ser el más diferenciado, presentando baja afinidad por la mayoría de antagonistas dopaminérgicos, por ejemplo, el raclopride, y exhibiendo una relativamente alta afinidad por el neuroléptico clozapina (*Missale, et al., 1998*).

La diferencia de afinidad que presentan los receptores de dopamina por su ligando endógeno puede permitir la activación de unos receptores o de otros en función de la cantidad de dopamina liberada (**Tabla 2**). Esta diversidad dentro de los receptores de dopamina es un reflejo de la diversidad funcional que ejerce este neurotransmisor, sobre todo si se considera la expresión diferencial de estos receptores dentro del SNC.

Familia	**D_1R- like**		**D_2R- like**		
Subtipo	D_1R	D_5R	D_2R	D_3R	D_4R
Proteína G	$G_{s/olf}$	$G_{s/olf}$	$G_{i/o}$	$G_{i/o}$	$G_{i/o}$
Mecanismo de transducción de señal	+ AC + PLC	+ AC	- AC + PLC - canales Ca^{2+}	- AC + PLC - canales Ca^{2+} + canales K^+	- AC + PLC
Moléculas efectoras	↑ AMPc ↑ PKA ↑ IP3	↑ AMPc	↓ AMPc ↑ IP_3 ↓ Ca^{2+} ↑ K^+	↓ AMPc ↑ IP_3 ↓ Ca^{2+} ↑ K^+ ↑ NKE*	↓ AMPc ↑ ác. araquid. ↑ NKE*
Afinidad por la dopamina K_D en nM	2340	261	2,8-474	4-27	28-450
Agonista	SKF-38393	NPA	Quinpirole	Bromocriptina	(-)Apomorfina
Antagonista	SCH-23390	SCH-23390	Raclopride	UH 232	Clozapina

*NKE: Na+ /K+ exchange: intercambiador Na+/K+.

Tabla 2: Resumen de las principales características de los diferentes subtipos de receptores de dopamina.

La expresión de los distintos subtipos ha sido determinada mediante la combinación de técnicas de unión de radioligandos y de hibridación *in situ*. Así ha sido demostrado que el receptor D_1 es el más abundante y su distribución es la más amplia de entre todos los receptores dopaminérgicos (*Dearry, et al., 1990*). Este receptor se encuentra en diversas regiones del cerebro como neuronas GABAérgicas del estriado que coexpresan sustancia P, núcleo accumbens, tubérculo olfatorio e hipotálamo (*Gerfen, et al., 1990*). El otro receptor D_1-*like*, el receptor D_5, presenta una distribución más restringida a regiones como el tálamo o el hipocampo (*Vallone, et al., 2000*; *Centonze, et al., 2003*). En cuanto a los receptores D_2-*like*, el receptor D_2 se expresa principalmente en núcleo accumbens, tubérculo olfatorio e hipocampo, tanto pre- como post-sinápticamente y su expresión es elevada en las neuronas GABAérgicas estriatopalidales. Este receptor actúa como autoreceptor en los terminales dopaminérgicos, donde regula la síntesis y liberación de dopamina (*Mercuri, et al., 1997*). El

receptor D_3 se localiza específicamente en las regiones límbicas del núcleo accumbens, con una localización post-sináptica en neuronas que expresan sustancia P y neurotensina. Por último, el receptor D_4 se expresa en interneuronas GABAérgicas tanto piramidales como no-piramidales de la corteza frontal e hipocampo y en el bulbo olfatorio, la amígdala y el mesencéfalo (*Missale, et al., 1998*).

En distintas situaciones patalógicas ha sido observada la existencia de diferencias cuantitativas en la expresión de los receptores de dopamina o bien en su señalización. Por ejemplo, los receptores D_1 ven incrementada su expresión en la esquizofrenia y su señalización varia en la enfermedad de Parkinson (*Paspalas, et al., 2013*). Por otro lado, la densidad de los receptores D_2 post-sinápticos se ve incrementada en la esquizofrenia y también en los enfermos de Parkinson no tratados con L-DOPA (*Matsukawa, et al., 2007; Reeves, et al., 2009*). Del mismo modo, un desequilibrio en la expresión de receptores D_1 y D_2 de dopamina está asociado con un aumento en la motivación por la búsqueda y consumo de sustancias con valor hedónico o drogas de abuso (*Volkow, et al., 2009; Sonntag, et al., 2014*).

1.3.3. Los ganglios basales

Los ganglios basales están constituidos por cinco núcleos principales en roedores: el estriado, la *substantia nigra*, el *globus pallidus*, el núcleo subtalámico y el núcleo entopeduncular (**Figura 20**). Estas estructuras están implicadas en muchos procesos mentales como las funciones motoras y sensoriales, el aprendizaje y memoria, aunque también ha sido descrita su implicación en funciones ejecutoras y en la toma de decisiones, en la motivación y las emociones (*Kim y Hikosaka, 2015*).

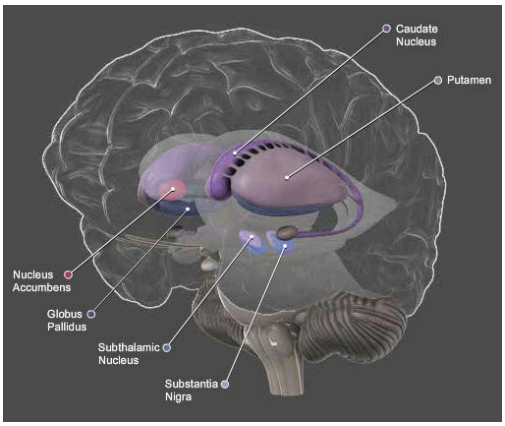

Figura 20: Localización de los núcleos que forman los ganglios basales. Imagen obtenida de *www.g2conline.org*

Cuando la región pre-frontal de la corteza cerebral, involucrada generalmente en la toma de decisiones y planificación, determina que una actividad motora debe ser ejecutada, envía señales activadoras a las áreas motoras. El cerebro contiene muchos generadores de patrones de movimientos, y cada uno de estos sirve para realizar un movimiento particular del cuerpo, como la locomoción/postura (*Takakusaki, 2004*), la vocalización (*Hage y Jürgens, 2006*) o alcanzar un objeto/sujetarlo (*Kinoshita, et al., 2012*). Por la acción de estímulos sensoriales concretos o de estados internos, estos mecanismos pueden trabajar independientemente para generar movimientos adaptativos, como por ejemplo, el reflejo vestíbulo-ocular. Sin embargo, el comportamiento general podría convertirse en incontrolable si estas áreas

motoras pudiesen activarse simplemente en base a sus propias reglas (*Kim y Hikosaka, 2015*). Para solucionar esta situación de manera eficiente el cerebro ha desarrollado un mecanismo que suprime todas las activaciones motoras inducidas por los generadores de patrones de movimientos. Las áreas motoras envían sus señales a través de los ganglios basales para refinar la elección de los músculos que participarán en el movimiento y para amplificar la actividad en las áreas motoras que dirigirán las contracciones musculares.

El estriado es la principal estructura de entrada de los ganglios basales y está funcionalmente subdividido en estriado dorsal y ventral. El estriado dorsal (núcleo caudado y putamen) se encuentra implicado en la ejecución y el aprendizaje de los actos motores complejos. El estriado ventral (núcleo accumbens) forma parte de los circuitos cerebrales implicados en la conversión de la motivación en acción. En el estriado más del 90% de las neuronas son GABAérgicas de proyección o *medium-size spiny neurons* y reciben dos vías de entrada que convergen en sus espinas dendríticas: por un lado, las neuronas dopaminérgicas del mesencéfalo, localizadas en la *substantia nigra pars compacta* y el área tegmental ventral y, por otro lado, las neuronas glutamatérgicas procedentes de áreas corticales, límbicas y talámicas (hipocampo y amígdala) (*Gerfen, et al., 2004; Heinsbroeck, et al., 2017*).

Por otro lado, todos los *outputs* eferentes del estriado que proyectan al tálamo son GABAérgicos e inhibitorios, son altamente activos continuamente (*Hikosaka, 2007*) y están conectados con los mecanismos motores. Estas eferencias salen desde dos estructuras, la *substantia nigra pars reticulata* (SNr) y el segmento interno del *globus pallidus* (GPi), dando lugar a dos vías: las neuronas estriatonigroentopedunculares (vía directa) y las neuronas estriatopalidales (vía indirecta). Humanos y monos con disfunciones en los ganglios basales normalmente presentan movimientos involuntarios, los cuales pueden ser causados por un mal funcionamiento de esta inhibición mediada por los núcleos SNr/GPi (*DeLong y Wichmann, 2007*). Los dos tipos de neuronas GABAérgicas estriatales se pueden distinguir neuroanatómicamente. Las neuronas estriatopalidales contienen el péptido encefalina y receptores de dopamina, predominantemente el subtipo D_2. Estas neuronas expresan, también, receptores A_1 y A_{2A} de adenosina. Las neuronas estriatonigroentopedunculares contienen dinorfina y sustancia P, receptores de dopamina, predominantemente de subtipo D_1 (*Alexander y Crutcher, 1990*) y receptores A_1 de adenosina, pero no receptores A_{2A} (*Schiffmann, et al., 2007*; *Ferré, et al., 2007*; *Fuxe, 2007*).

No obstante, estas vías inhibitorias deben ser reguladas en ciertos contextos, de lo contrario todos los movimientos quedarían suprimidos. Un problema en su regulación podría ser la causa de la aquinesia en pacientes de Parkinson (*Wichmann y DeLong, 1996*). La vía directa y la vía indirecta son las encargadas de la regulación del movimiento. La estimulación de la vía directa produce activación motora de los movimientos voluntarios, mientras que la activación de la vía indirecta produce inactivación motora, inhibiendo la aparición de componentes involuntarios en el movimiento. En la vía directa, las áreas motoras envían señales activadoras a los núcleos putamen y caudado del estriado. Las células de estos núcleos son GABAérgicas, de modo que al ser activadas mandan señales inhibitorias al GPi y a la SNr, inhibiendo así la actividad en estos núcleos, los cuales estaban bloqueando al núcleo ventrolateral del tálamo y evitando que se produjera actividad en las áreas motoras cerebrales. Simultáneamente, las señales enviadas por las áreas motoras a los núcleos caudado y putamen también activan la vía indirecta. Las neuronas GABAérgicas de esta vía envían señales inhibitorias al *globus pallidus* externo (GPe), reduciendo la actividad en este núcleo. EL GPe de manera basal envía señales inhibitorias al núcleo subtalámico (STN), de modo que, cuando se activa la vía indirecta, estas señales inhibitorias se ven reducidas, lo que provoca un aumento en la actividad del STN. Así, este núcleo puede enviar señales activadoras a ciertas partes del GPi

y a la SNr. Entonces, parte de estos núcleos envían señales inhibitorias al núcleo ventrolateral del tálamo, evitando así la activación de áreas motoras corticales que podrían competir con el movimiento voluntario. Un adecuado equilibrio entre las dos vías produce los movimientos normales, lo que se conoce como acción motora (*Hikida, et al., 2010*). La dopamina induce la activación de la actividad motora mediante receptores D_1 de las neuronas estriatonigroentopedunculares, mientras que deprime la actividad de las neuronas estriatopalidales actuando sobre los receptores D_2, produciendo indirectamente una actividad motora (*Grillner y Robertson, 2016*). La dopamina, por tanto, estimula el movimiento a través de dos vías, porque estimula la vía estimuladora e inhibe a la vía inhibidora (**Figura 21A**).

Algunos autores también hablan de la vía hiperdirecta (*Nambu, et al., 2002*), la cual actúa como supresora de movimientos ya en curso. Esta vía es mediada por el núcleo STN, y en ella neuronas glutamatérgicas excitadoras transmiten señales rápidamente de la corteza cerebral a los núcleos SNr y GPi, inhibiendo así el movimiento. Se considera que su principal función está relacionada con cambios comportamentales (*Isoda y Hikosaka, 2008*) en los que se suprimen movimientos rápidos y automáticos para que movimientos voluntarios puedan iniciarse.

La enfermedad de Parkinson está producida por la degeneración progresiva de las neuronas dopaminérgicas nigroestriatales que proyectan de la *substantia nigra* al caudado-putamen. Esta degeneración da lugar a una disminución de la liberación de dopamina en el estriado, que provoca una hipoactividad de las neuronas GABAérgicas estriatonigroentopedunculares (vía directa) y una hiperactividad de las neuronas GABAérgicas estriatopalidales (vía indirecta) debido a la ausencia de los efectos inhibitorios de la dopamina endógena (*Obeso, et al., 2008*), con el consiguiente descontrol de la actividad de los ganglios basales (**Figura 21B**). Los síntomas clínicos más relevantes incluyen bradiquinesia (lentitud en los movimientos), rigidez, temblor en reposo y alteraciones en el equilibrio. El tratamiento paliativo de esta enfermedad consiste en suministrar un precursor de dopamina, L-DOPA, que, aunque resulta efectivo en los primeros estadios de la enfermedad, acaba por perder la efectividad y provoca la aparición de complicaciones motoras como la discinesia (*Nutt, et al., 1990*). Actualmente existen avances importantes en el desarrollo de nuevos fármacos dopaminérgicos y no dopaminérgicos para la enfermedad de Parkinson, así como para las complicaciones motoras de las terapias en uso (*Schapira, et al., 2006*).

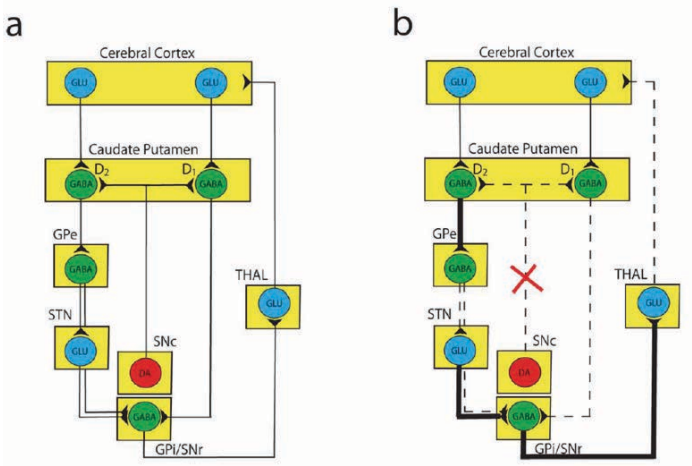

Figura 21. Funcionamiento de los ganglios basales. Existen dos vías de salida del estriado: la vía directa y la vía indirecta. **A)** Estado "normal" y **B)** Degeneración de la *substantia nigra pars compacta* en la enfermedad de Parkinson que provoca la disminución de la liberación de dopamina en el estriado. Imagen cedida por el Dr. Sergi Ferré.

La adenosina y la dopamina ejercen efectos opuestos en el estriado. La primera indicación de una interacción antagónica entre los receptores de adenosina y los de dopamina se obtuvo al analizar el comportamiento de animales modelo de la enfermedad de Parkinson (*Fuxe y Ungerstedt, 1974*). Se utilizaron los antagonistas no selectivos de adenosina, cafeína y teofilina, en combinación con L-DOPA y agonistas de los receptores de dopamina y se observó un aumento de la actividad motora producida por los fármacos dopaminérgicos. La heteromerización de los receptores A_{2A}-D_2, demostrada por primera vez por Canals y colaboradores en nuestro grupo (*Canals, et al., 2003*), tiene una gran relevancia en la enfermedad de Parkinson, siendo actualmente uno de los heterómeros más estudiados (*Ferré, et al., 2008*). En el cerebro, los receptores A_{2A} de adenosina y los D_2 de dopamina están altamente expresados en las neuronas GABAérgicas del estriado (*Schiffmann, et al., 2007*). Este tipo de neuronas representan prácticamente la mitad de la población neuronal del estriado y una mala función de éstas tiene un papel clave en la patogénesis de enfermedades de los ganglios basales como el Parkinson y la corea de Huntington, y probablemente en desordenes obsesivo-compulsivos y adicción a drogas (*Fuxe, et al., 2007*). En la línea de lo observado por Fuxe y Ungerstedt, los antagonistas de los receptores A_{2A} bloquean la acción de la adenosina endógena sobre el heterómero A_{2A}-D_2, provocando un incremento en la señalización mediada por el receptor D_2, además de disminuir la señalización inducida por la adenosina endógena (*Ferré, 2008*). Así pues, el tratamiento con L-DOPA y antagonistas de adenosina parece potenciar las acciones antiparkinsonianas de la L-DOPA, tanto en modelos animales (*Kanda, et al., 2000; Uchida, et al., 2015*) como en pacientes de esta enfermedad (*Hauser, et al., 2003*). Actualmente, para poder tratar esta enfermedad, muchos grupos de investigación están centrando sus esfuerzos en el descubrimiento de antagonistas selectivos del receptor A_{2A} de adenosina, como la istradefilina (o KW-6002), el cual ya se administra a enfermos de Parkinson (*Mizuno, et al., 2013*) o el SYN-115, identificado por los laboratorios farmacéuticos Hoffmann-La Roche, actualmente en fase clínica III (*Basu, et al., 2017*).

1.4. ADICCIÓN A LA COCAÍNA

1.4.1. El proceso de adicción

La adicción es una enfermedad crónica, devastadora y que afecta en cierto modo no solo al individuo afectado sino también a parientes, amigos y al conjunto de la sociedad. El *National Institute on Drug Abuse* (NIDA) estima que cada año el consumo de tabaco, alcohol y drogas ilícitas tiene un coste de más de 700 billones de dólares para la sociedad norte-americana, relacionados con costes médicos, baja productividad o crímenes, entre otros factores.

Frecuentemente, el termino adicción se relaciona con el abuso de sustancias psicoactivas, que afectan la función neuronal alterando el equilibrio químico del cerebro (*Joffe, et al., 2014*). El uso de estos agentes afecta al sistema de recompensa del cerebro, altera el comportamiento, la motivación y el estado de ánimo, la memoria y otros circuitos relacionados (*Joffe, et al., 2014*). Además, tiene la característica de incapacitar al adicto de abstenerse del uso de la sustancia adictiva a pesar de las consecuencias negativas que esta le aporta. Tales agentes incluyen el alcohol, el tabaco, los cannabinoides, los opiáceos, los estimulantes, los alucinógenos y las drogas de diseño, entre otros (*Joffe, et al., 2014*). También se incluyen adicciones que no requieren el consumo de ninguna sustancia, como el sexo, los juegos de azar y otros comportamientos (*DiLeone, et al., 2012*).

La adicción es una enfermedad crónica que se caracteriza por progresión cíclica a través de fases de recuperación y recaída (*Koob y Volkow, 2016*). El patrón de ingestión al inicio de la enfermedad es generalmente impulsivo y está motivado por un refuerzo positivo (sensación de euforia, bienestar, entre otros). A medida que la adicción progresa, la motivación por consumir la sustancia de abuso cambia hacia un refuerzo negativo, que aliviará los síntomas de abstinencia característicos de prácticamente todo tipo de adicción, pasando así a conductas compulsivas para obtener nuevas dosis de la sustancia de abuso. A la vez, el organismo del enfermo sufrirá una multitud de cambios que lo harán aún más susceptible a futuras recaídas. Si la adicción no es controlada, el tiempo transcurrido entre cada consumo se acorta a la vez que las dosis consumidas aumentan. Esto, junto con el hecho de que para el enfermo el único objetivo pasa a ser el consumo de la sustancia de abuso, llegando a olvidar la necesidad de ingerir alimentos o agua, llevan al sujeto a la muerte.

1.4.2. De coca a cocaína

Una sustancia psicotrópica es un agente químico que actúa sobre el sistema nervioso central, lo cual provoca cambios temporales en la percepción, el ánimo, el estado de conciencia y el comportamiento. A lo largo de la historia, los humanos han utilizado distintas sustancias psicotrópicas con fines ansiolíticos, euforizantes, depresivos, alucinógenos o estimulantes. Los psicoestimulantes son las sustancias psicotrópicas más utilizadas en el mundo. Un psicoestimulante puede definirse como una sustancia psicotrópica con la capacidad de estimular el SNC, aumentando los niveles de actividad motriz y cognitiva, reforzando el estado de vigilia, el estado de alerta y la atención. La cafeína y la nicotina son los psicoestimulantes más utilizados en la actualidad. La cafeína es el más aceptado socialmente, aproximadamente el 90% de la población de países industrializados la consume diariamente. Según el último informe de la Organización Mundial de la Salud, en el año 2015 aproximadamente había aproximadamente 1,1 billones de fumadores en el mundo. La nicotina es consumida a diario por el 25% de la población europea y el 19,5% de la población estadounidense. Estos porcentajes llegan a ser superiores en otras zonas del planeta como América del sur o Asia. Otras sustancias psicotrópicas como la cocaína, la metanfetamina o el éxtasis, por ejemplo, han sido consideradas ilegales, aunque este hecho no vaya siempre asociado a un bajo consumo, tal y como se deduce de los resultados presentados en el informe mundial sobre las drogas del 2016 en el que se calcula que cerca de 250 millones de personas entre 15 y 64 años consumieron drogas durante el año 2014, además del aumento significativo de las cantidades de estas drogas incautadas por las autoridades.

La cocaína es un extracto purificado de la planta de coca, *Erythroxylum coca*, procedente originariamente de América del sur. Las hojas de coca han formado parte de las culturas inca, aimara y quechua durante siglos. Hoy en día, en las culturas andinas aún es común masticar hoja de coca, así como beber mate de coca a pesar de las presiones gubernamentales para erradicar estas prácticas. Cuando se mastica, la hoja de coca actúa como estimulante, aporta sensación de euforia y elimina el apetito, la sed, el dolor y el cansancio. También ayuda a superar el mal de altura. Originalmente, la coca era administrada exclusivamente en forma de hoja o de infusión, hasta que en 1860 Albert Neiman aisló un extracto de la hoja de coca, la cocaína. Su utilización se extendió rápidamente por todo el mundo, convirtiéndose incluso en un ingrediente para productos como el vino de coca, enjuagues bucales o la Coca-Cola. Años más tarde aparecieron informes negativos respecto a su consumo, de modo que en 1903 esta marca de refrescos retiró la cocaína de sus productos.

Hoy en día, su posesión, cultivo y distribución son ilegales, exceptuando requisitos médicos o normas gubernamentales; sin embargo, su consumo se encuentra ampliamente extendido. En el informe del 2016 sobre sustancias de abuso elaborado por las Naciones Unidas se estima que cerca del 0,4% de la población mundial consume cocaína. Además, hay indicios de que el aumento de fabricación de esta droga observado en 2014 y 2015 podría seguir esta dinámica en el 2016. El consumo de cocaína tiene un coste muy elevado para toda la población. Aparte del problema sanitario que supone la adicción a cocaína, actualmente la adicción a esta droga se ha convertido también en un problema social, por un lado debido al gran número de vidas que se cobra, ya sean derivadas del consumo de la propia droga o por la corrupción y la violencia que gira en torno a las mafias asociadas a la producción y distribución de la cocaína, y por el otro al gasto de dinero público invertido en la lucha policial y judicial contra los narcotraficantes. Es por tanto una necesidad médica y social entender los mecanismos de acción de la cocaína y del proceso de adicción a esta droga para poder luchar contra ella.

Hasta la fecha, no ha sido encontrado un tratamiento altamente efectivo contra esta sustancia más allá del disulfiram, un fármaco utilizado para tratar el alcoholismo que inhibe la enzima dopamina β-hidroxilasa, reduciendo así los niveles de dopamina convertidos a norepinefrina (*Shorter, et al., 2013*). Otros investigadores han propuesto el tratamiento de la adicción a cocaína mediante la vacunación de los enfermos, estimulando el sistema inmune para crear anticuerpos específicos contra la molécula de cocaína, evitando así que esta llegue al cerebro (*Kosten y Domingo, 2013*). Los resultados obtenidos en ensayos clínicos han demostrado que los pacientes que presentan unos niveles altos de anticuerpos contra la cocaína reducen el consumo de esta sustancia, no obstante, solo el 38% de los pacientes vacunados llega a presentar suficientes anticuerpos en plasma, y solo durante unos 2 meses (*Kosten y Domingo, 2013*), siendo necesaria la mejora de este tratamiento para poderlo implementar. Otra línea de investigación es la que se centra en el desarrollo de nuevas técnicas para el tratamiento médico en situaciones de sobredosis aguda de cocaína: un ejemplo sería el propuesto por Schindler y Goldberg, en el que mediante ingeniería genética han sido modificados algunos enzimas involucrados en la destrucción de la cocaína (*Schindler y Goldberg, 2012*). Ha sido descrito que la vida media de la cocaína en ratas es relativamente corta, pudiendo oscilar entre quince minutos y una hora dependiendo de la vía de administración utilizada (*Nayak, et al., 1976*), y que una administración repetitiva podría prolongar el aumento en los niveles de dopamina y la vida media de la sustancia (*Volkow, et al., 1999*). Estudios recientes han revelado que la hidrólisis del éster de cocaína es la principal ruta de su catabolismo (*Chen, et al., 2017*), de modo que la modificación de los enzimas responsables de esta hidrólisis permitiría acelerar el metabolismo de la droga y antagonizar los efectos tóxicos y los efectos en el comportamiento provocados por la cocaína.

1.4.3. Mecanismo de acción de la cocaína

Existen evidencias de que diferentes drogas de abuso (cocaína, nicotina o morfina) provocan cambios neurobiológicos (*Areal, et al., 2015; Yuan, et al., 2015; Guegan, et al., 2016*). Los primeros estudios realizados revelaron que la cocaína inhibía la recaptación de monoaminas como la dopamina (*Moore, et al., 1977*; *Heikkila, et al., 1979*; *Ritz, et al., 1987*), la norepinefrina (*Moore, et al., 1977*) y la serotonina (*Ross y Renyi, 1967*). Sin embargo, aunque la cocaína actúa con el mismo grado de efecto en los transportadores de las tres monoaminas, la mayoría de

los efectos en el comportamiento (*De Wit y Wise, 1977*; *Colpaert, et al., 1978*; *Miczek, et al., 1982*) y la actividad motora (*Giros, et al., 1996*) de esta sustancia se atribuyen al bloqueo de la recaptación de dopamina y al consecuente aumento de la concentración de este neurotransmisor en el espacio sináptico. A finales de los años 80 la medición directa de la concentración de dopamina extracelular mediante técnicas de microdiálisis confirmó que las drogas de abuso compartían la propiedad de provocar un aumento de los niveles de dopamina en el núcleo accumbens (*Di Chiara e Imperato, 1988*). Actualmente, en modelos de primates no humanos ha sido observado que, una vez administrada la cocaína, los picos de dopamina aparecen a los cinco minutos y no se recuperan los niveles basales hasta los treinta minutos (*Bradberry, et al., 2000*). Así, inicialmente, los efectos observados por la cocaína eran explicados únicamente en base a la interacción de esta droga con el transportador de dopamina (DAT) presináptico. Mediante el modelaje molecular de DAT basado en la estructura cristalina de *Aquifex aeolicus* LeuT (Aa), un transportador de leucina homólogo en bacterias (*Beuming, et al., 2008*), ha sido postulada la unión de la cocaína a DAT. En este modelo son las hélices transmembrana 1, 3, 6 y 8 del transportador las que intervienen en la unión de la cocaína (**Figura 22**). Este centro de unión se superpone con el sitio de unión de la dopamina y las anfetaminas, explicando el bloqueo de la unión de la dopamina a DAT inducido por la cocaína (**Figura 22E**). Consecuentemente, si la dopamina no puede ser recaptada por DAT, los niveles de dopamina en el espacio sináptico se ven incrementados, induciendo una sobreestimulación de las vías dopaminérgias. Estos resultados cierran la puerta a la posibilidad de generar un inhibidor competitivo de la unión de cocaína, debido a que también se estaría compitiendo con la recaptación de dopamina.

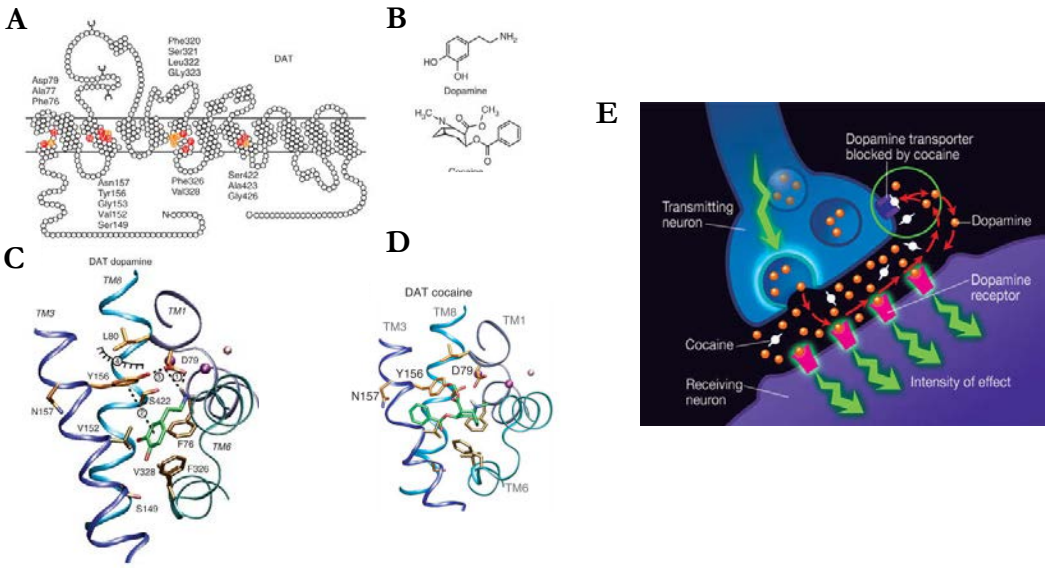

Figura 22. Esquema de la interacción de la cocaína y la dopamina con DAT. A) Representación del transportador de dopamina, DAT. Los círculos pintados corresponden a los lugares donde coincide la interacción de DAT con la dopamina y la cocaína. **B)** Estructuras químicas de la dopamina y la cocaína. **C)** Esquema de la interacción de DAT con la dopamina. **D)** Esquema de la interacción de DAT con la cocaína. Extraído de *Beuming, et al., 2008*. **E)** Mecanismo de acción clásico de la cocaína. Efecto del bloqueo de los transportadores de dopamina (DAT) por la cocaína. Extraído del *National Institute of Drug Abuse (NIDA).*

Si bien es cierto que el aumento de los niveles de dopamina es un mecanismo de acción común de las drogas de abuso, muchos trabajos han puesto de manifiesto que el aumento de este neurotransmisor tras la exposición a cocaína no es exclusivamente debido al bloqueo de DAT. Distintos estudios han demostrado que en condiciones fisiológicas la actividad fásica

de las neuronas dopaminérgicas de la VTA genera una señal de aprendizaje cuando tiene lugar una recompensa inesperada (*Schultz, et al., 1997*). El propósito de esta señal es promover un aprendizaje que permita obtener de nuevo esta recompensa. Cuando esta recompensa pasa a ser completamente predecible, las neuronas dopaminérgicas no se activan más, y el aprendizaje cesa (*Lüscher, et al., 2016*). La potencia farmacológica de las drogas de abuso es su capacidad para anular este sistema, generando un aprendizaje inapropiado que, a última instancia, lleva al consumo compulsivo de la droga a expensas de todos los demás comportamientos (*Lüscher, et al., 2016*). De modo que, en base a este modelo, la adicción a cocaína debe considerarse una enfermedad por aumento de función del sistema dopaminérgico. Si esto es cierto, una estimulación directa y sostenida de las neuronas dopaminérgicas, sin la participación del transportador DAT, debería tener efectos similares a los observados en animales adictos. Esto ha sido confirmado en estudios realizados mediante técnicas optogenéticas en animales en los que el transportador DAT no está bloqueado, observándose que la estimulación de las neuronas dopaminérgicas de la VTA induce a una preferencia de lugar inmediata (*Adamantidis, et al.,* 2011) y que la auto-estimulación directamente de estas mismas neuronas resulta en un refuerzo positivo para los ratones, los cuales apretarán la palanca cientos de veces por hora para recibir la ráfaga estimuladora (*Pascoli, et al., 2015*). Además, la inyección de una droga de abuso acaba con la auto-estimulación optogenética de las neuronas dopaminérgicas en estos ratones (*Pascoli, et al., 2015*). En la misma línea, otros estudios basados en modelos genéticos de ratones han cuestionado también el mecanismo clásico de acción de la cocaína. Tanto Hnasko y colaboradores, mediante ratones deficientes en dopamina (*Hnasko, et al., 2007*), como Rocha y colaboradores, mediante la generación de ratones transgénico *knok-out* para los transportadores de monoaminas (*Rocha, 2003*), fallaron en la prevención de la auto-administración de cocaína o preferencia de lugar asociada a esta droga.

Otro aspecto importante aún en estudio es el mecanismo de acción mediante el cual la cocaína induce uno de los principales efectos de su consumo, los cambios de comportamiento. Tras la exposición a esta droga de abuso se produce un incremento de la excitabilidad e hiperactividad, normalmente asociado a un aumento en la agresividad e irritabilidad en primera instancia, convirtiéndose en conductas erráticas y compulsivas a largo plazo. Un hipotético mecanismo inductor de los cambios de comportamiento consecuentes a la administración crónica de cocaína es una alteración de la plasticidad sináptica del cerebro. Además, estos cambios neurológicos dejan al adicto en una situación de vulnerabilidad a futuras recaídas (*Wolf, et al., 2016*). Han sido descritos diferentes cambios en la estructura de las dendritas tras el consumo de esta droga relacionados con los cambios de comportamiento (*Robinson y Kolb, 1999*; *Robinson, et al., 2001; Christian, et al., 2016; Zhu, et al., 2016*), que podrían ser debidos a alteraciones en la expresión de las proteínas de los neurofilamentos, las proteínas del citoesqueleto y/o las "*gap junctions*", todas ellas muy importantes para la estabilidad y la buena integración de los receptores en la sinapsis neuronal, o a la desregulación en los mecanismos que controlan la excitabilidad de las neuronas (*Creed, et al., 2016*).

Es importante destacar que los primeros estudios sobre la acción de la cocaína eran realizados en base a modelos celulares neuronales, sin embargo, a medida que han pasado los años, distintos grupos han empezado a utilizar modelos celulares no neuronales, en los que no se expresa el transportador DAT, para desarrollar sus investigaciones y, sin embargo, en estos trabajos también han sido observados efectos inducidos por la exposición a esta droga. Esto ha llevado a explorar la capacidad de la cocaína de interaccionar con otros elementos. Hoy en día es un hecho aceptado que la cocaína puede interaccionar con otras proteínas, un

ejemplo de ello son los receptores sigma. La cocaína interacciona con los receptores sigma a concentraciones fisiológicas (*Mesangeau, et al., 2008*), llegando éstos a ser propuestos como dianas terapéuticas para la lucha contra la adicción a la cocaína. Esta familia de proteínas está formada por los receptores sigma-1 y sigma-2. Todos estos resultados sugieren que hay distintos mecanismos de acción a través de los que la cocaína provoca un amplio abanico de efectos.

1.4.4. Receptores sigma-1 y sigma-2

El receptor sigma-1 es una proteína, aún hoy en día, muy enigmática. Originalmente este receptor fue reconocido como el sitio de unión a través del cual eran mediados los efectos psicomiméticos del agonista opioide SKF-10,047, sustancia que no se unía a los receptores κ-opioides ni a los μ-opioides, motivo por el que fue propuesto como un nuevo subtipo de receptor opioide (*Martin, et al., 1976*); sin embargo, la acción de los ligandos de sigma-1 no era bloqueada por los antagonistas opioides, naloxona y naltrexona, por lo que pasó a ser considerado un receptor huérfano no opioide (*Vaupel, 1983*). Finalmente, en el año 1996 el receptor sigma-1 fue clonado y se confirmó definitivamente como receptor no opioide (*Hanner, et al., 1996*). El receptor sigma-1 no presenta homología con ninguna otra proteína conocida de mamífero, pero comparte aproximadamente un 30% de identidad con la C7-C8 esterol isomerasa fúngica (*Cobos, et al., 2008*). El receptor sigma-1 ha sido recientemente cristalizado por Schmidt y colaboradores, mostrando una arquitectura trimérica con un único dominio transmebrana en cada protómero, además de una estructura hidrofóbica plana en el dominio carboxi-terminal que quedaría en contacto con la membrana lipídica (**Figura 23**) (*Schmidt, et al., 2016*).

El receptor sigma-1 se encuentra ampliamente distribuido en tejidos periféricos (*Stone, et al., 2006*) y en diferentes áreas del sistema nervioso central. En el cerebro se concentra en áreas implicadas en la memoria, las emociones y la función motora y sensorial (*Guitart, et al., 2004*). A nivel subcelular el receptor sigma-1, principalmente actúa como chaperona en el retículo endoplasmático (*Hayashi, et al., 2007*), pero también en las membranas plasmática, nuclear y mitocondrial (*Alonso, et al., 2000*). Este receptor, además de con cocaína, interacciona con diferentes sustancias entre las que destacan el haloperidol o los esteroides como la progesterona (*Hayashi, et al., 2003*), sin embargo, aún no ha sido determinado cuál es su ligando endógeno. El receptor sigma-1 no es un GPCR por lo que es complicado determinar lo que constituye un agonista o un antagonista, además, el hecho de que no señalice por si solo también dificulta la clasificación de sus ligandos. El ligando selectivo PRE-084 ha sido clasificado como agonista debido a su capacidad para disociar de manera dosis-dependiente el receptor sigma-1 de una binding immunoglobulin protein/78 kDa glucose-regulated protein (BiP/GPR-78) (*Hayashi, et al., 2007*), mientras el haloperidol ha sido clasificado como antagonista debido a su capacidad para inhibir completamente la disociación entre sigma-1R y BiP/GPR-78 causada por PRE-084. A pesar de no tener su propia maquinaria de señalización, una vez activado por ligandos este receptor opera vía translocación e interacciones proteína-proteína (*Su, et al., 2010*), regulando la señalización por calcio y la actividad de diversos canales iónicos (*Wu y Bowen, 2008*) y modulando diferentes receptores acoplados a proteína G (*Navarro, et al., 2010*; *Kim, et al., 2010*). Ha sido estudiada su implicación en diferentes desordenes fisiológicos como la depresión, la adicción a drogas, el dolor neuropático (*Schmidt, et al., 2016*) y también en enfermedades cardiovasculares (*Su, et al., 2010*). Recientemente ha sido descrita una mutación en este receptor como una de las

causas del desarrollo de la esclerosis amiotrófica lateral juvenil en humanos (*Al-Saif, et al., 2011*) así como de su posterior progresión (*Mavlyutov, et al., 2013*).

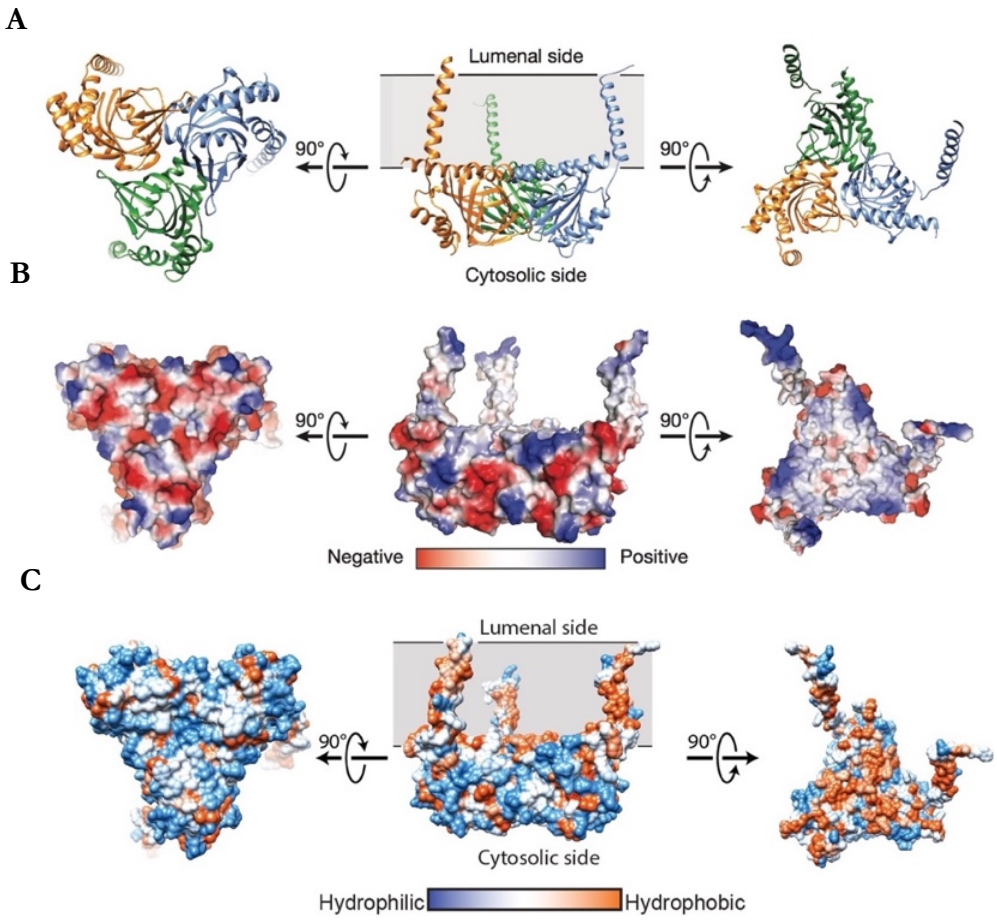

Figura 23. Estructura cristalina del receptor sigma-1. A) Imagen perpendicular al plano de la membrana plasmática. En una visión lateral, el receptor presenta una superficie plana asociada a la membrana. **B)** Modelo coloreado en función del potencial electrostático, que revela una superficie polar citosólica (lado izquierdo), y una superficie no polar que interaccióna con la membrana la cual es flaqueada por cargas positivas, sugiriendo que está parcialmente enterrada en la membrana. **C)** La estructura del receptor sigma-1 muestra una superficie hidrofóbica (azul) en la cara citosólica (izquierda), mientras que los dominios transmembrana y la superficie del receptor en contacto con la membrana son hidrofóbicos (naranja; panel izquierdo). En gris se representa el plano de la membrana plasmática. Extraído de *Schmidt, et al., 2016*.

El receptor sigma-1 se encuentra estrechamente relacionado con la acción de la cocaína en diferentes aspectos, como son la hiperlocomoción (*Menkel, et al., 1991; Barr, et al., 2015*), la sensibilización (*Ujike, et al., 1996*), el mecanismo de recompensa (*Romieu, et al., 2000*; *Romieu, et al., 2002*), las convulsiones y la letalidad (*Matsumoto, et al., 2001*). En comparación con otras drogas de abuso, la interacción entre la cocaína y el receptor sigma-1 es la más estudiada (*Hayashi y Su, 2005*) ya que esta droga posee una afinidad moderada por sigma-1 en ensayos de unión a radioligando (*Matsumoto, et al., 2003*) de modo que, igual que sucede con los transportadores de dopamina, la cocaína interacciona con los receptores sigma a concentraciones asumibles *in vivo*, sugiriendo pues que estos receptores pueden ser dianas terapéuticas para el desarrollo de fármacos anti-cocaína (*Matsumoto, et al., 2001*).

La reducción de los niveles de expresión del receptor sigma-1 en cerebro mediante oligonucleótidos *anti-sense* disminuye las acciones convulsivas y locomotoras de la cocaína

(*Matsumoto, et al., 2001*; *Matsumoto, et al., 2002*). También ha sido descrito que mientras agonistas del receptor sigma-1 potencian la toxicidad de la cocaína (*Matsumoto, et al., 2002*; *Matsumoto, et al., 2003*), antagonistas sintéticos del receptor sigma-1 disminuyen las acciones de la cocaína, así como sus efectos letales en diferentes modelos animales, sugiriendo su habilidad para bloquear los efectos psicomotores y tóxicos (*Matsumoto, et al., 2004*). Estos descubrimientos indican que las acciones de la cocaína, al menos en parte, pueden ser mediadas por su unión al receptor sigma-1.

De manera interesante, ha sido descrito que el receptor sigma-2 también se encuentra relacionado con los efectos de la cocaína (*Guo y Zhen, et al., 2015*). En 2007, Matsumoto y colaboradores observaron que el tratamiento con ligandos del receptor sigma-2 era capaz de atenuar algunos de los efectos sobre el comportamiento inducidos por la cocaína en ratones (Matsumoto, et al., 2007). Sin embargo, estos compuestos no tenían una alta especificidad para el receptor sigma-2. Un año más tarde Mésangeau y colaboradores sintetizaron una batería de ligandos selectivos para el receptor sigma-2 con la finalidad de ser utilizados como farmacoterapia contra la toxicidad de la cocaína (*Mésangeau, et al., 2008*). Recientemente ha sido observado que el tratamiento con antagonistas selectivos del receptor sigma-2 es capaz de contrarrestar la estimulación locomotora inducida por la cocaína en ratones (*Lever, et al., 2014*).

En la actualidad, existe un debate abierto sobre la identidad del receptor sigma-2. Inicialmente, la caracterización de sigma-2 recaía exclusivamente en ensayos de unión de radioligando en los que se bloqueaban previamente los receptores sigma-1 (*Hellewell, et al., 1994*). No fue hasta 2011 cuando Xu y colaboradores identificaron al *progesterone receptor membrane component-1* (PGRMC-1) como la entidad potencial del receptor sigma-2, mediante el diseño de una sonda específica para este receptor y posterior análisis de la proteína marcada con dicha sonda mediante espectrofotometría de masas (*Xu, et al., 2011*). Además, mediante técnicas de unión de radioligando observaron, por un lado, como tanto ligandos específicos del PGRMC-1 como ligandos específicos del receptor sigma-2 desplazaban la unión de [^{125}I]RHM-4, un radioligando de uso común para medir la densidad de receptores sigma-2. Y, por otro lado, observaron como al bloquear la expresión del PGRMC-1 mediante el uso de siRNA, se producía una disminución de la unión del radioligando [^{125}I]RHM-4 a la muestra (*Xu, et al., 2011*). Sin embargo, valores de 22 a 28 KDa han sido determinados para PGRMC-1 (*Meyer, et al., 1996*; *Peluso, et al., 2012*) mientras que un valor de solo 21,5 kDa había sido determinado para el receptor sigma-2 (*Hellewell, et al., 1994*). Estas diferencias podrían explicarse mediante procesos post-traduccionales o un fenómeno de *splicing* alternativo, pero han sembrado la duda en un grupo de investigadores. El receptor PGRMC-1 es una proteína citocromo b_5-*like* perteneciente a la familia de receptores de progesterona asociados a membrana (*membrane-associated progesterone receptor*, MAPR) (*Mifsud y Bateman, 2002; Cahill, 2007*). Sin embargo, PGRMC-1 no une directamente progesterona (*Min, et al., 2005*) y no muestra ninguna homología con los receptores de esteroides nucleares ni de membrana (*Mifsud y Bateman, 2002*). La resolución de la estructura cristalina del receptor PGRMC-1 muestra la existencia de un dominio de unión a grupos hemo y de una hélice transmembrana N-terminal mediante la cual se ancla a la membrana celular (*Kabe, et al., 2016*). En presencia de un grupo hemo, PGRMC-1 forma estructuras diméricas (*Kabe, et al., 2016*) (**Figura 24**). Hasta la fecha ha sido descrito que este receptor puede interaccionar con el *epidermal growth factor receptor* (EGFR) (*Ahmed, et al., 2010*), el citocromo P450 (*Hughes, et al., 2007*) o la proteína de unión a RNA, PAIR-BP1 (*plasminogen activator inhibitor 1 mRNA binding protein*) (*Peluso, et al., 2005*), entre otros.

El receptor sigma-2 se expresa en hígado, riñones, cerebro, pulmones, corazón, músculos y páncreas (*Gerdes, et al., 1998*; *Krebs, et al., 2000*). A nivel subcelular, mediante estudios de fluorescencia utilizando ligandos marcados, ha sido detectada la presencia del receptor en mitocondria, lisosomas, retículo endoplásmico y membrana plasmática, con la notable excepción del núcleo (*Zeng, et al., 2007*).

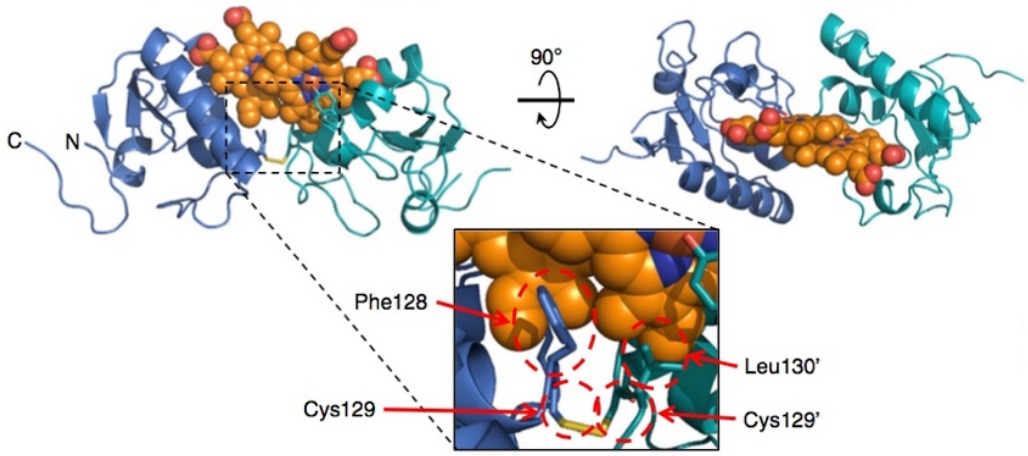

Figura 24. Estructura cristalina del receptor PGRMC-1/Sigma-2. Estructura dimérica del receptor PGRMC-1 formada por la unión de dos monómeros (pintados en azul y verde) a una molécula hemo (naranja). En la ampliación recuadrada se representan los residuos aminoacídicos implicados en la unión de la molécula hemo. Extraído de *Kabe, et al., 2016*.

Debido a su reciente clonación (*Xu, et al., 2011*) el papel del receptor sigma-2 aún está bien definido. El receptor sigma-2 se encuentra implicado en la proliferación celular y la biosíntesis de colesterol (*Rohe, et al., 2009; Ahmed, et al., 2012*). Además, ha sido definido como un biomarcador del estatus proliferativo de ciertos tumores (*Van Waarde, et al., 2015*). Ambos subtipos de receptores sigma están sobreexpresados en las células que de forma natural muestran una rápida proliferación, así como en células cancerosas. Particularmente el receptor sigma-2 es una diana interesante para detectar tumores, pues su nivel de expresión en células tumorales proliferativas es 10 veces mayor que en las células tumorales quiescentes (*Van Waarde, et al., 2010*). La activación del receptor sigma-2 a concentraciones del rango micromolar es capaz de inducir la muerte de distintas células cancerosas (*Crawford, et al., 2002*; *Berardi, et al., 2009*), induciendo la muerte celular vía apoptosis o por mecanismos independientes de apoptosis (*Mach, et al., 2013*; *Zeng, et al., 2014*). Así, se puede concluir que la inhibición de la proliferación tumoral requiere de la acción de agonistas del receptor sigma-2 (*Colabufo, et al., 2004*), sin embargo, ha sido descrito que es inhibida por antagonistas de PGRMC-1 (*Ahmed, et al., 2010*; *Jonhede, et al., 2010*). Esta contradicción puede ser más aparente que real, ya que el concepto de agonista o antagonista en los receptores sigma, al no tener señalización propia, no está bien definido. Algunos compuestos que originalmente fueron catalogados como agonistas de sigma pueden ser, en realidad, antagonistas, y *viceversa* (*Zeng, et al., 2014*).

La muerte celular inducida vía receptor sigma-2 es una de las áreas de investigación más activas alrededor de este receptor. No obstante, han aparecido estudios que lo relacionan con las acciones de la cocaína (*Garcés-Ramirez, et al., 2011*). En 2007 fue descrita una atenuación de los efectos conductuales inducidos por esta sustancia después del tratamiento con antagonistas del receptor sigma-2 (*Matsumoto, et al., 2007*). Lever y colaboradores también

describieron una atenuación de los efectos hiperlocomotores provocados por la cocaína en ratones tratados con antagonistas selectivos del receptor sigma-2 (*Lever, et al., 2014*).

Ha sido descrito que la cocaína puede interaccionar con el sistema dopaminérgico (*Navarro, et al., 2010*). Así, en un principio se hipotetizó que los ligandos de los receptores sigma-1 y sigma-2 podrían interferir en la señalización inducida por cocaína mediante los receptores de dopamina (*Romieu, et al., 2002, Kalivas, et al., 2004*). Esto fue confirmado por Navarro y colaboradores al demostrar la interacción molecular y funcional entre los receptores sigma-1 y D_1 de dopamina. El estudio evidenció que la interacción de la cocaína con el receptor sigma-1 potenciaba la activación de la adenilato ciclasa inducida por la activación del receptor de dopamina D_1 y bloqueaba la activación de la vía de las MAP kinasas. Este mecanismo era independiente del bloqueo de DAT (*Navarro, et al., 2010*).

1.4.5. Vía mesolímbica

La vía mesolímbica, o vía de la recompensa, es una de las vías dopaminérgicas del cerebro y el mecanismo cerebral que media la recompensa y proporciona placer al sujeto frente a una acción concreta. Es un circuito clave para asegurar la supervivencia del individuo pues al activarse aporta sensación de placer y bienestar, creando una asociación positiva con la acción que ha inducido a su activación (la ingesta de comida, beber cuando se tiene sed, el establecimiento de vínculos sociales con otros individuos o el sexo, entre otros). El placer que proporciona al sujeto su realización se torna suficiente motivo como para que se desee repetir la conducta.

La dopamina es el neurotransmisor predominante en el sistema mesolímbico, no obstante, también ha sido descrita la participación del glutamato y del GABA (*Steketee y Kalivas, 2011*). Esta vía está formada por el área tegmental ventral (VTA), el núcleo accumbens (NAc), conectando de este modo con el sistema límbico, y finalmente por la corteza prefrontal, formando así una interfaz motora-límbica que conecta procesos motivadores con acciones motoras (*Soares-Cunha, et al., 2016*). Neuronas dopaminérgicas proyectan desde la VTA hacia el núcleo accumbens y la corteza prefrontal, liberando dopamina y glutamato al sistema en respuesta a una acción motivadora (*McClure, et al., 2003; Tecuapetla, et al., 2010*). Estos neurotransmisores actúan como señal para iniciar respuestas de adaptación comportamental frente a la acción motivadora y promueven la neuroplasticidad, es decir, se inducen cambios celulares para establecer una asociación con dicha conducta (*Jay, 2003*). De este modo, se refuerzan las conexiones neuronales que involucran a esa acción concreta y, además, el organismo podrá emitir una respuesta más rápida si se reproduce la misma acción. La señal, al llegar al núcleo accumbens, establece una modulación de la conducta motivacional y establece una relación entre el evento motivador y las percepciones ambientales (*Sellings y Clarke, 2003*). El núcleo accumbens, a la vez, recibe aferencias de otros centros cerebrales asociados con la manifestación de emociones (amígdala e hipotálamo), memoria (hipocampo) e información motora de la corteza (*Di Ciano, et al., 2001; Steketee y Kalivas, 2011*). Todo esto servirá para afinar aún más la respuesta y preservar las conductas que han generado un estado positivo. Por otro lado, del núcleo accumbens proyectan neuronas GABAérgicas hacia la VTA, estableciendo así una inhibición en sentido inverso para modular el sistema (*Steketee y Kalivas, 2011*). Finalmente, el circuito mesolímbico está conectado con la corteza prefrontal, que a su vez mantiene conexiones con la corteza motora. A la corteza prefrontal llegan inervaciones dopaminérgicas procedentes de la VTA y a la vez, neuronas glutamatérgicas procedentes de la corteza prefrontal proyectan hacía la VTA y el núcelo accumebens *(Joffe, et al., 2014*). La corteza prefrontal es un lugar de asociación de importantes

funciones de mediación de la conducta: la elaboración de planes conductuales cognitivamente complejos, los procesos de toma de decisiones y la adecuación del comportamiento social adecuado a cada momento (*Yang y Raine, 2009*). Se considera que la actividad fundamental de esta región cerebral es la coordinación de pensamientos y acciones de acuerdo con metas internas (*Miller, et al., 2002*), así como de la intensidad de la respuesta que será emitida por el sujeto (*Bush, et al., 2002*) (**Figura 25**).

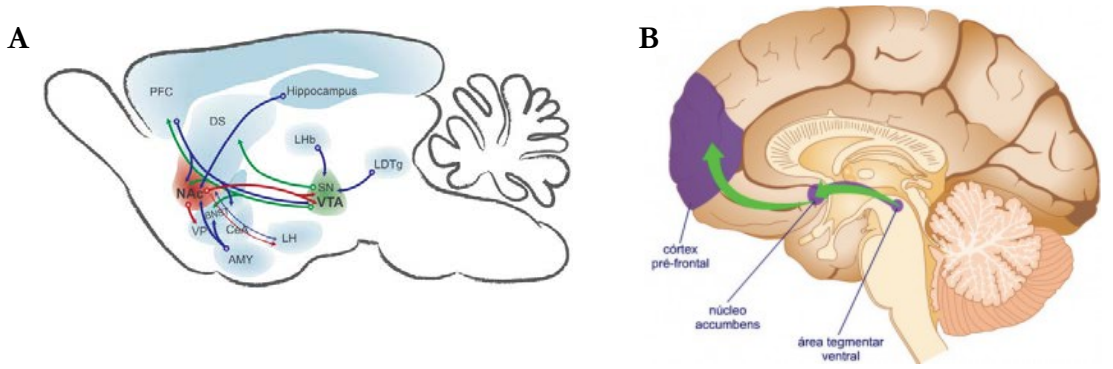

Figura 25. Representación esquemática del circuito de recompensa. A) En el cerebro de roedor. La transmisión dopaminérgica (flechas verdes) desde la VTA y la *substanctia nigra* (SN). En azul se representa la señalización glutamatérgica y en rojo la GABAérgica. AMY, amígdala; BNST, *bed nucleus of the stria terminalis*; CeA, núcleo central de la amígdala; DS, estriado dorsal; LDTg, *tegmentum* laterodorsal; LHb, habénula lateral; LH, hipotálamo lateral; PFC, corteza prefrontal; VP, *ventral pallidum*. Extraído de *Joffe, et al., 2014*. **B) En el cerebro humano.** Coloreado en lila se representan las estructuras implicadas y las conexiones dopaminérgicas están representadas por flechas verdes.

Como ha sido mencionado anteriormente, diferentes drogas euforizantes, entre ellas la cocaína, producen un fuerte aumento de los niveles de dopamina en el espacio sináptico con la consecuente sobre-activación de los circuitos neuronales donde la dopamina es el principal neurotransmisor, como la vía de la recompensa. A lo largo de los últimos 40 años multitud de estudios han relacionado los efectos de las drogas de abuso con la vía mesolímbica. Roberts y colaboradores describieron una inhibición en los efectos de recompensa de la cocaína en ratas con el núcleo accumbens lesionado (*Roberts, et al., 1977*). Más adelante, en estudios en ratas adictas a la cocaína, se determinó que el córtex prefrontal está implicado en la autoadministración de cocaína (*Goeders y Smith, 1983*), y unos años más tarde Pettit y Justice observaron una correlación entre la cocaína auto-administrada y los niveles de dopamina extracelular liberada en el núcleo accumbens en roedores (*Pettit y Justice, 1991*). En estudios más recientes en los que han sido combinados el tratamiento con antagonistas dopaminérgicos y la lesión del núcleo accumbens o regiones asociadas, ha sido observada también la relación de los efectos producidos por la cocaína y la vía mesolímbica (*Belin y Everitt, 2008; Will, et al., 2016*). Estos datos convierten la vía mesolímbica y el córtex prefrontal en las regiones más importantes para la integración de los efectos de la cocaína, aunque no son las únicas (*Bardo, et al., 1998*). Esta es la causa del elevado potencial adictivo de las drogas de abuso, el sujeto después del consumo de estas sustancias quiere repetir esta conducta repetidas veces para volver a alcanzar la misma sensación de placer.

1.4.6. Área tegmental ventral (VTA)

La VTA consiste en un grupo heterogéneo de neuronas agrupadas en distintos núcleos (*Phillipson, 1979*) en la base del mesencéfalo, adyacente a la *substantia nigra* (*Oades y Halliday, 1987*). La separación anatómica entre estas dos estructuras no es demasiado clara, no

obstante, sí que hay una diferencia más evidente al analizar hacia donde proyectan las neuronas de cada una de las dos regiones. Las neuronas de la VTA proyectan hacia numerosas áreas del cerebro como la habénula lateral, el núcleo accumbens o la corteza prefrontal (*Bariselli, et al., 2016; Morales y Margolis, 2017*), mientras que la de la *substantia nigra* proyecta hacia regiones del tálamo, el colículo superior y el núcleo caudado (*Nauta y Cole, 1978*). Esta diferencia respecto a la destinación de las aferencias de la VTA y la sustancia nigra provoca una divergencia en las funciones en las que está implicada cada una de estas dos zonas. La VTA se encuentra involucrada en las acciones cognitivas, en la motivación, el orgasmo, la recompensa, la adicción a drogas y las emociones relacionadas con el amor (*Morales y Margolis, 2017*). También ha sido observado que la VTA se encuentra implicada en distintos desordenes psiquiátricos, como la enfermedad de Alzheimer (*Trillo, et al., 2013*) o desórdenes de déficit de atención e hiperactividad (ADHD).

En la VTA, las neuronas dopaminérgicas representan un 55-65% del total (*German y Manaye, 1993*). No obstante, diversos tipos neuronales a través de sus *inputs* u *outputs* contribuyen a los procesos neurológicos adaptativos o patológicos relacionados con la motivación y la recompensa (*Bariselli, et al., 2016*). Recientes estudios han demostrado la existencia de poblaciones neuronales en la VTA que co-liberan dopamina y glutamato (*Stuber, et al., 2010*), dopamina y GABA (*Tritsch, et al., 2014*), o glutamato y GABA (*Root, et al., 2014*). Esta heterogeneidad de la población neuronal parece estar genéticamente programada en el estadio embrionario. De hecho, han sido descritos el establecimiento de gradientes de moléculas señalizadoras y de factores de transcripción que regulan la neurogenesis, migración y maduración de las neuronas del mesencéfalo (*Arenas, et al., 2015; Blaess y Ang, 2015*).

En esta región los receptores dopaminérgicos tienen un papel muy importante, y sin embargo coexisten con otros GPCR, tales como el receptor de *cortocotropin-releasing factor* (CRFR), involucrado principalmente en los procesos de estrés, el receptor de orexina (Ox_1R), involucrado en el apetito y en el sistema cerebral del sueño-vigilia, el receptor de grelina, la hormona del hambre, o con receptores moduladores como los receptores sigma-1 y sigma-2, que juegan un papel importante en los mecanismos de adicción a las drogas de abuso, concretamente, a la cocaína.

1.4.7. Receptor de *corticotropin-releasing factor* (CRFR)

El *Cortocotropin-releasing factor* (CRF) fue descubierto en 1981 por Vale y colaboradores (*Vale, et al., 1981*). Es un neuropéptido de 41 aminoácidos implicado en el balance homeostático, en la movilización de recursos y en la respuesta al estrés (*Bale y Vale, 2004*). También ha sido descrito su papel en la regulación de la ingesta y la saciedad (*Spina, et al., 1996; Zhang, et al. 2016*), la motilidad del tracto gastrointestinal (*Maillot, et al., 2000*), el tono vascular (*Terui, et al. 2001*), el desarrollo, la audición y la función cardíaca (*Okosi, et al., 1998*). El CRF media todas estas acciones por la unión a dos subtipos de receptores, CRF_1R y CRF_2R (*Bale y Vale, 2004*; *Hollenstein, et al., 2014*) (**Figura 26**). Se trata de dos GPCR de clase B con un 70% de identidad entre ellos, que provienen de distintos genes y expresan diferentes isoformas, debido a fenómenos de *splicing* alternativo, según el tejido donde se encuentren (*Bale y Vale, 2004*). Estos receptores están ampliamente distribuidos en el SNC y en tejidos periféricos (*Korosi, et al., 2006; Zorrilla, et al., 2014*).

El estrés incrementa la vulnerabilidad de los humanos a caer en conductas adictivas (*Sinha, 2008*). Distintos estudios muestran que agentes estresantes incrementan el comportamiento de búsqueda (*Sarnyai, et al., 2001*) y auto-administración de drogas de abuso (*Miczek, et al.,*

2008; Mantsch, et al., 2008). Los mecanismos moleculares que participan en la interacción entre el estrés y la auto-administración de cocaína aún están por determinar. Un posible candidato a establecer esta conexión es el CRF ya que fue demostrado que tanto el estrés como las drogas de abuso sensibilizaban las neuronas dopaminérgicas de la VTA a los *inputs* excitatorios, aumentado la fuerza de esta señalización mediante modificaciones sinápticas (*Saal, et al., 2003*) y este fenómeno podía ser reproducido al aplicar CRF en la VTA (*Ungless, et al., 2003*). Además, en la VTA de animales que habían sido puestos en contacto con cocaína previamente, pero no en animales *naive*, la liberación de CRF inducida por estrés incrementaba los niveles extracelulares de glutamato y de dopamina a lo largo de toda la vía de la recompensa (*Wang, et al., 2007; Holly, et al., 2015; Holly, et al., 2016*). A este núcleo llegan *inputs* de CRF desde el núcleo paraventricular y el prosencéfalo límbico (*Rodaros, et al., 2007*). Recientemente, ha sido demostrado que poblaciones de neuronas dopaminérgicas de la VTA expresan receptores de CRF (*Grieder, et al., 2014*), siendo el receptor CRF_1R el que está más implicado en los comportamientos de búsqueda de droga inducidos por estrés (*Lu, et al., 2003; Blacktop, et al., 2013*).

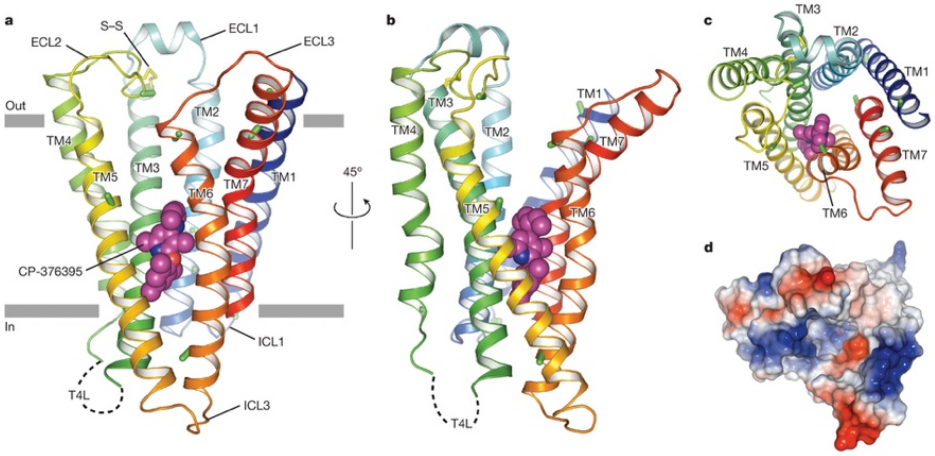

Figura 26. Estructura cristalina del receptor CRF_1R. A) B) C) Representación de la estructura del receptor en diferentes perspectivas. **D)** Representación del receptor desde el ángulo extracelular, la coloración representa el potencial electroestático de las diferentes regiones. Extraído de *Hollestein, et al., 2013*.

1.4.8. Receptor de Orexina (OX_1R)

Los neuropéptidos orexina-A (hypocretina-A) y orexina-B (hipocretina-B), de 33 y 28 aminoácidos respectivamente, fueron identificados por dos grupos distintos prácticamente de manera simultánea. Por un lado, Sakurai y colaboradores nombraron a este péptido orexina, derivado de "*orexis*", que en griego significa apetito (*Sakurai, et al., 1998*), mientras que de Lecea y colaboradores lo llamaron hipocretina, debido a que se sintetiza mayoritariamente en el hipotálamo y áreas adyacentes, y tiene cierto parecido al péptido secretina (*de Lecea, et al., 1998*). En la actualidad, aún no ha sido establecido oficialmente una de las dos nomenclaturas, motivo por el cual en la literatura se encuentran trabajos con uno u otro nombre para referirse al mismo neuropéptido.

Los péptidos Orexina-A y orexina-B tienen cerca de un 50% de homología entre sí, ya que provienen de un mismo precursor, la preproorexina (*Gotter, et al., 2012*). Además, la estructura de la orexina se encuentra altamente conservada en la mayoría de vertebrados (*Wong, et al., 2011*). Estos péptidos son diana de dos receptores distintos que forman el sistema

orexigénico, el receptor OX_1R y el receptor OX_2R. Estos receptores tienen distinta afinidad por la orexina. El receptor OX_1R tiene mayor afinidad por el péptido orexina-A que por la orexina-B. Mientras que el receptor OX_2R tiene afinidad similar por los dos péptidos (*Sakurai, et al., 1998*). Ambos tipos de receptores, además, parecen tener una distribución diferente en el sistema nervioso, lo que indica que pueden desempeñar papeles diferentes en las funciones fisiológicas de la orexina (*Scammell y Winrow, 2011*). Recientemente ha sido resuelta la estructura de los receptores de orexina-1 (*Yin, et al., 2016*) y orexina-2 (*Yin, et al., 2015*), lo que permitirá trabajar en el diseño de nuevos fármacos que puedan unirse específicamente a uno u otro receptor para fines terapéuticos.

Desde su descubrimiento, el sistema orexinérgico ha sido uno de los más estudiados, a pesar de la localización altamente restringida de las neuronas orexinérgicas en el hipotálamo; su inervación llega a muchas áreas distintas del cerebro, como el *locus coeruleus*, los núcleos de rafe o la VTA (*Mediavilla y Riscos, 2014*), participando en distintos mecanismos (*Peyron, et al., 1998; Messina, et al., 2016)*. El hipotálamo ha sido considerado tradicionalmente una región crítica en la conducta alimentaria y la regulación del metabolismo energético (*Bernardis y Bellinger, 1996*). Por ello, el hecho de que las neuronas orexinérgicas se concentren en esta región llevó desde un principio a relacionar a este neuropéptido con la ingesta de alimentos. Ha sido observado que la administración de orexina en áreas hipotalámicas, incluso en animales saciados, estimula la ingesta de alimentos, siendo mayor el efecto con la orexina-A que con la orexina-B (*Haynes, et al., 1999*; *Russell, et al., 2002*) y, por el contrario, al administrar un antagonista del receptor de orexina, ha sido observada una disminución en la ingesta de alimentos en estos animales (*Cole, et al., 2015*). Además, ha sido descrita la implicación de la orexina en el ciclo sueño-vigilia, disponiendo al cerebro en estado de conciencia; y ha sido comprobado que la administración intracerebroventricular de orexina prolonga el período de vigilia y reduce el tiempo de sueño (*Sakurai, 2007*). Finalmente, también ha sido relacionada la alteración de los niveles o del funcionamiento del sistema orexinérgico con la aparición de determinados trastornos clínicos, como la narcolepsia (*Mediavilla y Riscos, 2014*). Estas acciones en las que está implicada la molécula de orexina son mediadas por su unión y posterior activación de dos GPCR, el receptor de orexina-1 (OX_1R) y el receptor de orexina-2 (OX_2R), pertenecientes a la familia A, o *rhodopsin-like*, de GPCR (*Messina, et al., 2016*). (**Figura 27**).

La orexina también tiene un papel importante en los procesos de recompensa y en la adicción a sustancias de abuso (*Sakurai, 2014; Mahler, et al., 2014*). Como ya ha sido indicado anteriormente, las neuronas orexinérgicas del hipotálamo proyectan a diferentes regiones del núcleo accumbens y la VTA, que forman parte del sistema de recompensa (*Wise, 2002*). Ha sido descrito que las neuronas orexinérgicas del hipotálamo pueden ser activadas por estímulos de comida o de drogas de abuso, siendo su activación relevante en la dependencia a diferentes sustancias de abuso como morfina, heroína o cocaína (*Harris y Aston-Jones, 2006; Narita, et al., 2006; Cason, et al., 2010*). Diversos trabajos sostienen que existe una dicotomía en la función de la orexina relacionada con los dos receptores de orexina identificados. Por un lado, el receptor OX_2R estaría implicado en los mecanismos de sueño-vigilia (*Etori, et al., 2014*), mientras que el receptor OX_1R estaría implicado en los mecanismos relacionados con la recompensa y el apetito (*Mahler, et al. 2014*).

El sistema orexinérgico también se encuentra implicado en el proceso de recaída a través de la activación de la vía del estrés, la cual incluye la participación del receptor CRF. Ha sido observado que la administración de orexina-A induce una recaída dosis-dependiente de la búsqueda de cocaína, y que este comportamiento es evitado al tratar al animal con un antagonista no-selectivo de CRF. Además, un antagonista selectivo de OX_1R bloquea la

recaída inducida por estrés en animales en los que ya ha sido extinguido el comportamiento de búsqueda de cocaína (*Boutrel, et al., 2005*). La VTA es un área cerebral clave en la habilidad del sistema orexinérgico para promover la búsqueda de cocaína. Wang y colaboradores demostraron que la administración intra-VTA de orexina-A inducía la recaída en la auto-administración de cocaína, proceso que se asociaba a la liberación de glutamato y dopamina en la VTA (*Wang, et al., 2009*).

Hasta el momento, a pesar de que tanto el péptido CRF como la orexina-A se encuentran involucrados en la recaída en el consumo de cocaína inducida por estrés, sus mecanismos siempre han sido estudiados de forma independiente. Es de nuestro interés estudiar la relación que se establece entre ellos para intentar dar una explicación al mecanismo por el cual la adicción a las drogas de abuso está interconnectada con estos sistemas.

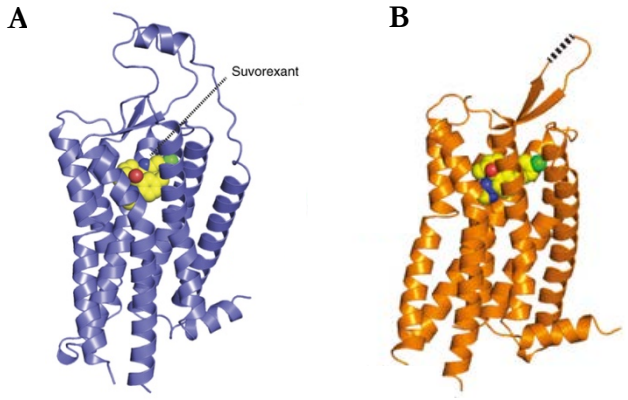

Figura 27. Estructura cristalina de los receptores OX_1R y OX_2R. A) Estructura del receptor OX_1R (azul) unido a una molécula de Suvorexant (amarillo). Extraído de *Yin, et al., 2016*. **B)** Estructura del receptor OX_2R (naranja) unido a una molécula de Suvorexant (amarillo). Extraído de *Yin, et al., 2015*.

1.4.9. Receptor de grelina (GHS-R)

La grelina es una hormona orexinérgica. Se trata de un péptido de 28 aminoácidos con una modificación posttraduccional, la acilación del residuo serina-3, necesaria para su activación (*Yang, et al., 2008*). Alrededor del 70 – 90% de la grelina que se detecta en plasma se encuentra en su forma no acilada, lo cual es explicado en parte por la corta vida media de la forma acilada, unos 8 minutos (*Kojima, et al., 1999*). La grelina actúa como señal interna para predisponer al sujeto a la ingesta de alimentos; este hecho le ha dado el nombre popular de "hormona del hambre". La grelina es sintetizada predominantemente por células endocrinas especializadas del estómago, las células oxínticas (*Kojima, et al., 1999*). Las células oxínticas son clasificadas como osciladores relacionados con el hambre, haciendo que los niveles de grelina en plasma se incrementen antes de la comida y disminuyan después de esta (*Cabral, et al., 2017*), fluctuando circadianamente (*Silver y Balsam, 2010*). El organismo, además, mediante distintos sensores como la reducción del volumen del estómago o la detección de un déficit calórico, entre otros, induce la síntesis de grelina. Este péptido tiene la capacidad de cruzar la barrera hematoencefálica, mecanismo aún por describir, y alcanzar los receptores de grelina localizados en áreas cerebrales específicas como el hipotálamo, el hipocampo, la amígdala, la VTA y regiones dopaminérgicas del mesencéfalo y del estriado (*Mason, et al., 2014*). Esta hormona estimula el apetito por su acción en el hipotálamo promoviendo la liberación hipofisiaria de la hormona de crecimiento (*Stanley, et al., 2005*). También induce respuestas en tejidos periféricos, incrementa la movilidad y secreción gástrica de HCl, modula la función

pancreática endocrina y el metablismo de la glucosa. Además, ha sido relacionada con diferentes efectos cardiovasculares (*Lilleness y Frishman, 2016*) y ha sido visto que promueve la proliferación de adipocitos del tejido adiposo blanco (*Wells, 2009; Lanfranco, et al., 2010*). La grelina actúa mediante su unión al receptor de grelina, un GPCR de la familia A que recibe el nombre de *growth hormone secretatogue* (GHS) *receptor*. Existen dos subtipos del receptor de grelina, el receptor de grelina 1a (GHS-R1a) y el receptor de grelina 1b (GHS-R1b), una variante truncada del receptor GHS-R1a al que le faltan los dominios transmembrana 6 y 7. La carencia de estos dos dominios transmembrana impide a la grelina interaccionar con este receptor, y además, al no tener concretamente el dominio transmembrana 6, no puede interaccionar con la proteína G, de modo que la grelina no puede ni activar ni señalizar a través de GHS-R1b (*Mary, et al., 2013*). Esta variante truncada del receptor de grelina había sido considerada un vestigio evolutivo sin ningún papel en la señalización mediada por grelina, no obstante, en los últimos años han aparecido estudios que empiezan a arrojar luz sobre el papel que desarrolla el GHS-R1b. Las células que expresan el receptor GHS-R1a también expresan el receptor GHS-R1b. Ha sido descrita la capacidad del receptor GHS-R1a para homodimerizar y heteromerizar con GHS-R1b; esta característica permitiría al receptor GHS-R1b regular de manera negativa la señalización mediada a través de GHS-R1a (*Mary, et al., 2013*). Han sido propuesto dos mecanismos distintos para la modulación negativa de GHS-R1b sobre GHS-R1a: por un lado, la retención intracelular de GHS-R1a cuando este se encuentra formando complejos con GHS-R1b debido a la incapacidad del receptor GHS-R1b de llegar a la membrana plasmática (*Chow, et al., 2012*), y por otro lado un mecanismo alostérico mediante el cual el complejo GHS-R1a-GHS-R1b produce un cambio conformacional en el receptor GHS-R1a, adquiriendo este una conformación que no le permite señalizar (*Mary, et al., 2013*). Estos mecanismos no tendrían por qué ser excluyentes (*Mary, et al. 2013*).

Como ha sido comentado con anterioridad, los receptores de grelina GHS-R1a y GHS-R1b coexisten en la VTA (*Zigman, et al., 2006*). La VTA, como ya ha sido descrito, tiene un papel muy importante en los mecanismos y conductas relacionados con la recompensa, incluidos los comportamientos cuya finalidad es obtener recompensas naturales como la comida (*Wise, 2002*). La vía de la recompensa se activa con la experiencia, la expectativa de recompensa o la exposición a estímulos placenteros (*Richardson y Gratton, 1998*). Es por ello que distintos trabajos proponen la grelina como un agente capaz de participar en la vía de la recompensa, regulando el apetito mediante la anticipación de las sensaciones que produce la ingesta de alimentos, generando así una expectativa y un refuerzo positivo. Abizaid y colaboradores observaron que la microinyección de un antagonista del receptor de grelina en la VTA era capaz de bloquear los efectos orexinérgicos que induce la administración periférica de grelina, además demostraron que la estimulación con grelina inducía un aumento en la liberación de dopamina en las neuronas de la VTA (*Abizaid, et al. 2006*) y del núcleo accumbens (*Jerlhag, et al., 2006; Abizaid y Horvath, 2008; Skibicka, et al., 2011*). También ha sido observado en ensayos de preferencia de lugar condicionado en ratones que estos animales pasan más tiempo en las zonas asociadas a una recompensa alimentaria, viéndose reducido este tiempo al tratar a los animales con un antagonista del receptor GHS-R1a y en ratones *knockout* para este mismo receptor (*Egecioglu, et al., 2010; Perello, et al., 2010*). Estos resultados ponen en evidencia el papel de la grelina en el sistema de recompensa. La constatación de la intervención de este péptido en la activación de la vía mesolímbica plantea nuevas cuestiones acerca de su posible papel en la adicción a drogas de abuso, concretamente a la cocaína. En este núcleo cerebral los receptores de grelina coinciden en el espacio con otros receptores clásicamente asociados a la adicción como los receptores dopaminérgicos o los receptores sigma. Deberá ser estudiado si existe una interacción entre ellos y determinar el papel funcional de esta.

Como ha sido comentando anteriormente, uno de los efectos observados tras el consumo de cocaína es la eliminación de la sensación de apetito. Este fenómeno ya era conocido por los chamanes de las antiguas civilizaciones andinas, y aún hoy en día el mascar hoja de coca o beber infusiones de coca es un recurso utilizado por trabajadores del ámbito rural de centro y sud-américa para afrontar las duras condiciones laborales a las que se ven sometidos. También entre los porteadores que realizan travesías a lo largo de la cordillera de los andes, y no pueden viajar cargando con grandes cantidades de comida, es frecuente el uso de la hoja de coca para apaciguar, entre otras cosas, la sensación de hambre. No obstante, a pesar del conocimiento popular de este fenómeno desconocemos las bases moleculares mediante las cuales la cocaína es capaz de modular los efectos de la grelina. Poder elucidar el mecanismo que se esconde tras este fenómeno es de gran interés, por ejemplo, para el futuro diseño de fármacos que permitan un control del apetito.

1.5. SENSORES DE CALCIO

1.5.1. Papel fisiológico del calcio en el organismo

Hasta el momento ha sido descrita la modulación de los GPCR mediante la interacción con otros GPCR, con isoformas del mismo receptor (GHS-R1a-GHS-R1b) o a través de receptores moduladores, como los receptores sigma-1 o sigma-2. No obstante, también ha sido descrito que los sensores de calcio pueden ejercer esta función sobre los GPCR.

El calcio es un segundo mensajero imprescindible para el correcto funcionamiento de todas las células. Participa en la transducción de señal, en la división celular, en la diferenciación y en la apoptosis (*Carafoli, 2002; Orrenius, et al., 2003*). Su concentración intracelular oscila desde niveles submicromolares hasta milimolares (*Tsien y Tsien, 1990; Ghosh, et al., 2017*). Estos cambios de concentración de los niveles del calcio son importantes para la regulación de diversos procesos, aunque también dependen de la velocidad específica, de la frecuencia o de la magnitud de la señal (*Zampese y Pizzo, 2012*). La combinación de cambios inducidos por el calcio y que caracterizan su señal son conocidos como "la firma del calcio" (*Hashimoto y Kudla, 2011*).

Si centramos nuestra atención en el SNC, la señalización mediada por calcio es fundamental para la comunicación entre neuronas (*Berridge, 1998*). La transmisión neuronal requiere un incremento muy rápido y muy localizado de la concentración de calcio en la zona pre- y post-sináptica. Una entrada masiva de calcio a la neurona post-sináptica contribuye a la plasticidad sináptica a corto y a largo plazo (*Catterall y Few, 2008; Mochida, et al., 2008*). La transcripción génica dependiente de calcio se encuentra involucrada en el control de procesos cruciales como el desarrollo, la maduración y el refinamiento de la sinapsis, debiendo estar estrictamente regulada (*Greer y Greenberg, 2008*). Es por ello que un amplio espectro de proteínas sensoras de calcio actúan como tampón para regular los niveles intracelulares de calcio, modulando y restringiendo el impacto espacial y temporal de este ion como segundo mensajero. Estas proteínas pues, juegan un papel central en la regulación de la señalización inducida por calcio (*Di Donato, et al., 2013*).

Las proteínas con capacidad para unir calcio se caracterizan por sufrir un cambio de conformación cuando varía la concentración de calcio en el medio. Este cambio de conformación permite la interacción del sensor con distintos efectores, y la transmisión de la información mediante fosforilaciones, o cambios en la expresión génica (*Hashimoto y Kudla,*

2011). Esto provoca, en último lugar, la modulación de la actividad neuronal (*McCue, et al., 2010*).

Existen diferentes proteínas de unión a calcio, con diferente distribución a nivel subcelular y tisular. En función del papel que desarrollan estas proteínas de unión a calcio se clasifican en tres gandes grupos: los sensores de calcio, como por ejemplo la calmodulina (CaM) (*Levine, et al., 1983*), se caracterizan por una baja afinidad por el calcio, sin embargo cuando unen calcio experimentan importantes cambios conformacionales, permitiendo así la interacción de los sensores con las distintas proteínas efectoras; el segundo grupo se encuentra formado por las proteínas tamponadoras, como por ejemplo, S100G o parvalbumina (*Schröder, et al., 1996*), estas proteínas tienen gran afinidad por el calcio aunque no muestran grandes cambios conformacionales, actuando únicamente como quelantes de calcio (*Schwaller, 2009*); en último lugar se describieron las proteínas estabilizadas por calcio, como por ejemplo la termolisina (*Buchanan, et al., 1986*). Las proteínas sensoras y tamponadoras de calcio se caracterizan por mostrar un domino *EF-hand*, mediante el cual unen calcio (*Mikhaylova, et al., 2011*). Este dominio consiste en 29 aminoácidos con una estructura formada por una hélice-α seguida de un *loop* que une otra hélice-α (*Burgoyne, 2007*). El motivo *EF-hand* fue caracterizado en la proteína parvalbúmina (*Krestsinger y Nockolds, 1973*), y se sabe que es uno de los dominios más comunes codificados por el genoma humano, estando presente en 122 proteínas.

En este trabajo nos centraremos en el estudio de los sensores de calcio a nivel del sistema nervioso central. Los sensores de calcio neuronales tienen como ancestro común la calmodulina (*Mikhaylova, et al., 2011*). Según la evolución y la historia de su descubrimiento, los sensores de calcio de la superfamilia de la CaM pueden separarse en dos grandes grupos: la superfamilia de los sensores de calcio neuronales (NCS); y la superfamilia caldendrin/calcium-binding proteins/Calneuron. Algunos autores utilizan un nombre más genérico para esta última superfamilia: las proteínas de unión a calcio neuronales (*neuronal calcium-binding proteins*, nCaBP) (*Mikhaylova, et al., 2011*). Al compartir un ancestro común, las proteínas que forman parte de estas superfamilias de sensores presentan una estructura parecida, con cuatro dominos *EF-hand* de unión a calcio, aunque no todos ellos son funcionales (*Mikhaylova, et al., 2011*). No obstante, a pesar de la homología estructural con la CaM, los NCS y los nCaBP presentan múltiples diferencias a nivel de secuencia aminoacídica. Además, las implicaciones funcionales de la unión del calcio a estas proteínas pueden ser completamente distintas. Este hecho incrementa el potencial y la versatilidad del ion calcio (*Ikura y Ames, 2006; Burgoyne, 2007*).

1.5.2. Calmodulina (CaM)

La superfamília de la calmodulina (CaM) engloba al grupo más numeroso de sensores de calcio (*Kawasaki, et al., 1998*). La CaM es la proteína más importante de esta superfamilia y probablemente el sensor de calcio intracelular más esencial. Su importancia se hace evidente por el hecho de que esta proteína es codificada en el genoma humano por tres genes independientes (*CALM1-3*) que codifican para proteínas idénticas (*Sorensen, et al., 2013*). También es indicativo de su relevancia el grado de conservación de esta proteína, la cual no ha sufrido cambios en su secuencia aminoacídica desde la aparición de los vertebrados (*Friedberg y Rhoads, 2001*). La calmodulina es una proteína relativamente pequeña, formada por 148 aminoácidos dispuestos en una estructura de hélice-α con dos dominios globulares, uno en el extremo N-terminal y otro en el extremo C-terminal; cada uno de los cuales contiene dos dominios *EF-hand* donde se unen las moléculas de calcio (*Sorensen, et al., 2013*)

con una afinidad de 5 – 10 microMolar (*Mikhaylova, et al., 2011*) (**Figura 28A**). El hecho de que los dominios N-terminal y C-terminal presenten una cinética de unión a calcio diferente incrementa aún más la versatilidad de este sensor (*Tadross, et al., 2008*), pudiendo unir hasta cuatro iones de calcio, sufriendo cambios conformacionales con cada nueva unión. Estos cambios le permiten unirse de forma específica a más de 120 proteínas (enzimas, canales iónicos, factores de transcripción y proteínas del citoesqueleto), ejerciendo una función de sensor o de transductor de señal (*Marcelo, et al., 2016*). Esta proteína tiene la capacidad de poder utilizar tanto el calcio citoplasmático como también las reservas de calcio del retículo endoplasmático o sarcoplasmático. Ciertas señales extracelulares como la insulina del páncreas, estímulos adipogénicos del tejido adiposo blanco u hormonas, entre otros, al unirse a sus respectivos receptores inducen un aumento en los niveles de calcio intracelular. La CaM, al unir calcio, puede interaccionar con diferentes efectores como proteínas quinasas *downstream*, las cuales promoverán el crecimiento celular, la regulación del balance energético, la síntesis de proteínas o la regulación de la expresión génica entre otras funciones (*Marcelo, et al., 2016*) (**Figura 28B**).

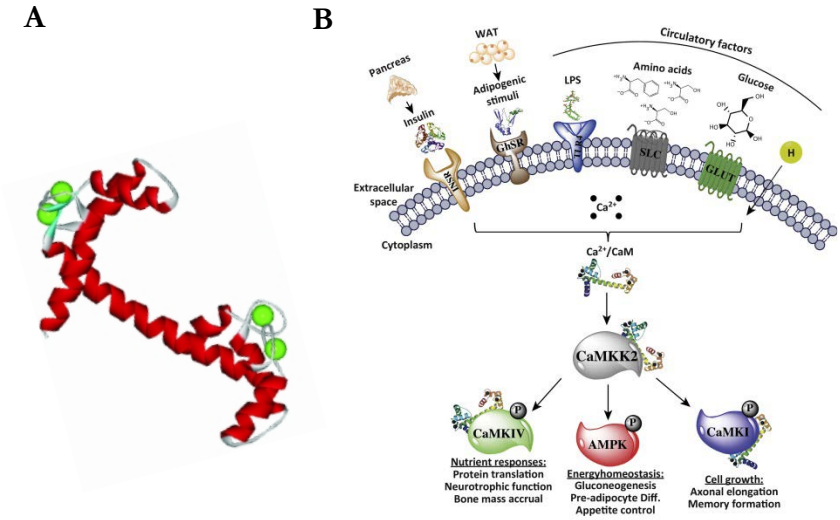

Figura 28. Calmodulina. A) Representación de la estructura de la CaM unida a cuatro iones de calcio (esferas verdes). Extraído de *McCue, et al., 2010*. **B)** Esquema de la cascada de señalización mediada por la CaM. Extraído de *Marcelo, et al., 2016*.

La CaM se expresa en todas las células eucariotas, aunque principalmente se localiza en cerebro y corazón, y en distintas estructuras subcelulares, desde la membrana plasmática hasta diferentes orgánulos como el retículo endoplasmático o la mitocondria. Este sensor se ha visto involucrado en distintos procesos relacionados con el metabolismo (*Marcelo, et al., 2016*), la apoptosis (*Ozcan y Tabas, 2010*), la inflamación (*Racioppi y Means, 2008; Ainscough, et al., 2015*), la contracción muscular (*Shen, et al., 2016*), la modulación del latido del corazón (*Sorensen, et al., 2013*), la memoria a largo plazo (*Limbäck-Stokin, et al., 2014*), el desarrollo del sistema nervioso (*Ghosh y Greenberg, 1995*), la respuesta inmune (*Racioppi y Means, 2008*), la proliferación celular y la autofagia (*Berchtold y Villalobo, 2014*), entre otros. Además, también ha sido relacionada la CaM con los procesos cancerosos debido al incremento de los niveles de esta proteína en las células tumorales (*Berchtold y Villalobo, 2014*).

En los últimos años ha sido descrito que este sensor de calcio es capaz de interaccionar con distintos receptores acoplados a proteína G, entre ellos el receptor metabotrópico 7 de glutamato (*El Far, et al., 2001*). Este receptor contiene un lugar de unión a la calmodulina en

su cola C-terminal del receptor, que coincide con el lugar de unión de la subunidad Gβγ de la proteína G (*El Far, et al., 2001*). Más adelante, Wang y colaboradores describieron la interacción de esta proteína con el tercer bucle intracelular del receptor μ-opioide (*Wang, et al., 1999*). En este estudio se concluyó que la calmodulina reducía la interacción del receptor μ-opioide con la proteína G, probablemente mediante un mecanismo de competencia (*Zhang, et al., 2005*). Más adelante, Turner y colaboradores demostraron mediante estudios de coinmunoprecipitación y la técnica de BRET en células vivas, la interacción de la CaM con el receptor de serotonina 5-HT_{1A} (*Turner, et al., 2004*). También fue descrita la interacción de la calmodulina con la región N-terminal del tercer bucle intracelular del receptor D_2 de dopamina en una zona comprometida en la interacción entre el receptor y la proteína G (*Bofill-Cardona, et al., 2000*). Posteriormente se demostró que la activación del receptor D_2 por agonistas específicos incrementaba la colocalización del receptor con la calmodulina endógena en células HEK-293T y en cultivos primarios neuronales (*Liu, et al. 2007*). Finalmente, no fue hasta el 2008 que se encontró *in vitro* un epítopo del extremo C-terminal del receptor A_{2A} de adenosina capaz de interaccionar con la CaM (*Woods, et al., 2008*). En este estudio se demostró que el epítopo de interacción del receptor D_2 de dopamina con la calmodulina no se veía modificado cuando el receptor de dopamina heteromerizaba con el receptor de adenosina A_{2A}, sugiriendo la posibilidad de que la CaM pudiese jugar un papel de *linker* para establecer la interacción entre estos dos receptores. Estudios posteriores confirmaron que la calmodulina puede oligomerizar con el heterómero de receptores A_{2A}-D_2 y modular su función de manera calcio-dependiente (*Navarro, et al., 2009; Ferré, et al., 2010*). Tal y como ha sido comentado anteriormente, el heterómero A_{2A}-D_2 juega un papel importante en la modulación de la actividad de las neuronas GABAérgicas, y es por ello que puede ser considerado una diana para el desarrollo de fármacos para desordenes neuropsiquiátricos como la enfermedad de Parkinson o adicción a drogas de abuso.

1.5.3. Neuronal calcium sensor (NCS)

Los miembros iniciales de esta superfamilia, la S-modulina, la visinina, la recoverina, la frecuentina/NCS-1, la proteína *visinin-like*-1 (VLP1) y la hipocalcina, fueron agrupados bajo la nomenclatura de sensores de calcio neuronales (NCS) en base a su capacidad por unir calcio y a la semejanza en su estructura. Esta nomenclatura fue utilizada por primera vez por De Castro y colaboradores el año 1995 (*De Castro, et al., 1995*). Posterioriormente, esta familia se ha ido expandiendo a partir de su ancestro común, la frecuentina (*McCue, et al. 2010*). Estas proteínas conservan únicamente un 20% de identidad con la calmodulina (*Burgoyne, 2007*), y sin embargo mantienen los cuatro dominios *EF-hand,* aunque la unión de calcio se produce únicamente a través de dos o tres de estos dominios (*Mikhaylova, et al., 2011*) (**Figura 29**).

Los sensores neuronales de calcio (NCS) regulan muchos procesos celulares tales como la neurotransmisión (*Pongs, et al., 1993*), la exocitosis (*McFerran, et al., 1998; Haynes, et al., 2005*), el aprendizaje (*Gomez, et al., 2001*), la plasticidad sináptica (*Sippy, et al., 2003*), la regulación de canales iónicos (*Weiss, et al., 2000*), la endocitosis de receptores (*Kabbani, et al., 2002*), el crecimiento (Hui, et al., 2006) y la supervivencia neuronal (*Nakamura, et al., 2006*). La gran variedad de funciones en las que estas proteínas se encuentran implicadas las ha relacionado con diferentes trastornos y enfermedades neurológicas como la epilepsia, la esquizofrenia, el Alzheimer o incluso el cáncer (*Braunewell, 2005*). Ha sido detectado un aumento en los niveles de la proteína NCS-1 en tejido cerebral de pacientes con esquizofrenia o con trastornos de bipolaridad (*Koh, et al., 2003*), lo que resultaría en un incremento en la excitabilidad neuronal,

un incremento de la concentración de calcio intracelular y consecuentemente, provocaría la muerte celular.

La proteína NCS-1 fue descubierta originalmente como frecuentina en *Drosophila melanogaster* (*Pongs, et al., 1993*) y fue nombrada NCS-1 unos años más tarde al considerarse que su expresión se encontraba restringida a células neuronales (*Nef, et al., 1995*). Estudios posteriores demostraron que NCS-1 puede encontrarse también en otros tipos celulares, aunque sus niveles de expresión son menores (*McFerran, et al., 1998; Kapp-Barnea, et al., 2003; Blasiole, et al., 2005*). Esta proteína se encuentra altamente conservada, con un 100% de identidad entre mamíferos y un 60% de identidad entre hongos y humanos (*Bourne, et al., 2001*). La afinidad de esta proteína por el calcio es de 440 nanoMolar, siendo superior a la de la CaM (*Mikhaylova, et al., 2009*). La unión de calcio se produce a través de tres de sus cuatro dominios *EF-hand* (**Figura 29**). Una vez unidas las moléculas de calcio, la proteína NCS-1 puede modificar dramáticamente la función de algunos GPCR (*Mikhaylova, et al., 2009*). Como ha sido mencionado anteriormente, ha sido descrita su capacidad para interaccionar y modificar la función de los receptores A_{2A} de adenosina (*Navarro, et al., 2012*) y D_2 de dopamina (*Pandalaneni, et al., 2015*).

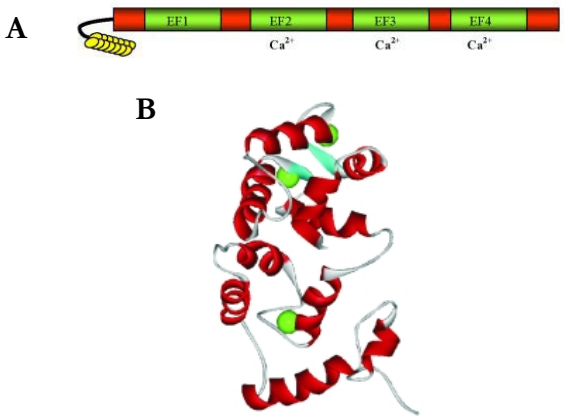

Figura 29. Estructura cristalina del sensor de calcio NCS-1. A) Representación esquemática de la proteína NCS-1, con los diferentes dominios EF-hand implicados con la unión de calcio. **B)** Estructura cristalina del sensor NCS-1 con moléculas de calcio unidas (esferas verdes). Adaptado de *McCue, et al., 2010*.

1.5.4. Neuronal calcium-binding proteins (nCaBP)

Todos los miembros de esta superfamilia tienen una estructura bipartida, por un lado presentan un extremo N-terminal no relacionado con otras proteínas conocidas y variable en cuanto a tamaño y estructura dentro de la misma familia y, por otro lado, un extremo C-terminal con cuatro dominios *EF-hand* que recuerda a los de la calmodulina, aunque la unión de calcio solo se produce a través de dos o tres de sus cuatro dominios *EF-hand* (*Mikhaylova, et al., 2009*). Respecto al extremo C-terminal, la caldendrina es el homólogo más cercano a la calmodulina expresado en cerebro, lo que lo convirtió en el miembro fundador de toda una familia génica nombrada CaBPs por Haeseleer y colaboradores (Seidenbecher, et al., 1998; *Haeseleer, et al., 2002*). Además, la variabilidad existente en el extremo N-terminal de estas proteínas es determinante para su localización subcelular y consecuentemente, su función (*Mikhaylova, et al., 2011*).

Principalmente, las nCaPB se encuentran restringidas a ciertas zonas del cerebro (*Bernstein, et al., 2003*), retina y oído (*Cui, et al., 2007*), solapándose con las zonas de expresión de NCS-1

(*Mikhaylova, et al., 2009*). La afinidad por el calcio no es homogénea en esta familia de sensores, siendo ligeramente inferior en el caso de la caldendrina, de 2,5 microMolar (*Mikhaylova, et al., 2006*), y superior en el caso de otras proteínas de esta superfamilia como la calneurona-1 y calneurona-2, de 200 nanoMolar (*Mikhaylova, et al., 2009*).

La CaM y los sensores nCaBP pueden interaccionar con proteínas diana similares, pero sus diferencias conllevan formas de regulación distintas. Por ejemplo, tanto la calmodulina como las nCaBP pueden unirse a canales de calcio dependientes de voltaje Ca_v1, en los que la unión de la calmodulina promueve una inactivación dependiente de calcio mientras que las nCaBP prolongan la apertura del canal (*Cui, et al., 2007*). Ha sido postulado que estos receptores se encuentran implicados en la regulación de los niveles intracelulares de calcio a través del control de los canales de calcio (*Zhou, et al., 2004*), la distribución subcelular de diferentes proteínas o la organización del citoesqueleto. No obstante, la funcionalidad de muchos de los miembros de esta superfamilia aún está por determinar.

Otras proteínas importantes de esta superfamilia son las calneuronas, calneurona-1 (caln-1) y calneurona-2 (caln-2), también conocidas como CaBP-7 y CaBP-8 respectivamente. Estas dos proteínas son muy parecidas entre ellas, con una secuencia de 219 y 215 aminoácidos respectivamente, conservando un 63% de identidad (*Mikhaylova, et al., 2006*). Recientemente han sido descritas dos isoformas de la caln-1 que presentan un domino N-terminal más largo. Estas son formadas por *splicing* alternativo dando lugar a dos proteínas de 261 y 293 aminoácidos. No obstante, la función de la extensión del dominio N-terminal aún está por determinar (*Hdrasky, et al., 2015*). De manera interesante, los bancos de datos muestran que la secuencia aminoacídica de las proteínas calneurona-1 y calneurona-2 son 100% idénticas entre humanos, rata y ratón. Este alto nivel de conservación indica que incluso la mitad C-terminal de las calneuronas tiene un significado funcional relacionado con su estructura (*Mikhyalova, et al., 2006*) (**Figura 30**). A pesar de que diferentes estudios han demostrado que la caldrendrina y las calneuronas están muy relacionada, algunos autores defienden, basándose en estudios filogenéticos, que las calneuronas constituyen una nueva subfamilia de sensores de calcio relacionados con la calmodulina y que la aparición de las proteínas relacionadas con la caldendrina y las relacionadas con la calneurona aparecieron a la vez durante la evolución de los vertebrados (*McCue, et al., 2010*). Las calneuronas se encuentran ampliamente distribuidas por el cerebro, coexistiendo con la caldendrina, con una prominente expresión a nivel neuronal pero no en células gliales, presentando una distribución muy similar en cerebro de rata y humano (*Hdrasky, et al., 2015*). A nivel subcelular, tanto la caln-1 como la caln-2 se detectan en fracciones de membrana y fracciones proteicas solubles esto sugiere que, a diferencia de la caldendrina, podrían interaccionar con proteínas citoplasmáticas.

Ambas calneuronas contienen únicamente dos dominios *EF-hand* funcionales y pueden unir calcio con una gran afinidad (*Mikhyalova, et al., 2006*), a diferencia de otras proteínas de la familia nCaBP, como la caldendrina, que al tener ciertos residuos aminoacídicos distintos en los dominios *EF-hand*, provocan la unión constitutiva del ion Mg^{2+} en lugar del ion de Ca^{2+} (*Wingard, et al., 2005*). La organización de los dominios *EF-hand* funcionales de las calneuronas es una característica exclusiva de estas proteínas que no coincide con lo observado en otros sensores de calcio (*Burgoyne, et al. 2004*). La presencia de los dominios *EF-hand* no funcionales, característica de las proteínas NCS y CaBP, se considera que puede ser debida a una mejora sustancial en la dinámica y la especificidad en la interacción con sus proteínas diana. Es por ello que se puede concluir que la estructura de los dominios *EF-hand* no funcionales del extremo C-terminal resulta indispensable para su función celular (*Mikhyalova, et al., 2006*). A estos dos sensores se les ha atribuido un papel regulador en la

síntesis de fosfolípidos y del tráfico de proteínas desde el complejo de Golgi hasta la membrana plasmática (*Mikhaylova, et al., 2009; Hradsky, et al., 2015*). No obstante, aún quedan funciones pendientes por determinar.

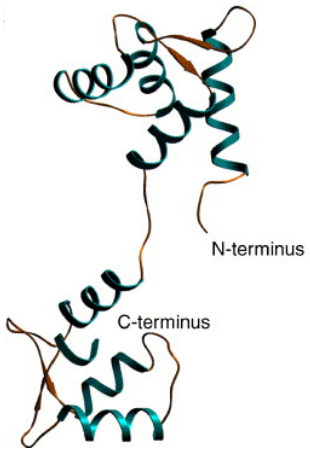

Figura 30. Predicción de la estructura de la proteína calneurona-1. Extraído de *Mikhyalova, et al., 2006*.

Entender las relaciones que se establecen entre estas proteínas, tanto GPCR, moduladores y sensores, en condiciones fisiológicas y en modelos de adición a cocaína, será crucial para elucidar los mecanismos moleculares mediante los cuales esta droga induce sus efectos tanto a corto como a largo plazo. Además, entender la sucesión de eventos que conducen de una toma inicial de la sustancia de abuso hasta una adicción ayudará al desarrollo de terapias efectivas que nos permitan luchar contra uno de los mayores problemas médicos y sociales de la actualidad.

OBJETIVOS

Actualmente es aceptada, por prácticamente la totalidad de la comunidad científica, la capacidad de los GPCR para interaccionar con otros GPCR formando homo- o heterooligómeros, así como con otras proteínas moduladoras o sensoras, confiriéndole al complejo nuevas propiedades farmacológicas diferentes a las de los receptores implicados cuando actúan por separado. Esto sugiere la necesidad de revisar y modificar toda la farmacología actual, basada fundamentalmente en el estudio de receptores monoméricos.

La importancia del estudio de los heterómeros es mayúscula a la hora de describir los mecanismos moleculares implicados en enfermedades asociadas a los GPCR, abriendo una nueva puerta al diseño de nuevas, y más eficaces, terapias. En la actualidad, la adicción a cocaína supone un grave problema médico y social que requiere de un esfuerzo por parte de la comunidad científica para llegar a elucidar las bases moleculares que se esconden tras esta devastadora enfermedad. En el grupo de investigación donde ha sido desarrollada esta Tesis, el estudio de la adicción a cocaína ha sido siempre una prioridad, llegando a romper el paradigma clásico de acción de la cocaína al demostrar que esta droga no solo provoca sus efectos al bloquear el transportador pre-sináptico DAT, sino que también produce parte de sus efectos al unirse al receptor sigma-1, el cual interacciona con el receptor D_1 de dopamina modulando su señalización. Con este precedente, el primer y segundo objetivos de esta Tesis han sido:

Objetivo 1. Investigar la formación de heterómeros entre los receptores D_1 y D_2 de dopamina y los moduladores sigma-1R y sigma-2R como un nuevo mecanismo de acción de la cocaína.

En multitud de trabajos ha sido descrita la estrecha relación entre la exposición a situaciones de estrés y la recaída en la búsqueda y el consumo de cocaína. Con el fin de investigar la relación existente entre los mecanismos de estrés y los mecanismos de adicción a cocaína ha sido propuesto el segundo objetivo de la Tesis:

Objetivo 2. Estudiar el efecto de la adicción a cocaína sobre el sistema de estrés, identificando cambios en la farmacología y expresión de los receptores CRF y Orexina-1.

Uno de los efectos observados posteriores al consumo de cocaína es la desaparición de la sensación de apetito. Sin embargo, a pesar de tratarse de un conocimiento ancestral transmitido de generación en generación, nunca ha sido estudiado el mecanismo molecular que relaciona la cocaína con la disminución del apetito. Una de las hormonas más importantes en la regulación del apetito es la grelina, conocida popularmente como la hormona del hambre. Esta hormona actúa mediante la unión al receptor GHS-R1a. No obstante, existe una segunda isoforma truncada del receptor de grelina incapaz de unir la hormona y de señalizar, el GHS-R1b. Esta isoforma truncada ha sido considerada un vestigio de la evolución durante muchos años, pero recientemente ha sido relacionada con un posible papel regulador sobre GHS-R1a. Es necesario entender el funcionamiento y regulación del sistema de la grelina para poder estudiar como la adicción a cocaína puede influir sobre la sensación de apetito. En este contexto, se han propuesto el tercer y cuarto objetivos de esta Tesis:

Objetivo 3: Describir el posible rol funcional y estructural de la isoforma GHS-R1b del receptor de grelina.

Objetivo 4: Investigar el efecto de la cocaína sobre el receptor GHS-R1a en células transfectadas y cultivos primarios de neuronas e identificar cambios en la expresión del receptor GHS-R1a en diferentes estadios de adicción a cocaína.

En la actualidad, la modulación de los GPCR mediante otras proteínas y sensores está adquiriendo una mayor relevancia. Uno de los segundos mensajeros más importantes a nivel celular es el Ca^{2+}. Ha sido descrita la modulación por Ca^{2+} del heterómero formado por los receptores A_{2A} de adenosina y D_2 de dopamina mediante la interacción con la proteína sensora de calcio calmodulina. Aunque la calmodulina es el sensor de calcio más estudiado, la célula posee otras proteínas sensoras de calcio que sufren un fuerte cambio conformacional en respuesta a incrementos citoplasmáticos de los niveles del ion. Estas proteínas confieren la posibilidad de una modulación mucho más fina de los GPCR ampliando la versatilidad de estos receptores. Dentro de este marco, el quinto objetivo de esta Tesis ha sido:

Objetivo 5: Determinar si las proteínas sensoras de calcio NCS-1, calneuron-1 y caldendrina interaccionan con el heterómero de receptores A_{2A} de adenosina – D_2 de dopamina e investigar el papel del Ca^{2+} en esta interacción.

El cambio conceptual de una farmacología clásica de homómeros de receptores a una nueva construida con heterómeros como entidades funcionales con características distintas a las de los receptores individuales nos conduce a la búsqueda de las bases estructurales y la arquitectura de estos nuevos complejos diméricos o de orden superior. La aparición de nuevas tecnologías ha permitido la descripción de la estructura cristalina de diferentes GPCR, así como de la interacción de los GPCR con la proteína G. El diseño de péptidos específicos contra las regiones transmembrana de los GPCR ha permitido conocer las interfases de interacción entre distintos GPCR, abriendo nuevas avenidas para el diseño de nuevas terapias más eficaces para el tratamiento de diversas patologías donde los heterómeros puedan verse involucrados. Con el fin de investigar la estructura cuaternaria de los heterómeros de receptores y las relaciones existentes entre los elementos que forman estos complejos ha sido tomado como modelo el heterómero A_1 de adenosina – A_{2A} de adenosina ya que constituye un paradigma en el campo de los heterómeros. En este contexto, el sexto y último objetivo de esta Tesis ha sido:

Objetivo 6. Investigar la estructura cuaternaria del heterómero de receptores A_1 y A_{2A} de adenosina, así como determinar la relación que se establece entre estos receptores y la proteína G heterotrimérica.

RESULTADOS

Gemma Navarro Brugal y Enric Isidre Canela Campos
Grupo de Neurobiología Molecular
Departamento de Bioquímica y Biomedicina Molecular
Av. Diagonal, 645
Edificio Prevosti, Planta -2
08028 Barcelona

La tesis doctoral de David Aguinaga Andrés "Interacción molecular y funcional entre receptores involucrados en la ingesta de alimentos y el consumo de drogas de abuso" se presenta como un compendio de publicaciones.

El manuscrito "**Cocaine inhibits dopamine D_2 receptor signaling via sigma-1-D_2 receptor heteromers**" ha sido publicado en *PLoS One* con un factor de impacto de 3.53. El manuscrito "**Sigma-2 receptors mediate cocaine effects on dopamine D_1 receptor signaling**" está en vías de preparación para ser enviado a *Molecular Psychiatry* con un factor de impacto de 13.31. El manuscrito "**Orexin - Corticotropin-releasing factor receptor heteromers in the ventral tegmental area as targets for cocaine**" ha sido publicado en *The Journal of Neuroscience* con un factor de impacto de 5.92. El manuscrito "**A significant role of the truncated ghrelin receptor GHS-R1b in ghrelin-induced signaling in neurons**" ha sido publicado en *The Journal of Biological Chemistry* con un factor de impacto de 4.26. El manuscrito "**Cocaine blocks ghrelin effects via interaction with sigma-1 receptors**" ha sido enviado a *Neuropsychopharmacology* con un factor de impacto de 6.39. El manuscrito "**Intracellular calcium levels determine differential modulation of allosteric interactions within G protein-coupled receptor heteromers**" ha sido publicado en *Chemistry & Biology* con un factor de impacto de 6.64. El manuscrito "**Quaternary structure of a G-protein-coupled receptor heterotetramer in complex with G_i and G_s**" ha sido publicado en *BioMed Central Biology* con un factor de impacto de 6.96. Finalmente, el manuscrito "**Cross-comunication between G_i and G_s in a G-protein-coupled receptor heterotetramer guided by a receptor C-terminal domain**" ha sido enviado a *Nature communications* con un factor de impacto de 11.32.

En el trabajo "**Cocaine inhibits dopamine D_2 receptor signaling via sigma-1-D_2 receptor heteromers**", el doctorando David Aguinaga Andrés ha llevado a cabo los experimentos correspondientes a la técnica de BRET. En el trabajo "**Sigma-2 receptors mediate cocaine effects on dopamine D_1 receptor signaling**" exceptuando la generación de animales adictos a cocaína y la posterior obtención de cortes cerebrales, el doctorando David Aguinaga Andrés ha realizado la totalidad del trabajo experimental. En el trabajo "**Orexin - Corticotropin-releasing factor receptor heteromers in the ventral tegmental area as targets for cocaine**" el doctorando David Aguinaga Andrés ha efectuado los experimentos correspondientes a la técnica de BRET. Así mismo, ha llevado a cabo la determinación de la señalización de la vía ERK1/2 y AKT mediante el uso de la técnica de Western blot. En el trabajo "**A significant role of the truncated ghrelin receptor GHS-R1b in ghrelin-induced signaling in neurons**" el doctorando David Aguinaga Andrés ha realizado los cultivos primarios de neuronas y ha efectuado la totalidad del trabajo experimental realizado en dichos cultivos primarios. En el trabajo "**Cocaine blocks ghrelin effects via interaction with sigma-1 receptors**", exceptuando la generación de animales adictos a cocaína y la posterior obtención de cortes cerebrales y el modelaje estructural, el doctorando David Aguinaga Andrés ha llevado a cabo la totalidad del trabajo experimental. En el trabajo "**Intracellular calcium levels determine differential modulation of allosteric interactions within G protein-coupled receptor heteromers**" el doctorando David Aguinaga Andrés ha realizado los cultivos primarios de neuronas. Además, ha efectuado todos los

experimentos correspondientes a la técnica de PLA. En el trabajo "**Quaternary structure of a G-protein-coupled receptor heterotetramer in complex with G_i and G_s**" el doctorando David Aguinaga Andrés ha llevado a cabo los experimentos correspondientes a la técnica de BRET. En el trabajo "**Cross-comunication between G_i and G_s in a G-protein-coupled receptor heterotetramer guided by a receptor C-terminal domain**" el doctorando David Aguinaga Andrés ha llevado a cabo los experimentos correspondientes a la técnica de BRET.

Barcelona, a 3 de abril de 2017

Dra. Gemma Navarro Brugal

Dr. Enric Isidre Canela Campos

Los resultados de la presente tesis están reflejados en los siguientes manuscritos:

- 3.1. Gemma Navarro, Estefanía Moreno, Jordi Bonaventura, Marc Brugarolas, Daniel Farré, **David Aguinaga**, Josefa Mallol, Antoni Cortés, Vicent Casadó, Carme Lluís, Sergi Ferré, Rafael Franco, Enric I. Canela y Peter J. McCormick. **Cocaine inhibits dopamine D_2 receptor signaling via sigma-1-D_2 receptor heteromers.**

  Manuscrito publicado en *PLoS One.*

- 3.2. **David Aguinaga**, Mireia Medrano, Ignacio Vega-Quiroga, Katia Gysling, Enric I. Canela, Gemma Navarro* y Rafael Franco*. **Sigma-2 receptors mediate cocaine effects on dopamine D_1 receptor signaling.**

  Manuscrito en preparación para ser enviado a *Molecular Psychiatry*.

- 3.3. Gemma Navarro*, César Quiroz*, David Moreno-Delgado*, Adam Sierakowiak, Kimberly McDowell, Estefanía Moreno, William Rea, Ning-Sheng Cai, **David Aguinaga**, Lesley A. Howell, Felix Hausch, Antonio Cortés, Josefa Mallol, Vicent Casadó, Carme Lluís, Enric I. Canela, Sergi Ferré y Peter McCormick. **Orexin - Corticotropin-releasing factor receptor heteromers in the ventral tegmental area as targets for cocaine.**

  Manuscrito publicado en *The Journal of Neuroscience.*

- 3.4. Gemma Navarro*, **David Aguinaga***, Edgar Angelats, Mireia Medrano, Estefanía Moreno, Josefa Mallol, Antonio Cortés, Enric I. Canela, Vicent Casadó, Peter J. McCormick, Carme Lluís y Sergi Ferré. **A significant role of the truncated ghrelin receptor GHS-R1b in ghrelin-induced signaling in neurons**.

  Manuscrito publicado en *The Journal of Biological Chemistry.*

- 3.5. **David Aguinaga**, Mireia Medrano, Edgar Angelats, Ignacio Vega-Quiroga, Katia Gysling, Enric I. Canela, Rafael Franco* y Gemma Navarro*. **Cocaine blocks ghrelin effects via interaction with sigma-1 receptors.**

  Manuscrito enviado a *Neuropsychopharmacology*.

- 3.6. Gemma Navarro, **David Aguinaga**, Estefanía Moreno, Johannes Hradsky, Pasham P. Reddy, Antoni Cortés, Josefa Mallol, Vicent Casadó, Marina Mikhaylova, Michel R. Kreutz, Carme Lluís, Enric I. Canela, Peter J. McCormick y Sergi Ferré. **Intracellular calcium levels determine differential modulation of allosteric interactions within G protein-coupled receptor heteromers.**

  Manuscrito publicado en *Chemistry & Biology.*

- 3.7. Gemma Navarro[*], Arnau Cordomí[*], Monika Zelman-Femiak[*], Marc Brugarolas, Estefanía Moreno, **David Aguinaga**, Laura Perez-Benito, Antoni Cortés, Vicent Casadó, Josefa Mallol, Enric I. Canela, Carme Lluís, Leonardo Pardo, Ana J. García-Sáez, Peter J. McCormick y Rafael Franco. **Quaternary structure of a G-protein-coupled receptor heterotetramer in complex with G_i and G_s**.

  Manuscrito publicado en *BioMed Central Biology*.

- 3.8. Gemma Navarro[*], Arnau Cordomí[*], Marc Brugarolas, Estefanía Moreno, **David Aguinaga**, Laura Perez-Benito, Sergi Ferré, Antoni Cortés, Vicent Casadó, Josefa Mallol, Enric I. Canela, Carme Lluís, Leonardo Pardo, Peter J. McCormick y Rafael Franco. **Cross-comunication between G_i and G_s in a G-protein-coupled receptor heterotetramer guided by a receptor C-terminal domain.**

  Manuscrito enviado a *Nature communications*.

*Estos autores han contribuido del mismo modo al correspondiente trabajo.

3.1. COCAINE INHIBITS DOPAMINE D_2 RECEPTOR SIGNALING VIA SIGMA-1-D_2 RECEPTOR HETEROMERS

Gemma Navarro, Estefanía Moreno, Jordi Bonaventura, Marc Brugarolas, Daniel Farré, **David Aguinaga**, Josefa Mallol, Antoni Cortés, Vicent Casadó, Carme Lluís, Sergi Ferré, Rafael Franco, Enric I. Canela y Peter J. McCormick.

Manuscrito publicado en *PLOS ONE*, abril 2013; 8(4).

En condiciones normales el cerebro mantiene un delicado equilibrio entre los *inputs* de recompensa controlado por las neuronas que contienen los receptores de la familia *D_1-like* de dopamina y los *inputs* aversivos procedentes de las neuronas que contienen los receptores *D_2-like* de dopamina. La cocaína es capaz de subvertir la entrada equilibrada de estos inputs mediante la alteración de la señalización celular de estas dos vías de tal manera que la vía de la recompensa donde se encuentra el receptor D_1 de dopamina, domina. En este trabajo se ofrece una explicación a nivel celular y bioquímico de cómo la cocaína puede lograr tal hecho. Explorando el efecto de la cocaína sobre la función de los receptores D_2 de dopamina, se presentan evidencias de la interacción molecular y funcional del receptor σ_1R con los receptores D_2 de dopamina. Mediante el uso de técnicas biofísicas, bioquímicas y de biología molecular, ha sido descubierto que los receptores D_2 (la isoforma larga del receptor D_2) puede formar complejos con los receptores σ_1R, un resultado específico de los receptores D_2, ya que los receptores D_3R y D_4R no forman heterómeros. Ha sido demostrado que los heterómeros del receptor σ_1R-D_2 consisten en oligómeros de orden superior, se encuentran en el estriado de ratón y que la cocaína, al unirse a los heterómeros del receptor σ_1R-D_2, inhibe la señalización *downstream* tanto en cultivos celulares como en neuronas estriatales de ratón. Por el contrario, en el cuerpo estriado de los animales *knockout* de σ_1R estos complejos no se encuentran y esta inhibición no se observa. En conjunto, estos datos muestran el mecanismo mediante el cual la exposición inicial a cocaína puede inhibir la señalización a través de las neuronas que contienen el receptor D_2, desestabilizando el delicado equilibrio de señalización que influye en la búsqueda de drogas que deriva de las neuronas que contienen el receptor D_1 y D_2 en el cerebro.

OPEN ACCESS Freely available online

PLOS ONE

Cocaine Inhibits Dopamine D_2 Receptor Signaling via Sigma-1-D_2 Receptor Heteromers

Gemma Navarro[1], Estefania Moreno[1], Jordi Bonaventura[1], Marc Brugarolas[1], Daniel Farré[1], David Aguinaga[1], Josefa Mallol[1], Antoni Cortés[1], Vicent Casadó[1], Carmen Lluís[1], Sergi Ferre[2], Rafael Franco[3☯], Enric Canela[1☯], Peter J. McCormick[1*☯]

1 Centro de Investigación Biomédica en Red de Enfermedades Neurodegenerativas (CIBERNED) and Institute of Biomedicine of the University of Barcelona (IBUB) and Department of Biochemistry and Molecular Biology, Faculty of Biology, University of Barcelona, Barcelona, Spain, **2** National Institute on Drug Abuse, Intramural Research Program, National Institutes of Health, Department of Health and Human Services, Baltimore, Maryland, United States of America, **3** Centro de Investigación Médica Aplicada, Universidad de Navarra, Pamplona, Spain

Abstract

Under normal conditions the brain maintains a delicate balance between inputs of reward seeking controlled by neurons containing the D_1-like family of dopamine receptors and inputs of aversion coming from neurons containing the D_2-like family of dopamine receptors. Cocaine is able to subvert these balanced inputs by altering the cell signaling of these two pathways such that D_1 reward seeking pathway dominates. Here, we provide an explanation at the cellular and biochemical level how cocaine may achieve this. Exploring the effect of cocaine on dopamine D_2 receptors function, we present evidence of σ_1 receptor molecular and functional interaction with dopamine D_2 receptors. Using biophysical, biochemical, and cell biology approaches, we discovered that D_2 receptors (the long isoform of the D_2 receptor) can complex with σ_1 receptors, a result that is specific to D_2 receptors, as D_3 and D_4 receptors did not form heteromers. We demonstrate that the σ_1-D_2 receptor heteromers consist of higher order oligomers, are found in mouse striatum and that cocaine, by binding to σ_1 -D_2 receptor heteromers, inhibits downstream signaling in both cultured cells and in mouse striatum. In contrast, in striatum from σ_1 knockout animals these complexes are not found and this inhibition is not seen. Taken together, these data illuminate the mechanism by which the initial exposure to cocaine can inhibit signaling via D_2 receptor containing neurons, destabilizing the delicate signaling balance influencing drug seeking that emanates from the D_1 and D_2 receptor containing neurons in the brain.

Citation: Navarro G, Moreno E, Bonaventura J, Brugarolas M, Farré D, et al. (2013) Cocaine Inhibits Dopamine D_2 Receptor Signaling via Sigma-1-D_2 Receptor Heteromers. PLoS ONE 8(4): e61245. doi:10.1371/journal.pone.0061245

Editor: Stefan Strack, University of Iowa, United States of America

Received November 5, 2012; **Accepted** March 8, 2013; **Published** April 18, 2013

Funding: This study was supported by grants from the Spanish Ministerio de Ciencia y Tecnología (SAF2009-07276, SAF2010-18472, SAF2011-23813), and by Intramural Funds of the National Institute on Drug Abuse to SF. PJM is a Ramón y Cajal Fellow. The funders had no role in study design, data collection and analysis, decision to publish, or preparation of the manuscript.

Competing Interests: The authors have declared that no competing interests exist.

* E-mail: pmccormick@ub.edu

☯ These authors contributed equally to this work.

Introduction

The striatum is the main input structure of the basal ganglia and consists of subcortical structures involved in the processing of information related with the performance and learning of complex motor acts and motivational processes and is altered in conditions such as Parkinson's, Huntington's and in drug addiction [1]. GABAergic striatal efferent neurons constitute more than 95% of the striatal neuronal population [2]. There are two major subtypes of GABAergic striatal efferent neurons: GABAergic dynorphinergic neurons, which express the peptide dynorphin and dopamine D_1 receptors and GABAergic enkephalinergic neurons, which express the peptide enkephalin and dopamine D_2 receptors [3]. In the case of drug addiction, and specifically cocaine, the dopaminergic pathway plays a critical role in the pathology [4,5], specifically, the two populations of D_1 and D_2 containing neurons. These two pathways can control novelty seeking and reward-dependent learning as well as having opposite effects on motor activity [6]. Early studies performed in D_1 receptor knockout mice showed the importance of dopamine D_1 receptor in cocaine action as the activation of D_1 receptors was an absolute requirement for the induction of the cellular and behavioral responses to cocaine [7]. In addition to opposing the locomotor effects of D_1, D_2 containing neurons also serve to oppose drug reinforcement [8]. In the context of cocaine it is known that the D_2 is essential for cocaine's effects [9] as D_2 receptors are required to enhance the rewarding properties of cocaine [10]. In D_2 $-/-$ mutant animals the release of dopamine evoked by cocaine injection is dramatically higher compared to WT animals, and an intact D_2-mediated signaling is required to elicit the rewarding and reinforcing effects of cocaine [11]. At the mechanistic level it was shown there is a switch from D_2 to a D_1 mediated increase on $GABA_A$-IPSC in cocaine treated rats [12], and in models of long-term cocaine treatment it has been shown that D_1 increases and D_2 levels decrease [13]. Finally, it has been shown that the activation of postsynaptic D_2 on striatopallidal neurons can facilitate drug reinforcement via inhibition of these neurons [8]. All of these studies point to a balance between D_1 and D_2 in

controlling the motivational processes and reinforcement in drugs of abuse, and specifically cocaine.

The initial mechanistic steps of cocaine binding and its effects on these two striatal populations of neurons (D_1 and D_2 receptor containing neurons) are not well understood. What is known is cocaine is able to exert part of its behavioral and cellular effect by elevating dopamine levels in the striatum [14]. It achieves this by binding to and inhibiting the presynaptic dopamine transporter (DAT) [15]. Cocaine is a high-affinity inhibitor of DAT and upon binding to DAT cocaine causes a rapid increase in extracellular dopamine levels. Although DAT inhibition is required for cocaine's effects, it is not the only required mechanism of action per the effects of D_1 and D_2 receptors discussed above. In fact, Cocaine is able to modulate dopamine signaling, via both the D_1 and D_2 family of dopamine receptors, which when activated can lead to stimulation or inhibition of signaling pathways. This provokes the question, how does cocaine seemingly influence two different receptor pathways? One potential answer lies in the fact that cocaine does not seem to bind the dopamine receptors directly but can bind to a receptor heteromer made up of the D_1-like receptor family member, D_1 and the σ_1-receptor [16]. Through this latter interaction, cocaine can potentiate D_1 receptor-mediated adenylyl cyclase activation, induce ERK1/2 phosphorylation and counteract the MAPK activation induced by D_1 receptor stimulation [16]. However, as discussed above, D_2 also plays a role in the early effects of cocaine. Here we explore the initial molecular events after cocaine exposure on the dopamine receptor D_2 like family and test the hypothesis that σ_1 receptor may provide the link between cocaine and the D_1 and D_2 receptor signaling balance.

Materials and Methods

Ethics Statement

The study received the approval of the Catalan Ethical Committee for Animal Use (CEAA/DMAH 4049 and 5664) and all procedures were performed to minimize animal suffering.

Fusion Proteins and Expression Vectors

Sequences encoding amino acids residues 1–155 and 155–238 of YFP Venus protein, and amino acids residues 1–229 and 230–311 of RLuc8 protein were subcloned in pcDNA3.1 vector to obtain the YFP Venus (nVenus, cVenus) and RLuc8 (nRLuc8, cRLuc8) hemi-truncated proteins expressed in pcDNA3.1 vector. The human cDNA for the long isoform of dopamine D_2 receptors (D_2 receptors), adenosine A_{2A} or σ_1 receptors cloned in pcDNA3.1 were amplified without their stop codons using sense and antisense primers harboring either unique *EcoRI* and *BamHI* sites (or *EcoRI* and *KpnI* sites for σ_1 receptor). The fragments were then subcloned to be in-frame with Rluc, EYFP or GFP^2 into the *EcoRI* and *BamHI* or *KpnI* restriction site of an Rluc-expressing vector (pRluc-N1, PerkinElmer, Wellesley, MA), an EYFP expressing vector (EYFP-N3; enhanced yellow variant of GFP; Clontech, Heidelberg, Germany) or an GFP^2 expressing vector (GFP^2-N2, Clontech) respectively, to give the plasmids that express receptors fused to either RLuc, YFP or GFP^2 on the C-terminal end of the receptor (D_2-RLuc, D_2-YFP, D_2-GFP^2, σ_1-Rluc, σ_1-YFP, A_{2A}-RLuc or A_{2A}-YFP receptors respectively). The human cDNAs for D_2 and σ_1 receptors cloned in pcDNA3.1 were amplified without its stop codon using sense and antisense primers harboring unique *KpnI* and *EcoRI* sites to clone D_2 and σ_1 receptors in pcDNA3.1-cVenus, pcDNA3.1-nVenus, pcDNA3.1-cRLuc8 or pcDNA3.1-nRLuc8. The amplified fragments were subcloned to be in-frame with the multiple cloning sites of the vectors to give the plasmids that express D_2 and σ_1 receptors fused to either nVenus, cVenus, nRLuc8 or cRLuc8 on the C-terminal end of the receptor (D_2-cVenus, D_2-nVenus, D_2-cRLuc8, D_2-nRLuc8, σ_1-nVenus, σ_1-cVenus, σ_1-nRluc8 or σ_1-cRluc8, respectively). When analyzed by confocal microscopy, it was observed that all fusion proteins showed similar subcellular distribution than naïve receptors (see results and results not shown). Fusion of RLuc and YFP to D_2 or A_{2A} receptors did not modify receptor function as previously determined by cAMP assays [17].

Cell Culture and Chemical Reagents

HEK-293T cells were grown in Dulbecco's modified Eagle's medium (DMEM) supplemented with 2 mM L-glutamine, 100 U/ml penicillin/streptomycin, and 5% (v/v) heat inactivated Fetal Bovine Serum (FBS) (all supplements were from Invitrogen, Paisley, Scotland, UK). CHO cell lines were maintained in α-MEM medium without nucleosides, containing 10% fetal calf serum, 50 μg/mL penicillin, 50 μg/mL streptomycin, and 2 mM L-glutamine (300 μg/mL). Cells were maintained at 37°C in an atmosphere of 5% CO_2, and were passaged when they were 80–90% confluent, i.e. approximately twice a week. HEK-293T or CHO cells were transiently transfected with the corresponding cDNAs by PEI (PolyEthylenImine, Sigma, St. Louis, MO, USA) method as previously described [18]or the corresponding siRNA by lipofectamine (Invitrogen™, Carlsbad, USA) method following the instructions of the supplier. siRNA that targets both human and rodent σ_1 RNA and a scrambled control siRNA were purchased from Invitrogen (catalog HSS 145543). All ligands used are diagrammed in Figure S1. Cocaine-HCl was purchased from Spanish Agencia del Medicamento n°: 2003C00220. PD144418 and PRE were purchased from Tocris, Bristol, UK. Quinpirole and raclopride were purchased from Sigma, St. Louis, MO, USA.

Immunocytochemistry

For immunocytochemistry, cells were fixed in 4% paraformaldehyde for 15 min and washed with PBS containing 20 mM glycine (buffer A) to quench the aldehyde groups. Then, after permeabilization with buffer A containing 0.2% Triton X-100 for 5 min, cells were treated with PBS containing 1% bovine serum albumin. After 1 h at room temperature, cells were labeled with the primary mouse monoclonal anti-Rluc receptor antibody (1/200, Millipore, CA, USA) or mouse monoclonal anti-σ_1 receptor antibody (1/200; Chemicon) for 1 h, washed, and stained with the secondary Cy3 donkey anti-mouse antibody (1/200, Jackson Immunoresearch Laboratories, West Grove, PA, USA). D_2 receptors fused to YFP protein were detected by their fluorescence properties. Samples were rinsed and observed in a Leica SP2 confocal microscope (Leica Microsystems, Mannheim, Germany).

BRET and BRET with BiFC Assays

HEK-293T cells growing in six-well plates were transiently co-transfected with a constant amount of cDNA encoding for the receptor fused to RLuc or nRLuc8 and cRLuc8 proteins and with increasingly amounts of cDNA corresponding to the receptor fused to YFP or nVenus and cVenus proteins (see figure legends). To quantify receptor-YFP expression or receptor-reconstituted YFP Venus expression, cells (20 μg protein) were distributed in 96-well microplates (black plates with a transparent bottom) and fluorescence was read in a Fluoro Star Optima Fluorimeter (BMG Labtechnologies, Offenburg, Germany) equipped with a high-energy xenon flash lamp, using a 10 nm bandwidth excitation filter at 400 nm reading. Receptor-fluorescence expression was determined as fluorescence of the sample minus the fluorescence of cells expressing the BRET donor alone. For BRET or BRET with

BiFC measurements, the equivalent of 20 μg of cell suspension were distributed in 96-well microplates (Corning 3600, white plates; Sigma) and 5 μM coelenterazine H (Molecular Probes, Eugene, OR) was added. After 1 minute for BRET or after 5 min for BRET with BiFC of adding coelenterazine H, the readings were collected using a Mithras LB 940 that allows the integration of the signals detected in the short-wavelength filter at 485 nm (440–500 nm) and the long-wavelength filter at 530 nm (510–590 nm). To quantify receptor-RLuc or receptor-reconstituted RLuc8 expression luminescence readings were also performed after 10 minutes of adding 5 μM coelenterazine H. Both fluorescence and luminescence of each sample were measured before every experiment to confirm similar donor expressions (about 150,000 luminescent units) while monitoring the increase acceptor expression (10,000–70,000 fluorescent units). The net BRET is defined as [(long-wavelength emission)/(short-wavelength emission)]-Cf where Cf corresponds to [(long-wavelength emission)/(short-wavelength emission)] for the donor construct expressed alone in the same experiment. BRET is expressed as mili BRET units, mBU (net BRET×1000).

SRET Assays

HEK-293T cells growing in six-well plates were transiently co-transfected with constant amounts of cDNAs encoding for both receptor fused to RLuc and GFP[2] proteins and with increasingly amounts of cDNA corresponding to the receptor fused to YFP protein and SRET was determined as previously described using a Mithras LB 40 [19].

Striatal Slices Preparation

Brains from WT littermates and σ_1 receptor KO CD1 albino Swiss male mice (8 weeks old, 25 g of weight) were generously provided by Laboratorios Esteve (Barcelona, Spain) [20]. Brains were rapidly removed from animals and striatal slices were obtained as previously indicated [16,21].

Coimmunoprecipitation

Striatal slices from WT littermates and σ_1 receptor KO mice were treated with medium or with 150 μM cocaine for 30 min. The striatal tissue was disrupted with a Polytron homogenizer in 50 mM Tris-HCl buffer, pH 7.4, containing a protease inhibitor mixture (1/1000, Sigma). The cellular debris was removed by centrifugation at 13,000 g for 5 min at 4°C, and membranes were obtained by centrifugation at 105,000 g for 1 h at 4°C. Membranes were solubilized in ice-cold immunoprecipitation buffer (phosphate-buffered saline (PBS), pH 7.4, containing 1% (v/v) Nonidet P-40) and incubated for 30 min on ice before centrifugation at 105,000 g for 1 h at 4°C. The supernatant (1 mg/ml of protein) was processed for immunoprecipitation as described in the immunoprecipitation protocol using a Dynabeads® Protein G kit (Invitrogen) using goat anti-D_2 receptor antibody (1:1000, Santa Cruz Biotechnology, Santa Cruz, CA). As negative control anti-FLAG antibody (1:1000, Sigma) was used. Protein was quantified by the bicinchoninic acid method (Pierce) using bovine serum albumin dilutions as standards. Immunoprecipitates were separated on a denaturing 10% SDS-polyacrylamide gel and transferred onto PVDF membranes. Membranes were blocked for 90 min in 5% Bovine (1% fat) dry milk and PBS-Tween 20 (0.05% V/V). The following primary antibodies were incubated overnight at 4°C in 5% milk and PBS-Tween 20 (0.05% V/V): mouse anti-D_2 receptor antibody (1:1000, Santa Cruz Biotechnology, Santa Cruz, CA) or mouse anti-σ_1 receptor antibody B-5 (sc-137075) (1:800, Santa Cruz Biotechnology, Santa Cruz, CA) and, after washing three times for 10 min in PBS Tween-20 (0.05% V/V), membranes were incubated with the secondary antibody rabbit anti-mouse-HRP (1:20,000, Dako, Glostrup, Denmark) for 1 h at room temperature in 5% milk and PBS-Tween 20 (0.05% V/V). After three washes with PBS Tween-20 (0.05% V/V) and a final wash with PBS, bands were detected with the addition of SuperSignal West Pico Chemiluminescent Substrate (Pierce) and visualized with a LAS-3000 (Fujifilm). Analysis of detected bands was performed by Image Gauge software (version 4.0) and Multi Gauge software (version 3.0).

In Situ Proximity Ligation Assays (PLA)

Striatal slices from WT and σ_1 receptor KO mice treated or not with 150 μM cocaine for 30 min, were mounted on slide glass and heteromers were detected using the Duolink II in situ PLA detection Kit (OLink; Bioscience, Uppsala, Sweden). Slices were thawed at 4°C, washed in 50 mM Tris-HCl, 0.9% NaCl pH 7.8 buffer (TBS), permeabilized with TBS containing 0.01% Triton X-100 for 10 min and successively washed with TBS. After 1 h incubation at 37°C with the blocking solution in a pre-heated humidity chamber, slices were incubated overnight in the antibody diluent medium with a mixture of equal amounts of the primary antibodies mouse anti-σ_1 receptor antibody B-5 (sc-137075, 1:500, see above) and the guinea-pig anti-D_2 receptor antibody (1:500 Sigma) which specificity for D_2 receptors was previously demonstrated [21]. Slices were washed as indicated by the supplier and incubated for 2 h in a pre-heated humidity chamber at 37°C with PLA probes detecting mouse or guinea pig antibodies, Duolink II PLA probe anti-mouse plus and Duolink II PLA probe anti-guinea minus (prepared following the instructions of the supplier) diluted in the antibody diluent to a concentration of 1:5. After washing at room temperature, slices were incubated in a pre-heated humidity chamber for 30 min at 37°C, with the ligation solution (Duolink II Ligation stock 1:5 and Duolink II Ligase 1:40). Detection of the amplified probe was done with the Duolink II Detection Reagents Red Kit. After exhaustively washing at room temperature as indicated in the kit, slices were mounted using the mounting medium with DAPI. The samples were observed in a Leica SP2 confocal microscope (Leica Microsystems, Mannheim, Germany). Images were opened and processed with Image J confocal.

Immunohistochemistry

Striatal slices from WT and σ_1 receptor KO mice were thawed at 4°C, washed in TBS, permeabilized with TBS containing 0.1% Triton X-100 for 10 min and successively washed with TBS. Slices were rocked in Blocking reagent 1% (Roche, Sant Cugat del Vallés, Spain) for 1 h at 37°C in a humidified atmosphere and incubated overnight at 4°C in a humidified atmosphere with the primary antibodies: mouse anti-σ_1 receptor antibody B-5 (sc-137075, 1:100, see above) or the guinea-pig anti-D_2 receptor antibody (1:100 Frontier Institute, Ishikari, Hokkaido, Japan), in 0.1% TBS-Tween, 0.1% BSA-Acetylated (Aurion, Wageningen, The Netherlands), 7% SND. Slices were washed in TBS-Tween 0.05% and left for 2 h at room temperature in a humidified atmosphere with the corresponding secondary antibodies: goat anti-mouse (1:200, Alexa Fluor 488, Invitrogen) and goat anti-guinea pig (1:200, Alexa Fluor 488, Invitrogen) in the same medium. Then, the slices were washed in TBS-Tween 0.05%, followed by a single wash in TBS before mounting in Mowiol medium (Calbiochem, Merck, Darmstadt, Germany), covered with a glass and left to dry at 4°C for 24 h. The sections were observed and imaged in a Leica SP2 confocal microscope.

cAMP Determination

Non transfected or transiently transfected CHO cells (see figure legends) were treated for 10 min with the indicated concentrations of D_2 receptor agonist quinpirole, 30 μM cocaine or 100 nM of the σ_1 receptor agonist PRE-084 alone or in combination. cAMP production was determined using [^{3}H]cAMP kit (Amersham Biosciences, Uppsala, Sweden) following the instructions from the manufacturer.

ERK 1/2 Phosphorylation Assays

WT and KO ice striatal slices were treated for the indicated time with the indicated concentrations of cocaine and/or D_2 receptor ligands, frozen on dry ice and stored at −80°C. When ERK1/2 phosphorylation assays were performed in cell cultures, CHO cells (48 h after transfection) were cultured in serum-free medium for 16 h before the addition of the indicated concentration of cocaine or/and D_2 receptor ligands for the indicated time. Both, cells and slices were lysed in ice-cold lysis buffer (50 mM Tris-HCl pH 7.4, 50 mM NaF, 150 mM NaCl, 45 mM β-glycerophosphate, 1% Triton X-100, 20 μM phenyl-arsine oxide, 0.4 mM $NaVO_4$ and protease inhibitor cocktail) and ERK 1/2 phosphorylation was determined as indicated elsewhere [16,22].

CellKey Label-free Assays

The CellKey system provides a universal, label-free, cell-based assay platform that uses cellular dielectric spectroscopy (CDS) to measure endogenous and transfected receptor activation in real time in live cells [23]. Changes in the complex impedance (DZ or dZ) of a cell monolayer in response to receptor stimulation were measured. Impedance (Z) is defined by the ratio of voltage to current as described by Ohm's law (Z = V/I). CHO cell clones stably expressing D_2 receptors were grown to confluence in a CellKey Standard 96 well microplate that contains electrodes at the bottom of each well. For untreated cells or for cells preincubated (overnight at 37°C) with PTx (10 ng/ml), medium was replaced by HBSS buffer (Gibco) supplemented with 20 mM HEPES 30 minutes prior to running the cell equilibration protocol. A baseline was recorded for 5 minutes and then cells were treated with increasing concentrations of the D_2 receptor agonist quinpirole or cocaine alone or in combination and data was acquired for the following 10 minutes. To calculate the impedance, small voltages at 24 different measurement frequencies were applied to treated or non-treated cells. At low frequencies, extracellular currents (iec) that pass around individual cells in the layer were induced. At high frequencies, transcellular currents (itc) that penetrate the cellular membrane were induced and the ratio of the applied voltage to the measured current for each well is the impedance. The data shown refer to the maximum complex impedance induced extracellular currents (Ziec) response to the ligand addition.

Results

σ_1 Receptors form Heteromers with Dopamine D_2 Receptors but not with the Other D_2-like Receptor Family Members

We first examined whether the receptors of the D_2-like family could directly interact with σ_1 receptors and thus be a target for cocaine binding. To do this we used the Bioluminescence Resonance Energy Transfer (BRET) technology in HEK-293T cells expressing a constant amount of D_2 (long isoform), D_3 or D_4 dopamine receptors fused to *Renilla Luciferase* (RLuc) and increasing amounts of σ_1 receptors fused to Yellow Fluorescence Protein (YFP). Clear BRET saturation curves were obtained in cells expressing D_2-RLuc receptors and increasing amounts of σ_1-YFP receptors with a $BRET_{max}$ of 55±7 mBU and a $BRET_{50}$ of 28±6 (Fig. 1a). In contrast, in cells expressing D_3-RLuc or D_4-RLuc and σ_1-YFP receptors a low and linear non-specific BRET signal was obtained thus confirming the specificity of the interaction between D_2-RLuc and σ_1-YFP receptors (Fig. 1b). As a further control, cells were cotransfected with σ_1-YFP receptors and adenosine A_{2A}-Rluc receptors and no specific BRET signal was obtained (Fig. 1a). These results indicate that σ_1 receptors selectively interact with dopamine D_2 receptors and not with the other members of the D_2-like receptor family.

The σ_1 receptors are predominantly found in the endoplasmic reticulum membrane and the plasma membrane [24] with one hypothesis that it may be acting as a chaperone protein [25]. The expression of σ_1 and D_2 receptors at the plasma membrane level was explored by analyzing the co-localization of both receptors by confocal microscopy. HEK-293T cells were used in the assays since they constitutively express σ_1 receptors, but not DAT [16]. As expected, a punctate σ_1 receptor staining in naïve (Fig. 1c left panels, top images) or cocaine-treated (Fig. 1c right panels, top images) HEK-293T cells was detected. After transfection of the cDNA corresponding to D_2 receptors, a co-localization of σ_1 receptor and D_2 receptors was detected at the plasma membrane level in cells not treated with cocaine (Fig. 1c left panels, bottom images) or in cells treated with 30 μM cocaine for 30 min (Fig. 1c right panels, bottom images).

Higher Order Complex Formation between σ_1 Receptors and Dopamine D_2 Receptors

Recent crystal structures have demonstrated that homodimers of GPCRs are possible, a fact that has been confirmed for dopamine D_2 receptors [26–30]. Considering that σ_1 may act as a chaperone like molecule we investigated the possible formation of higher order receptor complexes between σ_1 and D_2 receptor homomers. To test this we first needed to know whether σ_1-receptors could form dimers, something that had not been reported. First, we tested if σ_1 receptors can form dimers by BRET experiments in HEK-293T cells expressing a constant amount of σ_1-RLuc receptors and increasing amounts of σ_1-YFP receptors. A positive and saturable BRET signal was obtained with a $BRET_{max}$ of 165±35 mBU and a $BRET_{50}$ of 22±12 (Fig. 2a) indicating that σ_1-σ_1 homodimers can exist and demonstrating, for the first time, the oligomerization of σ_1 receptors. Next, we tested whether D_2 receptor homomers could interact with σ_1-receptors by a combined BRET and FRET assay termed Sequential Resonance Energy Transfer (SRET) [19]. This assay involves two sequential energy transfer events, one bioluminescent energy transfer between Rluc and a blue shifted GFP^2 and a second fluorescent energy transfer event between excited GFP^2 and YFP (see Fig. 2b top scheme). In HEK-293T cells expressing a constant amount of D_2-RLuc and D_2-GFP^2 receptors and increasing amounts of σ_1-YFP receptors, a net SRET saturation curve was obtained with a $SRET_{max}$ of 269±33 SU and a $SRET_{50}$ of 92±24 (Fig. 2b). Cells expressing constant amounts of adenosine A_{2A}-RLuc and A_{2A}-GFP^2 receptors and increasing amounts of σ_1-YFP receptors provided very low and linear SRET, according to the lack of interaction between A_{2A} receptors and σ_1 receptors. These results demonstrate that σ_1 receptors are able to form heteromers with D_2-D_2 receptor homomers. A net SRET saturation curve was also obtained using HEK-293T cells expressing constant amounts of σ_1-Rluc and D_2-GFP^2 and increasing amounts of σ_1-YFP ($SRET_{max}$: 140±8 SU; $SRET_{50}$: 9±3) but not when D_2-RLuc and D_2-GFP^2 receptors were

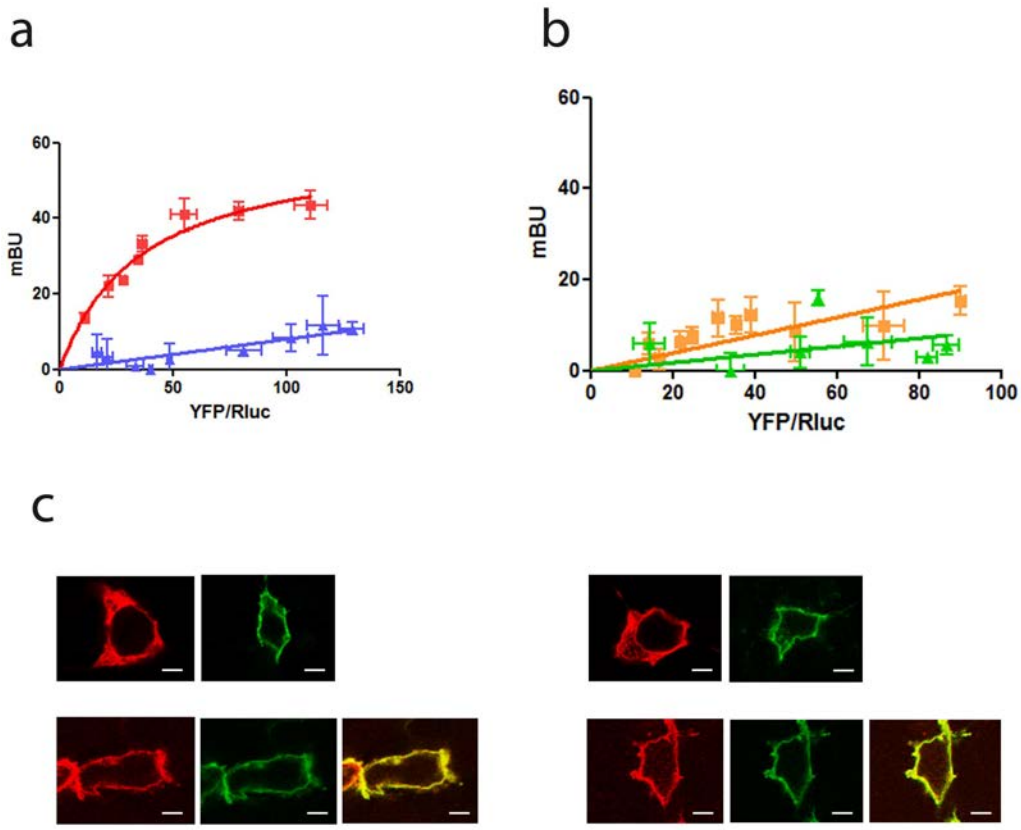

Figure 1. Molecular interaction between σ_1 receptors and D_2 receptors in living cells. BRET saturation experiments were performed with HEK-293T cells co-transfected with: (**a**) D_2-RLuc cDNA (0.4 μg, squares) or adenosine A_{2A}-RLuc cDNA as negative control (0.2 μg, triangles) and increasing amounts of σ_1-YFP cDNA (0.1 to 1 μg cDNA), (**b**) D_3-RLuc cDNA (0.5 μg, squares) or D_4-RLuc cDNA (0.5 μg, triangles) and increasing amounts of σ_1-YFP cDNA (0.1 to 1 μg cDNA). The relative amount of BRET acceptor is given as the ratio between the fluorescence of the acceptor minus the fluorescence detected in cells only expressing the donor, and the luciferase activity of the donor (YFP/Rluc). BRET data are expressed as means ± S.D. of five to six different experiments grouped as a function of the amount of BRET acceptor. In (**c**) confocal microscopy images of HEK-293T cells transfected with D_2-YFP or σ_1-RLuc (top panels) or co-transfected with D_2-YFP and σ_1-RLuc (bottom panels), treated (right images) or not (left images) with 30 μM cocaine for 30 min. σ_1 receptors (red) were identified by immunocytochemistry and D_2 receptors (green) were identified by its own fluorescence. Co-localization is shown in yellow. Scale bar:10 μm.
doi:10.1371/journal.pone.0061245.g001

replaced by A_{2A}-RLuc and A_{2A}-GFP[2] receptors (Fig. 2c). These results demonstrate that D_2 receptors are able to form heteromers with σ_1-σ_1 receptor homomers. Finally, we tested for a higher order interaction of receptor heteromers constituted by σ_1 and D_2 receptor homomers (σ_1-σ_1-D_2-D_2). This was done using a modified BRET assay that involves a double complementation assay [30]. A diagram showing the BRET with luminescence/fluorescence complementation approach (BRET with BiFC assay; see Methods) is shown in Figure 2d (top panel). Briefly, one receptor fused to the N-terminal fragment (nRluc8) and another receptor fused to the C-terminal fragment (cRluc8) of the Rluc8 act as BRET donor after Rluc8 reconstitution by a close receptor-receptor interaction and one receptor fused to an YFP Venus N-terminal fragment (nVenus) and another receptor fused to the YFP Venus C-terminal fragment (cVenus), act as BRET acceptor after YFP Venus reconstitution by a close receptor-receptor interaction. Accordingly, cells were co-transfected with a constant amount of the two cDNAs corresponding to D_2-nRluc8 and D_2-cRluc8 (equal amounts of the two cDNAs) and with a constant amount of the two cDNAs corresponding to σ_1-nVenus and σ_1-cVenus (equal amounts of the two cDNAs). Specific BRET would only be possible if RLuc reconstituted by D_2-nRluc8-D_2-cRluc8 dimerization is close enough to YFP Venus reconstituted by σ_1-nVenus-σ_1-cVenus dimerization. Higher order heterotetramers were in fact observed as evidenced by a positive BRET signal (Fig. 2d). As negative controls, cells expressing only three fusion proteins and the fourth receptor not fused provided neither a significant fluorescent signal nor a positive BRET (Figure 2d). Collectively these results indicate that σ_1-D_2 receptor heteromers seem to be constituted by the interaction of receptor homomers and the minimal structural unit is the σ_1-σ_1-D_2-D_2 receptor heterotetramer.

The Effect of σ_1 Receptor Ligands on σ_1-D_2 Receptor Heterotetramer

It is known that cocaine can bind to σ_1 [25,31,32]. We sought to measure the effect of cocaine binding to σ_1 receptors on σ_1-D_2 receptor heteromers using BRET. We performed BRET experiments in HEK-293T cells expressing a constant amount of D_2-RLuc receptors and increasing amounts of σ_1-YFP receptors in the presence or in the absence of cocaine. The BRET saturation curve was reduced when cells were treated for 30 min with 30 μM of cocaine ($BRET_{max}$: 35±6 mBU; $BRET_{50}$: 26±8) indicating that cocaine binding to σ_1 receptors induces structural changes in the σ_1-D_2 receptor heteromer. The cells treated (10 min) with the σ_1 agonist PRE084 (100 nM; $BRET_{max}$: 40±8 mBU; $BRET_{50}$:

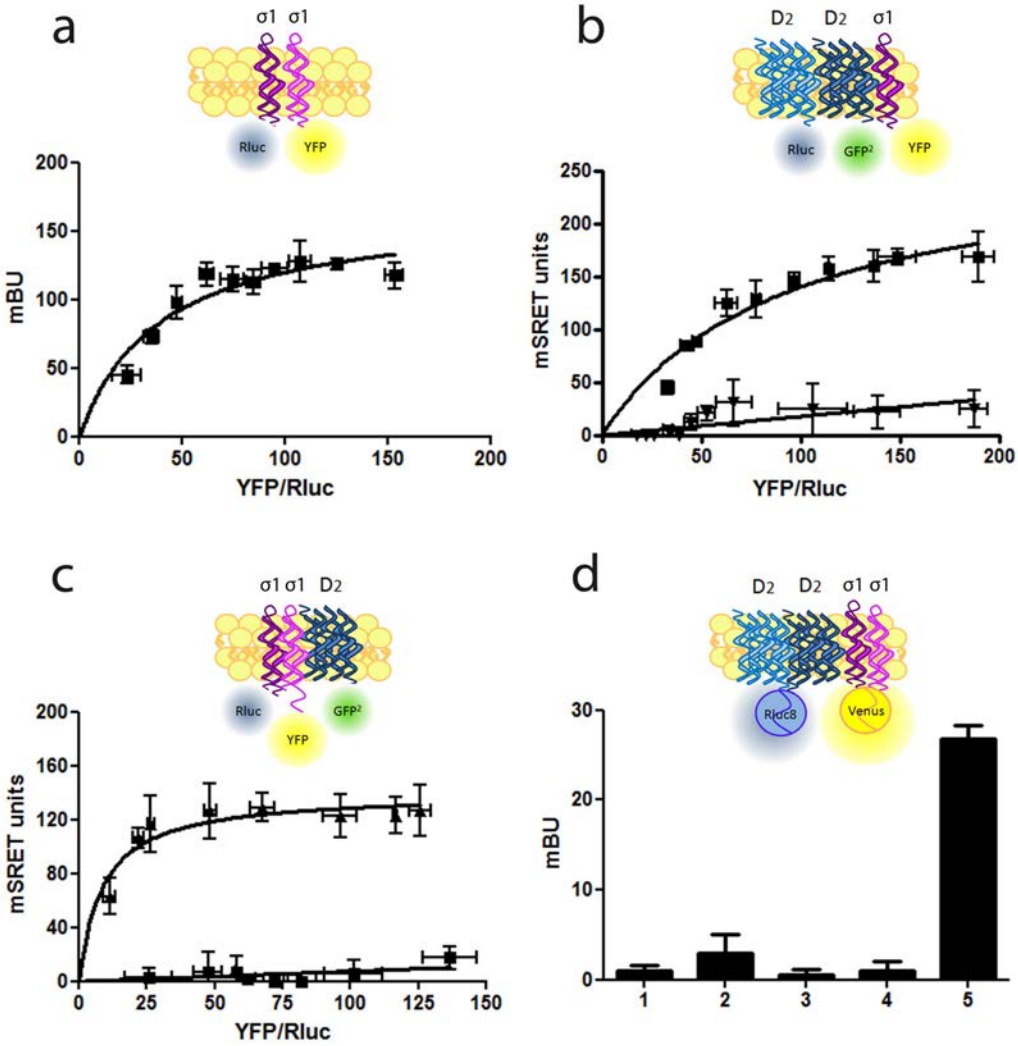

Figure 2. Higher order complex formation between σ_1 receptors and dopamine D_2 receptors in living cells. In (**a**) BRET saturation experiments were performed with HEK-293T cells co-transfected with σ_1-RLuc cDNA (0.2 μg) and increasing amounts of σ_1-YFP cDNA (0.1 to 0.6 μg cDNA). A schematic representation of a BRET process is shown at top in which the receptor fused to RLuc acts as donor and the receptor fused to YFP acts as acceptor. In (**b**) and (**c**) SRET saturation experiments were performed with HEK-293T cells co-transfected with: (b) a constant amount of D_2-RLuc (0.6 μg) and D_2-GFP^2 (1 μg) receptor cDNA (squares) or A_{2A}-RLuc (0.3 μg) and A_{2A}-GFP^2 (0.5 μg) receptor cDNA, as negative control (triangles), and increasing amounts of σ_1-YFP receptor (0.2 to 1.5 μg cDNA), (c) a constant amount of σ_1-Rluc (0.3 μg) and D_2-GFP^2 (1 μg) (triangles) or A_2-GFP^2 (0.5 μM) as negative control (squares) receptor cDNA and increasing amounts of σ_1-YFP receptor cDNA (0.2 to 1.5 μg). The relative amount of acceptor is given as the ratio between the fluorescence of the acceptor minus the fluorescence detected in cells only expressing the donor, and the luciferase activity of the donor (YFP/Rluc). A schematic representation of a SRET process is shown at top images in which two sequential energy transfer events between Rluc and GFP^2 (BRET process) and between GFP^2 and YFP (FRET process) occurs. In (**d**) BRET with luminescence/fluorescence complementation approach was performed measuring BRET in cells co-transfected with 1 μg of the two cDNAs corresponding to D_2-nRLuc8 and D_2-cRLuc8 and with 1.5 μg of the two cDNAs corresponding to σ_1-nVenus and σ_1-cVenus (5). As negative controls, cells transfected with the same amount of cDNA corresponding to D_2-nRLuc8, D_2-cRLuc8, σ_1-nVenus and cVenus (1), D_2-nRLuc8, D_2-cRLuc8, σ_1-cVenus and nVenus (2), D_2-nRLuc8, σ_1-nVenus, σ_1-cVenus and cRLuc8 (3), or D_2-cRLuc8, σ_1-nVenus, σ_1-cVenus and nRLuc8 (4) did not display any significant luminescence or positive BRET. A schematic representation of a BRET with luminescence/fluorescence complementation approach is given at the top image in which one receptor fused to the N-terminal fragment (nRluc8) and another receptor fused to the C-terminal fragment (cRluc8) of the Rluc8 act as BRET donor after Rluc8 reconstitution by a close receptor-receptor interaction and one receptor fused to an YFP Venus N-terminal fragment (nVenus) and another receptor fused to the YFP Venus C-terminal fragment (cVenus), act as BRET acceptor after YFP Venus reconstitution by a close receptor-receptor interaction. BRET or SRET data are expressed as means ± S.D. of five to six different experiments grouped as a function of the amount of BRET or SRET acceptor.

doi:10.1371/journal.pone.0061245.g002

31±6) but not with the antagonist PD144418 (1 μM; $BRET_{max}$: 48±3 mBU; $BRET_{50}$: 20±5) also showed a decrease in the BRET saturation curves. Interestingly, the σ_1 antagonist PD144418 is able to revert the effect induced by cocaine ($BRET_{max}$: 52±9 mBU; $BRET_{50}$: 31±7 in the presence of cocaine and PD144418) (Fig. 3a). To know if structural changes in σ_1-σ_1 receptor homomers or in D_2-D_2 receptor homomers can account for the ligand-induced effect on σ_1-D_2 receptor heteromers, we performed BRET experiments first in cells expressing σ_1-RLuc and σ_1–YFP receptors as indicated in Fig. 2a. Cells were treated for 10 min with 100 nM of the agonist PRE084 or 1 μM of the antagonist PD144418 or for 30 min with 30 μM of cocaine alone

or with 1 μM PD144418. As shown in Fig. 3b, no significant changes in $BRET_{max}$ or $BRET_{50}$ were observed. Then, changes in the BRET saturation curve obtained in cells expressing a constant amount of D_2-RLuc receptors and increasing amounts of D_2-YFP receptors ($BRET_{max}$: 44±3 mBU; $BRET_{50}$: 12±4) were analyzed. The BRET saturation curve changed in cells treated for 10 min with 100 nM of PRE084 ($BRET_{max}$: 27±5 mBU; $BRET_{50}$: 11±4) or 30 min with 30 μM of cocaine ($BRET_{max}$: 29±2 mBU; $BRET_{50}$: 19±5) but not in cells treated for 10 min with 1 μM of PD144418 ($BRET_{max}$: 44±3 mBU; $BRET_{50}$: 9±3). Again the antagonist, PD144418, was able to revert the effect induced by cocaine ($BRET_{max}$: 43±2 mBU; $BRET_{50}$: 16±3 in cells pre-treated with PD144418 and cocaine) (Fig. 3c). These data suggest structural changes in the complex brought about by binding of either the σ_1 agonist PRE084 or cocaine. To test whether the effect of PRE084 or cocaine on D_2-D_2 heteromers are due to the presence of σ_1 receptors, assays were performed in cells whose σ_1 receptor expression was knocked-down using an RNAi approach (Fig. 3d). When we transfected a specific small interfering RNA (siRNA), a robust silencing of σ_1 receptor expression was obtained (Fig. S2). The treatment with the specific siRNA completely abolished the effect of cocaine or PRE084 on the BRET saturation curve. The treatment with PD144418 or PD144418 and cocaine had no effect on these knocked-down cells (Fig. 3d). These results suggest that ligand binding to σ_1 receptors induces strong changes in the structure of the D_2-D_2 receptor homomers in the σ_1-D_2 receptor heteromers.

Cocaine Binding to σ_1 Receptors Modulates the D_2 Receptor Signaling in Transfected Cells

The cocaine-induced modifications of the quaternary structure of D_2 receptor homodimers in the σ_1-D_2 receptor heteromer described above suggest that cocaine can modulate the functionality of D_2 receptors. To study how cocaine affects D_2 receptor-mediated signaling, Chinese hamster ovary (CHO) cells were used as they provided a lower baseline of signaling for which to detect downstream changes and have been shown to constitutively express σ_1 receptors but not DAT [16]. The effect of cocaine on D_2 receptor agonist-induced, G protein-mediated signaling was measured using a label free assay that measures changes in cell impedance in response to stimulation. In CHO cells stably expressing D_2 receptors, increasing cocaine concentrations (10 nM to 100 μM) did not give any G protein-mediated signaling, neither $G_{i/0}$, G_S or G_q (Fig. 4a) as compared to known control receptors (Fig. S3). The signaling obtained upon D_2 receptor activation with the agonist quinpirole (0.1 nM to 1 μM) showed a G_i profile (increases in impedance) that was completely blocked when cells were treated with the G_i specific pertussis toxin (PTx) (Fig. 4b). We observed a small but significant decrease in the G_i activation induced by quinpirole when cells where pre-treated for 1 h with 30 μM cocaine (Fig. 4c). These results indicate that cocaine by itself is not able to induce a G protein-mediated signaling but can partially inhibit the ability of D_2 receptors to signal through G_i. A downstream consequence of G_i mediated signaling is the ability to decrease cAMP signaling. In addition to the label free experiments above we determined the levels of cAMP in CHO cells stably expressing D_2 receptors using forskolin and then measured whether cocaine was able to decrease the forskolin-induced cAMP formation. We found cocaine alone could not decrease the levels of cAMP after treatment with forskolin compared to the D_2 agonist quinpirole (Fig. 4d). However, cocaine significantly dampened the quinpirole-induced decreases of forskolin-mediated increases in cAMP levels (Fig. 4d). This effect was blocked when cells were transfected with siRNA against the σ_1 receptor (Fig. 4d), demonstrating that cocaine's ability to counteract the action of quinpirole was mediated by σ_1 receptors. Similar results were obtained when instead of cocaine the σ_1 receptor agonist PRE084 was used (Fig. S4) reinforcing the concept that σ_1 receptor ligands induce a significant decrease in the ability of D_2 receptors to signal through G_i.

Apart from G protein-mediated signaling, many GPCRs are able to signal in a G protein-independent way [33–37]. ERK 1/2 phosphorylation is one of the MAPK pathways that has been described to be activated in a G protein-independent and arrestin-dependent mechanism [36]. Several reports have highlighted the importance of ERK 1/2 activation in D_2 receptors containing neurons for the effects of cocaine [38–41]. We sought to understand how cocaine might influence σ_1-D_2 receptor heteromer-mediated ERK 1/2 signaling. Varying concentrations of cocaine and varying the time of treatment did not lead to any significant change in ERK 1/2 phosphorylation in response to cocaine in cells not expressing D_2 receptors (Fig. S5). Importantly, cocaine *per se* dose-dependently (Fig. S6a) and time-dependently (Fig. S6b) activated ERK 1/2 phosphorylation in cells expressing D_2 receptors. This effect was mediated by σ_1 receptors since it was strongly diminished in cells transfected with the σ_1 receptors siRNA (Figs. S6a and S6b). The D_2 receptor agonist quinpirole was also dose-dependently (Fig. S6c) and time-dependently (Fig. S6d) able to activate ERK 1/2 phosphorylation but, as expected, this effect was not mediated by σ_1 receptors since it was not diminished in cells transfected with the σ_1 receptors siRNA (Figs. S6c and S6d). These results point out that σ_1 or D_2 receptor activation in the σ_1-D_2 receptor heteromer induces ERK 1/2 phosphorylation. Thus, cocaine, like quinpirole, can act as an agonist at the MAPK activation level for the heteromer.

A property of some receptor heteromers is the ability of the antagonist of one receptor to block the function of the agonist of the partner receptor, a property defined as cross-antagonism [22,42]. In cells expressing D_2 receptors we looked for cross-antagonism among σ_1-D_2 receptor heteromers. Indeed we found the cocaine-induced ERK 1/2 phosphorylation was counteracted not only by the σ_1 receptor antagonist PD144418 (1 μM) but also by the D_2 receptor antagonist raclopride (10 μM) (Fig. 5a). Analogously, the D_2 receptor agonist quinpirole-induced ERK 1/2 phosphorylation was blocked by raclopride but also by PD144418 (Fig. 5b). These data suggest that antagonist binding leads to structural changes within the receptor heteromer that block signaling through the partner receptor. By definition an antagonist cannot signal on its own, therefore this cross-antagonism can only derive from the direct protein-protein interactions established between the receptors in the σ_1-D_2 receptor heteromer. This hypothesis is further supported by the fact that silencing cells of the σ_1 receptor led to a complete loss in this cross-antagonism. That is, the effect of PD144418 on quinpirole-induced ERK1/2 phosphorylation was not observed when cells were transfected with the siRNA for σ_1 receptors (Fig. 5b).

As mentioned above cocaine can inhibit DAT and increase the dopamine concentration in the striatum; so, in the presence of cocaine both receptors in the σ_1-D_2 receptor heteromer could be activated. Therefore we asked, what happens to ERK 1/2 phosphorylation after co-activation of both receptors? Surprisingly, a negative cross-talk was detected. When cells expressing D_2 receptors were treated with both 1 μM quinpirole and 30 μM cocaine there was a decrease in ERK 1/2 phosphorylation compared to quinpirole alone (Fig. 5c). This difference was not seen if the cells were depleted of σ_1 receptors via siRNA (Fig. 5c).

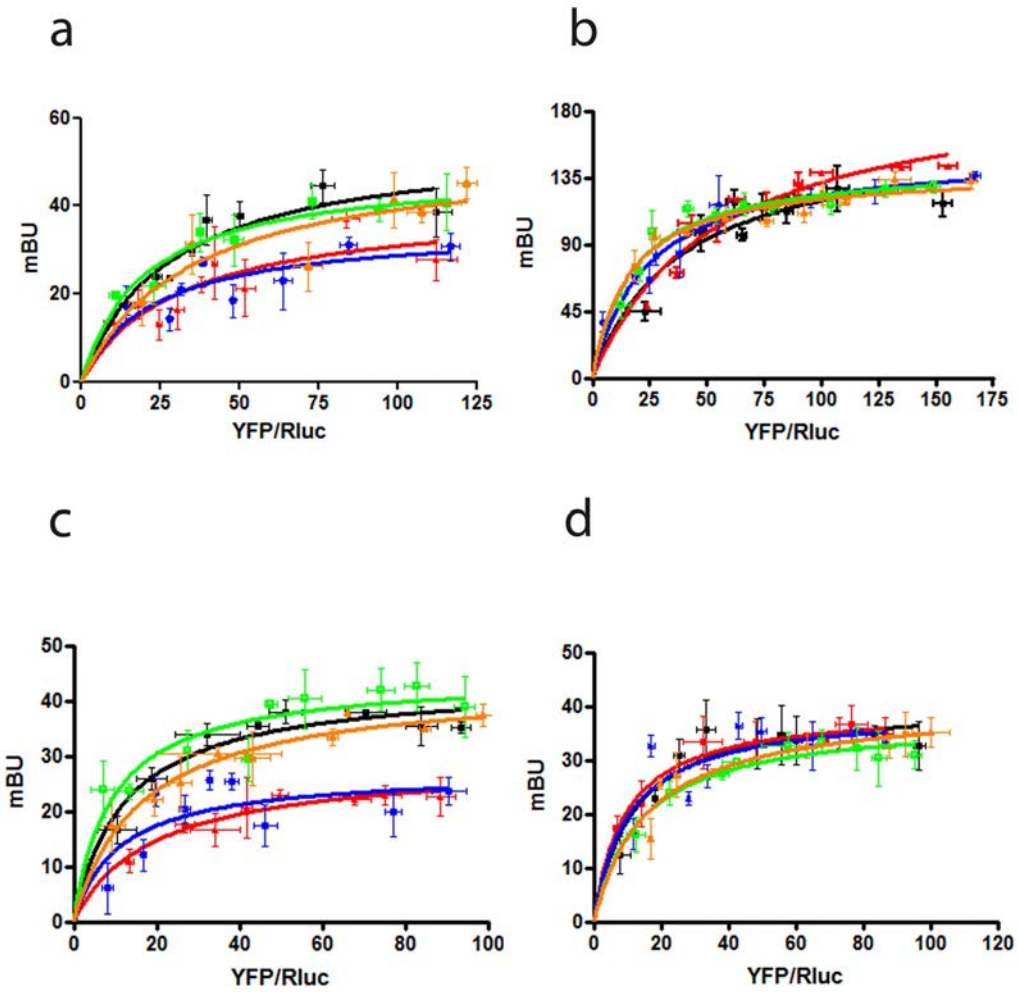

Figure 3. Effect of σ_1 receptor ligands on σ_1-D_2 receptor heteromer. BRET was measured in HEK-293T cells cotransfected with: (**a**) D_2–Rluc cDNA (0.4 μg) and increasing amounts of σ_1-YFP receptor cDNA (0.1 to 1 μg), (**b**) σ_1–Rluc cDNA (0.2 μg) and increasing amounts of σ_1-YFP receptor cDNA (0.1 to 1 μg), (**c**) D_2–Rluc cDNA (0.4 μg) and increasing amounts of D_2-YFP receptor cDNA (0.2 to 2 μg) or (**d**) siRNA corresponding to σ_1 receptor (see Methods), D_2–Rluc cDNA (0.4 μg) and increasing amounts of D_2-YFP receptor cDNA (0.2 to 2 μg)**,** not treated (black), treated for 30 min with 30 μM cocaine (red), treated for 10 min with 100 nM PRE084 (blue) or 1 μM PD144418 (green) or treated for 30 min with 30 μM cocaine and 1 μM PD144418 (orange)**.** The relative amount of BRET acceptor is given as the ratio between the fluorescence of the acceptor minus the fluorescence detected in cells only expressing the donor, and the luciferase activity of the donor (YFP/Rluc). BRET data are expressed as means ± SD of four to six different experiments grouped as a function of the amount of BRET acceptor.
doi:10.1371/journal.pone.0061245.g003

σ_1-D_2 Receptor Heteromers are Found in the Brain Striatum

The BRET experiments and the signaling experiments are all suggestive of functional complexes that can lead to changes in D_2 receptor function. However, all of these experiments were performed in transfected cells. To establish whether these complexes and their functional implications can be seen in tissue we obtained striatum from wild type (WT) and σ_1 knockout (KO) mice. The striatum express D_2 receptor containing neurons of the indirect motor pathway and is one of the key areas of the brain where cocaine imposes its effects. First we examined whether σ_1-D_2 receptor heteromers could be detected in native tissue. We performed Western blot experiments and found the expression of both receptors in the striatum of WT mice and the expression of D_2 receptors but not σ_1 receptors in the striatum of KO mice (Fig. 6a). Next we performed co-immunoprecipitation experiments and found the antibody against D_2 receptor could indeed co-precipitate D_2 receptors and σ_1 receptor (Fig. 6a) in WT mice striatum treated or not with 150 μM cocaine. This co-precipitation was not observed when tissue from σ_1 receptor KO animals was used (Fig. 6a). Although supportive of the BRET experiments above and highly suggestive of heteromers in striatum, we wanted to ensure that these complexes were not an artifact of the detergent solubilization. To test this we used the recently developed proximity ligation assay on slices of striatum from both WT and σ_1 KO mice [42]. Using immunohistochemistry, we first checked the expression of σ_1 receptors in WT animals but not in KO animals (Fig. S7) and the expression of D_2 receptors in both WT and KO animals (Fig. S8). Next we performed the proximity ligation assay on striatal slices from WT animals. The slices were treated or not with 150 μM cocaine and as shown in Figure 6 (b and d) a red punctate fluorescent staining was observed, indicating both receptors are indeed in a complex in mice striatum in the presence or absence of cocaine. As a negative control we repeated this with only one of the two primary antibodies, and staining was not seen (Fig. S9). As expected, the

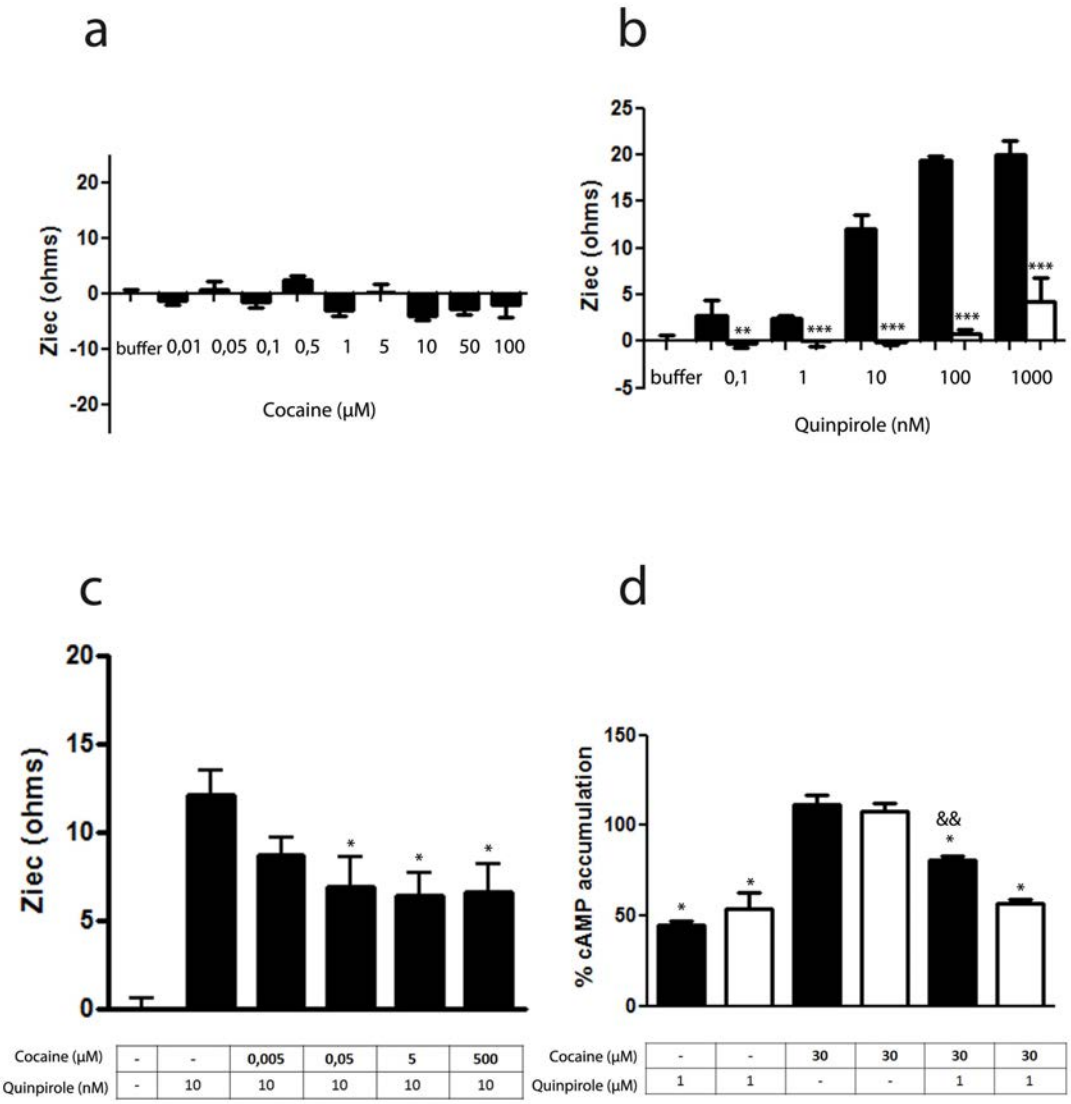

Figure 4. Cocaine binding to σ_1 receptor modulates the G_i-dependent D_2 receptor signaling in transfected cells. In (**a** to **c**) CellKey label-free assays were performed in CHO cells stable expressing D_2 receptors. In (a) cells were stimulated with buffer (B) or with increasing concentrations of cocaine. In (b) cells were preincubated (black columns) or not (white columns) with PTx (10 ng/ml) overnight and stimulated with buffer (B) or increasing concentrations of quinpirole. In (c) cells were stimulated with increasing concentrations of cocaine in the presence of 10 nM of quinpirole. In (d) cAMP production was determined in CHO cells stable expressing D_2 receptors not transfected (black columns) or transfected (white columns) with siRNA corresponding to σ_1 receptor (6.25 μg of oligonucleotides) and stimulated with 5 μM forskolin in absence (100%) or presence of 1 μM quinpirole, 30 μM cocaine alone or in combination. Percent of cAMP produced respect to 5 μM forskolin treatment was represented. Results are as mean ± S.E.M from 4–8 independent experiments. Statistical significance was calculated by one way ANOVA followed by Bonferroni multiple comparison test; in b $^{**}p<0.01$ and $^{***}p<0.005$ compared with cells not transfected with siRNA, in c $^{*}p<0.05$ compared with cells only treated with quinpirole, in d $^{\&\&}p<0.01$ compared to the corresponding quinpirole-treated cells and $^{*}p<0.05$ and $^{***}p<0.005$ compared with forskolin-treated cells (100%).
doi:10.1371/journal.pone.0061245.g004

red punctate fluorescent staining was not observed when the experiments were performed with striatal slices from σ_1 KO mice (Fig. 6c and e). These data further support the existence of σ_1-D_2 receptor heteromers in the striatum.

Cocaine Binding to σ_1 Receptors Modulates the D_2 Receptor Signaling in Mouse Brain Striatum

The above data provide strong evidence of σ_1-D_2 receptor heteromers in vivo but they do not say anything about the function of these complexes. We decided to test whether the negative cross-talk seen in signaling in transfected cells could also be found in the striatum. Striatum slices from WT and KO mice were tested for the effects of cocaine on ERK 1/2 phosphorylation. In co-transfected cells a strong and significant effect of cocaine was observed at 15 μM (see Fig. 5), a striatal level of the drug reached after pharmacologically significant doses of cocaine [43]. To allow diffusion into the tissue a ten-fold higher cocaine concentration, 150 μM, was then used to see clear effects in slices of mouse striatum. Both the D_2 receptor agonist quinpirole (1 μM) and cocaine (150 μM) induced ERK 1/2 phosphorylation in striatal slices from WT mice after 10 min activation (Fig. S10) or after 30 min activation (Fig. 7a). More interestingly, in striatal slices of WT mice, the co-activation with quinpirole and cocaine

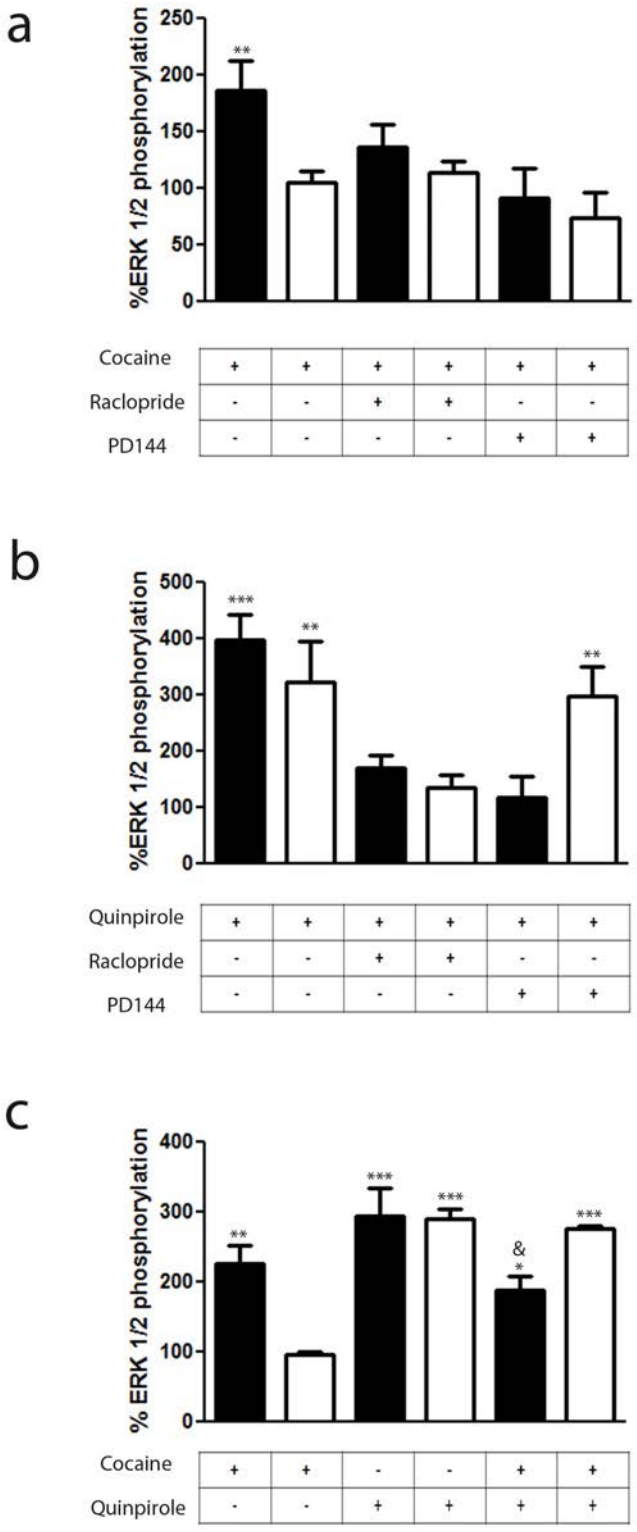

Figure 5. Cocaine binding to σ_1 receptor modulates the ERK 1/2 signaling in transfected cells. CHO cells were transfected with D_2 receptor cDNA (1 μg, black bars) or cotransfected (white bars) with D_2 receptor cDNA and σ_1 receptor siRNA (6.25 μg of oligonucleotides). Cells were incubated for 30 min (a) or 10 min (b) with medium (basal) or with 30 μM cocaine (a) or 1 μM quinpirole (b) in the absence or in the presence of 10 μM raclopride or 100 nM PD144418. In (**c**) cells were treated with medium (basal), 30 μM cocaine for 30 min, 1 μM quinpirole for 10 min or 30 μM cocaine for 30 min and, during the last 10 min, with 1 μM quinpirole. In all cases, ERK 1/2 phosphorylation is represented as percentage over basal levels (100%). Results are mean ± SEM of six to eight independent experiments performed in duplicate. Bifactorial ANOVA showed a significant (**$p<0.01$ and ***$P<0.005$) effect over basal.
doi:10.1371/journal.pone.0061245.g005

blocked ERK 1/2 phosphorylation (Figs. 7a and S10). Thus, the negative cross-talk between σ_1 and D_2 receptors on MAPK signaling detected in cotransfected cells was also observed in striatal samples from WT mice, meaning that the same biochemical fingerprint seen in transfected cells was also found in WT mice. When similar experiments were performed in striatal slices from mice lacking the σ_1 receptors, cocaine was unable to induce ERK 1/2 phosphorylation (Figs. 7a and S10) and quinpirole-induced ERK 1/2 phosphorylation was not modified by cocaine (Figs. 7a and S10). These results strongly support the existence of functional σ_1-D_2 receptor heteromers in the striatum and indicate that all detected cocaine effects are dependent on σ_1 receptors expression.

Discussion

The data presented in this paper lead to several major conclusions on the role σ_1 receptors play in modulating D_2 receptor upon cocaine exposure. First, D_2 receptors can form heteromers with σ_1 receptors, a result that is specific to D_2 receptors as the other members of the D_2-like family, D_3 and D_4 receptors, did not form heteromers. Second, these σ_1-D_2 receptor heteromers are found in mouse striatum and are functional. Third, σ_1-D_2 receptor heteromers consist of higher order oligomers with a minimal structure of σ_1-σ_1-D_2-D_2 receptor heterotetramers. Finally, cocaine, by binding to σ_1-D_2 receptor heteromers, inhibits downstream signaling in both cultured cells and in mouse striatum.

Cocaine intake elevates dopamine levels in the striatum, particularly in its more ventral part, the nucleus accumbens, which has been shown to be a preferential anatomical substrate for reward [44,45]. Cocaine exploits the dopaminergic system to elicit part of its behavioral and cellular effects [14]. Earlier studies have suggested that the presynaptic dopamine transporter (DAT) is the primary target for cocaine effects [46–49]. However, not all cocaine effects are mediated by a dopamine increase derived by the cocaine inhibition of DAT. Indeed, cocaine interacts with many proteins, and it is now well established that cocaine interacts with σ_1 receptors at physiologically relevant concentrations [50–55]. In fact, reducing brain σ_1 receptor levels with antisense oligonucleotides attenuates the convulsive and locomotor stimulant actions of cocaine [56,57] and antagonists for σ_1 receptors have also been shown to mitigate the actions of cocaine in animal models [50,58]. σ_1 receptors are highly expressed in the brain [24,59]. Within the caudate-putamen and nucleus accumbens (the dorsal and ventral parts of the striatum, respectively), brain regions that mediate the long-term effects of cocaine, it was demonstrated that repeated cocaine administration induces up-regulation of σ_1 receptors, a process mediated by dopamine D_1 receptors [60]. Indeed, we have demonstrated earlier the importance of the σ_1 and D_1 receptor interaction on the initial events upon cocaine exposure [16]. In addition, others have shown σ_1 can modulate signaling of a different GPCR family [61]. Through σ_1-D_1 receptor heteromers, cocaine robustly potentiated D_1 receptor-mediated adenylyl cyclase activation, providing a mechanism for D_1 receptor-mediated effects of cocaine [16]. In addition to DAT and D_1 receptors, our work here highlights the importance of σ_1 receptors. Our data suggest that it is σ_1 receptors that are able to

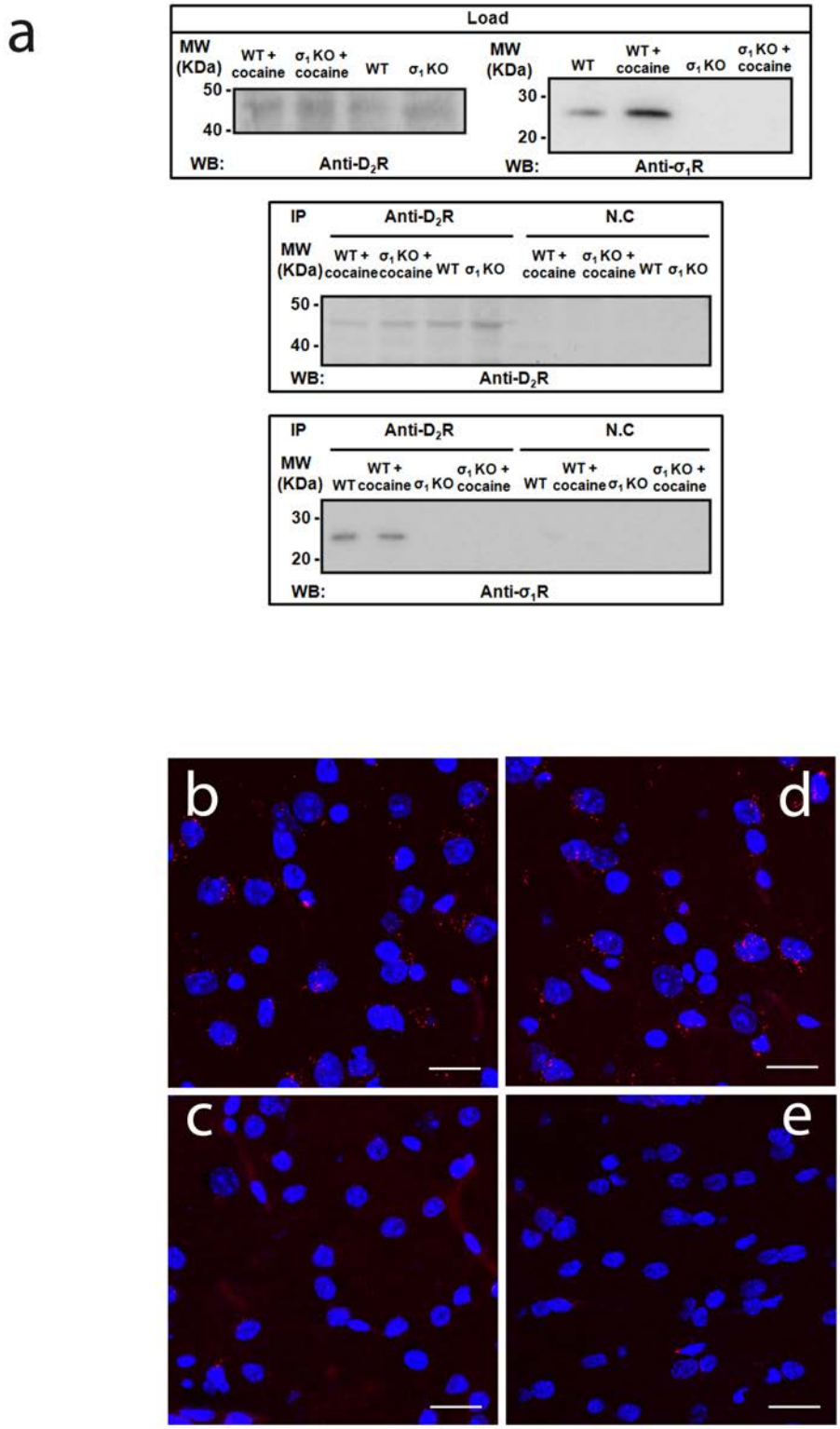

Figure 6. Expression of σ_1-D_2 receptor heteromers in the striatum. In (**a**) co-immunoprecipitation experiments are shown. Striatal slices from WT and KO mice were untreated or treated with 150 μM cocaine for 30 min. From slices solubilized striatal membranes (top panel) and immunoprecipitates with anti-D_2 receptor antibody or anti-FLAG antibody as negative control (NC) (middle and bottom panels) were analyzed by SDS-PAGE and immunoblotted using mouse anti-D_2 receptor antibody or mouse anti-σ_1 receptor antibody. IP: immunoprecipitation; WB: western blotting; MW, molecular mass. In (**b to e**) Proximity Ligation Assay (PLA) was performed as indicated in Materials and Methods, using WT (b and d) or KO (c and e) mouse striatal slices not treated (b and c) or treated (d and e) with 150 μM cocaine for 30 min. σ_1-D_2 receptor heteromers were visualized as red spots around blue colored DAPI stained nucleus. Scale bar: 20 μm.
doi:10.1371/journal.pone.0061245.g006

a

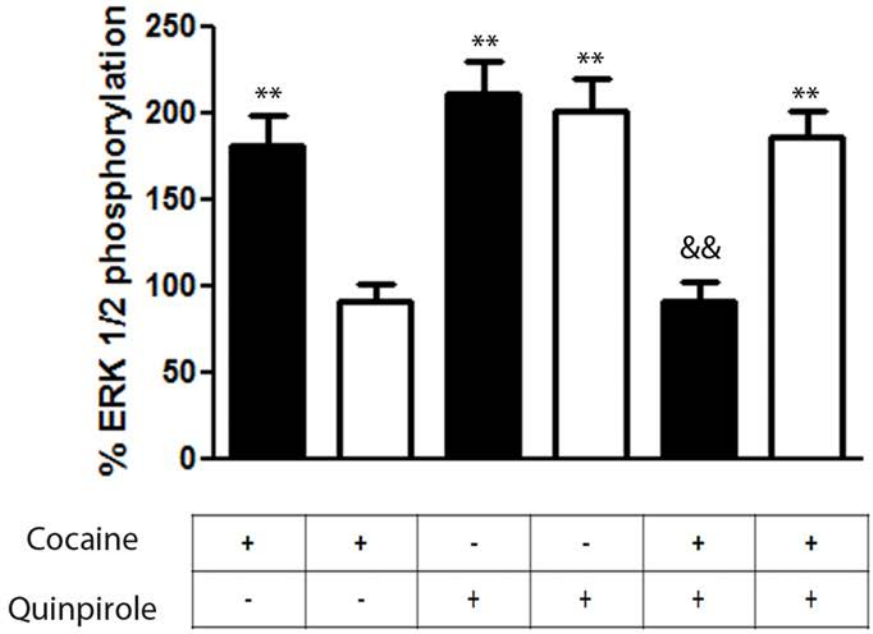
% ERK 1/2 phosphorylation
250
200
150
100
50
0
**
**
**
&&
**
Cocaine + + - - + +
Quinpirole - - + + + +

b

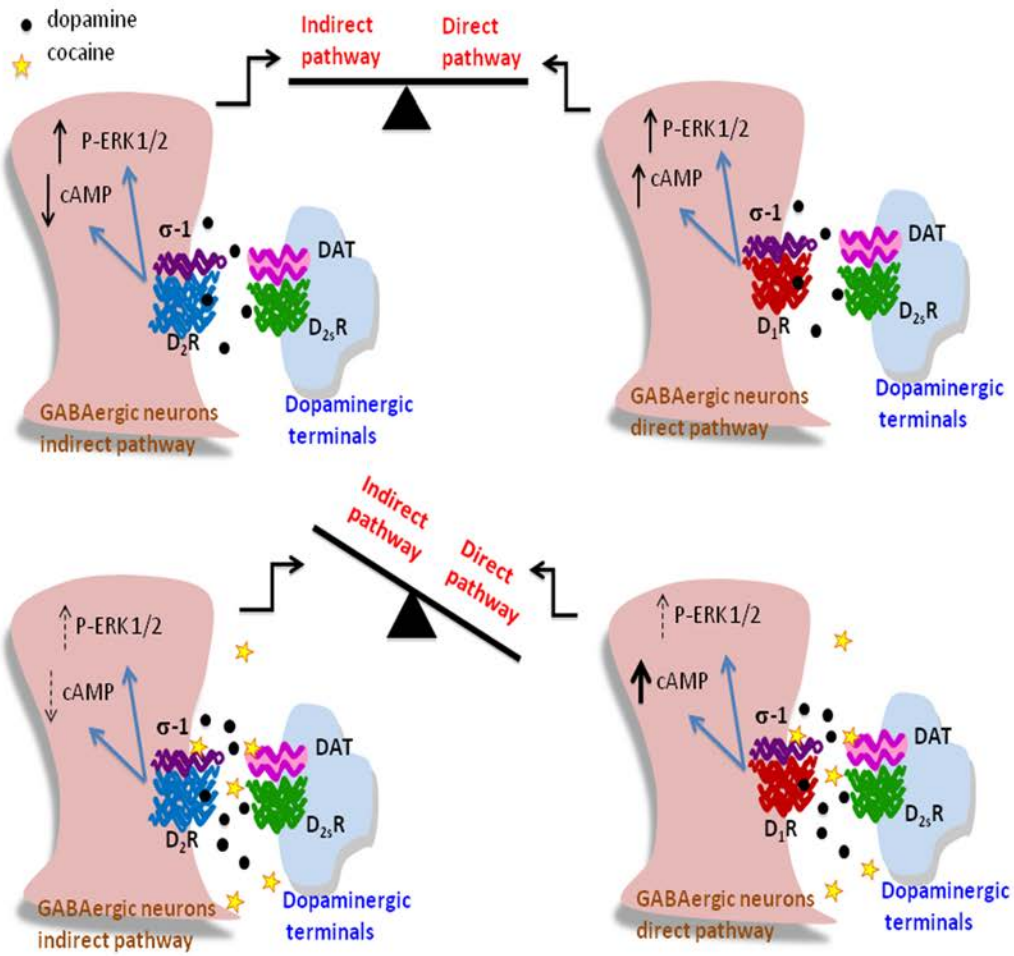
dopamine
cocaine
Indirect pathway
Direct pathway
P-ERK1/2
cAMP
σ-1
DAT
D2R
D2sR
D1R
GABAergic neurons indirect pathway
Dopaminergic terminals
GABAergic neurons direct pathway

Figure 7. Negative cross-talk between cocaine and the D_2 receptor agonist quinpirole on ERK 1/2 phosphorylation in mice striatum. In (**a**) WT (black bars) and σ_1 receptor KO (white bars) mouse striatal slices were treated with 1 μM quinpirole for 10 min, with 150 μM cocaine for 30 min or with cocaine for 30 min and, during the last 10 min, with quinpirole. Immunoreactive bands from six slices obtained from five WT or five KO animals were quantified for each condition. Values represent mean ± SEM of percentage of phosphorylation relative to basal levels found in untreated slices. No significant differences were obtained between the basal levels of the WT and the σ_1 receptor KO mice. Bifactorial ANOVA showed a significant (*$p<0.05$, **$p<0.01$, ***$p<0.005$) effect over basal. One-way ANOVA followed by Bonferroni post hoc tests showed a significant cocaine-mediated counteraction of quinpirole ($^{\&}p<0.05$, $^{\&\&}p<0.01$). In (**b**) a representative scheme summarizing the overall results is shown. Top images represent D_2 and D_1 receptors signaling in the indirect and direct striatal pathway neurons after dopamine binding. Bottom images represent the effect of cocaine increasing the dopamine by inhibiting dopamine transporters (DAT) and interacting with σ_1 receptors within σ_1-D_2 and σ_1-D_1 receptor heteromers, changing the dopamine receptor signaling.
doi:10.1371/journal.pone.0061245.g007

directly modulate the normally balanced D_1 and D_2 pathways via receptor-receptor interactions.

The cocaine effect on σ_1-D_2 receptor heteromer signaling is in contrast with the cocaine effect on σ_1-D_1 receptor heteromer signaling described by Navarro et al [16]. In the last case, the D_1 receptor-mediated activation of cAMP production was significantly increased by cocaine binding to a σ_1 protomer in the σ_1-D_1 receptor heteromers, resulting in a cocaine-induced increase in cAMP production. The results here described and those described by Navarro et al [16], point to the scenario that is shown in Figure 7b, where cocaine selectively leads to increased dopamine-induced signaling through the cAMP pathway in D_1 receptor-containing neurons and to depressed dopamine-induced inhibition of cAMP formation in D_2 receptor-containing neurons. Simultaneously, cocaine alters the levels of the initial ERK 1/2 phosphorylation signaling induced by dopamine in both D_1 receptor and D_2 receptor-containing neurons. These findings suggest that cocaine exposure leads to a deregulation of a normally balanced D_1/D_2 dopamine receptor signaling (Fig. 7b). The balance of D_1 and D_2 inputs is designed to avoid addictive behavior, thus its disruption would have long term consequences. The data presented here support a key role of σ_1 receptors in destabilizing this balance by increasing the D_1 receptor-mediated cAMP production and dampening the D_2 receptor signaling in σ_1-D_2 receptor heteromers, pushing the balance of inputs towards the D_1 containing, pro-reward and motivating pathway. Our data is supported by the results described by Durieux and colleagues where they found that striatal D_2R neurons can limit both locomotion and drug reinforcement and are organized in specific cell types [6,8]. Luo et al [9], have found in vivo evidence for the existence of D_1 and D_2 receptor-mediated cellular effects of cocaine (D_1 receptor-mediated increase in Ca^{2+} influx and D_2 receptor-mediated decrease in Ca^{2+} influx, using in vivo optical microprobe Ca^{2+} influx imaging), with significantly slower dynamics of the effect mediated by D_2 receptors. Taking into account our findings, the observations of Luo et al could in fact be linked with the signaling brake imposed by cocaine on the σ_1-D_2 receptor heteromer. Further, Ferraro et al. have found cocaine alone had no effect on striatal glutamate levels but when injected with a D_2 ligand there were significant changes [62]. Xu et al have shown that a σ_1 receptor ligand can reverse the effects of cocaine in rats strongly suggesting that blocking cocaine's actions via σ_1 receptor in σ_1-D_2 complexes could serve as an effective strategy to blunt the cellular signaling effects of cocaine [63]. Finally, Hiranita et al have shown that a combined strategy of blocking DAT and σ_1 is effective at reducing cocaine self-administration. However, in a follow up study this same group shows that after cocaine self-administration σ_1 receptor effects seem to be independent of dopamine pathways [54]. These are in line with our observations that the initial effects of cocaine disrupt the D_1/D_2 pathways. In summary, the results described here along with the highlighted previous studies support a model where the initial exposure to cocaine affects differently the direct (D_1 containing) and indirect (D_2 containing) pathways via σ_1 receptor heteromers which may significantly influence dopaminergic neurotransmission.

Supporting Information

Figure S1 Chemical structure of compounds used. a) cocaine, b) σ_1 receptor agonist PRE084, c) σ_1 receptor antagonist PD144418, d) D2 receptor agonist quinpirole, e) D2 receptor antagonist raclopride.
(TIF)

Figure S2 Effect of σ_1 receptor siRNA transfection on σ_1 receptor expression. Membranes from non-transfected HEK-293T cells (wt) or cells transfected with σ_1 receptor siRNA (6.25 μg of oligonucleotides) or irrelevant oligonucleotides (oligo, 6.25 μg of oligonucleotides) were analyzed by SDS/PAGE and immunoblotted with the anti-σ_1 receptor antibody. Values are mean ± SEM of three experiments. ***$P<0.001$ compared with non-transfected cells (one-way ANOVA followed by Bonferroni post hoc tests).
(TIF)

Figure S3 Control CellKey label-free assays. HEK-293T cells were stably transfected with the G_s protein-coupled adenosine A_{2A} receptor (a), the G_i protein-coupled adenosine A_1 receptor (b) or untransfected (c) in 96 well Cell-Key plates. Impedance changes were measured upon addition of 10 nM CGS 21680 (A_{2A} receptor agonist) in (a), 10 nM CPA (A_1 receptor agonist) in (b) or 50 nM thrombin (the agonist for the endogenous G_q protein-couples thrombin receptors) in (c). Plot shapes are consistent with the expected results for the respective G-proteins.
(TIF)

Figure S4 σ_1 receptor agonist modulates the D_2 receptor-mediated cAMP decreases. cAMP production was determined in CHO cells stable expressing D_2 receptors not transfected (black columns) or transfected (white columns) with siRNA corresponding to σ_1 receptor (6.25 μg of oligonucleotides). Cells were stimulated with 5 μM forskolin in absence (100%) or presence of 1 μM quinpirole, 100 nM PRE084 alone or in combination. Percent of cAMP produced respect to forskolin treatment was represented. Results are as mean ± S.E.M from five independent experiments. Statistical significance was calculated by one way ANOVA followed by Bonferroni multiple comparison test; ***$p<0.005$ compared with forskolin-treated cells (100%) and $^{\&\&}$ $p<0.01$ compared with the corresponding only quinpirole-treated cells.
(TIF)

Figure S5 Cocaine effect on ERK 1/2 phosphorylation in cells not expressing D_2 receptors. CHO cells were incubated with increasing cocaine concentrations for 30 min (a) or with 30 μM cocaine for increasing time periods (b). ERK1/2 phosphorylation is represented as percentage over basal levels (100%, non-treated cells). Results are mean ± SEM of three to four independent experiments performed in duplicate.

(TIF)

Figure S6 Cocaine-induced σ_1-D_2 receptor heteromer-mediated ERK 1/2 phosphorylation in transfected cells. CHO cells transfected with D_2 receptor cDNA (1 μg, black bars) or cotransfected (white bars) with D_2 receptor cDNA and σ_1 receptor siRNA (6.25 μg of oligonucleotides) were incubated with increasing cocaine concentrations for 30 min (a), with 30 μM cocaine for increasing time periods (b), with increasing quinpirole concentrations for 10 min (c) or with 1 μM quinpirole for increasing time periods (d). ERK1/2 phosphorylation is represented as percentage over basal levels (100%). Results are mean ± SEM of four to six independent experiments performed in duplicate. In all samples in (c) and (d) and samples without siRNA transfection in (a) and (b), Bifactorial ANOVA showed a significant ($p<0.01$) effect of cocaine or quinpirole over basal, and Bonferroni post hoc tests showed a significant counteraction of cocaine effect by siRNA (*$p<0.05$, **$p<0.01$ and ***$p<0.005$ compared with sample with the same treatment and with siRNA transfection).
(TIF)

Figure S7 Expression of σ_1 receptor in the striatum. WT (**a**) or σ_1 receptor KO (**b**) mouse striatal slices were processed for immunohistochemistry as indicated in Materials and Methods using an anti-σ_1 antibody. Cell nuclei were stained with DAPI (blue). Scale bar: 20 μm.
(TIF)

Figure S8 Expression of D_2 receptor in the striatum. WT (**a**) or σ_1 receptor KO (**b**) mouse striatal slices were processed for immunohistochemistry as indicated in Materials and Methods using an anti-D_2 antibody (green). Scale bar: 20 μm.
(TIF)

Figure S9 Negative controls for in situ proximity ligation assays. Negative controls for in situ proximity ligation assays (see Materials and Methods) were performed in WT mouse striatal slices incubated with only anti-σ_1 (**a**) or anti-D_2 (**b**) antibody as primary antibodies. Cell nuclei were stained with DAPI (blue). Scale bar: 20 μm.
(TIF)

Figure S10 Negative cross-talk between cocaine and the D_2 receptor agonist quinpirole on ERK 1/2 phosphorylation in mouse striatum. WT (black bars) and σ_1 receptor KO (white bars) mouse striatal slices were treated for 10 min with 1 μM quinpirole, with 150 μM cocaine or with both. Immunoreactive bands from six slices obtained from five WT or five KO animals were quantified for each condition. Values represent mean ± SEM of percentage of phosphorylation relative to basal levels found in untreated slices. No significant differences were obtained between the basal levels of the wild-type and the KO mice. Bifactorial ANOVA showed a significant (**$p<0.01$, ***$p<0.005$) effect over basal. One-way ANOVA followed by Bonferroni post hoc tests showed a significant cocaine-mediated counteraction of quinpirole ($^{\&\&\&}P<0.005$).
(TIF)

Acknowledgments

We would like to thank Jasmina Jiménez for technical help (University of Barcelona). We thank Laboratorios Esteve (Barcelona, Spain) for providing σ_1 receptor KO and WT mice brains.

Author Contributions

Conceived and designed the experiments: GN VC SF EC CL PJM. Performed the experiments: GN EM JB MB DF JM AC VC DA. Analyzed the data: GN EM VC SF EC CL PJM. Contributed reagents/materials/analysis tools: RF EC. Wrote the paper: EC SF CL PJM.

References

1. Kreitzer AC, Malenka RC (2008) Striatal plasticity and basal ganglia circuit function. Neuron 60: 543–554. doi:10.1016/j.neuron.2008.11.005.
2. Gerfen CR, Engber TM, Mahan LC, Susel Z, Chase TN, et al. (1990) D1 and D2 dopamine receptor-regulated gene expression of striatonigral and striatopallidal neurons. Science 250: 1429–1432.
3. Schiffmann SN, Vanderhaeghen JJ (1993) Adenosine A2 receptors regulate the gene expression of striatopallidal and striatonigral neurons. J Neurosci 13: 1080–1087.
4. Kalivas PW, Volkow ND (2005) The neural basis of addiction: a pathology of motivation and choice. Am J Psychiatry 162: 1403–1413. doi:10.1176/appi.ajp.162.8.1403.
5. Di Chiara G, Bassareo V (2007) Reward system and addiction: what dopamine does and doesn't do. Current Opinion in Pharmacology 7: 69–76. doi:10.1016/j.coph.2006.11.003.
6. Durieux PF, Schiffmann SN, De Kerchove d'Exaerde A (2012) Differential regulation of motor control and response to dopaminergic drugs by D1R and D2R neurons in distinct dorsal striatum subregions. EMBO J 31: 640–653. doi:10.1038/emboj.2011.400.
7. Xu M, Hu X-T, Cooper DC, Moratalla R, Graybiel AM, et al. (1994) Elimination of cocaine-induced hyperactivity and dopamine-mediated neurophysiological effects in dopamine D1 receptor mutant mice. Cell 79: 945–955. doi:16/0092-8674(94)90026-4.
8. Durieux PF, Bearzatto B, Guiducci S, Buch T, Waisman A, et al. (2009) D2R striatopallidal neurons inhibit both locomotor and drug reward processes. Nat Neurosci 12: 393–395. doi:10.1038/nn.2286.
9. Luo Z, Volkow ND, Heintz N, Pan Y, Du C (2011) Acute Cocaine Induces Fast Activation of D1 Receptor and Progressive Deactivation of D2 Receptor Striatal Neurons: In Vivo Optical Microprobe [Ca2+]i Imaging. The Journal of Neuroscience 31: 13180–13190. doi:10.1523/JNEUROSCI.2369-11.2011.
10. Welter M, Vallone D, Samad TA, Meziane H, Usiello A, et al. (2007) Absence of dopamine D2 receptors unmasks an inhibitory control over the brain circuitries activated by cocaine. Proceedings of the National Academy of Sciences of the United States of America 104: 6840–6845.
11. Rougé-Pont F, Usiello A, Benoit-Marand M, Gonon F, Vincenzo Piazza P, et al. (2002) Changes in extracellular dopamine induced by morphine and cocaine: Crucial control by D2 receptors. Journal of Neuroscience 22: 3293–3301.
12. Krawczyk M, Sharma R, Mason X, DeBacker J, Jones AA, et al. (2011) A Switch in the Neuromodulatory Effects of Dopamine in the Oval Bed Nucleus of the Stria Terminalis Associated with Cocaine Self-Administration in Rats. The Journal of Neuroscience 31: 8928–8935. doi:10.1523/JNEUROSCI.0377-11.2011.
13. Thompson D, Martini L, Whistler JL (2010) Altered ratio of D1 and D2 dopamine receptors in mouse striatum is associated with behavioral sensitization to cocaine. PLoS ONE 5: e11038. doi:10.1371/journal.pone.0011038.
14. De Mei C, Ramos M, Iitaka C, Borrelli E (2009) Getting specialized: presynaptic and postsynaptic dopamine D2 receptors. Curr Opin Pharmacol 9: 53–58. doi:10.1016/j.coph.2008.12.002.
15. Beuming T, Kniazeff J, Bergmann ML, Shi L, Gracia L, et al. (2008) The binding sites for cocaine and dopamine in the dopamine transporter overlap. Nat Neurosci 11: 780–789. doi:10.1038/nn.2146.
16. Navarro G, Moreno E, Aymerich M, Marcellino D, McCormick PJ, et al. (2010) Direct involvement of sigma-1 receptors in the dopamine D1 receptor-mediated effects of cocaine. Proc Natl Acad Sci USA 107: 18676–18681. doi:10.1073/pnas.1008911107.
17. Canals M, Marcellino D, Fanelli F, Ciruela F, De Benedetti P, et al. (2003) Adenosine A2A-Dopamine D2 Receptor-Receptor Heteromerization. Journal of Biological Chemistry 278: 46741–46749. doi:10.1074/jbc.M306451200.
18. González S, Moreno-Delgado D, Moreno E, Pérez-Capote K, Franco R, et al. (2012) Circadian-Related Heteromerization of Adrenergic and Dopamine D4 Receptors Modulates Melatonin Synthesis and Release in the Pineal Gland. PLoS Biol 10: e1001347. doi:10.1371/journal.pbio.1001347.
19. Carriba P, Navarro G, Ciruela F, Ferré S, Casadó V, et al. (2008) Detection of heteromerization of more than two proteins by sequential BRET-FRET. Nat Methods 5: 727–733. doi:10.1038/nmeth.1229.
20. Langa F, Codony X, Tovar V, Lavado A, Giménez E, et al. (2003) Generation and phenotypic analysis of sigma receptor type I (sigma 1) knockout mice. European Journal of Neuroscience 18: 2188–2196. doi:10.1046/j.1460-9568.2003.02950.x.
21. Moreno E, Hoffmann H, Gonzalez-Sepúlveda M, Navarro G, Casadó V, et al. (2011) Dopamine D1-histamine H3 receptor heteromers provide a selective link to MAPK signaling in GABAergic neurons of the direct striatal pathway. J Biol Chem 286: 5846–5854. doi:10.1074/jbc.M110.161489.

22. Moreno E, Vaz SH, Cai N-S, Ferrada C, Quiroz C, et al. (2011) Dopamine-Galanin Receptor Heteromers Modulate Cholinergic Neurotransmission in the Rat Ventral Hippocampus. J Neurosci 31: 7412–7423. doi:10.1523/JNEUROSCI.0191-11.2011.
23. Schroder R, Schmidt J, Blattermann S, Peters L, Janssen N, et al. (2011) Applying label-free dynamic mass redistribution technology to frame signaling of G protein-coupled receptors noninvasively in living cells. Nat Protocols 6: 1748–1760. doi:10.1038/nprot.2011.386.
24. Hayashi T, Su T (2005) The sigma receptor: evolution of the concept in neuropsychopharmacology. Curr Neuropharmacol 3: 267–280.
25. Kourrich S, Su T-P, Fujimoto M, Bonci A (2012) The sigma-1 receptor: roles in neuronal plasticity and disease. Trends Neurosci 35: 762–771. doi:10.1016/j.tins.2012.09.007.
26. Ng GYK, O'Dowd BF, Lee SP, Chung HT, Brann MR, et al. (1996) Dopamine D2 Receptor Dimers and Receptor-Blocking Peptides. Biochemical and Biophysical Research Communications 227: 200–204. doi:06/bbrc.1996.1489.
27. Lee SP, O'Dowd BF, Ng GYK, Varghese G, Akil H, et al. (2000) Inhibition of Cell Surface Expression by Mutant Receptors Demonstrates that D2 Dopamine Receptors Exist as Oligomers in the Cell. Molecular Pharmacology 58: 120–128.
28. Armstrong D, Strange PG (2001) Dopamine D2 Receptor Dimer Formation. Journal of Biological Chemistry 276: 22621–22629. doi:10.1074/jbc.M006936200.
29. Guo W, Shi L, Javitch JA (2003) The Fourth Transmembrane Segment Forms the Interface of the Dopamine D2 Receptor Homodimer. Journal of Biological Chemistry 278: 4385–4388. doi:10.1074/jbc.C200679200.
30. Guo W, Urizar E, Kralikova M, Mobarec JC, Shi L, et al. (2008) Dopamine D2 receptors form higher order oligomers at physiological expression levels. EMBO J 27: 2293–2304. doi:10.1038/emboj.2008.153.
31. Sharkey J, Glen KA, Wolfe S, Kuhar MJ (1988) Cocaine binding at [sigma] receptors. European Journal of Pharmacology 149: 171–174. doi:16/0014-2999(88)90058-1.
32. Maurice T, Su T-P (2009) The pharmacology of sigma-1 receptors. Pharmacol Ther 124: 195–206. doi:10.1016/j.pharmthera.2009.07.001.
33. Luttrell LM, Ferguson SS, Daaka Y, Miller WE, Maudsley S, et al. (1999) Beta-arrestin-dependent formation of beta2 adrenergic receptor-Src protein kinase complexes. Science 283: 655–661.
34. Shenoy SK, Lefkowitz RJ (2003) Multifaceted roles of beta-arrestins in the regulation of seven-membrane-spanning receptor trafficking and signalling. Biochem J 375: 503–515. doi:10.1042/BJ20031076.
35. Beaulieu J-M, Sotnikova TD, Marion S, Lefkowitz RJ, Gainetdinov RR, et al. (2005) An Akt/[beta]-Arrestin 2/PP2A Signaling Complex Mediates Dopaminergic Neurotransmission and Behavior. Cell 122: 261–273. doi:10.1016/j.cell.2005.05.012.
36. Shenoy SK, Drake MT, Nelson CD, Houtz DA, Xiao K, et al. (2006) beta-arrestin-dependent, G protein-independent ERK1/2 activation by the beta2 adrenergic receptor. J Biol Chem 281: 1261–1273.
37. DeWire SM, Ahn S, Lefkowitz RJ, Shenoy SK (2007) β-Arrestins and Cell Signaling. Annu Rev Physiol 69: 483–510. doi:10.1146/annurev.physiol.69.022405.154749.
38. Valjent E, Corvol J-C, Pages C, Besson M-J, Maldonado R, et al. (2000) Involvement of the Extracellular Signal-Regulated Kinase Cascade for Cocaine-Rewarding Properties. J Neurosci 20: 8701–8709.
39. Lu L, Koya E, Zhai H, Hope B, Shaham Y (2006) Role of ERK in cocaine addiction. Trends in Neurosciences 29: 695–703. doi:10.1016/j.tins.2006.10.005.
40. Lobo MK, Covington HE, Chaudhury D, Friedman AK, Sun H, et al. (2010) Cell Type-Specific Loss of BDNF Signaling Mimics Optogenetic Control of Cocaine Reward. Science 330: 385–390. doi:10.1126/science.1188472.
41. Hoffmann HM, Nadal R, Vignes M, Ortiz J (2012) Chronic cocaine self-administration modulates ERK1/2 and CREB responses to dopamine receptor agonists in striatal slices. Addict Biol 17: 565–575. doi:10.1111/j.1369-1600.2011.00353.x.
42. Callén L, Moreno E, Barroso-Chinea P, Moreno-Delgado D, Cortés A, et al. (2012) Cannabinoid Receptors CB1 and CB2 Form Functional Heteromers in Brain. J Biol Chem 287: 20851–20865. doi:10.1074/jbc.M111.335273.
43. Pettit HO, Pan HT, Parsons LH, Justice JB Jr (1990) Extracellular concentrations of cocaine and dopamine are enhanced during chronic cocaine administration. J Neurochem 55: 798–804.
44. Koob GF (2006) The neurobiology of addiction: a neuroadaptational view relevant for diagnosis. Addiction 101 Suppl 1: 23–30. doi:10.1111/j.1360-0443.2006.01586.x.
45. Di Chiara G, Bassareo V (2007) Reward system and addiction: what dopamine does and doesn't do. Curr Opin Pharmacol 7: 69–76. doi:10.1016/j.coph.2006.11.003.
46. Ritz MC, Lamb RJ, Goldberg SR, Kuhar MJ (1987) Cocaine receptors on dopamine transporters are related to self-administration of cocaine. Science 237: 1219–1223.
47. Giros B, Jaber M, Jones SR, Wightman RM, Caron MG (1996) Hyperlocomotion and indifference to cocaine and amphetamine in mice lacking the dopamine transporter. Nature 379: 606–612. doi:10.1038/379606a0.
48. Chen R, Tilley MR, Wei H, Zhou F, Zhou F-M, et al. (2006) Abolished cocaine reward in mice with a cocaine-insensitive dopamine transporter. Proc Natl Acad Sci USA 103: 9333–9338. doi:10.1073/pnas.0600905103.
49. Ferragud A, Velázquez-Sánchez C, Hernández-Rabaza V, Nácher A, Merino V, et al. (2009) A dopamine transport inhibitor with markedly low abuse liability suppresses cocaine self-administration in the rat. Psychopharmacology (Berl) 207: 281–289. doi:10.1007/s00213-009-1653-x.
50. Matsumoto RR, Liu Y, Lerner M, Howard EW, Brackett DJ (2003) Sigma receptors: potential medications development target for anti-cocaine agents. Eur J Pharmacol 469: 1–12.
51. Cobos EJ, Entrena JM, Nieto FR, Cendán CM, Del Pozo E (2008) Pharmacology and therapeutic potential of sigma(1) receptor ligands. Curr Neuropharmacol 6: 344–366. doi:10.2174/157015908787386113.
52. Kourrich S, Hayashi T, Chuang J-Y, Tsai S-Y, Su T-P, et al. (2013) Dynamic Interaction between Sigma-1 Receptor and Kv1.2 Shapes Neuronal and Behavioral Responses to Cocaine. Cell 152: 236–247. doi:10.1016/j.cell.2012.12.004.
53. Hiranita T, Soto PL, Tanda G, Katz JL (2010) Reinforcing Effects of σ-Receptor Agonists in Rats Trained to Self-Administer Cocaine. Journal of Pharmacology and Experimental Therapeutics 332: 515–524. doi:10.1124/jpet.109.159236.
54. Hiranita T, Mereu M, Soto PL, Tanda G, Katz JL (2013) Self-administration of cocaine induces dopamine-independent self-administration of sigma agonists. Neuropsychopharmacology 38: 605–615. doi:10.1038/npp.2012.224.
55. Katz JL, Su T-P, Hiranita T, Hayashi T, Tanda G, et al. (2011) A Role for Sigma Receptors in Stimulant Self Administration and Addiction. Pharmaceuticals (Basel) 4: 880–914. doi:10.3390/ph4060880.
56. Matsumoto RR, McCracken KA, Friedman MJ, Pouw B, De Costa BR, et al. (2001) Conformationally restricted analogs of BD1008 and an antisense oligodeoxynucleotide targeting sigma1 receptors produce anti-cocaine effects in mice. Eur J Pharmacol 419: 163–174.
57. Matsumoto RR, McCracken KA, Pouw B, Zhang Y, Bowen WD (2002) Involvement of sigma receptors in the behavioral effects of cocaine: evidence from novel ligands and antisense oligodeoxynucleotides. Neuropharmacology 42: 1043–1055.
58. Hiranita T, Soto PL, Kohut SJ, Kopajtic T, Cao J, et al. (2011) Decreases in cocaine self-administration with dual inhibition of the dopamine transporter and σ receptors. J Pharmacol Exp Ther 339: 662–677. doi:10.1124/jpet.111.185025.
59. Alonso G, Phan V, Guillemain I, Saunier M, Legrand A, et al. (2000) Immunocytochemical localization of the sigma(1) receptor in the adult rat central nervous system. Neuroscience 97: 155–170.
60. Zhang D, Zhang L, Tang Y, Zhang Q, Lou D, et al. (2005) Repeated cocaine administration induces gene expression changes through the dopamine D1 receptors. Neuropsychopharmacology 30: 1443–1454. doi:10.1038/sj.npp.1300680.
61. Kim FJ, Kovalyshyn I, Burgman M, Neilan C, Chien C-C, et al. (2010) Sigma 1 receptor modulation of G-protein-coupled receptor signaling: potentiation of opioid transduction independent from receptor binding. Mol Pharmacol 77: 695–703. doi:10.1124/mol.109.057083.
62. Ferraro L, Frankowska M, Marcellino D, Zaniewska M, Beggiato S, et al. (2012) A novel mechanism of cocaine to enhance dopamine d2-like receptor mediated neurochemical and behavioral effects. An in vivo and in vitro study. Neuropsychopharmacology 37: 1856–1866. doi:10.1038/npp.2012.33.
63. Xu Y-T, Robson MJ, Szeszel-Fedorowicz W, Patel D, Rooney R, et al. (2012) CM156, a sigma receptor ligand, reverses cocaine-induced place conditioning and transcriptional responses in the brain. Pharmacol Biochem Behav 101: 174–180. doi:10.1016/j.pbb.2011.12.016.

Figure S1

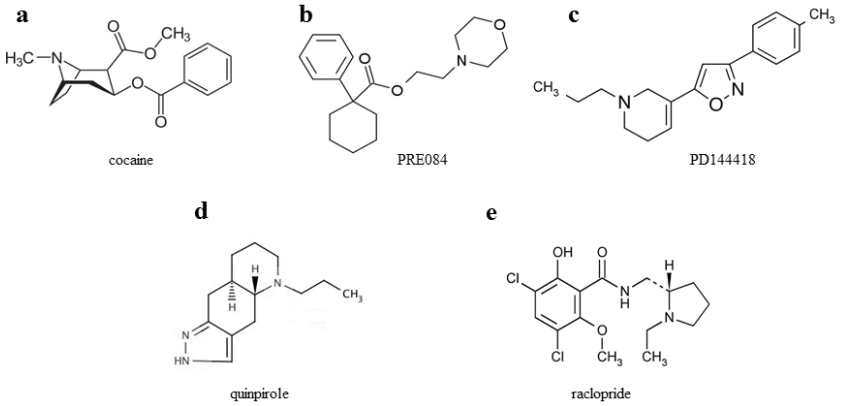

Figure S1. Chemical structure of compounds used. a) cocaine, **b)** σ1 receptor agonist PRE084, **c)** σ1 receptor antagonist PD144418, **d)** D_2 receptor agonist quinpirole, **e)** D_2 receptor antagonist raclopride.

Figure S2

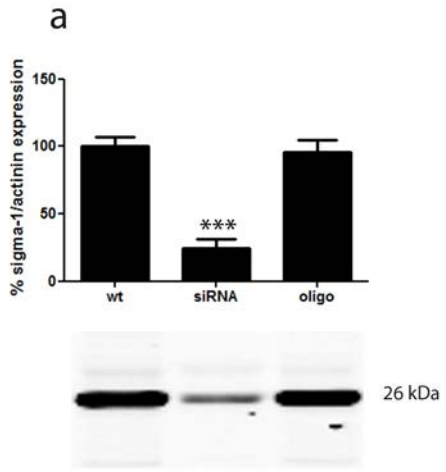

Figure S3

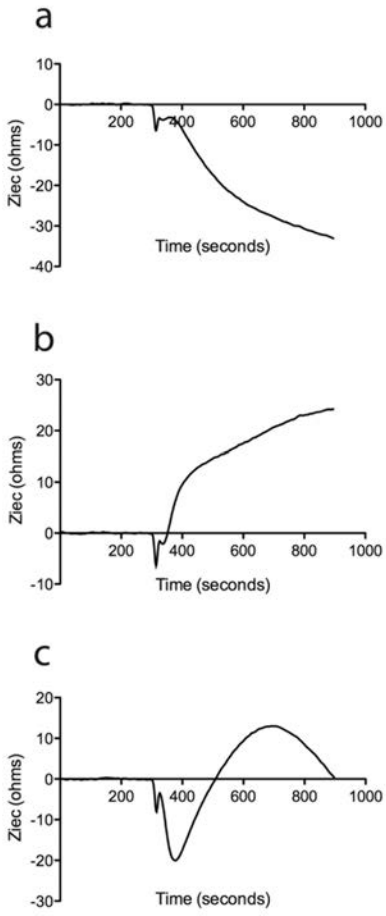

Figure S4

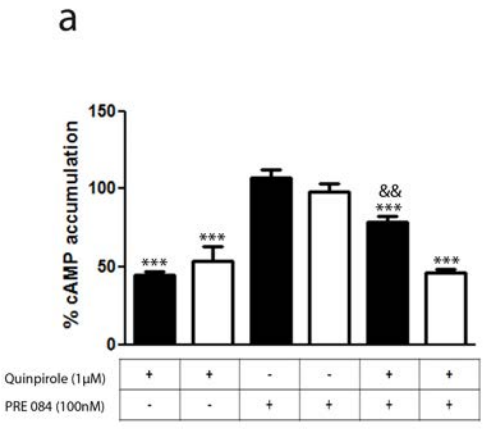

Figure S5

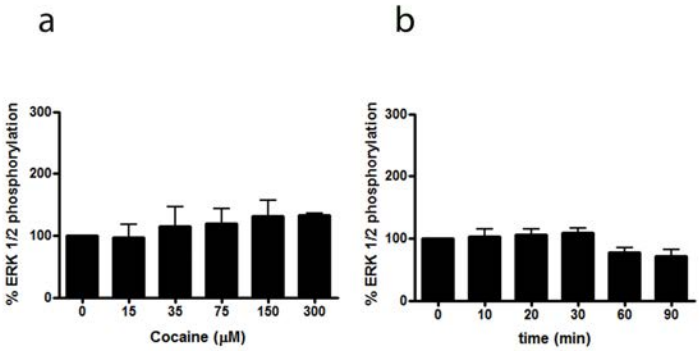

Figure S6

Figure S7

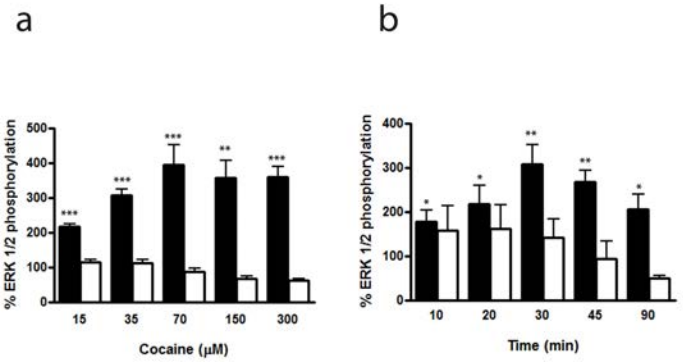

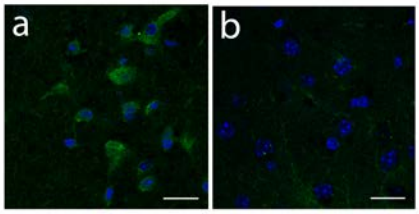

Figure S8

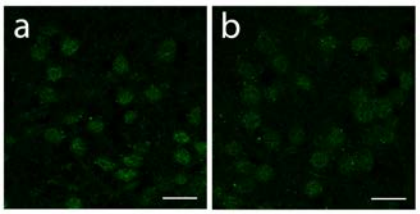

Figure S9

Figure S10

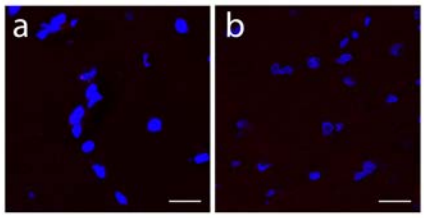

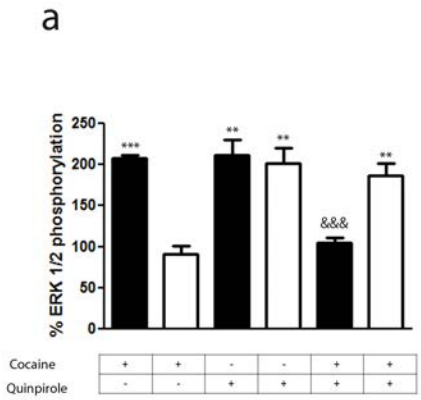

3.2. SIGMA-2 RECEPTORS MEDIATE COCAINE EFFECTS ON DOPAMINE D_1 RECEPTOR SIGNALING

David Aguinaga, Mireia Medrano, Ignacio Vega-Quiroga, Katia Gysling, Enric I. Canela, Gemma Navarro[*] y Rafael Franco[*].

[*]Coautores del manuscrito

Manuscrito en preparación para ser enviado a *Molecular Psychiatry*.

Los receptores sigma σ_1 y σ_2 son dianas de la cocaína. A pesar de compartir un nombre similar, los dos receptores no están relacionados estructuralmente y su papel fisiológico no se conoce aún. La cocaína aumenta los niveles de dopamina en el sistema motor y el de la recompensa en los que la dopamina es uno de los principales neurotransmisores. La droga también afecta a la señalización dopaminérgica mediante modificaciones alostéricas ejercidas por el σ_1R al interaccionar con los receptores D_1 y D_2 de dopamina. En este trabajo ha sido demostrado que el receptor σ_2 puede formar complejos heteroméricos con D_1R, pero no con D_2R. Sorprendentemente, los receptores σ_1, σ_2 y D_1 pueden formar heterotrímeros con propiedades particulares de señalización. La determinación de los niveles de AMPc y activación de MAP quinasas y los ensayos de Label-Free demuestran la existencia de interacciones alostéricas dentro del trímero. Es importante destacar que la presencia de σ_2R induce una transducción de señal sesgada (*biased*) ya que ligandos de σ_2R incrementan la señalización por AMPc mientras que reducen la activación de las MAP quinasas. Además, el efecto de σ_2R es opuesto al de σ_1R, sugiriendo que la señalización mediada por el receptor D_1 depende del equilibrio de la expresión de los receptores sigma y del grado de formación del trímero. Aunque el papel fisiológico es desconocido, el complejo heteromérico formado por los receptores σ_1, σ_2 y D_1 aparece como un mecanismo relevante para transmitir las acciones de la cocaína en los circuitos motores y de recompensa.

SIGMA-2 RECEPTORS MEDIATE COCAINE EFFECTS ON DOPAMINE D_1 RECEPTOR SIGNALING

David Aguinaga[1,2], Mireia Medrano[1,2], Ignacio Vega-Quiroga[4], Katia Gysling[4], Enric I. Canela[1,2], Gemma Navarro[1,3]* and Rafael Franco[1,2]*

[1]*Centro de Investigación en Red, Enfermedades Neurodegenerativas (CIBERNED). Instituto de Salud Carlos III. Madrid. Spain.*
[2]*Department of Biochemistry and Molecular Biomedicine. School of Biology. Universitat de Barcelona. Barcelona. Spain.*
[3]*Department of Biochemistry and Physiology. Faculty of Pharmacy. Universitat de Barcelona. Barcelona. Spain.*
[4]*Department of Cellular and Molecular Biology. Faculty of Biological Sciences. Pontificia Universidad Católica de Chile. Santiago. Chile.*

Corresponding author: Gemma Navarro, g.navarro@ub.edu

School of Pharmacy. Universitat de Barcelona. Diagonal 643.

Tel +34 934021213

SUMMARY

Sigma σ_1 and σ_2 receptors are targets of cocaine. Despite sharing a similar name the two receptors are structurally unrelated and their physiological role is not known. Cocaine increases dopamine levels in motor and reward central in which dopamine is one of the main neurotransmitters. The drug also affects dopaminergic signaling by allosteric modulations exerted by σ_1R interacting with dopamine D_1 and D_2 receptors. We here demonstrate that σ_2R may form heteroreceptor complexes with D_1 but not with D_2 receptors. Remarkably σ_1, σ_2 and D1 receptors may form heterotrimers with particular signaling properties. Determination of cAMP levels, and MAP kinase activation and label-free assays demonstrate allosteric interactions within the trimer. Importantly, the presence of σ_2R induces bias in signal transduction as σ_2R ligands increase cAMP signaling whereas reduce MAP kinase activation. Moreover, the effect of σ_2R is opposite to that of σ_1R, thus suggesting that the D_1 receptor-mediated signaling depends on the balance of sigma receptor expression and the degree of trimer formation. Although the physiological role is unknown the heteroreceptor complex formed by σ_1, σ_2 and D_1 receptors arise as relevant to convey the cocaine actions on motor control and reward circuits.

INTRODUCTION

Cocaine addiction is one of the major health and socio-economic problems in advanced societies. Cocaine consumption starts recreationally and the seeking behavior is sustained by an overall wellness sensation. Drug addiction results from plastic changes in brain areas having dopamine as main neurotransmitter, in particular in the *ventral tegmental area* (VTA). Importantly, the main consequence at the central nervous system (CNS) of cocaine consumption is an increase in the interneuronal dopamine levels, which is not restricted to the VTA but extends to other structures such as the basal ganglia. Inhibition of dopamine transporters was thought to be at the root of all the effects caused by this drug of abuse. However, there is solid evidence demonstrating that cocaine exerts effects by interacting sigma receptors. Two different sigma receptors have been identified. Despite the endogenous ligands are not known, despite the exact physiological role of sigma receptors is not known and despite their different structure, these receptors share the ability to bind cocaine. The interaction of sigma-1 (σ_1R) and the modulation of dopaminergic signaling by cocaine-σ_1R with dopamine receptors have been reported. In contrast, no study has been undertaking to know whether cocaine binding to σ_2R results in dopaminergic regulation.

The role of σ_1R as relevant target of cocaine was suspected due to the moderate affinity of the binding of the drug to the receptor (Matsumoto, et al., 2003; Hayashi and Su, 2005). It therefore appears that "physiologically" relevant concentrations of cocaine may both inhibit dopamine uptake and activate σ_1R. σ_1R is involved in the triggering of locomotor and convulsive actions of cocaine (Menkel, et al., 1991; Matsumoto, et al., 2001; Matsumoto, et al., 2002; Barr, et al., 2015). Furthermore, synthetic drugs acting as agonists and antagonists of σ_1R, respectively, potentiate (Matsumoto, et al., 2002; Matsumoto, et al., 2003) and reduce (Matsumoto, et al., 2004) cocaine actions. More recent studies have identified in both heterologous expression systems and natural sources an interaction between σ_1R and dopamine receptors (Navarro, et al., 2010; Moreno, et al., 2014). In 2007, Matsumoto et al. reported that treatment with synthetic drugs acting on σ_2R attenuated some of the effects of cocaine-induced behavior in mice (Matsumoto, et al., 2007). Although the selectivity od the compounds was poor, one year later Mésangeau et al. designed an approach to convert selective σ_1R ligands to σ_2R selective ligands that, importantly, showed anti-cocaine activity (Mésangeau, et al., 2008). Furthermore, it has been recently observed that treatment with σ_2R antagonists is capable of counteracting cocaine-induced locomotor stimulation in mice (Lever, et al., 2014) (Guo and Zhen, et al., 2015).

One important physiological consequence of cocaine intake is an increase in motor activity, which is controlled by the brain regions within the basal ganglia. Motor control is exerted by the direct and indirect pathways of basal ganglia and associated nuclei. Of the five types of dopamine receptors, the D_1 (D_1R) is enriched in the direct pathway whereas the D_2 (D_2R) is enriched in the indirect one. The balance of dopaminergic input in the two circuits results in fine tuning motor control. Locomotor hyperactivity resulting from cocaine consumption is likely reflecting a lack of balance in the two before mentioned circuits. The aim of this paper was to investigate how cocaine binding to σ_2R affects dopaminergic D_1R- and/or D_2R-medaited signaling. We first investigated whether σ_2R might interact with D_1R or with an D_2R and, subsequently, we assayed how cocaine could affect in a σ_1R-independent but σ_2R-dependent way the signal transduction triggered by agonist activation of D_1R or D_2R.

RESULTS

σ_2R may form heteromeric complexes with dopamine D_1 but not with dopamine D_2 receptors

Two different sigma receptors have been described, the non-opioid receptor, σ_1R, and the PGRMC-1 protein, also known as σ_2R. Despite the endogenous ligands are not known, the two sigma receptors may bind cocaine. While recent studies have demonstrated that σ_1R is involved in cocaine modulation of dopamine receptors function, a similar study on σ_2R-mediated modulation of dopaminergic signaling is lacking. We first evaluated in a heterologous expression system whether σ_2R may colocalize with dopamine receptors at the plasma membrane. Immunocytochemistry assays was undertaken in HEK-293T cells transfected expressing σ_2R fused to RLuc (1 μg cDNA) and either dopamine D_1R fused to YFP (1 μg cDNA) or dopamine D_2R fused to YFP (1 μg cDNA). The σ_2R expression was identified by a specific antibody against RLuc protein and a secondary Cy3 antibody while dopamine receptor-YFP expression was identified by the own fluorescence. D_1R (green) was detectable at the plasma membrane level while σ_2R (red) was expressed mainly both in intracellular structures and at the plasma membrane, where it colocalized (yellow) with D_1R. When a similar experiment was developed with D_2R, similar results were obtained indicating that D_2R and σ_2R colocalize in cell surface (Fig 1A). When the Immunocytochemical assays were performed in cells treated with cocaine 30 μM for 1 h previous to developing the experiment the level of colocalization between σ_2R and D_1R or D_2R was similar, indicating that cocaine pretreatment did not affect cell surface σ_2R and D_1R or D_2R expression and colocalization. Next, we determined whether σ_2R may form heteromeric complexes with dopamine D_1 or D_2 receptors. For this purpose, we took advantage of energy transfer assays and of *in situ* proximity ligation assays (PLA), which allows the identification of close proximity between two proteins (<17 nm) (Trifilieff et al., 2011). For PLA, HEK-293T cells expressing σ_2R (2 μg cDNA) and either D_1R (1 μg cDNA) or D_2R (1 μg cDNA) were treated with specific primary antibodies against σ_2R and against each of the dopamine receptors. Interestingly, the red punctuated signal around Hoechst-stained nuclei was much higher for D_1R and σ_2R (82% of stained cells) than for D_2R and σ_2R (27% of stained cells) (Fig 1B). Finally, we developed bioluminescence energy transfer assays in HEK-293T cells were transfected with 0.3 μg cDNA for D_1R-Rluc or 0.25 μg cDNA for D_2R-Rluc and increasing amounts of cDNA for σ_2R-YFP (0.5 to 4 μg). Interestingly, a saturable BRET curve was obtained ($BRET_{max}$ 50±3, $BRET_{50}$ 190±40) (Fig 2A) indicating a specific interaction between D_1R-σ_2R; in contrast, a linear signal was obtained between D_2R-σ_2R (Fig 2B) suggesting a lack of interaction between them. When the same experiments were realized in the presence of cocaine pretreatment for 1 h, similar results for the D_1R-Rluc/σ_2R-YFP donor/acceptor pair were obtained ($BRET_{max}$ 82 ± 10, $BRET_{50}$ 675 ± 201), indicating that cocaine does not affect the interaction.

Dopamine D_1R, σ_1R and σ_2R may form heterotrimeric complexes

Dopamine D_1 and σ_1 receptors may form heteromeric complexes in HEK-293T cells (Navarro et al 2010). To confirm that in our experimental conditions D_1R-Rluc (0.3 μg cDNA) may act as a donor of σ_1R-YFP (0.5 to 4.5 μg cDNA), BRET experiments were undertaken in co-transfected HEK-293T cells. A saturable curve was obtained indicating the interaction between σ_1R and D_1R. We then hypothesized that σ_1R and

σ_2R could be interacting together. Accordingly, BRET assays were performed in HEK-293T cells expressing a constant amount of σ_1R-Rluc (0.1 µg cDNA) and increasing amounts of σ_2R-YFP (1 to 6 µg cDNA). The unspecific linear signal obtained suggested that no interaction was occurring between the two sigma receptors. We then performed assays to investigated whether σ_1R and σ_2R competed for the binding to D_1R. BRET experiments were then developed in HEK-293T cells expressing a constant amount of σ_1R-Rluc (0.1 µg cDNA) and D_1-YFP (1.5 µg cDNA) and increasing amounts of non-fused σ_2R (0 to 5 µg cDNA). The results indicated that σ_2R was not able to displace σ_1R from the heteromer since the energy transfer between donor and acceptor was not altered (Fig. 2E). When a similar experiment was performed expressing a constant amount of D_1-Rluc (0.05 µg cDNA) and of σ_2R-YFP (0.3 µg cDNA) and increasing amounts of non-fused σ_1R (0 to 5 µg cDNA), the results indicated that low expression levels of σ_1R increase BRET signal, however, at high expression levels of σ_1R it is able to displace the σ_2R out of the heteromer, since a significative decrease in BRET signal is observed (Fig 2F). This result could reflect the formation of D_1R-σ_1R-σ_2R heterotrimeric complexes, where the interaction of σ_2R to the σ_1R-D_1R complex could create a structural change in turn leading to increasing the energy transfer between Rluc and YFP. Finally, Sequential Resonance Energy Transfer (SRET) assay, which permits detection of trimers (Carriba, et al., 2008), was developed in HEK-293T cells expressing a constant amount of σ_1R-Luc (0.2 µg cDNA) and of D_1R-YFP (1.5 µg cDNA) and increasing amounts of σ_2R-cherry (0.5 to 4 µg cDNA). The saturable SRET curve indicate that formation of σ_1R-D_1R-σ_2R heteromeric complexes is possible (Fig 2G, H).

σ_2R activation blocks dopamine D_1R signaling

The next aim was to characterize the functionality of the σ_1R-D_1R-σ_2R heterotrimer structure in HEK-293T cells treated with cocaine. It should be noted that σ_1R (Navarro, et al., 2010) and σ_2R (Johannessen, et al., 2011) are endogenously expressed levels in HEK-293T cells and, consequently, we used a siRNA approach to silence σ_1R or σ_2R expression thus impeding heterotrimer formation. When HEK-293T cells were transfected with D_1R and siRNA for σ_1R, the SKF-81297-induced increase in cAMP levels was inhibited by pre-treatment with cocaine 30 µM or with PB-28 (300 nM), indicating that cocaine decreases D_1R-mediated cAMP signaling function through its binding to σ_2R (Fig 3A). When HEK-293T cells were transfected with D_1R and siRNA for σ_2R, the results indicated that cocaine pre-treatment potentiated agonist-induced cAMP levels, which was evidence of cocaine action upon binding to the σ_1R (Fig 3B). The next set of results is consistent with a reciprocal modulation of signaling mediated by cocaine binding to σ_2R and σ_1R; while cocaine via σ_2R positively modulates cAMP levels, it inhibits cAMP signaling via σ_1R. Accordingly, no effect of cocaine was observed in HEK-293T expressing D_1R and the two endogenous sigma receptors (Fig 3C). The lack of modulation exerted by cocaine upon simultaneous binding to both σ_1R and σ_2R likely reflects a balance which would, in a physiological set-up, depend on the relative expression of the two sigma receptors. In fact, when HEK-293T cells were transfected with D_1R and both siRNA for σ_1R and σ_2R it was observed that cocaine or the specific σ_2R agonist, PB-28 (300 nM), had no effect, indicating that cocaine induced modulation over D_1R depends on σ_1R and σ_2R expression (Fig 3D).

We next investigated whether cocaine binding to σ_2R receptors could still modulate D_2R-mediated signaling. HEK-293T cells transfected with 1 μg of cDNA of D_2R and siRNA for σ_1R (3 μg siRNA), responded to the selective-D_2R agonist, sumanirole. In these cells the G_i-mediated decrease of 0.5 μM forskolin-induced cAMP accumulation due to $G_{\alpha i}$ coupling was not affect by cocaine pre-treatment (Fig 3E). These results agree with the lack of interaction between σ_2R and dopamine D_2R detected in Fig 2B. As a control, we confirmed that when the σ_1R-cocaine modulation over D_2R was assayed, cocaine was able to block the sumanirole-induced effect (Fig 3F). These results agree with those in Navarro, et al., 2013 in the sense that they reflect the consequence of a physical interaction between σ_1R and D_2R receptors. In agreement with this hypothesis, HEK-293T cells expressing D_2R and endogenous sigma receptors behaved as cells in which the σ_2R was silenced (Fig 3G). As a further control, HEK-293T cells treated with siRNAs to silence both sigma receptors showed no modulation by cocaine of D_2R-medaited signaling (Fig 3H), thus reinforcing the idea that that cocaine effect over D_2R depends on σ_1R expression.

σ_2R activation potentiates dopamine D_1R MAPK phosphorylation

To further understand the cocaine effect over D_1R it is required the evaluation of G-protein-independent signal transduction. Consequently, MAPK signaling was evaluated in HEK-293T cells transfected with 0.75 μg cDNA for D_1R and 3 μg siRNA for either σ_1R or σ_2R. In cells expressing D_1R with silenced σ_1R, i.e. expressing D_1R and σ_2R (Fig 4A), cocaine 30 μM pretreatment increased SFK-81297-induced ERK1/2 phosphorylation, while in cells with silenced σ_2R, i.e. expressing D_1R and σ_1R (Fig 4B), cocaine decreased agonist-induced ERK1/2 phosphorylation. These results are evidence of potentiation by cocaine-σ_2R of G-protein independent signaling, and potentiation by cocaine-σ_1R of G-protein dependent signaling. In cells expressing D_1R and the two sigma receptors, no effect of cocaine pretreatment on pERK1/2 levels was observed in agreement with the above-described balance resulting from reciprocal sigma-receptor-mediated cocaine effects (Fig 4C). As a further control, cocaine did not alter the SKF-81297-induced ERK1/2 phosphorylation in HEK-293T cells expressing D_1R and with silenced sigma receptors (Fig 4D). A similar experimental design was used to undertake label-free DMR assays. On the one hand, in cells expressing D_1R and σ_2R, cocaine blocked SKF-81297-induced increase in the DMR signal in a similar way as the selective σ_2R ligand, PB-28, did (Fig 4E). On the other hand, the SKF-81297 effect was potentiated by cocaine pretreatment in cells expressing D_1R and σ_1R (Fig 4F). Once more, cocaine modulation on D_1R-agonist-induced effects was not found in cells expressing D_1R and both sigma receptors (Fig 4G). As DMR in cells expressing D_1R mainly reflects Gs-coupling, these results are similar to those obtained in cAMP read-outs. Another control was performed to show that pretreatment with the σ_2R selective agonist, PB-28, did not results in any signal modulation in cells expressing D_1R and silenced σ_1R and σ_2R (Fig 4H).

σ_2R activation blocks dopamine D_1R-mediated signaling in striatal primary cultures of neurons

PLA was used to determine in striatal primary cultures of neurons whether D_1R-σ_2R complex expression was affected by cocaine pretreatment. Consequently, specific antibodies against D_1R and σ_2R were used in neurons treated or not with 30 μM cocaine for 30 min (Fig 5A). 32% of cells showed punctuated staining (with 2.2 red spots/cell containing spots) surrounding Hoechst-stained nuclei. These results indicate the

occurrence of D_1-σ_2 heteroreceptor complexes in striatal primary cultures of neurons. A control done in the absence of primary antibodies were missing led to 18% of labeled cells (with 1.2 red spots/cell containing spots). The percentage of positive cells after a 30-min treatment with cocaine was 30 (with 2 red spots/cell containing spots). Thus, cocaine pre-treatment did not significantly alter D_1R-σ_2R complex formation (Fig 5B). When PLA was developed to detect D_2R and σ_2R complexes, the results (19% with 1.3 red spots/cell containing spots) were similar to those in the negative control (20% with 1.4 red spots/ cell containing spots), i.e. no evidence of heterocomplex formation was obtained. Pretreatment with cocaine did not lead to the appearance of heteromeric complexes formed by D_2R and σ_2R. These results agree with the BRET assays that did not find sign of interaction between the D_1R-Rluc and σ_2R-YFP but between the D_1R-Rluc and σ_2R-YFP pair.

To demonstrate the effect of cocaine over D_1R-mediated signaling in a more physiological environment, we analyzed cAMP and MAPK signaling pathways in striatal primary cultures of neurons. As striatal neurons express the two sigma receptors, the siRNA approach was used to silence sigma receptor expression. On the one hand, in neurons transfected with siRNA for σ_1R, and consequently expressing D_1R and σ_2R, cocaine and PB-28 led to a decrease in agonist-induced cAMP levels and to an enhancement in MAPK signaling (Fig 5C, G). On the other hand, neurons transfected with the siRNA for σ_2R, and consequently expressing D_1R and σ_1R, cocaine but not PB-28 induced an increase in the cAMP signal and a decrease in the ERK1/2 phosphorylation signal in the ERK1/2 phosphorylation signal (Fig 5D, H). Most of these results agree with those obtained in the heterologous system. However, in striatal neurons expressing D_1R and both sigma receptors, cocaine treatment led to a net effect that showed predominance of σ_1R versus σ_2R.

D_1R-mediated signaling is modulated by σ_1R in acute cocaine treatment and by σ_2R in chronic cocaine treatment

In situ Proximity Ligation Assay (PLA) was used to identify D_1R-σ_1R and D_1R-σ_2R heteroreceptor complexes in 30μm slicers of Sprague-Dawley rats administrated i.p. with 15mg/kg of cocaine for 1 (acute) or 14 (chronic) days or vehicle (Fig. 6A). When striatal sections of vehicle-treated animals were analyzed, it was observed that 38.5% of cells showed D_1R-σ_1R complexes with 2.5 red spots/cell containing spots while only 25% of cells showed D_1R-σ_2R complexes with 2.1 dots/cell. When Sprague-Dawley rats were treated with cocaine for 2 days (acute condition), it was observed that both, the D_1R-σ_1R and the D_1R-σ_2R complexes expression increased (54% of cells showed red spots with 4.5 spots/cell containing spots and 33% of cells showed red spots with 2.3 spots/cell containing spots respectively). However, the D_1R-σ_1R complex doubled its expression while D_1R-σ_2R complex expression suffered a slight increase. Interestingly, in the case of Sprague-Dawley rats treated with cocaine for 10 days (chronic condition), the D_1R-σ_1R hetromeric complex expression was not affected (34% of cells showed red spots with 2.4 spots/cell containing spots) compared to control animals while the D_1R-σ_2R heteromer expression increased significantly (35% of cells containing spots with 3.4 spots/cell containing spots). These results indicate that acute cocaine treatment strongly increase D_1R-σ_1R complexes formation in striatal rat sections but chronic cocaine treatment only potentiates D_1R-σ_2R complex expression (Fig 6B). Then, we questioned if the cocaine-induced alterations in the D_1R-σ_1R and D_1R-σ_2R complexes expression correlated with signaling consequences. To do so, we analyzed SKF-81297-induced cAMP production in striatal primary cultures of neurons pretreated with vehicle

or cocaine for different times (from 0.5 hours to 7 days). Interestingly, it was observed that 0.5 h and 2 h of cocaine pretreatment potentiated SKF-81297-induced cAMP levels. These results were due to cocaine binding to the σ_1R, which activation induce a positive modulation over dopamine D_1R, as observed in transfected HEK-293T cells. However, in primary cultures of neurons, longer exposure to cocaine (from 1 day to 7 days) inhibited the SKF-81297-induced increase in cAMP levels (Fig 6E). This effect is associated to the D_1R-σ_2R complex, due to the σ_2R ability to counteract the SKF-induced increases of cAMP levels through D_1R, characterized in transfected HEK-293T cells. In order to determine if sigma receptors were responsible of cocaine-induced modulations over D_1R in primary striatal neurons, these cultures were transfected with siRNA for σ_1R or σ_2R. On the one hand and according with previous results, in primary cultures of neurons transfected with siRNA for σ_1R, and therefore expressing D_1R and σ_2R, cocaine pretreatment (0.5 h to 7 days) blocked SKF-induced accumulation of cAMP levels (Fig 6C). On the other hand, in primary neurons transfected with siRNA for σ_2R, and therefore expressing D_1R and σ_1R, 0.5 h and 2 h pretreatment of cocaine potenciated the SKF-81297-induced increases in cAMP levels. However, longer stimulations of cocaine (1 to 7 days) produced no effect (Fig 6D). These results suggest that in acute cocaine treatment D_1R form heteromers mainly with σ_1R, prevailing the D_1R-σ_1R-mediated signaling. While in chronic cocaine treatment the increase of σ_1R-D1 heteromeric complex expression observed in acute conditions disappear but the increase in the D_1R-σ_2R complex expression is maintained, being the σ_2R responsible of the cocaine modulation over dopaminergic D1R, prevailing then the D_1R-σ_2R-mediated signaling.

DISCUSSION

Sigma σ_1R and σ_2R are relevant for cocaine action as they modulate dopaminergic signaling. Despite cocaine may bind to the two receptors, they are not closely related and no other common structural properties have been identified. In what concerns modulation of receptor-mediated signaling, a relevant difference is the formation of heteroreceptor complexes of σ_1R with both D_1 and D_2 receptors (Navarro, et al 2010). We have previously reported that σ_1R mediate cocaine actions on both D_1R (Navarro, et al., 2010; Moreno, et al., 2014) and D_2R (Navarro, et al., 2014). In contrast, we here report that σ_2R can form heteromeric complexes with D_1R but not with D_2R.

The results here presented and those that we have already reported (Navarro et al., 2010; Navarro et al., 2013) show that in equivalent experimental setups cocaine pretreatment enhances D_1R-mediated cAMP accumulation and inhibit MAPK signaling via σ_1R while block D_1-mediated cAMP accumulation and enhances MAPK signaling via σ_2R in both HEK-293T cells and primary neuronal cultures.

D_1R may simultaneously form higher-order heteromeric complexes with σ_1R and σ_2R receptors, being σ_1R to displace σ_2R out of the heterotrimer, but not vice versa. Navarro and colleagues reported an increase in σ_1R receptor expression at the cell surface after cocaine acute exposure in cells (Navarro, et al., 2010). When this increase of σ_1R levels in plasma membrane occurs, σ_2R receptor is displaced from the D_1R-σ_2R or D_1R-σ_2R-σ_1R heteromeric complexes, thus increasing the number of D_1R-σ_1R heteromers potentiating the D_1R signaling, at the same time that σ_1R is dampening the D_2R signal (Navarro, et al., 2013), promoting the acute effects of cocaine. However, has been

observed that in more prolonged exposure to cocaine, D_1R dopamine receptor-mediated signaling corresponds to that previously determined for the D1R-σ_2R heteromer. These data suggest that the initial cocaine-induced overexpression at the cell membrane of σ_1R receptor is transient, once these levels decrease, due to internalization or any other mechanism yet unknown, is σ_2R the predominant receptor forming heteromers with dopamine D_1R, thus inducing long-term neural changes responsible for the establishment of cocaine addiction.

Motor control in the basal ganglia is achieved by a complex circuitry consisting of GABAergic neurons containing mostly D_1R (direct pathway) and GABAergic neurons containing mostly D_2R (indirect pathway). Fine motor control is achieved by a balance of dopaminergic signals, one via D_1R, which are G_s coupled, and another via D_2R, which are G_i coupled. Cocaine impairment of the motor control depends on direct/indirect pathway disbalance, but the underlying mechanism is not known. Although the scenario is complex, it is known that cocaine enhances cAMP levels in cells expressing D_1R-σ_1R (Navarro et al., 2010). Therefore, cocaine seems to be increasing the protein kinase A-DARPP 32-dependent dopaminergic output of the direct pathway. Via the same sigma receptor (σ_1R) forming heteromers with D_2R cocaine leads to an impairment of the dopaminergic output of the indirect pathway (Navarro et al., 2013). Further to the unbalance resulting from those σ_1–dependent effects, our results demonstrate that trimers of D_1, σ_1 and σ_2 receptors may be formed and that the effect of cocaine in those heteromers is to reduce the negative modulation exerted by D_1R-σ_1R complexes. The results also show that the MAPK signaling pathway is particularly targeted upon cocaine/dopamine activation of the receptors in the heteromer. Whereas cells expressing the D_1R-σ_1R heteromer, in the presence of cocaine, showed a decrease in the phosphorylation of ERK1/2, cells expressing the D_1R-σ_2R heteromer showed an enhanced MAP kinase activation. It is known that ERKs are involved in the plastic changes induced by the consumption of drugs of abuse (Radwanska, et al., 2005). Moreover, inhibition of ERK activation alters previously learned place preference in a paradigm of drug of abuse consumption, and activation of ERK1/2 is necessary to establish the association between the place preference and drug consumption (Valjent, et al., 2006; Du, et al., 2017). In this context knocking down ERK1 causes an increase in stimulus-dependent activation of ERK2 cocaine-induced psychomotor sensitization and cocaine-motivated place preference (Ferguson, et al., 2006). It should be noted that the temporal pattern of MAPK activation in the mouse brain is differently induced by addictive or non-addictive drugs (Valjent, et al., 2004). Interestingly, Zhang et al. have described that D_1 receptor promotes cocaine-induced long-term neuronal plasticity in the nucleus accumbens (Zhang, et al., 2016), however, the underlying mechanism in this phenomenon has not been described. According to the obtained results in our laboratory, and in accordance with the aforementioned studies, it is possible to suggest that the potentiation of MAP kinase pathway mediated by the D_1R-σ_2R heteromer may be the mechanism by which the σ_2R would induce long term neuronal plasticity, favoring the establishment of the addiction. The data obtained suggest a predominant role of the σ_1R in acute cocaine use and a more relevant role of σ_2R in the establishment of cocaine addiction. In any case, the relative expression of the two receptors in a given neuron seems important to determine the cell fate when the drug of abuse is consumed and to appropriately design successful therapeutic approaches to address drug seeking behavior.

As the two receptors seem to be constitutive, as they are widely expressed in the CNS, the net effects of cocaine on dopaminergic transmission would depend on the relative expression of the two sigma receptors. In terms of cocaine addiction, which courses with a marked increase of dopamine levels in motor control and reward brain regions, σ_1R are further potentiating the effects of the drug of abuse in acute consumption whereas σ_2R potentiates the drug effects in chronic conditions. In such a scenario antagonists of σ_1R would have potential to counteract acute effects of cocaine while antagonists of σ_2R would have potential to counteract cocaine chronic effects. Going deep inside, in brain slices of acute-cocaine treated rats has been observed a significant increase of both D_1R-σ_1R and D_1R-σ_2R heteromers with a prevalence of D_1R-σ_1R complexes. On the other hand, in brain slices of chronic-cocaine treated rats only D_1R-σ_2R heterocomplexes expression suffered a significant increase compared to control animals. In addition, in cocaine time-response experiments in striatal primary cultures it has been observed a switch in the modulatory effects of cocaine over SKF-induced cAMP levels. At short time of cocaine treatment, it was observed that cocaine pretreatment potentiated cAMP accumulation whereas, in cultures subjected to longer cocaine treatments D_1R suffered a negative modulation. Thus, in acute addiction to cocaine prevail D_1R-σ_1R heteromer-mediated signaling, but in more prolonged cocaine exposures over time, is the σ_2R the responsible of cocaine modulatory effects. Recently, Singer et al. have determined that 2 hours after cocaine exposure are initiated the neuronal plasticity mechanisms (Singer, et al., 2017). This result agrees with the observations detected in neuronal primary cultures and striatal brain slicers where there is a switch between σ_1R to σ_2R induced cocaine modulatory effects at 2 h of cocaine pretreatment. The mechanism of action described in this paper can not explain somehow the results obtained by Matsumoto et al. (Matsumoto, et al., 2007) and Lever et al. (Lever et al., 2014) in which σ_2R receptor antagonists block the cocaine-induced hyperlocomotor effects after cocaine administration. However, the ligands used in these works were not selective for the σ_2R receptor, Consequently, this attenuation observed following the administration of such antagonists could be due to σ_1R receptor blockade. Another possibility it would be that the increase of D_1R -σ_2 heteromeric complex detected in cocaine acute administration, that it seems not involved in the dopamine D_1 mediated signaling have a more significant role to that observed in the present manuscript, being σ_2 receptor expression necessary for acute cocaine treatment effects.

Recently, cocaine addiction has been addressed taking into account the 10-20% of neurons in the *nucleus accumbens* (NAc) that express both dopamine receptors, D_1R and D_2R (Perreault, et al., 2016). The increase of dopamine in this nucleus is fundamental for cocaine seeking behavior. When a cell expresses the two receptors, they readily form heteromers. Structural disruption of the dopamine D_1-D_2 receptor heteromer, using synthetic peptides targeting the heteroreceptor interfaces, induces as well as promotes, accelerates and exacerbates the incentive motivational and locomotor activating effects of cocaine in a self-administration paradigm. These findings suggest a model for tonic inhibition of basal and cocaine-induced reward (Perreault, et al., 2016). These data suggest that it would be worth investigating whether D_1R-D_2R heteroreceptor complex operation may be modulated by cocaine binding to σ_1R and/or to σ_2R. In summary, our results show that the dopaminergic-mediated drug addictive and motor actions of cocaine are likely resulting from a balance between cocaine-σ_1R and cocaine-σ_2R impact on effects derived from activation of D_1R, D_2R and D_1R-D_2R in *ad hoc* CNS circuits.

MATERIALS AND METHODS

Reagents

Cocaine-chlorhydrate was provided by the Spanish *Agencia del Medicamento* (Ref nº: 2003C00220). σ_2R ligands, PB-28, D_1R ligands, SKF-81297 and D_2R ligands, Sumanirole, were purchased from Tocris, Bristol, UK.

Fusion proteins and expression vectors

Human cDNAs for D_1R, D_2R, σ_1R or σ_2R cloned into pcDNA3.1, were amplified without their stop codons using sense and antisense primers harboring: *EcoRI* and *KpnI* sites to subclone D_1R, D_2R, σ_1R and σ_2R in pcDNA3.1RLuc vector (p*RLuc*-N1, PerkinElmer Life and Analytical Sciences, Wellesley, MA) or *HindIII* and *BamHI* sites to clone D_1R, D_2R, σ_1R and σ_2R in pEYFP-N1 vector (enhanced yellow variant of GPF; Clontech), or *EcoRI* and *BamHI* sites to clone σ_2R in a Cherry containing vector (pcDNA3.1Cherry). Amplified fragments were subcloned to be in-frame with restriction sites of p*RLuc*-N1, pEYFP-N1, or pcDNA3.1Cherry vectors to provide plasmids that express proteins fused to *Renilla* Luciferase (D_1R-Rluc, D_2R-Rluc, σ_1R-Rluc and σ_2R-Rluc), YFP (D_1R-YFP, D_2R-YFP, σ_1R-YFP and σ_2R-YFP) or Cherry (σ_2R-Cherry) on the C-terminal end.

Cell lines and transient transfection

HEK-293T human embryonic kidney cells were grown at 37 ºC in an atmosphere with 5% CO_2 in Dulbecco's modified Eagle's medium (DMEM) (Gibco, Thermo Fischer Scientific, Madrid, Spain) supplemented with 2 mM L-glutamine, 100 µl/ml sodium pyruvate, 100 U/ml penicillin/streptomycin, MEM Non-Essential Amino Acid Solution (1/100) and 5% (v/v) heat inactivated Fetal Bovine Serum (FBS) (all supplements were from Invitrogen, Paisley, Scotland, UK). Cells were transiently transfected with cDNA corresponding to receptors, fusion proteins, and siRNA, as detailed in an expanded view by the polyethylenimine (PEI; SigmaAldrich, Cerdanyola del Vallès, Spain) method. After the incubation cells were incubated in serum-free medium that after 4 hours was replaced by complete medium. Experiments were carried out 48 hours later.

Neuronal primary cultures

Primary cultures of striatal neurons were obtained from fetal Sprague Dawley rats of 19 days. Cells were isolated as described in Hradsky et al. (2013) and plated at a confluence of 40,000 cells/0.32 cm^2. Cells were maintained for 12 days in Neurobasal medium supplemented with 2 mM L-glutamine, 100 U/ml penicillin/streptomycin, and 2% (v/v) B27 supplement (Gibco) in 6-well microplates. Cells were transiently transfected with the corresponding siRNA (3 µg plasmid siRNA per well) using the Lipofectamine™ 2000 (Invitrogen, Life Technologies, Darmstadt, Germany). After the incubation cells were incubated in serum-free medium that after 4 h was replaced by complete medium. Experiments were carried out 48 h later.

Cocaine treatment of Sprague-Dawley rats

Male Sprague-Dawley rats weighing 200-220 g were selected for the experiments. Rats were kept in controlled environment with 12 h light-dark cycle at 21 ºC room temperature. Food and water were provided *ad libitum*. All experimental procedures were approved by the Ethics Committee of Faculty of Biological Sciences of "Pontificia Universidad Católica de Chile" and follow the international guidelines (NIH Guide for the Care and Use of Laboratory Animals. Rats keep housing and handling in colony for three days, and then were divided in two groups of experimental series, chronic cocaine-treated rats with respective control (saline) and acute cocaine rats. The chronic cocaine-treated rats administration protocol consisted of 15 mg/Kg, i.p. cocaine injections twice per day for 14 days as described by (Liu, et al., 2005), the acute cocaine-treated rats consist in one injection of 15 mg/kg, i.p. cocaine in the morning and afternoon. Daily administration of cocaine and saline solution was performed in both experimental series at the same time in the morning and afternoon (beginning at 11:00 A.M. and 5:00 P.M.).

Immunocytochemistry

HEK-293T cells were grown on glass coverslips. Samples were treated with 30 μM cocaine or vehicle for 30 minutes, then were washed with PBS, fixed in 4% paraformaldehyde for 15 minutes and washed with PBS containing 20 mM glycine to quench free aldehyde groups. After permeabilization with PBS-glycine buffer containing 0.2% Triton X-100 for 5 minutes, cells were blocked with PBS containing 1% bovine serum albumin (BSA) for 1 hour at room temperature. D_1R-YFP and D_2R-YFP were detected by its own fluorescence (wavelength 530 nm), and σ_2R-Rluc was stained using a primary mouse monoclonal anti-Rluc antibody (1/200, 1 h, room temperature, antibody from Millipore, CA, USA) washed and stained with the secondary Cyn3-conjugated donkey anti-mouse antibody (1/200, antibody from Jackson Immunoresearch Laboratories, West Grove, PA, USA). Nuclei were stained with Hoechst (1/100, SigmaAldrich, St. Louis, USA) and then samples were rinsed several times and mounted with Mowiol 30% (Calbiochem). Samples were observed in a Leica SP2 confocal microscope (Leica Microsystems, Mannheim, Germany).

Proximity ligation assay

For proximity ligation assays (PLAs), transfected cells and primary cultures of striatal neurons were grown on glass coverslips. Samples were treated with 30 μM cocaine or vehicle 30 minutes, then were washed with PBS and fixed in 4% paraformaldehyde for 15 minutes, washed with PBS containing 20 mM glycine, permeabilized with the same buffer containing 0.05% Triton X-100 for 5 minutes, and washed successively with PBS. Then samples were incubated at 37 ºC with the blocking solution for 1 hour. Heteromers were detected using the Duolink *in situ* PLA detection kit (OLink Bioscience, Bioscience, Uppsala, Sweden) following the instructions of the supplier. To detect both D_1R-σ_2R and D_2R-σ_2R heteromers, cells and primary cultures were incubated overnight with anti D_1R (1/100, SigmaAldrich, St. Louis, USA), anti σ_2R (1/100, SigmaAldrich, St. Louis, USA) and Hoechst (1/100, SigmaAldrich, St. Louis, USA) to stain nuclei or anti D_2R (1/100, Santa Cruz Biotechnology, Dallas, USA), anti σ_2R and Hoechst. Samples were processed using PLA probes that bind to the primary antibodies (Duolink II PLA probe anti-Mouse plus and Duolink II PLA probe anti-Goat

minus). Samples were observed in a Leica SP2 confocal microscope (Leica Microsystems, Mannheim, Germany) equipped with an apochromatic 63x oil-immersion objective (numerical aperture 1.4) and 405 and 561 nm laser lines. For each field of view a stack of two channels (one per staining) and 4 to 6 Z stacks with a step size of 1 μm were acquired. Quantification of the number of cells containing one or more red spots versus total cells (blue nuclei) and, in cells containing spots, of the number of red spots/cell ratio, was conducted using dedicated software known as Duolink ImageTool (ref: DUO90806, Sigma-Olink). This software has been developed for quantification of PLA signals and cell nuclei in images generated from fluorescence microscopy. One-way ANOVA followed by Dunnett's *post hoc* multiple comparison test was used to for statistical analysis.

Resonance energy transfer

For Bioluminescence resonance energy transfer (BRET), HEK-293T cells were transiently cotransfected with a constant amount of cDNA encoding for proteins fused to Rluc and increasing amounts of cDNAs corresponding to proteins fused to YFP (see figure legends). To normalize the amount of cell in the plates, protein concentration was determined using a Bradford assay kit (Bio-Rad, Munich, Germany) using bovine serum albumin dilutions as standards. To quantify protein YFP expression, cells (20 μg of protein) were distributed in 96-well microplates (black plates with a transparent bottom), and fluorescence was read in the FluoStar Optima Fluorimeter (BMG Labtech, Offenburg, Germany) equipped with a high-energy xenon flash lamp, using a 10 nm bandwidth excitation filter at 400 nm reading. Protein fluorescence expression was determined as fluorescence of the sample minus the fluorescence of cells expressing the BRET donor alone. For BRET measurements, the equivalent of 20 μg of cell suspension was distributed in 96-well microplates (Corning 3600, white plates; Sigma), and coelenterazine H (5 μM; Invitrogen) was added. After 1 minute, readings were obtained using a Mithras LB 940 (Berthold Technologies) that allows the integration of the signals detected in the short-wavelength filter at 485 nm and the long-wavelength filter at 530 nm. To quantify protein Rluc expression luminescence, readings were also performed 10 minutes after addition of coelenterazine H. For Sequential resonance energy transfer (SRET) assays, cells were transiently cotransfected with constant amounts of cDNA encoding for both receptor fused to Rluc and YFP proteins and with increasingly mounts of cDNA corresponding to the receptor fused to Cherry protein (see figure legends). After 48 hours of transfection, quantification were performed in parallel in aliquots of transfected cells (20 μg of protein): (1) quantification of receptor YFP or receptor Rluc expression was performed as indicated for BRET experiments; (2) for quantification of receptor-Cherry expression, cells were distributed in 96-well microplates (Corning black plates with a transparent bottom), and fluorescence was read in the FluoStar Optima Fluorimeter using a 10 nm bandwidth excitation filter at 590 nm reading; and (3) for quantification of SRET, cells were distributed in 96-well microplates (black plates with transparent bottom), and coelenterazine H (5 μM) was added. After 1 minute, the readings were collected using a FluoStar Optima Fluorimeter that allows the integration of the signals detected in the short-wavelength filter at 530 nm and the long-wavelength filter at 590 nm. Net BRET and net SRET were defined as [(long-wavelength emission)/(short-wavelength emission)] – C_f, where C_f corresponds to [(long-wavelength emission)/(short-wavelength emission)] for the Rluc construct expressed alone in the same experiment. Both fluorescence and luminescence of each

samples were measured before every experiment to confirm similar donor expressions (~100,000 bioluminescence units) while monitoring the increase in acceptor expression (1000-40,000 fluorescence units). BRET or SRET was expressed as milliBRET (mBU) or milliSRET (mSU) units (net BRET or SRET x 1000). Data were fitted to a nonlinear regression equation, assuming a single-phase saturation curve with GraphPad Prism software (GraphPad Software). The relative amount of BRET or SRET is given as a function of 100 x the ratio between the fluorescence of the acceptor (YFP or Cherry) and the Luciferase activity of the donor (Rluc).

Cytosolic cAMP determination

Forskolin dose-response curves in cells with different density were performed to select the most appropriate conditions of the assay, which were 5,000 HEK-293T cells, 7,500 neurons and 0.5 μM forskolin (Sigma). Transfected HEK-293T cells and neurons were incubated in serum-free medium for 3 hours before the experiment. Assays were performed in medium containing 50 μM zardaverine (Tocris Bioscience). Addition of reagents was performed when cells were already placed in 384-well microplates in medium. Then cells were preincubated with vehicle, the σ_2R agonist, PB-28 (300 nM) or cocaine (30 μM) for 15 minutes. Vehicle, the D_1R agonist, SKF-81297 (200 nM) or the D_2R agonist, sumanirole (500 nM) were then added, and, after 15 minutes of incubation period, vehicle or 5 μM forskolin was added. Readings were performed 15 minutes later using a homogeneous time-resolved fluorescence energy transfer (HTRF) method requiring the Lance Ultra cAMP kit (PerkinElmer) and fluorescence reading (at 635 nm) in a PHERAstar Flagship microplate equipped with an HTRF optical module (BMG Labtech).

ERK1/2 phosphorylation

To determine ERK1/2 phosphorylation, 40,000 HEK-293T cells/well or 50,000 neurons/well were plated in transparent Deltalab 96-well microplates and kept in the incubator for 48 hours. The medium was substituted by serum-free DMEM medium 2 to 4 hours before starting the experiment. Before addition of 200 nM of SKF-81297, agonist of D_1R, cells and neurons were pre-treated (10 minutes at 25 ºC) in serum-free medium with vehicle, PB-28 (300 nM) or cocaine (30μM). After 10 minutes of SKF-81297-induced activation to stop de reaction, cells and neurons were placed on ice and washed twice with cold PBS before addition of 30 μl of lysis buffer (15 minutes). Supernatants (10 μl) were placed in white ProxiPlate 384-well microplates, and ERK1/2 phosphorylation was determined using the AlphaScreen®SureFire® kit (Perkin Elmer) and the EnSpire® Multimode Plate Reader (PerkinElmer, Waltham, MA, USA).

Label-free dynamic Mass Redistribution assays (DMR)

HEK-293T cells and neuronal primary cultures were seeded in 384-well sensor microplates 24 hours before the assay to obtain 70-80% confluent monolayers constituted by 5,000 HEK-293T cells or 14,000 neurons per well. Previous to the assay, cells were washed twice with assay buffer (HBSS with 20 mM HEPES and 0.1% DMSO, pH 7.15) and incubated for 2 hours in 40 μl/well of assay-buffer in the reader at

24 ºC. Hereafter, the sensor plate was scanned and a baseline optical signature was recorded before adding 10 μl of vehicle, cocaine (30 μM) or PB-28 (300 nM) for 30 minutes followed by SKF-81297 (200 nm) addition. All compounds dissolved in assay buffer. Then, DMR responses were monitored for at least 3600 seconds using an EnSpire® Multimode Plate Reader (PerkinElmer Life and Analytical Sciences, Waltham, MA, USA). Sensitive measurements of changes in local optical density mimicking cellular mass movements induced upon receptor activation were detected using EnSpire Workstation Software v4.10, and curves were normalized with respect to the baseline.

Statistics

Sample sizes were between xx and xx, which our previous published work indicated are sufficient to perform appropriate statistical analysis. Parametric statistics (unpaired t test and one-way or repeated-measures ANOVA) were used, because the different groups analyzed showed normality and homogeneity of variance. GraphPad Prism software version 5 was used for the statistical analysis.

REFERENCES

Barr, J.L., Deliu, E., Brailoiu, G.C., Zhao, P., Yan, G., Abood, M.E., Unterwald, E.M., and Brailoiu, E. (2015). Mechanisms of activation of nucleus accumbens neurons by cocaine via sigma-1 receptor-inositol 1,4,5-trisphosphate-transient receptor potential canonical channel pathways. Cell Calcium *58*, 196–207.

Carriba, P., Navarro, G., Ciruela, F., Ferré, S., Casadó, V., Agnati, L., Cortés, A., Mallol, J., Fuxe, K., Canela, E.I., et al. (2008). Detection of heteromerization of more than two proteins by sequential BRET-FRET. Nat. Methods *5*, 727–733.

Du, Y., Du, L., Cao, J., Hölscher, C., Feng, Y., Su, H., Wang, Y., and Yun, K.-M. (2017). Levo-tetrahydropalmatine inhibits the acquisition of ketamine-induced conditioned place preference by regulating the expression of ERK and CREB phosphorylation in rats. Behav. Brain Res. *317*, 367–373.

Ferguson, S.M., Fasano, S., Yang, P., Brambilla, R., and Robinson, T.E. (2006). Knockout of ERK1 enhances cocaine-evoked immediate early gene expression and behavioral plasticity. Neuropsychopharmacology *31*, 2660–2668.

Guo, L., and Zhen, X. (2015). Sigma-2 receptor ligands: neurobiological effects. Curr. Med. Chem. *22*, 989–1003.

Hayashi, T., and Su, T. (2005). The sigma receptor: evolution of the concept in neuropsychopharmacology. Curr Neuropharmacol *3*, 267–280.

Johannessen, M., Fontanilla, D., Mavlyutov, T., Ruoho, A.E., and Jackson, M.B. (2011). Antagonist action of progesterone at σ-receptors in the modulation of voltage-gated sodium channels. Am. J. Physiol., Cell Physiol. *300*, C328-337.

Lever, J.R., Miller, D.K., Green, C.L., Fergason-Cantrell, E.A., Watkinson, L.D., Carmack, T.L., Fan, K.-H., and Lever, S.Z. (2014). A selective sigma-2 receptor ligand antagonizes cocaine-induced hyperlocomotion in mice. Synapse *68*, 73–84.

Matsumoto, R.R., Hewett, K.L., Pouw, B., Bowen, W.D., Husbands, S.M., Cao, J.J., and Newman, A.H. (2001a). Rimcazole analogs attenuate the convulsive effects of cocaine: correlation with binding to sigma receptors rather than dopamine transporters. Neuropharmacology *41*, 878–886.

Matsumoto, R.R., McCracken, K.A., Friedman, M.J., Pouw, B., De Costa, B.R., and Bowen, W.D. (2001b). Conformationally restricted analogs of BD1008 and an antisense oligodeoxynucleotide targeting sigma1 receptors produce anti-cocaine effects in mice. Eur. J. Pharmacol. *419*, 163–174.

Matsumoto, R.R., McCracken, K.A., Pouw, B., Zhang, Y., and Bowen, W.D. (2002). Involvement of sigma receptors in the behavioral effects of cocaine: evidence from novel ligands and antisense oligodeoxynucleotides. Neuropharmacology *42*, 1043–1055.

Matsumoto, R.R., Liu, Y., Lerner, M., Howard, E.W., and Brackett, D.J. (2003). Sigma receptors: potential medications development target for anti-cocaine agents. Eur. J. Pharmacol. *469*, 1–12.

Matsumoto, R.R., Gilmore, D.L., Pouw, B., Bowen, W.D., Williams, W., Kausar, A., and Coop, A. (2004). Novel analogs of the sigma receptor ligand BD1008 attenuate cocaine-induced toxicity in mice. Eur. J. Pharmacol. *492*, 21–26.

Matsumoto, R.R., Pouw, B., Mack, A.L., Daniels, A., and Coop, A. (2007). Effects of UMB24 and (+/-)-SM 21, putative sigma2-preferring antagonists, on behavioral toxic and stimulant effects of cocaine in mice. Pharmacol. Biochem. Behav. *86*, 86–91.

Menkel, M., Terry, P., Pontecorvo, M., Katz, J.L., and Witkin, J.M. (1991). Selective sigma ligands block stimulant effects of cocaine. Eur. J. Pharmacol. *201*, 251–252.

Mésangeau, C., Narayanan, S., Green, A.M., Shaikh, J., Kaushal, N., Viard, E., Xu, Y.-T., Fishback, J.A., Poupaert, J.H., Matsumoto, R.R., et al. (2008). Conversion of a highly selective sigma-1 receptor-ligand to sigma-2 receptor preferring ligands with anticocaine activity. J. Med. Chem. *51*, 1482–1486.

Moreno, E., Moreno-Delgado, D., Navarro, G., Hoffmann, H.M., Fuentes, S., Rosell-Vilar, S., Gasperini, P., Rodríguez-Ruiz, M., Medrano, M., Mallol, J., et al. (2014). Cocaine disrupts histamine H3 receptor modulation of dopamine D1 receptor signaling: σ1-D1-H3 receptor complexes as key targets for reducing cocaine's effects. J. Neurosci. *34*, 3545–3558.

Narita, M., Nagumo, Y., Hashimoto, S., Narita, M., Khotib, J., Miyatake, M., Sakurai, T., Yanagisawa, M., Nakamachi, T., Shioda, S., et al. (2006). Direct involvement of orexinergic systems in the activation of the mesolimbic dopamine pathway and related behaviors induced by morphine. J. Neurosci. *26*, 398–405.

Navarro, G., Moreno, E., Aymerich, M., Marcellino, D., McCormick, P.J., Mallol, J., Cortés, A., Casadó, V., Canela, E.I., Ortiz, J., et al. (2010). Direct involvement of sigma-1 receptors in the dopamine D1 receptor-mediated effects of cocaine. Proc. Natl. Acad. Sci. U.S.A. *107*, 18676–18681.

Navarro, G., Moreno, E., Bonaventura, J., Brugarolas, M., Farré, D., Aguinaga, D., Mallol, J., Cortés, A., Casadó, V., Lluís, C., et al. (2013). Cocaine inhibits dopamine D2 receptor signaling via sigma-1-D2 receptor heteromers. PLoS ONE *8*, e61245.

Perreault, M.L., Hasbi, A., Shen, M.Y.F., Fan, T., Navarro, G., Fletcher, P.J., Franco, R., Lanciego, J.L., and George, S.R. (2016). Disruption of a dopamine receptor complex amplifies the actions of cocaine. Eur Neuropsychopharmacol *26*, 1366–1377.

Radwanska, K., Caboche, J., and Kaczmarek, L. (2005). Extracellular signal-regulated kinases (ERKs) modulate cocaine-induced gene expression in the mouse amygdala. Eur. J. Neurosci. *22*, 939–948.

Singer, B.F., Bryan, M.A., Popov, P., Robinson, T.E., and Aragona, B.J. (2017). Rapid induction of dopamine sensitization in the nucleus accumbens shell induced by a single injection of cocaine. Behav. Brain Res. *324*, 66–70.

Trifilieff, P., Rives, M.-L., Urizar, E., Piskorowski, R.A., Vishwasrao, H.D., Castrillon, J., Schmauss, C., Slättman, M., Gullberg, M., and Javitch, J.A. (2011). Detection of antigen interactions ex vivo by proximity ligation assay: endogenous dopamine D2-adenosine A2A receptor complexes in the striatum. BioTechniques *51*, 111–118.

Valjent, E., Pagès, C., Hervé, D., Girault, J.-A., and Caboche, J. (2004). Addictive and non-addictive drugs induce distinct and specific patterns of ERK activation in mouse brain. Eur. J. Neurosci. *19*, 1826–1836.

Valjent, E., Corbillé, A.-G., Bertran-Gonzalez, J., Hervé, D., and Girault, J.-A. (2006). Inhibition of ERK pathway or protein synthesis during reexposure to drugs of abuse erases previously learned place preference. Proc. Natl. Acad. Sci. U.S.A. *103*, 2932–2937.

Zhang, L., Huang, L., Lu, K., Liu, Y., Tu, G., Zhu, M., Ying, L., Zhao, J., Liu, N., Guo, F., et al. (2016). Cocaine-induced synaptic structural modification is differentially regulated by dopamine D1 and D3 receptors-mediated signaling pathways. Addict Biol.

FIGURE LEGENDS

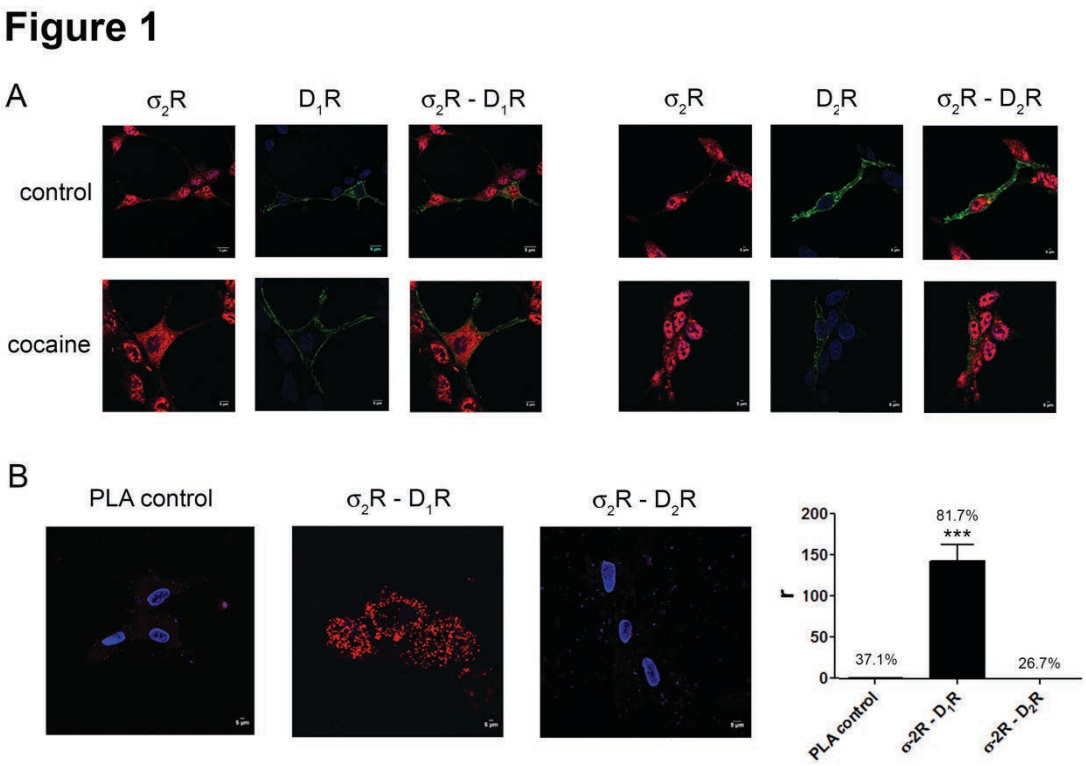

Figure 1. Expression of σ_2R-D_1R heteromeric complexes in an heterologous expression system.

To determine colocalization between σ_2R and dopamine D_1 or D_2 receptors, immunocytochemistry assays were performed in HEK-293T treated or not with cocaine 30 µM for 30 min previous to developing the experiment. HEK-293T cells expressing σ_2R-Rluc (1 µg cDNA), D_1R-YFP (1 µg cDNA), D_2R-YFP (1 µg cDNA), σ_2R-Rluc (1 µg cDNA) and D_1R-YFP (1 µg cDNA) or σ_2R-Rluc (1 µg cDNA) and D_2R-YFP (1 µg cDNA) were used. Dopamine receptors were detected by YFP fluorescence (green) and σ_2R was detected by a specific antibody against Rluc (1/100, Millipore, CA, USA) followed by a Cy3-secondary antibody (1/200, Jackson Immunoresearch Laboratories, West Grove, PA, USA) (red). Colocalization is shown in yellow (A). Scale bar 5 µm. *In situ* Proximity Ligation Assay (PLA) was developed in HEK-293T cells expressing D_1R (1 µg cDNA) or D_2R (1 µg cDNA) and σ_2R (1 µg cDNA) by the use of specific primary antibodies (1/100 dilution) against D_1R (SigmaAldrich, St. Louis, USA), D_2R (Santa Cruz Biotechnology, Dallas, USA) and/or σ_2R (SigmaAldrich, St. Louis, USA). Nuclei were stained with Hoechst (1/100, SigmaAldrich, St. Louis, USA). Confocal microscopy images (4 superimposed sections) were obtained showing D_1R-σ_2R or D_2R-σ_2R complexes as red spots (B). Scale bar 5 µm. Quantification of the PLA provides the ratio *r* values (number of red spots/cell containing spots) and the number of cells containing red spots, expressed in percentage versus the total number of cells (blue nucleus); shown above each bar. Data are the mean ± SEM of 4 different fields in 4 independent preparations. One way ANOVA and Dunnett's *post hoc* test showed statistically significant differences (***p <0.001).

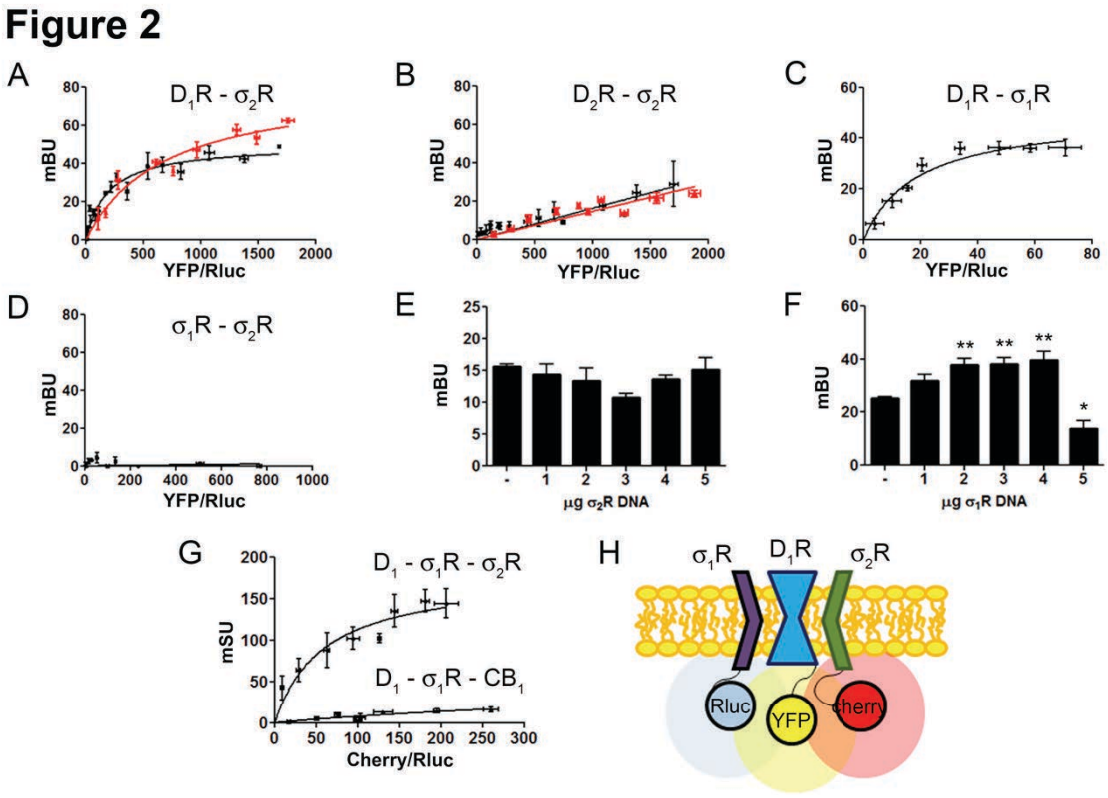

Figure 2. Identification of D_1R-σ_1R-σ_2R heteromers in a heterologous expression system.

Bioluminescence energy transfer (BRET) was developed in HEK-293T cells expressing i) a constant amount of D_1R-Rluc (0.3 µg cDNA) (A) or D_2R-Rluc (0.25 µg cDNA) (B) and increasing amounts of σ_2R-YFP (0.5 to 4 µg cDNA), or ii) a constant amount of D_1R-Rluc (0.3 µg cDNA) and increasing amounts (0.5 to 4.5 µg cDNA) of σ_1R-YFP (C) or iii) a constant amount of σ_1R-Rluc (0.1 µg cDNA) and increasing amounts of σ_2R-YFP (1 to 6 µg cDNA) (D). Cell were treated (red line) or not (black line) with 30 µM cocaine for 30 min. BRET is expressed as milli BRET units (mBU) and is given as the mean ± S.E.M. of 6 to 7 different experiments. Displacement experiments were developed in HEK-293T cells expressing a constant amount of σ_1R-Rluc (0.1 µg cDNA) and D_1-YFP (1.5 µg cDNA) and increasing amounts of unfused σ_2R (0 to 5 µg cDNA) (E) or a constant amount of D_1-Rluc (0.05 µg cDNA) and σ_2R-YFP (0.3 µg cDNA) and increasing amounts of unfused σ_1R (0 to 5 µg cDNA). Bioluminescence transfer of energy was quantified as milli BRET units (mBU) and is given as the mean ± S.E.M. of 8 to 10 different experiments. One way ANOVA and Dunnett's *post hoc* test showed statistically significant differences (*$p<0.05$, **$p<0.01$). Panel G: Sequential Resonance Energy Transfer (SRET) assay was developed in HEK-293T cells transfected with constant amounts of σ_1R-Rluc (0.2 µg cDNA) and D_1R-YFP (1.5 µg cDNA) and increasing amounts of σ_2R-RFP (0.5 to 4 µg cDNA). SRET is expressed as milli SRET units (mSU) and is given as the mean ± S.E.M. of 4 to 6 different experiments. Panel H: schematic representation of SRET.

Figure 3

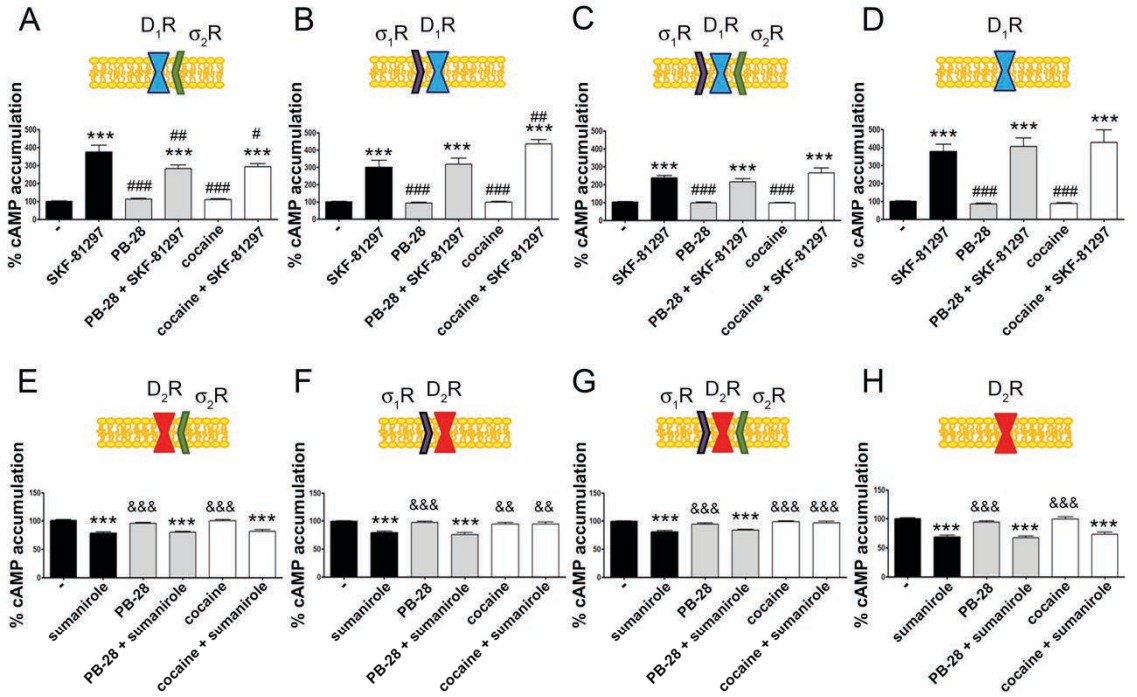

Figure 3. σ_2-D_1 receptor-mediated signaling in a heterologous expression system.

cAMP determination experiments were developed in HEK-293T cells expressing D_1R (A to D) or D_2R (E to H) in the presence or in the absence (C, G) of 3 µg siRNA for σ_1R (A, E), 3 µg siRNA for σ_2R (B, F) or both (D, H). Cells were pretreated with 30 µM cocaine, 300 nM PB-28 or vehicle 15 min prior to receptor activation using 200 nM SKF-81297 or 500 nM sumanirole. In cells expressing D_2R 0.5 µM forskolin was used to induce increases in cAMP levels. Basal [cAMP] is considered 100% in cells expressing D_1R, whereas forskolin-induced [cAMP] is considered 100% in cells expressing D_2R. Values are the mean ± S.E.M. of 12 to 15 different experiments. One way ANOVA followed by a Dunnett's multiple comparison *post hoc* test showed a significant effect of treatments versus control (***$p<0.001$), a significant effect of treatments versus SKF-81297 (#$p<0.05$, ##$p<0.01$ and ###$p<0.001$) and a significant effect of treatments versus sumanirole (&&$p<0.01$ and &&&$p<0.001$).

Figure 4

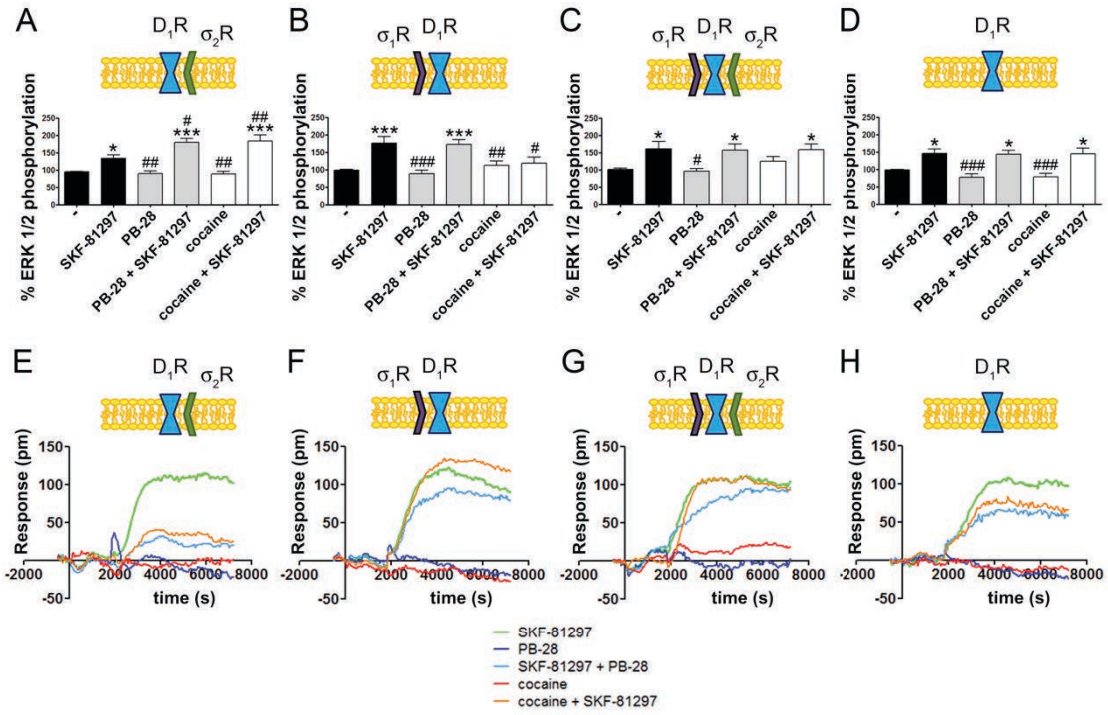

Figure 4. Cocaine effects on D_1R-mediated signaling.

Panels A-D: MAPK activation was recorded in HEK-293T cells transfected with 0.75 µg cDNA for D_1R in the presence or in the absence (C) of 3 µg siRNA for σ_1R (A), 3 µg siRNA for σ_2R (B) or both (D). Two hours before developing the experiment, the culture medium was replaced by non-supplemented DMEM. Then, cells were treated for 30 min with 30 µM cocaine, 300 nM PB-28 or vehicle followed by a 200 nM SKF-81297 stimulation (7 min). Values are the mean ± S.E.M. of 10 to 12 different experiments. One way ANOVA followed by a Dunnett's multiple comparison *post hoc* test showed a significant effect of treatments versus control (*p< 0.05, ***p< 0.01) and a significant effect of treatments versus SKF-81297 (#p<0.05, ##p<0.01 and ###p<0.001). Panels E- H: HEK-293T cells transfected with 0.75 µg cDNA for D_1R in the presence or in the absence (G) of 3 µg siRNA for σ_1R (E), 3 µg siRNA for σ_2R (F) or both (H) were treated with 30 µM cocaine (red), 300 nM PB-28 (dark blue) or vehicle (green) for 30 min previous to 200 nM SKF-81297 stimulation and real-time DMR signal recording (60 min).

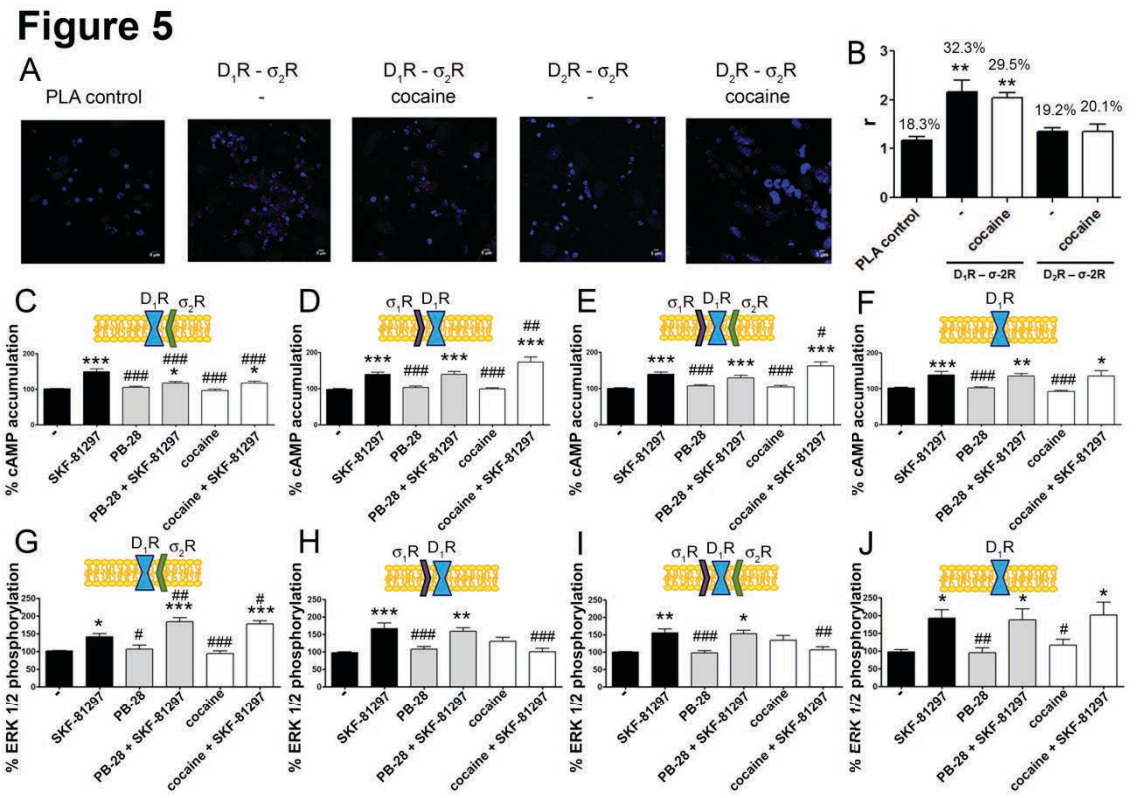

Figure 5. Expression and function of σ_2R-D_1R complexes in striatal primary cultures of neurons

PLA assay was developed in striatal primary cultures of neurons treated or not with cocaine 30 µM for 30 min previous to developing the experiment. σ_2R-D_1R or σ_2R-D_2R heteromeric complexes were detected by the use of specific antibodies (1/100 dilution) against σ_2R (SigmaAldrich, St. Louis, USA) and D_1R (SigmaAldrich, St. Louis, USA) or σ_2R and D_2R (Santa Cruz Biotechnology, Dallas, USA). Confocal microscopy images (4 superimposed sections) were obtained where nuclei were stained with Hoechst (1/100, SigmaAldrich, St. Louis, USA). Scale bar 5 µm. Quantification of the PLA provides the ratio *r* values (number of red spots/cell containing spots) and the number of cells containing red spots, expressed as the percentage of the total number of cells (blue nucleus); shown above each bar. Data are the mean ± SEM of 4 different fields in 4 independent preparations. One way ANOVA and Dunnett's multiple comparison *post hoc* test showed statistically significant differences versus control (**p<0.01). Panels C-J: primary cultures of striatal neurons, control (E, I) or transfected with siRNA for σ_1R (C, G), σ_2R (D, H) or both (F, J) were treated with 30 µM cocaine or 300 nM PB-28 prior to 200 nM SKF-81297 stimulation. cAMP levels (C to F) or MAPK activation l (G to J) were determined. Values are the mean ± S.E.M. of 10 to 15 different experiments. One way ANOVA followed by a Dunnett's multiple comparison *post hoc* test showed a significant effect of treatments versus not treated cells (*p<0.05, **p<0.01, ***p<0.001) and a significant effect of treatments versus SKF-81297 (#p<0.05, ##p<0.01 and ###p<0.001).

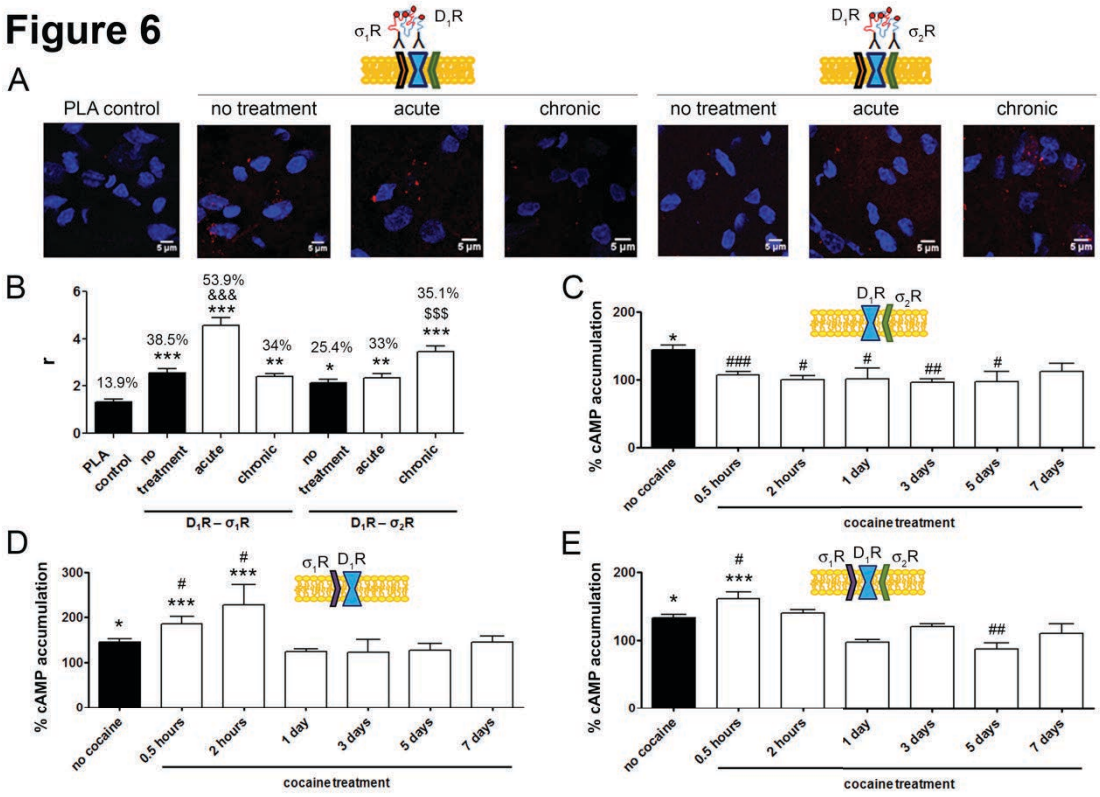

Figure 6. D_1R-mediated signaling is modulated by σ_1R in cocaine acute effect and by σ_2R in cocaine chronic effect.

PLA assay was developed in brain slices of male Sprague Dawley rats injected i.p with 15 mg/Kg of cocaine twice per day for 10 days (chronic treated rats) or for two days (acute treated rats) or with vehicle (control animals). D_1R-σ_1R or D_1R-σ_2R heteromeric complexes were detected by the use of specific antibodies against D_1R (1/100, SigmaAldrich, St. Louis, USA), σ_1R (1/100, Santa Cruz Biotechnology, Dallas, US) or σ_2R (1/100, SigmaAldrich, St. Louis, USA). Confocal microscopy images (4 superimposed sections) were obtained where nuclei were stained with Hoechst (1/100, SigmaAldrich, St. Louis, USA). Scale bar 5 µm. PLA quantifications provides the number of cells containing red spot, expressed as the percentage of the total number of cells (blue nucleus) and the ratio *r* values (number of red spots/cell containing spots). Data are the mean ± SEM of 6 different fields in 5 independent preparations. One way ANOVA and Dunnett's multiple comparison *post hoc* test showed statistically significant differences versus control (*p<0.05, **p<0.01, ***p<0.001), significant differences between acute treatments (&&&p<0.001) and significant differences between chronic treatments ($$$p<0.001). cAMP determination experiments were developed in primary culture of striatal neurons, transfected with 3 µg siRNA for σ_1R (C) or 3 µg siRNA for σ_2R (D) or control (E). Cultures were spitted in 9 groups and pretreated with vehicle or 30 µM for different time periods (from 0.5 hours to 7 days) prior to receptor activation using 200 nM SKF-81297. Basal [cAMP] is considered 100% (data not shown). Values are the mean ± S.E.M. of 2 different experiments. One way ANOVA followed by a Dunnett's multiple comparison *post hoc* test showed a significant effect of treatments versus basal (*p< 0.05, ***p< 0.001) and a significant effect of cocaine treatments (white bars) versus non-cocaine treated neurons (black bar) (#p<0.05, ##p<0.01 and ###p<0.001).

3.3. OREXIN - CORTICOTROPIN-RELEASING FACTOR RECEPTOR HETEROMERS IN THE VENTRAL TEGMENTAL AREA AS TARGETS FOR COCAINE

Gemma Navarro[*], César Quiroz[*], David Moreno-Delgado[*], Adam Sierakowiak, Kimberly McDowell, Estefanía Moreno, William Rea, Ning-Sheng Cai, **David Aguinaga**, Lesley A. Howell, Felix Hausch, Antonio Cortés, Josefa Mallol, Vicent Casadó, Carme Lluís, Enric I. Canela, Sergi Ferré y Peter McCormick.

[*]Coautores del manuscrito

Manuscrito publicado en *The Journal of Neuroscience*, abril 2015; 35(17):6639-6653.

La liberación de los neuropéptidos factor de liberación de corticotropina (CRF) y orexina-A en el área tegmental ventral (VTA) juegan un papel importante en la búsqueda de cocaína inducida por el estrés. En este trabajo se proporcionan evidencias de interacciones farmacológicamente significativas entre el CRF y la orexina-A que dependen de la oligomerización de los receptores CRF_1 (CRF_1R) y orexina-1 (OX_1R). Los heterómeros CRF_1R-OX_1R son los responsables de un *crosstalk* negative entre la orexina-A y el CRF como se demuestra en células transfectadas y de la VTA de rata, en las modulan significativamente la liberación dendrítica de dopamina. El receptor σ_1R, al que se puede unir cocaína, también se asocia con el heterómero CRF_1R-OX_1R. La unión de cocaína al complejo σ_1R-CRF_1R-OX_1R promueve una interrupción a largo plazo del *crosstalk* negativo entre la orexina-A y el CRF. A través de este mecanismo, la cocaína sensibiliza las células de la VTA a los efectos excitadores tanto del CRF como de la orexina-A, proporcionando así un mecanismo mediante el cual el estrés induce la búsqueda de cocaína.

Cellular/Molecular

Orexin–Corticotropin-Releasing Factor Receptor Heteromers in the Ventral Tegmental Area as Targets for Cocaine

Gemma Navarro,[1]* César Quiroz,[2]* David Moreno-Delgado,[1]* Adam Sierakowiak,[2] Kimberly McDowell,[2] Estefanía Moreno,[1] William Rea,[2] Ning-Sheng Cai,[2] David Aguinaga,[1] Lesley A. Howell,[3] Felix Hausch,[4] Antonio Cortés,[1] Josefa Mallol,[1] Vicent Casadó,[1] Carme Lluís,[1] Enric I. Canela,[1]† Sergi Ferré,[2]† and Peter J. McCormick[1,3]†

[1]Department of Biochemistry and Molecular Biology, Faculty of Biology, University of Barcelona, Center for Biomedical Research in Neurodegenerative Diseases Network and Institute of Biomedicine of the University of Barcelona, 08028 Barcelona, Spain, [2]Integrative Neurobiology Section, National Institute on Drug Abuse, Intramural Research Program, National Institutes of Health, Baltimore, Maryland 21224, [3]School of Pharmacy, University of East Anglia, Norwich, NR4 7TJ, United Kingdom, and [4]Max Planck Institute of Psychiatry, 80804 Munich, Germany

Release of the neuropeptides corticotropin-releasing factor (CRF) and orexin-A in the ventral tegmental area (VTA) play an important role in stress-induced cocaine-seeking behavior. We provide evidence for pharmacologically significant interactions between CRF and orexin-A that depend on oligomerization of CRF_1 receptor (CRF_1R) and orexin OX_1 receptors (OX_1R). CRF_1R–OX_1R heteromers are the conduits of a negative crosstalk between orexin-A and CRF as demonstrated in transfected cells and rat VTA, in which they significantly modulate dendritic dopamine release. The cocaine target σ_1 receptor (σ_1R) also associates with the CRF_1R–OX_1R heteromer. Cocaine binding to the σ_1R–CRF_1R–OX_1R complex promotes a long-term disruption of the orexin-A–CRF negative crosstalk. Through this mechanism, cocaine sensitizes VTA cells to the excitatory effects of both CRF and orexin-A, thus providing a mechanism by which stress induces cocaine seeking.

Key words: **cocaine; CRF receptor; GPCR heteromer; orexin receptor; sigma receptor**

Introduction

The 41 aa neuropeptide corticotropin-releasing factor (CRF) plays an important role in stress-induced drug-seeking behavior (Sarnyai et al., 2001). This depends primarily on CRF release in the ventral tegmental area (VTA), which receives CRF inputs from the paraventricular nucleus and the limbic forebrain (Rodaros et al., 2007). Stress and addictive drugs sensitize VTA dopaminergic neurons to the effects of excitatory inputs by common synaptic modifications (Saal et al., 2003), which can be reproduced by VTA application of CRF (Ungless et al., 2003). In the VTA of cocaine-experienced but not naive animals, stress-induced CRF release increases extracellular levels of glutamate and dopamine (Wang et al., 2005, 2007). Of the two known CRF receptors (CRF_1R and CRF_2R), CRF_1R is involved preferentially with stress-induced reinstatement of cocaine-seeking behavior and VTA dopamine release (Shaham et al., 1998; Lu et al., 2003; Lodge and Grace, 2005; Blacktop et al., 2011).

The 33- and 28-aa-long neuropeptides orexin-A (hypocretin-A) and orexin-B (hypocretin-B) are expressed within cell bodies in the lateral hypothalamus and adjacent perifornical area (Sakurai et al., 1998; de Lecea et al., 1998). These cells are the origin of an ascending arousal system that projects to the entire cortex, but apart from their well established role in arousal, orexins have a role in reward processes and substance-use disorders, which might depend on the dense orexinergic innervation of the dopaminergic cells of the VTA (Borgland et al., 2010; Mahler et al., 2014; Sakurai, 2014). A dichotomy in orexin function appears to be related to the two identified orexin receptors, with reward and arousal being associated closely with activation of OX_1R and OX_2R, respectively (Borgland et al., 2010; Mahler et al., 2014). The orexin–hypocretin system also drives cocaine reinstatement through activation of stress pathways, which includes the participation of CRF. Thus, central administration of orexin-A led to a dose-related reinstatement of cocaine seeking, which was prevented by a nonselective CRFR antagonist, and a selective OX_1R

Received Oct. 21, 2014; revised Feb. 18, 2015; accepted Feb. 23, 2015.

Author contributions: G.N., D.M.-D., C.Q., W.R., N.-S.C., D.A., L.A.H., F.H., A.C., J.M., V.C., C.L., E.I.C., S.F., and P.J.M. designed research; G.N., D.M.-D., C.Q., A.S., K.M., W.P.R., E.M., and P.J.M. performed research; G.N., D.M.-D., C.Q., W.R., E.M., C.L., S.F., and P.J.M. analyzed data; G.N., D.M.-D., C.Q., C.L., S.F., and P.J.M. wrote the paper.

This work was supported by intramural funds of the National Institute on Drug Abuse, from Spanish Ministry of Science and Technology Grants SAF2011-23813 and SAF2009-07276, Government of Catalonia Grant 2009-SGR-12, and Center for Biomedical Research in Neurodegenerative Diseases Network Grant CB06/05/0064. P.J.M. was supported through a Ramón y Cajal Fellowship. We thank Jasmina Jiménez for technical assistance.

The authors declare no competing financial interests.

*G.N., C.Q., and D.M.D. contributed equally to this manuscript.

†E.I.C., S.F., and P.J.M. are senior co-authors.

Correspondence should be addressed to either of the following: Dr. Sergi Ferré, Integrative Neurobiology Section, National Institute on Drug Abuse, Intramural Research Program, Triad Technology Building, 333 Cassell Drive, Baltimore, MD 21224, E-mail: sferre@intra.nida.nih.gov; or Dr. Peter J. McCormick, School of Pharmacy, University of East Anglia, Norwich Research Park, Norwich, NR4 7TJ, UK. E-mail: p.mccormick@uea.ac.uk.

DOI:10.1523/JNEUROSCI.4364-14.2015

 0270-6474/15/356639-15$15.00/0

antagonist blocked stress-induced reinstatement of previously extinguished cocaine-seeking behavior (Boutrel et al., 2005).

The same as for CRF, VTA is a key brain area involved in the ability of the orexinergic system to promote cocaine seeking. Intra-VTA administration of orexin-A reinstated cocaine self-administration, which was also associated with VTA glutamate and dopamine release (Wang et al., 2009). Intriguingly, although CRF and orexin-A are involved in stress-induced cocaine reinstatement by acting in the VTA, their mechanisms appeared independent (Wang et al., 2009). In the present study, we provide evidence for the existence of pharmacologically significant interactions between CRF and orexin-A that depend on CRF_1R–OX_1R oligomerization. CRF_1R–OX_1R heteromers are the conduits of a negative crosstalk between orexin-A and CRF observed in transfected cells and the VTA, in which they can significantly influence dendritic dopamine release. We also demonstrate that CRF_1R–OX_1R heteromers associate with σ_1 receptors (σ_1Rs) to form CRF_1R–OX_1R-σ_1R complexes and that cocaine binding to σ_1R in the complex promotes a long-term disruption of the orexin-A–CRF negative crosstalk. Through this mechanism, cocaine sensitizes VTA cells to the excitatory effects of both CRF and orexin-A.

Materials and Methods

Ligands and HIV transactivator of transcription-linked peptides. (−)-Cocaine HCl was purchased from Sigma and from the Spanish Agency of Medicine (number 2003C00220). σ_1R ligands PD144418 (1,2,3,6-tetrahydro-5-[3-(4-methylphenyl)-5-isoxazolyl]-1-propylpyridine oxalate) and PRE-084 2-(4-morpholinethyl) 1-phenylcyclohexanecarboxylate hydrochloride, CRF, orexins, SB334867 (*N*-(2-Methyl-6-benzoxazolyl)-*N*-1,5-naphthyridin-4-yl urea), and NBI27914 [5-chloro-*N*-(cyclopropylmethyl)-2-methyl-*N*-propyl-*N*′-(2,4,6-trichlorophenyl)-4,6-pyrimidinediamine hydrochloride] were purchased from Tocris Bioscience. To allow intracellular delivery, a peptide or protein can be fused to the cell-penetrating HIV transactivator of transcription (TAT) peptide (YGRKKRRQRRR; Schwarze et al., 1999). HIV TAT fused to a peptide with the amino acid sequence of a transmembrane domain (TM) of a GPCR can be inserted effectively into the plasma membrane as a result of both the penetration capacity of the TAT peptide and the hydrophobic property of the TM domain (He et al., 2011). HIV TAT-fused peptides with the amino acid sequences of OX_1R TM domains TM1, TM5, and TM7 were used (Genemad Synthesis). To obtain the right orientation of the inserted peptide, HIV TAT peptide was fused to the C terminus of OX_1R TM1, TM5, and TM7 peptides, with the following final amino acid sequences: WVLIAAYVAVFLIALVGNTLVYGRKKRRQRRR, SCFFFVTYLAPLGLMGMAYFQIFYGRKKRRQRRR, and YACFTFSHWLVYANSAANPIIYNFYGRKKRRQRRR, respectively.

Expression vectors, fusion proteins, and CRF_1R mutants. Sequences encoding amino acid residues 1-155 and 156-238 of yellow fluorescent protein (YFP) Venus protein were subcloned in pcDNA3.1 vector to obtain YFP Venus hemitruncated proteins. Human cDNAs for OX_1R, CRF_1R, ghrelin 1a receptors [growth hormone secretagogue 1a receptor ($GHS_{1a}R$)], or σ_1R, cloned into pcDNA3.1, were amplified without their stop codons using sense and antisense primers harboring the following: EcoRI and KpnI sites to clone CRF_1R, OX_1R, or $GHS_{1a}R$ in pcDNA3.1RLuc vector (p*RLuc*–N1; PerkinElmer Life and Analytical Sciences) or pEYFP–N1 vector (enhanced yellow variant of GFP; Clontech), HindIII and BamHI sites to clone σ_1R in pEYFP–N1 vector, or EcoRI and BamHI sites to clone CRF_1Rs and OX_1Rs in a Cherry containing vector (pcDNA3.1Cherry). Amplified fragments were subcloned to be in-frame with restriction sites of p*RLuc*–N1, pEYFP–N1, or pcDNA3.1Cherry vectors to provide plasmids that express proteins fused to *Renilla* Luciferase (RLuc), YFP, or Cherry on the C-terminal end (OX_1R–RLuc, CRF_1R–RLuc, OX_1R–YFP, CRF_1R–YFP, $GHS_{1a}R$–YFP, σ_1R–YFP, or CRF_1R–Cherry). Dr. Marian Castro (University of Santiago de Compostela, Santiago de Compostela, Spain) generously provided human β-arrestin 2–RLuc6 cDNA, cloned in pcDNA3.1 RLuc6 vector (pRLuc–N1; PerkinElmer Life and Analytical Sciences). For bimolecular fluorescence complementation (BiFC) experiments, human cDNA for CRF_1R was also subcloned into pcDNA3.1–nVenus to provide a plasmid that expresses the receptor fused to the hemitruncated nYFP Venus on the C-terminal end of the receptor (CRF1R–nVenus), and human cDNA for OX_1R was also subcloned into pcDNA3.1–cVenus to provide a plasmid that expresses the receptor fused to the hemitruncated cYFP Venus on the C-terminal end of the receptor (OX_1R–cVenus). Two CRF_1R mutants were used: (1) CRF_1R433, which lacks a large portion of the extracellular domain of the N terminus (amino acids 1–111) and is not able to bind ligands (Devigny et al., 2011); and (2) CRF_1R432, with H405P and A119L mutations in the 3 IL that confer enhanced constitutive activity.

Cell clones, cell culture, and transient transfection. HEK-293T cells were grown in DMEM (Gibco) supplemented with 2 mM L-glutamine, 100 μg/ml sodium pyruvate, 100 U/ml penicillin/streptomycin, minimal essential medium non-essential amino acids solution (1:100), and 5% (v/v) heat-inactivated fetal bovine serum (Invitrogen) and were maintained at 37°C in an atmosphere with 5% CO_2. Cells were transiently transfected with the corresponding fusion protein cDNA by the polyethylenimine (Sigma) method. For receptor–heteromer signaling, 0.4 μg of OX_1R–RLuc cDNA and 0.3 μg of CRF_1R–YFP cDNA were transfected, which provides 80–90% of maximum bioluminescence resonance energy transfer (BRET), as deduced from the BRET saturation curves (Fig. 1), indicating a high degree of receptor heteromerization. For the expression of $GHS_{1a}R$–YFP, equal amounts of $GHS_{1a}R$–YFP and $GHS_{1b}R$ cDNA were transfected to ensure $GHS_{1a}R$ expression at the cell membrane. HEK-293T stable cell lines expressing CRF_1R–YFP or OX_1R–YFP fusion proteins were created by transfection of the corresponding cDNA in a pcDNA3.1 plasmid. Antibiotic-resistant clones were isolated with 1000 μg/ml geneticin (Invitrogen), and, after an appropriate number of passages, stable cell lines were selected and grown as above indicated in the presence of 500 μg/ml geneticin. Sample protein concentration was determined as a control of cell number using a Bradford assay kit (Bio-Rad) with bovine serum albumin (BSA) dilutions as standards.

Fluorescence complementation assays. HEK-293T cells were cotransfected with 0.6 μM CRF_1R–nVenus cDNA and 0.6 μM OX_1R–cVenus cDNA; 48 h after transfection, cells were treated or not with the indicated HIV TAT–TM-fused peptides (4 μM) for 60 min at 37°C. To quantify protein-reconstituted YFP Venus expression, cells (20 μg of protein) were distributed in 96-well microplates (black plates with a transparent bottom; Porvair), and fluorescence was read in a Fluo Star Optima Fluorimeter (BMG Labtech) equipped with a high-energy xenon flash lamp, using a 10 nm bandwidth excitation filter at 400 nm reading. Protein fluorescence expression was determined as fluorescence of the sample minus the fluorescence of cells not expressing the fusion proteins.

Resonance energy transfer experiments. For BRET assays, HEK-293T cells were transiently cotransfected with a constant amount of cDNA encoding for proteins fused to RLuc and with increasing amounts of the cDNA corresponding to proteins fused to YFP. To quantify protein YFP expression, cells (20 μg of protein) were distributed in 96-well microplates (black plates with a transparent bottom), and fluorescence was read in the Fluo Star Optima Fluorimeter using a 10 nm bandwidth excitation filter at 400 nm reading. Protein fluorescence expression was determined as fluorescence of the sample minus the fluorescence of cells expressing the BRET donor alone. For BRET measurements, the equivalent of 20 μg of cell suspension were distributed in 96-well microplates (Corning 3600, white plates; Sigma), and coelenterazine H (5 μM; Invitrogen) was added. After 1 min, readings were obtained using a Mithras LB 940 (Berthold Technologies) that allows the integration of the signals detected in the short-wavelength filter at 485 nm and the long-wavelength filter at 530 nm. To quantify protein RLuc expression luminescence, readings were also performed 10 min after addition of coelenterazine H (5 μM). For sequential resonance energy transfer (SRET) assays, HEK-293T cells were transiently cotransfected with constant amounts of cDNAs encoding for both receptor fused to RLuc and YFP proteins and with increasingly amounts of cDNA corresponding to the receptor fused to Cherry protein. After 48 h of transfection, quantifications were performed in parallel in aliquots of transfected cells (20 μg of protein): (1) quantification of receptor YFP or receptor RLuc expression was performed as indicated for BRET experiments; (2) for quanti-

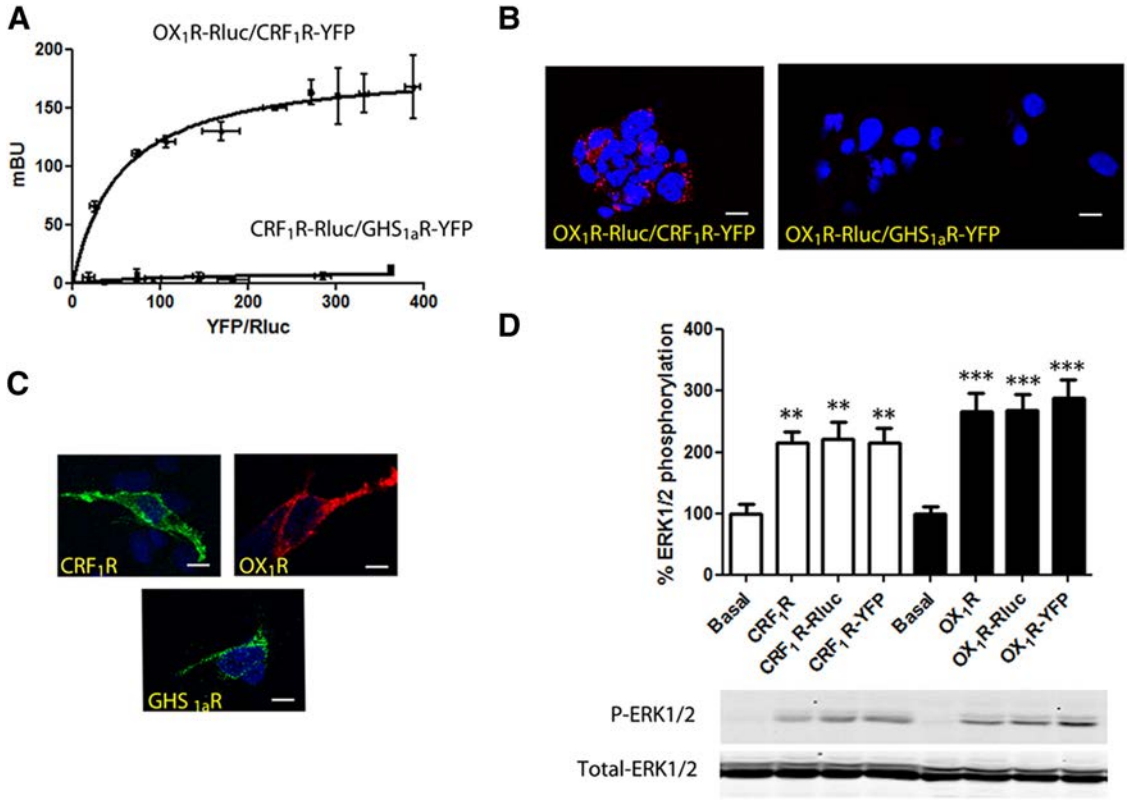

Figure 1. CRF_1R–OX_1R heteromers in transfected HEK-293T cells. ***A***, BRET saturation experiments in cells transfected with OX_1R–RLuc cDNA (0.4 μg) and increasing amounts of CRF_1R–YFP cDNA (0.05– 0.5 μg). Low and linear BRET is observed in cells transfected with OX_1R–RLuc cDNA (0.4 μg) and $GHS_{1a}R$–YFP cDNA (0.4 –2 μg). BRET, expressed as mBU, is given as a function of 1000 × ratio of fluorescence of the acceptor (YFP) and Luciferase activity of the donor (Rluc). Values are means ± SEMs of six to seven replications of one independent experiment per point. ***B***, Confocal microscopy images (superimposed sections) from PLA experiments performed in HEK-293T cells transfected with CRF_1R–YFP cDNA (0.3 μg) and OX_1R–RLuc cDNA (0.4 μg) (left) or $GHS_{1a}R$–YFP cDNA (2 μg) and OX_1R–RLuc cDNA (0.4 μg) (right). Heteromeric complexes appear as red spots and cell nuclei in blue (DAPI stained). Scale bars, 20 μm. ***C***, Confocal microscopy images of HEK-293T cells transfected with CRF_1R–YFP cDNA (0.3 μg; left), OX_1R–RLuc cDNA (0.4 μg; middle), or $GSH_{1a}R$–YFP (2 μg; right). YFP-fused receptors are identified by their own fluorescence (green) and OX_1R–RLuc by immunocytochemistry (red). Scale bars, 10 μm. ***D***, ERK1/2 phosphorylation in HEK-293T cells transfected with CRF_1R, CRF_1R–RLuc, or CRF_1R–YFP cDNA (0.3 μg; white columns) or with OX_1R, OX_1R–RLuc, or OX_1R–YFP cDNA (0.4 μg; black columns) were treated with CRF (100 nM) or orexin-A (50 nM), respectively. Values are means ± SEMs of seven experiments per group and are expressed as percentage of basal levels (100%). One-way ANOVA followed by Bonferroni's multiple comparison *post hoc* test shows significant agonist effect versus basal values (**$p < 0.01$ and ***$p < 0.001$). Representative Western blots are at the bottom.

fication of receptor Cherry expression, cells were distributed in 96-well microplates (Corning black plates with a transparent bottom), and fluorescence was read in the Fluo Star Optima Fluorimeter using a 10 nm bandwidth excitation filter at 590-nm reading; and (3) for quantification of SRET, cells were distributed in 96-well microplates (black plates with a transparent bottom), and coelenterazine H (5 μM) was added. After 1 min, the readings were collected using a using a Fluo Star Optima Fluorimeter that allows the integration of the signals detected in the short-wavelength filter at 530 nm and the long-wavelength filter at 590 nm. Net BRET and net SRET were defined as [(long-wavelength emission)/(short-wavelength emission)] − Cf, where Cf corresponds to [(long-wavelength emission)/(short-wavelength emission)] for the donor construct expressed alone in the same experiment. Both fluorescence and luminescence of each sample were measured before every experiment to confirm similar donor expressions (~100,000 bioluminescence units) while monitoring the increase in acceptor expression (1000–40,000 fluorescence units). BRET or SRET was expressed as milliBRET (mBU) or milliSRET (mSU) units (net BRET or SRET × 1000). Data were fitted to a nonlinear regression equation, assuming a single-phase saturation curve with GraphPad Prism software (GraphPad Software). The relative amount of BRET or SRET is given as a function of 100 × the ratio between the fluorescence of the acceptor (YFP or Cherry) and the Luciferase activity of the donor (RLuc).

Proximity ligation assay. For proximity ligation assays (PLAs), transfected cells were grown on glass coverslips and were fixed in 4% paraformaldehyde for 15 min, washed with PBS containing 20 mM glycine, permeabilized with the same buffer containing 0.05% Triton X-100, and washed successively with PBS. Heteromers were detected using the Duolink II *in situ* PLA detection Kit (OLink Bioscience) following the instructions of the supplier. To detect both OX_1R–RLuc–CRF_1R–YFP and OX_1R–RLuc–$GHS_{1a}R$–YFP heteromers, a mixture of equal amounts of rabbit anti-RLuc antibody (EMD Millipore) and mouse anti-YFP antibody (Santa Cruz Biotechnology) was used and incubated with anti-rabbit plus and anti-mouse minus PLA probes. Cells were mounted using the mounting medium with DAPI. The samples were observed in a Leica SP2 confocal microscope equipped with an apochromatic 63× oil-immersion objective (numerical aperture 1.4) and 405 and 561 nm laser lines. For each field of view, a stack of two channels (one per staining) and 9–15 Z stacks with a step size of 1 μm were acquired. Images were opened and processed with NIH Image J confocal.

Immunocytochemistry. Cells were fixed in 4% paraformaldehyde for 15 min and washed with PBS containing 20 mM glycine (buffer A) to quench the aldehyde groups. After permeabilization with buffer A containing 0.2% Triton X-100 for 5 min, cells were treated with PBS containing 1% BSA. After 1 h at room temperature, cells were labeled with the primary mouse monoclonal anti-RLuc receptor antibody (1:200; Millipore) for 1 h to detect OX_1R–RLuc, washed, and stained with the secondary Cy3 donkey anti-mouse antibody (1:200; Jackson ImmunoResearch). CRF_1R fused to YFP protein were detected by their fluorescence properties. The samples were rinsed several times and mounted with a medium suitable for immunofluorescence (30% Mowiol; Calbiochem). Samples were observed in a Leica SP2 confocal microscope.

Rat VTA slices. Male Sprague Dawley rats (2 months old; animal facility of the Faculty of Biology, University of Barcelona) were used. The

animals were housed two per cage and kept on a 12 h dark/light cycle with food and water available *ad libitum*, and experiments were performed during the light cycle. All procedures were approved by the Catalan Ethical Committee for Animal Use (CEAA/DMAH 4049 and 5664). Animals were killed by decapitation under 4% isoflurane anesthesia, and brains were rapidly removed, placed in ice-cold oxygenated (O_2/CO_2, 95%/5%) Krebs–HCO_3^- buffer (in mM: 124 NaCl, 4 KCl, 1.25 KH_2PO_4, 1.5 $MgCl_2$, 1.5 $CaCl_2$, 10 glucose, and 26 $NaHCO_3$, pH 7.4), and sliced at 4°C using a brain matrix (Zivic Instruments). VTA slices (500 μm thick) were kept at 4°C in Krebs–HCO_3^- buffer during the dissection; each slice was transferred into a 12-well plate with Corning Netwell inserts, containing 2 ml of ice-cold Krebs–HCO_3^- buffer. The temperature was raised to 23°C, and, after 30 min, the medium was replaced by 2 ml of fresh Krebs–HCO_3^- buffer (23°C). Slices were incubated under constant oxygenation (O_2/CO_2, 95%/5%) at 30°C for 4 h in an Eppendorf Thermomixer (5 Prime), and the medium was replaced by fresh Krebs–HCO_3^- buffer and incubated for 30 min before the addition of any agent. After incubation, the solution was discarded, and slices were frozen on dry ice and stored at −80°C until ERK1/2 phosphorylation was determined.

Akt and ERK1/2 phosphorylation. Cells or rat VTA slices were treated or not with the indicated ligands for the indicated time and were lysed by the addition of 300 μl of ice-cold lysis buffer (50 mM Tris-HCl, pH 7.4, 50 mM NaF, 150 mM NaCl, 45 mM β-glycerophosphate, 1% Triton X-100, 20 μM phenyl-arsine oxide, 0.4 mM $NaVO_4$, and protease inhibitor mixture). Cellular debris was removed by centrifugation at 13,000 × *g* for 5 min at 4°C, and the protein was quantified by the bicinchoninic acid method using BSA dilutions as standard. Akt or ERK1/2 phosphorylation was then determined by Western blot as described previously (Moreno et al., 2014), using a rabbit anti-phospho-Ser473 Akt antibody (1:2500; Signalway Antibody) for Akt phosphorylation or mouse anti-phospho-ERK1/2 antibody (1:2500; Sigma) and rabbit anti-ERK1/2 antibody that recognizes both phosphorylated and nonphosphorylated ERK1/2 (1:40,000; Sigma).

β-Arrestin 2 recruitment. Arrestin recruitment was determined as described previously (Moreno et al., 2014). Briefly, BRET experiments were performed in HEK-293T cells 48 h after transfection with the cDNA corresponding to the indicated receptors fused or not to the YFP and β-arrestin 2–RLuc cDNA (0.5 μg). Cells (20 μg protein) were distributed in 96-well microplates (Corning 3600, white plates with white bottom; Sigma) and were incubated with the indicated antagonist for 10 min and stimulated with the agonist for 10 min before the addition of coelenterazine H (5 μM; Invitrogen). After 1 min of adding coelenterazine H, BRET between β-arrestin 2–RLuc and receptor YFP was determined and quantified as described above.

cAMP production. Transfected HEK-293T cells were incubated in serum-free medium for 16 h before the experiment. Cells were preincubated for 15 min at 37°C with zardaverine (50 μM; Tocris Bioscience) and treated for 15 min with the indicated concentration of agonists in the presence or absence of forskolin (0.5 μM; Sigma). When indicated, receptor antagonists were preincubated 10 min before agonist addition. To stop the reaction, cells were placed on ice, washed with ice-cold PBS, and centrifuged at 2500 × *g* for 5 min at 4°C. The pellet was washed with ice-cold HBSS with 10 mM glucose and resuspended with 200 μl of $HClO_4$ (4%) for 30 min, and 1.5 M KOH was added to reach neutral pH. Samples were centrifuged at 15,000 × *g* for 30 min at 4°C, and the supernatant was frozen at −20°C. Accumulation of cAMP was measured with Cyclic AMP (^{3}H) Assay System (GE Healthcare) as described by the manufacturer.

Dynamic mass redistribution assays. Dynamic mass redistribution (DMR) was determined using an EnSpire Multimode Plate Reader (PerkinElmer Life and Analytical Sciences). Refractive waveguide grating optical biosensors, integrated in 384-well microplates, allow extremely sensitive measurements of changes in local optical density in a detecting zone up to 150 nm above the surface of the sensor. Cellular mass movements induced during receptor activation were detected by illuminating the underside of the biosensor with polychromatic light and measured as changes in wavelength of the reflected monochromatic light that is a sensitive function of the index of refraction. The magnitude of this wavelength shift (in picometers) is directly proportional to the amount of DMR. Briefly, 24 h before the assay, cells were seeded at a density of 5000 cells per well in 384-well sensor microplates with 30 μl of growth medium and cultured for 24 h (37°C, 5% CO_2) to obtain 70–80% confluent monolayers. Cells were washed twice with assay buffer (HBSS with 20 mM HEPES, pH 7.15) and incubated 2 h in 40 μl/well assay buffer with 0.1% DMSO at 24°C, the sensor plate was scanned, and a baseline optical signature was recorded before incubating the indicated antagonists for 30 min and adding 10 μl of agonist dissolved in assay buffer containing 0.1% DMSO. DMR responses were monitored for at least 8000 s. Kinetic results were analyzed using EnSpire Workstation Software version 4.10 (EnSpire Software), and curves were normalized with respect to the baseline.

In vivo *VTA dendritic dopamine release.* Male Sprague Dawley rats (3 months old; Charles River Laboratories) were used. Animals were housed two per cage and kept on a 12 h dark/light cycle with food and water available *ad libitum*. Experiments were performed during the light cycle. All animals used in the study were maintained in accordance with the guidelines of National Institutes of Health animal care, and the animal research conducted to perform this study was reviewed and approved by the National Institute on Drug Abuse Intramural Research Program Animal Care and Use Committee (Protocol 12-BNRB-73). Rats were deeply anesthetized with 3 ml/kg Equithesin [4.44 g of chloral hydrate, 0.972 g of Na pentobarbital, 2.124 g of $MgSO_4$, 44.4 ml of propylene glycol, 12 ml of ethanol, and distilled H_2O up to 100 ml of final solution (National Institute on Drug Abuse Pharmacy)] and implanted unilaterally in the VTA (coordinates in mm from bregma with a 10° angle in the coronal plane: anterior, 5.6; lateral, 2.4; vertical, 9) with a specially designed microdialysis probe that allows the direct infusion of large peptides within the sampling area. After surgery, rats were allowed to recover in hemispherical CMA-120 cages (CMA Microdialysis) equipped with two-channel overhead fluid swivels (Instech) connected to a sample collector (CMA 470; CMA). Twenty-four hours after implanting the probe, in the middle of the light period of the light/dark cycle, experiments were performed on freely moving rats in the same hemispherical home cages in which they recovered overnight from surgery. An ACSF (in mM: 144 NaCl, 4.8 KCl, 1.7 $CaCl_2$, and 1.2 $MgCl_2$) was pumped through the probe at a constant rate of 1 μl/min. After a washout period of 90 min, dialysate samples were collected at 20 min intervals. For peptide infusion, orexins and CRF were dissolved in ACSF to a final concentration of 10 μM, whereas HIV TAT-fused peptides were dissolved in 0.1% DMSO in ACSF to a final concentration of 30 μM (TM1 and TM5) or 60 μM (TM7). All peptides were injected with a 1 μl syringe (Hamilton) driven by an infusion pump and coupled with silica tubing (73 μm inner diameter; Polymicro) to the microdialysis probe infusion port (dead volume, 40 nl), which was primed with ACSF and plugged during implantation. All peptides were delivered at a rate of 16.6 nl/min. The OX_1R antagonist SB334667 was dissolved in sterile saline and administered intraperitoneally (10 mg/kg) 40 min before peptide infusion. The CRF_1R antagonist NBI27914 was dissolved in 5% DMSO in water and administered intraperitoneally (10 mg/kg) 40 min before peptide infusion. The σ_1R agonist PRE-084 was dissolved in ACSF at a concentration of 100 μM and was perfused through the microdialysis probe (reverse dialysis). Cocaine HCl was administered intraperitoneally 24 h before the start of the microdialysis experiment at a dose of 15 mg/kg. At the end of the experiment, rats were given an overdose of Equithesin, the brains were extracted and fixed in formaldehyde, and probe placement was verified using cresyl violet staining. Dopamine content was measured by HPLC coupled with a coulometric detector (5200a Coulochem III; ESA).

Statistics. Sample sizes were between 5 and 10, which our previous published work indicated are sufficient to perform appropriate statistical analysis. Parametric statistics (unpaired *t* test and one-way or repeated-measures ANOVA) were used, because the different groups analyzed showed normality and homogeneity of variance. GraphPad Prism software version 5 was used for the statistical analysis.

Results

Expression and functional characterization of heteromers between OX_1R and CRF_1R in transfected cells

BRET and PLA experiments were performed in HEK-293T cells transfected with OX_1R–RLuc and CRF_1R–YFP (Figs. 1*A*,*B*).

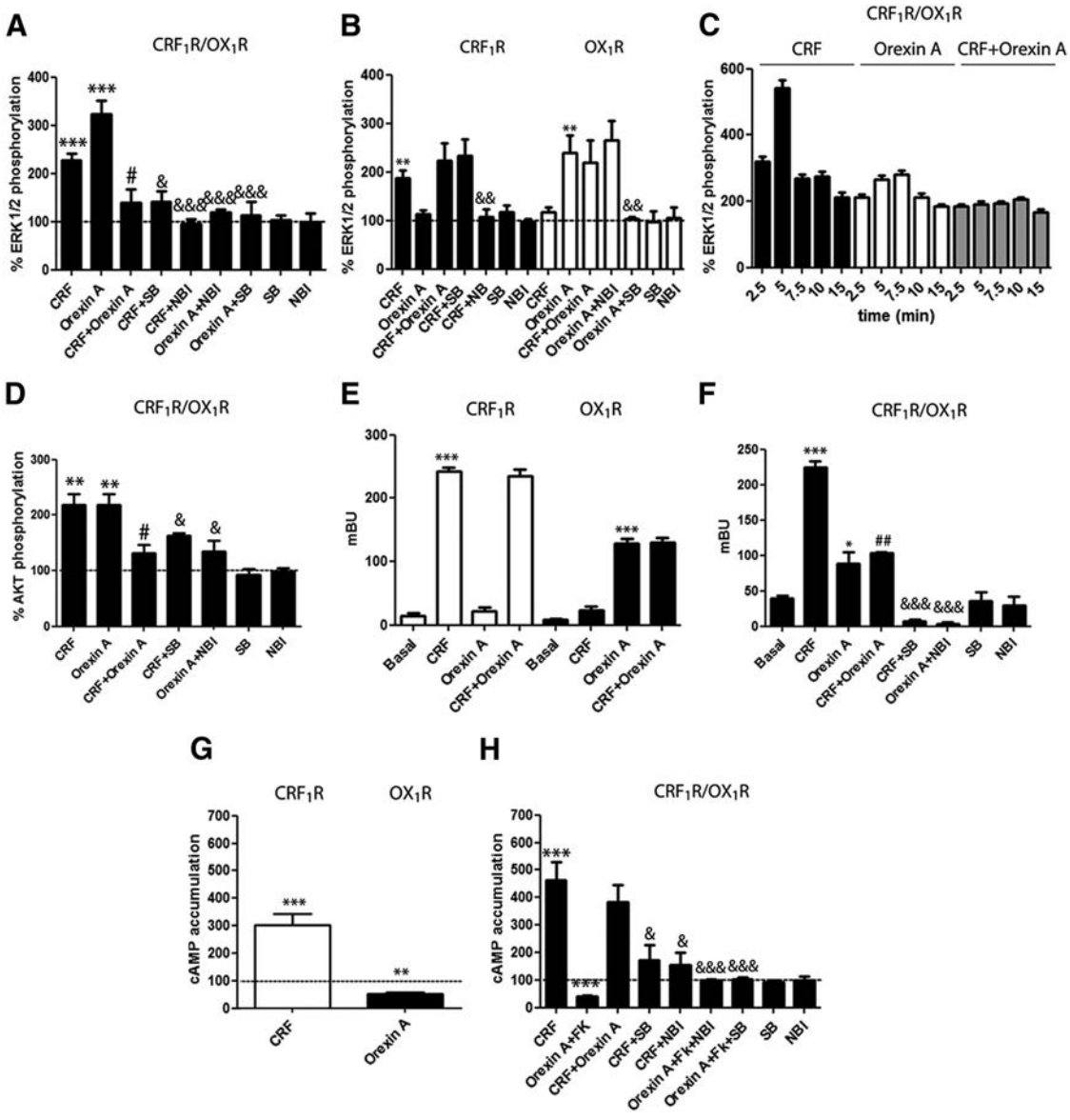

Figure 2. CRF_1R–OX_1R heteromer function in transfected HEK-293T cells. ***A–C***, ERK1/2 phosphorylation was performed in cells transfected with CRF_1R–YFP cDNA (0.3 μg; ***B***) or OX_1R–RLuc cDNA (0.4 μg; ***B***) or both (***A***, ***C***) pretreated (10 min) with vehicle, the OX_1R antagonist SB334667 (SB; 1 μM), or the CRF_1R antagonist NBI27914 (NBI; 1 μM), followed by treatment with medium, CRF (100 nM), orexin-A (50 nM), or both for 7 min (***A***, ***B***) or for 2.5, 5, 7.5, 19, and 15 min (***C***). Values are means ± SEMs of five to six experiments per group and are expressed as percentage of basal levels (100%; dotted line). ***D***, Akt phosphorylation was determined in cells transfected with CRF_1R–YFP cDNA (0.3 μg) and OX_1R–RLuc cDNA (0.4 μg), pretreated (10 min) with vehicle, the OX_1R antagonist SB334667 (SB; 1 μM), or the CRF_1R antagonist NBI27914 (NBI; 1 μM), followed by treatment (7 min) with medium, CRF (100 nM), orexin-A (50 nM), or both. Values are means ± SEMs of six to eight experiments per treatment and are expressed as percentage of basal levels (100%; dotted line). ***E***, ***F***, β-Arrestin 2 recruitment measured by BRET in cells transfected with CRF_1R–YFP cDNA (0.3 μg; ***E***, white bars) or OX_1R–YFP cDNA (0.4 μg; ***E***, black bars), or both (***F***) and β-arrestin 2–RLuc cDNA (0.5 μg). Cells were pretreated (10 min) with vehicle, SB334667 (SB; 1 μM), or NBI27914 (NBI; 1 μM), followed by treatment (7 min) with CRF (100 nM), orexin-A (50 nM), or both. Values are means ± SEMs of five to six experiments per treatment. ***G***, ***H***, cAMP accumulation was determined in cells transfected with CRF_1R–YFP cDNA (0.3 μg; ***G***, white bar) or OX_1R–RLuc cDNA (0.4 μg; ***G***, black bar), or both (***H***). Cells were pretreated (10 min) with vehicle, the OX_1R antagonist SB334667 (SB; 1 μM), or the CRF_1R antagonist NBI27914 (NBI; 1 μM), followed by treatment (7 min) with medium, CRF (100 nM), orexin-A (50 nM), or both. Values are means ± SEMs of six to eight experiments per treatment and expressed as increases of basal levels or as decreases of forskolin-induced cAMP accumulation (for orexin-A; 100%; dotted line). In ***A***, ***B***, ***D–F***, and ***H***, One-way ANOVA followed by Bonferroni's multiple comparison *post hoc* test shows significant single agonist effect versus basal values ($^{*}p < 0.05$, $^{**}p < 0.01$, and $^{***}p < 0.001$), or CRF plus orexin-A treatment versus CRF or orexin-A treatment ($^{\#}p < 0.05$) or antagonist plus agonist versus agonist with or without forskolin (FK; $^{\&}p < 0.05$, $^{\&\&}p < 0.01$, and $^{\&\&\&}p < 0.001$). In ***G***, unpaired Student's *t* test (two-tailed) shows significant difference of single agonist treatment versus basal values ($^{**}p < 0.01$ and $^{***}p < 0.001$).

These fusion proteins properly trafficked to the cell membrane, as shown by confocal microscopy (Fig. 1*C*), and were functional, as shown by comparing their ability to increase ERK1/2 phosphorylation with that of native receptors (Fig. 1*D*). BRET saturation curves were obtained in cells expressing OX_1R–RLuc and increasing amounts of CRF_1R–YFP (Fig. 1*A*), with $BRET_{max}$ of 186 ± 6 mBU and $BRET_{50}$ of 54 ± 7, indicating that these receptors can indeed form heteromers. As a negative control, a low and linear BRET was detected in cells expressing CRF_1R–RLuc and increasing amounts of $GHS_{1a}R$ fused to YFP (Fig. 1*A*). Accordingly, receptor heteromers were also visualized as red spots by using PLA in cells expressing OX_1R–RLuc and CRF_1R–YFP but not in cells expressing CRF_1R–RLuc and $GHSR_{1a}$–YFP (Fig. 1*B*).

CRF or the OX_1R agonist orexin-A induced ERK1/2 phosphorylation in cells coexpressing CRF_1R and OX_1R (Fig. 2*A*). Orexin-A-induced signaling was inhibited by the OX_1R antago-

nist SB334867 and the CRF_1R antagonist NBI27914, that did not modify basal levels by themselves, and vice versa, CRF-induced ERK1/2 phosphorylation was antagonized by both NBI27914 and SB334667. Thus, CRF_1R–OX_1R heteromers display cross-antagonism, a property seen in previous receptor heteromers (Guitart et al., 2014; Moreno et al., 2014). A negative crosstalk was also observed because ERK1/2 phosphorylation during coactivation of both receptors was significantly lower compared with that induced by single activation of either CRF_1R or OX_1R (Fig. 2*A*). Cross-antagonism and negative crosstalk were not attributable to either the lack of ligand specificity, because they were not observed in cells expressing single receptors (Fig. 2*B*), or a change in the shape of the time–response curve of ERK1/2 phosphorylation (Fig. 2*C*). Negative crosstalk and cross-antagonism were also observed at the level of Akt phosphorylation (Fig. 2*D*). β-Arrestin recruitment was also analyzed, because it has been shown to mediate ERK1/2 and Akt phosphorylation for several GPCRs (Kovacs et al., 2009). Orexin-A but not CRF significantly increased control BRET values in cells expressing β-arrestin 2–RLuc and OX_1R–YFP. Similarly, CRF but not orexin-A increased BRET values in cells expressing β-arrestin 2–RLuc and CRF_1R–YFP (Fig. 2*E*), indicating both the specificity of the ligands and the ability of these receptors to recruit β-arrestin 2 when activated. Significantly, not only CRF but also orexin-A significantly increased BRET values in cells expressing β-arrestin 2–RLuc, CRF_1R–YFP, and OX_1R (Fig. 2*F*). During coactivation with both agonists CRF and orexin-A, a negative crosstalk was observed at the level of β-arrestin 2 recruitment. Furthermore, cross-antagonism could also be demonstrated, and CRF-promoted and orexin-A-promoted β-arrestin 2 recruitment were counteracted by SB334867 and NBI27914, respectively (Fig. 2*F*).

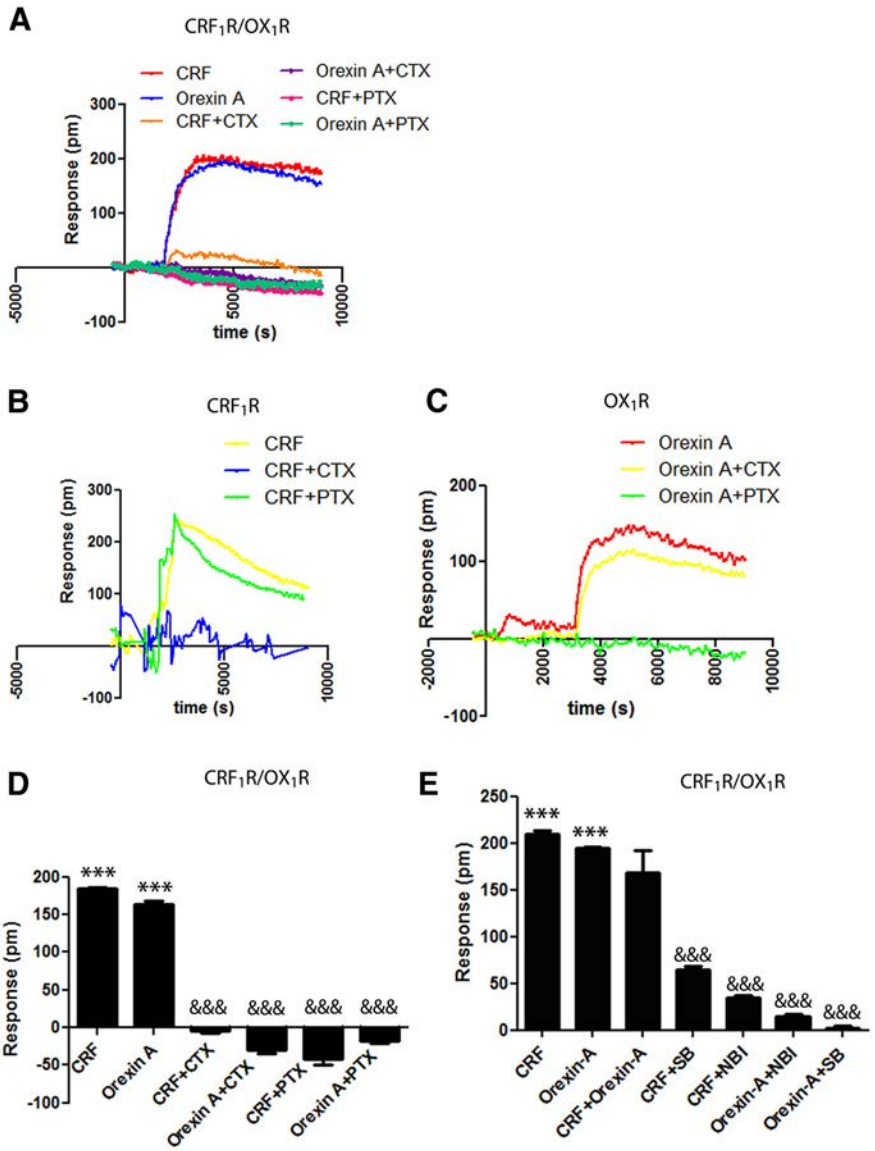

Figure 3. CRF_1R–OX_1R heteromer signaling detected by DMR. DMR was determined in HEK-293T cells stably transfected with OX_1R and transiently transfected with CRF_1R cDNA (0.3 μg; ***A***, ***D***, ***E***) or only stably transfected with OX_1R (***C***) or transiently transfected with CRF_1R cDNA (0.3 μg; ***B***). Cells were pretreated (overnight) with (***A–D***) vehicle, PTX (10 ng/ml), or CTX (100 ng/ml) or vehicle, the OX_1R antagonist SB334667 (SB; 1 μM) or the CRF_1R antagonist NB127914 (NBI; 1 μM), followed by treatment (7 min) with CRF (100 nM), orexin-A (50 nM), or both (***E***). ***A–C***, Representative picometer shifts of reflected light wavelength (picometers) versus time; each curve shows the mean of a representative optical trace experiment performed in triplicate. ***D***, ***E***, Maximum responses are derived from the resulting picometer shifts of reflected light wavelength (picometers) versus time curves. Values are means ± SEMs of four to five experiments per group. One-way ANOVA followed by Bonferroni's multiple comparison *post hoc* tests show significant agonist effect versus basal values (***$p < 0.001$), no significant effect of CRF plus orexin-A treatment versus CRF or orexin-A treatment, and significant effect of agonist plus antagonist or toxin treatment versus agonist alone ($^{\&\&\&}p < 0.001$).

Orexin-A decreased forskolin-stimulated cAMP in cells expressing OX_1R, indicating receptor coupling to a G_i-protein, and CRF promoted an increase in cAMP production in cells expressing CRF_1R, indicating receptor coupling to a G_s-protein (Fig. 2*G*). The same findings were observed in cells coexpressing OX_1R and CRF_1R, suggesting that the receptors can signal independently through their preferred G-proteins in the CRF_1R–OX_1R heteromer (Fig. 2*H*). Cross-antagonism could also be observed at the adenylyl-cyclase level in cells coexpressing OX_1R and CRF_1R. Thus, orexin-A-induced inhibition of forskolin-stimulated cAMP accumulation was counteracted not only by the OX_1R antagonist SB334867 but also by the CRF_1R antagonist NBI27914. Equally, CRF-induced cAMP accumulation was counteracted by both NBI27914 and SB334867 (Fig. 2*H*). A canonical G_s–G_i interaction at the adenylyl-cyclase level could not be observed during coactivation of both receptors with CRF and orexin-A, showing cAMP accumulation similar to that obtained with CRF alone (Fig. 2*H*). This would indicate a negative crosstalk by which CRF_1R activation counteracts OX_1R signaling through G_i in the CRF_1R–OX_1R heteromer. These findings were supported with experiments using label-free DMR technology, which allows measuring G-protein-mediated signaling in living cells. Agonist-induced time–response curves in the absence or presence of pertussis toxin (PTX) or cholera toxin (CTX) were obtained in cells expressing both OX_1R and CRF_1R (Fig. 3*A*). The maximum response in-

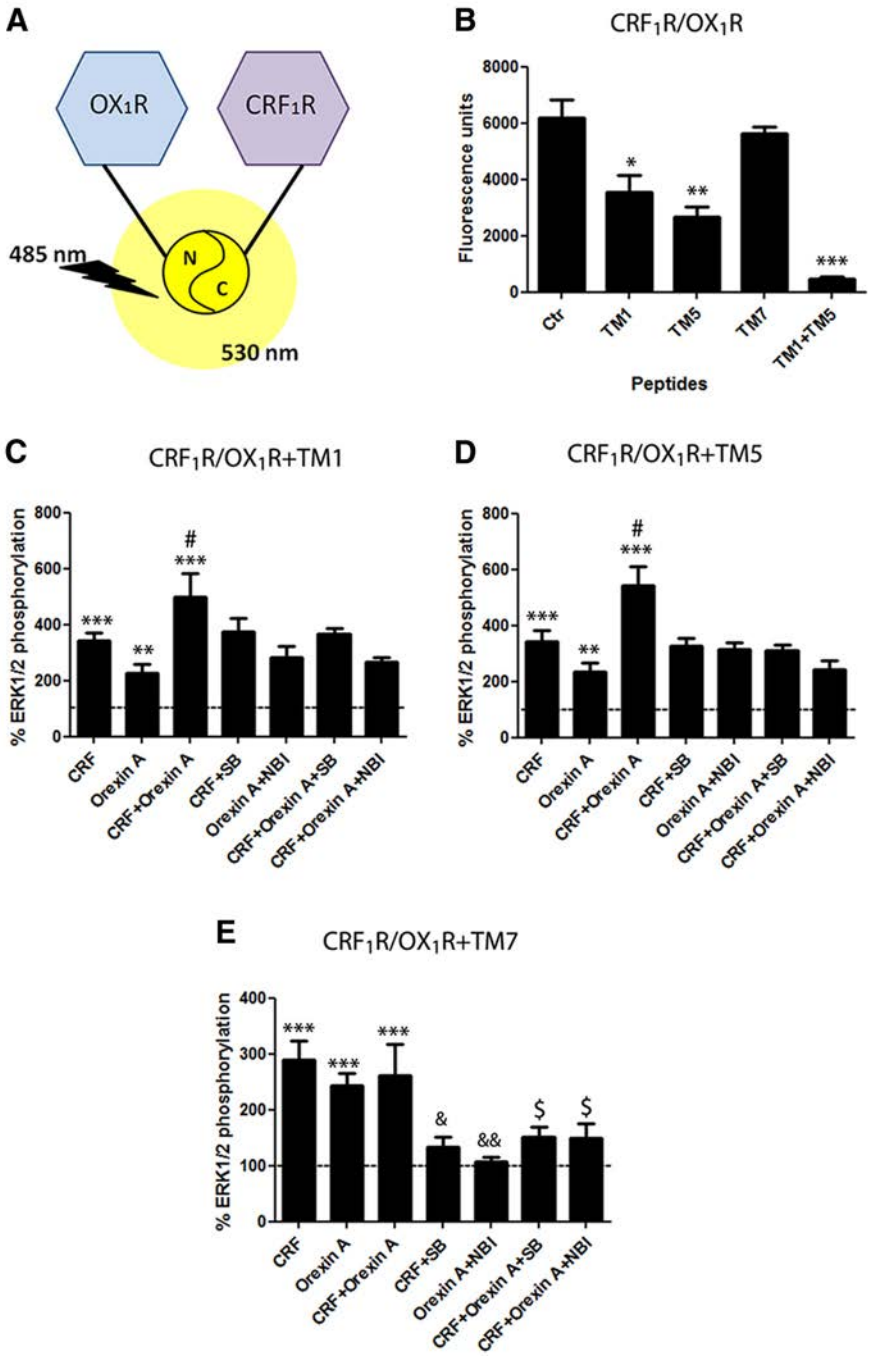

Figure 4. Effect of interfering synthetic peptides on the structure and function of CRF_1R–OX_1R heteromers. ***A***, Scheme showing BiFC. ***B***, Disruptive effect of HIV TAT-fused peptides with the amino acid sequences of OX_1R TM1, TM5, and TM7 on fluorescence emitted by HEK-293T cells cotransfected with CRF_1R–nVenus cDNA (0.6 μM) and OX_1R– cVenus cDNA (0.6 μM). Values (fluorescence at 530 nm) are means ± SEMs of six to seven experiments per group. One-way ANOVA followed by Bonferroni's multiple comparison *post hoc* test shows significant differences versus control (Ctr; $^{*}p < 0.05$, $^{**}p < 0.01$, and $^{***}p < 0.001$). ***C–E***, Disruptive effect of HIV TAT-fused peptides on ERK1/2 phosphorylation in HEK-293T cells transfected with CRF_1R cDNA (0.3 μg) and OX_1R cDNA (0.4 μg) preincubated (60 min) with OX_1R TM1, TM5, or TM7 (4 μM), pretreated (20 min) with vehicle, the OX_1R antagonist SB334667 (SB; 1 μM), or the CRF_1R antagonist NBI27914 (NBI; 1 μM), followed by treatment (7 min) with medium, CRF (100 nM), orexin-A (50 nM), or both. Values are means ± SEMs of five to six experiments expressed as percentage of basal (100%; dotted line). One-way ANOVA followed by Bonferroni's multiple comparison *post hoc* test shows significant differences of agonist treatment versus basal values ($^{**}p < 0.01$ and $^{***}p < 0.001$), CRF plus orexin-A treatment versus CRF or orexin-A treatment ($^{\#}p < 0.05$), one agonist plus antagonist versus agonist alone ($^{\&}p < 0.05$ and $^{\&\&}p < 0.01$), or both agonists plus NBI27914 versus CRF, or both agonists plus SB 334867 versus orexin-A ($^{\$}p < 0.05$).

duced by orexin-A or CRF (derived from time–response curves) was significantly inhibited with pretreatment with either PTX or CTX (Fig. 3*D*). Conversely, in cells only expressing CRF_1R, the effect of CRF was inhibited by CTX but not with PTX (Fig. 3*B*), whereas in cells only expressing OX_1R, the effect of orexin-A was only inhibited by PTX (Fig. 3*C*). These results demonstrate that the heteromer can interact simultaneously with both G_i- and G_s-proteins. Negative crosstalk and cross-antagonism were also observed by DMR. The effect (maximum response) of CRF or orexin-A was inhibited by both NBI27914 and SB334867, and the coactivation with CRF and orexin-A produced a lower response than the one obtained by single activation (Fig. 3*E*). These results suggest strongly that negative crosstalk and cross-antagonism observed for G-protein-dependent and β-arrestin-dependent signaling pathways constitute biochemical characteristics of CRF_1R–OX_1R heteromers.

BiFC experiments (Fig. 4*A*) were performed to check the ability of peptides with the amino acid sequence of OX_1R TM domains to destabilize CRF_1R–OX_1R heteromer, as described recently for the dopamine D_1–D_3 receptor heteromer (Guitart et al., 2014). HIV TAT peptides fused to OX_1R TM1, TM5, and TM7 peptides were used. Significant fluorescence could be detected in HEK-293T cells transfected with CRF_1R fused to the N-terminal fragment of YFP Venus (nVenus) and OX_1R fused to the C-terminal fragment YFP Venus (cVenus) as a result of YFP Venus reconstitution by CRF_1R–OX_1R heteromerization. Treatment with OX_1R TM1 and TM5 peptides alone or in combination, but not TM7, inhibited YFP Venus reconstitution, and the effect of TM1 plus TM5 was more pronounced than the effect obtained by either peptide alone (Fig. 4*B*). ERK1/2 phosphorylation crosstalk and cross-antagonism experiments were then performed in cells pretreated with OX_1R TM1 (Fig. 4*C*) or TM5 (Fig. 4*D*) peptides. Both peptides counteracted the negative crosstalk and cross-antagonism (Fig. 4*C*,*D*). Importantly, TM7 peptide, which was not able to alter the structure of CRF_1R–OX_1R in BiFC experiments, was also ineffective at counteracting the negative crosstalk and cross-antagonism (Fig. 4*E*). None of the peptides themselves significantly changed signaling from each of the receptors when activated alone with their respective agonists (Fig. 4*C*–*E*). These results demonstrate that the negative crosstalk and cross-antagonism depend on the integrity of the quaternary structure of the CRF_1R–OX_1R heteromer and, therefore, that constitute biochemical characteristics of the heteromer.

Two CRF_1R functional mutants were used to provide some insight about the conformational changes involved in the negative crosstalk between ligands binding to the CRF_1R–OX_1R heteromer: (1) a truncated mutant (CRF_1R433) that lacks a large part of the N-terminal domain and is not able to bind CRF but can still be activated by a small peptide that corresponds to the N-terminal part of CRF (peptide 14b, which binds to the juxtamembrane activating domain of CRF_1R; Devigny et al., 2011); and (2) a receptor that contains a mutation in the third intracellular loop and has enhanced constitutive activity (CRF_1R432). Both mutants were able to form heteromers with OX_1R as detected by BRET experiments without significant differences in $BRET_{max}$ and $BRET_{50}$ with respect to the CRF_1R (Fig. 5*A*,*B*). As expected, CRF or orexin-A did not induce ERK1/2 phosphorylation in HEK-293T cells expressing CRF_1R433 alone (Fig. 5*C*). Orexin-A, but not CRF, was able to signal in cells expressing CRF_1R433–OX_1R heteromers, but orexin-A-induced signaling was not modified by CRF or the CRF_1R antagonist NBI27914 (Fig. 5*D*,*E*). Nevertheless, in these cells, peptide 14b promoted ERK1/2 phosphorylation, and a negative crosstalk was observed between orexin-A and peptide 14b (Fig. 5*F*). These results indicate that an active conformation of the CRF_1R is involved with the negative crosstalk of receptor agonists in the CRF_1R–OX_1R heteromer. This was further corroborated using the CRF_1R432 mutant, which displays high constitutive activity. Single expression of CRF_1R432 showed increased basal ERK1/2 phosphorylation (compared with nontransfected cells), which could not be increased further by CRF (Fig. 5*G*). The same findings were also obtained in cells expressing CRF_1R432 and OX_1R (Fig. 5*H*). In addition, orexin-A did not increase MAPK signaling, in agreement with the active conformation of CRF_1R facilitating an allosteric inhibition of the orexin-A signaling (Fig. 5*H*).

CRF_1R–OX_1R heteromers in the VTA control dendritic dopamine release

In rat VTA slices, orexin-A and CRF promoted ERK1/2 phosphorylation (Fig. 6*A*), coactivation with orexin-A and CRF showed negative crosstalk, and both the CRF_1R antagonist NBI27914 and the OX_1R antagonist SB334867, which do not modify basal levels by themselves, antagonized the effect of orexin-A and CRF, thus showing cross-antagonism (Fig. 6*A*). Crosstalk and cross-antagonism disap-

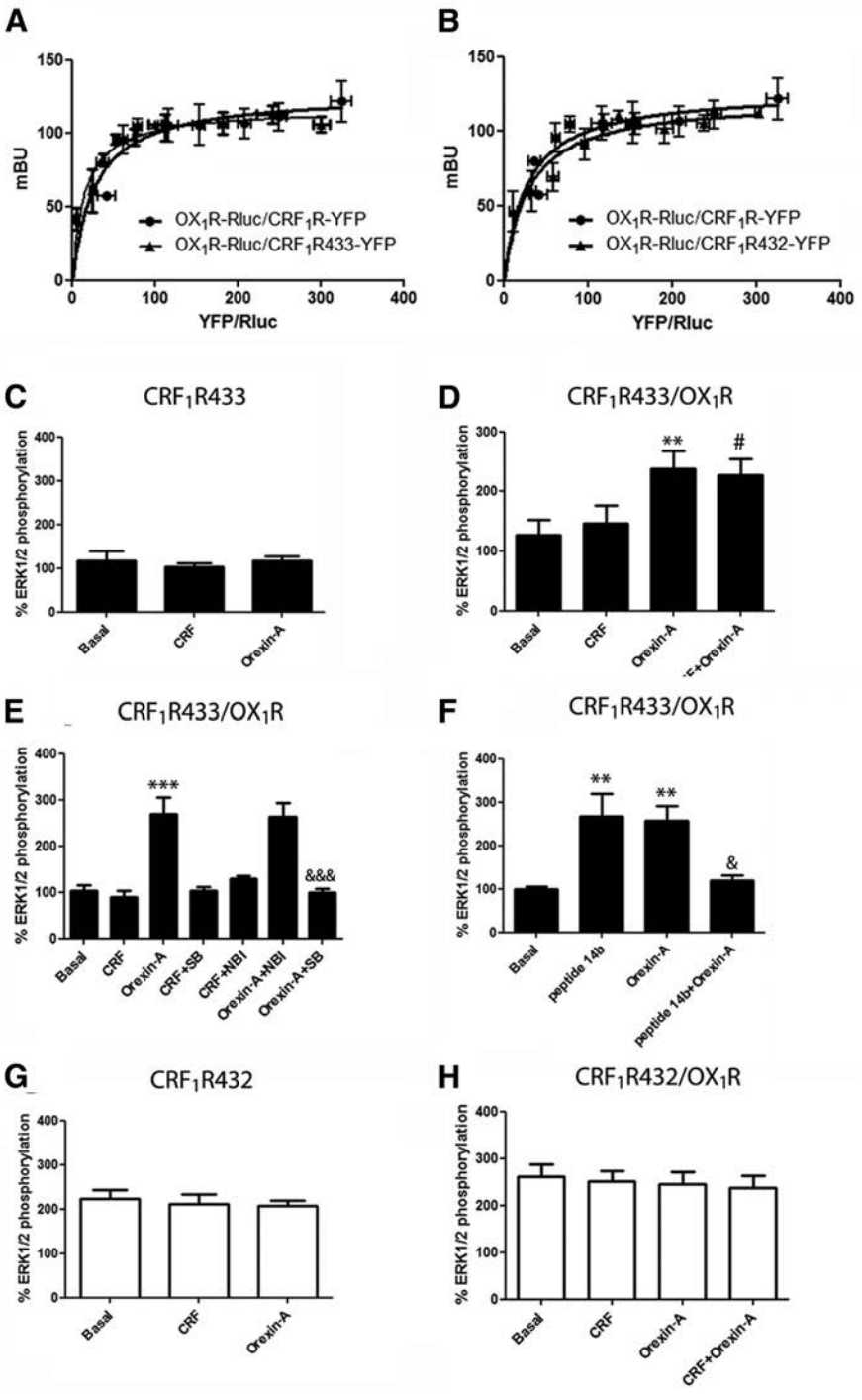

Figure 5. Involvement of the active conformation of CRF_1R with the negative crosstalk of receptor agonists in the CRF_1R–OX_1R heteromer. ***A***, ***B***, BRET saturation experiments in HEK-293T cells transfected with OX_1R–RLuc cDNA (0.2 μg) and increasing cDNA amounts (0.05–0.5 μg) of CRF_1R–YFP (circles), CRF1R433 mutant (triangles in ***A***), or CRF_1R432 mutant (triangles in ***B***). BRET is expressed as mBU as a function of 1000 × the ratio between fluorescence of the acceptor (YFP) and Luciferase activity of the donor (RLuc). Values are means ± SEMs of five to six replications of one independent experiment per point. ***C–F***, ERK1/2 phosphorylation in HEK-293T cells transfected with CRF1R433 mutant cDNA (0.3 μg; (***B***) alone or transfected with OX_1R cDNA (0.4 μg) pretreated (10 min) with vehicle, the OX_1R antagonist SB334667 (SB; 1 μM), or the CRF_1R antagonist NBI27914 (NBI; 1 μM), followed by treatment (7 min) with CRF (100 nM), orexin-A (50 nM), or both, or with peptide 14b (10 nM; ***C–E***). Values are means ± SEMs of five to six experiments per group expressed as percentage of basal (100%). One-way ANOVA followed by Bonferroni's multiple comparison *post hoc* test shows significant differences of single agonist treatment versus basal values ($^{**}p < 0.01$ and $^{***}p < 0.001$), CRF plus orexin-A treatment versus CRF or orexin-A treatment ($^{\#}p < 0.05$) or orexin-A plus SB334667 or peptide 14b versus orexin-A alone ($^{\&}p < 0.05$ and $^{\&\&\&}p < 0.001$). ***G***, ***H***, ERK1/2 phosphorylation in HEK-293T cells transfected with CRF1R432 mutant cDNA (0.3 μg; ***F***) alone or transfected with OX_1R (0.4 μg) treated (7 min) with vehicle or with CRF (100 nM), orexin-A (50 nM) or both (***G***). Values are means ± SEMs of five to six experiments per group expressed as percentage of basal values obtained in nontransfected cells (100%).

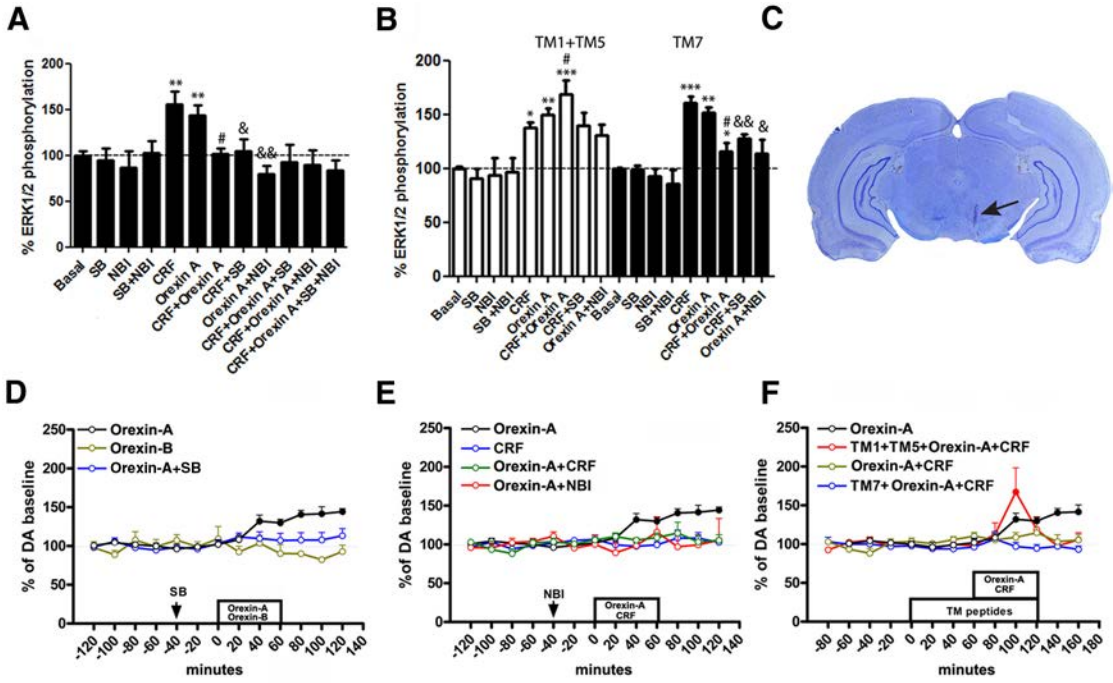

Figure 6. Expression and function of CRF_1R–OX_1R heteromers in the VTA. ***A***, ***B***, ERK1/2 phosphorylation in rat VTA slices preincubated (3 h) with vehicle (***A***) or HIV TAT-fused peptides with the amino acid sequences of OX_1R TM1 and TM5 (10 μM) or TM7 (20 μM) (30 min) with or without the OX_1R antagonist SB334667 (SB; 10 μM) or the CRF_1R antagonist NBI27914 (NBI; 10 μM), or both, followed by incubation (10 min) with vehicle, CRF (1 μM), orexin-A (1 μM), or both (***B***). Values are means ± SEMs of five to six experiments per group expressed as percentage of basal values (100%). One-way ANOVA followed by Bonferroni's multiple comparison *post hoc* test shows significant differences of agonist treatment versus basal values ($^{*}p < 0.05$, $^{**}p < 0.01$, and $^{***}p < 0.001$), CRF plus orexin-A treatment versus CRF or orexin-A treatment ($^{\#}p < 0.05$), or agonist plus antagonist treatment versus agonist alone ($^{\&}p < 0.05$ and $^{\&\&}p < 0.01$). ***C***, Representative coronal section of a rat brain (5.6 mm posterior from bregma), stained with cresyl violet, showing the track left by the tip of the modified microdialysis probe in the VTA (arrow). ***D***, ***E***, Dopamine (DA) levels in dialysates sampled from the VTA after slow infusion (1 μl/h) of orexin-A (1 μl, 10 μM), orexin B (1 μl, 10 μM), and/or CRF (1 μl, 10 μM) after previous systemic (intraperitoneal) administration of vehicle, SB334667 (SB; 10 mg/kg; ***D***), or NBI27914 (NBI; 10 mg/kg; ***E***) or with preinfusion and coinfusion (1 μl/h) of OX_1R TM1 plus TM5 (30 μM) or TM7 (60 μM) (***F***). Values are means ± SEMs of 7–10 experiments per group and are expressed as percentage of basal values (average of first 3 values before orexin-A or CRF infusion). A repeated measures ANOVA followed by Bonferroni's multiple comparison *post hoc* test showed significant difference (filled symbols, $p < 0.05$) versus the last basal values before orexin-A or CRF infusion. The same data on the effect of infusion of orexin-A alone are shown in ***D–F*** for comparison.

peared when VTA slices were treated with the CRF_1R–OX_1R destabilizing peptides OX_1R TM1 plus TM5 (10 μM; Fig. 6*B*), whereas the negative control TM7 peptide (at the same total peptide concentration, 20 μM) was ineffective (Fig. 6*B*), which demonstrates the presence of CRF_1R–OX_1R heteromers in the VTA.

To investigate the functional role of CRF_1R–OX_1R heteromers in the VTA, we analyzed dopamine release in the VTA using *in vivo* microdialysis experiments (Fig. 6*C–F*). Dendritic dopamine release by mesencephalic dopaminergic cells resembles that of the terminal regions, possessing a similar uptake mechanism and a finite releasable storage pool (Kita et al., 2009). Furthermore, local dopamine release in the VTA is a correlate of dopaminergic cell firing (Legault and Wise, 1999). Initial attempts to perfuse orexin-A through the dialysis probe (reverse dialysis) were unsuccessful, which included testing of different compositions of ACSF and different dialysis membranes of different materials and different cutoff, as analyzed with mass-spectrometry analysis of *in vitro*-recovered dialysates (data not shown). A specialized probe with an embedded silica infusion port was designed (Fig. 7) that allowed simultaneous constant slow delivery (1 μl/h) of large peptides (ligands and OX_1R TM peptides) in the same brain region where the microdialysis probe is sampling the extracellular concentration of dopamine. VTA infusion of orexin-A (10 μM) for 60 min produced dopamine release, which remained elevated >1 h after withdrawal (Fig. 6*D*). The average basal dialysate concentration of dopamine of a total of 121 animals was 2.37 ± 0.15 nM (mean ± SEM). This effect was attributable to selective activation of OX_1R, because it was not reproduced by a 10 μM infusion of the selective OX_2R agonist orexin-B (Sakurai et al., 1998; de Lecea et al., 1998) and was counteracted by the previous systemic administration of an effective dose (10 mg/kg, i.p.) of the selective OX_1R receptor antagonist SB334867 (Richards et al., 2008; Fig. 6*D*). The infusion of CRF (10 μM) or the systemic administration of an effective dose (10 mg/kg, i.p.) of the CRF_1R antagonist NBI27914 did not produce any significant change in the extracellular concentration of dopamine, but both counteracted the effect of orexin-A (Fig. 6*E*), demonstrating the negative crosstalk and cross-antagonism. These results strongly suggest that dendritic VTA dopamine release is under the control of CRF_1R–OX_1R heteromers. This was further demonstrated using CRF_1R–OX_1R destabilizing peptides. Infusion of OX_1R TM1 (30 μM) plus TM5 (30 μM) peptides but not the control TM7 peptide (at the same total peptide concentration, 60 μM) counteracted the orexin-A–CRF negative crosstalk (Fig. 6*F*). The effect of the TM peptides was not long lasting, probably because of a faster clearance compared with that of the larger and more hydrophilic orexin-A and CRF molecules. These results demonstrate that CRF_1R–OX_1R heteromers modulate VTA dopamine release.

CRF_1R–OX_1R heteromers are signaling units that can be modulated by cocaine in transfected cells and the VTA

In cells expressing CRF_1R and OX_1R, pretreatment for 2 h with 30 μM cocaine completely disrupted the negative crosstalk and

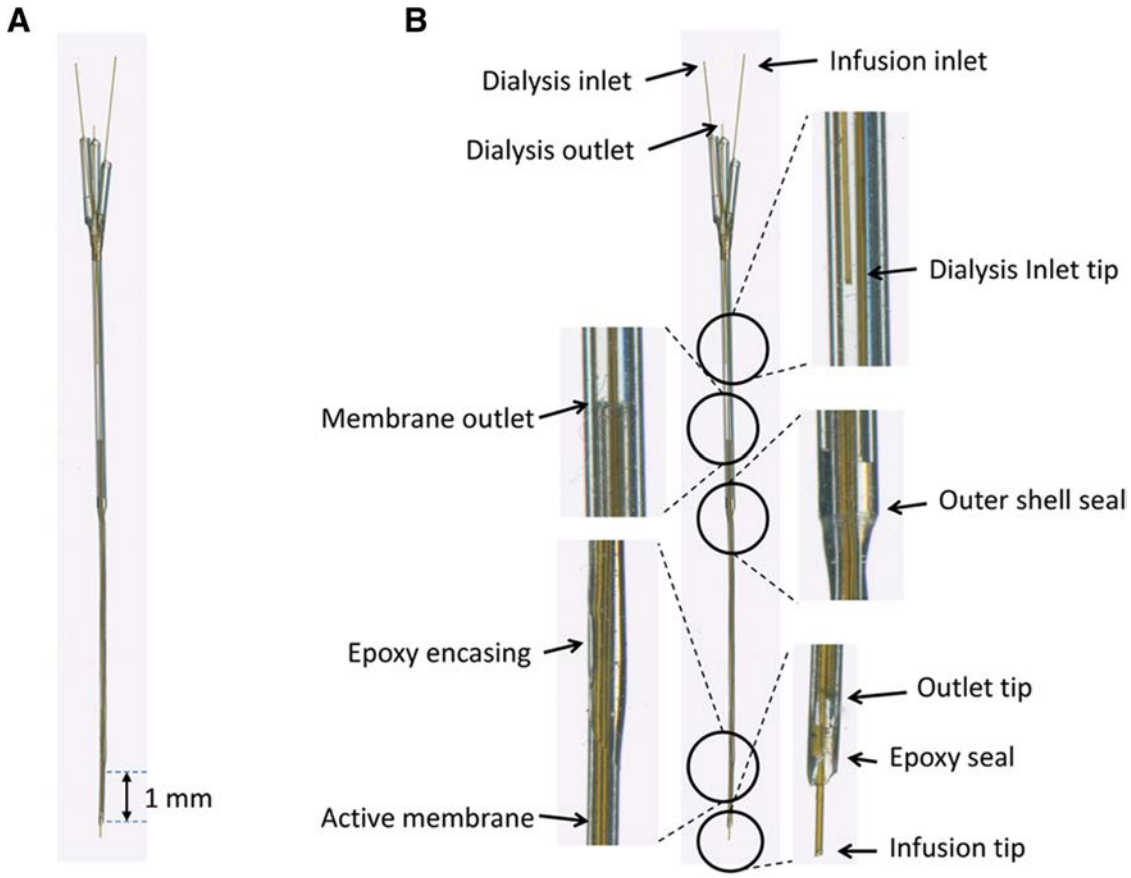

Figure 7. Microdialysis probe with infusion port. ***A***, Magnification showing the length of the dialysis membrane between dotted lines (1 mm). ***B***, Amplification of different parts of the probe (on a borosilicate glass model to show inner details). Internal tubing and infusion port are made of fused silica (40 mm internal diameter). The dialysis membrane (AN69) has a 20 kDa molecular weight cutoff. Seals are made of epoxy resin. The design allows the infusing of large peptides in the same brain region being analyzed for extracellular levels of dopamine.

cross-antagonism between CRF_1R and OX_1R ligands on MAPK signaling (Fig. 8*A*, black, bars) and β-arrestin 2 recruitment (Fig. 8*B*, black bars) that was seen in the absence of cocaine (Fig. 8*A*, *B*, white bars). Thus, cocaine blocks the allosteric intermolecular interactions in the CRF_1R–OX_1R heteromers that conduce the crosstalk and cross-antagonism between CRF_1R and OX_1R ligands.

We next explored the effect of cocaine in the rat VTA. The extracellular level of cocaine in the rat brain reached after pharmacologically significant doses is estimated to be 15 μM (Pettit et al., 1990). A higher cocaine concentration (100 μM) was then used to allow diffusion into the VTA slices. Cocaine pretreatment for 4 h counteracted the negative crosstalk of orexin-A and CRF on ERK1/2 phosphorylation. Furthermore, cross-antagonism of SB334867 or NBI27914 on ERK1/2 phosphorylation induced by CRF or orexin-A was not observed (Fig. 8*C*). Therefore, cocaine also disrupts the allosteric interactions within the CRF_1R–OX_1R heteromer in the VTA.

σ_1Rs mediate the disruptive effects of cocaine on CRF_1R–ORX_1R heteromer function

It has been found recently that cocaine can disrupt allosteric interactions between ligands in dopamine D_1–histamine H_3 receptor (H_3R) heteromers by acting on σ_1Rs that oligomerize with the heteromer (Moreno et al., 2014). We explored whether this mechanism could be involved in the disruptive effects of cocaine on CRF_1R–ORX_1R heteromer function. A saturable BRET curve was obtained in HEK-293T cells expressing CRF_1R–RLuc and increasing concentrations of σ_1R–YFP (Fig. 9*A*), indicating a direct interaction between σ_1R and CRF_1R. Cocaine produced a significant change in $BRET_{max}$ and $BRET_{50}$ BRET values (Fig. 9*A*), indicating a cocaine-induced change in the quaternary structure of the σ_1R–CRF_1R oligomers. Conversely, no significant BRET was detected in cells expressing OX_1R–RLuc and σ_1R–YFP in the absence or presence of cocaine (Fig. 9*B*). These results suggest that σ_1R can interact with CRF_1R–OX_1R heteromers by binding to CRF_1R in the heteromer. The heterotrimeric complex expression was demonstrated with SRET (Fig. 10*A*; Carriba et al., 2008). In HEK-293T cells expressing a constant amount of OX_1R–RLuc and σ_1R–YFP and increasing amounts of CRF_1R–Cherry, a net SRET saturation curve was obtained (Fig. 10*B*) with an $SRET_{max}$ of 0.31 $\pm$ 0.01 mSU and a $SRET_{50}$ of 0.08 $\pm$ 0.01. These results provide evidence for the existence of σ_1R–CRF_1R–OX_1R oligomers. Cocaine produced a significant change in $SRET_{max}$ and $SRET_{50}$ values ($SRET_{max}$ of 0.19 $\pm$ 0.03 mSU and a $SRET_{50}$ of 0.056 $\pm$ 0.002), indicating a cocaine-induced change in the quaternary structure of the σ_1R–CRF_1R–OX_1R oligomers. The involvement of σ_1R in the effects of cocaine on CRF_1R–OX_1R heteromers function in the VTA was demonstrated by using selective σ_1R ligands. In VTA slices, pretreatment for 4 h with the σ_1R agonist PRE-084 (Garcés-Ramírez et al., 2011) counteracted the negative crosstalk on ERK1/2 phosphorylation detected during CRF and orexin-A coadministration (Fig. 10*C*). Moreover, pretreatment with the σ_1R antagonist PD144418 (Akunne et al., 1997) blocked the effect of cocaine, and the negative cross-

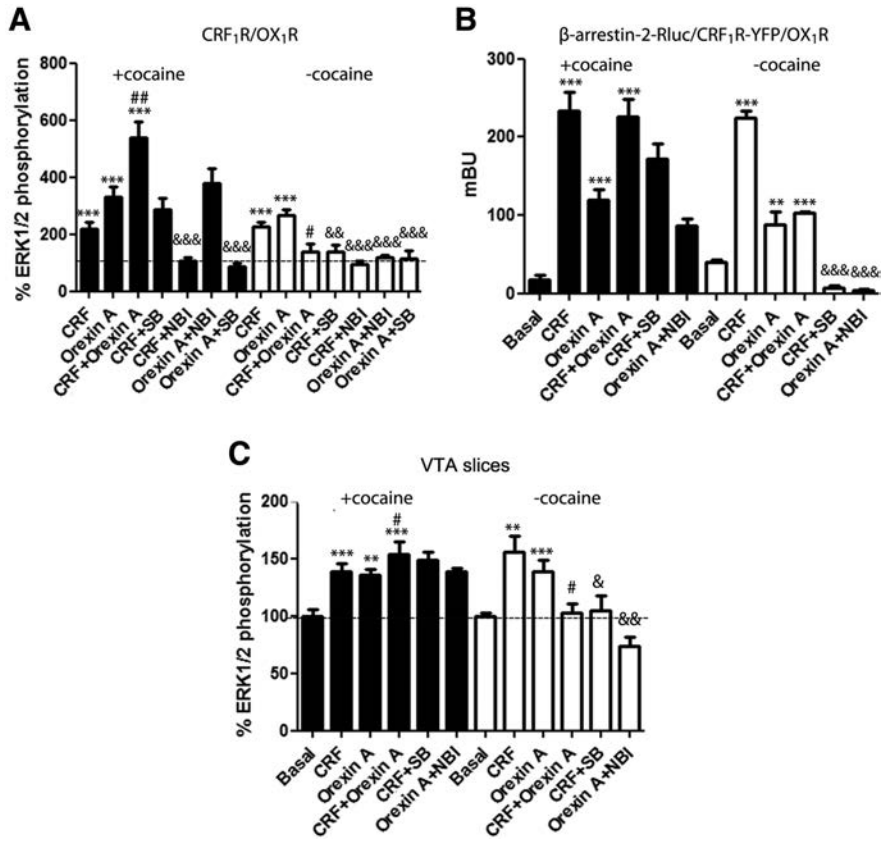

Figure 8. Cocaine-mediated disruption of negative crosstalk and cross-antagonism between CRF_1R and OX_1R ligands in CRF_1R–OX_1R heteromers in transfected cells and in the VTA. ***A***, ERK1/2 phosphorylation in HEK-293T cells transfected with CRF_1R–YFP cDNA (0.3 μg) and OX_1R–RLuc cDNA (0.4 μg) pretreated with (black bars) or without (white bars) cocaine (30 μM, 4 h) and (30 min) with vehicle, the OX_1R antagonist SB334667 (SB; 1 μM), or the CRF_1R antagonist NBI27914 (NBI; 1 μM), followed by treatment (10 min) with CRF (100 nM) or orexin-A (50 nM), or both. Values are means ± SEMs of six to seven experiments per group expressed as percentage of basal values (100%). One-way ANOVA followed by Bonferroni's multiple comparison *post hoc* test shows significant differences of agonist treatment versus basal values (**$p < 0.01$, ***$p < 0.001$), CRF plus orexin-A treatment versus CRF or orexin-A treatment ($^{\#\#}p < 0.01$), or agonist plus antagonist treatment versus agonist alone ($^{\&\&\&}p < 0.001$). ***B***, β-Arrestin 2 recruitment measured by BRET in HEK-293T cells transfected with CRF_1R–YFP cDNA (0.3 μg) and OX_1R cDNA (0.3 μg) and β-arrestin 2–RLuc cDNA (0.5 μg). Cells were pretreated (2 h) with cocaine (30 μM, black bars) or with medium (white bars) and (10 min) with vehicle, SB334667 (SB; 1 μM), or NBI27914 (NBI; 1 μM), followed by treatment (7 min) with CRF (100 nM), orexin-A (50 nM), or both. Values are means ± SEMs of five to six experiments per group. One-way ANOVA followed by Bonferroni's multiple comparison *post hoc* test shows significant differences of agonist treatment versus basal (**$p < 0.01$ and ***$p < 0.001$) or agonist plus antagonist treatment versus agonist alone ($^{\&\&\&}p < 0.001$). ***C***, ERK1/2 phosphorylation in rat VTA slices preincubated (4 h) with cocaine (100 μM, black bars) or with vehicle (white bars) and (30 min) with vehicle, SB334667 (SB; 10 μM), or NBI27914 (NBI; 10 μM), followed by treatment (10 min) with CRF (1 μM), orexin-A (1 μM) or both. Values are means ± SEMs of five to six experiments per group expressed as percentage of basal values (100%). One-way ANOVA followed by Bonferroni's multiple comparison *post hoc* test shows significant differences of agonist treatment versus basal values (**$p < 0.01$ and ***$p < 0.001$), CRF plus orexin-A treatment versus CRF or orexin-A treatment ($^{\#}p < 0.05$) or agonist plus antagonist treatment versus agonist alone ($^{\&}p < 0.05$ and $^{\&\&}p < 0.01$).

talk between CRF and orexin-A was still present with preincubation of cocaine and PD144418 (Fig. 10*D*).

Cocaine exerts its stimulant effects predominantly by its ability to block the dopamine transporter (DAT; Kita et al., 2009). To dissect the σ_1R effects in microdialysis experiments, we used the selective σ_1R agonist PRE-084, which reproduced the effects of cocaine in the *in vitro* experiments and has very low affinity for DAT (Garcés-Ramírez et al., 2011). Direct perfusion of the σ_1R agonist PRE-084 (100 μM) through the microdialysis probe did not modify the extracellular concentration of dopamine (Fig. 10*F*) but counteracted the negative crosstalk between orexin-A and CRF. Thus, in the presence of PRE-084, orexin-A plus CRF produced an increase in extracellular dopamine that was larger than the one induced by orexin-A alone (Fig. 10*E*). In fact, in the presence of PRE-084, orexin-A was more effective, particularly during the first two samples (40 min) after its infusion. Interestingly, CRF, which was ineffective by itself, also produced a prolonged significant elevation of extracellular dopamine during perfusion with the σ_1R agonist (Fig. 10*F*). These results match with the *in vitro* experiments and indicate the existence of a negative crosstalk between orexin-A and CRF, which is counteracted by σ_1R activation. These striking results are in total agreement with σ_1R–CRF_1R–OX_1R oligomers modulating VTA dopamine release.

We then studied whether one single administration of cocaine (15 mg/kg) could also reproduce the effects of the acute perfusion of the σ_1R agonist PRE-084 attributable to a long-term disruption of the allosteric interactions in the CRF_1R–OX_1R heteromer, as demonstrated recently for σ_1R–D_1R–H_3R oligomers (Moreno et al., 2014). In fact, a significant elevation in the extracellular concentration of VTA dopamine was observed after infusion of CRF or coinfusion of orexin-A and CRF (Fig. 10*G*).

Discussion

Class B GPCR CRF_1R has been shown previously to homomerize (Milan-Lobo et al., 2009) and also heteromerize with the class A GPCRs for vasopressin and its non-mammalian vertebrate homolog vasotocin in transfected cells (Mikhailova et al., 2007; Murat et al., 2012). Similarly, evidence has been reported for OX_1R homomerization and heteromerization in artificial cell systems (Ellis et al., 2006; Jäntti et al., 2014). However, although colocalized in the VTA, CRF_1R–OX_1R heteromerization has not been described, and, in fact, it has been argued that independent actions of CRF and orexin-A in the VTA are involved in reinstatement of cocaine seeking (Wang et al., 2009). In the present study, we demonstrate the existence of functional CRF_1R–OX_1R heteromers in transfected cells and the VTA, in which they exert a significant functional control of dopaminergic cells. By means of allosteric interactions within the CRF_1R–OX_1R heteromer, CRF and orexin-A antagonize each other's ability to signal and promote VTA dendritic dopamine release, indicating that this heteromer should play a significant role under stress conditions, during concomitant CRF and orexin-A VTA release. Additional important findings were the evidence for oligomerization of σ_1R with the CRF_1R–OX_1R heteromer and the ability of σ_1R agonists, including cocaine, to modify the quaternary structure of the heteromer to block the functional allosteric interactions between orexin-A and CRF within the heteromer.

Molecular interactions between CRF_1R and OX_1R were demonstrated in HEK-293T cells by using different approaches,

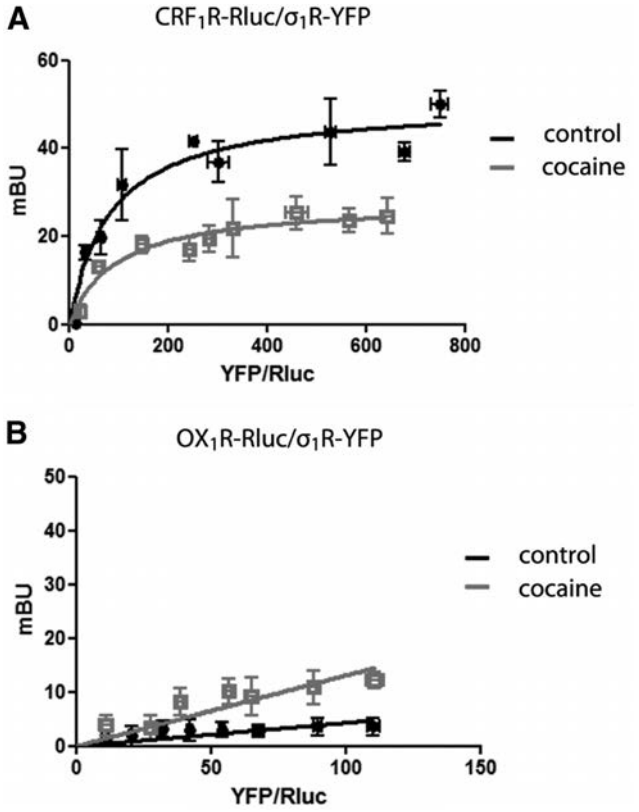

Figure 9. Interaction of σ_1R with CRF_1R. BRET saturation experiments in HEK-293T cells transfected with CRF_1R-RLuc cDNA (0.3 μg; ***A***) or OX_1R–RLuc cDNA (0.4 μg; ***B***) with increasing amounts of σ_1R–YFP cDNA (0.06 – 0.7 μg), in the absence (black curves) or presence (red curves) of cocaine (30 μM). BRET, expressed as mBU, is given as a function of 1000 × the ratio between the fluorescence of the acceptor (YFP) and the Luciferase activity of the donor (RLuc). Values are means ± SEMs of five to six experiments.

which included BRET, fluorescence complementation, and PLA, but also additional demonstration came from results of signaling experiments indicating the expression of CRF_1R–OX_1R heteromers at the membrane level. To our knowledge, the ability of an antagonist of one receptor to block the agonist-mediated signaling of another receptor has only been reported in the frame of receptor heteromerization (Ferré et al., 2014). Also, the ability of orexin-A to induce an interaction between β-arrestin 2–RLuc and CRF_1R–YFP indicates recruitment of β-arrestin 2 to the CRF_1R–OX_1R heteromer. Moreover, the surprising ability of PTX to counteract G_s-mediated CRF_1R signaling and that of CTX to block G_i-mediated OX_1R signaling indicate that the CRF_1R–OX_1R heteromer can interact simultaneously with both G_i and G_s proteins showing an interdependence of G_i and G_s protein function in the heteromer.

Demonstration of unique biochemical properties of a receptor heteromer requires their dependence on the structural integrity of the heteromer (Ferré et al., 2009, 2014), which can be destabilized, for instance, by interfering synthetic peptides with the amino acid sequence corresponding to some TM or intracellular domains of one of the protomers (Azdad et al., 2009; He et al., 2011; Guitart et al., 2014). BRET and complementation experiments in transfected cells demonstrated that specific OX_1R TM peptides and σ_1R agonists significantly modify the quaternary structure of the CRF_1R–OX_1R heteromer. Therefore, both were used as tools to interrogate the CRF_1R–OX_1R heteromer function. In fact, both OX_1R TM peptides and σ_1R agonists significantly counteracted negative crosstalk and cross-antagonism of CRF_1R and OX_1R ligands, demonstrating that they constitute biochemical properties of the CRF_1R–OX_1R heteromer. The application of the same tools *in situ* and *in vivo*, in VTA slices and in microdialysis experiments, further demonstrated the presence of CRF_1R–OX_1R heteromers in the VTA. The very different quantitative effect of OX_1R TM peptides versus σ_1R agonists observed *in vivo*, with a respective transient versus long-lasting (apparently irreversible) destabilization of CRF_1R–OX_1R-heteromer function, should be related to the different molecular mechanisms and different modifications of the quaternary structure of the heteromer involved. Particularly significant will be the elucidation of the apparently irreversible effect of σ_1R agonists, such as cocaine.

An important amount of experimental data demonstrates the involvement of σ_1R in many pharmacologic, including rewarding, effects of cocaine (Maurice and Su, 2009; Robson et al., 2012). Recent studies describe a role of oligomerization of σ_1R with D_1R or D_2R in the acute psychostimulants effects of cocaine (Navarro et al., 2010, 2013) and with voltage-gated Kv1.2 potassium channels in long-lasting behavioral responses (Kourrich et al., 2013). Also, oligomerization of σ_1R, D_1R, and H_3Rs (σ_1R–D_1R–H_3R heteromers) has been involved in the neurotoxic effects of cocaine (Moreno et al., 2014). Interestingly, when comparing the effects of cocaine binding with either σ_1R-D_1R–H_3R or σ_1R–CRF_1R–OX_1R oligomers, a common mechanism emerges, the loss of the allosteric interactions between ligands in the heteromer.

The present results strongly suggest that CRF_1R–OX_1R heteromers localized in the VTA convey the previously established significant control of dopaminergic cell function by CRF and orexin-A in cocaine-treated animals. The counteraction of the negative crosstalk between orexin-A and CRF in the VTA by the simultaneous application of the σ_1R agonist PRE-084 or by the previous administration of cocaine provides a mechanism by which CRF can only induce VTA dendritic dopamine release in animals exposed previously to cocaine (Wang et al., 2005). Under these conditions, CRF_1R-mediated signaling is not inhibited by a tonic activation of OX_1R by endogenous orexin-A. Counteraction of the allosteric interactions between agonists in the CRF_1R–OX_1R heteromer can also explain the apparent CRF-independent ability of orexin-A to release dopamine in the VTA and to induce cocaine seeking (Wang et al., 2009). Remarkably, in the present study, cocaine produced a modification of CRF_1R–OX_1R heteromer function that was observed 24 h after one single systemic administration. Very similar findings were reported recently for σ_1R–D_1R–H_3R oligomers, in which the ability of H_3R ligands to modulate D_1R-mediated signaling was also disrupted 24 h after one single systemic administration of cocaine (Moreno et al., 2014). Therefore, one single administration could explain some effects of cocaine attributed previously to its repeated administration.

Of the many new questions this study raises is the identification of the precise localization of CRF_1R–OX_1R heteromers in the VTA. Both receptors are potentially colocalized in dopaminergic cells and their glutamatergic afferents Borgland et al., 2010), in which CRF_1R–OX_1R heteromers could directly or indirectly control the extracellular levels of dopamine in the VTA. Second, our data indicate that, under basal conditions, the effects of CRF and orexin-A in the VTA are interdependent and mediated by CRF_1R–OX_1R heteromers, but they also suggest that endogenous σ_1R ligands should be able to act as cocaine and therefore promote independent effects of CRF and orexin-A. Those ligands and the conditions under which they are produced in the VTA

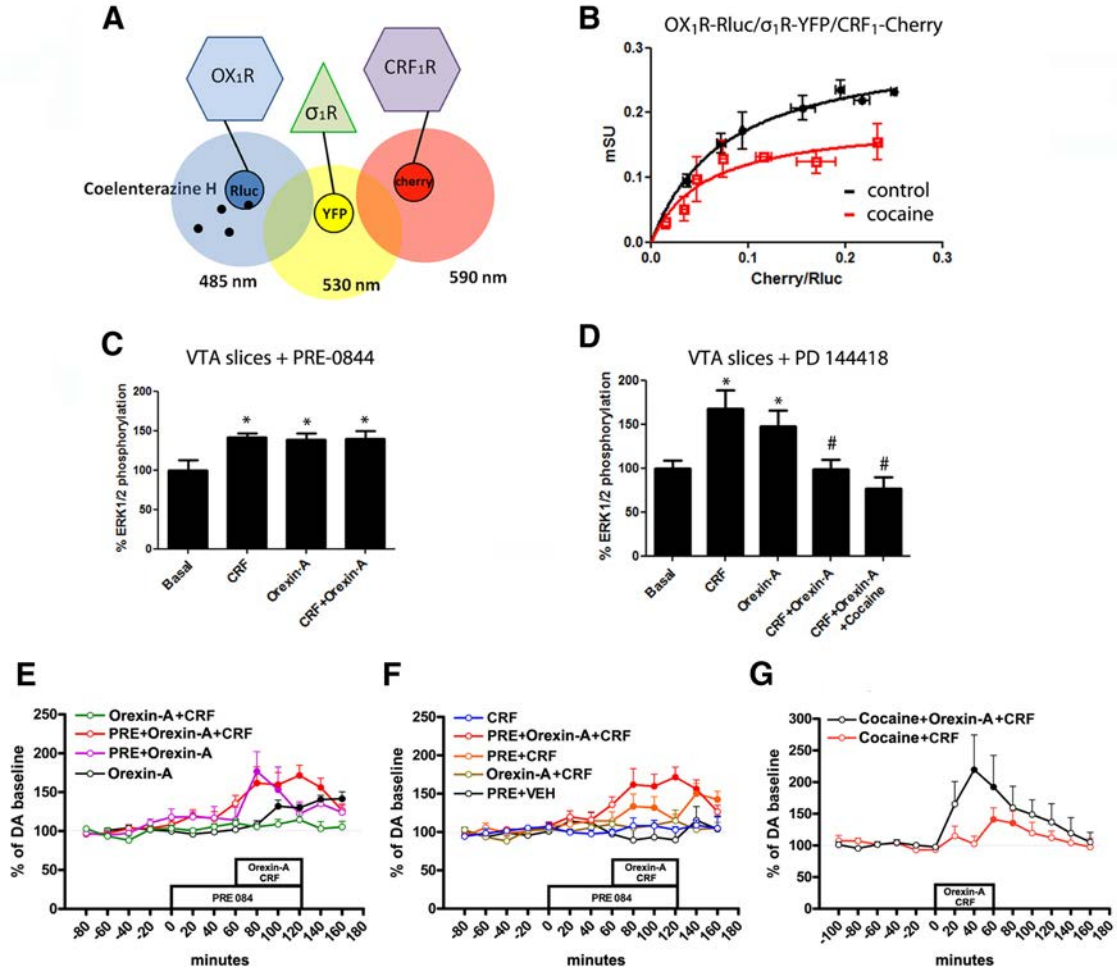

Figure 10. Involvement of σ_1R in the disruptive effect of cocaine on CRF_1R–OX_1R heteromer function. ***A***, Scheme showing SRET (see Results). ***B***, SRET saturation experiments in HEK-293T cells expressing a constant amount of OX_1R–RLuc cDNA (0.2 μg of cDNA transfected) and σ_1R–YFP cDNA (0.3 μg) and increasing amounts of CRF_1R–Cherry cDNA (0.05–0.6 μg) in controls (black curve) or cocaine-treated (30 min, 30 μM; red curve) cells. SRET, expressed as mSU, is given as a function of the ratio between the fluorescence of the acceptor (Cherry) and the Luciferase activity of the donor (RLuc). Values are means ± SEMs of seven to eight replications of one independent experiment per point. ***C***, ERK1/2 phosphorylation in rat VTA slices preincubated (4 h) with the σ_1R agonist PRE-084 (1 μM), followed by treatment (10 min) with CRF (1 μM), orexin-A (1 μM), or both. ***D***, ERK1/2 phosphorylation in rat VTA slices preincubated (4 h) with the σ_1R antagonist PD144418 (1 μM), with or without cocaine (100 μM), followed by treatment (10 min) with CRF (1 μM), orexin-A (1 μM), or both. In ***C*** and ***D***, values are means ± SEMs of five to six experiments per group expressed as percentage of basal values (100%). One-way ANOVA followed by Bonferroni's multiple comparison *post hoc* test showed significant differences versus basal (*$p < 0.05$) and CRF plus orexin-A treatment versus CRF or orexin-A treatment ($^{\#}p < 0.05$). ***E–G***, Dopamine (DA) levels in dialysates sampled from the VTA after slow infusion (1 μl/h) of orexin-A (1 μl, 10 μM) and/or CRF (1 μl, 10 μM) with preinfusion and coinfusion of the σ_1R agonist PRE-084 (PRE; 100 μM) or previous systemic (intraperitoneal) administration of cocaine (COC; 15 mg/kg; 24 h before the microdialysis experiment). Values are means ± SEMs of 7–10 experiments per group and are expressed as percentage of basal values (average of first 3 values before orexin-A or CRF infusion). A repeated-measures ANOVA (including only the basal value before orexin-A or CRF infusion) followed by Bonferroni's multiple comparison *post hoc* test showed significant differences (filled symbols, $p < 0.05$) versus the last basal values before orexin-A or CRF infusion. Data on the effect of infusion of orexin-A alone in ***E*** are the same shown in Figure 6*D–F*.

still need to be determined. Third is to understand the potential changes in σ_1R–CRF_1R–OX_1R oligomers in acute versus long-term exposure to cocaine. It has been shown that repeated cocaine exposure increases the levels of σ_1R in the brain (Robson et al., 2012), and cocaine-mediated upregulation of striatal σ_1R has been reported to increase the presence of σ_1–Kv1.2 oligomers at the plasma membrane, which has been suggested to be involved in sensitization to its psychostimulants effects (Kourrich et al., 2013). Therefore, upregulation of σ_1R in the VTA could increase the proportion of σ_1R–CRF_1R–OX_1R oligomers, leading to more profound cocaine-induced changes in the control of VTA dendritic dopamine release by CRF and orexin-A. Those changes could explain the CRF_1R-dependent augmented cocaine seeking in response to stress or CRF delivered into the VTA after long-access self-administration (Blacktop et al., 2011). Altogether, the present study demonstrates a significant functional and pharmacological role of σ_1R in the modulation of CRF_1R–OX_1R heteromers during physiological conditions and under conditions of acute cocaine administration and withdrawal. Addressing the study of σ_1R–CRF_1R–OX_1R oligomers in animal models of psychostimulant abuse should provide significant additional information that would support their role as new therapeutic targets.

References

Akunne HC, Whetzel SZ, Wiley JN, Corbin AE, Ninteman FW, Tecle H, Pei Y, Pugsley TA, Heffner TG (1997) The pharmacology of the novel and selective sigma ligand, PD 144418. Neuropharmacology 36:51–62. CrossRef Medline

Azdad K, Gall D, Woods AS, Ledent C, Ferré S, Schiffmann SN (2009) Dopamine D2 and adenosine A2A receptors regulate NMDA-mediated excitation in accum-

bens neurons through A2A-D2 receptor heteromerization. Neuropsychopharmacology 34:972–986. CrossRef Medline

Blacktop JM, Seubert C, Baker DA, Ferda N, Lee G, Graf EN, Mantsch JR (2011) Augmented cocaine seeking in response to stress or CRF delivered into the ventral tegmental area following long-access self-administration is mediated by CRF receptor type 1 but not CRF receptor type 2. J Neurosci 31:11396–11403. CrossRef Medline

Borgland SL, Ungless MA, Bonci A (2010) Convergent actions of orexin/hypocretin and CRF on dopamine neurons: emerging players in addiction. Brain Res 1314:139–144. CrossRef Medline

Boutrel B, Kenny PJ, Specio SE, Martin-Fardon R, Markou A, Koob GF, de Lecea L (2005) Role for hypocretin in mediating stress-induced reinstatement of cocaine-seeking behavior. Proc Natl Acad Sci U S A 102:19168–19173. CrossRef Medline

Carriba P, Navarro G, Ciruela F, Ferré S, Casadó V, Agnati L, Cortés A, Mallol J, Fuxe K, Canela EI, Lluís C, Franco R (2008) Detection of heteromerization of more than two proteins by sequential BRET-FRET. Nat Methods 5:727–233. CrossRef Medline

de Lecea L, Kilduff TS, Peyron C, Gao X, Foye PE, Danielson PE, Fukuhara C, Battenberg EL, Gautvik VT, Bartlett FS 2nd, Frankel WN, van den Pol AN, Bloom FE, Gautvik KM, Sutcliffe JG (1998) The hypocretins: hypothalamus-specific peptides with neuroexcitatory activity. Proc Natl Acad Sci U S A 95:322–327. CrossRef Medline

Devigny C, Perez-Balderas F, Hoogeland B, Cuboni S, Wachtel R, Mauch CP, Webb KJ, Deussing JM, Hausch F (2011) Biomimetic screening of class-B G protein-coupled. J Am Chem Soc 133:8927–8933. CrossRef Medline

Ellis J, Pediani JD, Canals M, Milasta S, Milligan G (2006) Orexin-1 receptor-cannabinoid CB1 receptor heterodimerization results in both ligand-dependent and -independent coordinated alterations of receptor localization and function. J Biol Chem 281:38812–38824. CrossRef Medline

Ferré S, Baler R, Bouvier M, Caron MG, Devi LA, Durroux T, Fuxe K, George SR, Javitch JA, Lohse MJ, Mackie K, Milligan G, Pfleger KD, Pin JP, Volkow ND, Waldhoer M, Woods AS, Franco R (2009) Building a new conceptual framework for receptor heteromers. Nat Chem Biol 5:131–134. CrossRef Medline

Ferré S, Casadó V, Devi LA, Filizola M, Jockers R, Lohse MJ, Milligan G, Pin JP, Guitart X (2014) Protein-coupled receptor oligomerization revisited: functional and pharmacological perspectives. Pharmacol Rev 66:413–434. CrossRef Medline

Garcés-Ramírez L, Green JL, Hiranita T, Kopajtic TA, Mereu M, Thomas AM, Mesangeau C, Narayanan S, McCurdy CR, Katz JL, Tanda G (2011) Sigma receptor agonists: receptor binding and effects on mesolimbic dopamine neurotransmission assessed by microdialysis. Biol Psychiatry 69:208–217. CrossRef Medline

Guitart X, Navarro G, Moreno E, Yano H, Cai NS, Sánchez-Soto M, Kumar-Barodia S, Naidu YT, Mallol J, Cortés A, Lluís C, Canela EI, Casadó V, McCormick PJ, Ferré S (2014) Functional selectivity of allosteric interactions within GPCR oligomers: the dopamine D1–D3 receptor heterotetramer. Mol Pharmacol 86:417–429. CrossRef Medline

He SQ, Zhang ZN, Guan JS, Liu HR, Zhao B, Wang HB, Li Q, Yang H, Luo J, Li ZY, Wang Q, Lu YJ, Bao L, Zhang X (2011) Facilitation of μ-opioid receptor activity by preventing δ-opioid receptor-mediated codegradation. Neuron 69:120–131. CrossRef Medline

Jäntti MH, Mandrika I, Kukkonen JP (2014) Human orexin/hypocretin receptors form constitutive homo- and heteromeric complexes with each other and with human CB1 cannabinoid receptors. Biochem Biophys Res Commun 445:486–490. CrossRef Medline

Kita JM, Kile BM, Parker LE, Wightman RM (2009) In vivo measurement of somatodendritic release of dopamine in the ventral tegmental area. Synapse 63:951–960. CrossRef Medline

Kourrich S, Hayashi T, Chuang JY, Tsai SY, Su TP, Bonci A (2013) Dynamic interaction between sigma-1 receptor and Kv1.2 shapes neuronal and behavioral responses to cocaine. Cell 152:236–247. CrossRef Medline

Kovacs JJ, Hara MR, Davenport CL, Kim J, Lefkowitz RJ (2009) Arrestin development: emerging roles for beta-arrestins in developmental signaling pathways. Dev Cell 17:443–458. CrossRef Medline

Legault M, Wise RA (1999) Injections of N-methyl-D-aspartate into the ventral hippocampus increase extracellular dopamine in the ventral tegmental area and nucleus accumbens. Synapse 31:241–249. CrossRef Medline

Lodge DJ, Grace AA (2005) Acute and chronic corticotropin-releasing factor 1 receptor blockade inhibits cocaine-induced dopamine release: correlation with dopamine neuron activity. J Pharmacol Exp Ther 314:201–206. CrossRef Medline

Lu L, Liu Z, Huang M, Zhang Z (2003) Dopamine-dependent responses to cocaine depend on corticotropin-releasing factor receptor subtypes. J Neurochem 84:1378–1386. CrossRef Medline

Mahler SV, Moorman DE, Smith RJ, James MH, Aston-Jones G (2014) Motivational activation: a unifying hypothesis of orexin/hypocretin function. Nat Neurosci 17:1298–1303. CrossRef Medline

Maurice T, Su TP (2009) The pharmacology of sigma-1 receptors. Pharmacol Ther 124:195–206. CrossRef Medline

Mikhailova MV, Mayeux PR, Jurkevich A, Kuenzel WJ, Madison F, Periasamy A, Chen Y, Cornett LE (2007) Heterooligomerization between vasotocin and corticotropin-releasing hormone (CRH) receptors augments CRH-stimulated 3′,5′-cyclic adenosine monophosphate production. Mol Endocrinol 21:2178–2188. CrossRef Medline

Milan-Lobo L, Gsandtner I, Gaubitzer E, Rünzler D, Buchmayer F, Köhler G, Bonci A, Freissmuth M, Sitte HH (2009) Subtype-specific differences in corticotropin-releasing factor receptor complexes detected by fluorescence spectroscopy. Mol Pharmacol 76:1196–1210. CrossRef Medline

Moreno E, Moreno-Delgado D, Navarro G, Hoffmann HM, Fuentes S, Rosell-Vilar S, Gasperini P, Rodríguez-Ruiz M, Medrano M, Mallol J, Cortés A, Casadó V, Lluís C, Ferré S, Ortiz J, Canela E, McCormick PJ (2014) Cocaine disrupts histamine H3 receptor modulation of dopamine D1 receptor signaling: σ1-D1–H3 receptor complexes as key targets for reducing cocaine's effects. J Neurosci 34:3545–3558. CrossRef Medline

Murat B, Devost D, Andrés M, Mion J, Boulay V, Corbani M, Zingg HH, Guillon G (2012) V1b and CRHR1 receptor heterodimerization mediates synergistic biological actions of vasopressin and CRH. Mol Endocrinol 26:502–520. CrossRef Medline

Navarro G, Moreno E, Aymerich M, Marcellino D, McCormick PJ, Mallol J, Cortés A, Casadó V, Canela EI, Ortiz J, Fuxe K, Lluís C, Ferré S, Franco R (2010) Direct involvement of sigma-1 receptors in the dopamine D1 receptor-mediated effects of cocaine. Proc Natl Acad Sci U S A 107:18676–18681. CrossRef Medline

Navarro G, Moreno E, Bonaventura J, Brugarolas M, Farré D, Aguinaga D, Mallol J, Cortés A, Casadó V, Lluís C, Ferre S, Franco R, Canela E, McCormick PJ (2013) Cocaine inhibits dopamine D2 receptor signaling via sigma-1-D2 receptor heteromers. PLoS One 8:e61245. CrossRef Medline

Pettit HO, Pan HT, Parsons LH, Justice JB Jr (1990) Extracellular concentrations of cocaine and dopamine are enhanced during chronic cocaine administration. J Neurochem 55:798–804. CrossRef Medline

Richards JK, Simms JA, Steensland P, Taha SA, Borgland SL, Bonci A, Bartlett SE (2008) Inhibition of orexin-1/hypocretin-1 receptors inhibits yohimbine-induced reinstatement of ethanol and sucrose seeking in Long-Evans rats. Psychopharmacology 199:109–117. CrossRef Medline

Robson MJ, Noorbakhsh B, Seminerio MJ, Matsumoto RR (2012) Sigma-1 receptors: potential targets for the treatment of substance abuse. Curr Pharm Des 18:902–919. CrossRef Medline

Rodaros D, Caruana DA, Amir S, Stewart J (2007) Corticotropin-releasing factor projections from limbic forebrain and paraventricular nucleus of the hypothalamus to the region of the ventral tegmental area. Neuroscience 150:8–13. CrossRef Medline

Saal D, Dong Y, Bonci A, Malenka RC (2003) Drugs of abuse and stress trigger a common synaptic adaptation in dopamine neurons. Neuron 37:577–582. CrossRef Medline

Sakurai T (2014) The role of orexin in motivated behaviours. Nat Rev Neurosci 15:719–731. CrossRef Medline

Sakurai T, Amemiya A, Ishii M, Matsuzaki I, Chemelli RM, Tanaka H, Williams SC, Richardson JA, Kozlowski GP, Wilson S, Arch JR, Buckingham RE, Haynes AC, Carr SA, Annan RS, McNulty DE, Liu WS, Terrett JA, Elshourbagy NA, Bergsma DJ, Yanagisawa M (1998) Orexins and orexin receptors: a family of hypothalamic neuropeptides and G protein-coupled receptors that regulate feeding behavior. Cell 92:573–585. CrossRef Medline

Sarnyai Z, Shaham Y, Heinrichs SC (2001) The role of corticotropin-releasing factor in drug addiction. Pharmacol Rev 53:209–243. Medline

Schwarze SR, Ho A, Vocero-Akbani A, Dowdy SF (1999) In vivo protein transduction: delivery of a biologically active protein into the mouse. Science 285:1569–1572. CrossRef Medline

Shaham Y, Erb S, Leung S, Buczek Y, Stewart J (1998) CP-154,526, a selective, non-peptide antagonist of the corticotropin-releasing factor1 receptor attenuates stress-induced relapse to drug seeking in cocaine- and heroin-trained rats. Psychopharmacology 137:184–190. CrossRef Medline

Ungless MA, Singh V, Crowder TL, Yaka R, Ron D, Bonci A (2003) Corticotropin-releasing factor requires CRF binding protein to potentiate NMDA receptors via CRF receptor 2 in dopamine neurons. Neuron 39: 401–407. CrossRef Medline

Wang B, Shaham Y, Zitzman D, Azari S, Wise RA, You ZB (2005) Cocaine experience establishes control of midbrain glutamate and dopamine by corticotropin-releasing factor: a role in stress-induced relapse to drug seeking. J Neurosci 25:5389–5396. CrossRef Medline

Wang B, You ZB, Rice KC, Wise RA (2007) Stress-induced relapse to cocaine seeking: roles for the CRF(2) receptor and CRF-binding protein in the ventral tegmental area of the rat. Psychopharmacology 193:283–294. CrossRef Medline

Wang B, You ZB, Wise RA (2009) Reinstatement of cocaine seeking by hypocretin (orexin) in the ventral tegmental area: independence from the local corticotropin-releasing factor network. Biol Psychiatry 65:857–862. CrossRef Medline

3.4. A SIGNIFICANT ROLE OF THE TRUNCATED GHRELIN RECEPTOR GHS-R1b IN GHRELIN-INDUCED SIGNALING IN NEURONS

Gemma Navarro[*], **David Aguinaga**[*], Edgar Angelats, Mireia Medrano, Estefanía Moreno, Josefa Mallol, Antonio Cortés, Enric I. Canela, Vicent Casadó, Peter J. McCormick, Carme Lluís y Sergi Ferré.

[*]Coautores del manuscrito

Manuscrito publicado en *The Journal of Biological Chemistry*, junio 2017; 291(25):13048-13062

Ha sido sugerido que el receptor de grelina truncado *growth hormone secretatogue* R1b (GHS-R1b), el cual no puede señalizar, simplemente ejercería un papel dominante negativo en el tráfico y la señalización del receptor de grelina completo y funcional (GHS-R1a). En este trabajo ha sido revelado un papel modulador más complejo de GHS-R1b. Una coexpresión diferencial de GHS-R1a y GHS-R1b, tanto en células HEK-293T como en cultivos de neuronas del estriado y del hipocampo, demuestran que GHS-R1b actúa como un modulador dual de la función de GHS-R1a: bajos niveles relativos de expresión de GHS-R1b potencian y altos niveles relativos de expresión de GHS-R1b inhiben la funcionalidad de GHS-R1a facilitando el tráfico hacia la membrana plasmática y ejerciendo un efecto alostérico negativo sobre la señalización de GHS-R1a, respectivamente. Ha sido detectado un acoplamiento preferencial a proteína $G_{i/o}$ por parte del complejo GHS-R1a-GHS-R1b en céulas HEK-293T y, inesperadamente, un acoplamiento $G_{s/olf}$ preferencial en cultivos de neuronas del estriado y del hipocampo. Un antagonista del receptor D_1 de dopamina (D_1R) bloquea la acumulación de cAMP inducida por grelina en las neuronas estriatales pero no del hipocampo, lo que indica la participación de D_1R en el acoplamiento GHS-R1a-$G_{s/olf}$ en el estriado. Los experimentos en células HEK-293T han demostrado que la co-expresión de D_1R promueve un cambio en el acoplamiento de la proteína G al receptor GHS-R1a, de $G_{i/o}$ a $G_{s/olf}$ pero sólo mediante coexpresión del receptor GHS-R1b. Además, los experimentos de transferencia de energía de resonancia mostraron que el receptor D_1 interacciona con GHS-R1a, pero solo en presencia de GHS-R1b. Por lo tanto, GHS-R1b no sólo determina la eficacia de la señalización del receptor GHS-R1a inducida por grelina, sino que también determina la capacidad de GHS-R1a para formar complejos oligoméricos con otros receptores, promoviendo cambios cualitativos profundos en la señalización inducida por grelina.

THE JOURNAL OF BIOLOGICAL CHEMISTRY VOL. 291, NO. 25, pp. 13048–13062, June 17, 2016
Published in the U.S.A.

A Significant Role of the Truncated Ghrelin Receptor GHS-R1b in Ghrelin-induced Signaling in Neurons*

Received for publication, January 11, 2016, and in revised form, April 6, 2016 Published, JBC Papers in Press, April 25, 2016, DOI 10.1074/jbc.M116.715144

Gemma Navarro[‡1,2], David Aguinaga[‡1], Edgar Angelats[‡], Mireia Medrano[‡], Estefanía Moreno[‡], Josefa Mallol[‡], Antonio Cortés[‡], Enric I. Canela[‡], Vicent Casadó[‡], Peter J. McCormick[§3], Carme Lluís[‡], and Sergi Ferré[¶4]

From the [‡]Department of Biochemistry and Molecular Biology, Faculty of Biology, University of Barcelona and Centro de Investigación Biomédica en Red sobre Enfermedades Neurodegenerativas, 08028 Barcelona, Spain, the [§]School of Pharmacy, University of East Anglia, Norwich Research Park, Norwich NR4 7TJ, United Kingdom, and the [¶]Integrative Neurobiology Section, National Institute on Drug Abuse, Intramural Research Program, Baltimore, Maryland 21224

The truncated non-signaling ghrelin receptor growth hormone secretagogue R1b (GHS-R1b) has been suggested to simply exert a dominant negative role in the trafficking and signaling of the full and functional ghrelin receptor GHS-R1a. Here we reveal a more complex modulatory role of GHS-R1b. Differential co-expression of GHS-R1a and GHS-R1b, both in HEK-293T cells and in striatal and hippocampal neurons in culture, demonstrates that GHS-R1b acts as a dual modulator of GHS-R1a function: low relative GHS-R1b expression potentiates and high relative GHS-R1b expression inhibits GHS-R1a function by facilitating GHS-R1a trafficking to the plasma membrane and by exerting a negative allosteric effect on GHS-R1a signaling, respectively. We found a preferential $G_{i/o}$ coupling of the GHS-R1a-GHS-R1b complex in HEK-293T cells and, unexpectedly, a preferential $G_{s/olf}$ coupling in both striatal and hippocampal neurons in culture. A dopamine D_1 receptor (D1R) antagonist blocked ghrelin-induced cAMP accumulation in striatal but not hippocampal neurons, indicating the involvement of D1R in the striatal GHS-R1a-$G_{s/olf}$ coupling. Experiments in HEK-293T cells demonstrated that D1R co-expression promotes a switch in GHS-R1a-G protein coupling from $G_{i/o}$ to $G_{s/olf}$, but only upon co-expression of GHS-R1b. Furthermore, resonance energy transfer experiments showed that D1R interacts with GHS-R1a, but only in the presence of GHS-R1b. Therefore, GHS-R1b not only determines the efficacy of ghrelin-induced GHS-R1a-mediated signaling but also determines the ability of GHS-R1a to form oligomeric complexes with other receptors, promoting profound qualitative changes in ghrelin-induced signaling.

Ghrelin is an orexigenic hormone, an internal signal for the animal to engage in food-directed behavior (1, 2). It is produced by stomach oxyntic cells, which provide plasma levels that fluctuate diurnally with a peak in the day and trough at night. Notably, oxyntic cells qualify as food-entrained oscillators, and ghrelin plasma levels increase during anticipated mealtimes and decrease after meals (1). These and other less well characterized central neuronal functions of ghrelin depend on its ability to cross the blood-brain barrier by still unclear mechanisms and reaching ghrelin receptors localized in specific brain areas, such as the hypothalamus, hippocampus, amygdala, mesencephalic dopaminergic regions, and striatum (2–4).

Ghrelin acts on the class A G protein-coupled receptor known as growth hormone secretagogue (GHS)[5] receptor or GHS-R1a. Cells expressing GHS-R1a also express GHS-R1b, a truncated variant of GHS-R1a lacking transmembrane domains 6 and 7. Ghrelin does not bind and therefore does not signal through GHS-R1b (5), and the role of this truncated "receptor" on ghrelin-mediated signaling is just beginning to be understood. Evidence has been provided for the ability of GHS-R1a to homodimerize and heterodimerize with GHS-R1b, which might allow GHS-R1b to produce a dominant negative effect on GHS-R1a signaling. Two different mechanisms have been invoked for the dominant negative function of GHS-R1b: intracellular retention by an inability of GHS-R1b to traffic to the plasma membrane (6, 7) and an allosteric mechanism that produces a conformational block of GHS-R1a in a non-signaling conformation (5). Those results were obtained from *in vitro* experiments in transfected cells and in reconstituted lipid vesicles, and, therefore, either mechanism could be involved in a physiological cellular environment. However, although both mechanisms do not seem exclusive, the intracellular retention of the GHS-R1a-GHS-R1b heteromer would render the reported complete blockade of G protein activation and β-arrestin recruitment (5) a fortuitous useless mechanism because both signaling pathways originate in the plasma membrane. The initial aim of this study was elucidating the mechanisms of GHS-R1b-mediated modulation of GHS-R1a in a neuronal environment and includes signaling experiments performed in a mammalian cell line and primary neurons in culture, with particular emphasis on the changes produced by manipulation of the relative expression of GHS-R1a and GHS-R1b in the plasma

* This work was supported by Spanish Ministerio de Ciencia y Tecnología Grant SAF2011-23813, government of Catalonia Grant 2014-SGR-1236, Centro de Investigación Biomédica en Red sobre Enfermedades Neurodegenerativas Grant CB06/05/0064, and intramural funds of the National Institute on Drug Abuse. The authors declare that they have no conflicts of interest with the contents of this article.

[1] Both authors contributed equally to this work.

[2] To whom correspondence may be addressed: Dept. of Biochemistry and Molecular Biology, Faculty of Biology, University of Barcelona, Diagonal 645, 08028 Barcelona, Spain. E-mail: dimartts@hotmail.com.

[3] Supported by a Ramon y Cajal fellowship.

[4] To whom correspondence may be addressed: Integrative Neurobiology Section, National Institute on Drug Abuse, Intramural Research Program, National Institutes of Health, Triad Technology Bldg., 333 Cassell Dr., Baltimore, MD 21224. E-mail: sferre@intra.nida.nih.gov.

[5] The abbreviations used are: GHS, growth hormone secretagogue; D1R, dopamine D_1 receptor; BRET, bioluminescence resonance energy transfer; SRET, sequence resonance energy transfer; DMR, dynamic mass redistribution; PTX, pertussis toxin; CTX, cholera toxin; ANOVA, analysis of variance; mBU, milliBRET unit; mSU, milliSRET unit.

membrane. The study reveals a significant and complex modulatory role of GHS-R1b in the trafficking and signaling of GHS-R1a that depends on the relative expression of both proteins. An unexpected additional finding in striatal and hippocampal neurons in culture was a predominant $G_{s/olf}$ protein-dependent signaling of ghrelin that, in striatal neurons, depended on dopamine D_1 receptor (D1R)-GHS-R1a-GHS-R1b heteromerization.

Experimental Procedures

Cell Lines and Neuronal Primary Cultures—HEK-293T cells were grown in DMEM (Gibco) supplemented with 2 mM L-glutamine, 100 μg/ml sodium pyruvate, 100 units/ml penicillin/streptomycin, minimum Eagle's medium non-essential amino acid solution (1/100) and 5% (v/v) heat-inactivated FBS (all supplements were from Invitrogen). Primary cultures of striatal, hippocampal, and cortical neurons were obtained from fetal Sprague-Dawley rats (embryonic day 19). Cells were isolated as described in Ref. 8 and plated at a confluence of 40,000 cells/0.32 cm^2 in 96-well plates for MAPK experiments and in 6-well plates for the other assays. Cells were maintained in Neurobasal medium supplemented with 2 mM L-glutamine, 100 units/ml penicillin/streptomycin, and 2% (v/v) B27 supplement (Gibco) in a 96-well plate for 12 days.

Vectors and Fusion Proteins—Sequences encoding amino acid residues 1-155 and 155-238 of the Venus variant of YFP and amino acid residues 1-229 and 230-311 of Rluc8 protein were subcloned in the pcDNA3.1 vector to obtain YFP and Rluc hemitruncated proteins. Human cDNAs for GHS-R1a, GHS-R1b, cannabinoid CB_1 receptor (CB1R), corticotropin-releasing factor CRF_1 receptor (CRF1R), or adenosine A_1 receptor (A1R), cloned into pcDNA3.1, were amplified without their stop codons using sense and antisense primers harboring EcoRI and KpnI sites to clone GHS-R1a, GHS-R1b and CRF1R in the pRLuc-N1 vector (pRLuc-N1, PerkinElmer Life Sciences) or in the pEYFP-N1 vector (enhanced yellow variant of GFP, Clontech); HindIII and BamHI sites to clone A1R in the pcDNA3.1cRluc8- vector; BamHI and EcoRI sites to clone CB1R in the pcDNA3.1RLuc vector; or EcoRI and KpnI sites to clone GHS-R1a receptors in a GFP^2-containing vector (p-GFP^2, Packard BioScience, Meridien, CT). Amplified fragments were subcloned to be in-frame with restriction sites of pRLuc-N1, pEYFP-N1, or p-GFP^2 vectors to provide plasmids that express proteins fused to RLuc, YFP, or GFP^2 on the C-terminal end (GHS-R1a-Rluc, GHS-R1b-Rluc, CB1R-Rluc, CRF1R-Rluc, GHS-R1a-YFP, GHS-R1b-YFP, or GHS-R1a-GFP^2). For bioluminescence resonance energy transfer (BRET) with bimolecular fluorescence and luminescence complementation (BiFC and BiLC) experiments, cDNA for GHS-R1b was subcloned into pcDNA3.1-nVenus and cDNA for GHS-R1a was subcloned into pcDNA3.1-cVenus to provide plasmids that express the receptor fused to the hemitruncated nYFP Venus or cYFP Venus on the C-terminal end of the receptor (GHS-R1b-nYFP and GHS-R1a-cYFP). Also, the cDNA for GHS-R1b was subcloned into pcDNA3.1-nRluc8 and the cDNA for GHS-R1a and A1R were subcloned into pcDNA3.1-cRluc8 to provide plasmids that express the receptor fused to the hemitruncated nRluc8 or cRluc8 on the C-terminal end of the receptor (GHS-R1b-nRluc, GHS-R1a-cRluc, and A1R-cRluc).

Cell Transfection—HEK-293T cells and neuronal primary cultures growing in 6-well dishes were transiently transfected with the corresponding protein cDNA by the PEI (Sigma-Aldrich, St. Louis, MO) method. Cells were incubated (4 h for HEK-293T cells and 6 h for neurons) with the corresponding cDNA together with PEI (5.47 mM in nitrogen residues) and 150 mM NaCl in a serum-starved medium. After 4 h, the medium was changed to a fresh complete culture medium. Forty-eight hours after transfection, cells were washed twice in quick succession in Hanks' balanced salt solution with 10 mM glucose, detached, and resuspended in the same buffer. Cells were maintained at 37 °C in an atmosphere of 5% CO_2.

Resonance Energy Transfer-based Assays—For BRET assays, HEK-293T cells were transiently co-transfected with a constant cDNA encoding for receptor-Rluc and with increasing amounts of cDNA corresponding to receptor-YFP or receptor-GFP^2. To control the cell number, the sample protein concentration was determined using a Bradford assay kit (Bio-Rad) using bovine serum albumin dilutions as standards. To quantify fluorescence proteins, cells (20 μg protein) were distributed in 96-well microplates (black plates with a transparent bottom), and the fluorescence was read in a Fluostar Optima fluorimeter (BMG Labtech, Offenburg, Germany) equipped with a high-energy xenon flash lamp using a 10-nm bandwidth excitation filter at 410 nm for receptor-GFP^2 reading or 485 nm for receptor-YFP reading. Receptor fluorescence expression was determined as fluorescence of the sample minus the fluorescence of cells expressing receptor-Rluc alone. For BRET measurements, the equivalent of 20 μg of cell suspension was distributed in 96-well white microplates with white bottoms (Corning 3600, Corning, NY) and 5 μM of coelenterazine H (for the YFP acceptor) or DeepBlueC (for the GFP^2 acceptor) (Molecular Probes, Eugene, OR) were added. Using DeepBlueC or coelenterazine H as substrates results in respective 410- and 485-nm emissions from Rluc, which allows the respective selective energy transfer to GFP^2 and YFP (14). One minute after adding coelenterazine H or immediately after addition of DeepBlueC, BRET was determined using a Mithras LB 940 reader (Berthold Technologies, DLReady), which allows the integration of the signals detected in the short-wavelength filter at 485 nm and the long-wavelength filter at 530 nm when YFP is the acceptor or the short-wavelength filter at 400 nm and the long-wavelength filter at 510 nm when GFP^2 is the acceptor. To quantify receptor-Rluc expression, luminescence readings were performed after 10 min of adding 5 μM of coelenterazine H irrespective of the acceptor used. Net BRET is defined as [(long-wavelength emission)/(short-wavelength emission)] − Cf, where Cf corresponds to [(long-wavelength emission)/(short-wavelength emission)] for the Rluc construct expressed alone in the same experiment. For BiFC and BiLC assays, HEK-293T cells were transiently co-transfected with a constant amount of cDNA encoding for proteins fused to nRluc8 or cRluc8 and with increasing amounts of the cDNA corresponding to proteins fused to nYFP Venus or cYFP Venus. The complemented YFP Venus or Rluc8 expression and BRET were quantified as described above. For sequence resonance energy transfer (SRET) assays (14), HEK-293T cells were transiently co-transfected with constant amounts of cDNAs encoding for both the

receptor fused to RLuc or GFP[2] and with increasingly amounts of cDNA corresponding to the receptor fused to YFP. Using aliquots of transfected cells (20 μg of protein), different determinations were performed in parallel: quantification of protein-YFP expression and quantification of protein-Rluc expression as described above. For SRET, cells were distributed in 96-well microplates, and 5 μM DeepBlueC was added. The SRET signal was collected using a Mithras LB 940 reader with detection filters for short wavelength (410 nm) and long wavelength (530 nm). By analogy with BRET, net SRET is defined as ((long wavelength emission)/(short wavelength emission)) − Cf, where Cf corresponds to long wavelength emission / short wavelength emission for cells expressing protein-Rluc and protein-GFP[2]. Linear unmixing was done for SRET quantification, taking into account the spectral signature to separate the two fluorescence emission spectra (11). SRET is expressed as milliSRET units (mSU; net SRET × 1000).

Immunocytochemistry—Transiently transfected HEK-293T cells were fixed in 4% paraformaldehyde for 15 min and washed with PBS containing 20 mM glycine (buffer A) to quench the aldehyde groups. After permeabilization with buffer A containing 0.2% Triton X-100 for 5 min, cells were treated with PBS containing 1% bovine serum albumin. After 1 h at room temperature, cells expressing receptor-Rluc were labeled with a primary mouse monoclonal anti-Rluc antibody (1/100, EMD Millipore, Darmstadt, Germany) for 1 h, washed, and stained with a secondary antibody for Cy3 donkey anti-mouse (1/100, Jackson ImmunoResearch Laboratories, Baltimore, MD). Receptors fused to YFP were detected by their fluorescence properties. Samples were rinsed and observed under a Leica SP2 confocal microscope or an SP5 confocal microscopy for DsRed (Leica Microsystems, Mannheim, Germany).

Western Blotting—To determine the GHS-R1a-YFP, GHS-R1b-YFP, or CB1R-YFP expression levels in transfected HEK-293T cells, equivalent amounts of cell protein (10 μg) were separated by electrophoresis on a denaturing 10% SDS-polyacrylamide gel and transferred onto PVDF fluorescence membranes. The membranes were probed with a mixture of a mouse anti-β-tubulin antibody (1:2000, Sigma-Aldrich) and a rabbit anti-YFP antibody (1:1000, Santa Cruz Biotechnology, Dallas, TX) and a mixture of IRDye 800 (anti-mouse) antibody (1:10,000; Sigma-Aldrich) and IRDye 680 (anti-rabbit) antibody (1:10,000; Sigma). Bands were scanned using an Odyssey infrared scanner (LI-COR Biotechnology, Lincoln, NE). Band densities were quantified using the scanner software, and the receptor level was normalized for differences in loading using tubulin protein band intensities.

Biotinylation Experiments—Cell surface proteins were biotinylated as described previously (9) using HEK-293T cells transiently expressing GHS-R1a-YFP and increasing amounts of GHS-R1b-Rluc or CB1R-Rluc or expressing increasing amounts of GHS-R1b-Rluc. Cells were washed three times with borate buffer (10 mM H_3BO_3 (pH 8.8) and 150 mM NaCl) and incubated with 50 μg/ml sulfo-NHS-LC-biotin (Thermo Fisher Scientific, Halethorpe, MD) in borate buffer for 5 min at room temperature. Cells were then washed three times in borate buffer and again incubated with 50 μg/ml sulfo-NHS-LC-biotin in borate buffer for 10 min at room temperature, followed by addition of 13 mM NH_4Cl for 5 min to quench the remaining biotin. Cells were washed in PBS, disrupted with three 10-s strokes in a Polytron, and centrifuged at 16,000 × *g* for 30 min. The pellet was solubilized in ice-cold radioimmune precipitation assay buffer (50 mM Tris-HCl, 1% Triton X-100, 0.2% SDS, 100 mM NaCl, 1 mM EDTA, and 0.5% sodium deoxycholate) for 30 min and centrifuged at 16,000 × *g* for 20 min. The supernatant was incubated with 80 μl streptavidin-agarose beads (Sigma-Aldrich) for 1 h with constant rotation at 4 °C. Beads were washed three times with ice-cold lysis buffer and aspirated to dryness with a 28-gauge needle. Subsequently, 50 μl of SDS-PAGE sample buffer (8 M urea, 2% SDS, 100 mM dithiothreitol, and 375 mM Tris (pH 6.8)) were added to each sample. Proteins were dissociated by heating to 37 °C for 2 h and resolved by SDS-polyacrylamide gel electrophoresis in 10% gels and immunoblotted as described above.

RT-PCR Assay—Total cellular RNA was isolated from neuronal cultures using a QuickPrep total RNA extraction kit (Amersham Biosciences, Piscataway, NJ). Total RNA (1 μg) was reverse-transcribed by random priming using the RNase H minus, point mutant, Moloney murine leukemia virus reverse transcriptase, following the protocol for two-step RT-PCR provided by Promega (Madison, WI). The resulting single-stranded cDNA was used to perform PCR amplification for GHS-R1a and GHS-R1b and GAPDH as an internal control of the PCR technique using TaqDNA polymerase (Promega). A rat GHS-R1a and GHS-R1b common forward primer (5′-GCTCTTCGTGGTGGGCATCT-3′) was used. To amplify GHS-R1a, the 5′-GAGAAGGATTCAAATCCTAGCA-3′ reverse primer was used, corresponding to a nucleotide sequence coding for transmembrane domain 7, not present in GHS-R1b. To amplify GHS-R1b, the 5′-TCAGCGGGTGCCAGGACTC-3′ reverse primer was used, corresponding to a nucleotide sequence coding for the five TM domain not present in GHS-R1a. To amplify GAPDH, the primers used were 5′-CATCCTGCACCACCAACTGCTTAG-3′ (forward) and 5′-GCCTGCTTCACCACCTTCTTGATG-3′ (reverse). RNA without reverse transcriptions did not yield any amplicons, indicating that there was no genomic DNA contamination.

Dynamic Mass Redistribution (DMR) Label-free Assays—Cell signaling was explored using an EnSpire® multimode plate reader (PerkinElmer Life Sciences) by a label-free technology. Refractive waveguide-grating optical biosensors, integrated in 384-well microplates, allow extremely sensitive measurements of changes in local optical density in a detecting zone up to 150 nm above the surface of the sensor. Cellular mass movements induced upon receptor activation were detected by illuminating the underside of the biosensor with polychromatic light and measured as changes in wavelength of the reflected monochromatic light that is a sensitive function of the index of refraction. The magnitude of this wavelength shift (in picometers) is directly proportional to the amount of DMR. Briefly, HEK-293T cells or neurons were seeded in 384-well sensor microplates to obtain 70–80% confluent monolayers. Prior to the assay, cells were washed twice with assay buffer (Hanks' balanced salt solution with 20 mM HEPES (pH 7.15)) and incubated for 2 h in the reader at 24 °C in 30 μl/well of vehicle (assay buffer with 0.1% DMSO). Hereafter, the sensor plate was

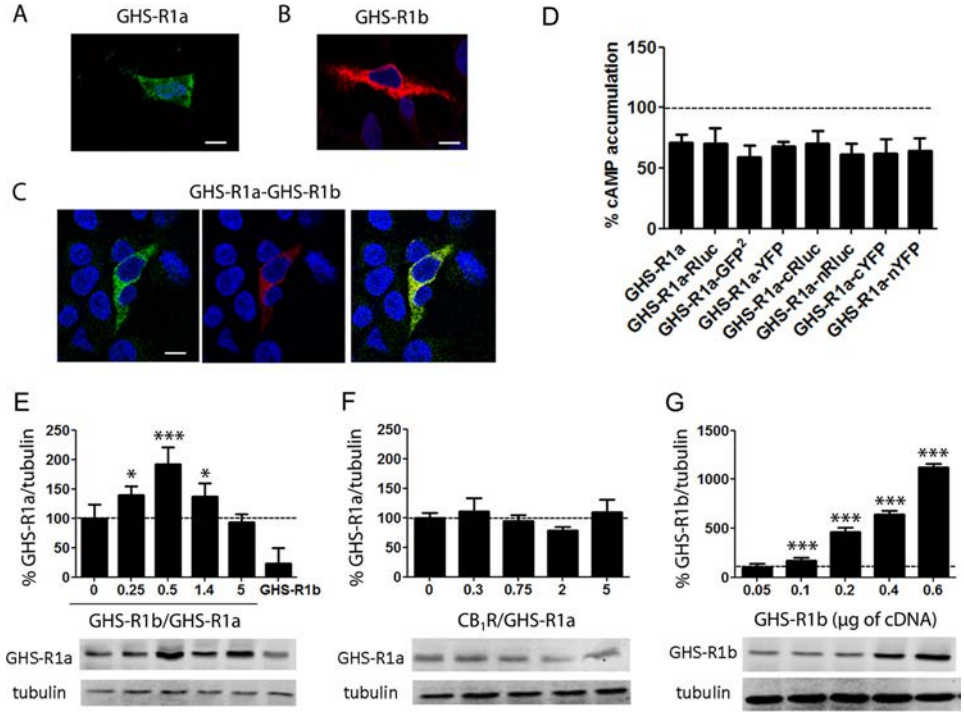

FIGURE 1. **GHS-R1b modulates plasma membrane expression of GHS-R1a in HEK-293T cells.** *A–C*, confocal microscopy images of HEK-293T cells transfected with GHS-R1a-YFP cDNA (1.5 μg), GHS-R1b-Rluc (0.5 μg), or both. GHS-R1a-YFP was identified by its own fluorescence (*green*) and GHS-R1b-Rluc by a monoclonal anti-Rluc primary antibody and a cyanine-3-conjugated secondary antibody (*red*). *C*, colocalization of both receptors is shown in *yellow*. Cell nuclei were stained with Hoechst (*blue*). *Scale bars* = 10 μm. *D*, cAMP was determined in HEK-293T cells transfected with cDNA (1.5 μg) from the indicated receptors or fusion proteins. Cells were exposed for 15 min to vehicle or ghrelin (100 nM) in the presence of forskolin (0.5 μM). Values are means ± S.E. of three to four experiments and expressed as decreases (percent) *versus* forskolin alone (100%, *dotted line*). No statistical differences between differently transfected cells were found by ANOVA followed by Bonferroni's corrections ($p > 0.05$). *E–G*, biotinylation experiments were performed in HEK-293T cells co-transfected with GHS-R1a-YFP cDNA (1 μg) and increasing amounts of GHS-R1b-Rluc cDNA (0–0.6 μg) or GHS-R1b-Rluc cDNA alone (0.5 μg) (*E*), GHS-R1a-YFP cDNA (1 μg) and increasing amounts of CB1R-Rluc cDNA (0–1 μg) (*F*), or increasing amounts of GHS-R1b-Rluc cDNA (0.05–0.6 μg) (*G*). Quantification of immunoreactive bands from four to six independent experiments is shown. Values represent mean ± S.E. of the percentage of GHS-R1a-YFP membrane expression *versus* control cells (cells not expressing GHS-R1b-Rluc or CB1R-Rluc) (*E* and *F*) or the percentage of GHS-R1b-Rluc membrane expression *versus* control cells (non-transfected cells) (*G*). Statistical differences of differently transfected cells were analyzed by ANOVA followed by Bonferroni's corrections. *, $p < 0.05$; ***, $p < 0.001$ compared with control cells. Representative Western blotting analyses are shown in the *bottom panels*.

scanned, and a baseline optical signature was recorded before adding 10 μl of test compound dissolved in vehicle. Then, DMR responses were monitored for at least 5000 s. Kinetic results were analyzed using EnSpire workstation software v. 4.10.

cAMP Accumulation—Homogeneous time-resolved fluorescence energy transfer assays were performed using the Lance Ultra cAMP kit (PerkinElmer Life Sciences). The optimal cell density was first established for an appropriate fluorescent signal by measuring the time-resolved FRET signal as a function of forskolin concentration using different cell densities. Forskolin dose-response curves were related to the cAMP standard curve to establish which cell density provides a response that covers most of the dynamic range of the cAMP standard curve. 5000 HEK-293T cells or neurons/well in 384-well microplates growing in medium containing 50 μM zardeverine were pretreated with the antagonists or the corresponding vehicle at 25 °C for 20 min and stimulated with agonists for 15 min before adding 0.5 μM forskolin or vehicle and incubating for an additional 15-min period. Fluorescence at 665 nm was analyzed on a PHERAstar Flagship microplate reader equipped with an homogeneous time-resolved fluorescence energy transfer optical module (BMG Labtech).

Intracellular Calcium Release—Cells were co-transfected with the cDNA for the indicated receptors and 3 μg of GCaMP6 calcium sensor (10) using the Lipofectamine 2000 (Thermo Fisher Scientific) method. 48 h after transfection, 150,000 HEK-293T cells/well in 96-well black, clear-bottom microtiter plates were incubated with Mg^{+2}-free Locke's buffer (pH 7.4) (154 mM NaCl, 5.6 mM KCl, 3.6 mM $NaHCO_3$, 2.3 mM $CaCl_2$, 5.6 mM glucose, and 5 mM HEPES) supplemented with 10 μM glycine, and receptor ligands were added as indicated. The fluorescence emission intensity of GCaMP6 was recorded at 515 nm upon excitation at 488 nm on the EnSpire® multimode plate reader for 335 s every 15 s and 100 flashes/well.

Arrestin Recruitment Assays—Arrestin recruitment was determined using BRET experiments as described above in HEK-293T cells expressing the cDNA corresponding to β-arrestin-2-Rluc (1 μg transfected), GHS-R1a-YFP (1.5 μg transfected) alone or with GHS-R1b (0.05–0.5 μg transfected) after the indicated treatment with ligands.

ERK1/2 Phosphorylation—HEK-293T cells (30,000 cells/well in 96-well plates) were treated with vehicle or the indicated ligand for the indicated time and were lysed by the addition of ice-cold lysis buffer (50 mM Tris-HCl (pH 7.4), 50 mM NaF, 150 mM NaCl, 45 mM β-glycerophosphate, 1% Triton X-100, 20 μM phenyl-arsine oxide, 0.4 mM $NaVO_4$, and protease inhibitor mixture). Cellular debris was removed by centrifugation at 13,000 × *g* for 5 min at 4 °C, and the protein was quantified by the

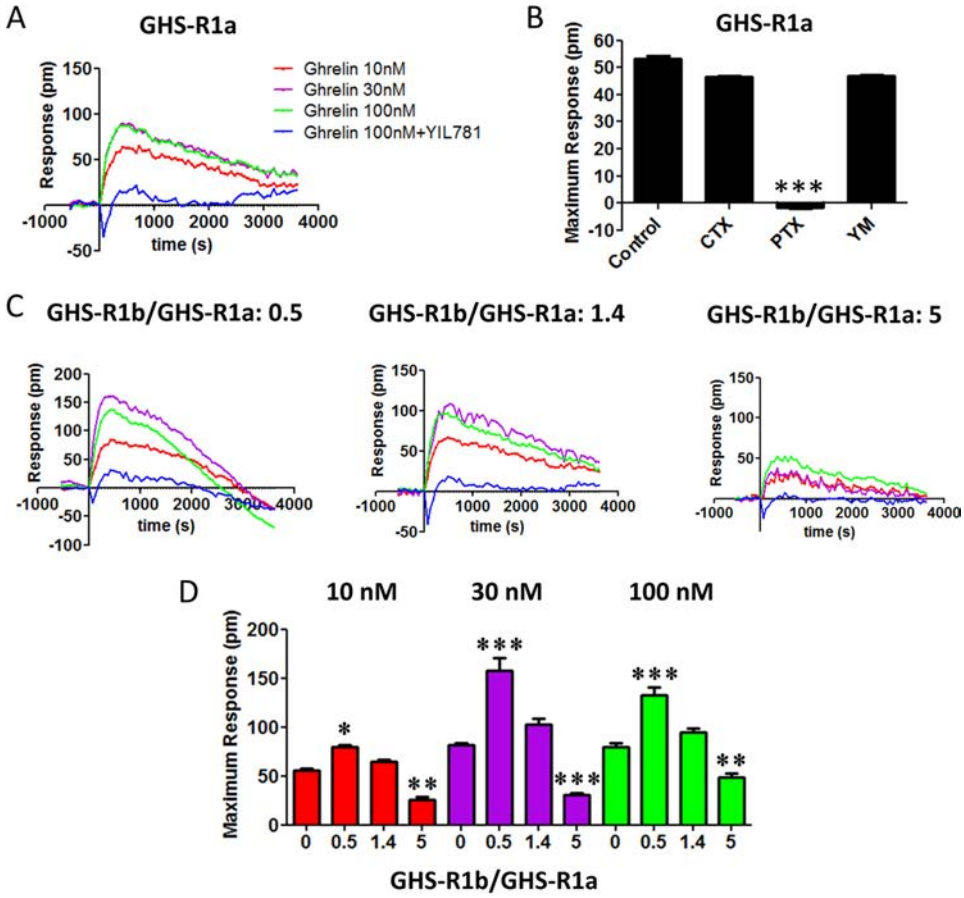

FIGURE 2. **GHS-R1b modulates GHS-R1a signaling detected by DMR in HEK-293T cells.** DMR was determined in HEK-293T cells transfected with GHS-R1a-YFP cDNA (1 μg) (*A* and *B*) or co-transfected with GHS-R1a-YFP cDNA (1 μg) and increasing amounts of GHS-R1b-Rluc cDNA (0.05–0.6 μg) to obtain a 0.5, 1.4, and 5 GHS-R1b-Rluc/GHS-R1a-YFP ratio (*C* and *D*). Cells were pretreated overnight with vehicle (*A*, *C*, and *D*) or with PTX (10 ng/ml), CTX (100 ng/ml), or the $G\alpha_q$ inhibitor YM254890 (*YM*, 1 μM) (*B*), followed by treatment (15 min) with vehicle or the GHS-R1a antagonist YIL781 (2 μM) and activated with increasing concentrations of ghrelin (10, 30, and 100 nM; *A*, *C*, and *D*) or with 30 nM ghrelin (*B*). Representative picometer (*pm*) shifts of reflected light wavelength *versus* time curves are shown in *A* and *C*. Each curve represents the mean of an optical trace experiment carried out in triplicate. *B*, maximum responses at 500 s are derived from the corresponding picometer shifts of reflected light wavelength *versus* time curves. *D*, maximum responses at 500 s induced by different ghrelin concentrations (10–100 nM) are compared for GHS-R1b-Rluc/GHS-R1a-YFP ratios from 0–5. Values are derived from the curves in *A* and *C*. Statistical differences of the effect of ghrelin between cells treated with PTX compared with vehicle-treated cells (*B*) or in cells transfected with different GHS-R1b/GHS-R1a ratios compared with cells only expressing GHS-R1a (*D*) were analyzed by ANOVA followed by Bonferroni's corrections. *, $p < 0.05$; **, $p < 0.01$; ***, $p < 0.001$.

bicinchoninic acid method using bovine serum albumin dilutions as the standard. Equivalent amounts of protein (10 μg) were separated by electrophoresis (10% SDS-polyacrylamide gel) and transferred onto PVDF fluorescence membranes. The membranes were probed with a mixture of a mouse anti-phospho-ERK1/2 antibody (1:2500, Sigma-Aldrich) and a rabbit anti-ERK1/2 antibody that recognizes both phosphorylated and non-phosphorylated ERK1/2 (1:40,000, Sigma-Aldrich), and bands were visualized by the addition of a mixture of IRDye 800 (anti-mouse) antibody (1:10,000, Sigma-Aldrich) and IRDye 680 anti-rabbit antibody (1:10,000, Sigma-Aldrich) and scanned by the Odyssey infrared scanner. Bands densities were quantified using the scanner software, and the level of phosphorylated ERK1/2 isoforms was normalized for differences in loading using the total ERK1/2 protein band intensities.

Results

GHS-R1b-mediated Modulation of GHS-R1a Expression at the Plasma Membrane in Transfected HEX-293T Cells—The role of GHS-R1b on GHS-R1a expression in the plasma membrane was evaluated first by analyzing GHS-R1a expression by immunocytochemistry and confocal microscopy in HEK-293T cells transfected with cDNA of GHS-R1a fused to YFP (GHS-R1a-YFP, 1 μg), GHS-R1b fused to Rluc (GHS-R1b-Rluc, 0.5 μg), or both. Both GHS-R1a-YFP (Fig. 1*A*, identified by its own fluorescence) and GHS-R1b-Rluc (Fig. 1*B*, identified by anti-Rluc and secondary Cy3 antibodies, see "Experimental Procedures"), when expressed alone, could be detected in intracellular structures and at the plasma membrane level. Some degree of co-localization could be observed upon GHS-R1a-YFP and GHS-R1b-Rluc co-transfection (Fig. 1*C*). Fused receptors retained the same degree of functionality compared with non-fused receptors (Fig. 1*D*). Biotinylation experiments using a non-membrane permeable biotin were performed to provide a more accurate determination of receptor expression at the plasma membrane. HEK-293T cells were co-transfected with GHS-R1a-YFP cDNA (1 μg) and increasing amounts of GHS-R1b-Rluc cDNA (0, 0.1, 0.2, 0.3, or 0.6 μg) or only with GHS-R1b-Rluc cDNA (0.3 μg). Total expression of GHS-R1a-YFP (YFP fluorescence, 20,000 ± 2000 units) did not significantly change by increasing the expression of GHS-R1b-Rluc (Rluc luminescence, 10,000–300,000 units). To determine the rela-

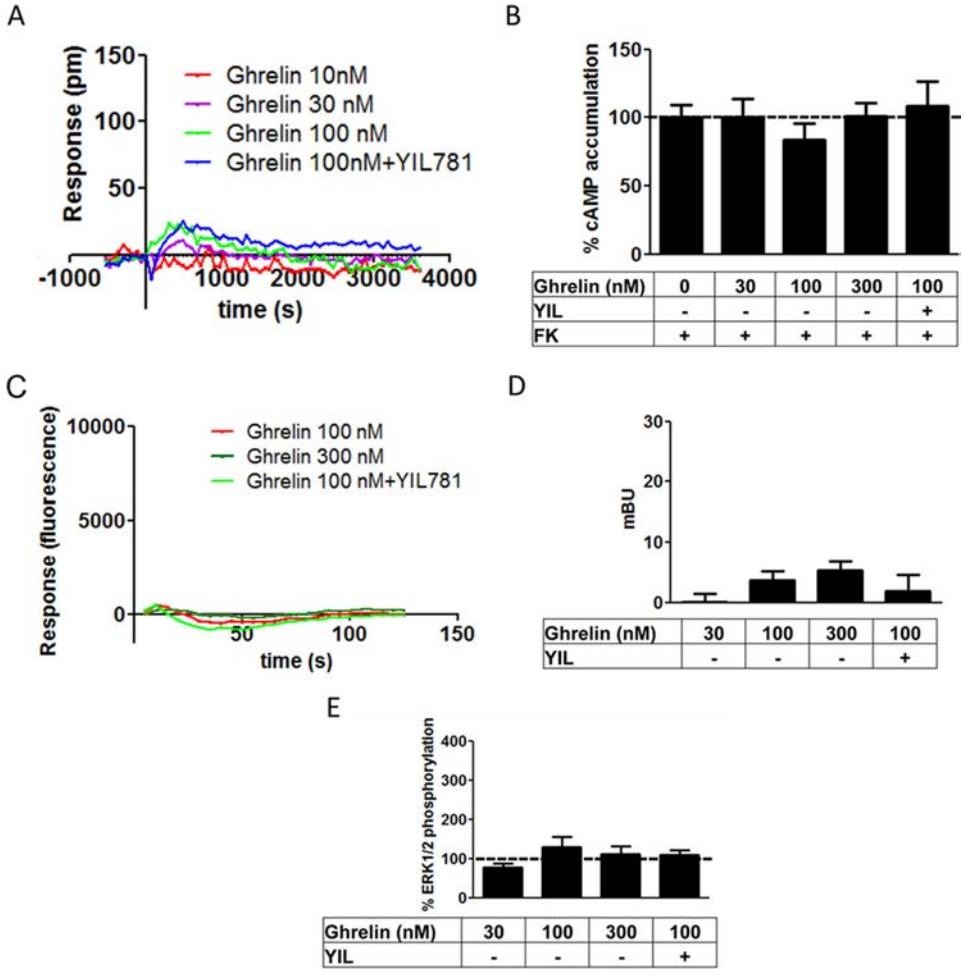

FIGURE 3. **Lack of functionality of GHS-R1b when expressed without GHS-R1a.** DMR (*A*), cAMP accumulation (*B*), cytosolic Ca^{2+} increases (*C*), β arrestin-2 recruitment (*D*), and ERK1/2 phosphorylation (*E*) were determined in HEK-293T cells transfected with 0.4 μg of GHS-R1b-Rluc cDNA. The cells were pretreated (15 min) with vehicle or the GHS-R1a antagonist YIL781 (*YIL*, 2 μM), followed by activation (15 min) with increasing concentrations of ghrelin in the absence (*A* and *C–E*) or presence (*B*) of 0.5 μM forskolin (*FK*). Values are means ± S.E. of four to five experiments. *pm*, picometer.

tive expression of GHS-R1b with respect to GHS-R1a (GHS-R1b/GHS-R1a) in transfected cells, we performed parallel experiments in which HEK-293T cells were transfected with increasing amounts of GHS-R1a-YFP cDNA (up to 1.5 μg) or GHS-R1b-YFP cDNA (up to 0.6 μg), and the relative total expression of receptors was calculated by Western blotting using an anti-YFP antibody. Linearity of transfected cDNA *versus* the Western blotting signal or *versus* fluorescence was obtained in both cases (transfected cDNA in micrograms *versus* fluorescence values in arbitrary units gave linear plots with slopes of 0.885 and 0.099, respectively), which allowed the accurate determination of the relative GHS-R1b/GHS-R1a expression ratio. Co-transfection with 1 μg of GHS-R1a-YFP and 0, 0.1, 0.2, 0.3, or 0.6 μg of GHS-R1b-YFP gave GHS-R1b/GHS-R1a ratios of 0, 0.25, 0.5, 1.4, and 5, respectively. Biotinylation experiments demonstrated that transfected GHS-R1a was always present in the plasma membrane, with or without co-transfection with GHS-R1b, and that co-transfection with GHS-R1b resulting in GHS-R1b/GHS-R1a ratios from 0.25–5 led to an inverted U shape in the relative expression of GHS-R1a in the plasma membrane (Fig. 1*E*). As a negative control, no changes in GHS-R1a expression at the plasma membrane were detected upon co-transfection with increasing amounts of CB1R-Rluc cDNA (Fig. 1*F*, the CB1R/GHS-R1a expression ratio was calculated as above using the slope value of 0.139 corresponding to linear plots of transfected CB1R-YFP cDNA in micrograms *versus* fluorescence values in arbitrary units). Furthermore, biotinylation also demonstrated a linear increase in the plasma membrane expression of GHS-R1b upon increasing transfected amounts of GHS-R1b-YFP cDNA (Fig. 1*G*). These data indicate that GHS-R1b differentially modulates GHS-R1a expression at the plasma membrane level as a function of GHS-R1b/GHS-R1a expression ratio.

GHS-R1b-mediated Modulation of GHS-R1a Signaling in Transfected HEK-293T Cells—The role of GHS-R1b on GHS-R1a signaling was evaluated in HEK-293T cells expressing the same amount of GHS-R1a-YFP (fluorescence, 20,000 ± 2000) and increasing amounts of GHS-R1b-Rluc (0–5 GHS-R1b/GHS-R1a ratio). First, the effect of GHS-R1b on GHS-R1a signaling was determined with a DMR label-free assay (see "Experimental Procedures"), which can detect ligand-induced changes in light diffraction in the bottom 150 nm of a cell monolayer mostly dependent on G protein-dependent signaling (12). Ghrelin (10, 30, and 100 nM) induced dose- and time-dependent signaling in cells only transfected with GHS-R1a-YFP, which was inhibited by the GHS-R1a antagonist YIL781

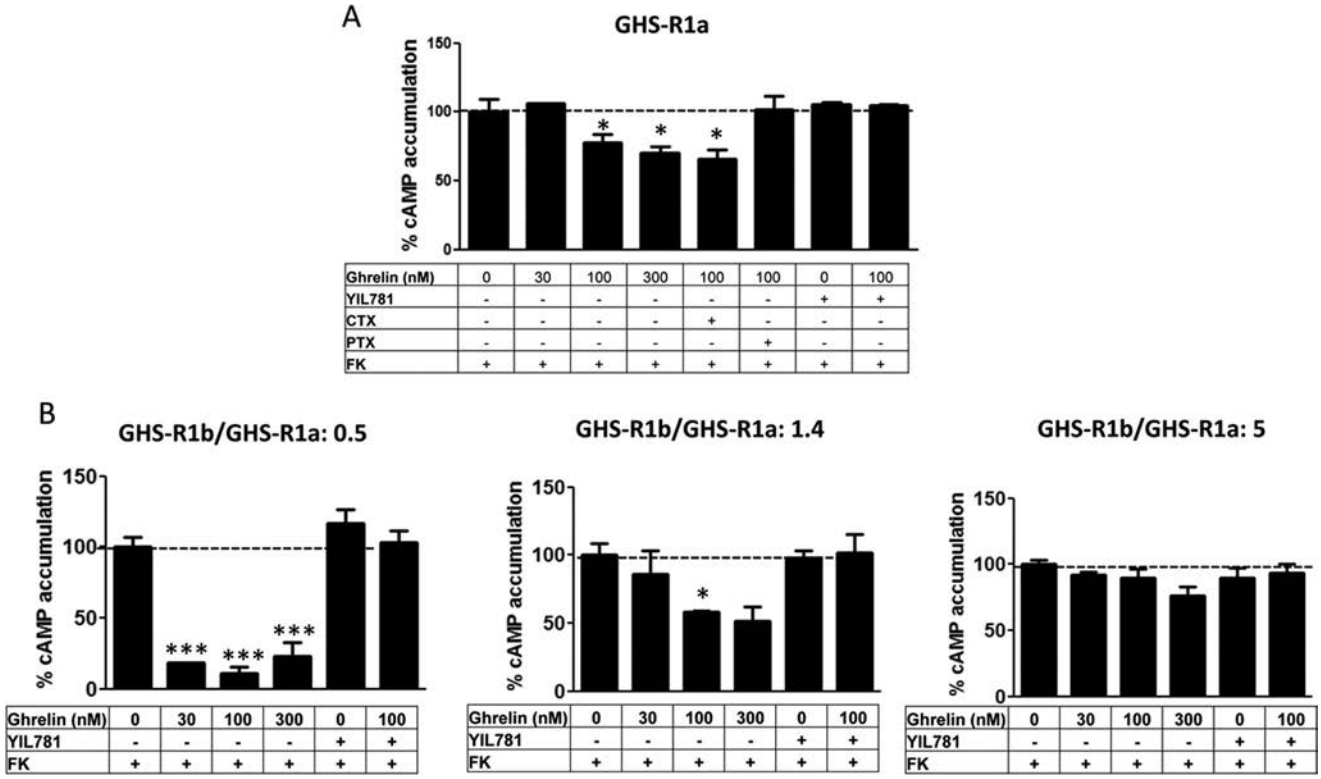

FIGURE 4. **GHS-R1b modulates GHS-R1a-mediated inhibition of adenylyl cyclase in HEK-293T cells.** cAMP accumulation was determined in HEK-293T cells transfected with GHS-R1a-YFP cDNA (1 μg) (*A*) or co-transfected with GHS-R1a-YFP cDNA (1 μg) and increasing amounts of GHS-R1b-Rluc cDNA (0.05–0.6 μg) to obtain a 0.5, 1.4, and 5 GHS-R1b-Rluc/GHS-R1a-YFP ratio (*B*). Cells were incubated overnight with vehicle or PTX (10 ng/ml) or for 2 h with CTX (100 ng/ml) and pretreated (15 min) with vehicle or the GHS-R1a antagonist YIL781 (2 μM), followed by activation (15 min) with ghrelin in the absence or presence of 0.5 μM forskolin (*FK*). Values are means ± S.E. of five to six experiments per treatment and expressed as decreases of forskolin-induced cAMP accumulation (100%, *dotted line*). Statistical differences of the effect of differently treated cells under different transfection conditions were analyzed by ANOVA followed by Bonferroni's corrections. *, $p < 0.05$; ***, $p < 0.001$ compared with the effect of forskolin alone.

(Fig. 2*A*). Ghrelin-induced DMR was completely blocked by pertussis toxin (PTX) but not by cholera toxin (CTX) or the G_q inhibitor YM254890 (Fig. 2*B*), indicating a predominant ghrelin-mediated $G_{i/o}$ protein coupling to GHS-R1a in HEK-293T cells. As expected, ghrelin did not produce any significant effect in cells only expressing GHS-R1b-Rluc (Fig. 3*A*). The ghrelin-mediated DMR signal was then analyzed upon three different GHS-R1b/GHS-R1a expression ratios: 0.5, 1.4, and 5. At a GHS-R1b/GHS-R1a expression ratio of 0.5, ghrelin was significantly more efficient than when the cells were only transfected with GHS-R1a (Fig. 2, *C* and *D*). Taking also into account the results of biotinylation experiments, these results suggest that low relative GHS-R1b expression potentiates ghrelin-induced $G_{i/o}$ protein-mediated signaling by facilitating GHS-R1a trafficking to the plasma membrane. However, progressively increasing the relative expression of GHS-R1b led to a progressive decrease in signaling that went down to an almost complete lack of effect of ghrelin with a GHS-R1b/GHS-R1a expression ratio of 5 (Fig. 2, *C* and *D*). This switch from facilitation to inhibition of ghrelin-induced $G_{i/o}$ protein-mediated signaling cannot be explained by a GHS-R1b-mediated modulation of GHS-R1a trafficking because plasma membrane expression of GHS-R1a was the same at the highest GHS-R1b/GHS-R1a expression ratio than in cells not co-transfected with GHS-R1b (Fig. 1*E*). According to the predominant coupling to $G_{i/o}$ protein, ghrelin dose-dependently decreased forskolin-induced cAMP accumulation in cells only expressing GHS-R1a (Fig. 4*A*). Again, this effect was not observed in cells only transfected with GHS-R1b (Fig. 3*B*), was inhibited by YIL781 (Fig. 4*A*), and was dependent on the GHS-R1b/GHS-R1a expression ratio, with ghrelin being more efficient, similarly efficient, and inefficient at expression ratios of 0.5, 1.4, and 5, respectively, compared with cells only transfected with GHS-R1a (Fig. 4*B*).

Ghrelin also induced a dose-dependent increase in cytosolic Ca^{2+} (Fig. 5, *A* and *B*), β arrestin-2 recruitment (Fig. 5*C*), and ERK1/2 phosphorylation (Fig. 5*D*) in HEK-293T cells only transfected with GHS-R1a. All measured ghrelin-activated signaling pathways were also inhibited by YIL781 (Fig. 5), and they were not observed in cells only transfected with GHS-R1b (Fig. 3, *C–E*). Importantly, these three signaling mechanisms were dependent on the GHS-R1b/GHS-R1a expression ratio (Fig. 5). As observed with DMR and cAMP accumulation experiments, at GHS-R1b/GHS-R1a expression ratios of 0.5, 1.4, and 5, ghrelin was more efficient, similarly efficient, and significantly less efficient or inefficient, respectively, compared with cells only transfected with GHS-R1a (Fig. 5).

Homodimers and Heterotetramers of GHS-R1a and GHS-R1b in HEK-293T-transfected Cells—Biotinylation and signaling experiments therefore did not support a preferential intracellular localization of GHS-R1b and GHS-R1a retention upon intracellular heteromerization with GHS-R1b as the basis for a dominant negative effect of GHS-R1b on GHS-R1a function (6, 7). Our results instead fit with a negative effect of GHS-R1b on

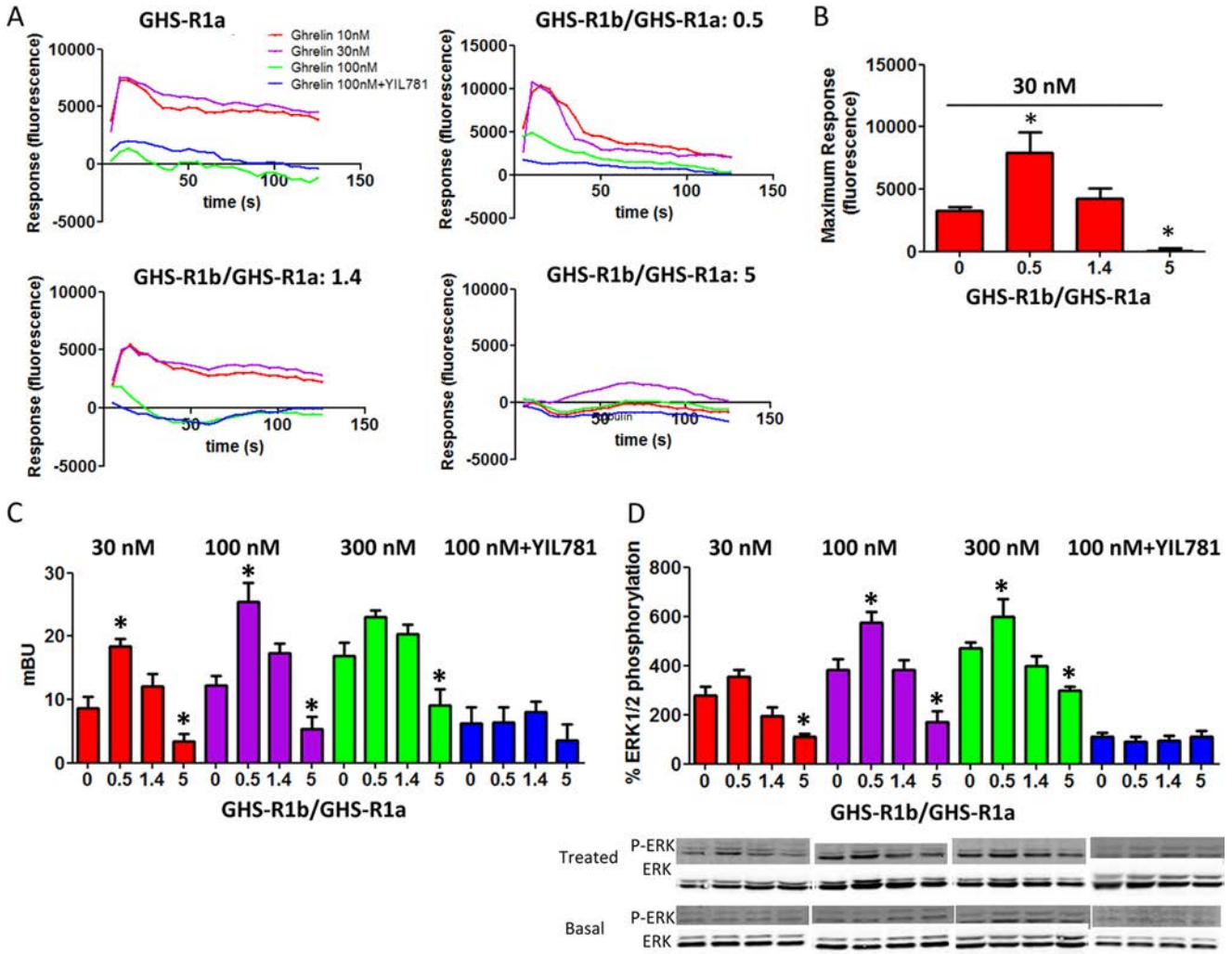

FIGURE 5. **GHS-R1b modulates GHS-R1a-mediated cytosolic Ca^{2+} increase, β arrestin-2 recruitment, and ERK1/2 phosphorylation.** *A* and *B*, HEK-293T cells were transfected with GHS-R1a-YFP cDNA (1 μg) or co-transfected with GHS-R1a-YFP cDNA (1 μg) and increasing amounts of GHS-R1b-Rluc cDNA (0.05–0.6 μg) to obtain a 0.5, 1.4, and 5 GHS-R1b-Rluc/GHS-R1a-YFP ratio. *A*, representative intracellular curves of Ca^{+2} release over time. *B*, values of maximal Ca^{+2} release (means ± S.E., $n = 4–6$) induced by 30 nM ghrelin were derived from the curves obtained at the different GHS-R1b-Rluc/GHS-R1a-YFP ratios. *C*, β-arrestin-2 recruitment (means ± S.E., $n = 5–7$) was measured by BRET experiments in cells transfected with 1 μg of β-arrestin-2-Rluc cDNA and 1 μg of GHS-R1a-YFP cDNA in the absence or the presence of GHS-R1b cDNA (0.05–0.6 μg). In all cases, cells were pretreated (15 min) with vehicle or the GHS-R1a antagonist YIL781 (2 μM), followed by activation with ghrelin (30, 100, or 300 nM). *D*, ERK1/2 phosphorylation from the same transfected cell groups and treatments as in *C*, expressed as a percentage over values found in non-transfected cells (means ± S.E., $n = 5–7$). Representative Western blotting analyses are shown in the *bottom panel*. Statistical differences of the effect of different GHS-R1b/GHS-R1a ratios under different treatment conditions were analyzed by ANOVA followed by Bonferroni's corrections. *, $p < 0.05$ compared with cells only expressing GHS-R1a.

GHS-R1a signaling upon heteromerization in the plasma membrane (5). Because GPCR homodimers seem to be a predominant species and oligomeric entities are viewed as multiples of dimers (13), we also investigated the possibility of homodimerization of GHS-1b and heteromerization of GHS-R1a and GHS-R1b homodimers. Saturable BRET curves were obtained in HEK-293T cells expressing a constant amount of GHS-R1a-Rluc and increasing amounts of GHS-R1a-GFP^2 (Fig. 6*A*, $BRET_{max}$ of 82 ± 6 mBU and $BRET_{50}$ of 55 ± 13 mBU) or a constant amount of GHS-R1b-Rluc and increasing amounts of GHS-R1b-YFP (Fig. 6*B*, $BRET_{max}$ of 124 ± 12 mBU and $BRET_{50}$ of 52 ± 16 mBU), strongly suggestive of homodimerization. As negative controls, linear plots with low BRET values were obtained using either CB1R-Rluc (Fig. 6*A*) or CRF1-Rluc (Fig. 6*B*). SRET assay was then used to evaluate the possibility of direct interactions between three receptor molecules, either two GHS-R1a and one GHS-R1b or two GHS-R1b and one GHS-R1a, as depicted in Fig. 6, *C* and *D*. In this assay, Rluc was fused to one of the receptor units to act as a BRET donor, GFP^2 was fused to a second receptor unit to act as a BRET acceptor and FRET donor, and YFP was fused to the third receptor unit to act as a FRET acceptor. The cDNA constructs were transfected in HEK-293T cells, and YFP emission was determined after adding DeepBlueC as luciferase substrate. Positive SRET saturation curves were obtained with transfection of a constant amount of GHS-R1b-Rluc and GHS-R1a-GFP^2 and increasing amounts of GHS-R1a-YFP (Fig. 6*C*) or increasing amounts of GHS-R1b-YFP (Fig. 6*D*), with $SRET_{max}$ values of 222 ± 18 mSU and 40 ± 5 mSU and $SRET_{50}$ values of 48 ± 14 mSU and 72 ± 20 mSU, respectively. As negative controls, linear plots with low SRET values were obtained when CB1R-Rluc was transfected as the BRET donor of GHS-R1a or GHS-R1b FRET pairs (Fig. 6, *C*

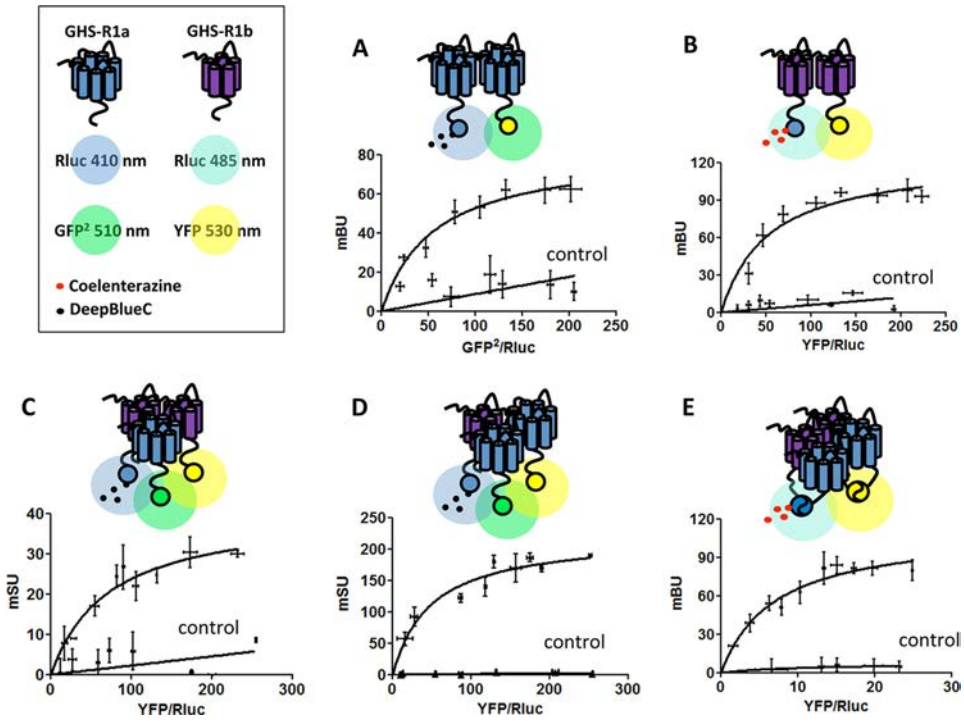

FIGURE 6. **Heterotetramers of GHS-R1a and GHS-R1b homodimers in HEK-293T cells.** *A* and *B*, GHS-R1a and GHS-R1b homodimers were detected by BRET saturation experiments in HEK-293T cells co-transfected with GHS-R1a-Rluc cDNA (1.5 μg) and increasing amounts of GHS-R1a-GFP^2 cDNA (0.5–3 μg) (*A*) or a constant amount of GHS-R1b-Rluc cDNA (0.3 μg) and increasing amounts of GHS-R1b-YFP (0.05–0.6 μg) (*B*). As negative controls, linear and low BRET values were obtained by transfecting the cDNA corresponding to either cannabinoid receptor CB_1R-Rluc (0.5 μg, *A*) or the corticotropin-releasing factor receptor $CRFR_1$-Rluc (0.3 μg, *B*) as BRET donors. *C* and *D*, positive SRET saturation curves were obtained in HEK-293T cells co-transfected with a constant amount of GHS-R1b-Rluc cDNA (0.4 μg) and GHS-R1a-GFP^2 cDNA (1.5 μg) and increasing amounts of GHS-R1b-YFP cDNA (0.5–3 μg, *C*) or GHS-R1a-YFP cDNA (0.05–0.5 μg, *D*). As SRET negative controls, linear and low SRET values were obtained when CB_1R-Rluc cDNA (0.4 μg) was transfected as BRET donor of GHS-R1a or GHS-R1b FRET pairs. *E*, the BiLFC saturation curve was obtained in HEK-293T cells co-transfected with equal amounts of cDNA corresponding to GHS-R1a-cRluc and GHS-R1b-nRluc (1.5 μg) and increasing amounts of GHS-R1a-cYFP and GHS-R1b-nYFP cDNAs (0.5–2.5 μg for each). As a negative control, linear and low BiLFC were obtained in cells transfected with adenosine A_1R-cRluc cDNA (0.2 μg) instead of GHS-R1a-cRluc cDNA. The relative amounts of BRET or SRET are given as a function of 100× the ratio between the fluorescence of the acceptor and the luciferase activity of the donor. BRET and SRET are expressed as milliBRET units or milliSRET units (*mSU*) and given as the means ± S.D. of four to five experiments grouped as a function of the amount of BRET or SRET acceptor.

and *D*). These results show the ability of GHS-R1a and GHS-R1b to assemble as heterotrimers and possibly heterotetramers. Support for heterotetramer formation was obtained by using BRET with double BiLC and BiFC assays (15, 16). In this assay, the two BRET sensors, the donor Rluc8 (a more efficient variant of Rluc) and the acceptor YFP Venus (a more efficient variant of YFP), are split into two hemiproteins, with each split sensor being fused to one of the four putative interacting receptors. BRET indicates reconstitution of both sensors and close proximity of the four receptors. A saturable BRET curve ($BRET_{max}$ of 111 ± 10 mBU and $BRET_{50}$ of 7 ± 2 mBU) was detected in HEK-293T cells co-transfected with equal amounts of GHS-R1a-cRluc and GHS-R1b-nRluc cDNAs and increasing amounts of GHS-R1a-cYFP and GHS-R1b-nYFP cDNAs (Fig. 6*E*). Negative controls were cells transfected with adenosine A1R-cRluc cDNA instead of GHS-R1a-cRluc cDNA (Fig. 6*E*). Collectively, these results indicate that GHS-R1a and GHS-R1b receptors can form oligomeric complexes that include heteromers of homodimers.

Differential GHS-R1b-mediated Modulation of GHS-R1a Signaling in Rat Striatal and Hippocampal Neurons—The significance of GHS-R1a-mediated signaling and its modulation by heteromerization with GHS-R1b was then addressed in primary neuronal cultures from the striatum and hippocampus, brain areas that express functional GHS-R1a receptors (3, 4). The relative expression of both GHS-R1a and GHS-R1b, determined by RT-PCR, was higher in striatal compared with hippocampal primary cultures (Figs. 7*A*). DMR was first analyzed to evaluate ghrelin-mediated signaling, and a dose-dependent response was obtained in both primary cultures (Fig. 7, *B–D*). Ghrelin was more potent and efficient in striatal than in hippocampal neurons, and its effects were counteracted by YIL781 in both preparations (Fig. 7, *B–D*). As shown in Fig. 7*A*, the relative expression of GHS-R1b was higher than GHS-R1a in striatal neurons, whereas the opposite, a higher relative expression of GHS-R1a than GHS-R1b, was observed in hippocampal neurons. Therefore, from the results obtained in HEK-293T cells, we anticipated that an increase in GHS-R1b expression could lead to opposite effects in hippocampal and striatal neurons. Indeed, in hippocampal primary cultures, transfection with increasing amounts of GHS-R1b cDNA (0.1 and 0.5 μg) led to a progressive significant increase in the efficacy of ghrelin-induced DMR (Fig. 8, *A* and *C*), whereas, in striatal primary cultures, GHS-R1b transfection led to the opposite effect (Fig. 8, *B* and *C*). By analyzing another signaling readout, cAMP accumulation, unexpected results were obtained compared with HEK-293T cells in both hippocampal and striatal primary cultures. Ghrelin produced an increase in cAMP production with an inverted U-shaped dose-response (maximal effect at about 100 nM), indicating an agonist-induced desensitization

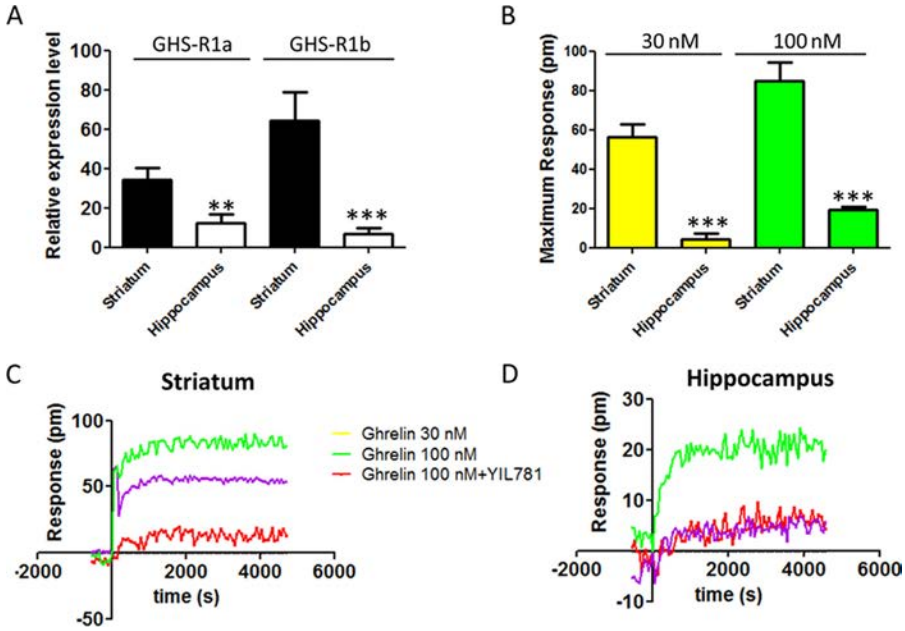

FIGURE 7. **Differential expression of GHS-R1a and GHS-R1b in striatal and hippocampal neurons in culture.** *A*, the relative expression of GHS-R1a and GHS-R1b was determined by RT-PCR using primary cultures of rat hippocampal (*white columns*) and striatal (*black columns*) neurons. *C* and *D*, DMR was determined in striatal (*C*) or hippocampal (*D*) neuronal primary cultures pretreated (30 min) with vehicle or the GHS-R1a antagonist YIL781 (2 μM) and followed by activation with ghrelin (30 or 100 nM). Representative picometer (*pm*) shifts of reflected light wavelength *versus* time curves are shown. Each curve represents the mean of an optical trace experiment carried out in triplicate. *B*, maximum responses of DMR at 2000 s induced by ghrelin (30 or 100 nM) are compared for striatal and hippocampal neuronal cultures. Values are means ± S.E. of five to seven experiments performed with independent primary cultures. Statistical differences of the expression of GHS-R1a and GHS-R1b and the effect of ghrelin between hippocampal compared with striatal cell cultures were analyzed by ANOVA followed by Bonferroni's corrections. **, $p < 0.01$; ***, $p < 0.001$.

effect (Fig. 8, *D* and *E*). This effect was blocked by YIL781 in both preparations (Fig. 8, *D* and *E*, *black columns*). The same as for DMR, in hippocampal and striatal primary cultures, transfection with increasing amounts of GHS-R1b cDNA (0.1 and 0.5 μg) led to a progressive significant increase and decrease, respectively, in the effect of ghrelin-induced cAMP accumulation (Fig. 8, *D* and *E*). The results also showed that, in neurons, GHS-R1b can positively or negatively modulate GHS-R1a function depending on the endogenous relative GHS-R1b/GHS-R1a expression ratio.

Dopamine D1R Interacts with GHS-R1a-GHS-R1b Heteromers, Promoting Coupling to $G_{s/olf}$ Protein—Previous studies have suggested that GHS-R1a-mediated signaling depends mostly on G_q coupling, although, in HEK-293T cells in this study, evidence for $G_{i/o}$ coupling has also been obtained (see "Discussion"). Similarly, ghrelin-induced cAMP-PKA signaling has also been reported but suggested to be independent of $G_{s/olf}$ proteins (see "Discussion"). The G protein subtype involved in ghrelin-induced cAMP accumulation in striatal and hippocampal neurons in culture was first investigated by using the $G_{s/olf}$ toxin CTX, the $G_{i/o}$ toxin PTX, and the G_q protein inhibitor YM254890. CTX, but not PTX or YM254890, prevented ghrelin-induced cAMP in both preparations (Fig. 9, *A* and *B*), identifying $G_{s/olf}$ as predominant G proteins coupled to GHS-R1a in neurons. Although CTX increased the basal levels of cAMP by about 2- to 3-fold, this cannot explain an apparent inhibition of the effect of ghrelin because of saturation on the activation of adenylyl cyclase because, under the same experimental conditions, forskolin increased cAMP levels by 10-fold (data not shown). A possible explanation for the unexpected preferential coupling of GHS-R1a to $G_{s/olf}$ in neurons *versus* $G_{i/o}$ in HEK-293T cells could be the presence in neuronal primary cultures of additional receptors that could interact with GHS-R1a or GHS-R1b. Indeed, dopamine D1R is a canonical mediator of adenylyl cyclase activation that has been reported to heteromerize with GHS-R1a (17, 18). We then investigated its possible involvement in ghrelin-mediated cAMP accumulation in neurons in culture. In fact, the D1R antagonist SCH23390 (1 μM), but not the dopamine D2R antagonist raclopride (1 μM), blocked ghrelin-induced cAMP accumulation in striatal but not hippocampal neurons in culture (Fig. 9, *C* and *D*). That D1R co-expression can promote a switch in G protein coupling of GHS-R1a from $G_{i/o}$ to $G_{s/olf}$ was then demonstrated in HEK-293T cells transfected with GHS-R1b-Rluc cDNA (0.2 μg), GHS-R1a-YFP cDNA (1 μg, GHS-R1b/GHS-R1a ratio of 1.4) and D1R cDNA (0.4 μg, Fig. 10*A*), or D2R cDNA (0.4 μg, Fig. 10*B*). In the presence of D1R, both ghrelin (100 nM) and the D1R agonist SKF81297 (100 nM) increased cAMP production, an effect that was blocked by CTX but not by PTX or the G_q inhibitor YM254890 (Fig. 10*A*). In the presence of D2R, both ghrelin (100 nM) and the D2R agonist quinpirole (1 μM) decreased cAMP production, an effect that was blocked by PTX but not by CTX or the G_q inhibitor YM254890 (Fig. 10*B*). Fig. 10*C* demonstrates agonist selectivity at the concentrations used in cAMP experiments using cells only transfected with single receptors. In cells transfected with GHS-R1a, GHS-R1b, and D1R, co-activation of GHS-R1a and D1R with ghrelin (100 nM) and SKF81297 (100 nM) did not produce an additive or synergistic effect (Fig. 10*D*), but blockade of either receptor with the D1R antagonist SCH23390 (1 μM) or the GHS-R1a antagonist YIL781 (1 μM) completely counteracted cAMP accumulation induced by both ghrelin and SKF81297 (Fig. 10*D*). Because the

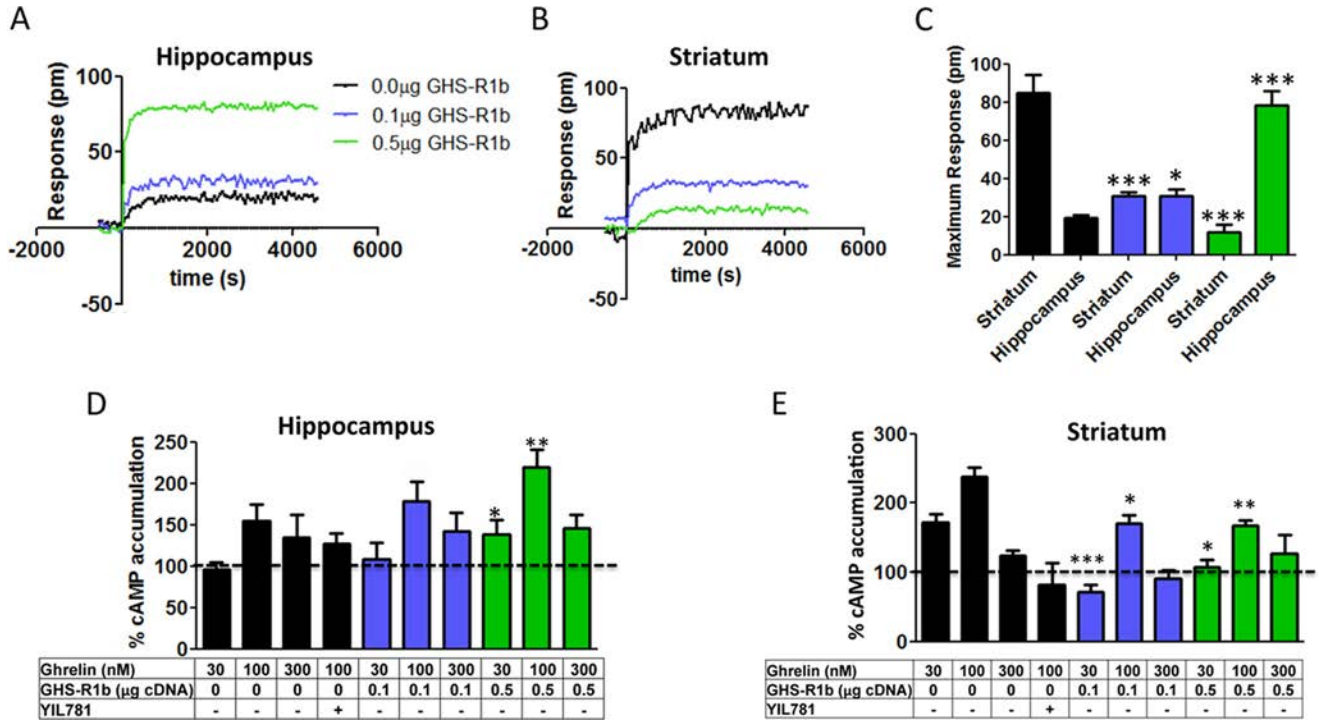

Ghrelin (nM)	30	100	300	100	30	100	300	30	100	300
GHS-R1b (μg cDNA)	0	0	0	0	0.1	0.1	0.1	0.5	0.5	0.5
YIL781	-	-	-	+	-	-	-	-	-	-

Ghrelin (nM)	30	100	300	100	30	100	300	30	100	300
GHS-R1b (μg cDNA)	0	0	0	0	0.1	0.1	0.1	0.5	0.5	0.5
YIL781	-	-	-	+	-	-	-	-	-	-

FIGURE 8. **GHS-R1b-mediated modulation of GHS-R1a signaling in striatal and hippocampal neurons.** *A–C*, DMR was determined in rat hippocampal (*A* and *C*) and striatal (*B* and *C*) primary cultures not transfected (*black*) or transfected with 0.1 μg (*blue*) or 0.5 μg (*green*) of GHS-R1b cDNA and activated with 100 nM ghrelin. Representative picometer (*pm*) shifts of reflected light wavelength *versus* time curves are shown in *A* and *B*. Each curve represents the mean of an optical trace experiment carried out in triplicate. *C*, ghrelin-induced maximum responses at 2000 s are compared for striatal and hippocampal neuronal cultures not transfected or transfected with 0.1 or 0.5 μg of GHS-R1b cDNA. Statistical differences between differently transfected cells for each type of culture were analyzed by ANOVA followed by Bonferroni's corrections. *, $p < 0.05$; ***, $p < 0.001$ compared with non-transfected cells. *D* and E, cAMP accumulation was determined in rat hippocampal (*D*) and striatal (*E*) primary cultures not transfected (*black*) or transfected with 0.1 μg (*blue*) or 0.5 μg (*green*) of GHS-R1b cDNA. Cells were pretreated (15 min) with vehicle or the GHS-R1a antagonist YIL781 (2 μM), followed by activation (15 min) with increasing ghrelin concentrations. Values are means ± S.E. of four to six experiments and expressed as percentage of values from non-stimulated cells (100%, *dotted line*). Statistical differences between differently transfected cells were analyzed by ANOVA followed by Bonferroni's corrections. *, $p < 0.05$; ***, $p < 0.001$ compared with non-transfected cells.

interactions between GHS-R1a and D1R ligands, particularly the cross-antagonism (see "Discussion"), strongly suggested oligomerization, we investigated this possibility with BRET experiments. In HEK-293T cells transfected with a constant amount of D1R-Rluc cDNA (0.4 μg) and increasing amounts of GHS-R1a-YFP cDNA (0.2–1.5 μg) (Fig. 11*A*) or GHS-R1b-YFP cDNA (0.1–0.6 μg) (Fig. 11*B*), low and linear plots were observed, consistent with nonspecific interactions. Similarly, low BRET values were obtained (at a YFP/Rluc ratio of 100) when cells where exposed to ghrelin, the D1R agonist SKF81297, or both (100 nM in all cases, Fig. 11, *C* and *D*). Nevertheless, a saturable BRET curve was obtained when cells were transfected with D1R-Rluc cDNA (0.4 μg), increasing amounts of GHS-R1b-YFP cDNA (0.1–0.6 μg), and GHS-R1a cDNA (0.8 μg), with $BRET_{max}$ and $BRET_{50}$ values of 36 ± 6 mBU and 93 ± 10 mBU, respectively (Fig. 11*E*, *black line*), indicating that D1R specifically interacts with GHS-R1a-GHS-R1b heteromers. In agreement, significant BRET values could only be obtained in cells transfected with D1R-Rluc cDNA (0.4 μg) and GHS-R1a-GFP^2 (1.0 μg) when co-transfected with increasing amounts of GHS-R1b cDNA (0.05–0.3 μg) (Fig. 11*F*). BRET saturation curves were also obtained in cells transfected with D1R-Rluc cDNA (0.4 μg), increasing amounts of GHS-R1b-YFP cDNA (0.1 to 0.6 μg), and GHS-R1a cDNA (0.8 μg) and treated with 100 nM SKF81297 (Fig. 11*E*, *red line*; $BRET_{max}$ and $BRET_{50}$ values of 34 ± 3 mBU and 25 ± 11 mBU, respectively), 100 nM ghrelin (Fig. 11*E*, *green line*; $BRET_{max}$ and $BRET_{50}$ values of 46 ± 3 mBU and 99 ± 12 mBU, respectively), or both (Fig. 11*E*, *blue line*; $BRET_{max}$ and $BRET_{50}$ values of 52 ± 3 mBU and 39 ± 9 mBU, respectively). The significant increase in $BRET_{max}$ upon treatment with ghrelin indicates a facilitation of energy transfer or an increase in heteromer formation, whereas the significant decrease in $BRET_{50}$ upon treatment with SKF81297 suggests an increase in the affinity of the interaction between receptors. Both effects, a significant increase in $BRET_{max}$ and a significant decrease in $BRET_{50}$, were observed upon co-treatment with ghrelin and SKF81297 (significant statistical differences in $BRET_{max}$ and $BRET_{50}$ compared with control non-treated cells were determined by ANOVA followed by Bonferroni's corrections: *, $p < 0.05$ in all cases). If D1R can only interact with GHS-R1a in the presence of GHS-R1b, the absence of GHS-R1b should disclose the properties that are dependent on GHS-R1a-GHR1b-D1R heteromerization. In fact, in cells transfected with D1R but only co-transfected with GHS-R1a, ghrelin (100 nM) did not produce cAMP accumulation, and YIL781 (1 μM) did not counteract cAMP accumulation induced by SKF81297 (100 nM) (Fig. 12). Together, the results from transfected HEK-293T cells provide a very plausible mechanism for the results obtained in striatal cells in culture, demonstrating that GHS-R1b determines the ability of GHS-R1a to form oligomeric complexes with D1R, which allows ghrelin to activate $G_{s/olf}$ protein-mediated signaling.

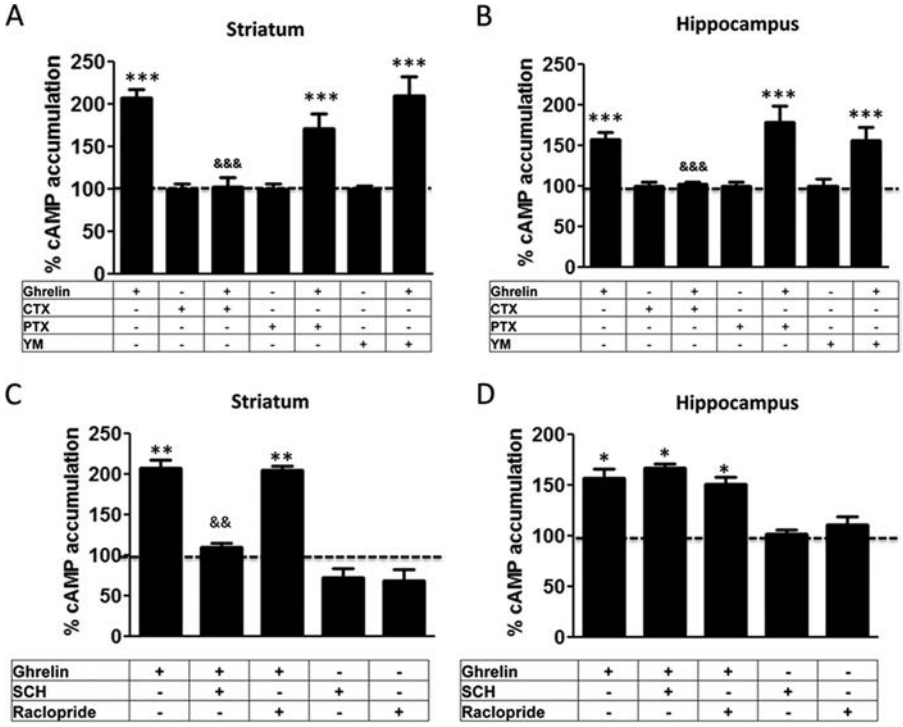

FIGURE 9. **$G_{s/olf}$-coupling of ghrelin receptors in striatal and hippocampal neurons.** *A* and *B*, cAMP accumulation was determined in rat striatal (*A*) and hippocampal (*B*) primary cultures incubated overnight with vehicle, PTX (10 ng/ml), or the $G\alpha_q$ inhibitor YM254890 (*YM*, 1 μM) or for 2 h with CTX (100 ng/ml). Cells were then treated with vehicle or ghrelin (100 nM). Values are means ± S.E. of three to four experiments and are expressed as percentage of the values of vehicle-treated cells (100%, *dotted line*). *C* and *D*, cAMP accumulation was determined in rat striatal (*A*) and hippocampal (*B*) primary cultures pretreated (15 min) with vehicle, the D1R antagonist SCH23390 (*SCH*, 1 μM), or the D2R antagonist raclopride (1 μM), followed by treatment (15 min) with vehicle or ghrelin (100 nM). Values are means ± S.E. of five to six experiments and are expressed as percentage of the values of vehicle-treated cells (100%, *dotted line*). Statistical differences between differently treated cells were analyzed by ANOVA followed by Bonferroni's corrections. *, $p < 0.05$; **, $p < 0.01$; ***, $p < 0.001$ compared with vehicle-treated cells. &&, $p < 0.01$ compared with ghrelin-treated cells.

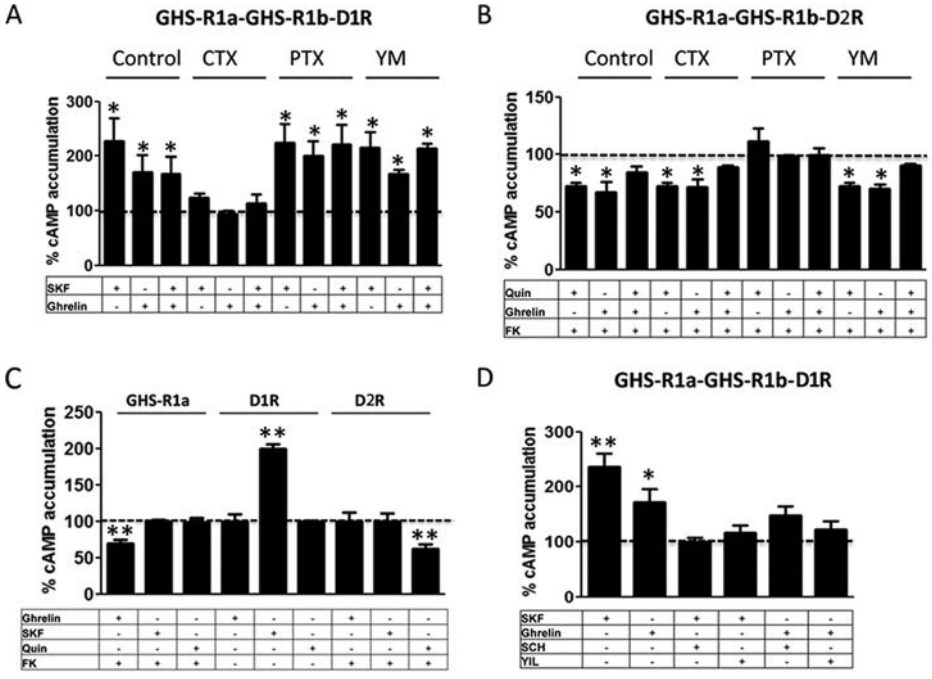

FIGURE 10. **D1R promotes GHS-R1a-GHS-R1b heteromers coupling to $G_{s/olf}$ protein.** cAMP accumulation was determined in HEK-293T cells transfected with GHS-R1b-Rluc cDNA (0.2 μg), GHS-R1a-YFP cDNA (1 μg), and D1R cDNA (0.4 μg, *A* and *D*) or D2R cDNA (0.4 μg, *B*) or single-transfected with the same amount of the indicated receptors (*C*). Cells were incubated overnight with vehicle, PTX (10 ng/ml), or the $G\alpha_q$ inhibitor YM254890 (*YM*, 1 μM) or for 2 h with CTX (100 ng/ml) and pretreated (15 min) with vehicle, the GHS-R1a antagonist YIL781 (*YIL*, 2 μM), or the D1R antagonist SCH23390 (*SCH*, 1 μM), followed by activation (15 min) with ghrelin (100 nM), the D1R agonist SKF81297 (*SKF*, 100 nM), or the D2R agonist quinpirole (*Quin*, 1 μM) alone or in combination in the absence (*A* and *D*) or presence (*B* and *C*) of forskolin (*FK*, 0.5 μM). Values are means ± S.E. of six to eight experiments and expressed as percentage of values of cells not treated with ghrelin (100%, *dotted line*). Statistical differences between differently treated cells were analyzed by ANOVA followed by Bonferroni's corrections. *, $p < 0.05$; **, $p < 0.01$ compared with vehicle-treated cells.

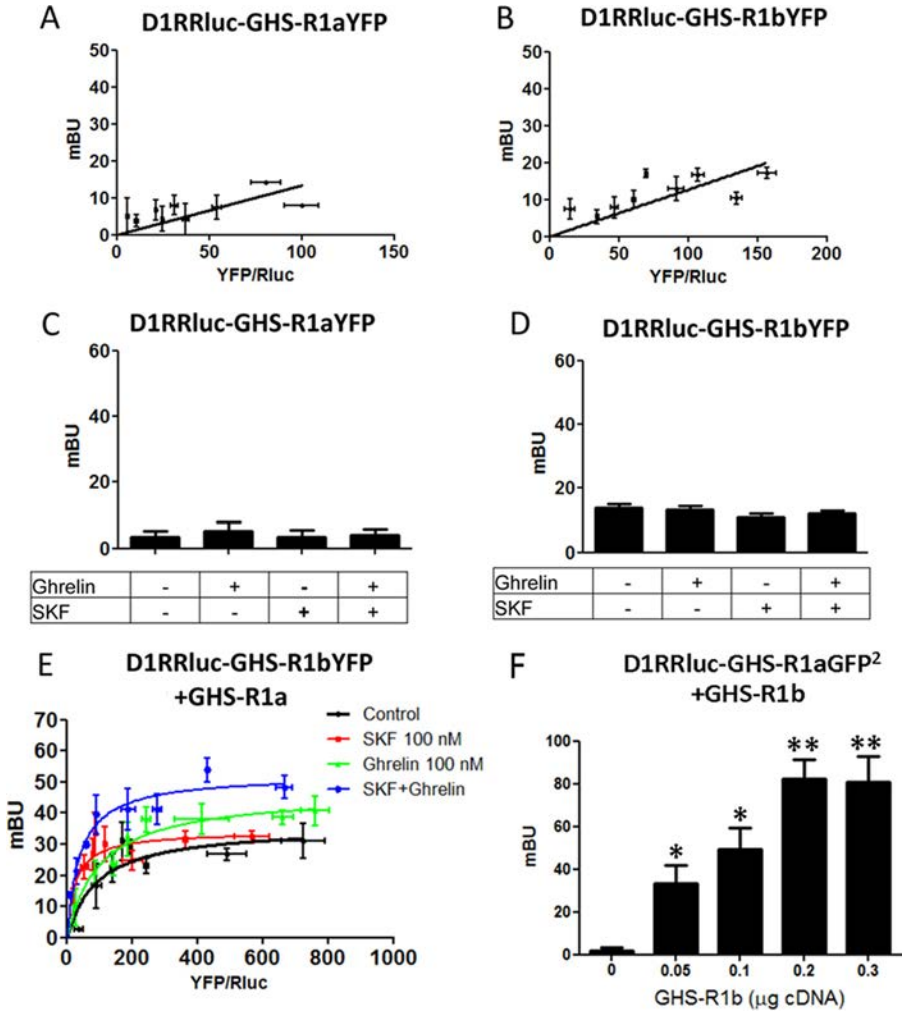

FIGURE 11. **Selective heteromerization of D1R with GHS-R1a-GH-R1b complexes.** BRET experiments in HEK-293T cells transfected with a constant amount of D_1R-Rluc cDNA (0.4 μg) and increasing amounts of GHS-R1a-YFP cDNA (0.2–1.5 μg, *A*) or GHS-R1b-YFP cDNA (0.1–0.6 μg, *B*). BRET at a YFP/Rluc ratio of 100 was also determined in cells not activated or activated with ghrelin (100 nM), the D_1R agonist SKF81297 (*SKF*, 100 nM), or both (*C* and *D*). *E*, BRET experiments were performed in HEK-293T cells transfected with D_1R-Rluc cDNA (0.4 μg), GHS-R1a cDNA (0.8 μg), and increasing amounts of GHS-R1b-YFP cDNA (0.1–0.6 μg), not stimulated (*black curve*), or stimulated with SKF81297 (*SKF*, 100 nM, *red curve*), ghrelin (100 nM, *green curve*), or both (*blue curve*). *F*, BRET experiments were performed in HEK-293T cells transfected with D_1R-Rluc cDNA (0.4 μg), GHS-R1a-GFP^2 cDNA (1.0 μg), and increasing amounts of GHS-R1b cDNA (0.05–0.3 μg). BRET values are given as a function of 100× the ratio between the fluorescence of the acceptor and the luciferase activity of the donor. BRET is expressed as milliBRET units and given as the means ± S.D. of four to six experiments grouped as a function of the amount of BRET acceptor. Statistical differences between differently transfected cells were analyzed by ANOVA followed by Bonferroni's corrections. *, $p < 0.05$; **, $p < 0.01$ compared with cells not transfected with GHS-R1b.

Discussion

Previous studies about the role of the truncated ghrelin receptor GHS-R1b only indicated a possible dominant negative effect, which could depend on its ability to retain the full and functional ghrelin receptor GHS-R1a in intracellular compartments (6, 7) or to stabilize GHS-R1a in a non-signaling conformation (5). This study does not support the intracellular mechanism as a main regulatory mechanism. Instead, it reveals a novel and complex modulatory role of GHS-R1b in the trafficking and signaling of GHS-R1a. First, GHS-R1b facilitates GHS-R1a trafficking to the plasma membrane with an efficiency that depends on a specific relative GHS-R1b/GHS-R1a expression ratio. With further increases in the GHS-R1b/GHS-R1a expression ratio, this facilitation declines and disappears. Thus, higher and probably non-physiological amounts of GHS-R1b seem to be necessary to promote intracellular retention of GHS-R1a (6, 7). Second, GHS-R1b impairs GHS-R1a signaling upon oligomerization at the plasma membrane. The correlation between the results obtained with biotinylation and signaling experiments in HEK-293T cells demonstrates that the main factor determining the potency of ghrelin-induced signaling is the stoichiometric relationship of both proteins in the plasma membrane. Therefore, GHS-R1b can act as a dual modulator of GHS-R1a function: low relative GHS-R1b expression potentiates and high relative GHS-R1b expression inhibits GHS-R1a function by facilitating GHS-R1a trafficking to the plasma membrane and by exerting a negative allosteric effect on GHS-R1a signaling, respectively. The ability of GHS-R1a homodimers to oligomerize with one or several (at least two) GHS-R1b protein molecules provides a frame for oligomerization to be involved in this fine-tuning, stoichiometry-dependent modulation of GHS-R1a function. Because GHS-R1a seems to be the minimal functional unit (19), one possible scenario is that one GHS-R1b molecule per one GHS-R1a

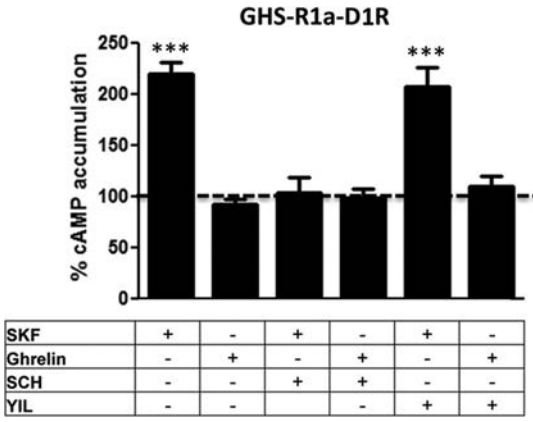

FIGURE 12. **Dependence on GHS-R1b for D1R-mediated modulation of GHS-R1a signaling.** cAMP accumulation was determined in cells transfected with GHS-R1a-YFP cDNA (1.5 μg) and D_1R cDNA (0.5 μg). Cells were treated with vehicle, ghrelin (100 nM), or SKF 81297 (*SKF*, 100 nM) with and without YIL781 (*YIL*, 2 μM) or SCH23390 (*SCH*, 1 μM). Values are means ± S.E. of four to six experiments and are expressed as percentage values from cells only treated with vehicle (100%, *dotted line*). Statistical differences between differently treated cells were analyzed by ANOVA followed by Bonferroni's corrections. **, $p < 0.01$; ***, $p < 0.001$ compared with cells treated only with vehicle.

homodimer facilitates trafficking but not a negative allosteric modulation of ghrelin, whereas two (or more) GHS-R1b molecules would not facilitate trafficking but would allosterically decrease ghrelin-mediated signaling.

To our knowledge, this is the first study that addresses the modulatory role of GHS-R1b on GHS-R1a signaling in primary neurons in culture that offers a more physiological model than previously used mammalian transfected cell lines. The results first indicate that endogenous relative expression of GHS-R1a and GHS-R1b are in the same range in primary neuronal cultures that in our experiments in HEK-293T transfected cells. Significantly, from the experiments in HEK-293T cells, predictable changes in ghrelin-induced signaling were demonstrated in striatal and hippocampal neurons in culture upon varying the relative levels of expression of GHS-R1b. Progressively increasing the expression of GHS-R1b in hippocampal and striatal cell cultures led to an increase and decrease in ghrelin-induced signaling, respectively, that depended on a respective initially low and high relative GHS-R1a/GHS-R1b expression ratio.

In isolation, the GHS-R1a receptor has been shown to couple to G_q proteins, resulting in activation of phospholipase C, inositol 1,4,5-trisphosphate, and Ca^{2+} mobilization (5, 19, 20), but it has also been reported to produce signaling dependent on pertussis toxin-sensitive $G_{i/o}$ proteins (21, 22). Thus, ghrelin seems to be able to activate different signaling pathways in a tissue-specific manner. In pituitary GH cells, GHS-R1a seems to couple preferentially to G_q, leading to stimulation of GH release, whereas, in islet pancreatic β cells, it couples to $G_{i/o}$ proteins, and its activation leads to inhibition of insulin release (23). It has also been reported that ghrelin can produce cAMP-PKA signaling, although this is generally not attributed to its canonically dependent stimulatory G_s protein (24–26). The use of selective G protein toxins and inhibitors demonstrated a preferential $G_{i/o}$ coupling of the GHS-R1a-GHS-R1b complex in HEK-293T cells and, unexpectedly, a preferential $G_{s/olf}$ coupling in both striatal and hippocampal neurons in culture. In HEK-293T cells, the same modulation by GHS-R1b was observed for GHS-R1a-mediated inhibition of adenylyl cyclase, β arrestin-2 recruitment, ERK1/2 phosphorylation, and cytosolic Ca^{2+} increase. Although a canonical G_q-coupled signaling, cytosolic Ca^{2+} increase can also be induced by G_i-associated $\beta\gamma$-dependent mechanisms, as demonstrated in several mammalian cell lines, including HEK-293 cells (27, 28). ERK1/2 phosphorylation could then depend on a downstream effect of cytosolic Ca^{2+} increase or β arrestin-2 recruitment (28, 29).

This study demonstrates that oligomerization with GHS-R1b confers the GHS-R1a-GHS-R1b complex the ability to heteromerize with D1R, allowing ghrelin to signal through $G_{s/olf}$. Thus, in HEK-293T cells transfected with GHS-R1a and GHS-R1b, co-transfection of D1R promoted a switch of ghrelin-mediated signaling from $G_{i/o}$ to $G_{s/olf}$ signaling. A previous study on transfected HEK-293 cells suggested that GHS-R1a can heteromerize and functionally interact with D1R but apparently without concomitant interaction with GHS-R1b. The same study also suggested that, within the GHS-R1a-D1R heteromer, ghrelin amplifies D1R signaling (17). A more recent study by the same research group also suggests that GHS-R1a-D1R heteromerization allows D1R to couple and signal through G_q proteins, again without the involvement of GHS-R1b (18). However, our BRET experiments show that GHS-R1a-D1R heteromerization depends on the presence of GHS-R1b in the complex. In cells co-transfected with D1R, GHS-R1a, and GHS-R1b, ghrelin (maximal effective concentration) does not potentiate and, if anything, decreases cAMP accumulation induced by SKF81297. Furthermore, a significant cross-antagonism, a common biochemical property of receptor heteromers, was also observed. This is the ability of an antagonist of one of the protomers to counteract the signaling induced by an agonist of the other protomer in a receptor heteromer (13). In cells transfected with GHS-R1a, GHS-R1b, and D1R, both the D1R antagonist SCH23390 and the GHS-R1a antagonist YIL781 were able to block both SKF81297- and ghrelin-induced cAMP increases. The cross-antagonism of SCH23390 on ghrelin-induced cAMP accumulation was also observed in striatal but not in hippocampal cells in culture. Furthermore, ghrelin-induced cAMP accumulation in striatal cells was dependent on the relative expression of GHS-R1b. The total correlation among the results obtained in HEK-293T and striatal cells indicates the presence of the same D1R-GHS-R1a-GHS-R1b complexes in striatal cells. In the hippocampus, although evidence for molecular and functional interactions between hippocampal GHS-R1a and D1R have been reported recently (18), receptors other than D1R might be responsible for coupling GHS-R1a-GHS-R1b heteromers to G_{s-olf} protein, suggesting that different complexes containing GHS-R1a-GHS-R1b heteromers can be differentially expressed in the brain.

In summary, GHS-R1b plays a much more active and complex role in ghrelin-induced signaling than previously assumed. This study indicates that the relative expression of GHS-R1b not only determines the efficacy of ghrelin-induced, GHS-R1a-mediated signaling but also determines the ability of GHS-R1a to form oligomeric complexes with other receptors, promoting profound qualitative changes in ghrelin-induced signaling.

Author Contributions—G. M., D. A., E. A., M. M., and E. M. performed the experiments and analyzed the data. G. N., D. A., J. M., A. C., E. I. C., V. C., P. J. M., C. L., and S. F. designed the experiments. G. M., C. L., and S. F. wrote the manuscript.

Acknowledgment—We thank Jasmina Jiménez for technical assistance.

References

1. Silver, R., and Balsam, P. (2010) Oscillators entrained by food and the emergence of anticipatory timing behaviors. *Sleep Biol. Rhythms* **8,** 120–136
2. Mason, B. L., Wang, Q., and Zigman, J. M. (2014) The central nervous system sites mediating the orexigenic actions of ghrelin. *Annu. Rev. Physiol.* **76,** 519–533
3. Andrews, Z. B. (2011) The extra-hypothalamic actions of ghrelin on neuronal function. *Trends Neurosci.* **34,** 31–40
4. Jang, J. K., Kim, W. Y., Cho, B. R., Lee, J. W., and Kim, J. H. (2013) Microinjection of ghrelin in the nucleus accumbens core enhances locomotor activity induced by cocaine. *Behav. Brain. Res.* **248,** 7–11
5. Mary, S., Fehrentz, J. A., Damian, M., Gaibelet, G., Orcel, H., Verdié, P., Mouillac, B., Martinez, J., Marie, J., and Banères, J. L. (2013) Heterodimerization with its splice variant blocks the ghrelin receptor 1a in a non-signaling conformation: a study with a purified heterodimer assembled into lipid discs. *J. Biol. Chem.* **288,** 24656–24665
6. Leung, P. K., Chow, K. B., Lau, P. N., Chu, K. M., Chan, C. B., Cheng, C. H., and Wise, H. (2007) The truncated ghrelin receptor polypeptide (GHS-R1b) acts as a dominant-negative mutant of the ghrelin receptor. *Cell Signal.* **19,** 1011–1022
7. Chow, K. B., Sun, J., Chu, K. M., Tai Cheung, W., Cheng, C. H., and Wise, H. (2012) The truncated ghrelin receptor polypeptide (GHS-R1b) is localized in the endoplasmic reticulum where it forms heterodimers with ghrelin receptors (GHS-R1a) to attenuate their cell surface expression. *Mol. Cell. Endocrinol.* **348,** 247–254
8. Hradsky, J., Mikhaylova, M., Karpova, A., Kreutz, M. R., and Zuschratter, W. (2013) Super-resolution microscopy of the neuronal calcium-binding proteins Calneuron-1 and Caldendrin. *Methods Mol. Biol.* **963,** 147–169
9. Ciruela, F., Soloviev, M. M., and McIlhinney, R. A. (1999) Cell surface expression of the metabotropic glutamate receptor type 1α is regulated by the C-terminal tail. *FEBS Lett.* **448,** 91–94
10. Chen, T. W., Wardill, T. J., Sun, Y., Pulver, S. R., Renninger, S. L., Baohan, A., Schreiter, E. R., Kerr, R. A., Orger, M. B., Jayaraman, V., Looger, L. L., Svoboda, K., and Kim, D. S. (2013) Ultrasensitive fluorescent proteins for imaging neuronal activity. *Nature* **499,** 295–300
11. Zimmermann, T., Rietdorf, J., Girod, A., Georget, V., and Pepperkok, R. (2002) Spectral imaging and linear un-mixing enables improved FRET efficiency with a novel GFP2-YFP FRET pair. *FEBS Lett.* **531,** 245–249
12. Schröder, R., Schmidt, J., Blättermann, S., Peters, L., Janssen, N., Grundmann, M., Seemann, W., Kaufel, D., Merten, N., Drewke, C., Gomeza, J., Milligan, G., Mohr, K., and Kostenis, E. (2011) Applying label-free dynamic mass redistribution technology to frame signaling of G protein-coupled receptors noninvasively in living cells. *Nat. Protoc.* **6,** 1748–1760
13. Ferré, S., Casadó, V., Devi, L. A., Filizola, M., Jockers, R., Lohse, M. J., Milligan, G., Pin, J. P., and Guitart X (2014) G protein-coupled receptor oligomerization revisited: functional and pharmacological perspectives. *Pharmacol. Rev.* **66,** 413–434
14. Carriba, P., Navarro, G., Ciruela, F., Ferré, S., Casadó, V., Agnati, L., Cortés, A., Mallol, J., Fuxe, K., Canela, E. I., Lluís, C., and Franco, R. (2008) Detection of heteromerization of more than two proteins by sequential BRET-FRET. *Nat. Methods* **5,** 727–733
15. Guitart, X., Navarro, G., Moreno, E., Yano, H., Cai, N. S., Sánchez-Soto, M., Kumar-Barodia, S., Naidu, Y. T., Mallol, J., Cortés, A., Lluís, C., Canela, E. I., Casadó, V., McCormick, P. J., and Ferré, S. (2014) Functional selectivity of allosteric interactions within G protein-coupled receptor oligomers: the dopamine D1-D3 receptor heterotetramer. *Mol. Pharmacol.* **86,** 417–429
16. Bonaventura, J., Navarro, G., Casadó-Anguera, V., Azdad, K., Rea, W., Moreno, E., Brugarolas, M., Mallol, J., Canela, E. I., Lluís, C., Cortés, A., Volkow, N. D., Schiffmann, S. N., Ferré, S., and Casadó, V. (2015) Allosteric interactions between agonists and antagonists within the adenosine A2A receptor-dopamine D2 receptor heterotetramer. *Proc. Natl. Acad. Sci. U.S.A.* **112,** E3609-E3618
17. Jiang, H., Betancourt, L., and Smith, R. G. (2006) Ghrelin amplifies dopamine signaling by cross talk involving formation of growth hormone secretagogue receptor/dopamine receptor subtype 1 heterodimers. *Mol. Endocrinol.* **20,** 1772–1785
18. Kern, A., Mavrikaki, M., Ullrich, C., Albarran-Zeckler, R., Brantley, A. F., and Smith, R. G. (2015) Hippocampal dopamine/DRD1 signaling dependent on the Ghrelin receptor. *Cell* **163,** 1176–1190
19. Damian, M., Mary, S., Maingot, M., M'Kadmi, C., Gagne, D., Leyris, J. P., Denoyelle, S., Gaibelet, G., Gavara, L., Garcia de Souza Costa, M., Perahia, D., Trinquet, E., Mouillac, B., Galandrin, S., Galès, C., Fehrentz, J. A., Floquet, N., Martinez, J., Marie, J., and Banères, J. L. (2015) Ghrelin receptor conformational dynamics regulate the transition from a preassembled to an active receptor:G_q complex. *Proc. Natl. Acad. Sci. U.S.A.* **112,** 1601–1606
20. Holst, B., Brandt, E., Bach, A., Heding, A., and Schwartz, T. W. (2005) Nonpeptide and peptide growth hormone secretagogues act both as ghrelin receptor agonist and as positive or negative allosteric modulators of ghrelin signaling. *Mol. Endocrinol.* **19,** 2400–2411
21. Dezaki, K., Kakei, M., and Yada, T. (2007) Ghrelin uses Galphai2 and activates voltage-dependent K^+ channels to attenuate glucose-induced Ca^{2+} signaling and insulin release in islet β-cells: novel signal transduction of ghrelin. *Diabetes* **56,** 2319–2327
22. Bennett, K. A., Langmead, C. J., Wise, A., and Milligan, G. (2009) Growth hormone secretagogues and growth hormone releasing peptides act as orthosteric super-agonists but not allosteric regulators for activation of the G protein $G\alpha_{o1}$ by the Ghrelin receptor. *Mol. Pharmacol.* **76,** 802–811
23. Dezaki, K. (2013) Ghrelin function in insulin release and glucose metabolism. *Endocr. Dev.* **25,** 135–143
24. Malagón, M. M., Luque, R. M., Ruiz-Guerrero, E., Rodríguez-Pacheco, F., García-Navarro, S., Casanueva, F. F., Gracia-Navarro, F., and Castaño, J. P. (2003) Intracellular signaling mechanisms mediating ghrelin-stimulated growth hormone release in somatotropes. *Endocrinology* **144,** 5372–5380
25. Cuellar, J. N., and Isokawa, M. (2011) Ghrelin-induced activation of cAMP signal transduction and its negative regulation by endocannabinoids in the hippocampus. *Neuropharmacology* **60,** 842–851
26. Sun, Y., Shi, N., Li, H., Liu, K., Zhang, Y., Chen, W., and Sun, X. (2014) Ghrelin suppresses Purkinje neuron P-type Ca^{2+} channels via growth hormone secretagogue type 1a receptor, the $\beta\gamma$ subunits of G_o-protein, and protein kinase a pathway. *Cell Signal.* **26,** 2530–2538
27. Dorn, G. W., 2nd, Oswald, K. J., McCluskey, T. S., Kuhel, D. G., and Liggett, S. B. (1997) α 2A-adrenergic receptor stimulated calcium release is transduced by G_i-associated $G\beta\gamma$-mediated activation of phospholipase C. *Biochemistry* **36,** 6415–6423
28. Della Rocca, G. J., van Biesen, T., Daaka, Y., Luttrell, D. K., Luttrell, L. M., and Lefkowitz, R. J. (1997) Ras-dependent mitogen-activated protein kinase activation by G protein-coupled receptors. Convergence of G_i- and G_q-mediated pathways on calcium/calmodulin, Pyk2, and Src kinase. *J. Biol. Chem.* **272,** 19125–19132
29. Kovacs J. J., Hara, M. R., Davenport, C. L., Kim, J., and Lefkowitz, R. J. (2009) Arrestin development: emerging roles for β-arrestins in developmental signaling pathways. *Dev. Cell* **17,** 443–458

3.5. COCAINE BLOCKS GHRELIN EFFECTS VIA INTERACTION WITH SIGMA-1 RECEPTORS

David Aguinaga, Mireia Medrano, Arnau Cordomí, Mireia Jiménez-Rosés, Edgar Angelats, Ignacio Vega-Quiroga, Katia Gysling, Leonardo Pardo, Enric I. Canela, Rafael Franco* y Gemma Navarro*

*Coautores del manuscrito

Manuscrito enviado a *Neuropsychopharmacology*.

Antes de ser una droga de abuso y convertirse en un importante problema de salud y socioeconómico, la cocaína era un suplemento natural de resistencia. Los pueblos indígenas conocían los beneficios de masticar hojas de coca, la desaparición del apetito uno de los más importantes. A pesar de este conocimiento, no se conocen los mecanismos moleculares subyacentes a la supresión del apetito por el consumo de cocaína. Ya que la cocaína se une a los receptores sigma-1 (σ_1R) que a su vez transmite algunos de los efectos de la droga, ha sido planteada la hipótesis que σ_1R podría interactuar molecular y/o funcionalmente con los receptores orexinérgicos. En este trabajo ha sido demostrada la formación de complejos heteroméricos formados por el receptor sigma-1 y el receptor de grelina GHS-R1a. El heterómero tiene propiedades particulares y es sensible a la cocaína cuando esta se une a sigma-1 en el complejo. La cocaína afecta a la expresión del heterómero en la superficie celular e inhibe la activación del receptor GHS-R1a por la hormona natural. También han sido proporcionadas evidencias de las interfases involucradas en las interacciones heteroméricas, y ha sido propuesta una posible estructura cuaternaria para este complejo que probablemente medie la supresión del apetito inducida por la cocaína.

COCAINE BLOCKS GHRELIN EFFECTS VIA INTERACTION WITH SIGMA-1 RECEPTORS.

David Aguinaga[1,2], Mireia Medrano[1,2], Arnau Cordomí[5], Mireia Jiménez-Rosés[5], Edgar Angelats[1,2], Ignacio Vega-Quiroga[4], Katia Gysling[4], Leonardo Pardo[5], Enric I. Canela[1,2], Rafael Franco[1,2]* and Gemma Navarro[1,3]*

[1]*Centro de Investigación en Red, Enfermedades Neurodegenerativas (CIBERNED). Instituto de Salud Carlos III. Madrid. Spain.*
[2]*Department of Biochemistry and Molecular Biomedicine. School of Biology. Universitat de Barcelona. Barcelona. Spain.*
[3]*Department of Biochemistry and Physiology. Faculty of Pharmacy. Universitat de Barcelona. Barcelona. Spain.*
[4]*Department of Cellular and Molecular Biology. Faculty of Biological Sciences. Pontificia Universidad Católica de Chile. Santiago. Chile.*
[5]*Laboratori de Medicina Computacional, Unitat de Bioestadística, Facultat de Medicina, Universitat Autònoma de Barcelona, 08193 Bellaterra, Spain;*

Corresponding author: Gemma Navarro, g.navarro@ub.edu

School of Pharmacy. Universitat de Barcelona. Diagonal 643.

Tel +34 934021213

SUMMARY

Before being a drug of abuse and become an important health and socio-economic issue, cocaine was an endurance natural supplement. Indigenous people chewing coca leaves known of the benefits, being lack of appetite one of the most important. Despite this knowledge, the molecular mechanisms underlying suppression of appetite by cocaine consumption are not known. As cocaine binds to sigma-1 receptors (σ1R) that in turn convey some of the effects of the drug, we hypothesized that σ1R could interact molecularly and/or functionally with orexinergic receptors. We here report the formation of heteromer complexes formed by σ1R and ghrelin GHS-R1a-receptors. The heteromer has specific properties and is sensitive to cocaine binding to its cognate receptor in the complex. Cocaine increase cell surface expression of the heteromer and inhibits GHS-R1a activation by the natural hormone. We also provide evidence for the interfaces involved in heteromer interactions, and propose a possible quaternary structure for this complex that likely mediates the cocaine-induced suppression of appetite.

INTRODUCTION

Used today as recreational drug, cocaine was first consumed by humans in the form of *Coca* leaves. Indeed, indigenous peoples of South American knew that chewing coca leaves was key for keeping their life style, especially in living within high mountains. Coca served to cope with the harsh living conditions, for instance when people had to travel long distances and cross Andean mountains with reduced weight and little food. Despite such ancient knowledge, i.e. the appetite suppressant action of cocaine consumption, the molecular basis of hunger dissipation by cocaine are not known. This report was undertaken to test the hypothesis of whether the well-known anorexic effect of cocaine is mediated by ghrelin receptors, which are key players in the central control of food/energy intake.

Ghrelin is a peptide hormone delivered by the stomach to the bloodstream in hungry conditions, being involved in the control of food intake and energy homeostasis. Its action is mediated by specific receptors that have received a variety of denominations, *inter alia* growth hormone-releasing peptide or growth hormone secretagogue receptor. Ghrelin receptors belong to the superfamily of G-protein-coupled receptors (GPCRs) and, up to date, only one type has been identified. However, this receptor show in human (also in pig) two known isoforms produced by alternative splicing: isoform 1a which contains seven transmembrane domains (GHS-R1a, 366 amino acids) and isoform 1b (GHS-R1b, 289 amino acids) which lacks the 5^{th} and 6^{th} transmembrane (TM) domains. These TM domains are required for ligand binding and coupling to heterotrimeric G proteins and, therefore, ghrelin cannot signal via GHS-R1b receptors (Mary, et al., 2013). The truncated variant seems to serve as modulator of GHS-R1a surface expression and signaling. In fact, GHS-R1b is expressed in the same cells than GHS-R1a and both isoforms interact to form heteromer receptor signaling units (Mary, et al., 2013). It has been reported that GHS-R1b guide surface expression of functional G-protein-coupled ghrelin receptors acting as a dual modulator of GHS-R1a function: low relative GHS-R1b expression potentiates GHS-R1a function (Navarro, et al., 2016) while high relative GHS-R1b expression negatively influences ghrelin action by allosteric interactions that within the GHS-R1a-GHS-R1b heteromer reduce the efficacy of the hormone (Chow, et al., 2012; Mary, et al., 2013). Although the purified GHS-R1a assembled into lipid discs is reportedly coupled to $G_{q/11}$ (Damian, et al., 2015, www.guidetopharmacology.org) the receptor may couple to non-$G_{q/11}$ heterotrimeric G proteins. We found a preferential Gi/o coupling of the GHS-R1a-GHS-R1b complex in HEK-293T cells and, a preferential Gs/olf coupling in both striatal and hippocampal neurons in culture (Navarro, et al., 2016). Heteromerization of GHS-R1a and GHS-R1b in heterologous expression systems is often needed for proper ghrelin-induced signaling. It should be noted that ghrelin receptors may form direct protein-protein interactions with a variety of GPCRs, *inter alia* with dopamine, melanocortin, prostanoid, serotonin, somatostatin and neurotensin receptors ((Borroto-Escuela, et al., 2014); see www.gpcr-hetnet.com and references therein).

The sigma 1 receptor (σ_1R) is an atypical type of membrane protein whose exact function remain unknown. It has been proposed as a pluripotent modulator in living cells (Su, et al., 2016), gaining momentum due to its potential as target against neuropathic pain (Corbera, et al., 2006; Mei & Pasternak, 2002; Sun, et al., 2016). Kruse et al. reviewed in 2016 the intriguing features of this protein, with no structural resemblance with any other membrane receptor, an occluded ligand binding site, and resemblance to a yeast enzyme, yeast sterol isomerase. In fact, the three-dimensional structure has been recently elucidated (Schmidt, et al., 2016). It consists in three σ_1R protomers, with a single

transmembrane domain and a C-terminal tail having a cupin-like β-barrel with a buried ligand-binding site that arrange into homotrimers. Due to the reports showing that σ_1R may interact with receptors for a variety of hormones/neurotransmitters (see below), it was tempting to speculate that its role may be the regulation of the expression and function of cell surface receptors. Remarkably, while the physiological function remains elusive and the endogenous ligand is yet to be discovered, σ_1R binds cocaine, mediating some effects of the drug (McCracken, et al., 1999; Skuza, 1999; Lever, et al., 2016). Thus, the design of drugs impeding the interaction of cocaine with σ_1R is proposed to reduce drug-seeking behavior (Matsumoto, et al., 2001). σ_1R-mediated cocaine actions in the central nervous system are dependent on molecular interactions with G-protein-receptors (GPCRs). We have identified cocaine binding to σ_1R receptors that in turn result in modulating the function of dopamine receptors by potentiating D_1R mediated adenylate cyclase signaling (Navarro, et al., 2010; Moreno, et al., 2014) and by inhibiting D_2R mediated signaling in striatal neurons, disrupting the delicate balance between inputs of reward seeking controlled by D_1R containing neurons and inputs of aversion coming from D_2R containing neurons (Navarro, et al., 2013). It has also been described that cocaine binding to σ_1R induce the disruption of the orexin and corticotropin releasing factor receptor negative cross-talk, playing an important role in the stress-induced cocaine-seeking behavior (Navarro, et al., 2015). In the present manuscript we questioned if σ_1R could interact and modulate the growth hormone secretagogue receptor 1a mediating the anorexigenic effects of cocaine in the central nervous system. Structural information on individual receptors and on GPCR macromolecular complexes already exist (See (Cordomí, et al., 2015) TIBS and references therein). In particular, it is becoming accepted that transmembrane regions are key factors on the receptor-receptor interacting interfaces. Thus, by the use of Transmembrane TAT-peptides of GHS-R1a and biophysical computational assays we have determined by the first time the heteromeric structure formed by σ_1R and a GPCR: the GHS-R1a.

RESULTS

GHS-R1a form heteromeric complexes with σ_1R

Immunocytochemical assays were first performed to detect whether colocalization between GHS-R1a and σ_1 receptors occurred in transfected HEK-293T cells. Cells were transfected with cDNAs for σ_1R fused to YFP (0.75 µg cDNA) and for GHS-R1a fused to Rluc (1,66 µg cDNA). In cells expressing only σ_1R-YFP the receptor was detected by YFP fluorescence, identifying the receptor in intracellular structures but also at the plasma membrane level (Fig. 1A). On the other hand, in HEK-293T cells expressing GHS-R1a-Rluc, the GHS-R1a was detected by a specific primary anti-Rluc and secondary Cy3 antibodies, being detected in intracellular structures and at the plasma membrane level. Interestingly, in HEK-293T cells coexpressing σ_1R-YFP (0.75 µg cDNA) and GHS-R1a-Rluc (1,66 µg cDNA), colocalization of both receptors was observed at the plasma membrane.

To identify a potential direct interaction between σ_1R and GHS-R1a, we developed BRET experiments, transfecting a constant amount of cDNA for σ_1R-Rluc (0.075 µg cDNA) and increasing amounts of cDNA for GHS-R1a-GFP^2 (0.5 to 3 µg cDNA). A saturation BRET curve was obtained thus indicating a specific interaction between σ_1R and GHS-1a ($BRET_{max}$ 371 ± 38 mBU, $BRET_{50}$ 68 ± 23) (Fig. 1C). In contrast, when adenosine A_{2A}-

GFP^2 (0.5 to 2.5 μg cDNA) was used instead of GHS-R1a receptor, a linear plot with low BRET values was obtained as negative control.

Quaternary structure of the σ1R-GHS-R1a heteroreceptor complex

The GHS-R1a receptor signaling cannot be explained without considering the possible homomeric and heteromeric complexes with additional GHS-R1a protomers and GHS-R1b (Chow, et al., 2012; Mary, et al., 2013; Navarro, et al., 2016). Consequently, we wanted to get a hint on the TM domains located in the receptor-receptor interacting interfaces. To fulfill this aim we designed peptides (whose exact sequence is provided in Methods) having receptor TM sequences and a sequence of the cell-penetrating HIV transactivator of transcription (TAT) that allows interaction with hydrophobic cell membrane domains. It has been also proved that synthetic peptides derived from TM segments can be used to disrupt interaction involving GPCRs (Ng, et al., 1996; Herbert, et al., 1996; Guitart, et al., 2014). We first transfected HEK-293T cells with GHS-R1a-nYFP (0.75 μg cDNA) and GHS-R1a-cYFP (0.5 μg cDNA) to find bimolecular complementation (approximately 4,000 units of fluorescence). When TM5 or TM6 but no other TM TAT peptides were included in the assays, the fluorescence decreased by two-fold (Fig. 2A). Such interference results indicated that GHS-R1a-GHS-R1a homomer formation likely occurred via TM5/TM6 domains. Similar results were obtained when the GHS-1a-GHS-1b receptor heterodimer interface was analyzed, i.e. the heteromer also involves TM5/6 interactions (Fig. 2B). Interestingly, when cells were transfected with cDNAs for GHS-R1a-nYFP and GHS-R1b-cYFP in the presence of GHS-R1a (Fig. 2C) it was observed that GHS-R1a-GHS-R1a homodimer interaction is stronger than GHS-R1a-GHS-R1b heterodimer interaction, forcing GHS-R1b receptor to interact by TM4 domain when TM5 and TM6 domains are occupied by another GHS-R1a receptor.

We then were interested to identify which transmembrane domains were involved in the interactions between σ_1R and GHS-R1a receptors. In HEK-293T cells coexpressing GHS-R1a-nYFP (0.75 μg cDNA) and σ_1R-cYFP (0.5 μg cDNA), fluorescence measurements of up to 4,000 units of fluorescence indicated bimolecular fluorescent complementation, BiFC, which demonstrated the formation of GHS-R1a-σ_1R complexes. Remarkably, when cells were treated for 4 h with TM1, TM2, TM5 or TM6 TAT-peptides, a significant decrease in fluorescence was detected (Fig. 2D) thus indicating the existence of two different interfaces between GHS-1a and σ_1 receptors involving either TM1/2 or TM5/6 of the GHS-1a receptor. When HEK-293T cells were transfected with σ_1R-cYFP (0.5 μg cDNA) and GHS-R1b-nYFP (the truncated isoform that lacks TM domains 6 and 7) (0.5 μg cDNA) a robust fluorescent signal (3,500 units) indicated that σ_1R is also able to interact with GHS-R1b. Treatment of these cells with HIV-peptides for GHS-R1a, TM1 and TM2 but not TM5 or TM6 TAT-peptides peptides significantly decreased the resulting fluorescence (Fig. 2E). The latter results also show that GHS-R1b can only bind σ_1R though the TM1/2 interface. In summary, the results obtained indicate that σ_1R may establish different interacting interfaces (TM1/2 and TM5/6) with GHS-R1a but only a TM1/2 interface with GHS-R1b.

Finally, to mimic physiological conditions as close as possible, cells were transfected with cDNAs for GHS-R1a-nYFP and σ_1R-cYFP in the presence of GHS-R1b (Fig. 2F). As anticipated, complementation was possible, and the fluorescence readings (5,000 fluorescence units) were higher than those obtained in the absence of GHS-R1a. Hence, it seemed that better interaction between GHS-R1a and σ_1R occurs when GHS-R1b is

present. Supporting this hypothesis, we found that in the presence of GHS-R1b, σ_1R only interact with GHS-R1a through the TM1/2 interface (Fig. 2E).

The crystal structure of σ_1R has been recently reported (Schmidt, et al 2016). The functional protein is seemingly constituted by an homotrimer. We constructed a computational model of the GHS-R1 dimer - σ_1R trimer – G protein system combining the presented biochemical experiments together with structural modelling (Fig 2G; see Methods section). According to the experiments with GHS-R1a-derived peptides above, σ1R can bind GHS-R1b through the TM1/2 interface and GHS-R1a through either the TM1/2 or the TM5/6 interfaces. Because GHS-R1a and GHS-R1b also employ the TM5/6 interface for homo/hetero-dimerization, we assumed that at normal expression levels, TM1/2 is the only possible interface for the GHS-R1- σ_1R complex as TM5/6 is occupied by the GHS-R1 homo/hetero-dimer. This model tells that it is not possible for one single GPCR (GHS-R1a or GHS-R1b) to simultaneously bind σ1R and the G protein because of steric clashes. Since GHS-R1a (but not GHS-R1b) is able to bind the G protein, the minimal unit requires one GHS-R1a protomer interacting with the G protein and a second protomer responsible for the binding of the σ_1R TM helix that could either be a second GHS-R1a or GHS-R1b. Interestingly, the model predicts that the cytoplasmic domain of a second σ_1R can contact the G_α subunit of the G_i protein, providing a possible mechanism for G protein modulation. Moreover, the GHS-R1a dimer has two free TM4/5 interfaces that may allow binding further GHS-R1a or GHS-R1b protomers, compatible with the stoichiometries previously reported (Navarro, et al., 2016).

Evidence of cocaine affecting cell surface GHS-R1a expression

As cocaine binds to σ_1R and these receptors can establish direct interactions with ghrelin receptors, we reasoned that cocaine could be affecting ghrelin-mediated signals. First, we investigated whether cocaine treatment would affect GHS-R1a expression. Cocaine was added (30 μM, 30 min) to cells expressing σ_1R and GHS-R1a receptors and Immunocytochemical assays were performed. Fig. 3A shows that plasma membrane expression of σ_1R increased when these cells were treated with a physiologically relevant dose of cocaine (30 μM) (Navarro et al., 2010). A similar increase was observed when cells were incubated with 100 nM of the σ_1 receptor ligand, PRE-084 for 30 min. Moreover, the expression of ghrelin receptors was not increased upon treatment with cocaine or PRE-084 but, interestingly, colocalization of the receptors at the cell surface increased when cells were treated with cocaine or PRE-084. These results indicate that not only cocaine, but also the σ_1R specific ligand PRE-084 are able to concomitantly affect coexpression of both receptors at the cell surface. Second, to evaluate the cocaine effect over σ_1R-GHS-R1a heteromerization, HEK-293T cells transfected with 0.075 μg cDNA for σ_1R-Rluc and 1.5 μg cDNA for GHS-R1a-GFP^2 were treated with 30 μM cocaine (red) or 100 nM PRE-084 (green) to find no differences in energy transfer recordings (comparing the different treatments with the control condition, Fig. 3B).

Cocaine treatment inhibits GHS-R1a signaling.

To evaluate the effect of cocaine on GHS-R1a-mediated signaling we first determined cAMP levels. It has been published that low concentrations of GHS-R1b expression significantly increase GHS-R1a signaling (Navarro, et al., 2016). Thus, to analyze GHS-R1a signaling pathways in HEK-293T cells, that do not express ghrelin receptors but endogenously express σ_1R (Navarro, et al., 2010), it has always been coexpressed GHS-R1a with low amounts of GHS-R1b. To evaluate cAMP levels, HEK-293T cells transfected with 1.66 μg cDNA for GHS-R1a and 0.25 μg cDNA for GHS-R1b were

stimulated with 100 nM ghrelin in the presence of 0.5 μM forskolin and a significant decrease in cAMP levels was observed (black) thus agreeing with the reported ghrelin receptor G_i coupling (www.guidetopharmacology.org) (Navarro, et al., 2016). The ghrelin effect on forskolin-induced cAMP levels was completely blocked by pre-treatment with the GHS-R1a selective antagonist, YIL-781 (2 μM) (blue). Interestingly, when cells were treated with 30 μM cocaine for 15 min (red) prior to ghrelin stimulation, the decrease in cAMP levels was reduced (Fig. 3C). Similar results were obtained when cells were pre-treated with 100 nM of PRE-084 (green), the σ_1R ligand, thus suggesting that cocaine-induced effects over GHS-R1a receptor could be due to cocaine interaction with σ_1 receptors. The proposed interaction between the C-terminus of σ_1R and $G_{\alpha,}$ could be the mechanism by which σ_1R regulates G_i in the complex (Fig 2E). Remarkably, the presented model constitutes the minimal signaling unit, as it is not possible that a single GHS-R1a protomer simultaneously binds G_i and σ_1R, and that a single σ_1R binds TMs 1 and 2 of the GHS-R1a and G_i.

ERK1/2 phosphorylation was subsequently analyzed. In HEK-293T cells transfected with 1.66 μg cDNA for GHS-R1a and 0.25 μg cDNA for GHS-R1b stimulation with 100 nM ghrelin increased by 80% ERK1/2 phosphorylation levels. Again, not only the treatment with YIL-781, but with cocaine or PRE-084, inhibited ghrelin effects (Fig. 3D). Indicating that cocaine not only affects the $G\alpha_i$-protein dependent pathway, but also $\beta\gamma$ dependent signaling.

Moreover, when HEK-293T cells expressing GHS-R1a, GHS-R1b and σ_1R were activated with 100 nM ghrelin, a characteristic trace of intracellular calcium transient was obtained (Fig. 3E). Analogously, Dynamic Mass Redistribution (DMR) recordings, which measure the changes in the wavelength of light passing through cell monolayer provided similar results (Fig. 3F). Moreover, 2 μM of the σ_1R antagonist, YIL-781, 30 μM cocaine or PRE-084 100 nM inhibited the ghrelin-induction of calcium released and DMR signal, in the same direction as the results obtained in cAMP levels and MAPK phosphorylation.

Cocaine inhibition of GHS-R1a receptor signaling are mediated by σ_1R

To check whether cocaine inhibition of ghrelin-induced signaling was due to its interaction with σ_1 receptors, HEK-293T cells expressing GHS-R1a (1.66 μg cDNA) and GHS-R1b (0.25 μg cDNA) were transfected with a siRNA designed to knock-down the σ_1 receptor expression (3 μg siRNA). Cells incorporating RNA responded to 100 nM ghrelin in both, forskolin-induced cAMP determination and ERK1/2 phosphorylation (black), with results similar to those in cells without the siRNA (Fig. 4A-B). However, in the presence of the siRNA, cocaine (red) or PRE-084 (green) had no effect on ghrelin-induced signals while pre-treatment with YIL-781 (blue) blocked ghrelin-induced GHS-R1a activation. Also, when HEK-293T cells expressing GHS-R1a were transfected with siRNA against σ_1R, ghrelin-induced a characteristic signal on calcium mobilization or on DMR recordings. Similarly, these stimulations were not affected by cocaine or PRE-084 pre-treatments while they were completely blocked by the ghrelin antagonist YIL-781. These results clearly indicate that cocaine effects over GHS-R1a receptor are mediated by σ_1 receptor.

Interfering TM1 TAT-peptide blocks the effect of cocaine on GHS-R1a function

Taking into account the structural data and that cocaine binds σ_1 but not ghrelin receptors, we hypothesized that the transfection of the TAT-peptide for ghrelin TM1 could abolish the cocaine effect. Accordingly, HEK-293T cells expressing GHS-R1a (1.66 µg cDNA) were treated during 4 h with 4µM of TAT-peptides for GHS-R1a TM1 or TM7. Next, cells were treated with 30 µM cocaine (red), 100 nM PRE-084 (green) or 1µM YIL-781 (blue) prior to ghrelin (100 nM) stimulation (Fig. 4E-H). The selective ghrelin receptor antagonist, YIL-781, blocked both, the decrease in cAMP levels and the characteristic DMR curve induced by ghrelin in TM1 and TM7 Tat-peptides treated cells. The results from cAMP accumulation and DMR assays indicated that, treatment with TM7, that did not alter GHS-R1a-nYFP-σ_1R-cYFP complementation and consequently was not involved in the GHS-R1a-σ_1R interface, showed similar results as that obtained in the absence of peptides, cells treated with cocaine or PRE-084 blocked GHS-R1a induced signaling (Fig. 4G, H). In contrast, the ghrelin effect was neither modulated by cocaine nor PRE-084 in TM1-treated cells (Fig. 4E, F). These results demonstrate that the disruption of the GHS-R1a-σ_1R interaction using TM1, alters the cocaine effect on ghrelin receptors, thus reinforcing the idea that cocaine modulates GHS-R1a receptor function via the σ_1 receptor.

Effect of cocaine treatment on striatal primary cultures of neurons.

Most of the cocaine effects in the CNS occur in the striatum (Joffe, et al., 2014, Borroto-Escuela, et al., 2017). Consequently, we moved to neuronal primary cultures of striatum to analyze the cocaine effects over GHS-R1a receptors in a more physiological environment. The *in situ* Proximity Ligation Assay (PLA), which allows the identification of interactions between two proteins in close proximity (<17 nm) (Borroto-Escuela, et al., 2011; Trifilieff, et al., 2011; Fuxe, et al., 2014) was used to identify GHS-R1a-σ_1R complexes, detected as punctuate red dots surrounding Hoechst-stained nuclei (Fig. 5A). In striatal primary cultures 43% of cells presented red dots with 2 dots/cell-containing dots. However, when these cells were treated with cocaine 30 µM for 30 min prior to developing the immunocytochemistry, the number of cells containing red dots and the number of dots/cell-containing dots increased significantly (54% of cells presented red dots with 3.2 dots/cell-containing dots). Indicating that cocaine pretreatment increase GHS-R1a-σ_1R complexes expression in striatal primary cultures of neurons (Fig 5A, B).

Then, cocaine effects over GHS-R1a signaling were analyzed in primary cultures of striatal neurons. Both, in cAMP determination and ERK1/2 phosphorylation assays, cocaine and PRE-084 counteracted the ghrelin-induction of GHS-R1a signaling in a similar way as the GHS-R1a specific antagonist YIL-781 (Fig. 5C, D). Such effect of cocaine was related to σ_1R modulation over GHS-R1a, as in striatal primary cultures treated with siRNA for σ_1R neither cocaine or PRE-084 had any effect (Fig. 5E, F).

Effect of cocaine administration on GHS-R1a-σ_1R heteromer expression in striatal sections from naïve and cocaine-treated animals

Following i.p. administration of 15 mg/kg cocaine for 1 (acute) or 14 (chronic) days, rats were sacrificed and 30 µm-thick striatal sections were obtained from each group of animals and from vehicle-treated animals. The *in situ* Proximity Ligation Assay (PLA) was used to identify GHS-R1a-σ_1R heteroreceptor complexes (Fig. 6A). When striatal sections of vehicle-treated animals were analyzed, it was observed that 11% of cells showed red dots with 1.6 dots/cell-containing dots (Fig 6B), indicating that around 10% of striatal cells expressed GHS-R1a-σ_1R complexes. Interestingly, in the case of the

chronic treatment the number of cells containing dots strongly increased to 61% and also the number of dots/cell-containing dots (2.7) compared to control cells. Remarkably, the cocaine acute treatment lead to values that were even higher than in the chronic condition (76% of cells containing dots and 3.2 dots/cell-containing dots). These results indicate that cocaine treatment increase GHS-R1a-σ_1R complexes formation in striatal rat sections with a maximum effect in acute conditions (Fig 6B).

DISCUSSION

σ_1R physiologic role as true receptor has not yet been demonstrated, however, synthetic agonists and antagonists are available for σ_1R. PRE-084 is considered a selective agonist due to its ability to dose-dependently dissociate σ_1R from a binding immunoglobulin protein/78 kDa glucose-regulated protein (BiP/GPR-78) (Hayashi & Su, 2007). Despite not having a specific signaling machinery, once activated by an agonist, σ_1R operate via translocation to the plasma membrane and via protein-protein-mediated modulation of cell responses (Su et al., 2016) involving calcium signaling and ion channels activation (Wu & Bowen, 2008). Of special interest here is the regulation of GPCR functionality. It has been published that σ1R is involved in the negative control that glutamate N-methyl-d-aspartate acid receptors (NMDARs) exert on opioid antinociception (Rodriguez-Muñoz, et al., 2015). Thus, σ1R antagonists would enhance antinociception and reduce neuropathic pain induced by μ-opioid receptors. Another example is the σ1R extent control of cannabinoid CB1-NMDAR receptors interaction which failure might constitute a vulnerability factor for cannabis abuse, potentially precipitating schizophrenia (Sanchez-Blazquez, et al., 2014). Even though the σ_1R endogenous ligand remain unknown, σ_1R can be activated by several drugs of abuse. Exposure of primary rat astrocytes to methamphetamine increased the expression of σ-1R, therefore in σ1R ko mice the drug could not induce astrocytes activation (Zhang et al., 2015). Upon demonstrating that cocaine may bind to the receptor even at doses attained at recreational use, σ_1R seem to mediate, at least in part, locomotor activation (Menkel et al., 1991; Barr et al., 2015), seizures (Matsumoto et al., 2001), drug sensitization (Ujike et al., 1996) and reward actions of the drug (Romieu et al., 2000; Pascal Romieu et al., 2002). Reduction of σ_1R receptor levels by injection of antisense nucleotides results in less convulsions (Matsumoto et al., 2002), whereas receptor agonism or antagonism respectively exacerbate or minimize drug effects (Matsumoto et al., 2002; Matsumoto et al., 2003; Matsumoto et al., 2004;). In 2004, Maurice T. and Romieu P. described thereafter that activation of the σ1R is also involved in the appetitive properties of cocaine, as measured using place preference conditioning in mice. However, the mechanism remained as a mystery. Today, our results show that σ_1R mediate the hunger-suppressive action of cocaine by interacting with the orexigenic ghrelin receptor.

The nucleus accumbens, one of the structures that conform the striatum, is part of the reward system. This system produces a pleasant sensation in front of food and other important actions for the individual survival (Kim & Hikosaka, 2015). The reward path is triggered by the expectation of a pleasurable stimulus, which is recognized by a solid foundation of previous experiences (Richardson and Gratton, 1998). Ghrelin receptors are expressed in the striatum (Engel, et al., 2015). Thus, the signal induced by ghrelin can activate the reward pathway inducing a pleasant sensation by generating expectations of food intake. Receptors controlling appetite were thus proposed as key in the central

control of food intake. Conditioned plate preference assays using both pharmacological and genetic models have shown that a lack of GHS-R1a receptor reduces the time of time spent in food reward spaces (Egecioglu, et al., 2010; Perello, et al., 2010). It is important to note that in these mesolimbic regions, the ghrelin receptor is coexpressed in neurons also containing cocaine-sensitive σ_1 receptors. From mechanistic and molecular point of views, this report highlights an interaction between σ_1R and GHS-R1a that is translated into a strong inhibition of grelin induced GHS-R1a signaling on G protein dependent signaling pathway, detected by cAMP accumulation and calcium release assays and also in the indirect signaling pathway, detected by MAPK phosphorylation and Dynamic Mass redistribution assays. It has been demonstrated in transfected HEK-293T cells and in striatum primary cultures of neurons that cocaine and σ_1R agonists pretreatment similarly inhibit ghrelin mediated signaling as compared to the GHS-R1a antagonist YIL. This effect is mediated by cocaine binding to σ_1 receptor as cocaine show no effect over grelin signaling in σ_1R-RNAi treated cells. Interestingly, other GPCR can be modulated by cocaine binding to σ_1R. Thus, cocaine is able to unbalance the striatum direct and indirect signaling pathways by altering the cell signaling of dopamine D_1 and D_2 receptors. While cocaine treatment potentiates the D_1R activation of adenylate cyclase and the subsequent increase in the cAMP levels, it counteracts the D_2R inhibition of adenylate cyclase activity. Toghether, D_1 reward seeking pathway dominates over aversion inputs coming from D2R neurons (Navarro, et al., 2013). The effect of cocaine binding to σ_1R on the CRF receptor-mediated signaling consists of a disruption of the orexin-A–CRF receptor negative crosstalk. We have proposed that this mechanism, which also requires a direct interaction of σ_1R and a GPCR, may explain how stress induces cocaine seeking (Navarro et al., 2015). Similarly, an interaction of σ_1R with dopamine D_1- histamine H_3 receptors heteromer, allows cocaine to block the histamine-mediated inhibition of dopaminergic output. Control by histamine of D_1 receptor-mediated signaling is broken in acute or self-administration paradigms and is restored by σ_1R antagonists (Moreno et al., 2014).

Kotagle and collaborators described that the potent orexigenic peptide neuropeptide Y (NPY) has been considered as a possible endogenous ligand for a subpopulation of sigma receptors (SigR) (Kotagale, et al., 2014), relating sigma receptors stimulation with hunger. Our results show that cocaine binding to σ_1R counteracts the feeling of hunger. Part of this effect could also be due to the competition between cocaine and NPY to interact σ_1R. The relevance of σ_1R-GHS-R1a interaction possibility becomes even more important by the finding that the heteromer expression is increased in both, acute and chronic conditions. However, it is more accused in acute conditions where striatum slicers of Sragues-Dawley rats injected for one day with cocaine, 15 mg/Kg, show three times more σ_1R-GHS-R1a heteromers than control animals.

Finally, a structural model of the interaction between σ_1R and a GPCR is presented which consists of a GHS-R1a homodimer, the heterotrimeric Gi protein and a σ_1R homotrimer. The model is compatible with the identified TM interfaces between the TM helix of one σ_1R and TM1/2 helices of GHS-R1a as well as between the cystoplasmic domain of a second σ_1R and Gi, and may explain the variety of effects due to σ_1R *activation* by specific agonists or cocaine by direct modulation of the G_i protein. The complex requires the existence of either GHS-R1a homodimers or GHS-R1a-GHS-R1b heterodimers that interact through the TM5/6 interface. When σ_1R is activated, conformational changes occur that restrict opening of the AH domain of the Gα subunit that is required for GDP-GTP exchange. This interaction could be the mechanism by which σ_1R blocks GHS-R1a-mediated signaling. Our proposed minimal model implies the interaction of two σ_1R protomers with one GHS-R1 homo/hetero-dimer. Still, the σ_1R homotrimer has two free

sites that would allow binding of two additional GHS-R1 homo/hetero-dimers. This suggests the possibility of the existence of higher order complexes between ghrelin and σ_1R receptors by the successive combination of these units. Clusters specialized in ghrelin-mediated signaling could thus be formed.

MATERIALS AND METHODS

Reagents

Cocaine-chlorhydrate was provided by the Spanish *Agencia del Medicamento* (Ref nº: 2003C00220). σ_1R ligand, PRE-084, and GHs-R1a ligands, ghrelin and YIL-781, were purchased from Tocris, Bristol, UK.

Fusion proteins and expression vectors

Sequences encoding amino acid residues 1–155 and 155–238 of the Venus variant of yellow fluorescence protein (Venus) were subcloned in the pcDNA3.1 vector to obtain complementary Venus n- and c-hemiproteins. Human cDNAs for GHS-R1a, GHS-R1b, or σ_1R, were amplified without their stop codons using sense and antisense primers harboring: EcoRI and KpnI sites to be subcloned in pcDNA3.1RLuc vector (p*RLuc*-N1 PerkinElmer, Wellesley, MA) or in a GFP^2 containing vector (p-GFP^2, Packard BioScience, Meridien, CT) to provide σ_1R-Rluc, GHS-R1a-Rluc, GHS-R1a-YFP, σ_1R-YFP or GHS-R1a-GFP^2 plasmids. Human cDNA for $A_{2A}R$ was subcloned into p-GFP^2 vector harboring HindIII and BamHI sites to provide the encoding A_{2A}-GFP^2 plasmid. For bimolecular fluorescence complementation (BiFC) experiments, cDNA for GHS-R1b, GHS-R1a and σ_1R were subcloned into pcDNA3.1-nVenus and pcDNA3.1-cVenus harboring EcoRI and KpnI sites to provide plasmids encoding GHS-R1b-nYFP, GHS-R1b-cYFP, GHS-R1a-nYFP and σ_1R-cYFP.

Cell lines, neuronal primary cultures and transient transfection

HEK-293T human embryonic kidney cells were grown in Dulbecco's modified Eagle's medium (DMEM) (Gibco) supplemented with 2 mM L-glutamine, 100 µg/ml sodium pyruvate, 100 U/ml penicillin/streptomycin, MEM Non-Essential Amino Acid Solution (1/100) and 5% (v/v) heat inactivated Fetal Bovine Serum (FBS) (all supplements were from Invitrogen, Paisley, Scotland, UK). Primary cultures of striatal neurons were obtained from fetal Sprague Dawley rats of 19 days. Cells were isolated as described in Hradsky et al. (2013) and plated at a confluence of 40,000 cells/0.32 cm^2. Cells were maintained for 12 days in Neurobasal medium supplemented with 2 mM L-glutamine, 100 U/ml penicillin/ streptomycin, and 2% (v/v) B27 supplement (GIBCO) in 6-well microplates. Cells were transiently transfected with the corresponding cDNAs using the PEI (PolyEthylenImine, SigmaAldrich, St. Louis, MO, USA) method or, in the case of the anti-σ_1R siRNA, with lipofectamine 2000 (Thermo Fisher Scientific). After transfection cells were incubated in serum-free medium that after 4 h was replaced by complete medium. Experiments were carried out 48 h later (unless otherwise indicated).

Immunocytochemistry

HEK-293T cells were fixed in 4% paraformaldehyde for 15 min and washed with PBS containing 20 mM glycine to quench free aldehyde groups. After permeabilization with PBS-glycine buffer containing 0.2% Triton X-100 for 5 min, cells were blocked with PBS containing 1% bovine serum albumin (1 h at room temperature). σ_1R-YFP was detected by its own fluorescence (wavelength 530 nm), and Rluc-containing proteins were stained using a mouse monoclonal anti-Rluc antibody (1/200, 1 h, room temperature, Millipore, CA, USA) and a Cyn3-conjugated donkey anti-mouse antibody (1/200, Jackson Immunoresearch Laboratories, West Grove, PA, USA). Nuclei were stained with Hoechst (1/100, SigmaAldrich, St. Louis, USA) and samples were mounted with Mowiol 30% (Calbiochem) and observed in a Leica SP2 confocal microscope (Leica Microsystems, Mannheim, Germany).

Resonance energy transfer

For Bioluminescence energy transfer (BRET) assays, HEK-293T cells were transiently transfected with a constant amount of cDNA for σ_1R-Rluc and increasing amounts of cDNAs for GHS-R1a-GFP[2] or A_{2A}-GFP[2]. To normalize the number of cells, protein concentration was determined using a Bradford assay kit (Bio-Rad, Munich, Germany) using bovine serum albumin dilutions as standards. To quantify fluorescence, cell suspensions were distributed in 96-well microplates (black with transparent bottom) and fluorescence was read in a Fluostar Optima Fluorimeter (BMG Labtech, Offenburg, Germany) equipped with a high-energy xenon flash lamp, using a 10 nm bandwidth excitation filter (400 nm). For BRET measurements, cell suspensions (20 µg protein) were distributed in 96-well white microplates (Corning 3600, Corning, NY), and 5 µM DeepBlueC (Molecular Probes, Eugene, OR) was added right before BRET signal acquisition using a Mithras LB 940 reader (Berthold Technologies, DLReady, Germany). To quantify receptor-Rluc expression, luminescence readings were performed after 10 minutes of adding 5 µM coelenterazine H. Net BRET is defined as [(long-wavelength emission)/(short-wavelength emission)]-C_f, where C_f corresponds to [(long-wavelength emission)/(short-wavelength emission)] for the Rluc protein when expressed individually. For bimolecular complementation (BiFC) assays, HEK-293T cells were transiently transfected with a constant amount of cDNA encoding for proteins fused to nVenus or cVenus and incubated for 4 h in complete DMEM containing the interfering TAT peptides (with similar sequences to those in TM1 to TM7 of GHS-R1a; see Table 1 for sequences). YFP resulting from complementation was detected by placing cells (20 µg protein) in 96-well microplates (black plates with a transparent bottom) and reading the fluorescence in a Fluostar Optima Fluorimeter (BMG Labtech, Offenburg, Germany) using a 30 nm bandwidth excitation filter (485 nm).

Cytosolic cAMP determination

Forskolin dose-response curves in different density of cells were performed to select the most appropriate conditions of the assay, which resulted in 5,000 HEK-293T cells, 7,500 neurons and 0.5 µM forskolin. Subsequently, assays were performed in medium containing 50 µM zardeverine, placing cells in 384-well microplates. Then, was done the preincubation with reagents (the σ_1R agonist, PRE-084, the GHS-R1a antagonist, YIL-781, or cocaine) for 15 min followed by Ghrelin addition (100 nM final concentration)

and, after 15 min incubation period 50 μM forskolin was added. Readings were performed 15 min later using a homogeneous time-resolved fluorescence energy transfer (HTRF) method requiring the Lance Ultra cAMP kit (PerkinElmer) and fluorescence readings (at 665 nm) in a PHERAstar Flagship microplate reader equipped with an HTRF optical module (BMG Labtech).

MAPK activation

To determine ERK1/2 phosphorylation, 40,000 HEK-293T cells/well or 50,000 neurons/well were plated in transparent Deltalab 96-well microplates and kept in the incubator for 48 h. The medium was substituted by serum-free DMEM medium 2 to 4 h before starting the experiment. Before addition of 100 nM ghrelin cells were pre-treated (10 min at 25°C) in serum-free medium with different reagents (the σ_1R agonist, PRE-084, the GHS-R1a antagonist, YIL-781, or cocaine). After 7 min of ghrelin-induced activation, cells were washed twice with cold PBS before the addition of 30 μL of Lysis Buffer (20 min). Supernatants (10 μL) were placed in white ProxiPlate 384-well microplates, and ERK1/2 phosphorylation was determined using the AlphaScreen®SureFire® kit (Perkin Elmer) and the EnSpire® Multimode Plate Reader (PerkinElmer, Waltham, MA, USA).

Intracellular calcium mobilization

HEK-293T cells were co-transfected with cDNA(s) for receptor(s) and 1 μg cDNA for the calmodulin-based calcium sensor, GCaMP6 (Chen et al., 2013). 48 h after transfection cells were detached using Mg^{+2}-free Locke's buffer pH 7.4 (154 mM NaCl, 5.6 mM KCl, 3.6 mM $NaHCO_3$, 2.3 mM $CaCl_2$, 5.6 mM glucose and 5 mM HEPES) supplemented with 10 μM glycine. 150,000 cells/well were plated in 96-well black, clear bottom, microtiter plates. Then, cells were incubated with the σ_1R agonist, PRE-084, the GHS-R1a antagonist, YIL-781, or cocaine for 10 min before ghrelin 100 nM addition. Upon excitation at 488 nm, real-time 515 nm fluorescence emission due to calcium-ion-complexed GCaMP6 was recorded at on the EnSpire® Multimode Plate Reader (every 5 s, 100 flashes per well).

Label-free dynamic Mass Redistribution assays (DMR)

HEK-293T cells and neuronal primary cultures were seeded in 384-well sensor microplates to obtain 70-80% confluent monolayers constituted by 10,000 HEK-293T cells or 14,000 neurons per well. Previous to the assay, cells were washed twice with assay buffer (HBSS with 20 mM HEPES and 0.1% DMSO, pH 7.15) and incubated for 2 h in 40 μL/well of assay-buffer in the reader at 24°C. Hereafter, the sensor plate was scanned and a baseline optical signature was recorded before adding 10 μL of cocaine (30 μM), PRE-084 (100 nM) or YIL-781 (2 μM) for 30min followed by ghrelin addition. All compounds dissolved in assay buffer. Then, DMR responses were monitored for at least 3600 s using an EnSpire® Multimode Plate Reader (PerkinElmer, Waltham, MA, USA). Sensitive measurements of changes in local optical density mimicking cellular mass movements induced upon receptor activation were detected using EnSpire Workstation Software v 4.10.

Proximity Ligation Assay

For Proximity Ligation assays (PLA), primary cultures of striatal neurons were fixed in 4% paraformaldehyde for 30 min and permeabilized in PBS containing 0.05% Triton X-100 (15 min). After 1 h incubation at 37°C with the blocking solution, primary cultures were incubated overnight with anti-σ_1R (1/100, Santa Cruz Biotechnology, Dallas, US), and anti-GHS-R1a antibody (1/100, AbCam, Cambridge, UK) in the presence of Hoechst (1/100, SigmaAldrich, St. Louis, USA) to stain nuclei. Cells were processed using the PLA probes that bind to the primary antibodies (Duolink II PLA probe anti-Mouse plus and Duolink II PLA probe anti-Goat minus) and heteroreceptor complex formation was detected using the Duolink II *in situ* PLA detection Kit (OLink; Bioscience, Uppsala, Sweden). Images were taken in a Leica SP2 confocal microscope (Leica Microsystems, Mannheim, Germany). For each field of view a stack of two channels (one per staining) and 4 to 6 Z stacks with a step size of 1 µm were acquired. Quantification of the number of cells containing one or more red dots versus total cells (blue nuclei) and of the number of red dots/ cell-containing dots: r ratio, was conducted using a dedicated software known as Duolink ImageTool (ref: DUO90806, Sigma-Olink). This software has been developed for PLA signals and cell nuclei quantification in images generated from fluorescence microscopy.

Cocaine treatment and fixed procedure

Male Sprague-Dawley rats weighing 200-220 g were selected for the experiments. Rats were kept in controlled environment with 12 h light-dark cycle at 21 ºC room temperature. Food and water were provided *ad libitum*. All experimental procedures were approved by the Ethics Committee of Faculty of Biological Sciences of "Pontificia Universidad Católica de Chile" and follow the international guidelines (NIH Guide for the Care and Use of Laboratory Animals). Rats keep housing and handling in colony for three days, and then were divided in two groups of experimental series, chronic cocaine-treated rats with respective control (saline) and acute cocaine rats. The chronic cocaine-treated rats administration protocol consisted of 15 mg/Kg, i.p. cocaine injections twice per day for 14 days as described by (Liu, et al., 2005), the acute cocaine-treated rats consist in one injection of 15 mg/kg, i.p. cocaine in the morning and afternoon. Daily administration of cocaine and saline solution was performed in both experimental series at the same time in the morning and afternoon (beginning at 11:00 A.M. and 5:00 P.M.).

Computational model of the GHS-R1a-σ_1R heteromer

σ_1R was modeled based on the recent crystal structure (PDB id 5HK1) (Schmidt, et al., 2016) using Modeller 9.12. The inactive form of the human GHS-R1a [UniProt: Q92847] was modelled based on the crystal structures of the neurotensin 1 receptor (PDB id 3ZEV; C-terminal part of the TM7 and the helix 8) (Egloff, et al., 2014), and (PDB id 4XES; other regions) (Krumm, et al., 2015). The human neurotensin 1 receptor which has 33% of sequence identity and 51% of sequence similarity with the human GHS-R1a. The active form of GHS-R1a was modelled by incorporating the active features present in the crystal structure of the β_2-adrenergic receptor (PDB id 3SN6) (Rasmussen, et al., 2011). The globular α-helical domain of the α-subunit was modeled in the "closed" conformation, using the crystal structure of AlF_4^-activated Gi (PDB id 1AGR) (Tesmer, et al., 1997). The GHS-R1a-σ_1R complex was constructed using protein-protein docking

with HADDOCK (van Zundert, et al., 2016), under the imposed experimental restrains that the TMs 1 and 2 of GHS-R1a contacts the single TM of σ_1R. The GHS-R1a homodimer was constructed based on the symmetric TM5/6 protein-protein interface observed in the crystal structure of the μOR (PDB id 4DKL) (Manglik, et al., 2012). The homotrimeric structure of σ_1R was modelled based on the recently relased structure (PDB id 5HK1) (Schmidt, et al 2016).

REFERENCES

Abizaid, A., and Horvath, T.L. (2008). Brain circuits regulating energy homeostasis. Regul. Pept. *149*, 3–10.

Abizaid, A., Liu, Z.-W., Andrews, Z.B., Shanabrough, M., Borok, E., Elsworth, J.D., Roth, R.H., Sleeman, M.W., Picciotto, M.R., Tschöp, M.H., et al. (2006). Ghrelin modulates the activity and synaptic input organization of midbrain dopamine neurons while promoting appetite. J. Clin. Invest. *116*, 3229–3239.

Barr, J.L., Deliu, E., Brailoiu, G.C., Zhao, P., Yan, G., Abood, M.E., Unterwald, E.M., and Brailoiu, E. (2015). Mechanisms of activation of nucleus accumbens neurons by cocaine via sigma-1 receptor-inositol 1,4,5-trisphosphate-transient receptor potential canonical channel pathways. Cell Calcium *58*, 196–207.

Borroto-Escuela, D.O., Van Craenenbroeck, K., Romero-Fernandez, W., Guidolin, D., Woods, A.S., Rivera, A., Haegeman, G., Agnati, L.F., Tarakanov, A.O., and Fuxe, K. (2011). Dopamine D2 and D4 receptor heteromerization and its allosteric receptor-receptor interactions. Biochem. Biophys. Res. Commun. *404*, 928–934.

Borroto-Escuela, D.O., Brito, I., Romero-Fernandez, W., Di Palma, M., Oflijan, J., Skieterska, K., Duchou, J., Van Craenenbroeck, K., Suárez-Boomgaard, D., Rivera, A., et al. (2014). The G protein-coupled receptor heterodimer network (GPCR-HetNet) and its hub components. Int J Mol Sci *15*, 8570–8590.

Borroto-Escuela, D.O., Narváez, M., Wydra, K., Pintsuk, J., Pinton, L., Jimenez-Beristain, A., Di Palma, M., Jastrzębska, J., Filip, M., and Fuxe, K. (2017). Cocaine self-administration specifically increases A2AR-D2R and D2R-sigma1R heteroreceptor complexes in the rat nucleus accumbens shell

Chow, K.B.S., Sun, J., Chu, K.M., Tai Cheung, W., Cheng, C.H.K., and Wise, H. (2012). The truncated ghrelin receptor polypeptide (GHS-R1b) is localized in the endoplasmic reticulum where it forms heterodimers with ghrelin receptors (GHS-R1a) to attenuate their cell surface expression. Mol. Cell. Endocrinol. *348*, 247–254.

Corbera, J., Vaño, D., Martínez, D., Vela, J.M., Zamanillo, D., Dordal, A., Andreu, F., Hernandez, E., Perez, R., Escriche, M., et al. (2006). A medicinal-chemistry-guided approach to selective and druglike sigma 1 ligands. ChemMedChem *1*, 140–154.

Cordomí, A., Caltabiano, G., and Pardo, L. (2012). Membrane Protein Simulations Using AMBER Force Field and Berger Lipid Parameters. J Chem Theory Comput *8*, 948–958.

Damian, M., Mary, S., Maingot, M., M'Kadmi, C., Gagne, D., Leyris, J.-P., Denoyelle, S., Gaibelet, G., Gavara, L., Garcia de Souza Costa, M., et al. (2015). Ghrelin receptor conformational dynamics regulate the transition from a preassembled to an active receptor: Gq complex. Proc. Natl. Acad. Sci. U.S.A. *112*, 1601–1606.

Cordomí, A., Navarro, G., Aymerich, M.S., and Franco, R. (2015). Structures for G-Protein-Coupled Receptor Tetramers in Complex with G Proteins. Trends Biochem. Sci. *40*, 548–551.

Egecioglu, E., Jerlhag, E., Salomé, N., Skibicka, K.P., Haage, D., Bohlooly-Y, M., Andersson, D., Bjursell, M., Perrissoud, D., Engel, J.A., et al. (2010). Ghrelin increases intake of rewarding food in rodents. Addict Biol *15*, 304–311.

Egloff, P., Hillenbrand, M., Klenk, C., Batyuk, A., Heine, P., Balada, S., Schlinkmann, K.M., Scott, D.J., Schütz, M., and Plückthun, A. (2014). Structure of signaling-competent neurotensin receptor 1 obtained by directed evolution in Escherichia coli. Proc. Natl. Acad. Sci. U.S.A. *111*, E655-662.

Engel, J.A., Nylander, I., and Jerlhag, E. (2015). A ghrelin receptor (GHS-R1A) antagonist attenuates the rewarding properties of morphine and increases opioid peptide levels in reward areas in mice. Eur Neuropsychopharmacol *25*, 2364–2371.

Fuxe, K., Tarakanov, A., Romero Fernandez, W., Ferraro, L., Tanganelli, S., Filip, M., Agnati, L.F., Garriga, P., Diaz-Cabiale, Z., and Borroto-Escuela, D.O. (2014). Diversity and Bias through Receptor-Receptor Interactions in GPCR Heteroreceptor Complexes. Focus on Examples from Dopamine D2 Receptor Heteromerization. Front Endocrinol (Lausanne) *5*, 71.

Guitart, X., Navarro, G., Moreno, E., Yano, H., Cai, N.-S., Sánchez-Soto, M., Kumar-Barodia, S., Naidu, Y.T., Mallol, J., Cortés, A., et al. (2014). Functional selectivity of allosteric interactions within G protein-coupled receptor oligomers: the dopamine D1-D3 receptor heterotetramer. Mol. Pharmacol. *86*, 417–429.

Hayashi, T., and Su, T.-P. (2007). Sigma-1 receptor chaperones at the ER-mitochondrion interface regulate Ca (2+) signaling and cell survival. Cell *131*, 596–610.

Herbert, T. E., Moffett, S., Morello, J.-P., Loisel, T. P., Bichet, D. G., Barret, C. and Bouvier, M. (1996). A peptide derived from a β2-adrenergic receptor transmembrane domain inhibits both receptor dimerization and activation.

Jerlhag, E., Egecioglu, E., Dickson, S.L., Andersson, M., Svensson, L., and Engel, J.A. (2006). Ghrelin stimulates locomotor activity and accumbal dopamine-overflow via central cholinergic systems in mice: implications for its involvement in brain reward. Addict Biol *11*, 45–54.

Joffe, M.E., Grueter, C.A., and Grueter, B.A. (2014). Biological substrates of addiction. Wiley Interdiscip Rev Cogn Sci *5*, 151–171.

Kim, F.J., Kovalyshyn, I., Burgman, M., Neilan, C., Chien, C.-C., and Pasternak, G.W. (2010). Sigma 1 receptor modulation of G-protein-coupled receptor signaling: potentiation of opioid transduction independent from receptor binding. Mol. Pharmacol. *77*, 695–703.

Kim, H.F., and Hikosaka, O. (2015). Parallel basal ganglia circuits for voluntary and automatic behaviour to reach rewards. Brain *138*, 1776–1800.

Kotagale, N.R., Upadhya, M., Hadole, P.N., Kokare, D.M., and Taksande, B.G. (2014). Involvement of hypothalamic neuropeptide Y in pentazocine induced suppression of food intake in rats. Neuropeptides *48*, 133–141.

Krumm, B.E., White, J.F., Shah, P., and Grisshammer, R. (2015). Structural prerequisites for G-protein activation by the neurotensin receptor. Nat Commun *6*, 7895.

Kruse, A. (2016). Structural Insights into Sigma1 Function. Handb Exp Pharmacol.

Lever, J.R., Fergason-Cantrell, E.A., Watkinson, L.D., Carmack, T.L., Lord, S.A., Xu, R., Miller, D.K., and Lever, S.Z. (2016). Cocaine occupancy of sigma1 receptors and dopamine transporters in mice. Synapse *70*, 98–111.

Liu, J., Yu, B., Orozco-Cabal, L., Grigoriadis, D.E., Rivier, J., Vale, W.W., Shinnick-Gallagher, P., and Gallagher, J.P. (2005). Chronic cocaine administration switches corticotropin-releasing factor2 receptor-mediated depression to facilitation of glutamatergic transmission in the lateral septum. J. Neurosci. *25*, 577–583.

Manglik, A., Kruse, A.C., Kobilka, T.S., Thian, F.S., Mathiesen, J.M., Sunahara, R.K., Pardo, L., Weis, W.I., Kobilka, B.K., and Granier, S. (2012). Crystal structure of the μ-opioid receptor bound to a morphinan antagonist. Nature *485*, 321–326.

Mary, S., Fehrentz, J.-A., Damian, M., Gaibelet, G., Orcel, H., Verdié, P., Mouillac, B., Martinez, J., Marie, J., and Banères, J.-L. (2013). Heterodimerization with Its splice variant blocks the ghrelin receptor 1a in a non-signaling conformation: a study with a purified heterodimer assembled into lipid discs. J. Biol. Chem. *288*, 24656–24665.

Matsumoto, R.R., Hewett, K.L., Pouw, B., Bowen, W.D., Husbands, S.M., Cao, J.J., and Newman, A.H. (2001). Rimcazole analogs attenuate the convulsive effects of cocaine: correlation with binding to sigma receptors rather than dopamine transporters. Neuropharmacology *41*, 878–886.

Matsumoto, R.R., McCracken, K.A., Pouw, B., Zhang, Y., and Bowen, W.D. (2002). Involvement of sigma receptors in the behavioral effects of cocaine: evidence from novel ligands and antisense oligodeoxynucleotides. Neuropharmacology *42*, 1043–1055.

Matsumoto, R.R., Liu, Y., Lerner, M., Howard, E.W., and Brackett, D.J. (2003). Sigma receptors: potential medications development target for anti-cocaine agents. Eur. J. Pharmacol. *469*, 1–12.

Matsumoto, R.R., Gilmore, D.L., Pouw, B., Bowen, W.D., Williams, W., Kausar, A., and Coop, A. (2004). Novel analogs of the sigma receptor ligand BD1008 attenuate cocaine-induced toxicity in mice. Eur. J. Pharmacol. *492*, 21–26.

Maurice, T., and Romieu, P. (2004). Involvement of the sigma1 receptor in the appetitive effects of cocaine. Pharmacopsychiatry *37 Suppl 3*, S198-207.

McCracken, K.A., Bowen, W.D., and Matsumoto, R.R. (1999). Novel sigma receptor ligands attenuate the locomotor stimulatory effects of cocaine. Eur. J. Pharmacol. *365*, 35–38.

Mei, J., and Pasternak, G.W. (2002). Sigma1 receptor modulation of opioid analgesia in the mouse. J. Pharmacol. Exp. Ther. *300*, 1070–1074.

Menkel, M., Terry, P., Pontecorvo, M., Katz, J.L., and Witkin, J.M. (1991). Selective sigma ligands block stimulant effects of cocaine. Eur. J. Pharmacol. *201*, 251–252.

Moreno, E., Moreno-Delgado, D., Navarro, G., Hoffmann, H.M., Fuentes, S., Rosell-Vilar, S., Gasperini, P., Rodríguez-Ruiz, M., Medrano, M., Mallol, J., et al. (2014). Cocaine disrupts histamine H3 receptor modulation of dopamine D1 receptor signaling: σ1-D1-H3 receptor complexes as key targets for reducing cocaine's effects. J. Neurosci. *34*, 3545–3558.

Navarro, G., Moreno, E., Aymerich, M., Marcellino, D., McCormick, P.J., Mallol, J., Cortés, A., Casadó, V., Canela, E.I., Ortiz, J., et al. (2010). Direct involvement of sigma-1 receptors in the dopamine D1 receptor-mediated effects of cocaine. Proc. Natl. Acad. Sci. U.S.A. *107*, 18676–18681.

Navarro, G., Moreno, E., Bonaventura, J., Brugarolas, M., Farré, D., Aguinaga, D., Mallol, J., Cortés, A., Casadó, V., Lluís, C., et al. (2013). Cocaine inhibits dopamine D2 receptor signaling via sigma-1-D2 receptor heteromers. PLoS ONE *8*, e61245.

Navarro, G., Quiroz, C., Moreno-Delgado, D., Sierakowiak, A., McDowell, K., Moreno, E., Rea, W., Cai, N.-S., Aguinaga, D., Howell, L.A., et al. (2015). Orexin-corticotropin-releasing factor receptor heteromers in the ventral tegmental area as targets for cocaine. J. Neurosci. *35*, 6639–6653.

Navarro, G., Aguinaga, D., Angelats, E., Medrano, M., Moreno, E., Mallol, J., Cortés, A., Canela, E.I., Casadó, V., McCormick, P.J., et al. (2016). A Significant Role of the Truncated Ghrelin Receptor GHS-R1b in Ghrelin-induced Signaling in Neurons. J. Biol. Chem. *291*, 13048–13062.

Ng, G.Y., O'Dowd, B.F., Lee, S.P., Chung, H.T., Brann, M.R., Seeman, P., and George, S.R. (1996). Dopamine D2 receptor dimers and receptor-blocking peptides. Biochem. Biophys. Res. Commun. *227*, 200–204.

Perello, M., Sakata, I., Birnbaum, S., Chuang, J.-C., Osborne-Lawrence, S., Rovinsky, S.A., Woloszyn, J., Yanagisawa, M., Lutter, M., and Zigman, J.M. (2010). Ghrelin increases the rewarding value of high-fat diet in an orexin-dependent manner. Biol. Psychiatry *67*, 880–886.

Pronk, S., Páll, S., Schulz, R., Larsson, P., Bjelkmar, P., Apostolov, R., Shirts, M.R., Smith, J.C., Kasson, P.M., van der Spoel, D., et al. (2013). GROMACS 4.5: a high-throughput and highly parallel open source molecular simulation toolkit. Bioinformatics *29*, 845–854.

Rasmussen, S.G.F., DeVree, B.T., Zou, Y., Kruse, A.C., Chung, K.Y., Kobilka, T.S., Thian, F.S., Chae, P.S., Pardon, E., Calinski, D., et al. (2011). Crystal structure of the β2 adrenergic receptor-Gs protein complex. Nature *477*, 549–555.

Richardson, N.R., and Gratton, A. (1998). Changes in medial prefrontal cortical dopamine levels associated with response-contingent food reward: an electrochemical study in rat. J. Neurosci. *18*, 9130–9138.

Rodríguez-Muñoz, M., Sánchez-Blázquez, P., Herrero-Labrador, R., Martínez-Murillo, R., Merlos, M., Vela, J.M., and Garzón, J. (2015). The σ1 receptor engages the redox-regulated HINT1 protein to bring opioid analgesia under NMDA receptor negative control. Antioxid. Redox Signal. *22*, 799–818.

Romieu, P., Martin-Fardon, R., and Maurice, T. (2000). Involvement of the sigma1 receptor in the cocaine-induced conditioned place preference. Neuroreport *11*, 2885–2888.

Romieu, P., Phan, V.L., Martin-Fardon, R., and Maurice, T. (2002). Involvement of the sigma (1) receptor in cocaine-induced conditioned place preference: possible dependence on dopamine uptake blockade. Neuropsychopharmacology *26*, 444–455.

Sánchez-Blázquez, P., Rodríguez-Muñoz, M., Herrero-Labrador, R., Burgueño, J., Zamanillo, D., and Garzón, J. (2014). The calcium-sensitive Sigma-1 receptor prevents cannabinoids from provoking glutamate NMDA receptor hypofunction: implications in antinociception and psychotic diseases. Int. J. Neuropsychopharmacol. *17*, 1943–1955.

Schmidt, H.R., Zheng, S., Gurpinar, E., Koehl, A., Manglik, A., and Kruse, A.C. (2016). Crystal structure of the human σ1 receptor. Nature *532*, 527–530.

Skibicka, K.P., Hansson, C., Alvarez-Crespo, M., Friberg, P.A., and Dickson, S.L. (2011). Ghrelin directly targets the ventral tegmental area to increase food motivation. Neuroscience *180*, 129–137.

Skuza, G. (1999). Effect of sigma ligands on the cocaine-induced convulsions in mice. Pol J Pharmacol *51*, 477–483.

Su, T.-P., Hayashi, T., Maurice, T., Buch, S., and Ruoho, A.E. (2010). The sigma-1 receptor chaperone as an inter-organelle signaling modulator. Trends Pharmacol. Sci. *31*, 557–566.

Su, T.-P., Su, T.-C., Nakamura, Y., and Tsai, S.-Y. (2016). The Sigma-1 Receptor as a Pluripotent Modulator in Living Systems. Trends Pharmacol. Sci. *37*, 262–278.

Sun, H., Shi, M., Zhang, W., Zheng, Y.-M., Xu, Y.-Z., Shi, J.-J., Liu, T., Gunosewoyo, H., Pang, T., Gao, Z.-B., et al. (2016). Development of Novel Alkoxyisoxazoles as Sigma-1 Receptor Antagonists with Antinociceptive Efficacy. J. Med. Chem. *59*, 6329–6343.

Tesmer, J.J., Berman, D.M., Gilman, A.G., and Sprang, S.R. (1997). Structure of RGS4 bound to AlF4--activated G(i alpha1): stabilization of the transition state for GTP hydrolysis. Cell *89*, 251–261.

Trifilieff, P., Rives, M.-L., Urizar, E., Piskorowski, R.A., Vishwasrao, H.D., Castrillon, J., Schmauss, C., Slättman, M., Gullberg, M., and Javitch, J.A. (2011). Detection of antigen interactions ex vivo by proximity ligation assay: endogenous dopamine D2-adenosine A2A receptor complexes in the striatum. BioTechniques *51*, 111–118.

Ujike, H., Kuroda, S., and Otsuki, S. (1996). sigma Receptor antagonists block the development of sensitization to cocaine. Eur. J. Pharmacol. *296*, 123–128.

van Zundert, G.C.P., Rodrigues, J.P.G.L.M., Trellet, M., Schmitz, C., Kastritis, P.L., Karaca, E., Melquiond, A.S.J., van Dijk, M., de Vries, S.J., and Bonvin, A.M.J.J. (2016). The HADDOCK2.2 Web Server: User-Friendly Integrative Modeling of Biomolecular Complexes. J. Mol. Biol. *428*, 720–725.

Wu, Z., and Bowen, W.D. (2008). Role of sigma-1 receptor C-terminal segment in inositol 1,4,5-trisphosphate receptor activation: constitutive enhancement of calcium signaling in MCF-7 tumor cells. J. Biol. Chem. *283*, 28198–28215.

Zhang, Y., Lv, X., Bai, Y., Zhu, X., Wu, X., Chao, J., Duan, M., Buch, S., Chen, L., and Yao, H. (2015). Involvement of sigma-1 receptor in astrocyte activation induced by methamphetamine via up-regulation of its own expression. J Neuroinflammation *12*, 29.

Zigman, J.M., Jones, J.E., Lee, C.E., Saper, C.B., and Elmquist, J.K. (2006). Expression of ghrelin receptor mRNA in the rat and the mouse brain. J. Comp. Neurol. *494*, 528–548.

Table 1. Chemical structure of interfering peptides containing a sequence homologous to that of transmembrane domains (TM) of GHS-R1a and the TAT GRKKRRQRRR sequence of the human immunodeficiency virus in its correct orientation (as for the C-N in-out or out-in topology of each TM domain crossing the plasma membrane).

T**M1**
APLLAGVTATSVALFVVGIAGNLLTMLVV-GRKKRRQRRR
TM2
RRRQRRKKRG-LYLSSMAFSDLLIFLSMPLDLV
TM3
FQFVSESSTYATVLTITALSV-GRKKRRQRRR
TM4
RRRQRRKKRG-VKLVIFVIWAVAFSSAGPIFVL
TM5
LLTVMVWVSSIFFFLPVFSLTVLYSLI--GRKKRRQRRR
TM6
RRRQRRKKRG-MLAVVVFAFILCWLPFHVGRYLF
TM7
YCNLVSFVLFYLSAAINPILYNIM--GRKKRRQRRR

FIGURE LEGENDS

Figure 1

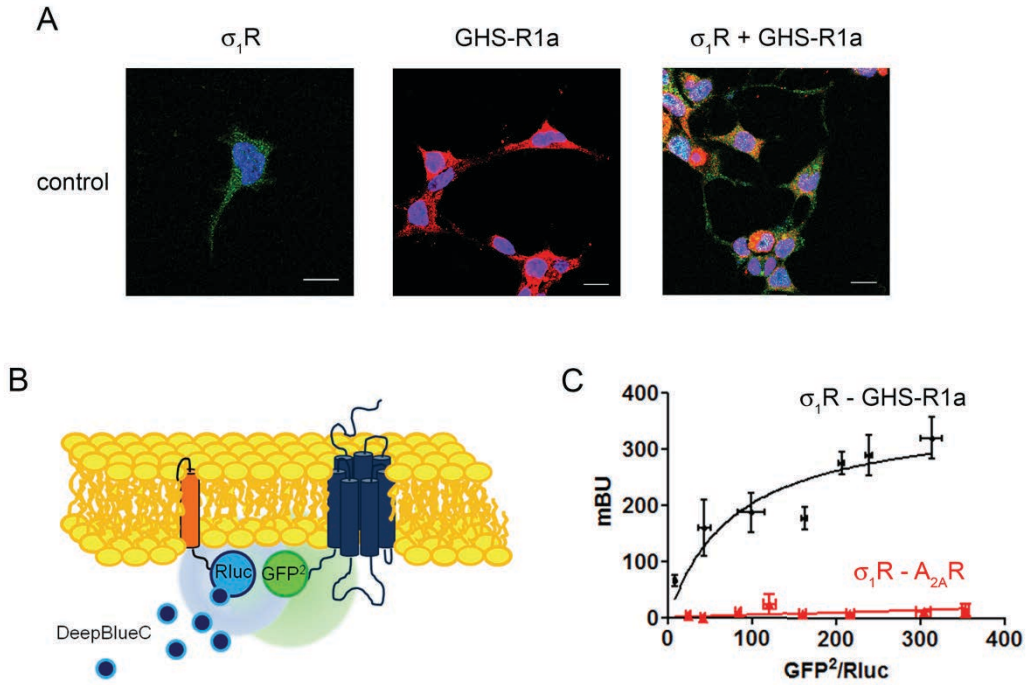

Figure 1. GHS-R1a interact with σ_1R forming σ_1R-GHS-R1a heteroreceptor complexes.

Panel A**:** HEK-293T cells expressing σ_1R-YFP, GHS-R1a-Rluc or both, were monitored by the YFP fluorescence (green) or using a monoclonal anti-Rluc primary antibody and a cyanine-3-conjugated secondary antibody (red). Colocalization is shown in yellow. Nuclei were stained with Hoechst (1/100, xxx) (blue). Scale bar 10 µm. Panel B: Scheme of BRET^2. Panel C: HEK-293T cells were transfected with a constant amount of cDNA (0.075 µg) for σ_1Rluc and increasing amounts of GHS-R1a-GFP^2 (from 0.5 µg to 3 µg cDNA) or A_{2A}R-GFP^2 (from 0.5 µg to 2.5 µg cDNA) as negative control. Values are the mean ± S.E.M. from 6 to 8 different experiments.

Figure 2

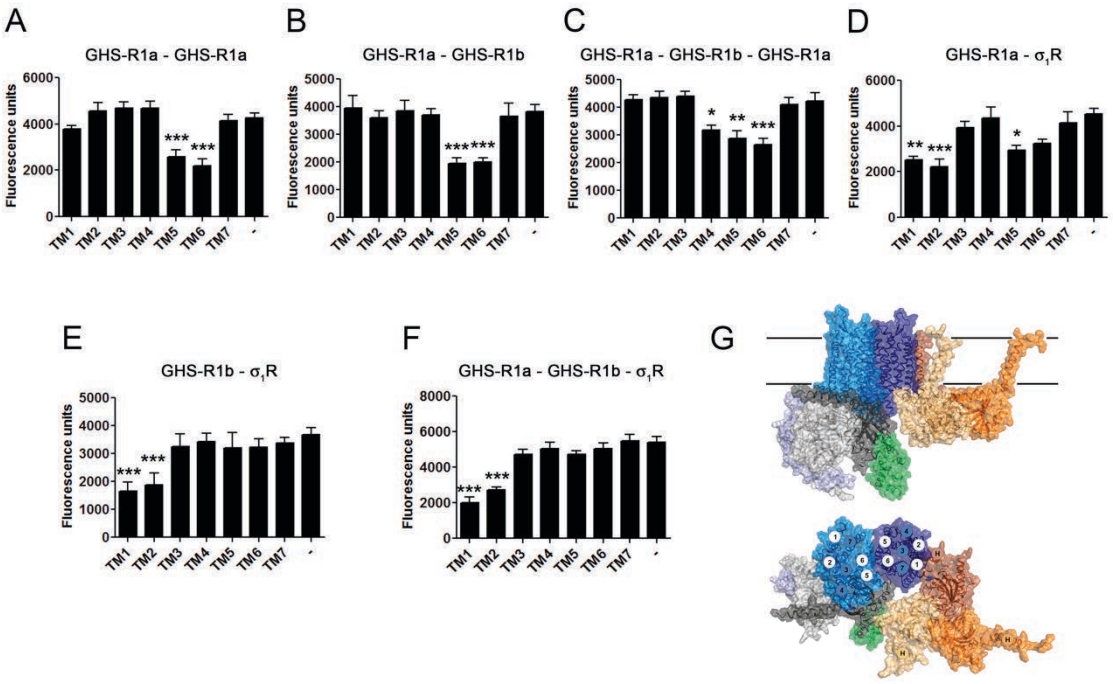

Figure 2. Effect of interfering peptides on the σ_1R-GHS-R1a interaction.

BiFC complementation experiments were performed in HEK-293T cells transfected with 0.75 µg cDNA for GHS-R1a-nYFP and 0.75 µg cDNA for GHS-R1a-cYFP (A), with 0.75 µg cDNA for GHS-R1a-nYFP and 0.75 µg cDNA for GHS-R1b-cYFP (B) with 0.75 µg cDNA for GHS-R1a-nYFP and 0.75 µg cDNA for GHS-R1b-cYFP in the presence of 1.5 µg cDNA for GHS-R1a-nYFP (C) with 0.75 µg cDNA for GHS-R1a-nYFP and 0.75 µg cDNA for σ_1R-cYFP (D), , with 0.5 µg cDNA for GHS-R1b-nYFP and 0.5 µg cDNA for σ_1R-cYFP (E) or with 0.75 µg cDNA for GHS-R1a-nYFP and 0.75 µg cDNA for GHS-R1b-cYFP (F) in the presence of 1.5 µg cDNA of GHS-R1a not fused. Prior to fluorescence determination, cells were treated with each of the interfering peptides (TM1 to TM7, 4 µM) during 4 h. Values are the mean ± S.E.M. from 8 to 10 different experiments. One-way ANOVA followed by Dunnett's *post-hoc* test showed a significant effect of treatments versus control conditions. *p<0.05, **p<0.01 and ***p<0.001. Panel E: Structural model consisting of a GHS-R1a homodimer (GHS-R1a G_α-bound: light blue, GHS-R1a G_α-unbound: dark blue) in complex with a σ_1R homotrimer (in red, orange and yellow) coupled to G_i (Gα Ras-like domain: light grey, Gα alpha helical domain: green, Gβ: dark grey and Gγ: purple) viewed from the extracellular side (top) or from the membrane (bottom). Proteins are displayed with a transparent surface and a cartoon. TM helices are indicated by circles (GHS-R1a: 1-7, σ_1R: H).

Figure 3

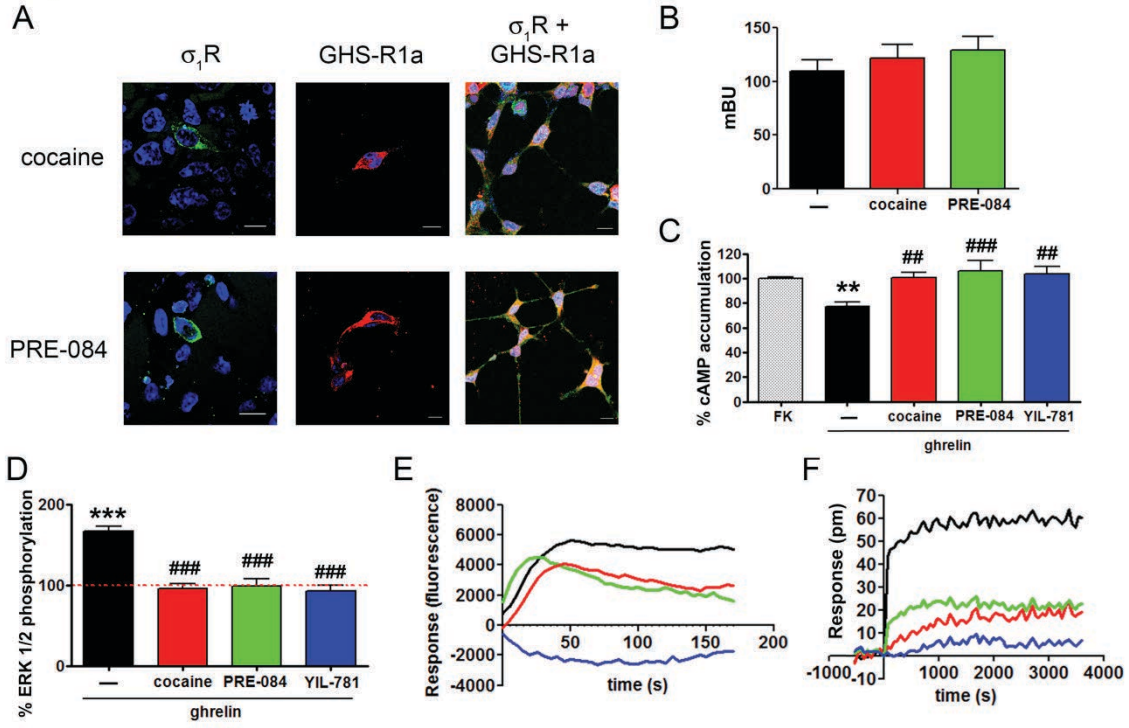

Figure 3. Cocaine effects on ghrelin-mediated signaling.

Panel A**:** HEK-293T cells transfected with 0.75 µg cDNA for σ_1R-YFP, 1.66 µg cDNA for GHS-R1a-Rluc or both were treated with 30 µM cocaine or 100 nM PRE-084, then were monitored by the YFP fluorescence (green) or using a monoclonal anti-Rluc primary antibody and a cyanine-3-conjugated secondary antibody (red). Colocalization is shown in yellow. Nuclei were stained with Hoechst (blue). Scale bar 10 µm. Panel B: HEK-293T cells were transfected with 0.075 µg cDNA for σ_1R-Rluc and 1.5 µg cDNA for GHS-R1a-GFP[2] and treated with 30 µM cocaine, 100 nM PRE-084 or vehicle for 30 min. Afterwards, the energy transfer signal was measured. Values are the mean ± S.E.M. of 7 different experiments. One-way ANOVA followed by Dunnett's *post-hoc* test did not show any significant effect of treatments versus control. Panels C-F: HEK-293T cells were transfected with 1.66 µg GHS-R1a cDNA and 0.25 µg GHS-R1b cDNA and treated with 30 µM of cocaine (red), 100 nM of the σ_1R agonist, PRE-084 (green), 2 µM of the GHS-R1a antagonist, YIL-781 (blue), or vehicle (black). Cells were then treated with ghrelin 100 nM followed by 0.5 µM forskolin only in cAMP accumulation assay (C). ERK1/2 phosphorylation (D) was analyzed using an AlphaScreen®SureFire® kit (Perkin Elmer). Fluorescence of the GCaMP6 sensor was used to monitor cytosolic calcium mobilization (E), and real-time label-free DMR tracings (F) representing the picometer-shifts of reflected light wavelength were recorded in an EnSpire® Multimode Plate Reader (PerkinElmer, Waltham, MA, USA). Values are the mean ± S.E.M. from 8 to 11 different experiments. One-way ANOVA followed by Dunnett's *post-hoc* test showed a significant effect of treatments versus forskolin (cAMP assays, C) or control (pERK1/2 assays, D), **p<0.01 and ***p<0.001, and a significant effect of treatments versus ghrelin, ##p<0.01 and ###p<0.001.

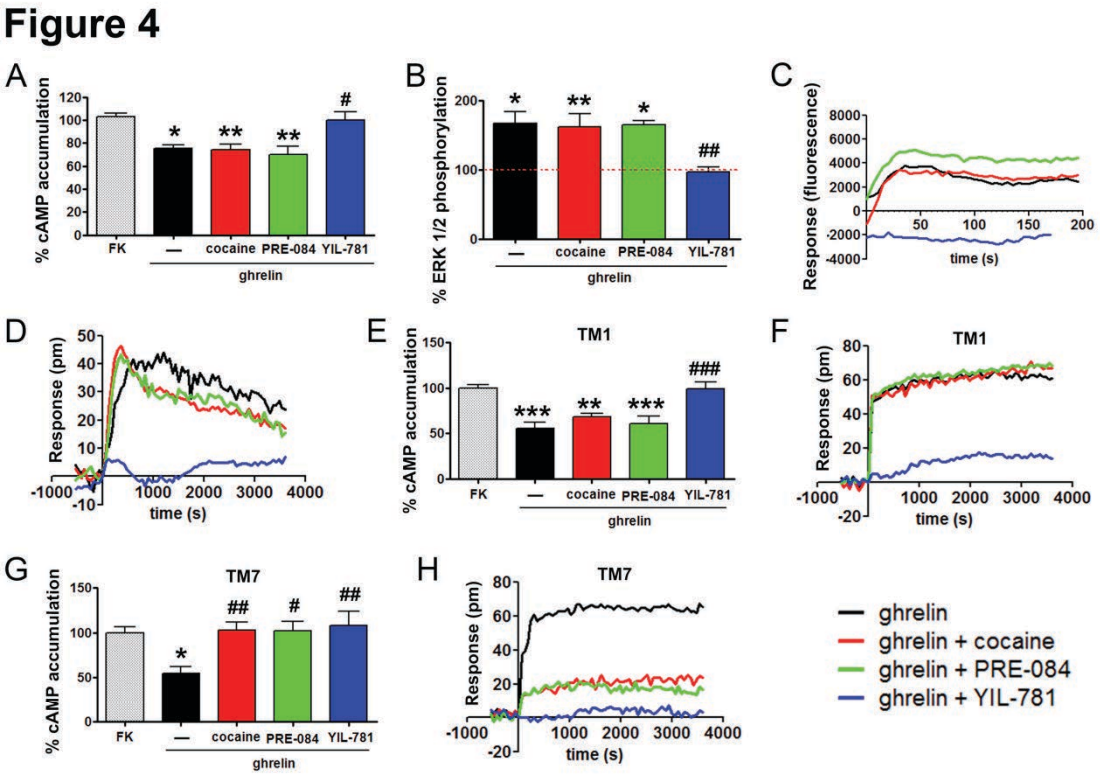

Figure 4. Cocaine effects over GHs-R1a signaling depended on σ_1R expression.

Panels A-D: HEK-293T cells were transfected with 1.66 µg GHS-R1a cDNA, 0.25 µg GHS-R1b cDNA and 3 µg siRNA for σ_1R. These cells were treated with 30 µM of cocaine (red), 100 nM of the σ_1R agonist, PRE-084 (green), 2µM of the GHS-R1a antagonist, YIL-781 (blue), or vehicle (black) followed by 100 nM of ghrelin stimulation and forskolin 0.5 µM in cAMP accumulation. Then, cAMP levels (A) pERK1/2 (B) calcium ion (C) and DMR (D) signals were recorded. Values are the mean ± S.E.M. from 8 to 11 different experiments. One-way ANOVA followed by Dunnett's *post-hoc* test showed a significant effect of treatments versus forskolin (cAMP assays, A) or control (pERK1/2 assays, B), *p<0.05, **p<0.01, and a significant effect of treatments versus ghrelin, #p<0.05, ##p<0.01. Panels E-F: HEK-293T cells expressing GHS-R1a (0.5 µg cDNA) were treated for 4h with TM1 (E, F) or TM7 (G, H) TAT-peptides. Cells were subsequently treated with 30 µM cocaine (red), 100 nM PRE-084 (green), 1 µM YIL-781 (blue) or vehicle (black). Cells were then treated with 100 nM ghrelin and 0.5 µM forskolin only in cAMP experiments and cAMP levels (E, G) were determined 15 min afterwards while in F and H, traces representing DMR signal variation over time are represented. Values are the mean ± S.E.M. of 6 different experiments. One-way ANOVA followed by Dunnett's *post-hoc* test showed a significant effect of treatments versus forskolin, *p<0.05, **p<0.01 and ***p<0.001, and a significant effect of treatments versus ghrelin, #p<0.05, ##p<0.01 and ###p<0.001.

Figure 5

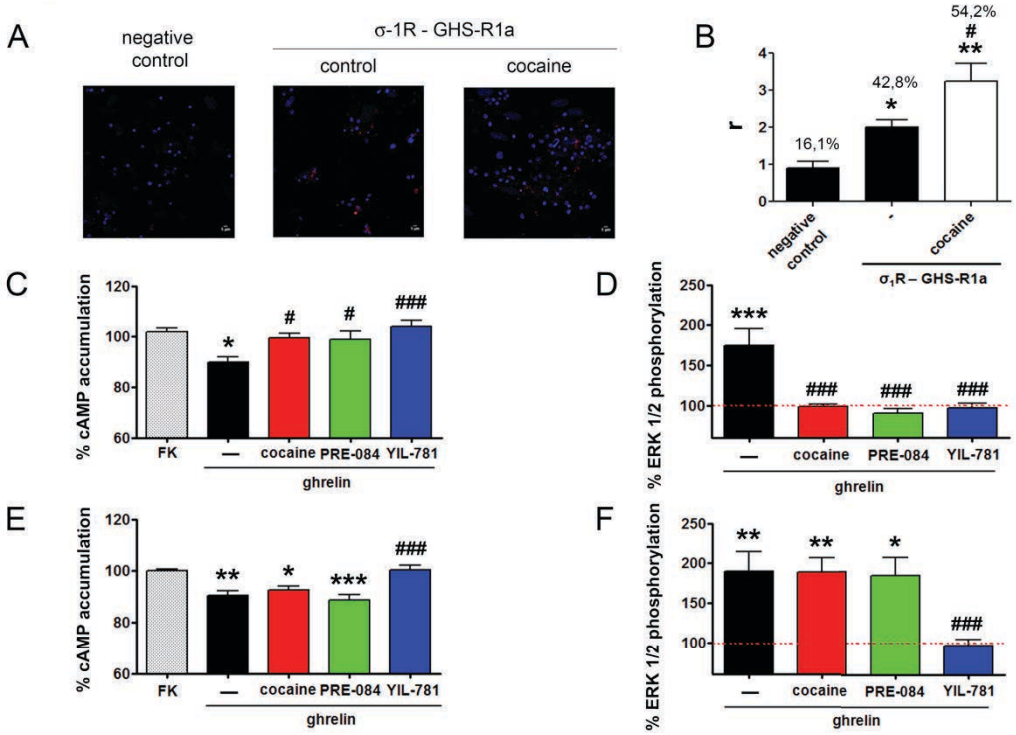

Figure 5. Cocaine treatment inhibited GHs-R1a signaling in striatal neurons primary cultures.

GHS-R1a-σ_1R heteromeric complexes were identified in striatal primary cultures treated with 30 µM cocaine, 100 nM PRE-084 or vehicle and detected by the use of a polyclonal anti-σ_1R primary antibody (1/100, Santa Cruz Biotechnology, Dallas, US) and a polyclonal anti-ghrelin primary antibody (1/100, AbCam, Cambridge, UK) in the presence of Hoesch (1/100, xxx) and then treated with the PLA probes (See Methods). Panel A: Representative PLA confocal images showing GHS-R1a-σ_1R complexes as red dots surrounding Hoechst-stained nuclei. Scale bar: 5 µm. Panel B: Percentage of positive cells (containing one or more red dots; from cells in 5-6 different fields), and number (r) of red dots/cell-containing dots in primary cultures of striatal neurons. One-way ANOVA followed by Dunnett's *post-hoc* test showed a significant effect of treatments versus the negative control, *p<0.05, **p<0.01, and a significant effect of treatments versus the untreated cells, #p<0.05. Panels C-F: neuronal striatal primary cultures transfected (E-F) or not (C-D) with 3 µg siRNA for σ_1R were treated with 30 µM cocaine (red) cocaine, 100 nM of the σ_1R agonist, PRE-084 (green), 2 µM of the GHS-R1a antagonist, YIL-781 (blue), or vehicle (black) previous to 100 nM ghrelin addition. cAMP accumulation was induced after forskolin 0.5 µM addition 15 after ghrelin stimulation (C, E). ERK1/2 phosphorylation (D, F) was analyzed using an AlphaScreen®SureFire® kit (Perkin Elmer). Values are ± S.E.M. from 6 to 8 different experiments. One-way ANOVA followed by Dunnett's *post-hoc* test showed a significant effect of treatments versus forskolin (cAMP assays, C, E) or control (pERK1/2 assays, D, F), *p<0.05, **p<0.01 and ***p<0.001, and a significant effect of treatments versus ghrelin, #p<0.05 and ###p<0.001.

Figure 6

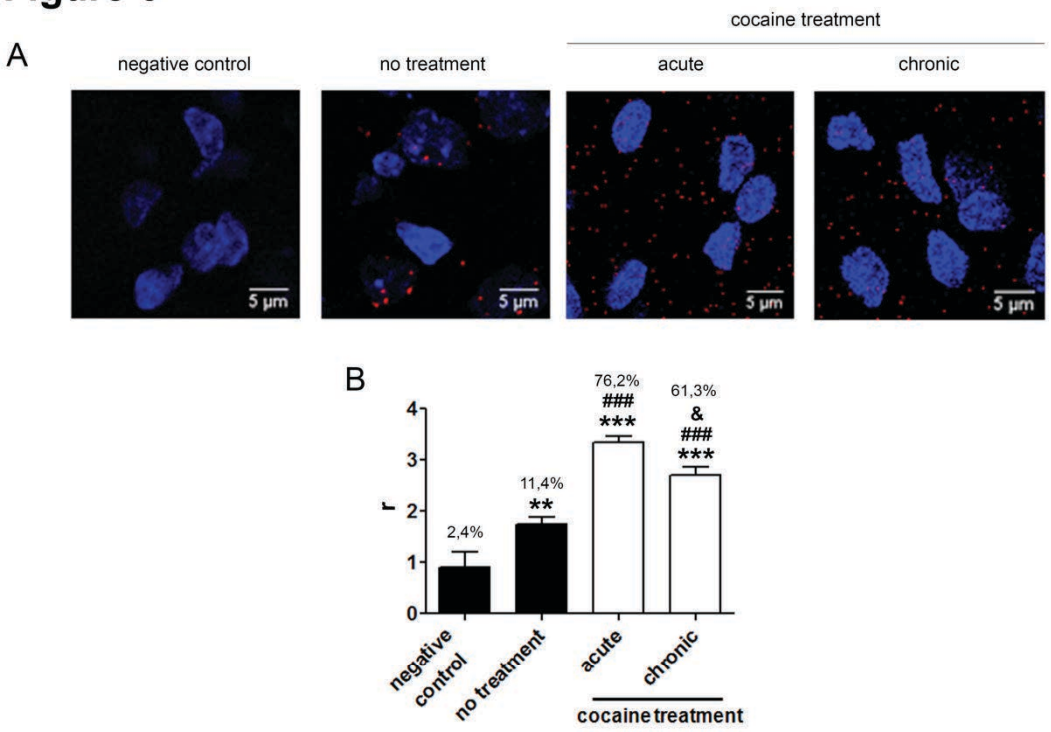

Figure 6. Acute and chronic cocaine treatments increase the GHS-R1a-σ_1R heteromers expression in Sprague Dawley rats.

Male Sprague Dawley rats were i.p. administrated with vehicle (control) or 15 mg/kg cocaine for 1 (acute) or 14 (chronic) days. To identify σ1-GHS-R1a complexes from each condition, rats were sacrificed and 30 µm-thick striatal sections were obtained and treated with a polyclonal anti-σ_1R primary antibody (1/100, Santa Cruz Biotechnology, Dallas, US) and a polyclonal anti-ghrelin primary antibody (1/100, AbCam, Cambridge, UK) in the presence of Hoesch (1/100, xxx) and then treated with the PLA probes (See Methods). Representative PLA confocal images showing GHS-R1a-σ_1R complexes as red dots surrounding Hoechst-stained nuclei are shown for each condition (Fig 6A). Scale bar: 5 µm. Panel B: percentage of positive cells (containing one or more red dots; from cells in 4-6 different fields), and number (r) of red dots/cell-containing dots in rat striatal slicers. One-way ANOVA followed by Dunnett's *post-hoc* test showed a significant effect of treatments versus the negative control, *p<0.05, **p<0.01, a significant effect of treatments versus the untreated cells, #p<0.05, and a significant effect of chronic treatment versus acute treated slicers, &p<0.05.

3.6. INTRACELLULAR CALCIUM LEVELS DETERMINE DIFFERENTIAL MODULATION OF ALLOSTERIC INTERACTIONS WITHIN G PROTEIN-COUPLED RECEPTOR HETEROMERS

Gemma Navarro, **David Aguinaga**, Estefanía Moreno, Johannes Hradsky, Pasham P. Reddy, Antoni Cortés, Josefa Mallol, Vicent Casadó, Marina Mikhaylova, Michel R. Kreutz, Carme Lluís, Enric I. Canela, Peter J. McCormick y Sergi Ferré.

Manuscrito publicado en *Chemistry & Biology*, noviembre 2014; 21:1546-1556.

La importancia farmacológica del heterómero entre los receptores de adenosina A_{2A} ($A_{2A}R$) y dopamina D_2 (D_2R) está bien establecida y es considerado como un objetivo importante para el tratamiento de la enfermedad de Parkinson y otros trastornos neuropsiquiátricos. Sin embargo, los factores fisiológicos que controlan sus propiedades bioquímicas características son todavía desconocidos. En este trabajo ha sido demostrado que diferentes niveles intracelulares de Ca^{2+} ejercen una modulación diferencial del heterómero A_{2A}-D_2 en la señalización mediada por la adenilato ciclasa y las MAPK en células estriatales. Esto depende de la capacidad de altos y bajos niveles de Ca^{2+} para promover una interacción selectiva del heterómero con las proteínas neuronales de unión a Ca^{2+}, NCS-1 y calneurona-1, respectivamente. Estas proteínas de unión a Ca^{2+} modulan de forma distinta interacciones alostéricas dentro del heterómero A_{2A}-D_2, constituyendo un dispositivo celular único que integra señales extracelulares (adenosina y dopamina) e intracelulares (Ca^{2+}) para producir una respuesta funcional específica.

CellPress

Chemistry & Biology
Article

Intracellular Calcium Levels Determine Differential Modulation of Allosteric Interactions within G Protein-Coupled Receptor Heteromers

Gemma Navarro,[1,*] David Aguinaga,[1] Estefania Moreno,[1] Johannes Hradsky,[2] Pasham P. Reddy,[2] Antoni Cortés,[1] Josefa Mallol,[1] Vicent Casadó,[1] Marina Mikhaylova,[2,3] Michael R. Kreutz,[2] Carme Lluís,[1] Enric I. Canela,[1,6] Peter J. McCormick,[1,4,6] and Sergi Ferré[5,6,*]

[1]Department of Biochemistry and Molecular Biology, Faculty of Biology, University of Barcelona, Centro de Investigación Biomédica en Red Sobre Enfermedades Neurodegenerativas and Institute of Biomedicine of the University of Barcelona (IBUB), Barcelona 08028, Spain
[2]Research Group Neuroplasticity, Leibniz-Institute for Neurobiology, Magdeburg 39118, Germany
[3]Cell Biology, Utrecht University, Utrecht 3584, the Netherlands
[4]School of Pharmacy, University of East Anglia, Norwich NR4 7TJ, UK
[5]Integrative Neurobiology Section, National Institute on Drug Abuse, Intramural Research Program, Department of Health and Human Services, National Institutes of Health, Baltimore, MD 21224, USA
[6]Co-senior author
*Correspondence: dimartts@hotmail.com (G.N.), sferre@intra.nida.nih.gov (S.F.)
http://dx.doi.org/10.1016/j.chembiol.2014.10.004

SUMMARY

The pharmacological significance of the adenosine A_{2A} receptor ($A_{2A}R$)-dopamine D_2 receptor (D_2R) heteromer is well established and it is being considered as an important target for the treatment of Parkinson's disease and other neuropsychiatric disorders. However, the physiological factors that control its distinctive biochemical properties are still unknown. We demonstrate that different intracellular Ca^{2+} levels exert a differential modulation of $A_{2A}R$-D_2R heteromer-mediated adenylyl-cyclase and MAPK signaling in striatal cells. This depends on the ability of low and high Ca^{2+} levels to promote a selective interaction of the heteromer with the neuronal Ca^{2+}-binding proteins NCS-1 and calneuron-1, respectively. These Ca^{2+}-binding proteins differentially modulate allosteric interactions within the $A_{2A}R$-D_2R heteromer, which constitutes a unique cellular device that integrates extracellular (adenosine and dopamine) and intracellular (Ca^{+2}) signals to produce a specific functional response.

INTRODUCTION

G protein-coupled receptors (GPCR) heteromers are defined as macromolecular complexes composed of at least two functional receptor units with biochemical properties that are different from those of its individual receptors (Ferré et al., 2009). Allosteric mechanisms are responsible for a multiplicity of unique pharmacological properties of GPCR heteromers (Ferré et al., 2014). One of the most reproduced allosteric modulations in a GPCR heteromer is an antagonistic interaction by which adenosine A_{2A} receptor ($A_{2A}R$) agonists decrease the affinity of dopamine D_2 receptor (D_2R) agonists in the $A_{2A}R$-D_2R heteromer (Ferré et al., 1991). $A_{2A}R$-D_2R heteromers were one of the first GPCR heteromers detected in the brain. They are localized in the striatum, in the GABAergic striato-pallidal neurons, where they play a seminal role controlling basal ganglia function and dysfunction (Ferré et al., 2011).

Apart from modulation of ligand affinity, GPCR oligomers enable ligands to exert different intrinsic efficacy (power of the agonist to induce a functional response independent of its affinity for the receptor) for different signaling pathways (functional selectivity) (Ferré et al., 2014). Thus, allosteric changes in the functional response of an agonist can be mediated by changes in affinity and/or intrinsic efficacy. This principal can be observed in the $A_{2A}R$-D_2R heteromer, where a decrease in D_2R agonist affinity could not alone explain the ability of $A_{2A}R$ agonists to abolish the decrease in excitability of GABAergic striato-pallidal neurons induced by high concentrations of D_2R agonists, sufficient to overcome their decreased affinity (Azdad et al., 2009).

$A_{2A}R$ and D_2R couple preferentially to $G_{s/olf}$ and G_i proteins, respectively, and several studies have reported an antagonistic interaction reciprocal to the $A_{2A}R$-D_2R allosteric modulations, the ability of D_2R ligands to potently inhibit $A_{2A}R$ agonist-mediated adenylyl-cyclase (AC) activation (Kull et al., 1999; Hillion et al., 2002). It is not known if this canonical interaction between G_s- and G_i-mediated signaling pathways takes place in the frame of the $A_{2A}R$-D_2R heteromer, as suggested for dopamine D_1-D_3 receptor heteromers (Guitart et al., 2014), or if it depends on separate receptor populations (Ferré et al., 2011). But if it is a property of the $A_{2A}R$-D_2R heteromer, we do not know the physiological factors that modulate these reciprocal interactions, determining the final neuronal response.

Intracellular Ca^{2+} levels are a physiological factor that modulates neuronal activity and GPCR function. The Ca^{2+}-binding protein calmodulin (CaM) has been shown to interact and modulate $A_{2A}R$ and D_2R function in the $A_{2A}R$-D_2R heteromers, but without altering the allosteric interactions between $A_{2A}R$ and D_2R ligands (Navarro et al., 2009; Ferré et al., 2010). CaM is an ancestor of a superfamily of Ca^{2+}-binding proteins, which includes neuronal members classified in neuronal Calcium Binding

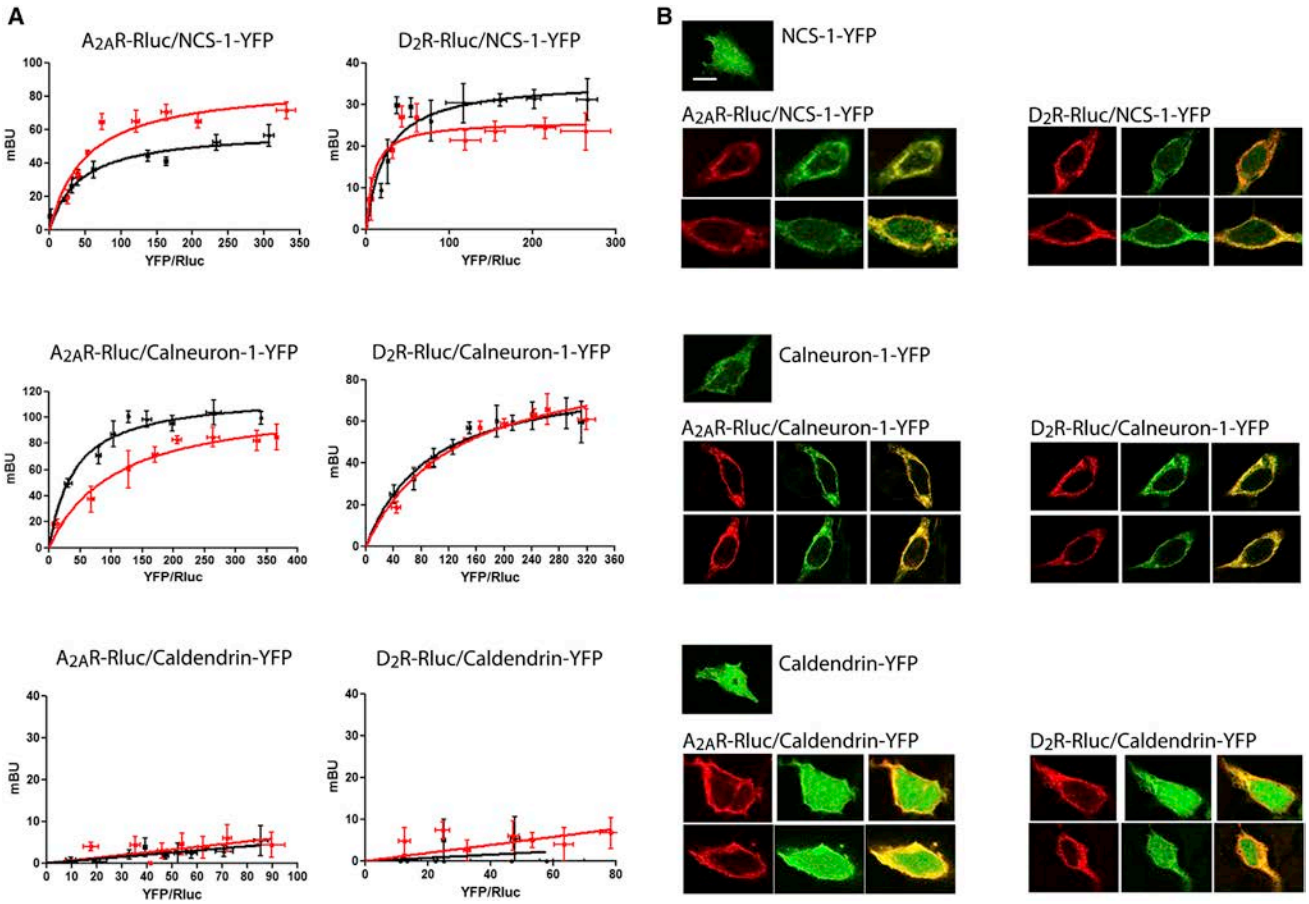

Figure 1. NCS-1 and Calneuron-1, but Not Caldendrin, Interact with $A_{2A}R$ and D_2R

(A) BRET saturation experiments in HEK293T cells transfected with $A_{2A}R$-Rluc cDNA (0.2 μg; left graphs) or D_2R-Rluc cDNA (0.4 μg; right graphs) and increasing amounts of NCS-1-YFP cDNA (0.2 to 0.8 μg; top graphs), calneuron-1-YFP cDNA (0.4 to 1.2 μg; middle graphs), or caldendrin-YFP cDNA (0.2 to 1 μg; bottom graphs), in the absence (black curves) or in the presence (red curves) of 1 μM ionomycin. The relative amount of BRET is given as a function of 1,000 × the ratio between the fluorescence of the acceptor (YFP) and the luciferase activity of the donor (Rluc). BRET is expressed as miliBRET units (mBU) and is given as means ± SEM of five to seven different experiments grouped as a function of the amount of BRET acceptor.

(B) Confocal microscopy images of HEK293T cells transfected with NCS-1-YFP cDNA (0.5 μg; top panels), calneuron-1-YFP cDNA (0.7 μg; middle panels), or caldendrin-YFP cDNA (0.5 μg; bottom panels), cotransfected or not with $A_{2A}R$-RLuc cDNA (0.4 μg; left panels) or D_2R-Rluc cDNA (0.6 μg; right panels). Receptors were identified by immunocytochemistry (red) and proteins fused to YFP were identified by its own fluorescence (green). Colocalization is shown in yellow in merge figures. Scale bar, 10 μm.

Proteins (CaBPs, such as caldendrin and calneuron-1) and the Neuronal Calcium Sensor (NCS) proteins (such as NCS-1) (Mikhaylova et al., 2011). NCS-1, caldendrin, and calneuron-1 have overlapping expression in the brain and have been shown to dramatically modify GPCR function (Mikhaylova et al., 2009). NCS-1 is also known to interact and modify the function of $A_{2A}R$ and D_2R (Kabbani et al., 2002; Saab et al., 2009; Navarro et al., 2012). We therefore studied if neuronal Ca^{2+}-binding proteins could provide the pursued modulators of the allosteric interactions in the $A_{2A}R$-D_2R heteromers.

RESULTS

NCS-1 and Calneuron-1 Directly Interact with $A_{2A}R$-D_2R Heteromers

Bioluminescence resonance energy transfer (BRET) experiments were performed in HEK293T cells in which one of the receptors is fused to the bioluminescent protein *Renilla* Luciferase (RLuc) and the Ca^{2+}-binding protein to a yellow fluorescent protein (YFP). Protein interactions were detected by saturable BRET curves in cells expressing a constant amount of $A_{2A}R$-Rluc or D_2R-Rluc and increasing amounts of NCS-1-YFP or calneuron-1-YFP (Figure 1A, top and middle graphs). $BRET_{max}$ and $BRET_{50}$ values were, respectively, 59.6 ± 4 mBU and 42.4 ± 9 for the pair $A_{2A}R$-Rluc-NCS1-1-YFP; 35.8 ± 4 mBU and 23.4 ± 5 for the pair D_2R-Rluc-NCS-1-YFP; 118.1 ± 7 mBU and 40.5 ± 7 for the pair $A_{2A}R$-Rluc-calneuron-1-YFP; and 51.9 ± 10 mBU and 25.7 ± 7 for the pair D_2R-Rluc-calneuron-1-YFP. Very low and linear BRET was detected in cells expressing a constant amount of $A_{2A}R$-Rluc or D_2R-Rluc and increasing amounts of caldendrin-YFP (Figure 1A, bottom graph), showing the inability of caldendrin to interact with $A_{2A}R$ or D_2R, and the specificity of NCS-1 and calneuron-1 interactions. Increasing intracellular Ca^{2+} levels with ionomycin produced noticeable changes in

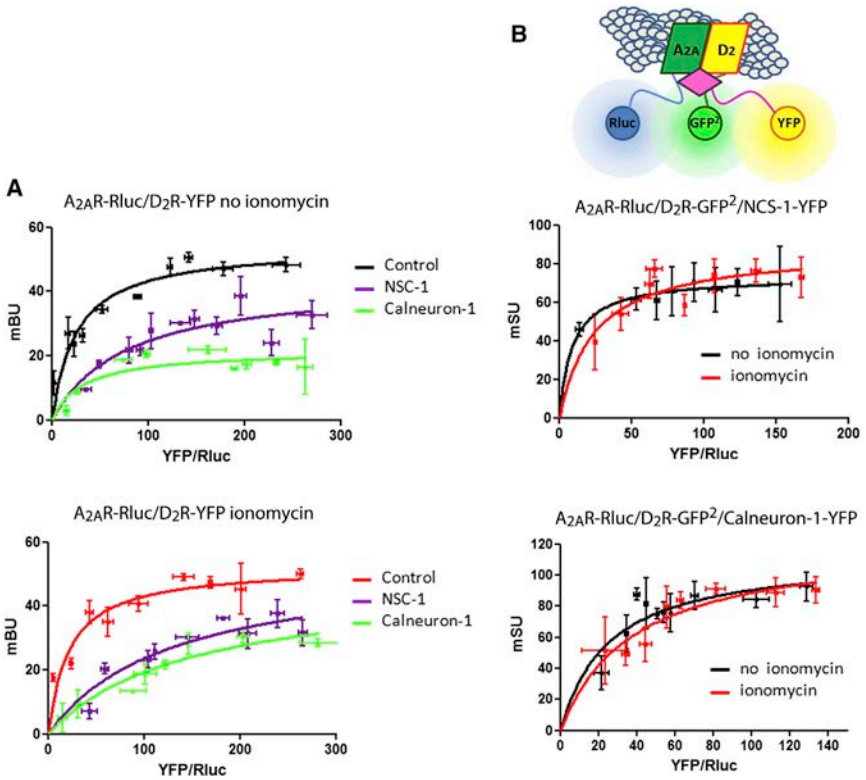

Figure 2. NCS-1 and Calneuron-1 Interact with $A_{2A}R$-D_2R Heteromers

(A) BRET saturation experiments in HEK293T cells transfected with $A_{2A}R$-Rluc cDNA (0.2 μg) and increasing amounts of D_2R-YFP cDNA (0.1 to 1 μg) with or without NCS-1 cDNA (0.7 μg) or calneuron-1 cDNA (1 μg), in the absence (top graph) or in the presence (bottom graph) of 1 μM ionomycin.

(B) Sequential resonance energy transfer (SRET) saturation experiments in HEK293T cells transfected with $A_{2A}R$-Rluc cDNA (0.3 μg), D_2R-GFP^2 cDNA (0.4 μg), and increasing amounts of NCS-1-YFP cDNA (0.3 to 0.8 μg; top graph) or calneuron-1-YFP cDNA (0.5 to 1.5 μg; bottom graph), in the absence (black curves) or presence (red curves) of 1 μM ionomycin. Scheme shows SRET with the sequential BRET (Rluc as donor and GFP^2 as acceptor) and FRET (GFP^2 as donor and YFP as acceptor) processes. BRET or SRET are expressed as miliBRET or miliSRET units (mBU, mSU), respectively, and given as a function of 1,000 × the ratio between the fluorescence of the acceptor (YFP) and the luciferase activity of the donor (Rluc). Values are means ± SEM of six to eight different experiments.

the BRET curves for the pairs $A_{2A}R$-Rluc-NCS-1-YFP, D_2R-Rluc-NCS-1-YFP, and A_{2A}-Rluc-calneuron-1-YFP (Figure 1A, top and middle graphs), indicating that Ca^{2+} binding to NCS-1 or calneuron-1 induces structural changes in the respective complexes. In accordance with the BRET data, the intracellular distribution of NCS-1 dramatically changed to a plasma membrane distribution after $A_{2A}R$ or D_2R coexpression (Figure 1B, top panel). Calneuron-1 expressed alone showed a membrane localization that was maintained in the presence of $A_{2A}R$ or D_2R with a high degree of colocalization (Figure 1B, middle panel). Caldendrin did not change its intracellular distribution when coexpressed with either receptor (Figure 1B, bottom panel).

Heteromers were detected by saturable BRET curves in cells expressing a constant amount of $A_{2A}R$-Rluc and increasing amounts of D_2R-YFP in the absence or in the presence of ionomycin (Figure 2A). Coexpression of calneuron-1 or NCS-1 induced structural changes in the heteromer detected as changes in the BRET curve shape (Figure 2A). This suggested oligomerization between $A_{2A}R$-D_2R heteromers and the Ca^{2+}-binding proteins, which was further supported by sequential resonance energy transfer (SRET) experiments (Carriba et al., 2008). Rluc was fused to $A_{2A}R$ to act as a BRET donor, GFP^2 was fused to D_2R to act as a BRET acceptor and as a FRET donor, and YFP was fused to NCS-1 or to calneuron-1 to act as a FRET acceptor as diagrammed in Figure 2B (top scheme). In cells expressing a constant amount of $A_{2A}R$-Rluc and D_2R-GFP^2 and increasing amounts of NCS-1-YFP (Figure 2B, middle graph) or calneuron-1-YFP (Figure 2B, bottom graph), a positive SRET saturation curve was obtained in the absence (black curves) or in the presence (red curves) of ionomycin, with a $SRET_{max}$ of 73.3 ± 2 mSU and $SRET_{50}$ of 8.9 ± 2 or $SRET_{max}$ of 88.2 ± 9 mSU and $SRET_{50}$ of 24.1 ± 6 for the $A_{2A}R$-D_2R-NCS-1 complex in the absence or in the presence of ionomycin, respectively, and a $SRET_{max}$ of 113.2 ± 14 mSU and $SRET_{50}$ of 25.1 ± 7 or $SRET_{max}$ of 122.6 ± 15 mSU and $SRET_{50}$ of 38.5 ± 10 for the $A_{2A}R$-D_2R-calneuron-1 complex in the absence or in the presence of ionomycin, respectively. Therefore, both NCS-1 and calneuron-1 bind to $A_{2A}R$-D_2R heteromers independently of the presence of Ca^{2+}.

To investigate if membrane localization of the Ca^{2+}-binding proteins, mediated by C-terminal transmembrane domain in calneuron-1 and N-terminal myristoylation of NSC-1 (Hradsky et al., 2011), are necessary for the interaction with $A_{2A}R$ and D_2R, we used a calneuron-1 construct truncated in its C terminus (calneuron-1ΔCT) (Hradsky et al., 2011) and an N-terminal myristoylation-deficient NCS-1 mutant. No BRET signal was detected in cells expressing $A_{2A}R$-Rluc or D_2R-Rluc and increasing amounts of mutant calneuron-YFP (Figure S1A, top graphs, available online). Very low and linear BRET values were also obtained in cells expressing $A_{2A}R$-Rluc or D_2R-Rluc and increasing amounts of mutant NCS1-YFP (Figure S1A, bottom graphs).

NCS-1 and Calneuron-1 Compete for the Binding to $A_{2A}R$ and D_2R

Competition BRET experiments were performed in which energy transfer between $A_{2A}R$-Rluc-NCS-1-YFP was measured in the presence of increasing concentrations of calneuron-1 with or without ionomycin (Figure 3A, left graph). In both conditions, calneuron-1 dose-dependently lowered the energy transfer, indicating competition between both Ca^{2+}-binding proteins for $A_{2A}R$. Similar results were obtained with D_2R. NCS-1 reduced

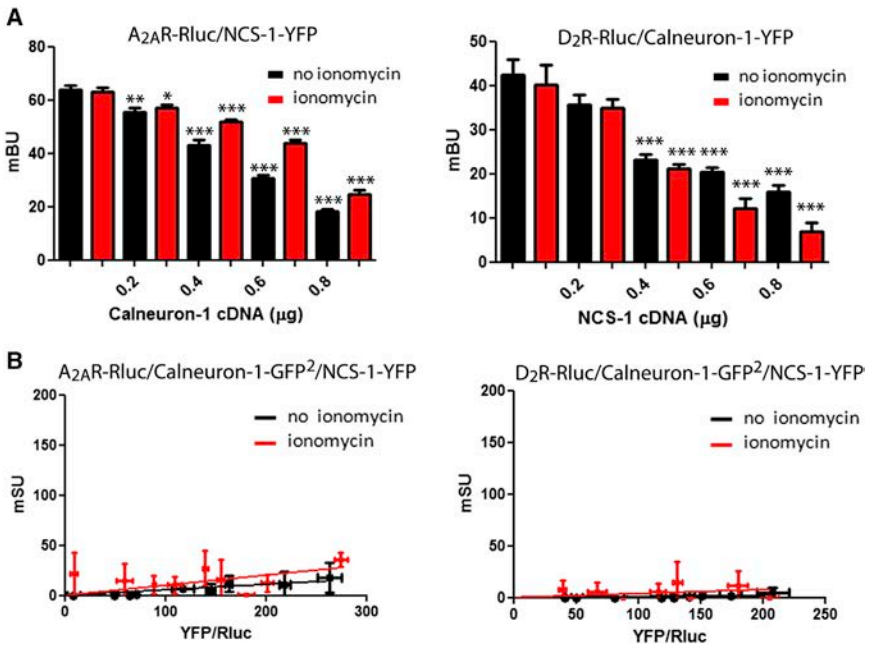

Figure 3. NCS-1 and Calneuron-1 Compete for Binding to $A_{2A}R$ and D_2R

(A) BRET competition experiments in HEK293T cells transfected with $A_{2A}R$-Rluc cDNA (0.2 μg) and NCS-1-YFP cDNA (0.7 μg) with increasing amounts of calneuron-1 cDNA (0.2 to 0.8 μg; left graph) or with D_2R-Rluc cDNA (0.3 μg) and calneuron-1-YFP cDNA (1 μg; right graph) with increasing amounts of NCS-1 cDNA (0.2 to 0.8 μg, right graph) in the absence (black bars) or presence (red bars) of 1 μM ionomycin. BRET, expressed as miliBRET units (mBU), is given as means ± SEM of six to eight different experiments. One-way ANOVA followed by post hoc Dunnett's multiple comparisons: *$p < 0.05$, **$p < 0.01$, and ***$p < 0.001$ versus BRET in the absence of NCS-1 or calneuron-1.

(B) SRET in HEK293T cells transfected $A_{2A}R$-Rluc cDNA (0.2 μg; left graphs) or D_2R-Rluc cDNA (0.3 μg; right graph), and calneuron-1-GFP^2 cDNA (0.4 μg) and increasing amounts of NCS-1-YFP cDNA (0.2 to 0.8 μg) in the absence (black lines) or presence (red lines) of 1 μM ionomycin. The relative amount of SRET, expressed as miliSRET units (mSU), is given as a function of 1,000 × the ratio between the fluorescence of the acceptor (YFP) and the luciferase activity of the donor (Rluc). Values are means ± SEM of four to six different experiments.

the energy transfer between D_2R-Rluc and calneuron-1-YFP in the absence or presence of ionomycin (Figure 3A, right graph). Therefore, NCS-1 and calneuron-1 bind and compete for the same binding sites on $A_{2A}R$ and D_2R. In agreement, low and linear SRET curves were obtained in the absence or in the presence of ionomycin in cells expressing $A_{2A}R$-Rluc-calneuron-1-GFP^2-NCS-1-YFP or D_2R-Rluc-calneuron-1-GFP^2-NCS-1-YFP (Figure 3B).

BRET saturation values were significantly diminished when a mutant $A_{2A}R$ fused to Rluc in which the sequence $_{199}$RIFLAARRQ$_{207}$ (localized in the cytoplasm, at the end of TM5) was mutated to $_{199}$RIFLAAAAQ$_{207}$ ($A_{2A}R^{A205\text{-}A206}$ receptor) was coexpressed with either NCS-1-YFP or calneuron-1-YFP (Figure S1B). NCS-1 and calneuron-1 thus interact with the third intracellular loop (3IL) of $A_{2A}R$. This was confirmed by surface plasmon resonance measurements showing the in vitro interaction between the Ca^{2+}-binding proteins and glutathione S-transferase (GST) fused to a peptide with the amino acid sequence corresponding to the third intracellular loop of the $A_{2A}R$ (GST-$A_{2A}R$-IL3) (Figure S2, top graphs). The sequence corresponding to amino acids 428–443 in the C-terminal domain of the D_2R has been involved in NCS-1 binding (Kabbani et al., 2002). In agreement, a complete loss of BRET was observed when a D_2R mutant lacking this sequence ($D_2R^{428–443}$) fused to Rluc was coexpressed with NCS-1-YFP (Figure S1C, top left graph). In addition, a significant but partial modification of the D_2R-Rluc/calneuron-1 BRET saturation curve was obtained with $D_2R^{428–443}$-Rluc (Figure S1C, top right graph). A partial modification of the D_2R-Rluc/calneuron-1 BRET saturation curve was also obtained with the short isoform of D_2R fused to Rluc ($D_{2S}R$-Rluc, which lacks an Arg-rich epitope in the middle of the 3IL of the long isoform) (Figure S1C, bottom right graph). On the other hand, no significant differences were observed between $D_{2S}R$-Rluc/NCS-1 BRET saturation curves (Figure S1C, bottom left graph). These results reinforce the assumption that the C-terminal domain of D_2R is sufficient for NCS-1 binding and indicate that both the C-terminal domain and the 3IL of D_2R are involved in calneuron-1 binding. The role of the D_2R C-terminal domain in the interaction with both Ca^{2+}-binding proteins was confirmed with surface plasmon resonance measurements using a peptide with the amino acid sequence of the C-terminal domain of the D_2R coupled to the biosensor (Figure S2, bottom graphs).

Differential Modulation by NCS-1 and Calneuron-1 of Allosteric Interactions within $A_{2A}R$-D_2R Heteromers

In HEK293T cells expressing $A_{2A}R$ alone or $A_{2A}R$ and D_2R, the $A_{2A}R$ agonist CGS 21680 (100 nM) induced ERK1/2 phosphorylation, which was completely blocked by the protein kinase A inhibitor H89 (Figure S3), indicating a G protein-cAMP-PKA-dependent $A_{2A}R$-mediated mitogen-activated protein kinase (MAPK) activation. In cells expressing $A_{2A}R$ and the D_2R, CGS 21680 and the D_2R agonist quinpirole (1 μM) induced a similar degree of ERK1/2 phosphorylation, in the presence or absence of ionomycin (Figure 4A, black bars). The absence of additive effect indicates the presence of moderate negative crosstalk, a negative allosteric interaction between both ligands within the $A_{2A}R$-D_2R heteromer. Similar effects were observed in cells expressing NCS-1, in the absence or in the presence of ionomycin, (Figure 4A, gray bars), as well as in cells expressing calneuron-1, but only in the absence of ionomycin (Figure 4A, left graph, white bars). In the presence of calneuron-1 and ionomycin, a strong negative crosstalk was observed, without an increase of ERK1/2 phosphorylation over basal level and with significantly lower values upon coadministration of CGS 21680 plus quinpirole compared with CGS 21680 alone (Figure 4A, right graph, white bars). As negative control, this effect was not observed when using the truncated mutant of calneuron-1, not able to bind to the $A_{2A}R$ or D_2R (Figure S4A). These results suggest that at high, but not low, intracellular levels of Ca^{2+},

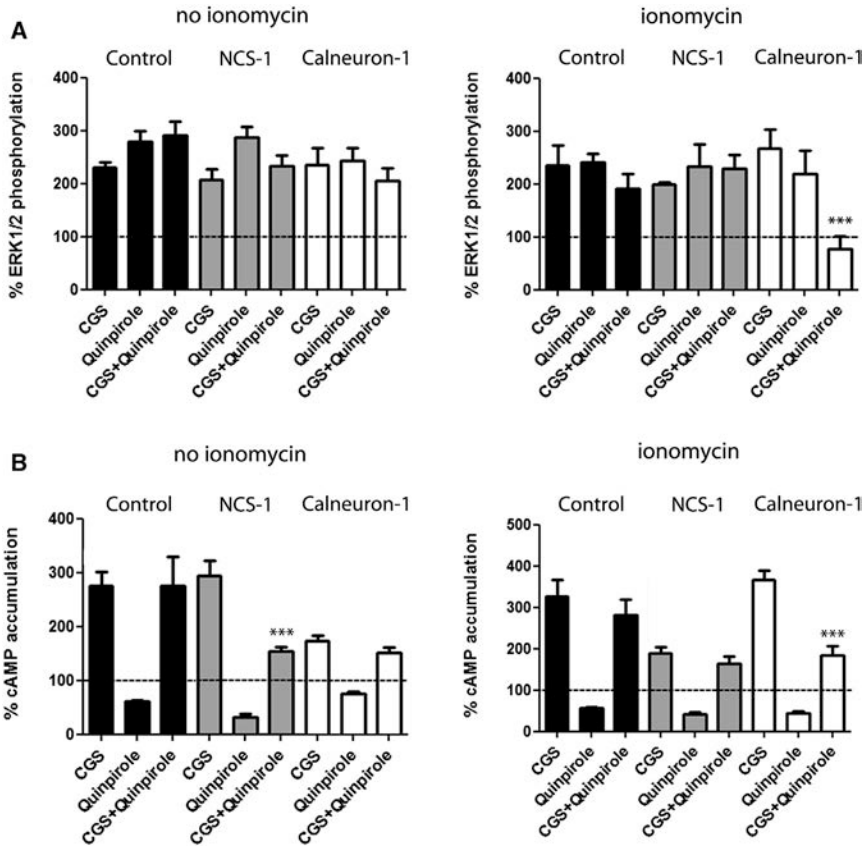

Figure 4. Modulation by NCS-1 and Calneuron-1 of $A_{2A}R$-D_2R Heteromer Signaling in Transfected Cells

(A) ERK1/2 phosphorylation in HEK293T cells transfected with $A_{2A}R$-Rluc cDNA (0.3 μg) and D_2R-YFP cDNA (0.5 μg) alone (black bars) or also transfected with NCS-1 cDNA (0.4 μg cDNA; gray bars) or calneuron-1 cDNA (0.6 μg; white bars) after administration of the $A_{2A}R$ agonist CGS 21680 (CGS, 100 nM), the D_2R agonist quinpirole (1 μM), or both, in the absence or presence of ionomycin (left and right graphs, respectively). ERK1/2 phosphorylation levels are expressed as a percentage over basal.

(B) Levels of cAMP in HEK293T cells transfected with $A_{2A}R$-Rluc cDNA (0.3 μg) and D_2R-YFP cDNA (0.5 μg) alone (black bars) or also transfected with NCS-1 cDNA (0.4 μg cDNA; gray bars) or calneuron-1 cDNA (0.6 μg; white bars) after administration of the $A_{2A}R$ agonist CGS 21680 (CGS, 100 nM), the D_2R agonist quinpirole (1 μM), or both, in the absence or presence of ionomycin (left and right graphs, respectively). Levels of cAMP after CGS alone or after CGS plus quinpirole are expressed as a percentage over basal; cAMP after quinpirole alone are expressed as percentage of decreases with respect to cAMP induced by forskolin (0.5 μM); basal and forskolin-induced cAMP were given as 100% and represented by a dotted line. Values are mean ± SEM of four to six different experiments. One-way ANOVA followed by post hoc Dunnett's multiple comparisons: ***$p < 0.001$ versus CGS 21680 treatment.

calneuron-1 selectively facilitates a reciprocal negative allosteric interaction between CGS-21680 and quinpirole at the level of MAPK signaling in the $A_{2A}R$-D_2R heteromer.

In HEK293T cells expressing $A_{2A}R$ and D_2R receptors, CGS 21680 (100 nM) increased cyclic AMP (cAMP) accumulation and quinpirole (1 μM) decreased forskolin-induced cAMP accumulation in the absence or in the presence of ionomycin (Figure 4B, black bars). However, quinpirole did not counteract CGS 21680-induced cAMP accumulation (Figures 4B, black bars), indicating the existence of a strong negative allosteric modulation by which CGS 21680 significantly decreases the intrinsic efficacy of quinpirole as inhibitor of AC signaling. This modulation was also observed in cells expressing calneuron-1 in the absence of ionomycin (Figure 4B, left graph, white bars) and in cells expressing NCS-1, but in the presence of ionomycin (Figure 4B, right graph, white bars). In contrast, quinpirole was able to reduce cAMP accumulation induced by CGS 21680 in cells expressing calneuron-1 in the presence of ionomycin (Figure 4B, right graph, white bars) and in cells expressing NCS-1 but in the absence of ionomycin (Figure 4B, left graph, gray bars). As negative controls, the ability of quinpirole to counteract cAMP accumulation induced by CGS 21680 in the presence of ionomycin and calneuron-1 was not detected in cells expressing mutants of $A_{2A}R$ or D_2R not able to bind calneuron-1 (Figure S4B, left graph). These results suggest binding of calneuron-1 to both receptors in the $A_{2A}R$-D_2R heteromer is necessary to exert its modulation. The ability of quinpirole to counteract cAMP accumulation induced by CGS 21680 in the presence of NCS-1 and in the absence of ionomycin was not observed in cells expressing $A_{2A}R$ and the D_2R mutant not able to bind NCS-1 (Figure S4B, right graph). But in contrast to calneuron-1, the effect was observed for heteromers constituted by wild-type D_2R and the $A_{2A}R$ mutant not able to bind NCS-1 (Figure S7B, right graph), indicating that binding of NCS-1 to D_2R, but not to the $A_{2A}R$, in the heteromer is sufficient to exert its modulation.

Ca^{2+} Levels Determine the Binding of NCS-1 and Calneuron-1 to $A_{2A}R$-D_2R Heteromers in Striatal Neurons

Proximity ligation assay (PLA) was used to confirm the expression of endogenous $A_{2A}R$-D_2R complexes in the primary cultures (Trifilieff et al., 2011). $A_{2A}R$-D_2R complexes could be observed as punctate red spots in neurons visualized by phase contrast and DAPI-stained nuclei (Figure 5A). The staining was observed in a high percentage of cells (>90%), but not in negative controls in which one of the primary antibodies was omitted (Figure S5, control neurons). To evaluate the role of endogenous NCS-1 and calneuron-1 in the modulation of $A_{2A}R$-D_2R heteromer function, ERK1/2 phosphorylation was determined in neurons transfected with small hairpin RNA (shRNA) against NCS-1 or calneuron-1 mRNA. Knockdown efficiency compared with control was verified by immunoblotting with specific antibodies against calneuron-1 or NCS1 and anti-tubulin antibodies as loading control (Figure S6). The transfection rate of calneuron-1 shRNA was analyzed by determination of GFP expression induced by

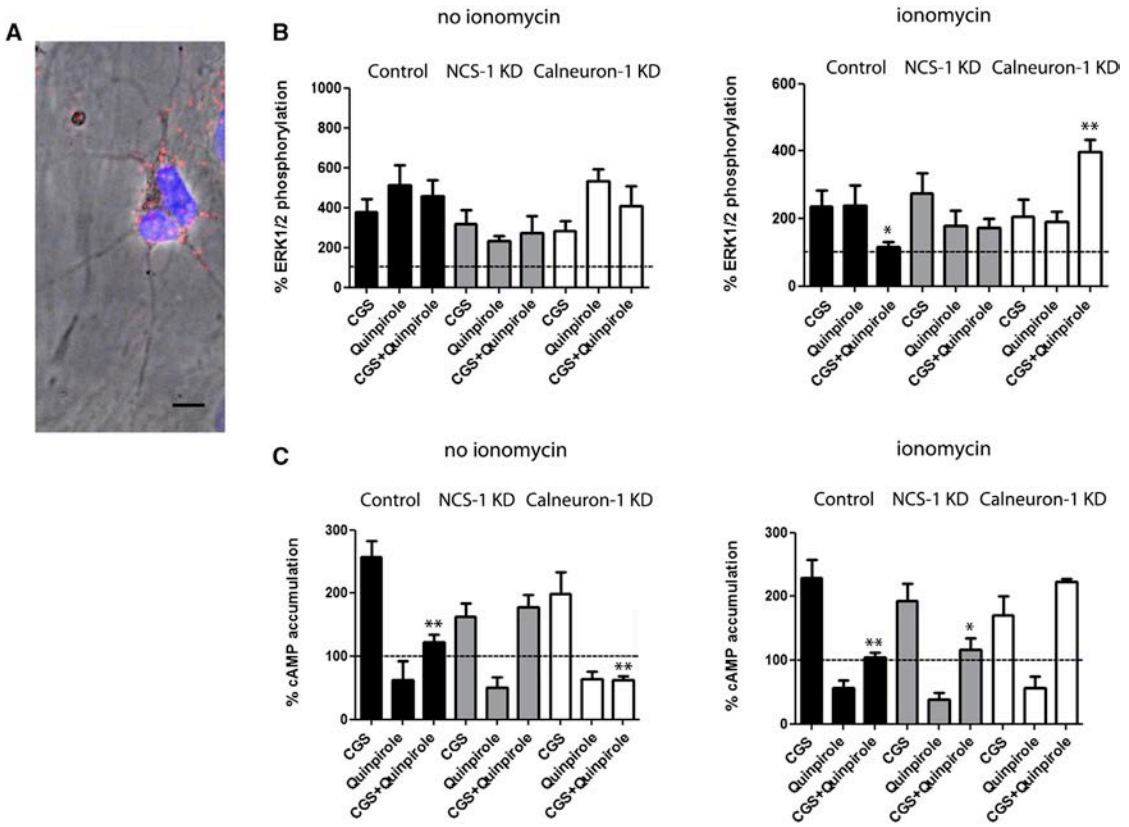

Figure 5. Modulation by NCS-1 and Calneuron-1 of $A_{2A}R$-D_2R Heteromer Signaling in Primary Cultures of Rat Striatal Neurons

(A) $A_{2A}R$-D_2R heteromers detected by proximity ligation assay and confocal microscopy images (superimposed sections) in rat striatal neurons in culture. $A_{2A}R$-D_2R heteromers are seen as red and cell nuclei in blue (Hoesch stain). Scale bars, 20 μm.

(B) ERK1/2 phosphorylation in striatal primary cultures not transfected or transfected with NCS-1 shRNA cDNA (1.5 μg; gray bars) or with calneuron-1 shRNA cDNA (1.5 μg; white bars) after administration of the $A_{2A}R$ agonist CGS 21680 (CGS, 100 nM), the D_2R agonist quinpirole (1 μM), or both, in the absence or presence of ionomycin (left and right graphs, respectively). ERK1/2 phosphorylation levels are expressed as a percentage over basal.

(C) Levels of cAMP in striatal primary cultures not transfected or transfected with NCS-1 shRNA cDNA (1.5 μg; gray bars) or with calneuron-1 shRNA cDNA (1.5 μg; white bars) after administration of the $A_{2A}R$ agonist CGS 21680 (CGS, 100 nM), the D_2R agonist quinpirole (1 μM), or both, in the absence or presence of ionomycin (left and right graphs, respectively). Levels of cAMP after CGS alone or after CGS plus quinpirole are expressed as a percentage over basal; cAMP after quinpirole alone are expressed as percentage of decreases with respect to cAMP induced by forskolin (0.5 μM); basal and forskolin-induced cAMP were given as 100% and represented by a dotted line.

In (A), values are expressed as a percentage over basal (100%, dotted line), as means ± SEM of four to six different experiments; one-way ANOVA followed by post hoc Dunnett's multiple comparisons: *$p < 0.05$ and **$p < 0.01$ versus CGS alone. In (B) and (C), values are means ± SEM of four to six different experiments; one-way ANOVA followed by post hoc Dunnett's multiple comparisons: *$p < 0.05$ and **$p < 0.01$ versus CGS 21680 treatment.

the same plasmid under a different promoter (about 10,000 fluorescence units over basal background), and the expression of the NCS-1 shRNA was determined by cotransfection with an empty GFP vector (about 8,000 fluorescence units over basal). Coadministration of CGS 21680 and quinpirole showed a partial or complete negative allosteric modulation between both ligands in the absence or in the presence of ionomycin, respectively (Figure 5B, black bars). This was equivalent to the negative allosteric modulation of $A_{2A}R$ and D_2R ligands demonstrated in transfected HEK293T cells. In fact, the complete negative allosteric modulation was observed in the presence of ionomycin (Figure 5B, right panel, black bars), which would be expected to depend on calneuron-1 (see Figure 4A, right panel, white bars). Indeed, tonic blockade of the negative crosstalk by endogenous calneuron-1 could be demonstrated, as silencing its expression led to a complete loss of the allosteric interaction in the presence of ionomycin (Figure 5B, right graph, white bars). Neither blockade of the expression of calneuron-1 in the absence of ionomycin (Figure 5B, left graph, white bars) nor blockade of the expression of NCS-1 in the presence or absence of ionomycin (Figure 5B, gray bars) significantly modified the effect of coadministration of CGS 21680 and quinpirole on ERK1/2 phosphorylation in striatal cells in culture.

CGS 21680 induced cAMP accumulation and quinpirole decreased forskolin-induced cAMP accumulation in the absence or in the presence of ionomycin (Figure 5C, black bars). Furthermore, quinpirole was able to reduce CGS 21680-induced cAMP in the absence or in the presence of ionomycin (Figure 5C, black bars). Thus, CGS 21680 could not significantly decrease the intrinsic efficacy of quinpirole as an inhibitor of AC signaling. Remarkably, the ability of CGS 21680 to fully

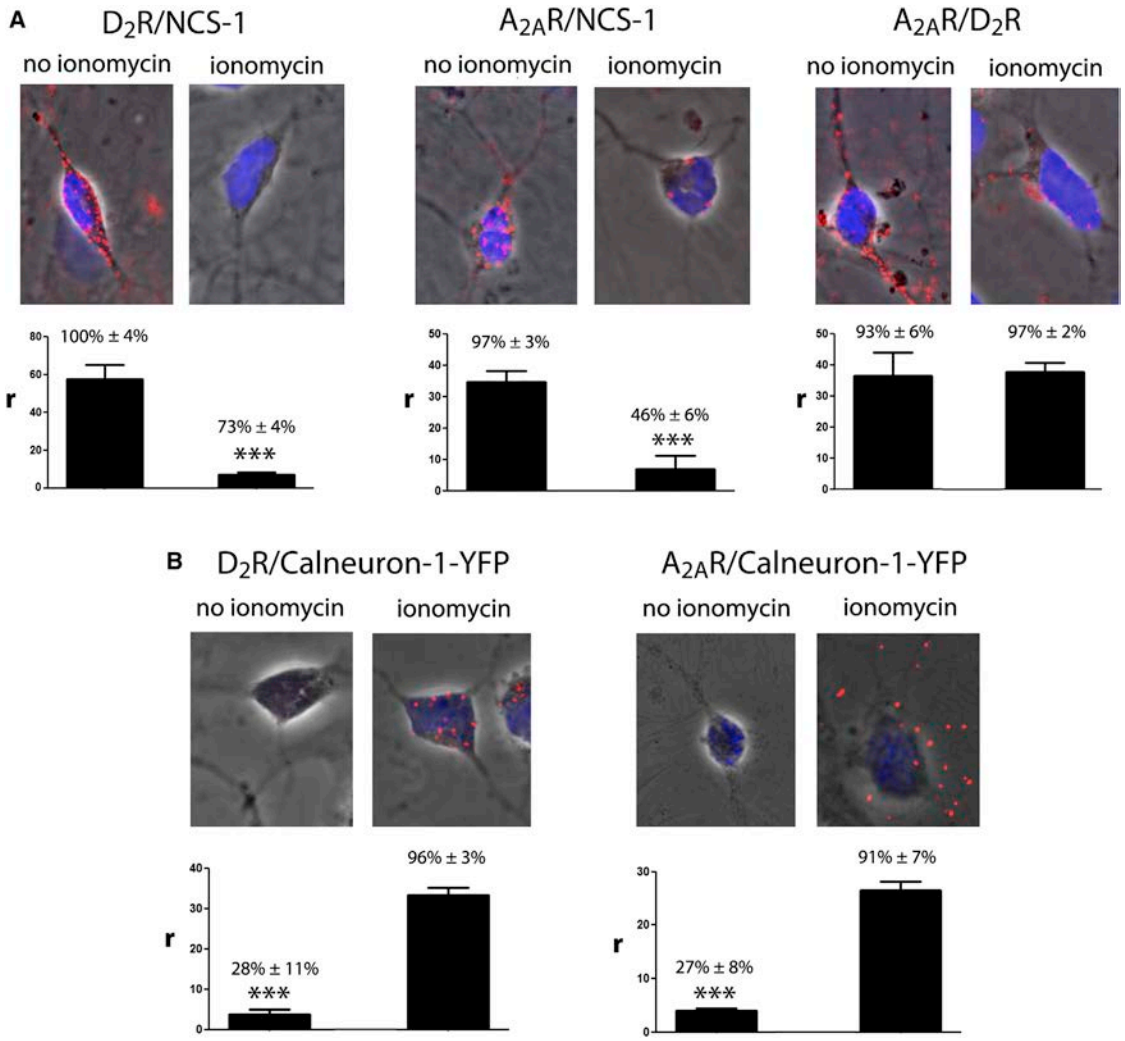

Figure 6. Interactions of NCS-1 and Calneuron-1 with $A_{2A}R$-D_2R Heteromers in Striatal Neurons Depend on Intracellular Ca^{+2} Levels

(A) Proximity ligation assay and confocal microscopy images (superimposed sections) in rat striatal neurons in culture, using primary antibodies for D_2R and NCS-1 (left), $A_{2A}R$ and NCS-1 (middle), and $A_{2A}R$ and D_2R (right), in the absence or presence of ionomycin (1 μM).

(B) PLA and confocal microscopy images (superimposed sections) in rat striatal neurons in culture transfected with calneuron-1-YFP cDNA (1 μg), using primary antibodies for D_2R and YFP (left) and $A_{2A}R$ and YFP (right), in the absence or presence of ionomycin (1 μM). Receptor heteromers and receptor-Ca^{2+}-binding protein complexes appear as red clusters in neurons detected by phase contrast. Cell nuclei were stained with Hoesch (blue). The bar graphs represent PLA quantification: r values represent number of red spots/cell containing spots and percentage values represent the percentage of cells containing one or more red spots respect to the total number of cells. Data (% of positive cells or r) are means ± SEM of counts in 20–30 different neurons of three independent preparations. One-way ANOVA and followed by Bonferroni post hoc test: ***$p < 0.001$ compared with no ionomycin (in A) or ionomicin (in B) of r values.

counteract the inhibitory effect of quinpirole appeared with blockade of the expression of NCS-1 in the absence of ionomycin (Figure 5C, left graph, gray bars) and with blockade of calneuron-1 expression in the presence of ionomycin (Figure 5C, right graph, white bars). These results are in complete agreement with those obtained in HEK293T cells. In striatal cells, however, intracellular Ca^{2+} levels determine which neuronal Ca^{2+}-binding protein interacts with the $A_{2A}R$-D_2R heteromer.

PLA was also used to confirm the ability of Ca^{2+} levels to determine which Ca^{2+}-binding protein interacts with the $A_{2A}R$-D_2R heteromer in striatal neurons. Because of the lack of antibodies sufficiently specific for calneuron-1, only interactions with endogenous NCS-1 could be addressed. D_2R-NCS-1 (Figure 6A, left panels), $A_{2A}R$-NCS-1 (Figure 6A, middle panels), and $A_{2A}R$-D_2R (Figure 6A, left panels) complexes were readily observed in the absence of ionomycin as punctate red spots visualized by phase contrast and with DAPI-stained nuclei. As negative controls, red spots were not observed in the presence of only one of the primary antibodies (Figure S8; NCS-1 KD). The staining was observed in a high percentage of cells (Figure 6A, bar graphs). Although PLA can only assess close proximity between two proteins, the detection of $A_{2A}R$-NCS-1, D_2R-NCS-1, and $A_{2A}R$-D_2R complexes supports that $A_{2A}R$-D_2R-NCS-1 complexes are expressed in the same striatal neurons at low Ca^{2+} levels. Importantly, in the presence of ionomycin, red spots were only observed for $A_{2A}R$-D_2R complexes (Figure 6A, right

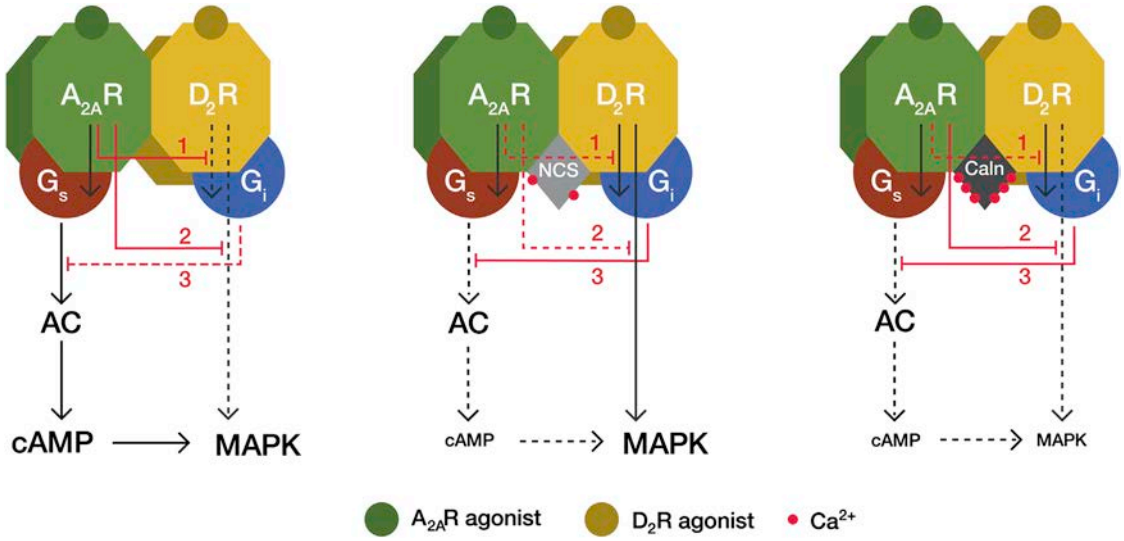

Figure 7. Model Representing the Differential Role of NCS-1 and Calneuron-1 in $A_{2A}R$-D_2R Heteromer Signaling

Depending on the intracellular Ca^{+2} levels, the neuronal Ca^{+2}-binding proteins NCS-1 (NCS) and calneuron-1 (Caln) exert a differential modulation of $A_{2A}R$-D_2R heteromer signaling. In the absence of Ca^{+2}-binding proteins, the D_2R agonist cannot counteract the ability of the $A_{2A}R$ agonist to induce cAMP accumulation (3), due to an allosteric modulation by which $A_{2A}R$ activation inhibits D_2R-mediated G protein-dependent signaling (1). Under these conditions, $A_{2A}R$ activation also inhibits the D_2R agonist-mediated G protein-independent MAPK activation (2). These two allosteric modulations (1 and 2) are absent when NCS-1 binds to the receptor heteromer in the presence of low intracellular Ca^{+2} levels. Under these conditions, coactivation of both receptors in the heteromer does not produce cAMP accumulation, but still induces MAPK activation. When calneuron-1 binds to $A_{2A}R$-D_2R heteromer, the allosteric modulation at the level of G protein-dependent signaling (1) is selectively disrupted and the allosteric modulation at the level of G protein-independent signaling (2) is maintained. This results in very low activation of both MAPK signaling and cAMP production upon coactivation of both receptors in the heteromer, since $A_{2A}R$ agonist-mediated MAPK activation (which is dependent on AC signaling) is also inhibited (3).

panels), and not for D_2R-NCS-1 (Figure 6A, left panels) or $A_{2A}R$-NCS-1 (Figure 6A, middle panels) complexes. To determine whether high Ca^{2+} levels promote calneuron-1 binding to the heteromer, and circumventing the lack of specific calneuron-1 antibodies suitable for PLA, we transfected calneuron-1-YFP and used a specific anti-YFP antibody. $A_{2A}R$-calneuron-1-YFP and D_2R-calneuron-1-YFP complexes could be readily observed by PLA in the presence, but not in the absence, of ionomycin (Figure 6B). The staining was observed in a high percentage of cells only in the presence of ionomycin (Figures 6B, bar graphs). These results from PLA experiments are in complete agreement with low and high Ca^{2+} levels promoting NCS-1 and calneuron-1 binding to the $A_{2A}R$-D_2R heteromer, respectively.

DISCUSSION

The present results provide general findings about the physiological modulation of GPCR heteromer function. First, they demonstrate that in neurons, different Ca^{+2} levels can determine the binding of different neuronal Ca^{+2}-binding proteins to a GPCR heteromer. Second, they demonstrate that the binding of different neuronal Ca^{+2}-binding proteins can promote or disrupt different allosteric modulations in a GPCR heteromer. Third, we show that these differential effects allow a selective modulation of specific GPCR heteromer-dependent signaling pathways.

The strikingly similar results of signaling experiments obtained from HEK293T transfected cells and striatal cells in culture allows us to formulate an heuristic model, which encapsulates previous biochemical findings in the frame of the heteromer, such as a canonical antagonistic G_s-G_i interaction at the level of AC signaling between $A_{2A}R$ and D_2R (Kull et al., 1999; Hillion et al., 2002; Kudlacek et al., 2003), a predominant G protein-cAMP-PKA-dependent $A_{2A}R$-mediated MAPK activation (present results and Klinger et al., 2002; Canals et al., 2005) and a predominant G protein independent MAPK activation mediated by D_2R when coexpressed with $A_{2A}R$ (Huang et al., 2013). Finally, the model assumes the recently proposed tetrameric structure of receptor heteromers (Ferré et al., 2014; Guitart et al., 2014).

The model proposes two independent $A_{2A}R$-mediated inhibitions of two different D_2R-mediated signaling pathways: MAPK activation (G protein independent) and AC inhibition (G protein dependent) (Figure 7). Accumulation of cAMP only occurs upon single or predominant activation of the $A_{2A}R$ in the heteromer, i.e., with low concentrations of dopamine. Under these conditions, the well-known $A_{2A}R$-agonist mediated decrease of the affinity of D_2R agonists counteracts any D_2R-mediated signaling through the heteromer, including AC inhibition. Coactivation with high concentrations of dopamine or D_2R-specific agonists should surmount the decrease in affinity induced by $A_{2A}R$ agonists and allow D_2R agonists to inhibit AC activity. However, in HEK293T transfected cells in the absence of Ca^{+2}-binding proteins, coactivation of both receptors produced similar cAMP levels than those promoted by the $A_{2A}R$ agonist, indicating that it is also possible to observe an $A_{2A}R$ agonist-induced allosteric modulation of the intrinsic efficacy of D_2R agonists (Figure 7, left panel). This modulation, nevertheless, is disrupted with low and high Ca^{+2} levels in the presence of NCS-1 and calneuron-1, respectively, and the modulation is absent in striatal neurons in culture with low or high intracellular Ca^{+2} levels (because of the

endogenous binding of NCS-1 or calneuron-1, respectively). Low levels of cAMP are then produced upon coactivation of the heteromer under these conditions (Figure 7, middle and right panels). Low Ca^{+2} levels (with NCS-1 binding), but not high Ca^{+2} levels (with calneuron-1 binding), disrupt the $A_{2A}R$-mediated negative crosstalk of the D_2R-mediated MAPK activation (Figure 7, middle and right panels). In summary, the allosteric modulation mediated by neuronal Ca^{+2}-binding proteins determines that in the $A_{2A}R$-D_2R heteromer a preferential activation of $A_{2A}R$ leads to both cAMP accumulation and MAPK signaling; upon coactivation of $A_{2A}R$ and D_2R, the presence of low intracellular Ca^{+2} levels leads only to MAPK signaling, and at high Ca^{+2} levels, coactivation leads to a very diminished $A_{2A}R$-D_2R heteromer-mediated signaling response.

Previous reports have shown that, depending on the neuronal function under study, coactivation of $A_{2A}R$ and D_2R leads to significant inhibition of $A_{2A}R$ or D_2R-mediated response, indicating the existence of reciprocal interactions between both receptors that modulate different functional responses. In the striatum, stimulation of $A_{2A}R$ counteracts a D_2R agonist-induced inhibitory modulation of NMDA receptor-mediated effects (Azdad et al., 2009; Higley and Sabatini, 2010), which are dependent on an increase in intracellular Ca^{+2} levels. On the other hand, the ability of $A_{2A}R$ to activate AC seems to be normally restrained by a strong tonic inhibitory effect of endogenous dopamine on striatal D_2R, which efficiently inhibits $A_{2A}R$-mediated AC activation (Svenningsson et al., 1999). To explain the coexistence of these simultaneous reciprocal antagonistic interactions between striatal $A_{2A}R$ and D_2R, we previously postulated their mediation by two different populations of $A_{2A}R$, forming and not forming heteromers with D_2R (Ferré et al., 2011). The present results allow understanding the coexistence of these interactions considering only one predominant population of $A_{2A}R$, which forms heteromers with D_2R. This could account for different G protein-dependent or G protein-independent functional responses, which could be differentially modulated by intracellular Ca^{+2} levels. Apart from adenosine and dopamine, the Ca^{+2}-dependent modulation of $A_{2A}R$-D_2R heteromer function allows further integration of other neurotransmitter systems such as glutamate (through NMDA receptor activation) and acetylcholine (through G_q-coupled muscarinic receptors) (Tozzi et al., 2011).

SIGNIFICANCE

The present study demonstrates that GPCR heteromers are cellular devices that provide a very elaborate integration and modulation of signals from different neurotransmitters that ultimately depends on physiological factors such as intracellular Ca^{+2} levels. Ca^{+2} levels, through different Ca^{+2}-binding proteins, determine functional selectivity within the $A_{2A}R$-D_2R heteromer, which is an important target for the treatment of Parkinson's disease and other neuropsychiatric disorders.

EXPERIMENTAL PROCEDURES

Vectors, Fusion Proteins, and Mutant Proteins

The cDNA constructs encoding human $A_{2A}R$, D_2R, $D_{2\ s}R$, or calmodulin in pcDNA3 vectors were subcloned in pEYFP-N1(enhanced yellow variant of GFP; Clontech, Heidelberg, Germany), pRluc-N1 (PerkinElmer, Wellesley, MA), or pGFP-2-N1 (Biosignal) vectors as previously described (Navarro et al., 2009) to generate $A_{2A}R$-YFP, $A_{2A}R$-Rluc, $A_{2A}R$-GFP^2, D_2R-YFP, D_2R-Rluc, $D_{2\ s}R$-Rluc, or D_2R-GFP^2 fusion proteins. cDNA constructs encoding NCS-1 or caldendrin in pcDNA3 vectors were subcloned in pEYFP-N1 or in pGFP-2-N1 vectors as previously described (Navarro et al., 2012) to generate NCS-1-YFP, caldendrin-YFP, or NCS-1-GFP^2 fusion proteins. The cDNA for calneuron, cloned into pcDNA3.1, was amplified without its stop codons using sense and antisense primers harboring unique BamHI and HindII sites to clone calneuron-1 in pcDNA3.1RLuc vector or HindIII and BamHI to clone in pEYFP-N1 vector or to clone in pGFP-2-N1 vector. The amplified fragments were subcloned to be in-frame with restriction sites of the corresponding vectors to give the plasmids that express calneuron-1-RLuc, calneuron-1-YFP, or calneuron-1-GFP^2. The sequence ^{199}RIFLAARRQ^{207} in the cytoplasm at the end of TM5 of human $A_{2A}R$ was mutated to ^{199}RIFLAAAAQ^{207} to obtain the $A_{2A}R^{A205\text{-}A206}$ as previously described (Navarro et al., 2010). The $D_2R^{428\text{-}443}$ was generated by deletion of the last 16 amino acids from the D_2R and subcloned harboring EcoRI and KpnI restriction sites in pRluc-N1. Calneuron-1 construct truncated in the C terminus (calneuron-1ΔCT) and N-terminal myristoylation-deficient NCS-1 mutant in which YFP is fused to the N terminus of NCS-1 were obtained as described elsewhere (Hradsky et al., 2011). Fusion proteins corresponding to mutant proteins were obtained following the methodology above described.

Primary Cultures of Rat Striatal Neurons, Cell Lines, and Transfection

Primary cultures of striatal neurons were obtained from fetal Sprague Dawley rats of 19 days. Striatal cells were isolated as described in Hradsky et al. (2013) and plated at a confluence of 40,000 cells/0.32 cm^2. Cells were grown in Neurobasal medium supplemented with 2 mM L-glutamine, 100 U/ml penicillin/streptomycin, and 2% (v/v) B27 supplement (GIBCO) in a 96-well plate for 12 days. HEK293T cells were grown in Dulbecco's modified Eagle's medium (DMEM) supplemented with 2 mM L-glutamine, 100 U/ml penicillin/streptomycin, and 5% (v/v) heat inactivated fetal bovine serum (Invitrogen). Primary cultures or HEK293T cells were cultured in the corresponding growth medium in the absence of ionomycin or in the presence of 1 μM of ionomycin. Striatal neurons and HEK293T cells were transfected with the plasmids encoding receptors and/or calcium binding proteins by the PEI (PolyEthylenImine) method as previously described (Carriba et al., 2008).

Resonance Energy Transfer Experiments

Resonance energy transfer experiments are described in other studies (Carriba et al., 2008; Navarro et al., 2009, 2010, 2012), in figure legends, and in Supplemental Information.

Surface Plasmon Resonance

Surface plasmon resonance measurements were performed on a Biacore X100 system (GE Healthcare) to determine the interaction of calcium binding proteins with GST coupled to $A_{2A}R$ third intracellular loop (GST-$A_{2A}R$-IL3) or with D_2R C-terminal domain peptide (P14416, pos. 432-443, peptide purchased from PSL) coupled to a CM5 sensor chip according to the manufacturer's protocol (D_2R-Cterm). Surface plasmon resonance is described in other studies (Catimel et al., 1997; Mikhaylova et al., 2009) and in figure legends (Figure S2).

Immunocytochemistry

Immunocytochemistry assays were performed as previously described (Navarro et al., 2009) using the primary antibodies mouse anti-$A_{2A}R$ (1/200; Millipore) or mouse anti-D_2R (1/200; Santa Cruz Biotechnology) and stained with the secondary antibodies Cy3 anti-mouse (1/200; Jackson ImmunoResearch). NCS-1, calneuron-1, or caldendrin fused to YFP protein were detected by its fluorescence properties. Samples were observed in a Leica SP2 confocal microscope (Leica Microsystems).

Knockdown Endogenous Calneuron-1 or NCS-1 in Primary Cultures of Rat Striatal Neurons

Primary striatal neurons growing in six-well dishes were transfected with the PEI method to knock down the NCS-1 or calneuron-1 expression using

calneuron-1 shRNAII (1xconstruct #2; genecopoeia) with psi-HIV-H1 backbone and eGFP as a marker or pSuper-NCS-1 vector. Cells were incubated for 6–8 hr with the cDNA and the PEI (5.47 mM in nitrogen residues) and 150 mM in NaCl in serum-starved medium. After 6–8 hr, the medium was replaced with a complete culture medium. Forth-eight hours after transfection, the GFP^2 fluorescence signal was detected to test the transfection efficiency. Striatal neurons were then detached and calneuron-1 and NCS-1 expression was detected by western blotting (see Results).

Cell Signaling

The cAMP concentration was determined by homogeneous time-resolved fluorescence (HTRF) energy transfer assay. Lance Ultra cAMP kit (PerkinElmer), based on a europium chelate-labeled cAMP tracer, was used. Cells (4,000 cells/well for transfected HEK293T cells or 6,000 cells/well for primary cultures of striatal neurons) were stimulated with agonists for 15 min in serum-starved DMEM medium supplemented with 50 μM zardeverine, 5 mM HEPES, and 0.1% BSA with or without 1 μM ionomycin, before adding 0.5 μM forskolin or vehicle, and incubating for an additional 15 min period. Fluorescence at 665 nm was analyzed on a PHERAstar Flagship microplate reader equipped with an HTRF optical module (BMG Labtechnologies). ERK 1/2 phosphorylation was determined using the AlphaScreen SureFire kit (Perkin Elmer) following the instructions of the supplier and using an EnSpire Multimode Plate Reader (PerkinElmer). Cells (30,000 cells/well for transfected HEK293T cells or 40,000 cells/well for primary cultures) were seeded in white ProxiPlate 384-well microplates, pretreated at 25°C for 20 min with vehicle or antagonists in serum-starved DMEM medium supplemented or with 1 μM ionomycin and stimulated for an additional 7 min with the indicated agonists.

Proximity Ligation Assays

Heteromers were detected using the Duolink II in situ PLA detection Kit (OLink; Bioscience) following the instructions of the supplier. Primary cultures of striatal neurons were grown on glass coverslips and were fixed in 4% paraformaldehyde for 15 min, washed with PBS containing 20 mM glycine to quench the aldehyde groups, permeabilized with the same buffer containing 0.05% Triton X-100 for 5 min, and successively washed with PBS. After 1 hr incubation at 37°C with the blocking solution in a preheated humidity chamber, primary cultures were incubated overnight in the antibody diluent medium with a mixture of equal amounts of mouse monoclonal anti-$A_{2A}R$ antibody (1:200, Millipore) and the goat polyclonal anti-D_2R antibody (1:200, Santa Cruz) to detect $A_{2A}R$-D_2R heteromers, with the goat polyclonal anti-D_2R antibody and a polyclonal rabbit anti-NCS-1 antibody (1:200, FL190, Santa Cruz) to detect D_2R-NCS-1 complexes, with mouse monoclonal anti-$A_{2A}R$ antibody and the rabbit polyclonal anti-NCS-1 antibody to detect $A_{2A}R$-NCS-1 complexes, with goat polyclonal anti-D_2R antibody and rabbit anti-GFP antibody (1/200, Molecular Probes) to detect D_2R-calneuron-1-YFP complexes or mouse monoclonal anti-$A_{2A}R$ antibody, and rabbit anti-GFP antibody to detect $A_{2A}R$-calneuron-1-YFP complexes. Cells were processed using the PLA probes detecting mouse and goat antibodies (Duolink II PLA probe anti-Mouse plus and Duolink II PLA probe anti-Goat minus), goat and rabbit antibodies (Duolink II PLA probe anti-Goat plus and Duolink II PLA probe anti-Rabbit minus), or mouse and rabbit antibodies (Duolink II PLA probe anti-Mouse plus and Duolink II PLA probe anti-Rabbit minus) diluted in the antibody diluent to a concentration of 1:5. Ligation and amplification were done as indicated by the supplier, and cells were mounted using the mounting medium with Hoechst (1/200; Sigma). Samples were observed in a Leica SP2 confocal microscope (Leica Microsystems) equipped with an apochromatic 63X oil-immersion objective (N.A. 1.4) and 405 nm and a 561 nm laser lines. For each field of view, a stack of two channels (one per staining) and four to eight Z stacks with a step size of 1 μm were acquired. A quantification of cells containing one or more red spots versus total cells (blue nucleus) and, in cells containing spots, the ratio r (number of red spots/cell) were determined considering a total of 25–40 cells from 10–20 different fields using the ImageJ confocal program. Nuclei and red spots were counted on the maximum projections of each image stack. One-way ANOVA followed by Dunet's post hoc multiple comparison test was used to compare the values (% of positive cells or r spots/cell) obtained for each pair of receptors.

SUPPLEMENTAL INFORMATION

Supplemental Information includes Supplemental Experimental Procedures and six figures and can be found with this article online at http://dx.doi.org/10.1016/j.chembiol.2014.10.004.

AUTHOR CONTRIBUTIONS

G.N., M.M., M.R.K., A.C., J.M., V.C., C.L., E.I.C., P.J.M., and S.F. contributed to research design. G.N., D.A., E.M., J.H., P.P.R., and M.M. contributed to experiments. G.N., D.A., E.M., J.H., P.P.R., M.M., C.L., P.J.M., and S.F. contributed to data analysis. G.N., M.M., C.L., P.J.M., and S.F. contributed to the writing of the manuscript.

ACKNOWLEDGMENTS

This work was supported by the intramural funds of the National Institute on Drug Abuse, from the Spanish "Ministerio de Ciencia y Tecnología" (SAF2011-23813), the Government of Catalonia (2009-SGR-12), CIBERNED (CB06/05/0064), the German Research Foundation (SFB779/TPB8, DFG Kr1879/3-1), the Leibniz Foundation (Pakt f. Forschung), a European Molecular Biology Organization Long-Term Fellowship (to M.M., EMBO ALTF 884-2011), the European Commission (EMBOCOFUND2010, GA-2010-267146), a Marie Curie Actions (Intra-European Fellowship), and a "Ramón y Cajal" Fellowship (to P.J.M.).

Received: August 13, 2014
Revised: October 3, 2014
Accepted: October 6, 2014
Published: November 6, 2014

REFERENCES

Azdad, K., Gall, D., Woods, A.S., Ledent, C., Ferré, S., and Schiffmann, S.N. (2009). Dopamine D2 and adenosine A2A receptors regulate NMDA-mediated excitation in accumbens neurons through A2A-D2 receptor heteromerization. Neuropsychopharmacology *34*, 972–986.

Canals, M., Angulo, E., Casadó, V., Canela, E.I., Mallol, J., Viñals, F., Staines, W., Tinner, B., Hillion, J., Agnati, L., et al. (2005). Molecular mechanisms involved in the adenosine A and A receptor-induced neuronal differentiation in neuroblastoma cells and striatal primary cultures. J. Neurochem. *92*, 337–348.

Carriba, P., Navarro, G., Ciruela, F., Ferré, S., Casadó, V., Agnati, L., Cortés, A., Mallol, J., Fuxe, K., Canela, E.I., et al. (2008). Detection of heteromerization of more than two proteins by sequential BRET-FRET. Nat. Methods *5*, 727–733.

Catimel, B., Nerrie, M., Lee, F.T., Scott, A.M., Ritter, G., Welt, S., Old, L.J., Burgess, A.W., and Nice, E.C. (1997). Kinetic analysis of the interaction between the monoclonal antibody A33 and its colonic epithelial antigen by the use of an optical biosensor. A comparison of immobilisation strategies. J. Chromatogr. A *776*, 15–30.

Ferré, S., von Euler, G., Johansson, B., Fredholm, B.B., and Fuxe, K. (1991). Stimulation of high-affinity adenosine A2 receptors decreases the affinity of dopamine D2 receptors in rat striatal membranes. Proc. Natl. Acad. Sci. USA *88*, 7238–7241.

Ferré, S., Baler, R., Bouvier, M., Caron, M.G., Devi, L.A., Durroux, T., Fuxe, K., George, S.R., Javitch, J.A., Lohse, M.J., et al. (2009). Building a new conceptual framework for receptor heteromers. Nat. Chem. Biol. *5*, 131–134.

Ferré, S., Woods, A.S., Navarro, G., Aymerich, M., Lluís, C., and Franco, R. (2010). Calcium-mediated modulation of the quaternary structure and function of adenosine A2A-dopamine D2 receptor heteromers. Curr. Opin. Pharmacol. *10*, 67–72.

Ferré, S., Quiroz, C., Orru, M., Guitart, X., Navarro, G., Cortés, A., Casadó, V., Canela, E.I., Lluis, C., and Franco, R. (2011). Adenosine A(2A) Receptors and A(2A) Receptor heteromers as key players in striatal function. Front. Neuroanat. *5*, 36.

Ferré, S., Casadó, V., Devi, L.A., Filizola, M., Jockers, R., Lohse, M.J., Milligan, G., Pin, J.P., and Guitart, X. (2014). G protein-coupled receptor oligomerization revisited: functional and pharmacological perspectives. Pharmacol. Rev. *66*, 413–434.

Guitart, X., Navarro, G., Moreno, E., Yano, H., Cai, N.S., Sanchez, M., Kumar-Barodia, S., Naidu, Y., Mallol, J., Cortes, A., et al. (2014). Functional selectivity of allosteric interactions within GPCR oligomers: the dopamine D_1-D_3 receptor heterotetramer. Mol. Pharmacol. *86*, 417–429.

Higley, M.J., and Sabatini, B.L. (2010). Competitive regulation of synaptic Ca2+ influx by D2 dopamine and A2A adenosine receptors. Nat. Neurosci. *13*, 958–966.

Hillion, J., Canals, M., Torvinen, M., Casado, V., Scott, R., Terasmaa, A., Hansson, A., Watson, S., Olah, M.E., Mallol, J., et al. (2002). Coaggregation, cointernalization, and codesensitization of adenosine A2A receptors and dopamine D2 receptors. J. Biol. Chem. *277*, 18091–18097.

Hradsky, J., Raghuram, V., Reddy, P.P., Navarro, G., Hupe, M., Casado, V., McCormick, P.J., Sharma, Y., Kreutz, M.R., and Mikhaylova, M. (2011). Post-translational membrane insertion of tail-anchored transmembrane EF-hand Ca2+ sensor calneurons requires the TRC40/Asna1 protein chaperone. J. Biol. Chem. *286*, 36762–36776.

Hradsky, J., Mikhaylova, M., Karpova, A., Kreutz, M.R., and Zuschratter, W. (2013). Super-resolution microscopy of the neuronal calcium-binding proteins Calneuron-1 and Caldendrin. Methods Mol. Biol. *963*, 147–169.

Huang, L., Wu, D.D., Zhang, L., and Feng, L.Y. (2013). Modulation of A_2a receptor antagonist on D_2 receptor internalization and ERK phosphorylation. Acta Pharmacol. Sin. *34*, 1292–1300.

Kabbani, N., Negyessy, L., Lin, R., Goldman-Rakic, P., and Levenson, R. (2002). Interaction with neuronal calcium sensor NCS-1 mediates desensitization of the D2 dopamine receptor. J. Neurosci. *22*, 8476–8486.

Klinger, M., Kudlacek, O., Seidel, M.G., Freissmuth, M., and Sexl, V. (2002). MAP kinase stimulation by cAMP does not require RAP1 but SRC family kinases. J. Biol. Chem. *277*, 32490–32497.

Kudlacek, O., Just, H., Korkhov, V.M., Vartian, N., Klinger, M., Pankevych, H., Yang, Q., Nanoff, C., Freissmuth, M., and Boehm, S. (2003). The human D2 dopamine receptor synergizes with the A2A adenosine receptor to stimulate adenylyl cyclase in PC12 cells. Neuropsychopharmacology *28*, 1317–1327.

Kull, B., Ferré, S., Arslan, G., Svenningsson, P., Fuxe, K., Owman, C., and Fredholm, B.B. (1999). Reciprocal interactions between adenosine A2A and dopamine D2 receptors in Chinese hamster ovary cells co-transfected with the two receptors. Biochem. Pharmacol. *58*, 1035–1045.

Mikhaylova, M., Reddy, P.P., Munsch, T., Landgraf, P., Suman, S.K., Smalla, K.H., Gundelfinger, E.D., Sharma, Y., and Kreutz, M.R. (2009). Calneurons provide a calcium threshold for trans-Golgi network to plasma membrane trafficking. Proc. Natl. Acad. Sci. USA *106*, 9093–9098.

Mikhaylova, M., Hradsky, J., and Kreutz, M.R. (2011). Between promiscuity and specificity: novel roles of EF-hand calcium sensors in neuronal Ca2+ signalling. J. Neurochem. *118*, 695–713.

Navarro, G., Aymerich, M.S., Marcellino, D., Cortés, A., Casadó, V., Mallol, J., Canela, E.I., Agnati, L., Woods, A.S., Fuxe, K., et al. (2009). Interactions between calmodulin, adenosine A2A, and dopamine D2 receptors. J. Biol. Chem. *284*, 28058–28068.

Navarro, G., Ferré, S., Cordomi, A., Moreno, E., Mallol, J., Casadó, V., Cortés, A., Hoffmann, H., Ortiz, J., Canela, E.I., et al. (2010). Interactions between intracellular domains as key determinants of the quaternary structure and function of receptor heteromers. J. Biol. Chem. *285*, 27346–27359.

Navarro, G., Hradsky, J., Lluís, C., Casadó, V., McCormick, P.J., Kreutz, M.R., and Mikhaylova, M. (2012). NCS-1 associates with adenosine A(2A) receptors and modulates receptor function. Front. Mol. Neurosci. *5*, 53.

Saab, B.J., Georgiou, J., Nath, A., Lee, F.J., Wang, M., Michalon, A., Liu, F., Mansuy, I.M., and Roder, J.C. (2009). NCS-1 in the dentate gyrus promotes exploration, synaptic plasticity, and rapid acquisition of spatial memory. Neuron *63*, 643–656.

Svenningsson, P., Fourreau, L., Bloch, B., Fredholm, B.B., Gonon, F., and Le Moine, C. (1999). Opposite tonic modulation of dopamine and adenosine on c-fos gene expression in striatopallidal neurons. Neuroscience *89*, 827–837.

Tozzi, A., de Iure, A., Di Filippo, M., Tantucci, M., Costa, C., Borsini, F., Ghiglieri, V., Giampà, C., Fusco, F.R., Picconi, B., and Calabresi, P. (2011). The distinct role of medium spiny neurons and cholinergic interneurons in the D_2/A_2A receptor interaction in the striatum: implications for Parkinson's disease. J. Neurosci. *31*, 1850–1862.

Trifilieff, P., Rives, M.L., Urizar, E., Piskorowski, R.A., Vishwasrao, H.D., Castrillon, J., Schmauss, C., Slättman, M., Gullberg, M., and Javitch, J.A. (2011). Detection of antigen interactions ex vivo by proximity ligation assay: endogenous dopamine D2-adenosine A2A receptor complexes in the striatum. Biotechniques *51*, 111–118.

Chemistry & Biology, Volume *21*

Supplemental Information

Intracellular Calcium Levels Determine Differential Modulation of Allosteric Interactions within G Protein-Coupled Receptor Heteromers

Gemma Navarro, David Aguinaga, Estefania Moreno, Johannes Hradsky, Pasham P. Reddy, Antoni Cortés, Josefa Mallol, Vicent Casadó, Marina Mikhaylova, Michael R. Kreutz, Carme Lluís, Enric I. Canela, Peter J. McCormick, and Sergi Ferré

SUPPLEMENTAL FIGURES

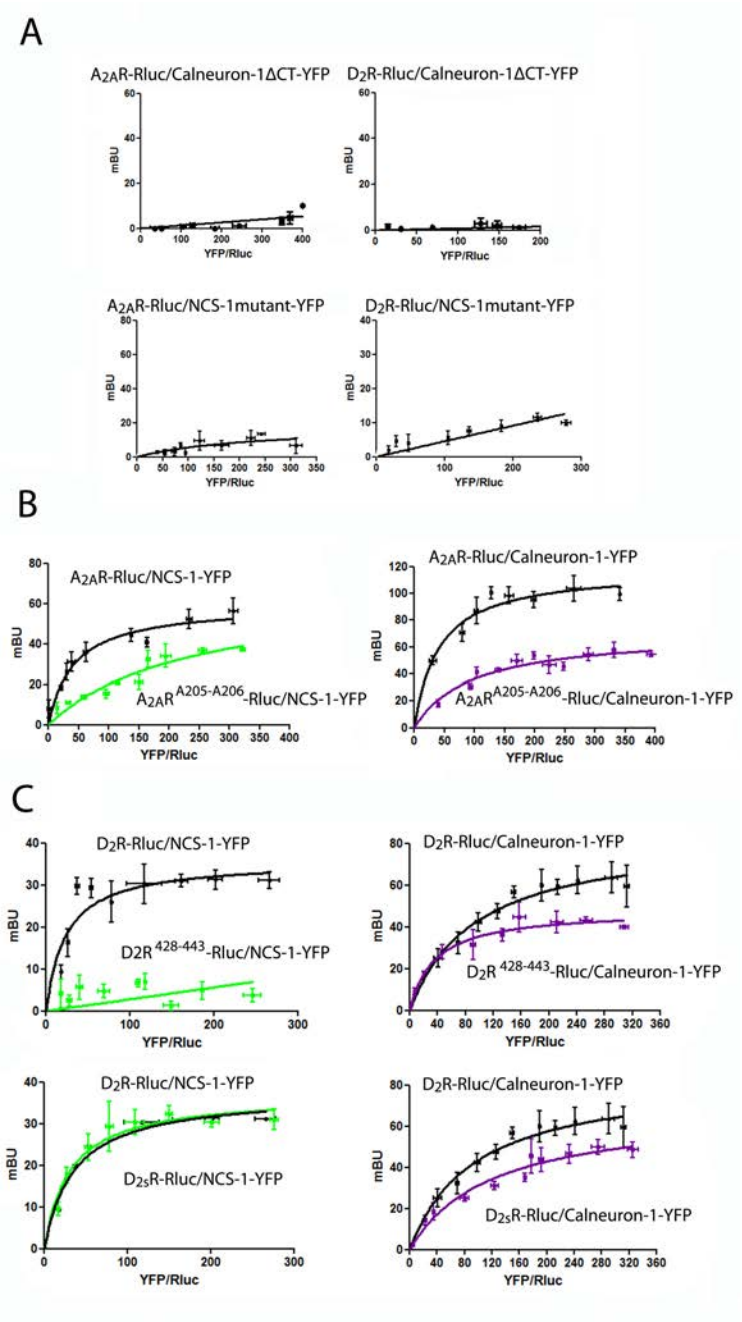

Figure S1, related to Figures 2 and 3. Molecular determinants involved in NCS-1 or calneuron-1 interaction with $A_{2A}R$ and D_2R

A. BRET experiments in HEK-293T cells in cells transfected with $A_{2A}R$-Rluc cDNA (0.2 µg; left panels) or D_2R-Rluc cDNA (0.3 µg; right panels) and calneuron-1ΔCT-YFP cDNA (0.4 µg to 1.2 µg; bottom panels) or myristoylation-deficient YFP-NCS-1 cDNA (0.2 µg to 0.8 µg; bottom panels). **B.** BRET saturation experiments in HEK-293T cells transfected with mutant $A_{2A}R^{A205\text{-}A206}$-Rluc cDNA (0.2 µg) and increasing amounts of NCS-1-YFP cDNA (0.2 µg to 0.8 µg; green curve) or calneuron-1-YFP cDNA (0.4 µg to 1.2 µg; purple curve) and compared

with control cells transfected with $A_{2A}R$ cDNA (0.2 µg; black curves). **C.** BRET saturation experiments in HEK-293T cells transfected with mutant $D_2R^{428-443}$-Rluc cDNA (0.25 µg; top graphs) or $D_{2s}R$-Rluc cDNA (0.25 µg; bottom graphs) and increasing amounts of NCS-1-YFP cDNA (0.2 µg to 0.8 µg; green curves) or calneuron-1-YFP cDNA (0.4 µg to 1.2 µg; purple curves) and compared with control cells transfected with D_2R cDNA (0.3 µg; black curves). BRET, expressed as miliBRET units (mBU), is given as a function of 1000 x the ratio between the fluorescence of the acceptor (YFP) and the luciferase activity of the donor (Rluc). Values are means ± S.E.M. of 5 to 7 different experiments.

A

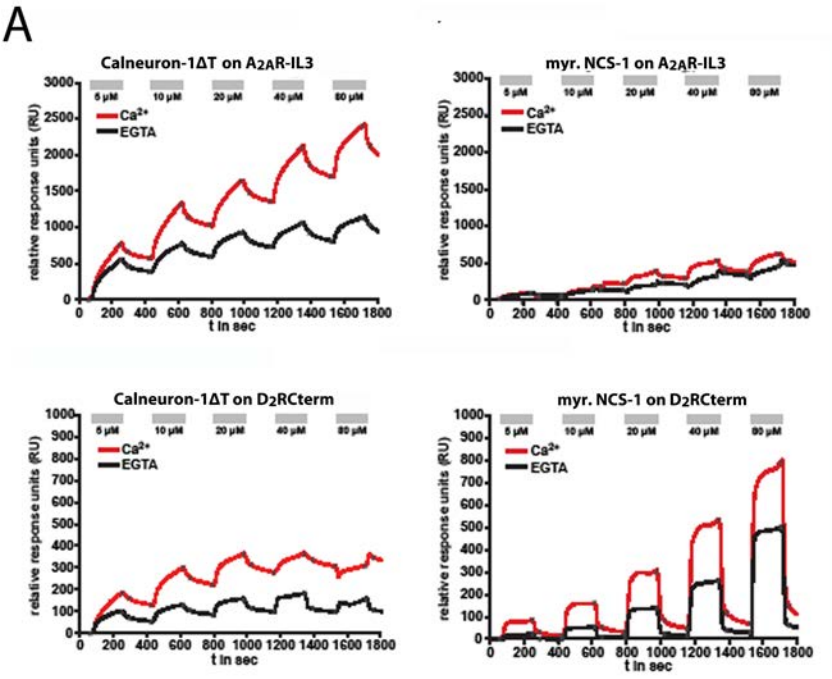

B

	Molar binding activity	
Protein	Calcium	EGTA
$A_{2A}R$-IL3/myr. NCS-1	$3.6x\ 10^2$	$3.2x\ 10^2$
$A_{2A}R$-IL3/Calneuron-1ΔT	$7.2x\ 10^2$	$3.6x\ 10^2$
D_2RCterm/myr. NCS-1	$6.1x10^3$	$2.8x10^3$
D_2RCterm/Calneuron-1ΔT	$6.3x10^3$	$2.1x10^3$

Figure S2, related to Figures 2 and 3. The NCS-1 and calneuron-1 binding to $A_{2A}R$ third intracellular loop and to D_2R C-terminal domain determined by surface plasmon resonance

A. Net sensograms corresponding to the interaction of His_6SUMO-calneuron-1ΔCT and myristoylated NCS-1 on immobilized GST-$A_{2A}R$-IL3 and D_2R-Cterm using surface plasmon resonance (SPR). Surface plasmon resonance was performed in single cycle mode using increasing amounts of injected His_6SUMO-calneuron-1ΔCT (calneuron-1ΔCT) or myristoylated NCS-1 (myr. NCS-1), shown in the grey boxes on top of each sensogram. Sensograms were recorded in single cycle mode at a flow rate of 10 µl/min and with 180 s analyte injections at concentrations of 5 µM, 10 µM, 20 µM, 40 µM and 80 µM. All runs were

performed in HBS-P buffer supplemented with 500 µM Ca^{2+}/1 mM Mg^{2+} (red traces) or 2 mM EGTA/1 mM Mg^{2+} (black traces) Net sensograms were calculated by subtracting response units obtained after analyte injections on control surfaces (GST for GST-A_{2A}R-IL3 and blank CM5 surface for D_2R-Cterm) and in case of His_6SUMO-calneuron-1ΔCT also of response units obtained from injections of the His_6SUMO-tag only. The molar binding activity (MBA) was calculated from the stability point of last injection considering the molecular mass of the analyte as well as the amount of ligand immobilized on the surface of the sensor chip surface as described by Catimel at al. (1997). Stability points used to calculate the molar binding activity (MBA) are shown in grey crosses on the individual traces. In all cases higher response units (RUs) were obtained in the presence of Ca^{2+}. **B.** Molar binding activities.

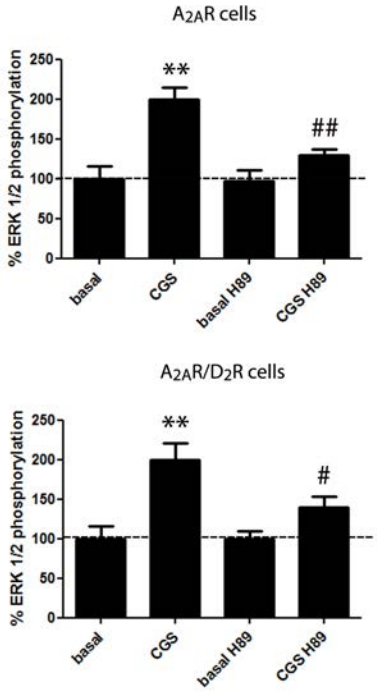

Figure S3, related to Figure 7. G-protein-cAMP-PKA-dependent A_{2A}R-mediated MAPK activation

ERK1/2 phosphorylation in HEK-293T cells transfected with A_{2A}R-Rluc cDNA (0.3 µg) alone (top graph) or A_{2A}R-Rluc cDNA (0.3 µg) and D_2R-YFP cDNA (0.5 µg) (bottom graph). Cells were pre-treated or not with the PKA inhibitor H98 (10 µM for 30 min) and were stimulated with the A_{2A}R agonist CGS 21680 (CGS; 100 nM). ERK1/2 phosphorylation levels are expressed as percentage over basal, represented by a dotted line. Values are given as means ± S.E.M. of 6 different experiments. One way ANOVA followed by a Bonferroni multiple comparison *post hoc* test: $^{**}p < 0.01$, compared to basal; $^{\#}p < 0.05$ and $^{\#\#}p < 0.01$, compared to CGS alone.

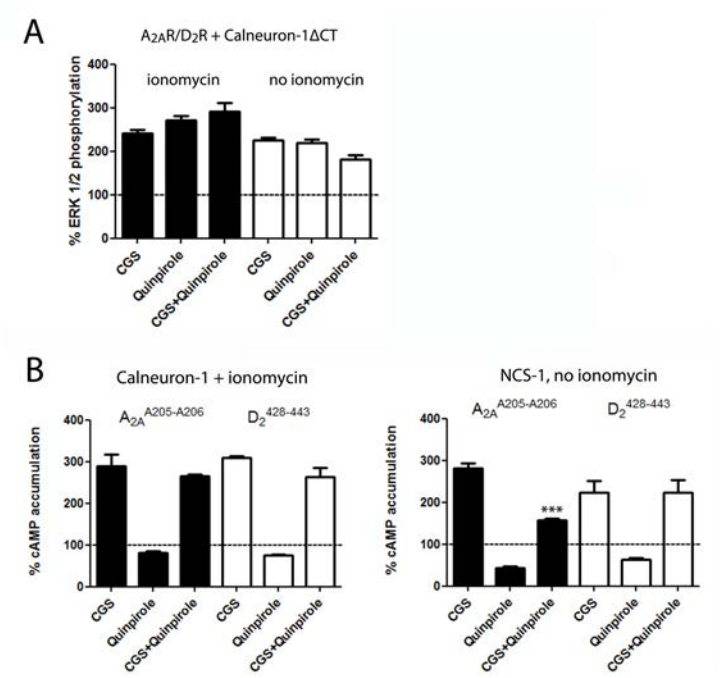

Figure S4, related to Figure 4. Specificity of NCS-1- and calneuron-1-mediated modulation of the signaling of $A_{2A}R$-D_2R heteromer in transfected cells

A. ERK1/2 phosphorylation in HEK-293T cells transfected with $A_{2A}R$-Rluc cDNA (0.3 µg), D_2R-YFP cDNA (0.4 µg) and calneuron-1ΔCT cDNA (0.6 µg). Cells were not stimulated (basal, dotted line) or stimulated with the $A_{2A}R$ agonist CGS 21680 (CGS; 100 nM), the D_2R agonist quinpirole (1 µM) in the absence (black bars) or the presence (white bars) of ionomycin (1 µM). **B.** In the left graph, cAMP accumulation in HEK-293T cells transfected with $A_{2A}R^{A205\text{-}A206}$-Rluc mutant cDNA (0.3 µg), D_2R-YFP cDNA (0.4 µg) and calneuron-1 cDNA (0.6 µg) (black bars) or $A_{2A}R$-Rluc cDNA (0.3 µg), $D_2R^{428\text{-}443}$-YFP mutant cDNA (0.4 µg) and calneuron-1 cDNA (0.6 µg) (white bars) in the presence of ionomycin (1 µM). In the right graph, HEK-293T cells transfected with $A_{2A}R^{A205\text{-}A206}$-Rluc mutant cDNA (0.3 µg), D_2R-YFP cDNA (0.4 µg) and NCS-1 cDNA (0.5 µg) (black bars) or $A_{2A}R$-Rluc cDNA (0.3 µg), $D_2R^{428\text{-}443}$-YFP mutant cDNA (0.4 µg) and NCS-1 cDNA (0.5 µg of cDNA transfected) (white bars) in the absence of ionomycin. Cells were stimulated with the $A_{2A}R$ agonist CGS 21680 (CGS; 100 nM) or the D_2R agonist quinpirole (1 µM) or both. In **A**, values are expressed as the percentage of basal (100%, dotted line) and are means ± S.E.M. of 4 to 6 different experiments. In **B**, cAMP accumulation is expressed as the percentage of basal or forskolin values (dotted line) and are means ± S.E.M. of 4 to 6 different experiments. One way ANOVA followed by Dunnett's multiple comparison *post hoc* test: ***$p < 0.001$ compared to CGS alone.

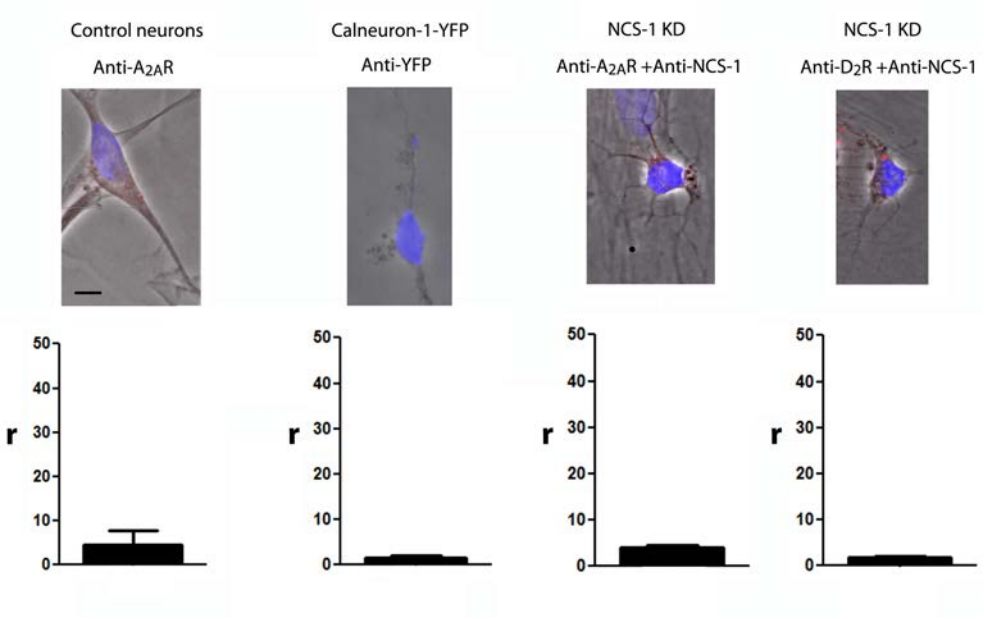

Figure S5, related to Figures 5 and 6. Negative controls for PLA experiments in neuronal primary cultures

In situ proximity ligation assays *(*PLA) in primary cultures of rat striatal neurons with calneuron-1-YFP cDNA (1 μg) or NCS-1 shRNA cDNA (1.5 μg). PLA was performed with primary antibodies against $A_{2A}R$, GFP, $A_{2A}R$ and NCS-1 or D_2R and NCS-1. Confocal microscopy images are shown (superimposed sections) in which very few red clusters appear in neurons detected by phase contrast. Scale bars = 20 μm. Cell nuclei were stained with Hoesch (blue). Bars represent the quantification of ratio *r* values (number of red spots/cell containing spots) corresponding to the different conditions. Data are means ± SEM of counts in 20-30 different neurons of three independent preparations.

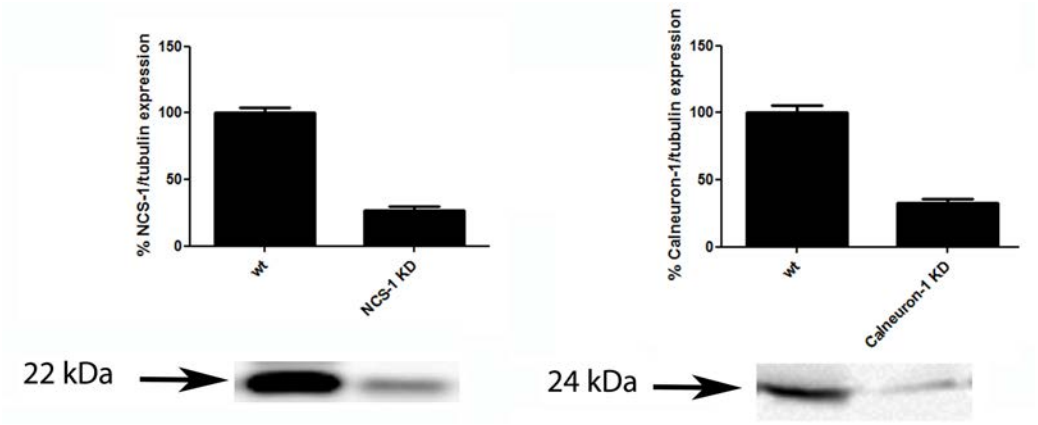

Figure E6, related to Figures 5 and 6. Silencing NCS-1 or calneuron-1 on rat striatal neurons

Rat striatal primary cultures not transfected (wt) or transfected with NCS-1 shRNA cDNA (NCS-1 KD; 1.5 μg) or calneuron-1 shRNA cDNA (calneuron-1 KD, 1.5 μg). Membranes from primary cultures were analyzed by SDS-PAGE and immunoblotted with anti-NCS-1 or anti-calneuron-1 antibodies. Representative Western blots are shown.

SUPPLEMENTAL EXPERIMENTAL PROCEDURES

Resonance Energy Transfer experiments

For Bioluminescence Resonance Energy Transfer (BRET) experiments, HEK-293T cells transiently co-transfected with a constant amount of cDNA encoding for the protein fused to RLuc and with increasingly amounts of cDNA corresponding to the protein fused to YFP (see figure legends) were used after 48 h transfection. To quantify protein-YFP expression, fluorescence of cells (20 µg protein) was read in a Fluoro Star Optima Fluorimeter (BMG Labtechnologies, Offenburg, Germany) equipped with a high-energy xenon flash lamp, using a 10 nm bandwidth excitation filter at 400 nm reading. For BRET measurements, 5 µM of coelenterazine H (Molecular Probes, Eugene, OR) was added to the equivalent of 20 µg of cell suspension. After 1 minute, the readings were collected using a Mithras LB 940 that allows the integration of the signals detected in the short-wavelength filter at 485 nm and the long-wavelength filter at 530 nm. To quantify protein-RLuc expression, luminescence readings were also performed after 10 minutes of adding 5 µM coelenterazine H. The net BRET is defined as [(long-wavelength emission)/(short-wavelength emission)]-Cf where Cf corresponds to [(longwavelength emission)/(short-wavelength emission)] for the donor construct expressed alone in the same experiment. Data were fitted to a non-linear regression equation, assuming a single-phase saturation curve with GraphPad Prism software (San Diego, CA, USA). BRET is expressed as miliBRET units, mBU (net BRET x 1000).

For Sequential Resonance Energy Transfer (SRET) assays, HEK-293T cells were transiently co-transfected with constant amounts of cDNAs encoding for both proteins fused to RLuc and GFP^2 and with increasingly amounts of cDNA corresponding to the protein fused to YFP. In SRET, the oxidation of the Rluc substrate DeepBlueC by protein-Rluc triggers protein-GFP^2 excitation (BRET), which triggers a subsequent excitation of protein-YFP (FRET). Emission of YFP after addition of DeepBlueC is only possible if the three fusion proteins are in close proximity (<10 nm), allowing sequential bioluminescent and fluorescent resonance energy transfer to occur. Cells were used 48 h post-transfection. Using aliquots of transfected cells (20 µg of protein), different determinations were performed in parallel: (i) Quantification of protein-YFP expression was performed as indicated in BRET experiments. (ii) For quantification of protein-Rluc expression cells were distributed in 96-well microplates (Corning 3600, white plates with White bottom), and luminescence was determined 10 min after addition of 5 µM coelenterazine H in a Mithras LB 940 multimode reader. (iii) For SRET, cells were distributed in 96-well microplates (Corning 3600, white plates with white bottom), and 5 µM DeepBlueC (Molecular Probes, Eugene, OR) was added. The SRET signal was collected using a Mithras LB 940 reader with detection filters for short wavelength (410 nm) and long wavelength (530 nm). By analogy with BRET, net SRET is defined as ((long wavelength emission)/(short wavelength emission)) - Cf, where Cf corresponds to long wavelength emission/short wavelength emission for cells expressing protein-Rluc and protein-GFP^2. Linear unmixing was done for SRET quantification, taking into account the spectral signature to separate the two fluorescence emission spectra. SRET is expressed as miliSRET units, mSU (net SRET x 1000). Data were fitted as in BRET experiments.

3.7. QUATERNARY STRUCTURE OF A G-PROTEIN-COUPLED RECEPTOR HETEROTETRAMER IN COMPLEX WITH G_I AND G_S

Gemma Navarro[*], Arnau Cordomí[*], Monika Zelman-Femiak[*], Marc Brugarolas, Estefanía Moreno, **David Aguinaga**, Laura Perez-Benito, Antoni Cortés, Vicent Casadó, Josefa Mallol, Enric I. Canela, Carme Lluís, Leonardo Pardo, Ana J. García-Sáez, Peter J. McCormick y Rafael Franco.

[*]Coautores del manuscrito

Manuscrito publicado en *BioMed Central Biology*, abril 2016; 14:26.

Los receptores acoplados a proteína G (GPCR), en forma de monómeros o homodímeros que se unen a proteínas G heterotriméricas son fundamentales en la transferencia de estímulos extracelulares a las vías de señalización intracelular. Distintos GPCRs también pueden interaccionar para formar heterómeros que son nuevas unidades de señalización. A pesar del crecimiento exponencial en el número de estructuras cristalinas de GPCR resueltas, las propiedades estructurales del heterómero permanecen desconocidas. En este trabajo han sido utilizados experimentos de seguimiento de una sola partícula en células que expresan receptores funcionales de adenosina A_1-A_{2A} fusionados a proteínas fluorescentes para mostrar la pérdida de movimiento browniano del receptor A_1 en presencia del receptor A_{2A} y una preponderancia a nivel de superficie celular de los complejos heteroméricos 2:2 (dímero de dímeros). Mediante sistemas de modelaje computacional, ayudado por ensayos de transferencia de energía por resonancia bioluminiscente para estudiar la homomerización y heteromerización y el acoplamiento a la proteína G, han sido predichas las regiones de interacción y ha sido propuesta una estructura cuaternaria del tetrámero de GPCRs en complejo con dos proteínas G. La combinación de resultados apunta a una arquitectura molecular formada por un heterotetrámero en forma de rombo, que está unido a dos proteínas G heterotriméricas distintas (G_i y G_s) y que interactúan simultáneamente con el complejo. Estos nuevos resultados constituyen un avance importante en la comprensión de la complejidad molecular relacionada con la función de los GPCRs.

Navarro et al. BMC Biology (2016) 14:26
DOI 10.1186/s12915-016-0247-4

BMC Biology

RESEARCH ARTICLE Open Access

Quaternary structure of a G-protein-coupled receptor heterotetramer in complex with G_i and G_s

Gemma Navarro[1,2,3†], Arnau Cordomí[4†], Monika Zelman-Femiak[5,6†], Marc Brugarolas[1,2,3], Estefania Moreno[1,2,3], David Aguinaga[1,2,3], Laura Perez-Benito[4], Antoni Cortés[1,2,3], Vicent Casadó[1,2,3], Josefa Mallol[1,2,3], Enric I. Canela[1,2,3], Carme Lluís[1,2,3], Leonardo Pardo[4†], Ana J. García-Sáez[5,6,7†], Peter J. McCormick[1,2,3,8*†] and Rafael Franco[1,2,3*†]

Abstract

Background: G-protein-coupled receptors (GPCRs), in the form of monomers or homodimers that bind heterotrimeric G proteins, are fundamental in the transfer of extracellular stimuli to intracellular signaling pathways. Different GPCRs may also interact to form heteromers that are novel signaling units. Despite the exponential growth in the number of solved GPCR crystal structures, the structural properties of heteromers remain unknown.

Results: We used single-particle tracking experiments in cells expressing functional adenosine A_1-A_{2A} receptors fused to fluorescent proteins to show the loss of Brownian movement of the A_1 receptor in the presence of the A_{2A} receptor, and a preponderance of cell surface 2:2 receptor heteromers (dimer of dimers). Using computer modeling, aided by bioluminescence resonance energy transfer assays to monitor receptor homomerization and heteromerization and G-protein coupling, we predict the interacting interfaces and propose a quaternary structure of the GPCR tetramer in complex with two G proteins.

Conclusions: The combination of results points to a molecular architecture formed by a rhombus-shaped heterotetramer, which is bound to two different interacting heterotrimeric G proteins (G_i and G_s). These novel results constitute an important advance in understanding the molecular intricacies involved in GPCR function.

Keywords: GPCR, Heterotetramer, Heterotrimeric G protein, Single-particle tracking, BRET, Molecular modeling

Background

G-protein-coupled receptor (GPCR) oligomerization is heavily supported by recent biochemical and structural data [1–6]. Optical-based techniques are instrumental in studying the dynamics and organization of receptor complexes in living cells [7]. For instance, total internal reflection fluorescence microscopy shows that 30 % of muscarinic M1 receptors exist as dimers (with no evidence of higher oligomers) that undergo interconversion with monomers on a timescale of seconds [8]. Similarly, the β_1-adrenergic receptors (β_1-AR) are expressed as a mixture of monomers and dimers whereas β_2-adrenergic receptors (β_2-AR) have a tendency to form dimers and higher-order oligomers [9]. Moreover, the monomer-dimer equilibrium of the chemoattractant *N-formyl* peptide receptor at a physiological level of expression lies within a timescale of milliseconds [10]. Together, these studies in heterologous systems show that a given GPCR is present in a dynamic equilibrium between monomers, dimers, and higher-order oligomers.

Studies in a broad spectrum of GPCRs [11–14] show that these receptors may form heteromers. GPCR heteromers are defined as novel signaling units with functional properties different from homomers and they represent a completely new field of study [15]. Innovative crystallographic techniques have permitted researchers to obtain crystal structures of GPCR families A, B, C, and F, bound to either agonists, antagonists, inverse agonists or allosteric modulators; in the form of monomers or homo-oligomers; and in complex with a G protein or

* Correspondence: p.mccormick@uea.ac.uk; rfranco123@gmail.com
†Equal contributors
[1]Centro de Investigación Biomédica en Red sobre Enfermedades Neurodegenerativas (CIBERNED), Madrid, Spain
Full list of author information is available at the end of the article

with a ß-arrestin [16]. However, crystal structures of GPCR heteromers have not yet been obtained. Here, we propose a quaternary structure of a heteromer, taking into account the molecular stoichiometry and the interacting G proteins. Adenosine A_1-A_{2A} receptor (A_1R-$A_{2A}R$) complexes constitute a paradigm in the GPCR heteromer field because A_1R is coupled to G_i and $A_{2A}R$ to G_s; that is, they transduce opposite signals in cyclic adenosine monophosphate (cAMP)-dependent intracellular cascades. First described as a concentration-sensing device in striatal glutamatergic neurons [17], the A_1R-$A_{2A}R$ heteromer is thought to function as a G_s/G_i-mediated switching mechanism by which low and high concentrations of adenosine inhibit and stimulate, respectively, glutamate release [17, 18]. The structural basis of this switch is key to understanding heteromer function and the biological advantage behind the GPCR heteromerization phenomenon. Here, we have devised the molecular architecture of the adenosine A_1R-$A_{2A}R$ heteromer in complex with G proteins using a combination of microscope-based single-particle tracking, molecular modeling, and energy transfer assays in combination with molecular complementation. The results point to A_1 and A_{2A} receptors organizing into a rhombus-shaped heterotetramer that couples to G_i and G_s. The overall structure is very compact and provides interacting interfaces for GPCRs and for G proteins.

Results and discussion

Reciprocal restriction of adenosine receptor motion in the plasma membrane

To examine the dynamics of A_1R-$A_{2A}R$ heteromers in the plasma membrane of a living cell, the motion of the receptors tagged with fluorescent proteins (A_1R-green fluorescent protein [GFP] or $A_{2A}R$-mCherry) was measured by real-time single-particle tracking (SPT) (Fig. 1). Examples of fluorescent images and individual particle trajectories are shown in Additional file 1: Figure S1. Analysis of data corresponding to 500 A_1R-GFP particles showed a linear relationship between the mean square displacement (MSD) versus time lag in the trajectories of up to 1600 single fluorescent particles (Fig. 1a, c). This is typical for Brownian diffusion, indicating a lack of restrictions in A_1R-GFP motion. Co-expression of $A_{2A}R$-mCherry (Fig. 1b) led to a reduction in the lateral mobility of A_1R-GFP, which became confined to plasma membrane regions of 0.461 ± 0.004 μm in diameter. Its diffusion coefficient decreased from 0.381 ± 0.002 $\mu m^2/s$ to 0.291 ± 0.003 $\mu m^2/s$ ($p = 0.002$, one-tailed t-test). Similarly, A_1R-GFP also decreased the $A_{2A}R$-mCherry diffusion coefficient from 0.317 ± 0.002 $\mu m^2/s$ to 0.143 ± 0.005 $\mu m^2/s$ ($p < 0.0001$) (Fig. 1d–f). $A_{2A}R$ moved within a confinement zone of 0.941 ± 0.007 μm in diameter that was reduced to 0.360 ± 0.001 μm ($p < 0.0001$) when both receptors were co-expressed. We conclude from these mobility comparisons that reciprocally restricted motion of the individual receptor particles must be due to A_1R-$A_{2A}R$ receptor-receptor interactions.

Stoichiometry of A_1 and A_{2A} receptor heterocomplexes

The stoichiometry of the fluorescent receptors on the cell surface can be calculated from the brightness distribution of the individual particles [19] (see "Methods"). In cells expressing A_1R-GFP, we found the majority of clusters to consist of either two (~47 %) or four (~34 %) receptors, and clusters with one or three receptors were scarce (~10 % and ~9 %, respectively) (Additional file 2: Figure S2A and black bars in Additional file 2: Figure S2C). In the case of $A_{2A}R$-mCherry, the stoichiometry analysis showed that the clusters mostly expressed trimers (45 %), with dimers (29 %) and tetramers (12 %) the second and third most common populations (Additional file 2: Figure S2D and black bars in Additional file 2: Figure S2F). Remarkably, this stoichiometry for either A_1 or A_{2A} receptors was altered when the partner receptor was also expressed. In cells co-expressing A_1R-GFP and $A_{2A}R$-mCherry, the dimer population increased (57 % for A_1R-GFP and 49 % for $A_{2A}R$-mCherry, blue bars in Additional file 2: Figures S2C, F) and became the predominant species (Additional file 2: Figures S2B, C, E, F).

In order to focus the analysis on heteromer complexes, we identified clusters containing both receptors (individual yellow dots in Fig. 1g, displaying both GFP and mCherry fluorescence). In ~1000 analyzed co-localized clusters that consisted of a mixture of A_1-GFP and A_{2A}-Cherry (yellow dots in Fig. 1g), we found a similar high amount of dimers of A_1R (75 %, left panel in Fig. 1h and green bar in Fig. 1i) and $A_{2A}R$ (74 %, right panel in Fig. 1h and red bar in Fig. 1i). Trimers and tetramers of A_1R, and monomers and tetramers of $A_{2A}R$, were in the minority or negligible (see Fig. 1h, i). In summary, given that the percentage of dimers of either A_1R-GFP or $A_{2A}R$-mCherry in the yellow dots (which show co-localization of the two receptors) was similar and high (~75 %), the heterotetramer containing two A_1Rs and two $A_{2A}R$s must have been the most predominant species. To our knowledge, this is the first stoichiometry data for a GPCR heteromer in living cells.

Arrangement of G proteins interacting with A_1 and A_{2A} receptors

Monomeric GPCRs are capable of activating G proteins [20]. However, recent findings suggest that one GPCR homodimer bound to a single G protein may be a common functional unit [21]. Thus, an emerging question is how G proteins couple to GPCR heteromers. Because A_1R selectively couples to G_i and $A_{2A}R$ to G_s [22], the

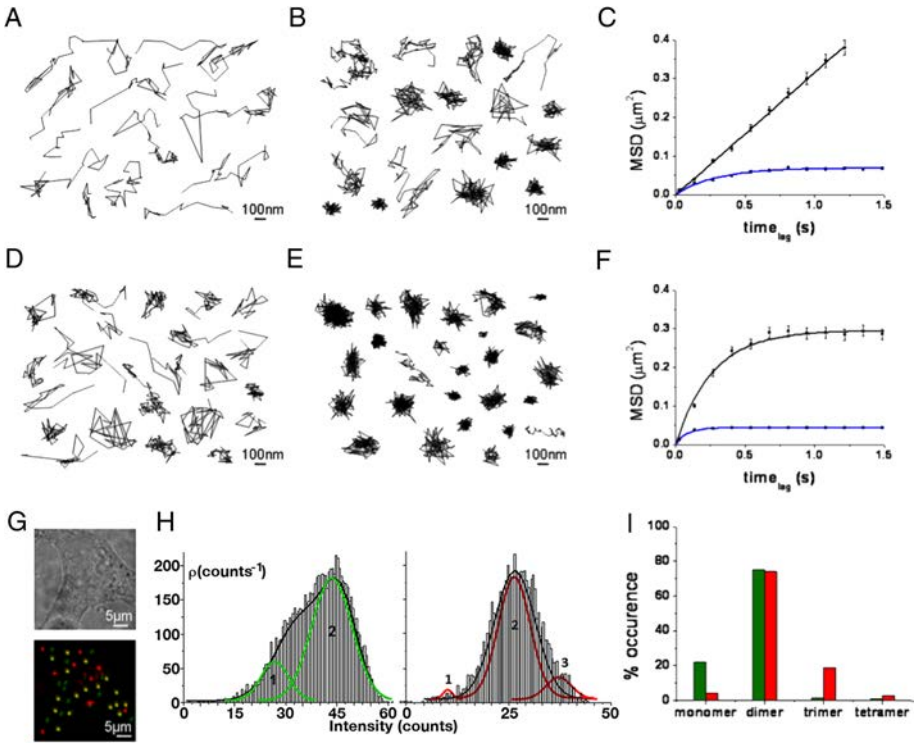

Fig. 1 Cell surface mobility of A_1R-GFP and A_{2A}R-mCherry. Individual trajectories of particles containing GFP fused to the C-terminus of A_1R (A_1-GFP) (**a** and **b**) or mCherry fused to the C-terminus of A_{2A}R (A_{2A}-mCherry) (**d** and **e**) on HEK-293T cells expressing A_1-GFP (a), A_{2A}-mCherry (d) or both (b and e). The trajectory and the fluorescence intensity of the individual particles were recorded over time using total internal reflection microscopy (TIRFM) and an electron multiplying charged-coupled device (EMCCD) camera recording. Receptor motion was determined by plotting (versus time lag) the mean square displacement (*MSD*) of A_1-GFP (**c**) in the absence (*black line*) or presence of A_{2A}-mCherry (*blue line*), or A_{2A}-mCherry (**f**) in the presence (*black line*) or presence of A_1-GFP (*blue line*). Data sets were fitted to mathematical models of free and confined diffusion for A_1R and A_{2A}R respectively. **g** Co-localization of A_1-GFP and A_{2A}-mCherry is observed (*yellow dots*). Scale bar: 100 nm. **h** Distribution of the fluorescence signal of A_1-GFP (*left*) and A_{2A}-mCherry (*right*) within co-localized receptors (*yellow dots* in g). Curves approximately delineate the number of monomers, dimers, or trimers within the co-localized complex. **i** Stoichiometry analysis performed for co-localized A_1-GFP and A_{2A}-mCherry receptor particles co-expressed in HEK-293T cells (*yellow dots* in g). *Green* corresponds to A_1-GFP and *red* to A_{2A}-mCherry

working hypothesis was that both G_i and G_s proteins may couple to the A_1R-A_{2A}R heterotetramer. To test this hypothesis, we used bioluminescence resonance energy transfer (BRET) assays [23]. In agreement with the SPT experiments (see above), homodimers and heterodimers were detected by BRET assays in cells expressing A_1R fused with *Renilla* luciferase (A_1R-Rluc) or yellow fluorescent protein (A_1R-YFP) (Fig. 2a), A_{2A}R-Rluc and A_{2A}R-YFP (Fig. 2b), or A_1R-Rluc and A_{2A}R-YFP (Fig. 2e). Neither A_1R-Rluc nor A_{2A}R-YFP interacted with the ghrelin receptor 1a fused to YFP (GHS1a-YFP), used as a control as a protein unable to directly interact with these adenosine receptors (Fig. 2a, b). In order to test the presence of the two G proteins in the heterotetramer, we transfected cells with minigenes that code for peptides blocking either G_i or G_s binding to GPCRs [24]. In addition, cells were treated with pertussis or cholera toxins that catalyze ADP-ribosylation of G_i or G_s. Clearly, treating cells with pertussis toxin, or expressing the minigene-coded peptide that blocks α_i coupling, reduced the value of $BRET_{max}$ for A_1R-A_1R homodimers (Fig. 2a) and for A_1R-A_{2A}R heterodimers (Fig. 2e) but not for A_{2A}R-A_{2A}R homodimers (Fig. 2b). This indicates that G_i is coupled to A_1R in both the homodimer and the heterodimer. Similarly, blocking G_s-receptor interaction using cholera toxin or a minigene-coded peptide that blocks α_S coupling reduced $BRET_{max}$ for A_{2A}R-A_{2A}R homodimers (Fig. 2b) and for A_1R-A_{2A}R heterodimers (Fig. 2e) but not for A_1R-A_1R homodimers (Fig. 2a). Interestingly, BRET curves showed sensitivity to both cholera and pertussis toxins in cells expressing either A_1R-Rluc-A_1R-YFP and A_{2A}R (Fig. 2c) or A_{2A}R-Rluc-A_{2A}R-YFP and A_1R (Fig. 2d). Functionality of constructs and controls in cells expressing minigenes, and in cells expressing the ghrelin GHS1a receptor instead of one of the adenosine receptors, are shown in Additional file 3: Figure S3. To further confirm that G_i binds A_{2A}R in the receptor heteromer, the energy transfer between Rluc fused to the N-terminal domain of the α-subunit of G_i (G_i-Rluc) and A_{2A}R-YFP was analyzed in

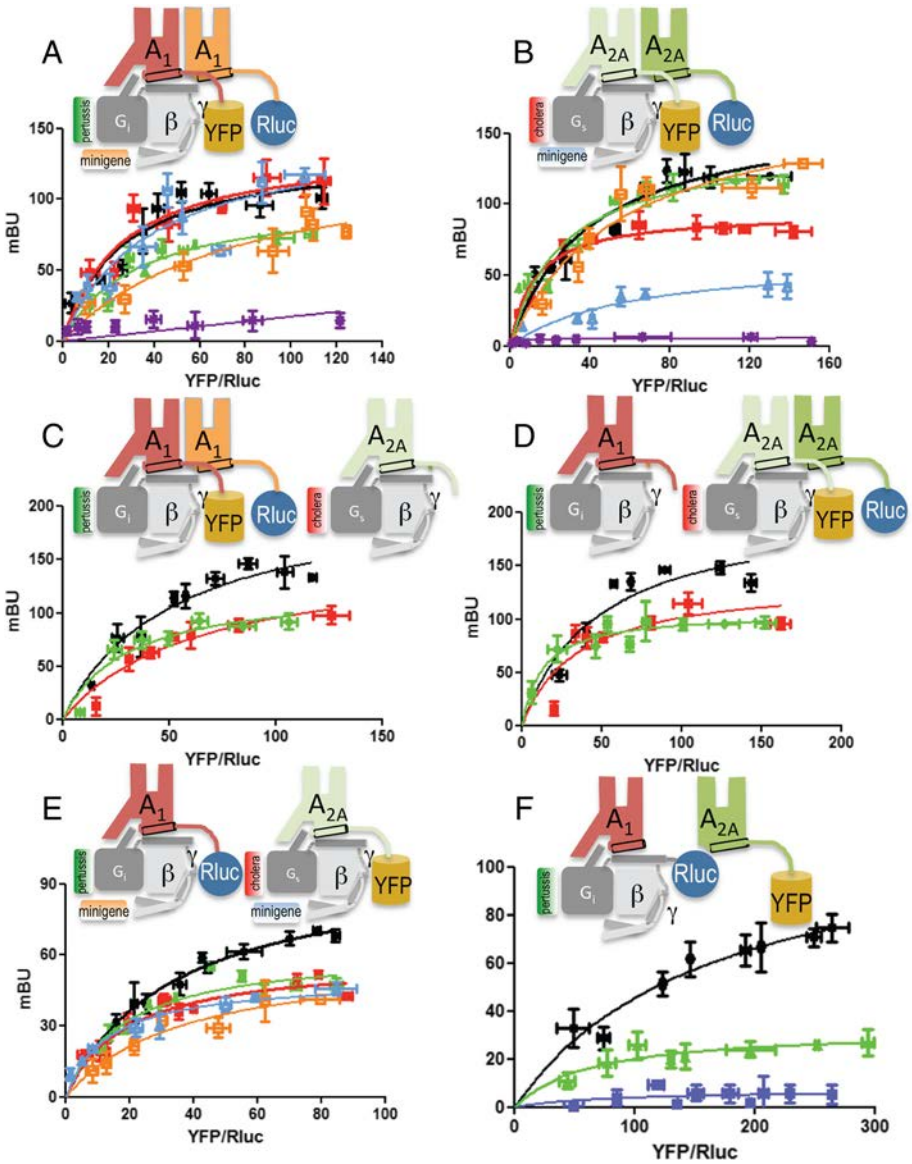

Fig. 2 Influence of G proteins on A_1R and $A_{2A}R$ homodimerization and heterodimerization. B Bioluminescence resonance energy transfer (BRET) saturation curves were performed in HEK-293T cells 48 h post-transfection with (**a**, **c**) 0.3 μg of cDNA corresponding to A_1R-Rluc and increasing amounts of A_1R-YFP (0.1–1.5 μg cDNA) or GHS1a-YFP (0.25–2 μg cDNA) as negative control (a, *purple line*), without (a) or with (c) 0.15 μg of cDNA corresponding to $A_{2A}R$; (**b**, **d**) 0.2 μg of cDNA corresponding to $A_{2A}R$-Rluc and increasing amounts of $A_{2A}R$-YFP (0.1–1.0 μg cDNA) or GHS1a-YFP (0.25–2 μg cDNA) as negative control (b, *purple line*), without (b) or with (d) 0.5 μg of cDNA corresponding to A_1R; (**e**) 0.3 μg of cDNA corresponding to A_1R-Rluc and increasing amounts of A_{2AR}-YFP (0.1–1.0 μg cDNA); and (**f**) 0.5 μg of cDNA corresponding to A_1R (except control *blue curves* that were obtained in cells not expressing A_1R), 2 μg of cDNA corresponding to G_i-Rluc, and increasing amounts of $A_{2A}R$-YFP (0.1–0.5 μg cDNA). In panels a, b, and e, cells were also transfected with 0.5 μg of cDNA corresponding to the G_i-related (*orange curves*) or G_s-related (*blue curves*) minigenes. Cells were treated for 16 h with medium (*black curves*), with 10 ng/ml of pertussis toxin (*green curves*), or with 100 ng/ml of cholera toxin (*red curves*) prior to BRET determination. To confirm similar donor expressions (approximately 100,000 bioluminescence units) while monitoring the increase in acceptor expression (1000–40,000 fluorescence units), the fluorescence and luminescence of each sample were measured before energy transfer data acquisition. MiliBRET unit (*mBU*) values are the mean ± standard error of the mean of four to six different experiments grouped as a function of the amount of BRET acceptor. In each panel (*top*) a cartoon depicts the proteins to which Rluc and YFP were fused and the presence or not of partner receptors and/or G_s or G_i proteins [schemes in c to f are not intended to illustrate on stoichiometry because the predominant form in cells expressing the two receptors was the heterotetramer containing two A_1 and two A_{2A} receptors (see "Results")]

cells co-expressing or not co-expressing A_1R (Fig. 2f). A hyperbolic BRET curve was observed in the presence of A_1R, but not in its absence, indicating that G_i and G_s are bound to their respective receptor homodimers within the A_1R-$A_{2A}R$ heteromer.

Further, two complementary BRET experiments were performed to determine the orientation of G_i and G_s within the A_1R-$A_{2A}R$ heterocomplex. First, Rluc and YFP were respectively fused to the N-terminal domains of the α-subunit of G_i (α_i-Rluc) and G_s (α_s-YFP) (Fig. 3, bar a); second, they were fused to the N-terminal domain of the γ-subunit (γ-Rluc and γ-YFP) (Fig. 3, bar b). We observed significant energy transfer between γ-Rluc and γ-YFP in cells co-expressing A_1R and $A_{2A}R$ (Fig. 3, bar b) but minimal amounts in negative-control cells (Fig. 3, bars c and d). In cells expressing either A_1R or $A_{2A}R$, the energy transfer between γ-Rluc and γ-YFP was also low (Fig. 3, bars e and f), suggesting that dimers but not tetramers were the most prevalent form of surface receptors in single-transfected cells. These results in co-transfected cells corroborate the 2:2 stoichiometry obtained from analysis of the fluorescence in single particles and are consistent with G_i and G_s binding to these A_1R-$A_{2A}R$ heterotetramers.

Molecular model of G_i and G_s bound to the A_1R-$A_{2A}R$ heterotetramer

To identify the orientation of the G protein in the receptor homodimer, we combined energy transfer assays between α_s-Rluc (Rluc at the N-terminus of the G protein α-subunit) and $A_{2A}R$-YFP (Fig. 4a) with information on transmembrane (TM) interfaces based on crystal structures of GPCRs [3, 4], which have been recently summarized [25]. The observed high-energy transfer using α_s-Rluc and $A_{2A}R$-YFP indicated close proximity between the N-tail of the α-subunit of G_s and the C-tail of $A_{2A}R$. Interestingly, Rluc and YFP in the "monomeric" $A_{2A}R$-G_s complex (see "Methods") point toward distant positions in space (Fig. 4b). Therefore, the observed BRET should occur between Rluc in the G protein α-subunit and a second $A_{2A}R$-YFP protomer. Among all described TM interfaces for receptor homodimerization (see Additional file 4: Figure S4), we propose the TM4/5 interface, which is observed in the oligomeric structure of β_1-AR [4] and in structures derived from coarse-grained molecular dynamics (MD) simulations [26]. In fact, this is the only interface that favors BRET between α_s-Rluc and a second $A_{2A}R$-YFP protomer in a homodimer (Fig. 4c). The homologous A_1R homodimer was built using the same TM4/5 interface as for $A_{2A}R$ (see Additional file 4: Figure S4 and its legend).

The remaining possible TMs able to form heteromeric interfaces are TM1 and TM5/6 (Fig. 5). Both are possible inter-GPCR interfaces as observed in the structure of the μ-opioid receptor (μ-OR) [3]. To discern between these two possibilities, a bimolecular fluorescence complementation strategy was undertaken. For this purpose,

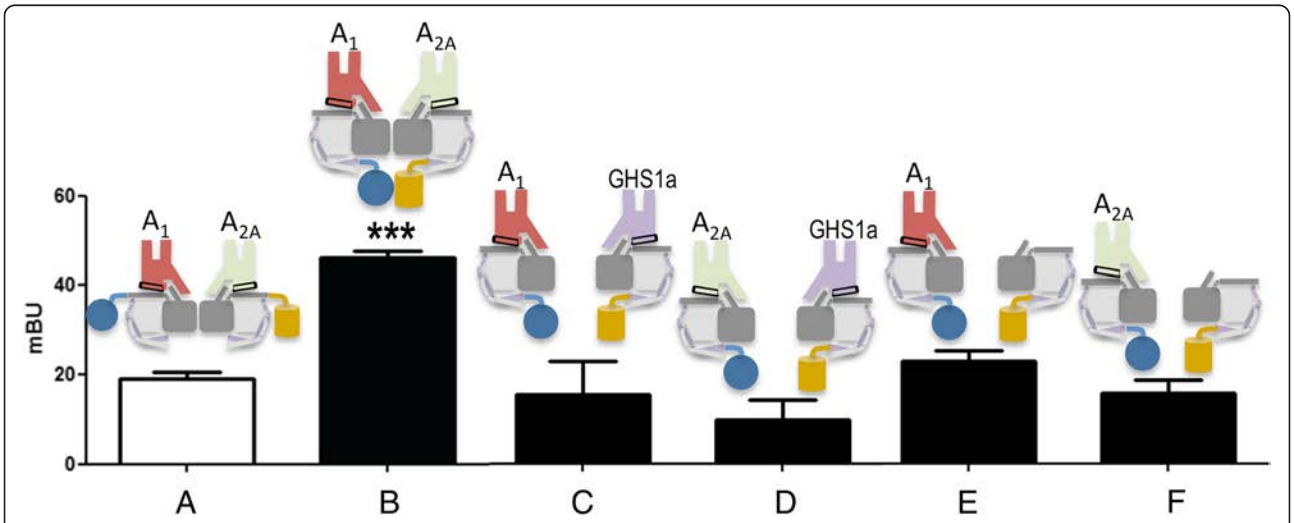

Fig. 3 G_s and G_i coupling to adenosine A_1R-$A_{2A}R$ heterocomplexes. Bioluminescence resonance energy transfer (BRET) experiments were performed in HEK-293T cells 48 h post-transfection with (**a**, **b**) 0.2 μg of cDNA corresponding to A_1R and 0.15 μg of cDNA corresponding to $A_{2A}R$; (**c**, **d**) 0.2 μg of cDNA corresponding to A_1R or 0.15 μg of cDNA corresponding to $A_{2A}R$ and 0.4 μg of cDNA corresponding to growth hormone secretagogue receptor GHS1a; (**e**) 0.2 μg of cDNA corresponding to A_1R; or (**f**) 0.15 μg of cDNA corresponding to $A_{2A}R$. Cells were also transfected with 2 μg of cDNA corresponding to the α-subunit of G_i fused to Rluc and increasing amounts of cDNA corresponding to the α-subunit of G_s fused to YFP (a) or 0.3 μg of cDNA corresponding to the γ-subunit fused to Rluc and increasing amounts of cDNA corresponding to the γ-subunit fused to YFP (b–f). Maximum miliBRET unit (*mBU*) values are the mean ± standard error of the mean of four different experiments. A scheme showing the protein to which Rluc and YFP were fused is provided (*top*). ***$p < 0.001$ by one-way ANOVA with post - hoc Dunnett's test

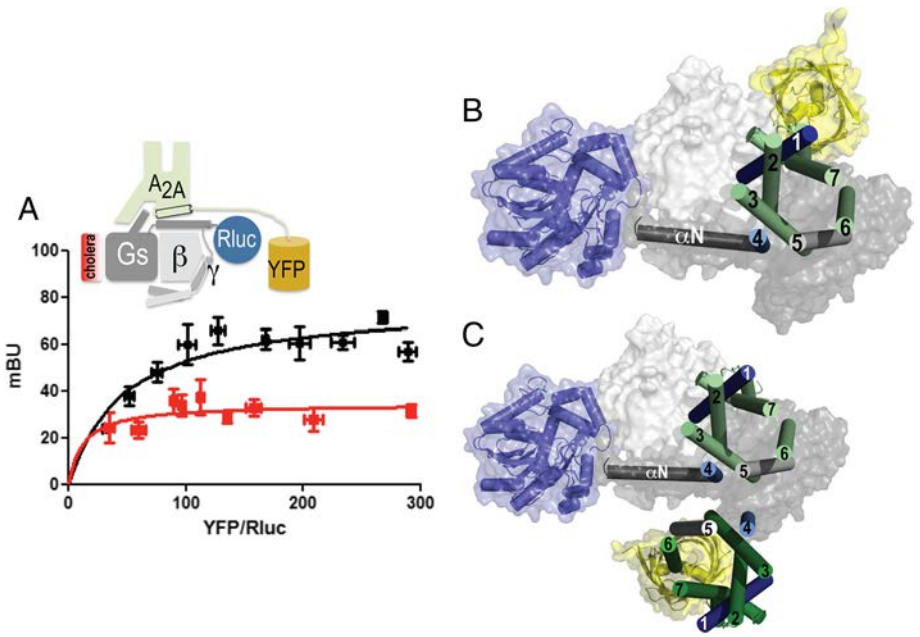

Fig. 4 Orientation of a G protein in a receptor homodimer. Bioluminescence resonance energy transfer (BRET) saturation experiments were performed in HEK-293T cells transfected with 2 μg of cDNA corresponding to the α-subunit of G_s fused to Rluc and increasing amounts of A_{2A}R-YFP (0.1–0.5 μg) cDNA. **a** BRET measurements in cells pretreated for 16 h with medium (*black line*) or with 100 ng/ml of cholera toxin (*red line*). Both fluorescence and luminescence of each sample were measured before every experiment to confirm similar donor expressions (approximately 50,000 bioluminescence units) while monitoring the increase in acceptor expression (1000–10,000 fluorescence units). miliBRET unit (*mBU*) values are the mean ± standard error of the mean of four to five different experiments grouped as a function of the amount of BRET acceptor. A scheme of the placement of donor and acceptor BRET moieties is provided (*top*). **b** Molecular model of the A_{2A}R-G_s complex. Rluc (*blue*) is attached to the N-terminal αN helix of G_s (*gray*), and YFP (*yellow*) is attached to the C-terminal domain of A_{2A}R (*light green*) (see Additional file 9: Figure S9 for details). **c** Arrangement of A_{2A}R homodimers modeled via the TM4/5 interface as observed in the oligomeric structure of β_1-AR [4]. The A_{2A}R protomer bound to α_s is shown in *light green*, whereas the second A_{2A}R-YFP protomer is shown in *dark green*. The molecular model in panel c (BRET between Rluc in G_s α subunit and YFP in a second A_{2A}R protomer; center-to-center distance between Rluc and YFP of 6.5 nm), in contrast to the model shown in panel B (BRET between Rluc in G_s α subunit and YFP in the G-protein bound A_{2A}R protomer; center-to-center distance between Rluc and YFP of 8.3 nm), would favor the observed high-energy transfer (see panel a) between α_s-Rluc and A_{2A}R-YFP

the N-terminal fragment of Rluc8 was fused to A_1R (A_1R-nRluc8) and its C-terminal domain to A_{2A}R (A_{2A}R-cRluc8), which only upon complementation can act as a BRET donor (Rluc8). The BRET acceptor protein was obtained upon complementation of the N-terminal fragment of YFP Venus protein fused to A_1R (A_1R-nVenus) and its C-terminal domain fused to A_{2A}R (A_{2A}R-cVenus). When all four receptor constructs were transfected, we obtained a positive and saturable BRET signal ($BRET_{max}$ of 35 ± 2 mBU and $BRET_{50}$ of 16 ± 3 mBU) that was not obtained for negative controls (Additional file 5: Figure S5). Figure 5a, b shows that the hemi-donor (A_1R-nRluc8 and A_{2A}R-cRluc8) and the hemi-acceptor (A_1R-nVenus and A_{2A}R-cVenus) moieties, placed at the C-terminus of the receptors, can only complement if A_1R-A_{2A}R heterodimerization occurs via the TM5/6 interface. The TM4/5 interface for homodimerization and the TM5/6 interface for heterodimerization give a rhombus-shaped tetramer organization (Fig. 5a). Remarkably, cell pre-incubation with either pertussis or cholera toxins decreased the $BRET_{max}$ by 35 % (Fig. 5c), further suggesting that both G_s and G_i proteins bind to the A_1R-A_{2A}R heterotetramer.

We next evaluated, using computational tools, whether the proposed A_1R-A_{2A}R heterotetramer could couple to both G_i and G_s proteins. Clearly, the external protomers of the proposed A_1R-A_{2A}R heterotetramer can bind to G_i and G_s proteins (Fig. 5d). This model positions the α-subunits of G_i and G_s in close contact, facing the interior of the tetrameric complex, while the N-terminal α-helices of α_i and α_s point outside the complex. The N-terminal α-helices of the γ-subunits are in close proximity, facing the inside (Additional file 6: Figure S6), which explains the significant energy transfer observed between γ-Rluc and γ-YFP (Fig. 3, bar b). The model provides experimental insights into the structural arrangement of heteromers consisting of two GPCRs and coupled to two G proteins, the possibility of which has recently been discussed [25]. We used MD simulations to study the stability of this complex. Additional file 7:

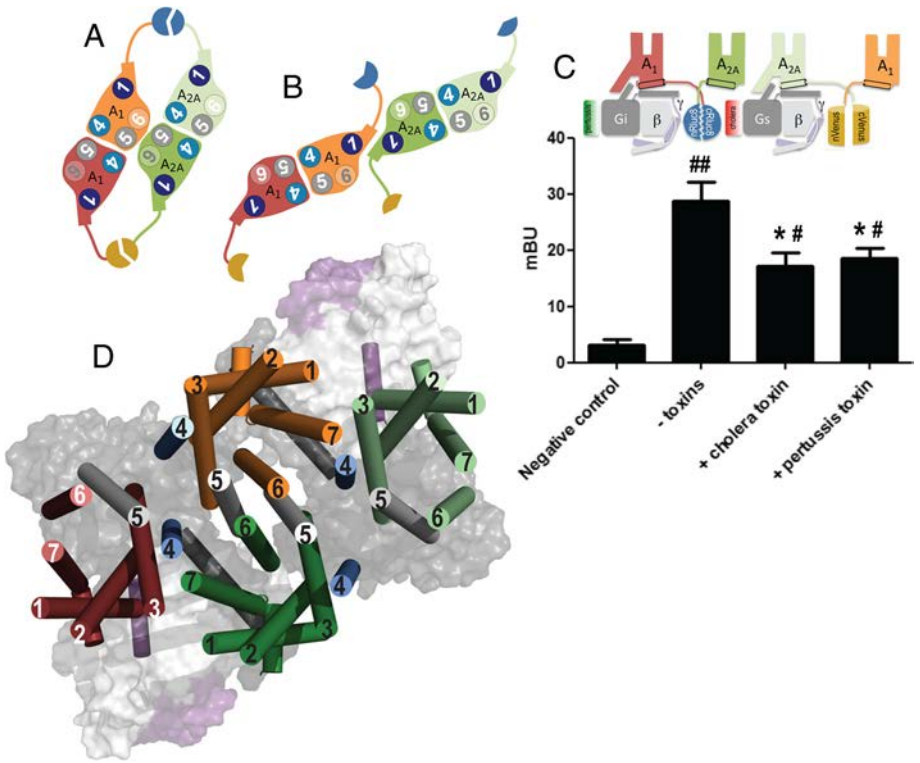

Fig. 5. Bioluminescence resonance energy transfer (BRET)-aided construction of a model consisting of G_i and G_s bound to an A_1R-$A_{2A}R$ heterotetramer. **a**, **b** A_1R-$A_{2A}R$ tetramer built using TM5/6 (a) or TM1 (b) inter-receptor interfaces modeled as in the structure of the μ opioid receptor [3]. TM helices 1, 4, and 5, involved in receptor dimerization, are highlighted in *dark blue*, *light blue*, and *gray*, respectively. nRluc8 and cRluc8 are shown in *blue* and nVenus and cVenus in *dark yellow*. **c** BRET and bimolecular fluorescence complementation experiments were performed in HEK-293T cells transfected with 1.5 μg of cDNA corresponding to A_1R-cRluc8 and $A_{2A}R$-nRluc8, and 1.5 μg of cDNA corresponding to A_1R-nVenus and $A_{2A}R$-cVenus. As the negative control, cells were transfected with 1 μg of cDNA corresponding to nRluc8 and 1.5 μg of cDNA corresponding to $A_{2A}R$-nRluc8, A_1R-nVenus, and $A_{2A}R$-cVenus. Cells were treated for 16 h with medium (– *toxins*), 10 ng/ml of pertussis toxin (+ *pertussis*), or 100 ng/ml of cholera toxin (+ *cholera*) prior to BRET determination. The relative amount of BRET is given as in Fig. 4 and values are the mean ± standard error of the mean of three different experiments. Student's t-test showed statistically significant differences with respect to the control ($^{\#}p < 0.05$, $^{\#\#}p < 0.01$) and a significant effect in the presence of either toxin over BRET in the absence of toxins ($^{*}p < 0.05$). A schematic representation at the *top* shows the protein to which the hemi luminescent or fluorescent proteins were fused. **d** Molecular model of the A_1R-$A_{2A}R$ tetramer in complex with G_i and G_s. A_1R bound to G_i is shown in *red*, G_i-unbound A_1R is shown in *orange*, $A_{2A}R$ bound to G_s is shown in *dark green*, G_s-unbound $A_{2A}R$ is shown in *light green*, and the α, β-, and γ-subunits of G_i and G_s are shown in *dark gray*, *light gray*, and *purple*, respectively. Transmembrane helices 4 and 5 are highlighted in *light blue* and *gray*, respectively

Figure S7 shows root-mean-square deviations (rmsd) on protein α-carbons throughout the MD simulation, as well as key intermolecular distances among protomers and G proteins. Clearly, both the A_1R protomer bound to G_i and the A_1R protomer that does not interact with it maintained a close structural similarity (rmsd ≈ 0.3 nm) relative to the initial structures. Similar results were obtained for the $A_{2A}R$ protomers (bound and unbound to G_s) (Additional file 7: Figure S7A). The fact that rmsd values of the whole system, formed by the A_1R-$A_{2A}R$ heterotetramer bound to G_i and G_s, are of the order of 0.6 nm indicates that the initial structural model is maintained during the MD simulation (Additional file 7: Figure S7A). As a consequence, selected intermolecular distances among protomers and G proteins remain constant during the MD simulation (Additional file 7: Figure S7B). A key aspect in the assembly of the heterotetramer is the TM interfaces for homodimerization (TM4/5) and heterodimerization (TM5/6). Additional file 8: Figure S8B shows rmsd values of the four-helix bundle forming the TM4/5 and TM5/6 interfaces, the initial and final snapshots of these bundles, and the evolution of the A_1R-$A_{2A}R$ heterotetramer during the MD simulation. Clearly, the rather small structural variations of these four-helix bundles, also reflected by rmsd <0.3 nm, suggest a stable complex. Notably, the TM5/6 four-helix bundle seems more stable than the TM4/5 bundles, as shown by its lower rmsd value. Additional file 8: Figure S8B, C depicts contact maps of the TM4/5 and TM5/6 interfaces, as well as the evolution of the network of hydrophobic interactions within these interfaces during the MD simulation.

Conclusions

For more than a decade, experimental evidence has supported the occurrence of homo-oligomers and hetero-oligomers of GPCRs [21]. However, our basic understanding of what makes heteromers different from homomers remains unknown. Our results, studying adenosine receptors as a model heteromer, point to three important new findings. First, the predominant stoichiometry in cells expressing A_1R-$A_{2A}R$ heteromers is 2:2; that is, a dimer of dimers (tetramer). Second, two different heterotrimeric G proteins can couple to heteromers, the overall complex constituting a functional unit. Third, the molecular orientation within the heteromer complex affords various qualitatively different interfaces; the two more relevant are the inter-protomer heteromeric interface and the inter-G-protein interface. Presumably, the two interfaces provide the key characteristic of heteromers: the ability of one protomer/G-protein complex to influence the signaling of the other. Surely, allosteric effects occurring between heteroreceptors and between G_s and G_i proteins are due to conformational changes transmitted along the intimately interacting molecules in the complex. In our controlled cell transfection system, which expressed a low density of receptors, minor species formed by monomers and trimers were found in addition to a predominance of tetramers in the plasma membrane, strongly supporting the occurrence of an in vivo dynamic distribution of receptors.

Adenosine was, from an evolutionary point of view, one of the first extracellular regulators given that it is involved in energy and nucleic acid metabolisms. Adenosine A_1 and A_{2A} receptors are expressed in almost every mammalian organ and tissue. In the heart, where adenosine plays a key role in both inotropic and chronotropic regulation, A_1R-mediated cardioprotection did not occur in $A_{2A}R$ knockout mice, suggesting an interaction between A_1 and A_{2A} receptors. In neurons, A_1 and A_{2A} receptors show co-localization, leading to inter-receptor interactions unveiled by pharmacological treatments. For instance, Okada et al. [27] showed that cAMP-dependent protein kinase A plays a role in the regulation of hippocampal serotonin release mediated by both A_1 and A_{2A} receptors. Similarly, the control of γ-amino butyric acid transport in astrocytes was attributed to the expression of A_1R-$A_{2A}R$ heteromers and to a specific mechanism by which the heteromer signals via G_i or G_s depending on the concentration of adenosine [28]. The structural basis of the differential signaling by the heteromer/G-protein macromolecular complex likely implies communication at the receptor-receptor level but also between G_s and G_i. Because the binding of two G proteins to a heterodimer is not feasible due to steric clashes [25], our finding that the A_1R-$A_{2A}R$ heterotetramer may bind to both G_s and G_i provides a structural framework to interpret experimental data.

Methods

Total internal reflection microscopy and single-particle data analysis

Single-particle imaging and tracking were performed on a Nikon Total Internal Reflection Fluorescence (TIRF) system, as detailed in Additional file 11: Supplementary Methods. Typically, 500 readouts of a 512 × 512-pixel region, the full array of the CCD chip, were acquired. For single-particle data analysis, parameters were calculated by applying the equations described in Additional file 11: Supplementary Methods.

Cell culture and transient transfection

HEK-293T cells were grow at 37 °C in Dulbecco's modified Eagle's medium (DMEM) (Gibco, Thermo Fischer Scientific, Madrid, Spain) supplemented with 2 mM L-glutamine, 100 U/ml penicillin/streptomycin, and 5 % (v/v) heat-inactivated fetal bovine serum (FBS) (all supplements were from Invitrogen, Paisley, UK). Cells were transiently transfected with cDNA corresponding to receptors, fusion proteins, $A_{2A}R$ mutants, or G-protein minigene vectors obtained as detailed in an expanded view by the polyethylenimine (PEI; SigmaAldrich, Cerdanyola del Vallès, Spain) method. Sample protein concentration was determined using a Bradford assay kit (Bio-Rad, Munich, Germany) using bovine serum albumin dilutions as standards. For single-particle imaging, cells were seeded into six-well plates containing glass coverslips (No. 1, round, 24 mm; Assistent, Sondheim, Germany) or into the Lab-Tek Chambered #1.0 Borosilicate Coverglass System (Nunc, Thermo Fisher Scientific, Schwerte, Germany). Cell transient transfections were performed with Lipofectamine™ 2000 (Invitrogen, Life Technologies, Darmstadt, Germany) or FuGENE 6 (Roche Applied Science, Indianapolis, IN, USA) and the application of 0.1–0.2 μg plasmid DNA per well. Before each experiment, cells were washed three times with 200 μL phenol red-free DMEM.

Plasmids

DNA sequences encoding amino acid residues 1–155 and 155–238 of YFP Venus protein, and amino acids residues 1–229 and 230–311 of RLuc8 protein were subcloned in the pcDNA3.1 vector to obtain the YFP Venus and RLuc8 hemi-truncated proteins. The human cDNAs for adenosine receptors, $A_{2A}R$ and A_1R, cloned into pcDNA3.1, were amplified without their stop codons using sense and antisense primers harboring unique EcoRI and BamHI sites to clone receptors into the pcDNA3.1RLuc vector (p*RLuc*-N1; PerkinElmer, Wellesley, MA, USA), and EcoRI and KpnI to clone $A_{2A}R$, A_1R, or GHS1a into the pEYFP-N1 vector (enhanced yellow variant of GFP; Clontech, Heidelberg, Germany). $G_{\alpha s}$ cloned into the *SFV1* vector, $G_{\alpha i}$ cloned into the pcDNA3.1 vector, or G_γ cloned into the *pEYFP-C1* vector were amplified

without their stop codons using sense and antisense primers harboring unique *Hind*III and *Bam*HI sites to clone them into the pcDNA3.1-Rluc vector, or EcoRI and KpnI to clone $G_{\alpha s}$ into the pEYFP-N1 vector. The amplified fragments were subcloned to be in-frame with restriction sites of the pcDNA3.1RLuc or pEYFP-N1 vectors to give plasmids that expressed proteins fused to RLuc or YFP on the N-terminal end ($G_{\alpha s}$-RLuc, $G_{\alpha i}$-RLuc, G_{γ}-RLuc, $G_{\alpha s}$-YFP, and G_{γ}-YFP) or the C-terminal end (A_1R-RLuc, $A_{2A}R$-RLuc, A_1R-YFP, $A_{2A}R$-YFP, and GHS1a-YFP). The human cDNAs for A_1R or GHS1a were subcloned into pcDNA3.1-nRLuc8 or pcDNA3.1-nVenus to give plasmids that expressed A_1R or GHS1a fused to either nRLuc8 or nYFP Venus on the C-terminal end of the receptor (A_1R-nRLuc8 and A_1R-nVenus or GHS1a-nRLuc8 and GHS1a-nVenus). The cDNAs for human A_{2A} or GHS1a receptors were subcloned into pcDNA3.1-cRLuc8 or pcDNA3.1-cVenus to give plasmids that expressed receptors fused to either cRLuc8 or cYFP Venus on the C-terminal end of the receptor ($A_{2A}R$-cRLuc8 and $A_{2A}R$-cVenus or GHS1a-cRLuc8 and GHS1a-cVenus). Expression of constructs was tested by confocal microscopy and the receptor-fusion protein functionality by measuring ERK1/2 phosphorylation and cAMP production, as described previously [13, 14, 17, 29].

"Minigene" plasmid vectors are constructs designed to express relatively short polypeptide sequences following their transfection into mammalian cells. Here, we used minigene constructs encoding the carboxyl-terminal 11-amino acid residues from G_{α} subunits of $G_{i1/2}$ (G_i minigene) or G_s (G_s minigene) G proteins; the resulting peptides inhibit G-protein coupling to the receptor and consequently inhibit the receptor-mediated cellular responses as previously described [24]. The cDNA encoding the last 11 amino acids of human G_{α} subunit corresponding to $G_{i1/2}$ (I K N N L K D C G L F) or G_s (Q R M H L R Q Y E L L), inserted in a pcDNA3.1 plasmid vector, were generously provided by Dr Heidi Hamm.

Energy transfer assays

For BRET and complementation BRET assays, HEK-293T cells were transiently cotransfected with a constant amount of cDNA encoding for proteins fused to RLuc, nRLuc8, or cRLuc8, and with increasing amounts of the cDNA corresponding to proteins fused to YFP, nYFP Venus, or cYFP Venus (see figure legends). To quantify protein-YFP expression or protein-reconstituted YFP Venus expression, cells (20 μg protein) were distributed in 96-well microplates (black plates with a transparent bottom) and fluorescence was read in a FLUOstar OPTIMA Fluorimeter (BMG Labtechnologies, Offenburg, Germany) equipped with a high-energy xenon flash lamp, using a 10 nm bandwidth excitation filter at 400 nm reading. Protein fluorescence expression was determined as the fluorescence of the sample minus the fluorescence of cells expressing the BRET donor alone. For BRET measurements, the equivalent of 20 μg of cell suspension were distributed in 96-well microplates (Corning 3600, white plates; Sigma) and 5 μM coelenterazine h (Molecular Probes, Eugene, OR, USA) was added. After 1 min for BRET or after 5 min for BRET with bimolecular fluorescence complementation, the readings were collected using a Mithras LB 940 that allows the integration of the signals detected in the short-wavelength filter at 485 nm (440–500 nm) and the long-wavelength filter at 530 nm (510–590 nm). To quantify protein-RLuc or protein-reconstituted RLuc8 expression, luminescence readings were also performed 10 min after adding 5 μM coelenterazine h. The net BRET was defined as [(long-wavelength emission)/(short-wavelength emission)] – Cf, where Cf corresponds to [(long-wavelength emission)/(short-wavelength emission)] for the donor construct expressed alone in the same experiment. BRET is expressed as miliBRET units (mBU; net BRET × 1000).

Computational model of the A_1R-$A_{2A}R$ tetramer in complex with G_i and G_s

The crystal structure of inactive $A_{2A}R$ [PDB:4EIY] [30] was used for the construction of human $A_{2A}R$ [UniProt:P29274] and A_1R [UniProt:P30542] homology models using Modeller 9.12 [31]. These receptors share 51 % of sequence identity and 62 % of sequence similarity, excluding the C-terminal after helix 8. Intracellular loop 3 (ICL3) of $A_{2A}R$ (Lys209–Gly218) and A_1R (Asn212–Ser219) were modeled using Modeller 9.12 [31] using ICL3 of squid rhodopsin [PDB:2Z73] as a template. The C-terminus tails of A_1R, containing 16 amino acids (Pro311–Asp326), and of $A_{2A}R$, containing 102 amino acids (Gln311–Ser412), were modeled as suggested for the oxoeicosanoid receptor (OXER) [32] (see Additional file 9: Figure S9 for details). The N-terminus of A_1R and $A_{2A}R$ were not included in the model. The "active" conformations of A_1R bound to G_i and $A_{2A}R$ bound to G_s were modeled using the crystal structure of β_2-AR in complex with G_s [PDB:3SN6] [33]. The globular α-helical domain of the α-subunit was modeled in the "closed" conformation [34], using the crystal structure of [AlF_4^-]-activated G_i [PDB:1AGR]. The location of YFP [PDB:2RH7] attached to the C-tail of $A_{2A}R$ was determined as suggested for the OXER [32] (see Additional file 9: Figure S9 for details). Rluc [PDB:2PSD] and YFP were fused to the to the N-terminus of the α-subunits and γ-subunits of G_i and G_s by a covalent bond. The structures of adenosine receptor oligomers were modeled via the TM4/5 interface for homodimerization, using the oligomeric structure of the β_1-AR [PDB:4GPO] [4], or via the TM5/6 interface for

heterodimerization, using the structure of the μ-OR [PDB:4DKL] [3]. The G_i-bound A_1R and G_s-bound $A_{2A}R$ protomers were rotated 10° to avoid the steric clash of the N-terminal helix of G_i and G_s with the C-terminal helix (Hx8) of G_s-unbound $A_{2A}R$ and G_i-unbound A_1R, respectively. This computational model, without Rluc and YFP, was placed in a rectangular box containing a lipid bilayer (814 molecules of 1-palmitoyl-2-oleoyl-sn-glycero-3-phosphocholine - POPC -) with explicit solvent (102,973 water molecules) and a 0.15 M concentration of Na^+ and Cl^- (1762 ions). This initial complex was energy-minimized and subsequently subjected to a 10 ns MD equilibration, with positional restraints on protein coordinates. These restraints were released and 500 ns of MD trajectory were produced at constant pressure and temperature (see Additional file 10: Movie M1). Computer simulations were performed with the GROMACS 4.6.3 simulation package [35], using the AMBER99SB force field as implemented in GROMACS and Berger parameters for POPC lipids. This procedure has been previously validated [36].

Availability of data and materials

The crystal structures 4EIY, 2Z73, 3SN6, 1AGR, 2RH7, 2PSD, 4GPO, and 4DKL are available from PDB (http://www.rcsb.org). All other relevant data are within the paper and its Additional files.

Additional files

Additional file 1: Figure S1. Examples of receptor trajectories in HEK-293T cells. Images of cells expressing A_1R-GFP (A) and of particular trajectories of A_1R-GFP-containing (B) or $A_{2A}R$-mCherry-containing (C) particles. (TIF 1164 kb)

Additional file 2: Figure S2. Graphical description of the stoichiometry of A_1R-GFP, $A_{2A}R$-mCherry or both A_1-GFP and A_{2A}-mCherry. The fluorescence intensity signal distribution (gray area) detected for more than 7000 independent observations is given for HEK-293T cells expressing A_1-GFP (A), A_{2A}-mCherry (D), or both A_1-GFP and A_{2A}-mCherry (B, E). The stoichiometry analysis was performed for A_1-GFP (A, B) and A_{2A}-mCherry (D, E). Curves approximately delineating the amount of monomers, dimers, trimers, and tetramers are displayed in green for A_1-GFP (A, B) and in red for A_{2A}-mCherry (D-E). The occurrence on the cell surface of monomers, dimers, trimers, and tetramers for A_1-GFP (C) expressed alone (black bars) or in the presence of A_{2A}-mCherry (blue bars) and for A_{2A}-mCherry (F) expressed alone (black bars) or in the presence of A_1-GFP (blue bars) was calculated by stoichiometry analysis from results shown in A, B, D, and E. (TIF 455 kb)

Additional file 3: Figure S3. Controls of cAMP production and BRET assays in cells expressing minigenes and in cells expressing the ghrelin GHS1a receptor instead of one of the adenosine receptors. (A,B) cAMP determination in HEK-293T cells transfected with (A) 0.3 μg of cDNA corresponding to A_1R or (B) with 0.2 μg of cDNA corresponding to $A_{2A}R$ with (control) or without 0.5 μg of cDNA corresponding to minigenes coding for peptides blocking either Gi or Gs binding. Cells were stimulated with the A_1R agonist N^6-Cyclopentyladenosine (CPA) (10 nM, red bars) in the presence of 0.5 μM forskolin (Fk) or with the $A_{2A}R$ agonist 4-[2-[[6-Amino-9-(N-ethyl-β-D-ribofuranuronamidosyl)-9H-purin-2-yl]amino]ethyl]benzenepropanoic acid hydrochloride (CGS-21680) (200 nM, blue bars). Values expressed as % of the forskolin-treated cells (CPA reduces forskolin-induced cAMP levels, red bars) or of the basal (CGS 21680 *per se* enhances cAMP levels, blue bars) are given as mean ± SD (n = 4–8). One-way ANOVA followed by a Bonferroni post - hoc test showed a significant effect of CPA when compared with that of forskolin (red bars, $^{***}p < 0.001$) or of CGS 21680 when compared to basal cAMP levels (blue bars, $^{\#\#}p < 0.01$, $^{\#\#\#}p < 0.001$). (C, D) BRET saturation curves were performed in HEK-293T cells transfected with (C) 0.3 μg cDNA coding for A_1R-Rluc, increasing amounts of cDNA coding for A_1R-YFP (0.1–1.5 μg cDNA), and 0.4 μg cDNA coding for GHS1a, or (D) with 0.2 μg of cDNA coding for $A_{2A}R$-Rluc, increasing amounts of cDNA coding for $A_{2A}R$-YFP (0.1–1.0 μg cDNA), and 0.5 μg cDNA coding for to GHS1a. Prior to BRET determination, cells were treated for 16 h with medium (black curves), with 10 ng/ml of pertussis toxin (green curves), or with 100 ng/ml of cholera toxin (red curves). mili BRET units (mBU) are given as the mean ± SD (n = 4–6 different experiments grouped as a function of the amount of BRET acceptor). (TIF 1418 kb)

Additional file 4: Figure S4. Possible interfaces in $A_{2A}R$ homodimers in complex with G_s. In A–E, the $A_{2A}R$ homodimer was modeled through TM4 using the H_1-receptor structure as template (A), through TM5 using the structure of squid rhodopsin (B), through TM4/5 using the β_1-receptor structure (C), and via TM5/6 (D) and TM1 (E) using the μ-OR structure. TM helices 1, 4, and 5 involved in receptor dimerization are highlighted in dark blue, light blue, and gray, respectively. $A_{2A}R$ protomers bound to G_s (in gray) are shown in light green, whereas G_s-unbound $A_{2A}R$ protomers are shown in dark green. Rluc (blue) is attached to the N-terminal αN helix of G_s, and YFP (yellow) is attached to the C-terminal domain of the G_s-unbound $A_{2A}R$ protomer (light green). It is important to note that the position of YFP is highly dependent on the orientation of the long and highly flexible C-tail of $A_{2A}R$ (102 amino acids, Gln311–Ser412), which was modeled as described for the OXER [32] (see Additional file 9: Figure S9 for details). Despite these limitations, we can crudely estimate the approximate distances between the center of mass of Rluc and YFP as 4.6, 10.1, 6.5, 11.6, and 8.3 nm for panels A–E, respectively. Thus, among all these possible dimeric interfaces, only the molecular models depicted in panels A (TM4 interface) and C (TM4/5 interface) would favor the observed high-energy transfer between G_s-Rluc and $A_{2A}R$-YFP (Fig. 4a in main paper). However, there is a steric clash between the N-terminal helix of Gs and the dark-green protomer in the TM4 interface. Accordingly, we have modeled $A_{2A}R$ homodimerization via the TM4/5 interface. Unfortunately, similar experiments with cells transfected with G_i-Rluc and A_1R-YFP could not be accomplished because of a lack of receptor expression (not shown); it is likely that the shorter C-tail of A_1R (16 amino acids, Pro311–Asp326) could not accommodate YFP in the presence of G_i in the right three-dimensional structure. The A_1R homodimer was built using the same TM4/5 interface as for $A_{2A}R$. (TIF 3135 kb)

Additional file 5: Figure S5. BRET assays in cells expressing fusion proteins containing hemi-Rluc8 and hemi-Venus moieties fused to adenosine receptors or containing the ghrelin GHS1a receptor instead of one of the adenosine receptors. (A) Saturation BRET curve in HEK-293T co-transfected with 1.5 μg of the two cDNAs corresponding to A_1R-cRLuc8 and $A_{2A}R$-nRLuc8 and with increasing amounts of cDNAs corresponding to A_1R-nVenus and $A_{2A}R$-cVenus (equal amounts of the two cDNAs). $BRET_{max}$ was 35 ± 2 mBU and $BRET_{50}$ was 16 ± 3 mBU. BRET in cells expressing cRluc8 instead of A_1R-cRluc8 gave a linear, non-saturable signal. (B) Comparison of BRET responses using complementary and non-complementary pairs, or replacing one adenosine receptor with the ghrelin GHS1a (gn) receptor. Data are mean ± SD of three different experiments grouped as a function of the amount of BRET acceptor. $^{***}p < 0.001$ with respect to BRET in cells expressing adenosine receptors and hemi-Rluc8 and hemi-Venus proteins. (TIF 398 kb)

Additional file 6: Figure S6. Details of the relative position of Rluc and YFP in a receptor heterotetramer interacting with two G proteins. Computational-based model of G_s and G_i bound to the adenosine A_1R-$A_{2A}R$ heterotetramer. Rluc and YFP fused to the N-terminal domain of the G_α-subunits point toward different positions in space (A), whereas Rluc and YFP fused to G_γ-subunits are close (B). The color code of the proteins is depicted in the adjacent schematic representations (TM4 and TM5 of GPCR protomers are in light blue and gray, respectively). (TIF 6445 kb)

Additional file 7: Figure S7. Molecular dynamics (MD) simulation of the adenosine A_1R-$A_{2A}R$ heterotetramer in complex with G_i and G_s. (A) Root-mean-square deviations (rmsd) on protein α-carbons of the whole system (black solid line), of the two A_1Rs (orange and red

solid lines), of the two A_{2A}Rs (light and dark green solid lines), of G_i (gray solid line), and of G_s (gray dotted line) throughout the MD simulation. This color scheme matches with the color of the different proteins depicted in the two adjacent schematic representations. (B) Intermolecular distances between the N-terminal helices of the γ-subunit of Gi and Gs (magenta line), the N-terminal helices of the α-subunit of G_i and G_s (gray line), the N-terminal helix of the α-subunit of G_i and the C-terminal helix (Hx8) of inactive A_1R (orange line), the N-terminal helix of the α-subunit of G_s and the C-terminal Hx8 of inactive A_{2A}R (green line), the C-terminal Hx8 of A_1R and A_{2A}R (blue lines). These computed intermolecular distances are depicted as double arrows in the two adjacent schematic representations. (TIF 6973 kb)

Additional file 8: Figure S8. Evolution of TM4/5 and TM5/6 interfaces as devised from MD simulations of the adenosine A_1R-A_{2A}R heterotetramer in complex with G_i and G_s. (A) Representative snapshots (20 structures collected every 25 ns) of the TM domains of A_1R bound to G_i (red), G_i-unbound A_1R (orange), A_{2A}R bound to G_s (dark green), and G_s-unbound A_{2A}R (light green). TM helices 4 and 5 are highlighted in light blue and gray, respectively. Initial (at 0 ns, transparent cylinders) and final (at 500 ns, solid cylinders) snapshots of TM interfaces are shown for homodimerization (TM4/5, within rectangles) and heterodimerization (TM5/6, within a circle) bundles. TM helices 4 (light blue), 5 (gray), and 6 (orange and green) are highlighted. (B) Root-mean-square deviations (rmsd) on protein α-carbons of the four-helix bundles forming the TM5/6 interface (orange solid line), TM4/5 interface of A_1R (blue dotted line), and TM4/5 interface of A_{2A}R (blue solid line) throughout the MD simulation. (C) Contact maps of the TM4/5 interface (rectangles in panel A) in the A_1R or A_{2A}R homodimer (left and right panels) and of the TM5/6 interface (circle in panel A) in the A_1R-A_{2A}R heterodimer (middle panel). Darker dots show more frequent contacts. (D) Detailed view of the extensive network of hydrophobic interactions (mainly of aromatic side chains) within the TM4/5 (left and right panels) and TM5/6 (middle panel) interfaces. The amino acids are numbered following the generalized numbering scheme of Ballesteros and Weinstein [37, 38]. This allows easy comparison among residues in the 7TM segments of different receptors. (TIF 4004 kb)

Additional file 9: Figure S9. Positioning YFP in the C-tail of A_{2A}R. The complex between the A_{2A}R protomer (in light green) and G_s (α-subunit in dark grey and yellow, β-subunit in light gray, and γ-subunit in purple) was constructed from the crystal structure of β_2 in complex with G_s [33]. Although the exact conformation of the A_{2A}R C-tail (102 amino acids, Gln311–Ser412) cannot unambiguously be determined, its orientation was modeled as in the C-tail of squid rhodopsin [39], which contains the conserved amphipathic helix 8 that runs parallel to the membrane and an additional cytoplasmic helix 9. Thus, the C-tail of A_{2A}R expands (see solid light green line) and points intracellularly toward the N-termini of the γ-subunit as suggested for OXER [32]. The laboratory of Kostenis has shown that the C-terminal of OXER, labeled with Rluc (OXER-Rluc), gets close to the N-terminal of the γ-subunit, labeled with GFP (γ-GFP) [32]. Analogously, we propose that YFP attached to the C-tail of A_{2A}R is positioned near the N-termini of the γ-subunit (in purple). (TIF 2395 kb)

Additional file 10: Movie M1. Assembly of adenosine A_1 and A_{2A} receptors in complex with two G proteins and MD simulation of the system. The assembly of G_s and G_i bound to the adenosine A_1R-A_{2A}R heterotetramer was subjected to 500 ns of MD simulation in a rectangular box containing the system, the lipid bilayer, explicit solvent, and ions. A_1R protomers are in orange and red, A_{2A}R protomers in light and dark green, G_α in white, G_β in gray, and G_γ in purple. For easier visualization of protomer-protomer interfaces, TMs 4 and 5 are highlighted in blue and white, respectively. (MPEG 87870 kb)

Additional file 11: Supplementary methods. (DOCX 72 kb)

Competing interests
The authors declare that they have no competing interests.

Authors' contributions
GN performed the molecular biology. GN, MB, EM, and DA perfomed BRET experiments. MZ-F performed single-particle tracking experiments. AC and LP-B performed molecular modeling studies. AC, VC, JM, and EIC analyzed the data. CL, LP, AJG-S, PJM, and RF designed the experiments, supervised the work in the respective laboratories and wrote the manuscript.. All authors read and approved the final manuscript.

Acknowledgments
We acknowledge the technical help provided by Jasmina Jiménez (CIBERNED, University of Barcelona). This study was supported by grants from the Spanish Ministerio de Ciencia y Tecnología (SAF2009-07276, SAF2010-18472, SAF2011-23813, SAF2013-48271-C2-2-R; those grants may include FEDER funds), the Max Planck Society, the German Cancer Research Center, and the German Ministry for Education and Research (BMBF). PJM and LP participate in the European COST Action CM1207 (GLISTEN). Authors gratefully acknowledge the computer resources provided by the Barcelona Supercomputing Center - Centro Nacional de Supercomputación.

Author details
[1]Centro de Investigación Biomédica en Red sobre Enfermedades Neurodegenerativas (CIBERNED), Madrid, Spain. [2]Institute of Biomedicine of the University of Barcelona (IBUB), Barcelona, Spain. [3]Department of Biochemistry and Molecular Biomedicine, Faculty of Biology, University of Barcelona, Barcelona 08028, Spain. [4]Laboratori de Medicina Computacional, Unitat de Bioestadística, Facultat de Medicina, Universitat Autònoma de Barcelona, 08193 Bellaterra, Spain. [5]Max Planck Institute for Intelligent Systems, Heisenbergstrasse 3, 70569 Stuttgart, Germany. [6]German Cancer Research Center, Bioquant, Im Neuenheimer Feld 267, 69120 Heidelberg, Germany. [7]Interfaculty Institute of Biochemistry, Hoppe-Seyler-Strasse 4, 72076 Tübingen, Germany. [8]School of Pharmacy, University of East Anglia, Norwich NR4 7TJ, UK.

Received: 26 September 2015 Accepted: 16 March 2016
Published online: 05 April 2016

References
1. Fung JJ, Deupi X, Pardo L, Yao XJ, Velez-Ruiz GA, Devree BT, et al. Ligand-regulated oligomerization of beta(2)-adrenoceptors in a model lipid bilayer. EMBO J. 2009;28:2384–92.
2. Albizu L, Cottet M, Kralikova M, Stoev S, Seyer R, Brabet I, et al. Time-resolved FRET between GPCR ligands reveals oligomers in native tissues. Nat Chem Biol. 2010;6:587–94.
3. Manglik A, Kruse AC, Kobilka TS, Thian FS, Mathiesen JM, Sunahara RK, et al. Crystal structure of the micro-opioid receptor bound to a morphinan antagonist. Nature. 2012;485:321–6.
4. Huang J, Chen S, Zhang JJ, Huang XY. Crystal structure of oligomeric β1-adrenergic G protein-coupled receptors in ligand-free basal state. Nat Struct Mol Biol. 2013;20:419–25.
5. Lane JR, Donthamsetti P, Shonberg J, Draper-Joyce CJ, Dentry S, Michino M, et al. A new mechanism of allostery in a G protein-coupled receptor dimer. Nat Chem Biol. 2014;10:745–52.
6. Vinals X, Moreno E, Lanfumey L, Cordomi A, Pastor A, de La Torre R, et al. Cognitive impairment induced by delta9-tetrahydrocannabinol occurs through heteromers between cannabinoid cb1 and serotonin 5-ht2a receptors. PLoS Biol. 2015;13:e1002194.
7. Kasai RS, Kusumi A. Single-molecule imaging revealed dynamic GPCR dimerization. Curr Opin Cell Biol. 2014;27:78–86.
8. Hern JA, Baig AH, Mashanov GI, Birdsall B, Corrie JE, Lazareno S, et al. Formation and dissociation of M1 muscarinic receptor dimers seen by total internal reflection fluorescence imaging of single molecules. Proc Natl Acad Sci U S A. 2010;107:2693–8.
9. Calebiro D, Rieken F, Wagner J, Sungkaworn T, Zabel U, Borzi A, et al. Single-molecule analysis of fluorescently labeled G-protein-coupled receptors reveals complexes with distinct dynamics and organization. Proc Natl Acad Sci U S A. 2013;110:743–8.
10. Kasai RS, Suzuki KG, Prossnitz ER, Koyama-Honda I, Nakada C, Fujiwara TK, et al. Full characterization of GPCR monomer-dimer dynamic equilibrium by single molecule imaging. J Cell Biol. 2011;192:463–80.
11. Vilardaga JP, Nikolaev VO, Lorenz K, Ferrandon S, Zhuang Z, Lohse MJ. Conformational cross-talk between alpha2A-adrenergic and mu-opioid receptors controls cell signaling. Nat Chem Biol. 2008;4:126–31.
12. Fribourg M, Moreno JL, Holloway T, Provasi D, Baki L, Mahajan R, et al. Decoding the signaling of a GPCR heteromeric complex reveals a unifying mechanism of action of antipsychotic drugs. Cell. 2011;147:1011–23.
13. Gonzalez S, Moreno-Delgado D, Moreno E, Perez-Capote K, Franco R, Mallol J, et al. Circadian-related heteromerization of adrenergic and dopamine D(4) receptors modulates melatonin synthesis and release in the pineal gland. PLoS Biol. 2012;10:e1001347.

14. Navarro G, Ferre S, Cordomi A, Moreno E, Mallol J, Casado V, et al. Interactions between intracellular domains as key determinants of the quaternary structure and function of receptor heteromers. J Biol Chem. 2010;285:27346–59.
15. Ferre S, Baler R, Bouvier M, Caron MG, Devi LA, Durroux T, et al. Building a new conceptual framework for receptor heteromers. Nat Chem Biol. 2009;5:131–4.
16. Venkatakrishnan AJ, Deupi X, Lebon G, Tate CG, Schertler GF, Babu MM. Molecular signatures of G-protein-coupled receptors. Nature. 2013;494:185–94.
17. Ciruela F, Casado V, Rodrigues RJ, Lujan R, Burgueno J, Canals M, et al. Presynaptic control of striatal glutamatergic neurotransmission by adenosine A1-A2A receptor heteromers. J Neurosci. 2006;26:2080–7.
18. Orru M, Bakesova J, Brugarolas M, Quiroz C, Beaumont V, Goldberg SR, et al. Striatal pre- and postsynaptic profile of adenosine A(2A) receptor antagonists. PLoS One. 2011;6:e16088.
19. Harms GS, Cognet L, Lommerse PH, Blab GA, Kahr H, Gamsjager R, et al. Single-molecule imaging of l-type Ca(2+) channels in live cells. Biophys J. 2001;81:2639–46.
20. Whorton MR, Bokoch MP, Rasmussen SG, Huang B, Zare RN, Kobilka B, et al. A monomeric G protein-coupled receptor isolated in a high-density lipoprotein particle efficiently activates its G protein. Proc Natl Acad Sci U S A. 2007;104:7682–7.
21. Ferre S, Casado V, Devi LA, Filizola M, Jockers R, Lohse MJ, et al. G protein-coupled receptor oligomerization revisited: functional and pharmacological perspectives. Pharmacol Rev. 2014;66:413–34.
22. Fredholm BB, IJzerman AP, Jacobson KA, Linden J, Muller CE. International Union of Basic and Clinical Pharmacology. LXXXI. Nomenclature and classification of adenosine receptors–an update. Pharmacol Rev. 2011;63:1–34.
23. Carriba P, Navarro G, Ciruela F, Ferre S, Casado V, Agnati L, et al. Detection of heteromerization of more than two proteins by sequential BRET-FRET. Nat Methods. 2008;5:727–33.
24. Gilchrist A, Li A, Hamm HE. G alpha COOH-terminal minigene vectors dissect heterotrimeric G protein signaling. Sci STKE. 2002;2002:pl1.
25. Cordomi A, Navarro G, Aymerich MS, Franco R. Structures for G-protein-coupled receptor tetramers in complex with G proteins. Trends Biochem Sci. 2015;40:548–51.
26. Mondal S, Johnston JM, Wang H, Khelashvili G, Filizola M, Weinstein H. Membrane driven spatial organization of GPCRs. Sci Rep. 2013;3:2909.
27. Okada M, Nutt DJ, Murakami T, Zhu G, Kamata A, Kawata Y, et al. Adenosine receptor subtypes modulate two major functional pathways for hippocampal serotonin release. J Neurosci. 2001;21:628–40.
28. Cristovao-Ferreira S, Navarro G, Brugarolas M, Perez-Capote K, Vaz SH, Fattorini G, et al. A1R-A2AR heteromers coupled to Gs and G i/0 proteins modulate GABA transport into astrocytes. Purinergic Signal. 2013;9:433–49.
29. Canals M, Marcellino D, Fanelli F, Ciruela F, de Benedetti P, Goldberg SR, et al. Adenosine A2A-dopamine D2 receptor-receptor heteromerization: qualitative and quantitative assessment by fluorescence and bioluminescence energy transfer. J Biol Chem. 2003;278:46741–9.
30. Liu W, Chun E, Thompson AA, Chubukov P, Xu F, Katritch V, et al. Structural basis for allosteric regulation of GPCRs by sodium ions. Science. 2012;337:232–6.
31. Marti-Renom MA, Stuart AC, Fiser A, Sanchez R, Melo F, Sali A. Comparative protein structure modeling of genes and genomes. Annu Rev Biophys Biomol Struct. 2000;29:291–325.
32. Blattermann S, Peters L, Ottersbach PA, Bock A, Konya V, Weaver CD, et al. A biased ligand for OXE-R uncouples Gα and Gβγ signaling within a heterotrimer. Nat Chem Biol. 2012;8:631–8. doi: 10.1038/nchembio.962. Epub 2012 May 27.
33. Rasmussen SG, DeVree BT, Zou Y, Kruse AC, Chung KY, Kobilka TS, et al. Crystal structure of the β2 adrenergic receptor-Gs protein complex. Nature. 2011;477:549–55.
34. Chung KY, Rasmussen SG, Liu T, Li S, DeVree BT, Chae PS, et al. Conformational changes in the G protein Gs induced by the β2 adrenergic receptor. Nature. 2011;477:611–5.
35. Pronk S, Pall S, Schulz R, Larsson P, Bjelkmar P, Apostolov R, et al. GROMACS 4.5: a high-throughput and highly parallel open source molecular simulation toolkit. Bioinformatics. 2013;29:845–54.
36. Cordomi A, Caltabiano G, Pardo L. Membrane protein simulations using AMBER force field and Berger lipid parameters. J Chem Theory Comput. 2012;8:948–58.
37. Ballesteros JA, Weinstein H. Integrated methods for the construction of three dimensional models and computational probing of structure-function relations in G-protein coupled receptors. Methods Neurosci. 1995;25:366–428.
38. Isberg V, de Graaf C, Bortolato A, Cherezov V, Katritch V, Marshall FH, et al. Generic GPCR residue numbers - aligning topology maps while minding the gaps. Trends Pharmacol Sci. 2015;36:22–31.
39. Murakami M, Kouyama T. Crystal structure of squid rhodopsin. Nature. 2008;453:363–7.

3.8. CROSS-COMUNICATION BETWEEN G_I AND G_S IN A G-PROTEIN-COUPLED RECEPTOR HETEROTETRAMER GUIDED BY A RECEPTOR C-TERMINAL DOMAIN

Gemma Navarro[*], Arnau Cordomí[*], Marc Brugarolas, Estefanía Moreno, **David Aguinaga**, Laura Perez-Benito, Sergi Ferré, Antoni Cortés, Vicent Casadó, Josefa Mallol, Enric I. Canela, Carme Lluís, Leonardo Pardo, Peter J. McCormick y Rafael Franco.

[*]Coautores del manuscrito

Manuscrito enviado a *Nature communications*.

Los heterómeros de receptores acoplados a proteína G (GPCR) tienen propiedades únicas cuya base molecular permanece desconocida. La activación de los receptores de adenosina A_1 (A_1R) o A_{2A} ($A_{2A}R$) en las células, que pueden formar heterómeros A_1R-$A_{2A}R$ (A_1-A_{2A}Het), conduce a la señalización canónica dependiente de la proteína G (AMPc) e independiente (β-arrestina). Los ensayos de acumulación de AMPc y de reclutamiento de β-arrestina muestran que la activación del $A_{2A}R$ impide la señalización a través del A_1R en el A_1-A_{2A}Het. Este bloqueo cruzado no ha sido observado en ausencia de la activación del $A_{2A}R$ por agonistas, en la ausencia del dominio C-terminal del $A_{2A}R$, o en la presencia de péptidos sintéticos que rompen la interfaz heteromérica del heterómero A_1-A_{2A}. Por lo tanto, en este trabajo ha sido identificado un nuevo mecanismo de transducción de señal, en el que la cola C-terminal del receptor $A_{2A}R$ influye en la señalización mediada por la proteína G_i del receptor A_1R. Este mecanismo proporciona la base molecular para el funcionamiento del heterómero A_1R-$A_{2A}R$ como dispositivo de detección de la concentración de adenosina que modula las señales tanto del A_1R como del $A_{2A}R$.

CROSS-COMMUNICATION BETWEEN G_I AND G_S IN A G-PROTEIN-COUPLED RECEPTOR HETEROTETRAMER GUIDED BY A RECEPTOR C-TERMINAL DOMAIN

Gemma Navarro[1,2,3]*, Arnau Cordomí[4]*, Marc Brugarolas[1,2,3], Estefanía Moreno[1,2,3], David Aguinaga[1,2,3], Laura Pérez-Benito[4], Sergi Ferre[5], Antoni Cortés[1,2,3], Vicent Casadó[1,2,3], Josefa Mallol[1,2,3], Enric I. Canela[1,2,3], Carme Lluís[1,2,3], Leonardo Pardo[4,&], Peter J. McCormick[1,2,3,6&] and Rafael Franco[3,&]

[1]*Centro de Investigación Biomédica en Red sobre Enfermedades Neurodegenerativas.* [2]*Institute of Biomedicine of the University of Barcelona (IBUB).* [3]*Department of Biochemistry and Molecular Biology, Faculty of Biology, University of Barcelona, Barcelona, 08028 Spain;* [4]*Laboratori de Medicina Computacional, Unitat de Bioestadística, Facultat de Medicina, Universitat Autònoma de Barcelona, 08193 Bellaterra, Spain;* [5]*Integrative Neurobiology Section, National Institute on Drug Abuse, National Institutes of Health, Baltimore, MD 21224, USA;* [6]*School of Veterinary Medicine, University of Surrey, Guildford GU2 7AL.*

*These authors contributed equally to this work

[&]These authors equally supervised this work

Corresponding authors:

Leonardo Pardo: leonardo.pardo@uab.es, Peter J. McCormick: p.mccormick@surrey.ac.uk, Rafael Franco: rfranco@ub.edu

Short Title: Cross-communication between G proteins

ABSTRACT

G-protein-coupled receptor (GPCR) heteromers have unique properties whose molecular basis remains unknown. Activation of adenosine A_1 or A_{2A} receptors (A_1R or $A_{2A}R$) in cells, which can form A_1R-$A_{2A}R$ heteromers (A_1-A_{2A}Het), leads to canonical G-protein-dependent (adenylate cyclase-mediated) and independent (ß-arrestin-mediated) signaling. cAMP accumulation and ß-arrestin recruitment assays show that activation of $A_{2A}R$ impedes signaling via the A_1R in the A_1-A_{2A}Het. This cross-blockade is not observed in the absence of $A_{2A}R$ activation by agonists, in the absence of the C-terminal domain of $A_{2A}R$, or in the presence of synthetic peptides that disrupt the heteromeric interface of A_1-A_{2A}Het. Our data has identified a new mechanism of signal transduction that implies a cross-communication between G_i and G_s proteins guided by the C-terminal tail of the $A_{2A}R$. This mechanism provides the molecular basis for the operation of the A_1-A_{2A}Het as an adenosine-concentration sensing device that modulates the signals of both A_1R and $A_{2A}R$.

INTRODUCTION

Adenosine is a purine nucleoside whose relevance in the central nervous system is large part due to its role in regulating neurotransmitter release [1]. The effects of adenosine are mediated by specific G-protein-coupled receptors (GPCRs) that are named due to their interaction with intracellular heterotrimeric $G_{\alpha\beta\gamma}$ proteins. The endogenous adenosine ligand acts on four receptor subtypes: A_1R, $A_{2A}R$, $A_{2B}R$ and A_3R. Convergent and compelling evidence show that GPCRs may form complexes constituted by a number of equal (homo) or different (hetero) molecules [2]. As agreed in the field, a GPCR heteromer displays characteristics that are different from those of the constituting protomers, thus giving rise to novel functional entities [3]. Adenosine receptors have been used as a paradigm in the study of receptor homo and heteromerization (see http://www.gpcr-hetnet.com/ and references therein). For instance, A_1R, which is G_i-coupled, and $A_{2A}R$, which is G_s-coupled, form a functional heteromer [4].

The A_1R-$A_{2A}R$ heteromer (A_1-A_{2A}Het) is found presynaptically in cortical glutamatergic terminals innervating the striatum and functions as a switch that differentially senses high and low concentrations of adenosine in the inter-synaptic space. Since adenosine has higher affinity for A_1R than for $A_{2A}R$, low concentrations bind predominantly to A_1R, engaging a G_i-mediated signaling, whereas higher adenosine concentrations also bind to $A_{2A}R$, engaging a G_s-mediated signaling [4]. The physiological role of such a concentration-sensing device is remarkable as it allows adenosine to fine-tune modulate the release of neurotransmitters from presynaptic terminals. However, the mechanism by which A_1-A_{2A}Het integrates both G_i- and G_s-dependent signals is not yet understood. We have recently shown, using a combination of single-particle tracking experiments, bioluminescence resonance energy transfer (BRET) assays and computer modeling, that the (minimal) functional A_1-A_{2A}Het/G protein unit is composed by a compact rhombus-shaped heterotetramer (with A_1R and $A_{2A}R$ homodimers), which is bound to two different interacting heterotrimeric G proteins (G_s and G_i) [5]. In the present study, we aim to understand the molecular intricacies underlying the signaling mediated by A_1-A_{2A}Het, in which i) both receptors constituting the heteromer are activated by the same endogenous agonist and ii) it is coupled to two different G proteins with opposed effect, i.e. one mediating the inhibition of the adenylate cyclase (G_i) and another mediating the activation of the

enzyme (G_s). Our data identifies a new mechanism of signal transduction and provide the molecular basis to understand the unique properties of this heteromer, in which the C terminal tail of the $A_{2A}R$ influences the Gi-mediated signaling of the partner A_1R receptor.

RESULTS

Homodimerization of A_1R and $A_{2A}R$ occurs through the TM4/5 interface and heterodimerization via TM5/6 in the A_1-A_{2A}Het

Our recently published BRET-aided computational model of the A_1-A_{2A}Het predicted the TM interfaces involved in homo- (TM4/5) and hetero-dimerization (TM5/6) [5]. To further confirm this arrangement, we used synthetic peptides with the sequence of TM domains of the $A_{2A}R$ (abbreviated TM1 to TM7), fused to the cell-penetrating HIV transactivator of transcription (TAT) peptide [6], to alter inter-protomer interactions in the A_1-A_{2A}Het. These peptides were first tested in Bimolecular Fluorescence Complementation (BiFC) assays in HEK-293T cells expressing receptors fused to two complementary halves of YFP (cYFP and nYFP) (see Methods). We detected fluorescence in HEK-293T cells transfected with cDNAs for $A_{2A}R$-nYFP, $A_{2A}R$-cYFP, and non-fused A_1R (control in Fig. 1A), indicating the formation of the $A_{2A}R$-$A_{2A}R$ homodimer. Notably, in the presence of interference peptides, we observed fluorescence decreased only with TM4 and TM5 (Fig. 1A). These results therefore confirmed the TM 4/5 interface for $A_{2A}R$ homodimerization. Similarly, we detected fluorescence in cells expressing A_1R-nYFP and $A_{2A}R$-cYFP (control in Fig. 1B), indicating formation of the A_1-A_{2A}Het. This fluorescence was only reduced in the presence of TM4, TM5 and TM6 peptides (Fig. 1B). These results reinforce our previously proposed compact rhombus-shaped arrangement of protomers in which heteromerization of A_1-A_{2A}Het occurs via the TM5/6 interface (Fig. 1F). The fluorescence decrease induced by TM4 could indicate that the correct homomerization is a requisite for A_1-A_{2A}Het occurs or that the TM4 peptide interferes with interactions of the TM 4 of the external protomer of the $A_{2A}R$ homodimer with the internal protomer of the A_1R homodimer (Fig. 1F) [5]. Next we evaluated whether receptor activation, by the A_1R-selective agonist N^6-cyclopentyladenosine (CPA), the $A_{2A}R$-selective agonist 4-[2-[[6-Amino-9-(N-ethyl-β-D-ribofuranuronamidosyl)-9H-purin-2-yl]amino]ethyl] benzenepropanoic acid (CGS-21680) or both, modify the heteromer TM interface. As clearly shown in Figs. 1C-1E, none of the agonists alone (Figs. 1C, D) or in combination (Fig. 1E) modified the effect of the TM peptides relative to the ligand-free experiments. Therefore, no rearrangements of the TM interface in A_1-A_{2A}Het occurred upon receptor activation. This is compatible with our proposal that both G_i and G_s proteins are bound to the external protomers of the A_1-A_{2A}Het, because, with this arrangement, the agonist-

induced outward movement of TM6, opening a cavity for the binding of the C-terminal α5 helix of the G-protein [7], does not interfere with the involvement of the TM 5/6 interface in heteromerization [8].

Next we investigated if interfering TM peptides, which are able to alter the quaternary structure of the A_1-A_{2A}Het as demonstrated by BiFC experiments, are also able to disrupt the heteromer. To do this, Proximity Ligation Assays (PLA) were performed in HEK-293T cells expressing A_1R and A_{2A}R. The PLA assay is a powerful technique to detect protein-protein interactions that permits assessing proximity between proteins (GPCR protomers in our case), within an oligomer, with high resolution (< 40 nm). A_1-A_{2A}Het was observed as red punctate staining (Fig. 2). Pretreatment of cells with TM4, TM5, TM6 and TM7 of A_{2A}R did not decreased PLA staining (Fig. 2), indicating that interfering peptides can alter the quaternary structure of the heteromer but cannot disrupt heteromerization.

The complex formed by G_s, G_i and the A_1-A_{2A}Het as a signal transduction unit

We tested whether the A_1-A_{2A}Het can signal through G_s- and G_i-dependent pathways by measuring cAMP levels in cells expressing both A_1R and A_{2A}R. The A_1R-selective agonist CPA decreased forskolin-induced cAMP due to a G_i coupling, and the A_{2A}R-selective agonist CGS21680 increased cAMP due to a G_s coupling (Fig. 3A, control), indicating that both receptors signal via their cognate G protein. We performed the same experiments in cells treated with pertussis (PTX) or cholera (CTX) toxins, which alter G_i- and G_s-mediated signaling, respectively, and in cells transfected with minigenes that encode for peptides blocking the interaction of the receptor with the α subunits of G_i or G_s [9]. As expected, we observed blockade of CPA-induced cAMP decrease by either PTX (Fig. 3A) or the G_i-specific minigene (Fig. 3B), and blockade of CGS21680-induced cAMP increase by CTX (Fig. 3A) or the G_s-specific minigene (Fig. 3B). Strikingly, PTX or G_i-specific minigene (blocking G_i-receptor interaction) also blocked the CGS21680-induced cAMP increase (Fig. 3A, B). Moreover, CTX or G_s-specific minigene (blocking G_s-receptor interaction) also blocked the CPA-induced cAMP decrease (Fig. 3A, B). Control experiments using these agonists in cells expressing only A_1R or A_{2A}R did not show any crossover effect with either toxins or minigenes (Figs. S1A-D). These results demonstrate that both A_1R- and A_{2A}R-mediated signaling in the A_1-A_{2A}Het are dependent on the functional integrity of both G_i and G_s proteins. This

cross-communication could depend on the ability of α subunits of G_i and G_s coupled to the A_1-A_{2A}Het to establish molecular interactions (see below).

To further test this cross-communication between G proteins in the G_s-G_i-heterotetramer signaling unit, we resolved the real-time signaling signature by using a label-free method, based on optical detection of dynamic changes in cellular density following receptor activation [10]. The magnitude of the signaling by CPA or by CGS 21680 significantly decreased when cells co-expressing both receptors were pre-treated in both cases with either PTX or CTX (Fig. 3D). This phenomenon was not observed in cells only expressing A_1R (Fig. S1E) or A_{2A}R (Fig. S1F). Again, these results indicate the simultaneous coupling of interacting G_s and G_i proteins within the A_1-A_{2A}Het.

Simultaneous activation of both A_1R and A_{2A}R with CPA and CGS21680, respectively, increased cAMP to similar levels to those obtained with CGS21680 alone and the signal of co-activated receptors was inhibited by both PTX and CTX (Fig. 3C). Therefore, A_1R agonist was able to decrease forskolin-induced cAMP and yet was unable to decrease A_{2A}R-mediated increases of cAMP. Consequently, when both receptors are co-activated in the heterotetramer, only the A_{2A}R-mediated, but not the A_1R-mediated signaling occurs. This finding was confirmed in label-free experiments, showing that receptor co-activation with CPA and CGS 21680 did not increase the time-response curve with respect to the activation with CGS 21680 (Fig. 3D green lines).

It has been shown that the mechanism for receptor-catalyzed nucleotide exchange in G proteins involves a large-scale opening of the α-helical domain (αAH) of the α-subunit, from the Ras domain, allowing GDP to freely dissociate [11-14]. Notably, our proposed model of the A_1-A_{2A}Het positions the α_iAH and α_sAH domains facing each other (Figs. 3E-F). The fact that both G_s- and G_i-specific toxins and G_s- and G_i-specific minigenes affect both G_s- and G_i-mediated coupling in the A_1-A_{2A}Het suggests that the proposed large-scale conformational changes of αAH domains could be mutually dependent. We used molecular dynamics (MD) simulations of the A_1-A_{2A}Het in complex with G_s and G_i to evaluate intermolecular distances between the α_sAH and α_iAH domains in the open and closed conformations (Fig. S2). Double electron–electron resonance (DEER) distance distributions between spin labels attached to Arg90 (α_iAH domain) and Glu238 (Ras domain) of G_i (the distance between Cα atoms is termed d[Arg90α_i-Glu238α_i] in the manuscript) or Asn112 (α_sAH) and Asn261 (Ras)

of G_s (d[Asn112α_s-Asn261α_s]) permitted to faithfully monitor the equilibrium between open (distance of ~40Å) and closed (~20Å) conformation of the αAH domain [14]. The intermolecular distance between the α_sAH and α_iAH domains was measured as the distance between the Cα atoms of Arg90 of α_i and Asn112 of α_s (d[Arg90α_i-Asn112α_s]). This d[Arg90α_i-Asn112α_s] intermolecular distance between α_iAH in the closed conformation (d[Arg90α_i-Glu238α_i]=11 Å, yellow line in Fig. S2B) and α_sAH in the closed conformation (d[Asn112α_s-Asn261α_s]=14 Å, green line in Fig. S2B) has an average value of 108 Å for inactive A_1-A_{2A}Het (dark red line in Fig. S2B, left panel in Fig. 3E). Activation of A_{2A}R would trigger the opening of α_sAH (d[Asn112α_s-Asn261α_s]=52 Å, green line in Fig. S2C, middle panel in Fig. 3E), necessary for GDP/GTP exchange, decreasing the d[Arg90α_i-Asn112α_s] distance between α_iAH and α_sAH to 60 Å (dark red line in Fig. S2C). Similar conclusions would be obtained by activation of A_1R (not shown). This indicates that both receptors can signal via their cognate G protein by opening their αAH domain. However, in the compact rhombus-shaped A_1-A_{2A}Het model, simultaneous opening of both αAH domains (co-activation with CPA and CGS 21680) would not be possible due to a steric clash in such open conformations (Fig. 3E, right panel). Due to this steric clash, MD simulations of this open α_iAH-open α_sAH conformation in the absence of interference peptides (see below) was not performed.

Next we investigated whether the correct formation of the A_1-A_{2A}Het is a necessary condition for the crosstalk between the G_s- and G_i- signaling units using the interference peptides (TM4, TM5 and TM6, which alter receptor heterodimerization, and TM7 as a negative control). Remarkably, pretreatment of cells expressing A_1-A_{2A}Het with the interference peptides did not change receptor signaling when only one receptor is activated (Fig. 4A). Interestingly, in the presence of TM4, TM5 and TM6 peptides, simultaneous activation of both A_1R and A_{2A}R with CPA and CGS21680, respectively, allows CPA to decrease CGS21680-stimulated cAMP (Fig. 4A), in contrast to experiments in the absence of interference peptides (Fig. 4A, control) or TM 7 used as a negative control (Fig. 4A). Thus, modification of the quaternary structure of the A_1-A_{2A}Het with peptides that interfere with the heteromer interface abolishes inhibition of A_1R by A_{2A}R in the G_s-G_i-heterotetramer signaling unit. These experimental results suggest that synthetic peptides inserted between A_1R and A_{2A}R protomers, which are

not able to disrupt the heteromer as seen by PLA (see Fig. 2), increase the distance between G_i and G_s. This would allow the simultaneous opening of α_iAH and α_sAH domains for GDP dissociation. In order to verify this hypothesis, we modeled the A_1-A_{2A}Het with the TAT-fused peptide TM 6 altering the heteromeric interface between A_1R and A_{2A}R, in complex with G_s (open α_sAH, d[Asn112α_s-Asn261α_s]=56 Å, green line in Fig. S2D) and G_i (open α_iAH, d[Arg90α_i-Glu238α_i]=52 Å, yellow line in Fig. S2D). Due to the insertion of TM 6, the distance between the binding site of A_1R and A_{2A}R increases by 17 Å, from 14 Å in the absence of TM 6 (black line in Figs. S2B-C) to 31 Å in the presence of TM 6 (black line in Fig. S2D). This increase in the distance between heteromers also moves the intracellular α_iAH and α_sAH domains apart, thus, permitting their simultaneous opening (d[Arg90α_i-Asn112α_s]=10 Å, dark red line in Fig. S2D, Fig. 4B) for GDP/GTP exchange.

Recruitment of β-arrestin-2 by the A_1-A_{2A}Het

Recruitment of β-arrestins by the A_1-A_{2A}Het, a signaling that is G-protein independent (Fig. S3A), was also analyzed. We used BRET assays to detect the interaction between a GPCR protomer and β-arrestin-2. Thus, cells were transfected with cDNAs of β-arrestin-2 fused to *Renilla* Luciferase (Arr-Rluc) as BRET donor and A_1R or A_{2A}R fused to YFP (A_1R-YFP, A_{2A}R-YFP) as BRET acceptor. Control experiments in cells expressing only A_1R-YFP or A_{2A}R-YFP and Arr-Rluc show the ability of both receptors to recruit ß-arrestin-2 when expressed alone and the specificity of the agonist (Fig. S3B). Similar experiments in cells additionally expressing non-fused A_{2A}R (Arr-Rluc/A_1R-YFP+A_{2A}R) or non-fused A_1R (Arr-Rluc/A_{2A}R-YFP+A_1R) were performed (Fig. S3B). Interestingly, in cells expressing Arr-Rluc, A_{2A}R-YFP and non-fused A_1R (control in Fig. 5A and Fig. S3B) or Arr-Rluc, A_1R-YFP and non-fused A_{2A}R (Fig. S3B), similar degree of BRET was induced by CGS-21680 (white bars) or by CGS-21680 plus CPA (scratched bars). This suggests that agonist binding to A_{2A}R inhibits the CPA ability to recruit β-arrestin-2. In order to rationalize these results, we have used the recent crystal structure of rhodopsin bound to visual arrestin-1 [15] to model the A_1-A_{2A}Het in complex with β-arrestin-2. The finger loop of arrestin, which adopts a short α-helix, is inserted into the intracellular cavity of the external protomer, whereas the C-domain of arrestin points towards the internal protomer of the homodimer (Fig. 5B). The A_1-A_{2A}Het quaternary structure permits, similarly to the simultaneous binding of G_i

and G_s to the heterotetramer, the binding of two arrestin molecules to the external protomers of both A_1R and $A_{2A}R$. Moreover, the model of A_1-A_{2A}Het in complex with G_i and β-arrestin-2 (Fig. 5B) shows no steric clashes between G_i (bound to A_1R) and arrestin (bound to $A_{2A}R$). These results suggest that sustained activation of G_s ($G_{\beta\gamma}$ moving away from $G_{\alpha s}$ to facilitate the interaction of $G_{\alpha s}$ with the catalytic domain of adenylate cyclase) by agonist binding to $A_{2A}R$, enables β-arrestin-2 recruitment to $A_{2A}R$. As stated above, within the A_1-A_{2A}Het, CPA cannot activate G_i in the presence of the $A_{2A}R$ agonist CGS-21680 (Fig. 3), and consequently, CPA does not trigger additional β-arrestin-2 recruitment to A_1R (control in Fig. 5A and Fig. S3B).

Using the TAT-fused synthetic peptides we investigated whether the quaternary structure of the A_1-A_{2A}Het determines its putative selective $A_{2A}R$-dependent ß-arrestin-2 recruitment. Pretreatment of cells expressing Arr-Rluc, $A_{2A}R$-YFP and non-fused A_1R with TM4, TM5 and TM6 peptides, but not in the absence of peptides (control) or with the TM7 peptide (negative control), allowed to detect positive BRET (recruitment of ß-arrestin-2) not only when cells were treated with the $A_{2A}R$ selective agonist CGS-21680 (white bars), but also when treated with the A_1R selective agonist CPA (black bars) (Fig. 5A). Importantly, when these cells were co-activated by CPA and CGS-21680 (scratched bars), BRET measurement in the presence of TM4, TM5, or TM6, but not in the absence of peptides or TM7, increased significantly relative to the values obtained by the action of a single agonist (Fig. 5A). These results indicate that alteration of the A_1R-$A_{2A}R$ heteromer interface within the A_1-A_{2A}Het allows simultaneous recruitment of β-arrestin-2 to A_1R and $A_{2A}R$ when both receptors are activated. Interference peptides abolish cross-communication of G proteins, permitting CPA to activate G_i ($G_{\beta\gamma}$ moving away from $G_{\alpha i}$) and recruitment of β-arrestin-2 to A_1R, as well as G_s activation by CGS-21680 ($G_{\beta\gamma}$ moving away from $G_{\alpha s}$) and simultaneous recruitment of β-arrestin-2 to $A_{2A}R$.

The C-terminal domain of $A_{2A}R$ is responsible for the dominant $A_{2A}R$-mediated signaling

A major difference between A_1R and $A_{2A}R$ is the length of the intracellular C-terminal domain (16 amino acids in A_1R versus 102 in $A_{2A}R$). The short C-terminal tail of the A_1R does not have any known specific function, while the C-terminus of $A_{2A}R$, albeit dispensable for ligand binding [16], dimerization [17], and agonist induced cAMP signaling

[18], influences constitutive signaling [19]. Due to the shorter C-terminus of A_1R and the proposed orientation of the C-tail of $A_{2A}R$ toward α_sAH (see Fig. S4A for details), we speculated that the C-terminus of $A_{2A}R$ could modulate the prevailing G_s-mediated signaling upon A_1R and $A_{2A}R$ co-activation. To test this hypothesis, we engineered two $A_{2A}R$ mutants, one lacking most of the C-terminal end ($A_{2A}^{\Delta CT}R$) and another lacking the last 40 amino acids ($A_{2A}^{\Delta 40}R$). First, we tested whether these truncated versions of the $A_{2A}R$ could form heteromers with the A_1R. We observed similar BRET saturation curves in HEK-293T cells expressing a constant amount of A_1R-Rluc cDNA and increasing amounts of either $A_{2A}R$-YFP, $A_{2A}^{\Delta 40}R$-YFP or $A_{2A}^{\Delta CT}R$-YFP, indicating that $A_{2A}^{\Delta 40}R$ and $A_{2A}^{\Delta CT}R$ form heteromers with A_1R (Fig. 6A; $BRET_{max}$ in mU: 91±3 $A_{2A}R$, 99±3 $A_{2A}^{\Delta 40}R$ and 90±8 $A_{2A}^{\Delta CT}R$). Second, we measured cAMP production in cells expressing A_1R and wild-type or truncated $A_{2A}R$ receptors (Fig. 6B). Truncated $A_{2A}R$ were able to signal as wild-type receptors. Interestingly, the dominant G_s-mediated signaling when A_1R and $A_{2A}R$ are co-activated decreased progressively with the shortening of the $A_{2A}R$ C-tail (Fig. 6B, scratched bars). In fact, CPA was able to inhibit CGS-21680-induced cAMP accumulation when truncated receptors were expressed, showing that in these heteromers A_1R were functional. Fig. 6D shows a detailed view of the orientation of the C-tail (102 amino acids, Gln311-Ser412) of both $A_{2A}R$ protomers in the A_1-A_{2A}Het, which was modeled as suggested for the OXER [20], together with the structure of ß-arrestin-2 in complex with V2 vasopressin receptor [21] (see Fig. S4 for details). The fact that the C-tail of the α_s-unbound $A_{2A}R$ protomer points toward the α_sAH domain, suggests that this C-tail is influencing the conformational changes required to open the α_sAH, and thus controlling the balance between G_s and G_i activation. Next, we measured β-arrestin recruitment by BRET assay in cells expressing A_1R and wild-type or truncated $A_{2A}R$ receptors. In cells expressing non-fused A_1R, Arr-Rluc and $A_{2A}R$-YFP or $A_{2A}^{\Delta 40}R$-YFP or $A_{2A}^{\Delta CT}R$-YFP, the A_1R agonist CPA was able to increase BRET values when the heteromer is formed only with $A_{2A}R$ truncated receptors and, in these conditions, co-activation with CPA and CGS-21860 induced a BRET increase higher than the one obtained with CGS-21680 alone (Fig. 6C). These results indicate that the selective $A_{2A}R$-dependent β-arrestin-2 recruitment in the A_1-A_{2A}Het decreases progressively with the shortening of the $A_{2A}R$ C-tail (Fig. 6C).

DISCUSSION

As previously reviewed, [2,3,19] the intercommunication between protomers of a GPCR heteromer, can be observed at the level of agonist binding, ligand-induced cross-conformational changes between receptor protomers, and the binding of GPCR-associated proteins, including heterotrimeric G proteins and β-arrestins. The intercommunication between protomers is a consequence of a defined quaternary structure that is responsible for the specific functional characteristics of the heteromer. For GPCR heteromers constituted by different receptors, sensing the same hormone and producing opposite signaling effects, such as A_1-A_{2A}Het, is not obvious to understand how a defined quaternary structure can allow this dual behavior. A_1-A_{2A}Het acts as a concentration-sensing device that allows adenosine to signal by one or the other receptor to fine-tune modulate the release of neurotransmitters from presynaptic terminals. In the present study, we solved this question by discovering a new mechanism of signal transduction, a cross-communication between G_i and G_s in the G-protein-coupled A_1-A_{2A}Het guided by the A_{2A}R C-terminal domain.

We have shown that cross-communication between G_i and G_s proteins involves the formation of a GPCR heterotetramer (i.e., one homodimer of A_1R and one of A_{2A}R) that has a 2:2:1:1 (A_{2A}R:A_1R:G_s:G_i) stoichiometry. From our data, it is deduced that the cross-talk between G_i and G_s resides on the structural constraints surrounding the mechanism for GDP/GTP exchange, which involves the opening of the αAH domain of the α-subunit of any given G protein. We propose that cross-communication in the G_s-G_i-heterotetramer signaling unit is a property associated with a specific quaternary structure, the compact rhombus-shaped A_1-A_{2A}Het (the TM 4/5 interface for homodimerization and the TM 5/6 interface for heterodimerization), which positions the α_iAH and α_sAH domains in close proximity, making their conformational changes mutually dependent in a way that simultaneous opening of both αAH domains would not be possible due to a steric clash in such open conformations. Alterations of this quaternary structure of the A_1-A_{2A}Het by insertion of synthetic peptides between A_1R and A_{2A}R blocks this cross-communication without disrupting the heteromer and permits simultaneous activation of G_i and G_s in the heteromer. Since the cross-talk between G_i and G_s resides on the structural constraints imposed by a defined TM interfaces in the heteromer it is important to note that other heterotetramers, mainly those sensing different hormones, with different quaternary structure might not display

this cross-communication among G proteins. Moreover, although from a structural point of view A_1-A_{2A}Het is capable to recruit not only two G proteins but also two ß-arrestin proteins, the cross-talk between G_i and G_s, in which G_s activation inhibits de simultaneous activation of G_i, blocks A_1R agonist-promoted arrestin recruitment. Alteration of the A_1-A_{2A}Het by insertion of synthetic peptides between A_1R and A_{2A}R facilitates simultaneous activation of G_i and G_s and the corresponding binding of two ß-arrestin molecules to A_1R and A_{2A}R. Our finding that G_i is dependent on G_s-mediated signaling strengthens the conclusion that cross-talk across G proteins is a potential important functional property of GPCR heteromers. Remarkably, when both receptors are co-activated in this heterotetramer, only the A_{2A}R-mediated, but not the A_1R-mediated signaling occurs. We show that the ability of blunting A_1R-mediated signaling when G_s is engaged is dependent of the long C-terminus of the A_{2A}R. In the absence of A_{2A}R activation by agonists, or in the absence of the C-terminal domain of A_{2A}R, the A_1R-mediated signaling via G_i is totally functional. The most straightforward hypothesis is that the opening of α_sAH parallels a movement of the C-tail to block the opening of α_iAH.

Adenosinergic signaling in mammalians is important for energy and temperature homeostasis and for neuroregulation. Multiplicity of adenosine actions is due to a balance between the expression of specific receptors and producing/degrading enzymes and to the biological diversity due to a membrane network established by the interaction among purinergic receptors [22]. Ciruela et al. [4] first identified the occurrence of heteromers formed by A_1R-G_i- and A_{2A}-G_s-coupled adenosine receptors that participate in the regulation of glutamate release by neurons projecting from the cortex to the striatum. The same A_1-A_{2A}Het can be found in astrocytes modulating the transport of γ-amino butyric acid (GABA) [23]. Differently from the modulation of neuronal glutamate release, the A_1R-G_i-coupled receptor activates and the A_{2A}R-G_s-coupled inhibits in the modulation of GABA transport. Under conditions of high extracellular adenosine concentrations, such as hypoxic conditions [24], the nucleoside will bind to both the high (A_1R) and the low (A_{2A}R) affinity receptors in the heteromer, and the predominant A_{2A}R-mediated signaling via G_s will result in counteraction of astrocytic GABA transport. Our results show that the asymmetric signaling is possible because the long C-terminus of A_{2A}R blunts G_i-mediated signaling. We have therefore elucidated the mechanism by which the A_1-A_{2A}Het functions as an adenosine-concentration sensing

device that can promotes even opposite signaling responses depending on the extracellular concentration of adenosine. The molecular mechanism involves the C-terminal domain of the activated G_s-coupled $A_{2A}R$, which hinders the activation of A_1R-mediated G_i activation.

METHODS

Cell culture and transient transfection

HEK-293T cells were grown at 37ºC in in Dulbecco's modified Eagle's medium (DMEM) (Gibco) supplemented with 2 mM L-glutamine, 100 U/ml penicillin/streptomycin, and 5% (v/v) heat inactivated Fetal Bovine Serum (FBS) (all supplements were from Invitrogen, Paisley, Scotland, UK). Cells were transiently transfected with cDNA corresponding to receptors, fusion proteins, $A_{2A}R$ mutant constructs or minigene vectors using PEI (PolyEthylenImine, SigmaAldrich, Cerdanyola del Vallés, Spain) as described elsewhere [25].

Expression vectors, $A_{2A}R$ mutants and minigenes

Sequences encoding amino acid residues 1-155 or 155-238 of YFP-Venus protein, were subcloned in pcDNA3.1 to obtain the YFP Venus hemi-truncated proteins (nYFP and cYFP). The human cDNAs for $A_{2A}R$, mutant $A_{2A}R$ or A_1R, cloned into pcDNA3.1, were amplified without their stop codons using sense and antisense primers harboring unique EcoRI and BamHI sites to subclone receptors in pcDNA3.1RLuc vector (p*RLuc*-N1 PerkinElmer, Wellesley, MA) and EcoRI and KpnI to subclone receptors in pEYFP-N1 (enhanced yellow variant of GFP; Clontech, Heidelberg, Germany), pcDNA3.1-nVenus or pcDNA3.1-cVenus vectors. The amplified fragments were subcloned to be in-frame with restriction sites of the corresponding vectors to give the plasmids that express receptors fused to RLuc, YFP, nYFP or cYFP on the C-terminal end (A_1R-Rluc, $A_{2A}R$-Rluc, A_1R-YFP, $A_{2A}R$-YFP, $A_{2A}{}^{\Delta 40}R$-YFP, $A_{2A}{}^{\Delta CT}R$-YFP, A_1R-nYFP, A_{2A}-nYFP and A_{2A}-cYFP). Expression of constructs was tested by confocal microscopy and the receptor-fusion protein functionality by second messengers, ERK1/2 phosphorylation and cAMP production as described previously [4,26-28]. Mutants with a deletion of aa 372 to aa 412 ($A_{2A}{}^{\Delta 40}R$) or aa 321 to aa 412 ($A_{2A}{}^{\Delta CT}R$) on the C-terminal domain of $A_{2A}R$ were generated as previously described [29]. "Minigene" plasmid vectors are constructs designed to express relatively short polypeptide sequences following their transfection into mammalian cells. Here we used minigene constructs encoding 11 amino acid residues from the C-terminus sequence of α subunit of $G_{i1/2}$ or G_s. The peptides coded by every minigene inhibits the coupling of the G ($G_{i1/2}$ or G_s) protein to the receptor and, consequently, it inhibits the G-protein-mediated cellular response, as previously described [9]. The cDNA encoding the last 11 amino acids of human G_α subunit

corresponding to $G_{i1/2}$ (IKNNLKDCGLF) or G_s (QRMHLRQYELL), inserted in a pcDNA 3.1 plasmid vector were generously provided by Dr. Heidi Hamm.

TAT-TM peptides

Peptides with the sequence of transmembrane domains (TM) of $A_{2A}R$ fused to the HIV transactivator of transcription (TAT) peptide (YGRKKRRQRRR) were used as oligomer-disrupting molecules (synthesized by Genemad Synthesis Inc. San Antonio, TX). The cell-penetrating TAT peptide allows intracellular delivery of fused peptides [6]. The TAT-fused TM peptide can then be inserted effectively into the plasma membrane because of the penetration capacity of the TAT peptide and the hydrophobic property of the TM moiety [30]. To obtain the right orientation of the inserted peptide, the HIV-TAT peptide was fused to the C-terminus or to the N-terminus as indicated:

VYITVELAIAVLAILGNVLVCWAVWYGRKKRRQRRR for TM1,
YGRKKRRQRRRYFVVSLAAADIAVGVLAIPFAITI for TM2,
LFIACFVLVLTQSSIFSLLAIAIYGRKKRRQRRR for TM3,
YGRKKRRQRRRAKGIIAICWVLSFAIGLTPMLGW for TM4,
MNYMVYFNFFACVLVPLLLMLGVYLYGRKKRRQRRR for TM5,
YGRKKRRQRRRLAIIVGLFALCWLPLHIINCFTFF for TM6,
LWLMYLAIVLSHTNSVVNPFIYAYYGRKKRRQRRR for TM7.

Bimolecular fluorescence complementation assay (BiFC)

HEK-293T cells were transiently transfected with equal amounts of the cDNA for fusion proteins of the hemi-truncated Venus (1 μg of each cDNA). 48 h after transfection cells were treated for 4 h at 37º with medium or TAT-peptides (4 μM) before plating 20 μg of protein in 96-well black microplates (Porvair, King's lynn, UK). To quantify reconstituted YFP Venus expression, fluorescence at 530 nm was read in a Fluoro Star Optima Fluorimeter (BMG Labtechnologies, Offenburg, Germany) equipped with a high-energy xenon flash lamp, using a 10 nm bandwidth excitation filter at 400 nm reading. Protein fluorescence expression was determined as fluorescence of the sample minus the fluorescence of cells not expressing the fusion proteins (basal). Cells expressing receptor-cVenus and nVenus or receptor-nVenus and cVenus showed similar fluorescence levels than non-transfected cells.

Bioluminescence resonance energy transfer (BRET)

HEK-293T cells were transiently transfected with a constant amount of cDNA for Rluc fusion proteins and increasing amounts of cDNA for YFP fusion proteins. 48h after transfection 20 µg of cell suspension were plated in 96-well black microplates for fluorescence detection or in 96-well white microplates for BRET readings and Rluc quantification. YFP fluorescence at 530 nm was quantified in a Fluoro Star Optima Fluorimeter as above described. BRET signal was collected 1 minute after addition of 5 µM coelenterazine H (Molecular Probes, Eugene, OR) using a Mithras LB 940. The integration of the signals detected in the short-wavelength filter at 485 nm and the long-wavelength filter at 530 nm was recorded. To quantify protein-RLuc expression, luminescence readings were also performed after 10 minutes of adding 5 µM coelenterazine H. The net BRET is defined as [(long-wavelength emission)/(short-wavelength emission)]-Cf where Cf corresponds to [(longwavelength emission)/(short-wavelength emission)] for the donor construct expressed alone in the same experiment. BRET is expressed as milli BRET units (mBU; net BRET x 1,000). To calculate maximum BRET ($BRET_{max}$) from saturation curves, data were fitted to a nonlinear regression equation, assuming a single-phase saturation curve with GraphPad Prism software (San Diego, California, US).

Proximity ligation assay (PLA)

HEK293T cells were grown on glass coverslips and fixed in 4% paraformaldehyde for 15 min, washed with phosphate-buffered saline (PBS) containing 20 mM glycine, permeabilized with the same buffer containing 0.05% Triton X-100, and successively washed with TBS. Heteromers were detected using the Duolink II in situ PLA detection Kit (OLink; Bioscience, Uppsala, Sweden) following supplier's instructions. A mixture of the primary antibodies [mouse anti-$A_{2A}R$ antibody (1:100; 05-717, Millipore, Darmstadt, Germany) and rabbit anti-A_1R antibody (1:100; ab82477, Abcam, Bristol, UK) was used to detect A_1-A_{2A}Het together with PLA probes detecting mouse or rabbit antibodies. Then, samples were processed for ligation and amplification with a Detection Reagent Red and were mounted using a DAPI-containing mounting medium. Samples were analyzed in a Leica SP2 confocal microscope (Leica Microsystems, Mannheim, Germany) equipped with a 405 nm and a 561 nm laser lines. For each field of view a stack of two channels (one per staining) and 4 to 6 Z-stacks with a step size of

1 µm were acquired. Images were opened and processed with Image J software (National Institutes of Health, Bethesda, MD).

cAMP determination assays

HEK-293T cells expressing adenosine receptors were incubated for 4 h in serum-free medium containing 50 µM zardeverine. Cells were plated in 384-well white microplates (1500 cells/well), pre-treated with toxins or the corresponding vehicle for the indicated time and stimulated with agonists for 15 min before adding medium or 0.5 µM forskolin, and incubating for an additional 15 min period. cAMP production was quantified by a TR-FRET (Time-Resolved Fluorescence Resonance Energy Transfer) methodology using the LANCE Ultra cAMP kit (PerkinElmer) and fluorescence at 665 nm was analyzed on a Pherastar Flagship Microplate Reader (BMG Labtech, Ortenberg, Germany).

Dynamic-mass-redistribution (DMR) assays

The heteromer-induced cell signaling signature was determined using an EnSpire® Multimode Plate Reader (PerkinElmer, Waltham, MA, USA) by a label free technology. Refractive waveguide grating optical biosensors, integrated in 384-well microplates, allow extremely sensitive measurements of changes in local optical density in a detecting zone up to 150 nm above the surface of the sensor. Cellular mass movements induced upon receptor activation were detected by illuminating the underside of the biosensor with polychromatic light and measured as changes in wavelength of the reflected monochromatic light that is a sensitive function of the index of refraction. The magnitude of this wavelength shift (in picometers) is directly proportional to the amount of DMR. Briefly, 24 h before the assay, cells were seeded at a density of 7,500 cells per well in 384-well sensor microplates with 40 µl growth medium and cultured for 24 h (37°C, 5% CO_2) to obtain 70-80% confluent monolayers. Previous to the assay, cells were pre-treated with medium or toxins as indicated and incubated 2 h in 40 µl per well of assay-buffer (HBSS with 20 mM HEPES, pH 7.15) in the reader at 24°C. Hereafter, the sensor plate was scanned and a baseline optical signature was recorded before adding 10 µl of receptor agonist dissolved in assay buffer containing 0.1% DMSO and DMR responses were monitored for at least 8,000 s. Data were analyzed using EnSpire Workstation Software v 4.10.

Computational modeling

The structural model of the A_1-A_{2A}Het bound to G_s (closed α_sAH domain) and G_i (closed α_iAH domain) was taken from our previous work [5]. This previous structural model contains a A_{2A}R-based homology model of A_1R. However, the structure of the adenosine A_1R has recently been revealed [31]. An intermediate conformation (obtained using the g_morph tool of the GROMACS package [32]) between the closed αAH domain (PDB id 1AGR) and the conformation observed in the crystal structure of the β_2-AR in complex with Gs (PDB id 3SN6) was used to model the open αAH domain (Fig. S2A). This conformation is supported by double electron-electron resonance spectroscopy, deuterium-exchange and electron microscopy data [12-14]. The active state of β-arrestin-2 was built using a multi-template alignment combining the structure of the active β-arrestin-1 (PDB id 4JQI) [21] and the structure of rhodopsin in complex with visual ß-arrestin (PDB id 4ZWJ) [15]. Structural models of the A_1-A_{2A}Het bound to β-arrestin-2 were modeled using the crystal structure of rhodopsin bound to β-arrestin (PDB id 4ZWJ) [15]. The structure of TM6 of A_{2A}R fused to the cell-penetrating TAT peptide was modeled from the structure of A_{2A}R. Molecular models of the A_1-A_{2A}Het with the TAT-fused TM6 peptide, disrupting the heteromeric interface between A_1R and A_{2A}R, in complex with G_s (open α_sAH domain) and G_i (open α_iAH domain) was built from the structure of A_1-A_{2A}Het. The conformation of the C-tail of A_{2A}R, containing 102 amino acids (Gln311–Ser412), cannot be unambiguously determined. It was modeled as suggested for the oxoeicosanoid receptor (OXER) [20], together with the structure derived from the human V2 vasopressin receptor in complex with ß-arrestin-2 [21] (see Fig. S4 for details). Modeller 9.12 was used to build these models [33]. These molecular models of A_1-A_{2A}Het in complex with G_s and G_i or ß-arrestin, in the absence or presence of the TAT-fused TM6 peptide, were embedded in a pre-equilibrated box containing a lipid bilayer (~800 POPC molecules) with explicit solvent (~110,000 waters) and 0.15 M concentration of Na^+ and Cl^- (~1,800 ions). These initial complexes were energy-minimized and subsequently subjected to a 21 ns MD equilibration, with positional restraints on protein coordinates. These restraints were released and 500 ns of MD trajectory were produced at constant pressure and temperature. Computer simulations were performed with the GROMACS 4.6.3 simulation package [32], using the AMBER99SB force field as implemented in GROMACS and Berger parameters for POPC lipids. This procedure has been previously validated [34].

ACKNOWLEDGMENTS

We would like to thank Jasmina Jiménez for technical help (University of Barcelona). This study was supported by grants from the Spanish *Ministerio de Economía y Competitividad* (SAF2015-74627-JIN, SAF2016-77830-R). PJM and LP participate in the European COST Action CM1207 (GLISTEN).

REFERENCES

1. Thompson, S.M., Haas, H.L. & Gahwiler, B.H. Comparison of the actions of adenosine at pre- and postsynaptic receptors in the rat hippocampus in vitro. *J. Physiol.* **451**, 347-63 (1992).
2. Franco, R., Martinez-Pinilla, E., Lanciego, J.L. & Navarro, G. Basic Pharmacological and Structural Evidence for Class A G-Protein-Coupled Receptor Heteromerization. *Front. Pharmacol.* **7**, 76 (2016).
3. Ferre, S. et al. Building a new conceptual framework for receptor heteromers. *Nat. Chem. Biol.* **5**, 131-4 (2009).
4. Ciruela, F. et al. Presynaptic control of striatal glutamatergic neurotransmission by adenosine A1-A2A receptor heteromers. *J. Neurosci.* **26**, 2080-7 (2006).
5. Navarro, G. et al. Quaternary structure of a G-protein-coupled receptor heterotetramer in complex with Gi and Gs. *BMC Biol.* **14**, 26 (2016).
6. Schwarze, S.R., Ho, A., Vocero-Akbani, A. & Dowdy, S.F. In vivo protein transduction: delivery of a biologically active protein into the mouse. *Science* **285**, 1569-72 (1999).
7. Rasmussen, S.G. et al. Crystal structure of the beta2 adrenergic receptor-Gs protein complex. *Nature* **477**, 549-55 (2011).
8. Cordomi, A., Navarro, G., Aymerich, M.S. & Franco, R. Structures for G-Protein-Coupled Receptor Tetramers in Complex with G Proteins. *Trends Biochem. Sci.* **40**, 548-51 (2015).
9. Gilchrist, A., Li, A. & Hamm, H.E. G alpha COOH-terminal minigene vectors dissect heterotrimeric G protein signaling. *Sci. STKE* **2002**, pl1 (2002).
10. Schroder, R. et al. Applying label-free dynamic mass redistribution technology to frame signaling of G protein-coupled receptors noninvasively in living cells. *Nat. Protoc.* **6**, 1748-60 (2011).
11. Van Eps, N. et al. Interaction of a G protein with an activated receptor opens the interdomain interface in the alpha subunit. *Proc. Natl. Acad. Sci. U S A* **108**, 9420-4 (2011).
12. Chung, K.Y. et al. Conformational changes in the G protein Gs induced by the beta2 adrenergic receptor. *Nature* **477**, 611-5 (2011).
13. Westfield, G.H. et al. Structural flexibility of the G alpha s alpha-helical domain in the beta2-adrenoceptor Gs complex. *Proc. Natl. Acad. Sci. U S A* **108**, 16086-91 (2011).
14. Dror, R.O. et al. SIGNAL TRANSDUCTION. Structural basis for nucleotide exchange in heterotrimeric G proteins. *Science* **348**, 1361-5 (2015).
15. Kang, Y. et al. Crystal structure of rhodopsin bound to arrestin by femtosecond X-ray laser. *Nature* **523**, 561-7 (2015).
16. Piersen, C.E., True, C.D. & Wells, J.N. A carboxyl-terminally truncated mutant and nonglycosylated A2a adenosine receptors retain ligand binding. *Mol. Pharmacol.* **45**, 861-70 (1994).
17. Canals, M. et al. Homodimerization of adenosine A2A receptors: qualitative and quantitative assessment by fluorescence and bioluminescence energy transfer. *J. Neurochem.* **88**, 726-34 (2004).
18. Palmer, T.M. & Stiles, G.L. Identification of an A2a adenosine receptor domain specifically responsible for mediating short-term desensitization. *Biochemistry* **36**, 832-8 (1997).
19. Klinger, M. et al. Removal of the carboxy terminus of the A2A-adenosine receptor blunts constitutive activity: differential effect on cAMP accumulation

and MAP kinase stimulation. *Naunyn Schmiedebergs Arch. Pharmacol.* **366**, 287-98 (2002).
20. Blattermann, S. et al. A biased ligand for OXE-R uncouples Galpha and Gbetagamma signaling within a heterotrimer. *Nat. Chem. Biol.* **8**, 631-8 (2012).
21. Shukla, A.K. et al. Structure of active beta-arrestin-1 bound to a G-protein-coupled receptor phosphopeptide. *Nature* **497**, 137-41 (2013).
22. Schicker, K. et al. A membrane network of receptors and enzymes for adenine nucleotides and nucleosides. *Biochim. Biophys. Acta* **1793**, 325-34 (2009).
23. Cristovao-Ferreira, S. et al. A1R-A2AR heteromers coupled to Gs and G i/0 proteins modulate GABA transport into astrocytes. *Purinergic Signal.* **9**, 433-49 (2013).
24. Lopes, L.V., Sebastiao, A.M. & Ribeiro, J.A. Adenosine and related drugs in brain diseases: present and future in clinical trials. *Curr. Top. Med. Chem.* **11**, 1087-101 (2011).
25. Carriba, P. et al. Detection of heteromerization of more than two proteins by sequential BRET-FRET. *Nat. Methods* **5**, 727-33 (2008).
26. Canals, M. et al. Adenosine A2A-dopamine D2 receptor-receptor heteromerization: qualitative and quantitative assessment by fluorescence and bioluminescence energy transfer. *J. Biol. Chem.* **278**, 46741-9 (2003).
27. Gonzalez, S. et al. Circadian-related heteromerization of adrenergic and dopamine D(4) receptors modulates melatonin synthesis and release in the pineal gland. *PLoS Biol.* **10**, e1001347 (2012).
28. Navarro, G. et al. Interactions between intracellular domains as key determinants of the quaternary structure and function of receptor heteromers. *J. Biol. Chem.* **285**, 27346-59 (2010).
29. Burgueno, J. et al. The adenosine A2A receptor interacts with the actin-binding protein alpha-actinin. *J. Biol. Chem.* **278**, 37545-52 (2003).
30. He, S.Q. et al. Facilitation of mu-opioid receptor activity by preventing delta-opioid receptor-mediated codegradation. *Neuron* **69**, 120-31 (2011).
31. Glukhova, A. et al. Structure of the Adenosine A1 Receptor Reveals the Basis for Subtype Selectivity. *Cell* **168**, 867-877 e13 (2017).
32. Pronk, S. et al. GROMACS 4.5: a high-throughput and highly parallel open source molecular simulation toolkit. *Bioinformatics* **29**, 845-54 (2013).
33. Marti-Renom, M.A. et al. Comparative protein structure modeling of genes and genomes. *Annu. Rev. Biophys. Biomol. Struct.* **29**, 291-325 (2000).
34. Cordomi, A., Caltabiano, G. & Pardo, L. Membrane Protein Simulations Using AMBER Force Field and Berger Lipid Parameters. *J. Chem. Theory Comput.* **8**, 948-958 (2012).

FIGURES

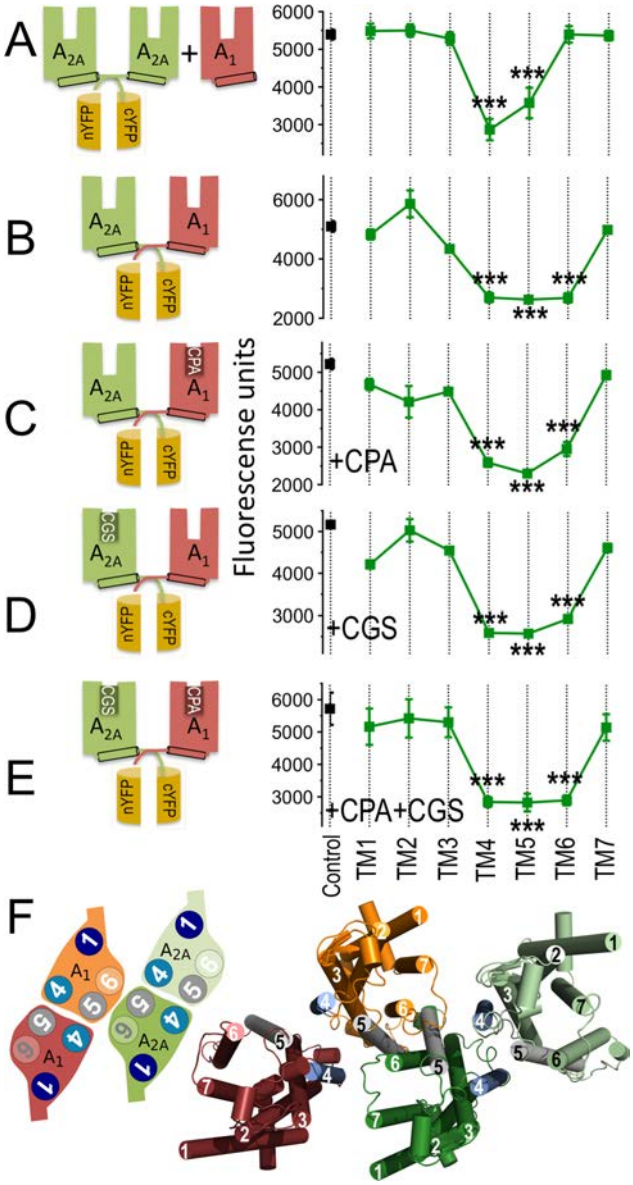

Figure 1. Effect of interfering peptides on the A_1-A_{2A}Het structure determined by Bimolecular Fluorescence Complementation (BiFC) assays.

In (A-E) BiFC assays were performed in HEK-293T cells transfected with cDNAs (1 µg) for A_{2A}R-nYFP, A_{2A}R-cYFP and non-fused A_1R (A) or A_{2A}R-cYFP and A_1R-nYFP (B-E). Cells were pre-treated for 4 h with medium (control) or with 4 µM of A_{2A}R TM synthetic peptides (TM1 to TM7, see Methods) before being not activated (A, B) or activated for 10 min with the A_1R agonist CPA (C, 100 nM), the A_{2A}R agonist CGS-21680 (D, 100 nM) or both (E). Fluorescence was read at 530 nm. Values are the mean ± SEM of 12-15 independent experiments per treatment. One-way ANOVA followed by a Dunnett's multiple comparison tests showed a significant fluorescence decrease

over control values (***p<0.001). In each panel, there is a schematic representation of the BiFC pairs and conditions. In (F) schematic slice (left) and cartoon (right) representations of the A_1-A_{2A}Het built using the predicted experimental interfaces.

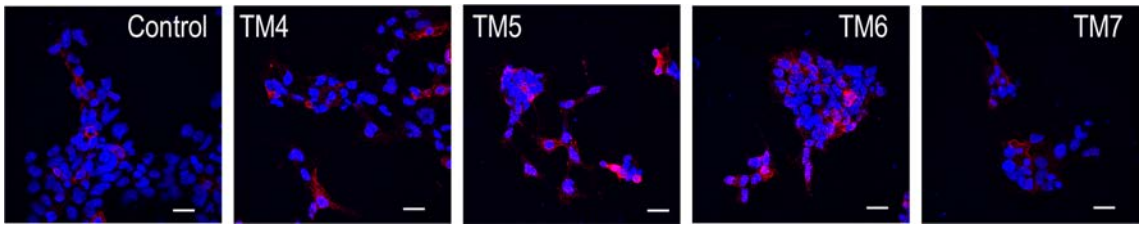

Figure 2. Effect of interfering peptides on the A_1-A_{2A}Het structure determined by Proximity Ligation Assays (PLA)

Confocal microscopy images (superimposed sections) are shown in which A_1-A_{2A}Het appears as red spots. HEK-293T cells expressing A_1R and A_{2A}R were treated for 4 h with medium (control) or 4 μM of indicated TM peptides of A_{2A}R; cell nuclei were stained with DAPI (blue); scale bars: 10 μm.

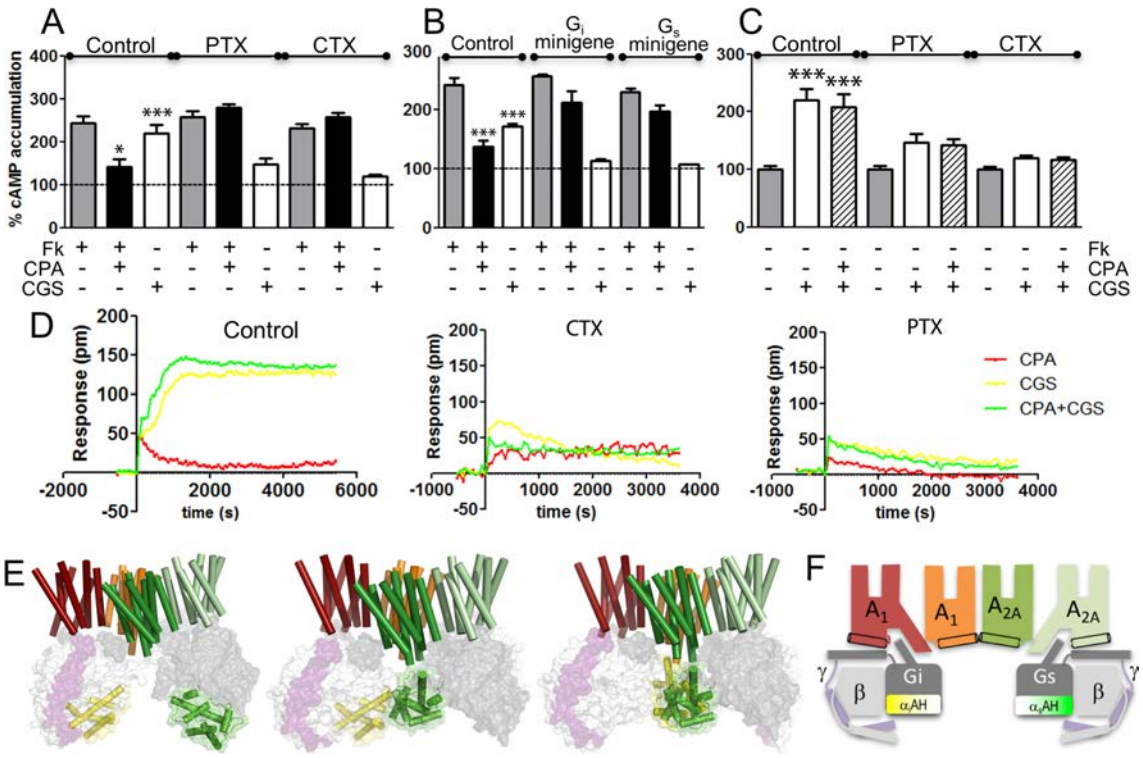

Figure 3. Receptor signaling through the A_1-A_{2A}Het.

In (A, C, D) HEK-293T cells transfected with 0.4 µg of A_1R and A_{2A}R cDNAs were pre-treated with medium (control), overnight with pertussis toxin (PTX, 10 ng/ml) or for 1h with cholera toxin (CTX, 100 ng/mL) before stimulation with medium (basal; dotted line in A, gray bars in C, or 0 response in D), with forskolin (Fk, 0.5 µM, gray bars in A), with forskolin and the A_1R agonist CPA (100nM, black bars in A), with only CPA (red line in D), with the A_{2A}R agonist CGS-21680 (CGS, 100nM, white bars in A, C; yellow line in D) or with CPA and CGS 21680 (scratched bars in C, green line in D). In (B) HEK-293T cells transfected with 0.4 µg of A_1R and A_{2A}R cDNAs in the absence (control) or in the presence of 0.5 µg of cDNA corresponding to the minigene related to G_i (G_i minigene) or G_s (G_s minigene) alpha subunits were stimulated as indicated in A. Increases in cAMP levels (A, B, C) were expressed over non-stimulated cells (basal, 100%). Values are the mean ± SEM of 6-8 experiments per group. One-way ANOVA followed by the Bonferroni's *post hoc* test showed a significant effect over basal in samples only treated with CGS 21680 or over forskolin only stimulated cells in samples in the presence of forskolin ($^{*}p < 0.05$, $^{***}p < 0.001$). In the dynamic mass redistribution analysis (D) the resulting picometer-shifts of reflected light wavelength (pm) against the time were monitored. Each curve is the means of a representative optical trace experiment carried out in triplicates. In (E, F) molecular models of A_1R-A_{2A}R

heteromers in complex with G_i and G_s are shown. The color code of the depicted proteins is: A_1R bound to G_i is shown in red, G_i-unbound A_1R is shown in orange, $A_{2A}R$ bound to G_s is shown in light green, G_s-unbound $A_{2A}R$ is shown in dark green, and the α, β-, and γ-subunits of G_i and G_s are shown in dark gray, light gray, and purple, respectively. TMs 4 and 5 are highlighted in light blue and gray, respectively. The α-helical domains α_iAH and α_sAH are shown in green and yellow, respectively. (E) shows α_iAH and α_sAH in the closed conformation (left panel, which corresponds to non-activated receptors, see Fig. S2B). Activation of $A_{2A}R$ by the selective agonist CGS-21680 triggers the open α_sAH (middle panel, see Fig. S2C), facilitating GDP/GTP exchange, and G_s-mediated intracellular signaling. The right panel shows that, simultaneously, the open conformation of α_sAH and α_iAH is not feasible due to a steric clash. (F) is a schematic representation of the complex.

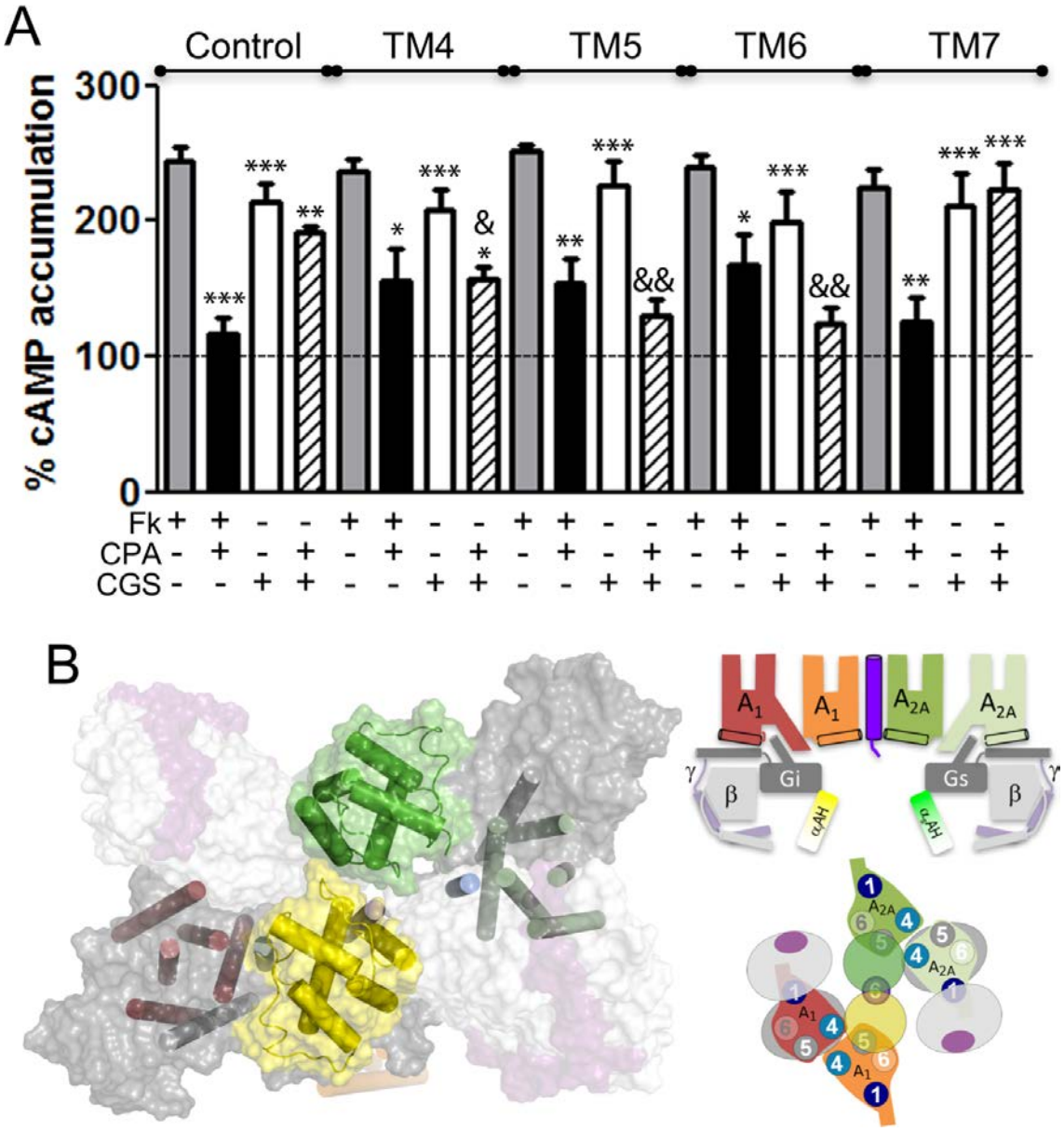

Figure 4. Effect of interfering peptides on receptor signaling

In (A) cAMP production was determined in HEK-293T cells transfected with 0.4 µg of A_1R and $A_{2A}R$ cDNAs. Cells were treated for 4 h with medium (control) or with 4 µM $A_{2A}R$ TM synthetic peptides (TM1 to TM7, see Methods). Cells were non-stimulated (basal, dotted line) or stimulated with forskolin (Fk, 0.5 µM, gray bars), with forskolin and the A_1R agonist CPA (100nM, black bars), the $A_{2A}R$ agonist CGS-21680 (CGS, 100nM, white bars) or with CPA and CGS 21680 (scratched bars). Increases in cAMP levels were expressed as percentage over non-stimulated cells (basal, 100%). Values

represent the mean ± SEM of 7-8 experiments per condition. One-way ANOVA followed by the Bonferroni's *post hoc* test showed a significant effect over basal in samples only treated with CGS 21680 or over forskolin only stimulated cells in samples in the presence of forskolin ($^{*}p < 0.05$, $^{***}p < 0.001$) or a significant effect of CPA plus CGS over CGS stimulated cells ($^{\&}p < 0.05$, $^{\&\&}p < 0.01$). In (B) molecular model of the A_1R and $A_{2A}R$ homodimers with the TAT-fused TM6 interference peptide disrupting the heteromeric interface (see Fig. S2D), in complex with G_s (open α_sAH domain) and G_i (open α_iAH domain), viewed from the intracellular site. The TAT-TM6 peptide is shown in purple whereas the color code of the depicted proteins is as in Fig. 3. This color scheme matches with the color of the different proteins depicted in the adjacent schematic representation.

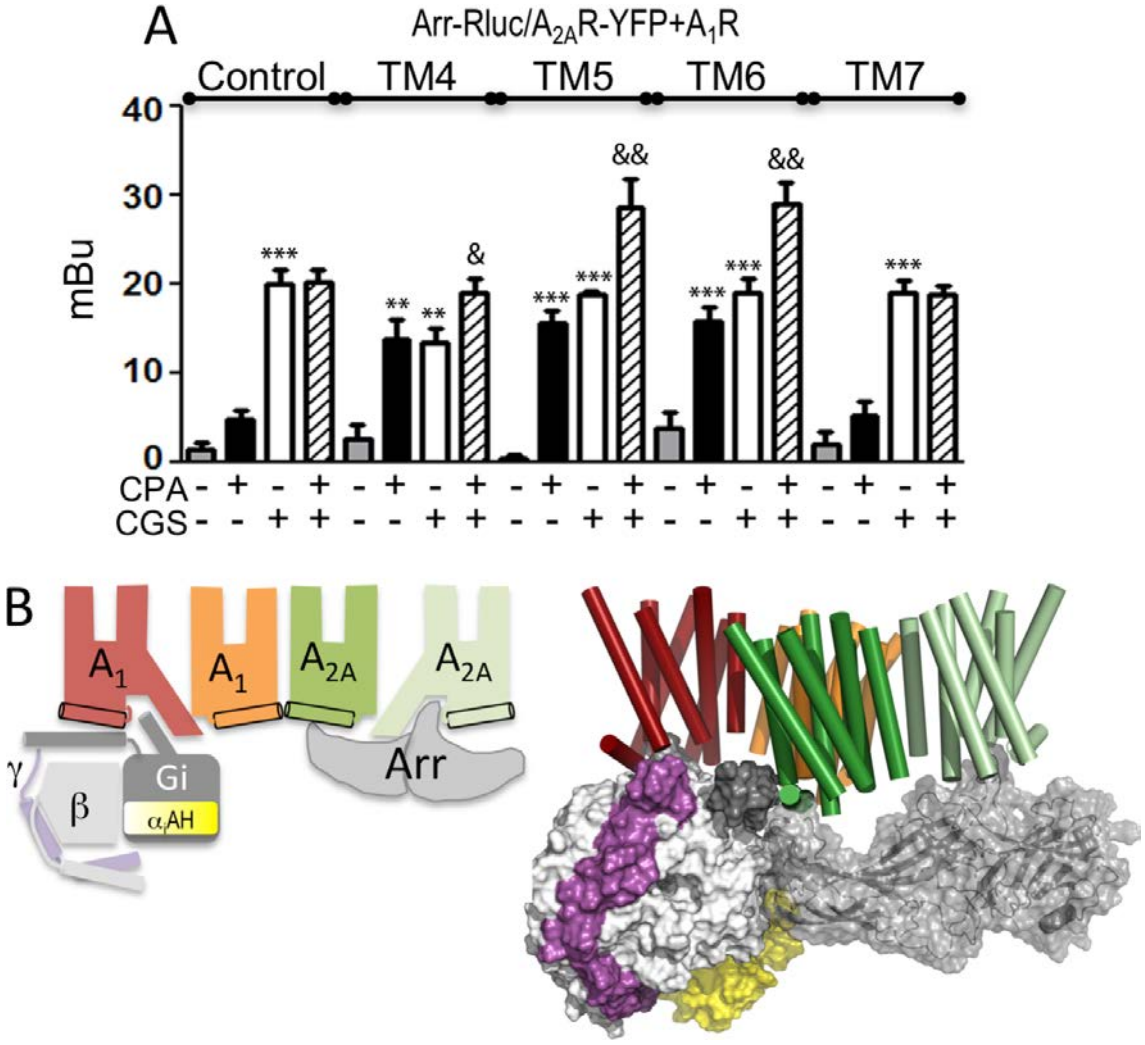

Figure 5. Effect of interfering peptides on recruitment of β-arrestin-2

In (A) receptor agonist-induced β-arrestin-2 recruitment was measured by BRET experiments. HEK-293T cells were transfected with the cDNAs for β-arrestin-2-Rluc (Arr-Rluc, 0.5 μg cDNA), A_{2A}-YFP (0.4 μg cDNA) and A_1R (0.4 μg cDNA). Cells were not treated (control) or treated for 4 h with 4 μM $A_{2A}R$ TM synthetic peptides (TM4, TM5, TM6 and TM7, see Methods) before addition of medium (basal, gray bars) or 100 nM of either the A_1R agonist CPA (black bars), the $A_{2A}R$ agonist CGS-21680 (CGS, white bars) or both (scratched bars). Positive BRET was expressed as mBU (see Methods). Values are the mean ± SEM of 7-8 experiments per condition. One-way ANOVA followed by the Bonferron's *post hoc* test showed significant differences over basal (**p<0.01, ***p<0.001) or CPA plus CGS over CGS stimulated cells ($^{\&}$p<0.05, $^{\&\&}$p<0.01). In (B) molecular model of A_1-A_{2A}Het in complex with G_i bound to A_1R and β-arrestin-2 bound to $A_{2A}R$. Arrestin is shown in gray, whereas the color code of the

depicted proteins is as in Fig. 3. This color scheme matches with the color of the different proteins depicted in the adjacent schematic representation.

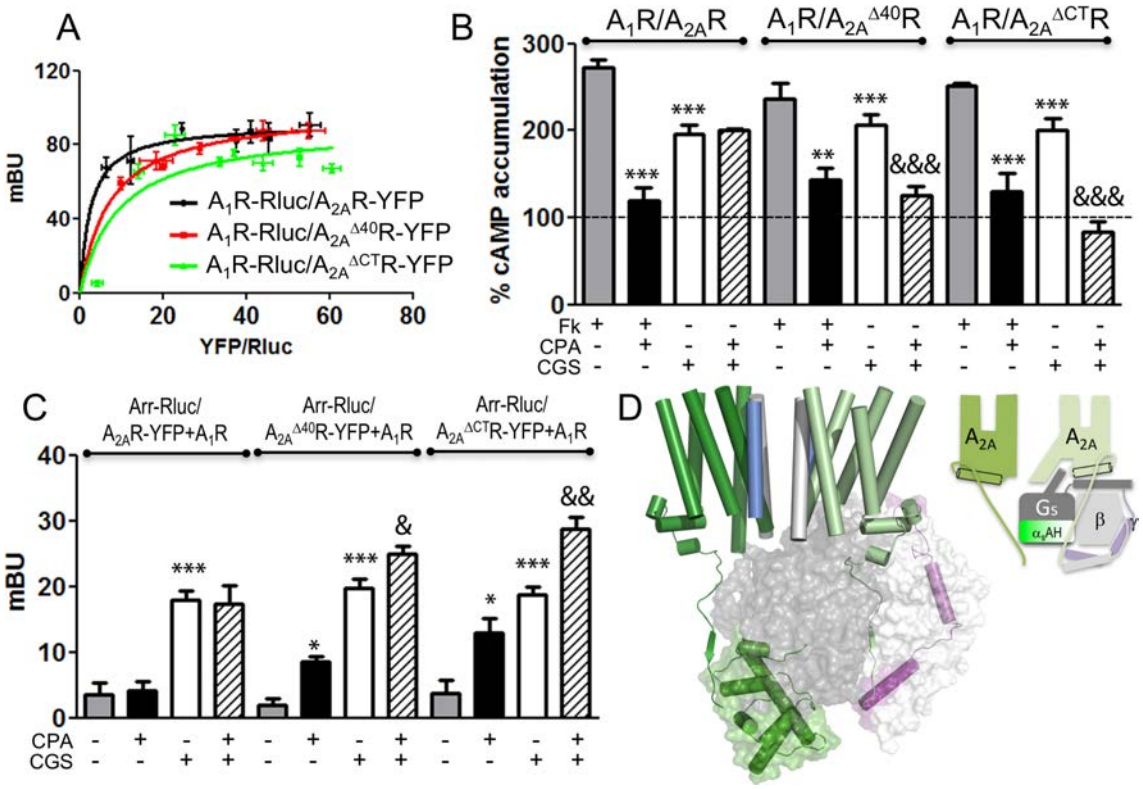

Figure 6. The influence of the C-terminal domain of $A_{2A}R$ in the signaling properties of the A_1-A_{2A}Het.

In (A) BRET assays were carried out in HEK-293T cells expressing a constant amount of A_1-Rluc (0.4 µg cDNA transfected) and increasing amounts (0.1 to 0.7 µg cDNA transfected) of mutant $A_{2A}R$: $A_{2A}^{\Delta 40}R$-YFP or $A_{2A}^{\Delta CT}R$-YFP. BRET saturation curves were obtained in which the relative amount of BRET is given as a function of 100 x the ratio between the fluorescence of the acceptor (YFP) and the luciferase activity of the donor (Rluc). BRET is expressed as milli BRET units (mBU) and are the mean ± SEM of 5 to 7 different experiments grouped as a function of the amount of BRET acceptor. In (B) HEK-293T cells expressing A_1R (0.4 µg cDNA transfected) and $A_{2A}R$ (0.3 µg cDNA transfected), $A_{2A}^{\Delta 40}R$ (0.3 µg cDNA transfected) or $A_{2A}^{\Delta CT}R$ (0.3 µg cDNA transfected) were non-stimulated (basal, dotted line) or stimulated with forskolin (Fk, 0.5 µM, gray bars), with forskolin and the A_1R agonist CPA (100nM, black bars), the $A_{2A}R$ agonist CGS-21680 (CGS, 100nM, white bars) or with CPA and CGS 21680 (scratched bars). Increases in cAMP levels were expressed over non-stimulated cells (basal). Values are the mean ± SEM of 6-8 experiments per group. One-way ANOVA

followed by the Bonferroni's *post hoc* test showed a significant effect over basal in CGS 21680 stimulated samples or over forskolin only stimulated cells in samples in the presence of forskolin ($^{**}p < 0.01$, $^{***}p < 0.001$) or CPA plus CGS over CGS stimulated cells ($^{\&\&\&}p<0.001$). In (C) HEK-293T cells were transfected with the cDNAs for β-arrestin-2-Rluc (Arr-Rluc, 0.5 μg cDNA), A_1-YFP (0.4 μg cDNA,) and $A_{2A}R$ (0.3 μg cDNA transfected), $A_{2A}{}^{\Delta 40}R$ (0.3 μg cDNA transfected) or $A_{2A}{}^{\Delta CT}R$ (0.3 μg cDNA transfected). Cells were non-stimulated or stimulated with CPA, CGS-21680 or both as indicated in B. Positive BRET was expressed as mBU (see Methos). Values are the mean ± SEM of 7-8 experiments per condition. One-way ANOVA followed by the Bonferron's *post hoc* test showed significant differences over non-stimulated cells (basal, grey bars) (*p<0.05, ***p<0.001) or CPA plus CGS over CGS stimulated cells ($^{\&}p<0.05$, $^{\&\&}p<0.01$). In (D) molecular model of the $A_{2A}R$ homodimer in complex with G_s. TMs 4 and 5, involved in homo-dimerization, are highlighted in light blue and gray, respectively, whereas the color code of the depicted proteins is as in Fig. 3 (this color scheme matches with the color of the different proteins depicted in the adjacent schematic representation). The C-tail of the G_s α-subunit-unbound $A_{2A}R$ protomer is near α_sAH (shown in the closed conformation) and might modulate the conformational change.

SUPPLEMENTARY FIGURES

CROSS-COMMUNICATION BETWEEN G_I AND G_S IN A G-PROTEIN-COUPLED RECEPTOR HETEROTETRAMER GUIDED BY A RECEPTOR C-TERMINAL DOMAIN

Gemma Navarro[1,2,3]*, Arnau Cordomí[4]*, Marc Brugarolas[1,2,3], Estefanía Moreno[1,2,3], David Aguinaga[1,2,3], Laura Pérez-Benito[4], Sergi Ferre[5], Antoni Cortés[1,2,3], Vicent Casadó[1,2,3], Josefa Mallol[1,2,3], Enric I. Canela[1,2,3], Carme Lluís[1,2,3], Leonardo Pardo[4,&], Peter J. McCormick[1,2,3,6&] and Rafael Franco[3,&]

[1]Centro de Investigación Biomédica en Red sobre Enfermedades Neurodegenerativas. [2]Institute of Biomedicine of the University of Barcelona (IBUB). [3]Department of Biochemistry and Molecular Biology, Faculty of Biology, University of Barcelona, Barcelona, 08028 Spain; [4]Laboratori de Medicina Computacional, Unitat de Bioestadística, Facultat de Medicina, Universitat Autònoma de Barcelona, 08193 Bellaterra, Spain; [5]Integrative Neurobiology Section, National Institute on Drug Abuse, National Institutes of Health, Baltimore, MD 21224, USA; [6]School of Veterinary Medicine, University of Surrey, Guildford GU2 7AL.

*These authors contributed equally to this work

[&]These authors equally supervised this work

Corresponding authors:

Leonardo Pardo: leonardo.pardo@uab.es, Peter J. McCormick: p.mccormick@surrey.ac.uk, Rafael Franco: rfranco@ub.edu

Short Title: Cross-communication between G proteins

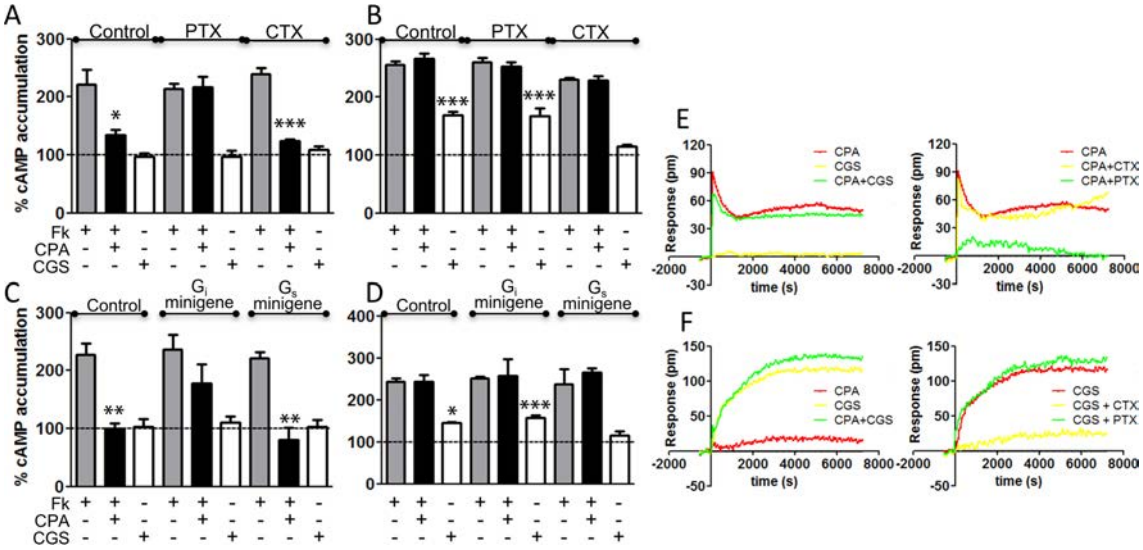

Supplementary Figure S1. Receptor signaling through A_1R and $A_{2A}R$

In (A, B) cAMP determination were performed in HEK-293T cells transfected with the cDNA (0.5 μg) for A_1R (A) or $A_{2A}R$ (B). Cells were pre-treated with medium (control), overnight with pertussis toxin (PTX, 10 ng/ml), or 1 h with cholera toxin (CTX, 100 ng/mL) and were no-stimulated (basal, dotted line) or stimulated with forskolin (Fk, 0.5 μM, gray bars), with forskolin and 100 nM of CPA (black bars) or with 100 nM of CGS-21680 (white bars). In (C, D) cells were transfected as in A, B respectively and not co-transfected (control) or co-tranfected with the cDNAs (0.5 μg) for mini-genes coding for peptides that block the coupling to either G_s or G_i. Cells were stimulated as indicated above. Increases in cAMP levels were expressed over basal. Values are means ± SEM of 5-6 experiments per group. One-way ANOVA followed by the Bonferroni's *post hoc* test showed a significant effect respect to basal in samples only stimulated with CGS 21680 or respect to forskolin only stimulated cells in samples in the presence of forskolin ($^{*}p < 0.05$, $^{**}p < 0.01$, $^{***}p < 0.001$). In (E, F) dynamic mass redistribution analyses were performed in cells transfected and stimulated as indicated in A and B. The resulting picometer-shifts of reflected light wavelength (pm) against time were monitored. Each curve is the means of a representative optical trace experiment carried out in triplicates.

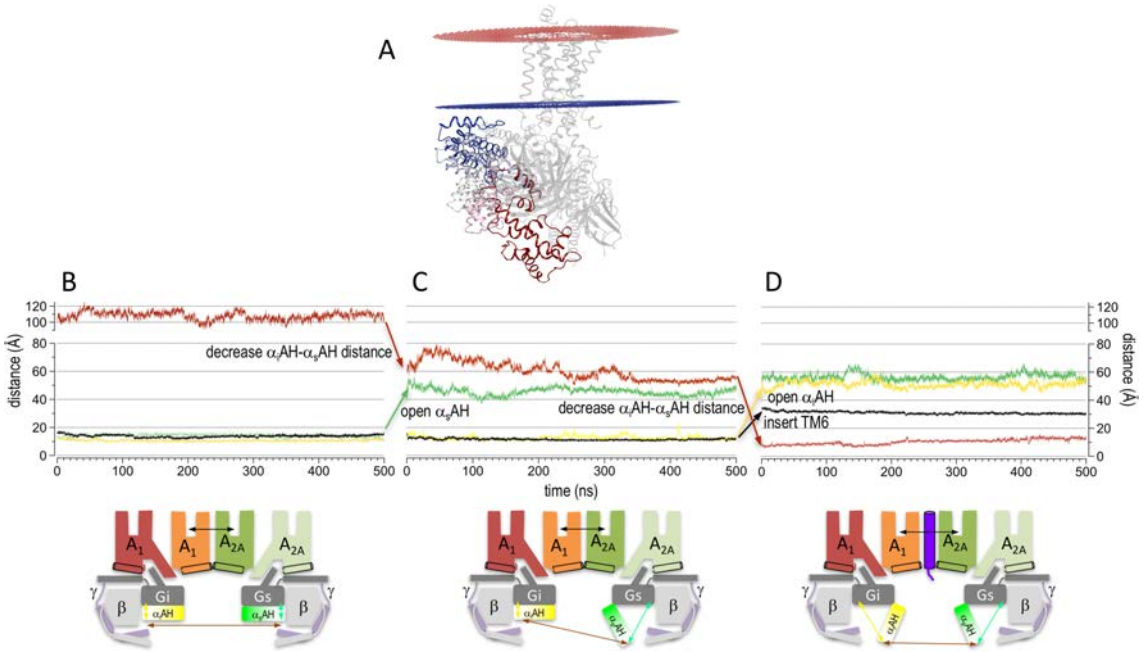

Supplementary Figure S2. Evolution of α_sAH and α_iAH in the molecular dynamics simulation of A_1-A_{2A}Het in complex with G_i and G_s

In (A) the α_sAH domain of the α_s-subunit in the crystal structure of the β_2-AR in complex with G_s (in blue) (PDB id 3SN6) and in a G_i-based homology model (PDB id 1AGR) of the α_s-subunit in the closed conformation (red) are shown. Intermediate conformations (light blue, white, light red) between these two structures were obtained using the g_morph tool of the GROMACS package. The open conformation of the α_sAH domain (white) was selected from these intermediate conformations in such a manner that the distance (d[Asn112α_s-Asn261α_s]) between the Cα atoms of Asn112 (in the α_sAH domain) and Asn261 (Ras domain) is ~40Å, as observed in DEER distance distributions between spin labels attached to these amino acids[1]. Similar procedure was used to model open and closed conformations of the α_i-subunit (not shown). The selected open conformation of α_iAH also reproduces a distance (d[Arg90α_i-Glu238α_i]) between the Cα atoms of Arg90 (α_iAH domain) and Glu238 (Ras domain) of ~40Å [1]. In (B-D) Intermolecular distances between the Cα atoms of Arg90 (α_iAH domain) and Glu238 (Ras domain) of G_i (d[Arg90α_i-Glu238α_i], in yellow), Asn112 (α_sAH) and Asn261 (Ras) of G_s (d[Asn112α_s-Asn261α_s], in green), Arg90 (α_iAH) and Asn112 (α_sAH) (d[Arg90α_i-Asn112α_s], in dark red), and between the center of mass of the binding site of the G_i-unbound A_1R and G_s-unbound A_{2A}R protomers (in black) during the MD simulations of A_1-A_{2A}Het in complex with G_i and G_s in the closed α_iAH-closed

α_sAH (B), closed α_iAH-open α_sAH (C), and open α_iAH-open α_sAH (D) conformations. The open α_iAH-open α_sAH simulation is performed in the presence of the TAT-fused peptide TM 6 altering the heteromeric interface between A_1R and $A_{2A}R$. These computed intermolecular distances are depicted as double arrows in the adjacent schematic representations.

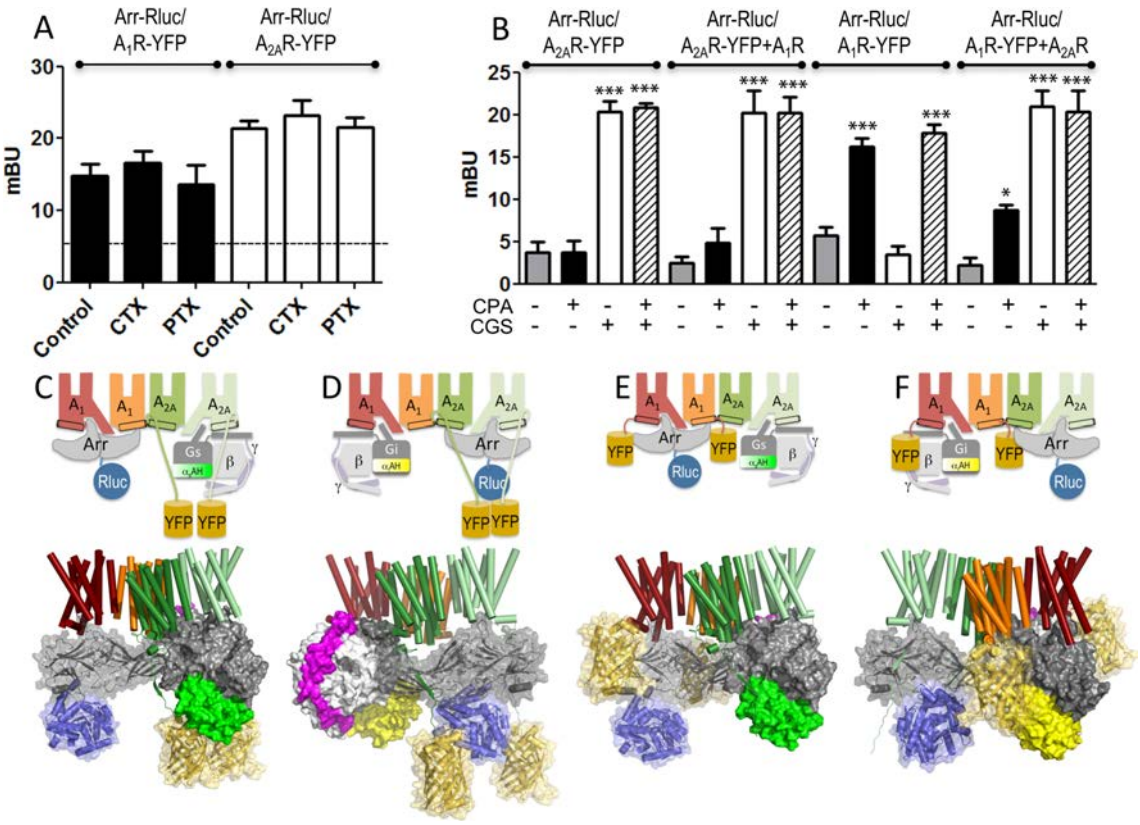

Supplementary Figure S3. Recruitment of β-arrestin-2 by the A_1-A_{2A}Het

In (A, B) receptor agonist-induced β-arrestin-2 recruitment was measured by BRET experiments. HEK-293T cells were transfected with the cDNAs for β-arrestin-2-Rluc (Arr-Rluc, 0.5 µg cDNA) and A_1-YFP (0.4 µg cDNA, black bars), A_{2A}-YFP (0.4 µg cDNA), A_1R (0.4 µg cDNA) or A_{2A}R (0.4 µg cDNA) as indicated in the panels. Cells were not treated (control) or treated overnight with pertussis toxin (PTX, 10 ng/ml) or cholera toxin (CTX, 100 ng/mL) (A). Cells were stimulated with medium (basal, dotted line in panel A and gray bars in panel B), the A_1R agonist CPA (100nM, black bars), the A_{2A}R agonist CGS-21680 (CGS, 100nM, white bars) or both (scratched bars). Positive BRET was expressed as mBU (see Methods). Values are the mean ± SEM of 7-8 experiments per condition. One-way ANOVA followed by the Bonferron's *post hoc* test showed significant differences over basal (***p<0.001). In (B) positive BRET was observed when cells expressing Arr-Rluc and A_1R-YFP were activated with the A_1R agonist CPA but not with the A_{2A}R agonist CGS-21680 and CGS-21680 did not modify the CPA signaling. Analogously, positive BRET was observed when cells expressing Arr-Rluc and A_{2A}R-YFP were activated with CGS-21680 but not with CPA and CPA did not modify CGS-21680 signaling. However, in cells expressing Arr-Rluc, A_1R-YFP and non-fused A_{2A}R, the ability of CPA to increase BRET by recruitment of ß-arrestin-

2 to A_1R, was diminished compared to cells not expressing $A_{2A}R$. These results suggest that the presence of $A_{2A}R$-G_s in the heteromer modifies the position of YFP fused to the C-terminal domain of A_1R or/and Rluc fused to the C-term of ß-arrestin-2 in a way that energy transfer diminished. Moreover, CGS-21860 was able to increase BRET in cells expressing Arr-Rluc, A_1R-YFP and non-fused $A_{2A}R$ to a similar level to cells only expressing Arr-Rluc and $A_{2A}R$-YFP (white bars). This indicates that Arr-Rluc bound to non-fused $A_{2A}R$ can energy transfer to the arrestin-unbound A_1R-YFP acceptor. Energy transfer is not observed when CPA binds to non-fused A_1R in cells expressing Arr-Rluc, $A_{2A}R$-YFP and non-fused A_1R (black bars).

In (C-F) molecular models of Arr-Rluc, $A_{2A}R$-YFP and non-fused A_1R (C, D) or Arr-Rluc, A_1R-YFP and non-fused $A_{2A}R$ (E, F) with Arr-Rluc bound to A_1R (C, E) or $A_{2A}R$ (D, F) and G_i bound to A_1R (D, F) or G_s bound to $A_{2A}R$ (C, E) were given to explain the above described results. These molecular models show that Arr-Rluc bound to A_1R cannot transfer energy to $A_{2A}R$-YFP because the long C-tail of $A_{2A}R$ position YFP near the α_sAH domain or the N-term of the γ-subunit (see Fig. S4), far from Rluc (panel C). In contrast, Arr-Rluc bound to $A_{2A}R$ can transfer energy to A_1R-YFP because the short C-tail of the α_i-unbound A_1R protomer positions YFP in close proximity to Rluc (panel F, which is rotated 180º relative to panels C-E to visualize the proximity of YFP and Rluc).

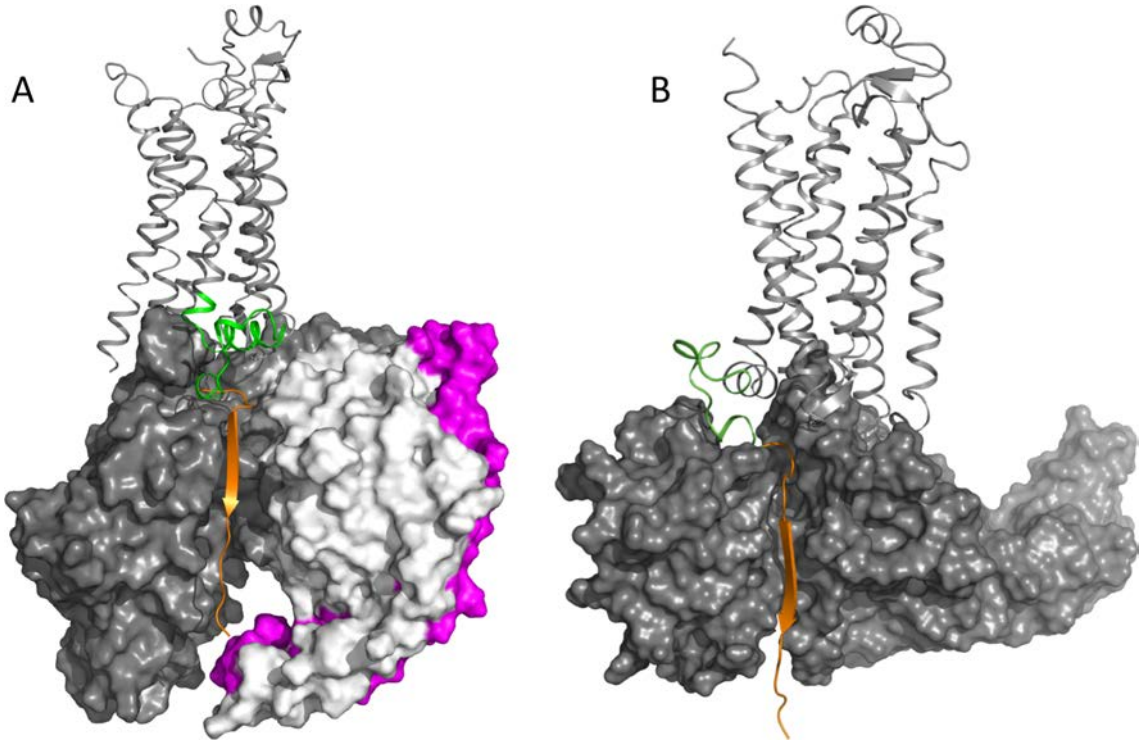

Supplementary Figure S4. Modeling the orientation of the C-tail of $A_{2A}R$

Although the exact conformation of the $A_{2A}R$ C-tail (102 amino acids, Gln311-Ser412) cannot unambiguously be determined, its orientation was modeled using a combination of structural templates. First, the C-tail of squid rhodopsin[2], which contains the conserved amphipathic helix 8 that runs parallel to the membrane and an additional cytoplasmic helix 9, was used to model 13 amino acids (Ser305-Ala317 in green). Second, the C-tail of the human V2 vasopressin receptor, determined in complex with ß-arrestin-2[3], was used to model 18 amino acids (Gly318-Ser335 in orange). The laboratory of Kostenis has shown that the C-term of OXER, labeled with Rluc (OXER-Rluc), gets close to the N-term of the γ-subunit, labeled with GFP (γ-GFP)[4]. Thus, the modeled orientation of the C-tail of $A_{2A}R$ accomplishes simultaneously two restraints imposed by the G protein and arrestin: it is positioned near the N-termini of the γ-subunit of G_s (in purple) as suggested for the OXER (panel A) and it extends the N-domain β-sandwich fold of arrestin, binding as an antiparallel β-strand, as suggested for V2 vasopressin receptor (panel B).

REFERENCES

1. Dror, R.O. et al. SIGNAL TRANSDUCTION. Structural basis for nucleotide exchange in heterotrimeric G proteins. *Science* **348**, 1361-5 (2015).
2. Murakami, M. & Kouyama, T. Crystal structure of squid rhodopsin. *Nature* **453**, 363-7 (2008).
3. Shukla, A.K. et al. Structure of active beta-arrestin-1 bound to a G-protein-coupled receptor phosphopeptide. *Nature* **497**, 137-41 (2013).
4. Blattermann, S. et al. A biased ligand for OXE-R uncouples Galpha and Gbetagamma signaling within a heterotrimer. *Nat. Chem. Biol.* **8**, 631-8 (2012).

RESUMEN DE RESULTADOS Y DISCUSIÓN

Tradicionalmente se consideraba que los GPCR eran entidades monoméricas, y funcionaban exclusivamente como tal. No obstante, en las últimas décadas han sido obtenidos resultados que apoyan la teoría de que estos receptores pueden formar complejos homoméricos y heteroméricos (*Angers, et al., 2000; Bouvier, 2001; Milligan y Bouvier, 2005; Ferré, et al., 2009; Navarro, et al., 2016*). Aun así, actualmente en la comunidad científica todavía existe debate acerca de la heteromerización entre receptores GPCR y el papel que esta tiene en la señalización y funcionalidad celular.

Es aceptado entre los investigadores que los GPCR de la familia C forman homo- o heterodímeros constitutivamente (*Kniazeff, et al., 2011*). Sin embargo, estudios realizados con GPCR de la familia A (*rhodopsin-like*) cuestionan que esta dimerización sea constitutiva y requerida para la activación de la proteína G. Para evaluar si la dimerización era estrictamente necesaria fueron realizados ensayos en nanodiscos que contenían una entidad monomérica de GPCR. En estos experimentos se observó que los receptores β_2-adrenérgico, el receptor de rodopsina y los receptores μ-opioides podían funcionar como monómeros (*Bayburt, et al., 2007; Whorton, et al, 2007; Kuszak, et al., 2009; Bayburt, et al., 2011*). Hay que puntualizar que las conclusiones obtenidas en los ensayos realizados utilizando como modelo los nanodiscos han sido muy cuestionadas, pues el microambiente en estos se considera una extracción muy alejada de la realidad. Sin embargo, los defensores de la funcionalidad de los GPCR como entidad monomérica vieron aumentados sus apoyos cuando se demostró que miembros de 7 dominios TM de la familia C de los GPCR aislados monoméricamente eran capaces de unir la proteína G (*El Moustaine, et al., 2012*). No obstante, en este último estudio, se observó que la inducción de la señalización mediante la proteína G tras la exposición a ligandos sí requería de la estructura dimérica de los GPCR (*El Moustaine, et al., 2012*). A pesar de ello, todos estos resultados no excluyen la posibilidad de que los GPCR de clase A puedan formar oligómeros de forma espontánea en células vivas, tal y como ha sido demostrado con receptores de la familia C de GPCR. De hecho, recientemente ha sido demostrado que los tres GPCR que funcionaban como unidades monoméricas en nanodiscos existen en conformaciones estructurales de orden superior en células vivas. Fung y colaboradores encontraron evidencias de la existencia de oligómeros, mayoritariamente tetrámeros, estables del receptor β_2-adrenérgico (*Fung, et al., 2009*). A favor de la opinión de los autores que defienden la necesidad de la dimerización de los GPCR, juegan las recientes obtenciones de las estructuras cristalinas de alta resolución de algunos receptores. Es interesante destacar que precisamente algunos de los GPCR que inicialmente se consideraba que funcionaban monoméricamente han sido cristalizados como dímeros y/o tetrámeros, siendo el caso de los receptores μ-opioides (*Manglik, et al., 2012*) y κ-opioides (*Wu, et al., 2012*), o los β_1-adrenérgicos (*Huang, et al., 2013*).

La investigación en el campo de la oligomerización ha avanzado mucho en los últimos años. Mediante el uso de técnicas biofísicas como las de transferencia de energía por resonancia han sido obtenidos muchos resultados que apoyan la existencia de los homo- y heterotetrámeros de GPCR en células vivas. No obstante, estas técnicas han quedado limitadas en la predicción de la estequiometria de los oligómeros y su posible dinámica natural (*Ferré, et al., 2014*). Por ello, a lo largo de esta tesis han sido utilizadas, además de estas técnicas clásicas, otras más novedosas como i) el *Single-particle imaging and tracking* (SPT), mediante la cual ha sido posible explorar la dinámica de estos oligómeros ii) el ensayo de ligación por proximidad (PLA), técnica que permite detectar heterómeros, no sólo en modelos celulares donde han sido sobreexpresados los receptores de interés, sino también en cultivos primarios iii) la elaboración de modelos computacionales mediante los cuales, en base a la estructura cristalina de los receptores, ha sido predicho como se establecen las interacciones proteína-proteína iiii) la puesta a punto de distintas técnicas para el estudio de la señalización inducida por estos receptores al formar heterómeros como la *Dynamic Mass Redistribution* (DMR), que detecta cambios en la estructura citoesquelética de las células por acción del acoplamiento de las proteínas G a los receptores pertinentes cuando las células son expuestas a distintos ligandos, las técnicas de cuantificación de producción de AMPc, la

determinación de la activación de la vía de las MAPK detectando la fosforilación de las ERK1/2; o la técnica para determinar la liberación de calcio intracelular mediante la transfección del sensor GCaMP6.

El conocimiento de las nuevas propiedades adquiridas por los receptores al formar complejos heteroméricos con otros receptores, u otras proteínas, es de vital importancia para dar explicación a muchos mecanismos fisiológicos, así como para el diseño de nuevos fármacos. Se estima que el 40% de los fármacos comercializados actualmente modulan la actividad de los GPCR (*Lu y Wu, 2016*), sin embargo, muchos de estos fármacos han sido diseñados en base a la funcionalidad monomérica del GPCR de interés, obviando que, al interaccionar con otros receptores o proteínas, su función puede ser completamente opuesta. Los heterómeros también pueden ejercer un papel modulador de un receptor sobre otro, potenciando o bloqueando al receptor principal. En estos casos se podrían encontrar nuevas dianas terapéuticas con un menor grado de efectos secundarios actuando sobre los receptores moduladores. Un claro ejemplo es el fármaco antiparkinsoniano K2006 (*Mizuno, et al., 2013*). El descubrimiento de los heterómeros ha abierto una nueva avenida de posibilidades farmacológicas que puede llegar a aumentar y mejorar considerablemente la farmacología actual. Entender cómo se establecen las modulaciones entre unos receptores y otros posibilitará también en un futuro el desarrollo de tratamientos preventivos para distintos trastornos psicológicos, como la adicción a drogas.

Uno de los principales objetivos de esta tesis ha sido estudiar y aportar nuevos datos para el entendimiento del funcionamiento de la adicción a sustancias psicoestimulantes, concretamente la cocaína. La adicción a esta droga es un grave problema a nivel mundial. En primera instancia es un problema en los países productores, normalmente países sud-americanos, por toda la corrupción y violencia que gira en torno a las mafias que obtienen, producen y distribuyen la droga. Además, los "laboratorios" clandestinos donde esta sustancia es generada normalmente son operados por personal no cualificado, entre los cuales suelen encontrarse menores de edad, con todos los riesgos que esto comporta. Una vez el producto llega al mercado, normalmente países del denominado "primer mundo", aparecen otro tipo de problemas para la sociedad, como el gasto médico derivado del consumo de cocaína, la exclusión social de los consumidores habituales y la consiguiente marginación y aparición de conductas violentas. Es importante destacar que este problema que muchas veces nos parece lejano es mucho más cercano de los que nosotros creemos. España se mantiene, junto a otros países como el Reino Unido o Francia, a la cabeza de la Unión Europea en el consumo de cocaína entre los jóvenes, a pesar de que el uso de estas sustancias sigue disminuyendo des del máximo alcanzado en 2008. Estos datos revelan la cara más oscura de la sociedad en la que vivimos y exponen claramente que existe una serie de problemas muy graves aún por entender y, por lo tanto, aún por resolver. Es por eso que parte de los resultados de esta tesis buscan aportar luz a este gran agujero negro. El grupo de investigación en el que ha sido desarrollada la Tesis doctoral, se encuentra trabajando en esta misma línea de investigación para poder llegar a obtener conocimiento suficiente de los mecanismos de la adicción y promover terapias válidas para reparar el daño que estas sustancias pueden llegar a causar en el individuo y en la sociedad.

Tradicionalmente el estudio de los efectos de la cocaína había sido realizado en torno al campo de la drogadicción mediante estudios comportamentales en los que se analizaba como respondía el sujeto a procesos como la abstinencia, la recaída, la búsqueda de la droga…, después de una toma de cocaína más o menos prolongada. Era evidente que las respuestas observadas a nivel de conducta respondían a efectos bioquímicos y genéticos (cambios en la expresión y actividad de algunos genes), de modo que la adicción a cocaína empezó también a estudiarse a nivel molecular. Los primeros estudios bioquímicos, indicaron que la cocaína inducía múltiples efectos sobre la transmisión dopaminérgica, explotando dicho sistema para provocar parte de sus efectos

conductuales y celulares (*De Mei, et al., 2009*). Más concretamente, fue determinado que el consumo de esta droga elevaba los niveles de dopamina en el estriado, sobre todo en la parte del núcleo accumbens, estructura muy importante en la vía de la recompensa (*Singer, et al., 2017*). A raíz de estos primeros estudios se describió que la cocaína bloqueaba el transportador presináptico de dopamina, DAT, inhibiendo la recaptación de dopamina del espacio sináptico e induciendo una sobreestimulación de los receptores dopaminérgicos (*Ritz, et al., 1987*). Sin embargo, no todos los efectos producidos por la cocaína eran explicables por la interacción de la cocaína con DAT. Nuevas investigaciones demostraron la interacción de la cocaína con otras proteínas y receptores. Actualmente está establecido que la cocaína interacciona con el receptor sigma-1 a las concentraciones fisiológicas alcanzadas en un consumo normal (*Matsumoto, et al., 2003*). De hecho, la reducción del receptor sigma-1 en cerebro utilizando un oligonucleótido *antisense* atenúa las acciones estimuladoras convulsivas y locomotoras inducidas por la cocaína (*Matsumoto, et al., 2001*), mientras que el uso de antagonistas para el receptor sigma-1 mitiga las acciones de la cocaína en distintos modelos animales (*Hiranita, et al., 2011*). El receptor sigma-1 está altamente expresado en cerebro (*Hayashi y Su, 2005*), con una mayor expresión en el caudado-putámen y el núcleo accumbens, la parte dorsal y ventral del estriado, respectivamente. Estas regiones se encuentran implicadas en los efectos de la cocaína a largo plazo. Ha sido demostrado que la administración repetida de cocaína inducia una sobreexpresión de receptores sigma-1, un proceso mediado por los receptores de dopamina D_1 (*Zhang, et al., 2005*). En base a estos resultados, nuestro grupo de investigación demostró la interacción entre los receptores D_1 y sigma-1 en los eventos iniciales de la exposición a cocaína (*Navarro, et al., 2010*). En este trabajo fue descrita la capacidad del receptor sigma-1 para unirse al homómero de receptores D_1-D_1 y modular su funcionalidad tanto en células vivas, como también en cortes de estriado de cerebro.

El estriado es la estructura principal de los ganglios basales. Las neuronas eferentes estriatales GABAérgicas constituyen más del 95% de la población neuronal del estriado (*Heinsbroeck, et al., 2017*), y se separan en dos subtipos mayoritarios: las neuronas GABAérgicas dinorfinérgicas, las cuales expresan el péptido dinorfina y receptores D_1 de dopamina, dando lugar a la vía directa, y las neuronas GABAérgicas encefalinérgicas, que expresan el péptido encefalina y los receptores D_2 de dopamina, formando la vía indirecta (*Grillner y Robertson, 2016*). Los ganglios basales se encuentran involucrados en el procesamiento de información relacionada con la ejecución y el aprendizaje motor, actuando en procesos motivacionales, siendo esta estructura una de las zonas más afectadas en adicciones a drogas de abuso (*Kreitzer y Malenka, 2008; Lovinger y Alvarez, 2017*). En el caso de la adicción a drogas, y especialmente a cocaína, la vía dopaminérgica juega un papel crítico en la patología (*Di Chiara y Bassareo, 2007*), específicamente las dos poblaciones de neuronas que contienen los receptores D_1 y D_2. La estimulación de las neuronas que expresan los receptores D_1 potencian los efectos de recompensa de la cocaína, mientras que la estimulación de las neuronas que contienen los receptores D_2 los atenúa (*Hikida, et al., 2010*). Ha sido demostrado que la activación del receptor D_1 es estrictamente necesaria para la inducción de las respuestas celulares y conductuales de la cocaína (*Xu, et al., 1994*). Por otra parte, las neuronas que contienen el receptor D_2 se oponen a los efectos locomotores y de refuerzo promovidos por los receptores D_1 (*Durieux, et al., 2009*). En concreto, en animales mutantes D_2 -/-, se observó que la liberación de dopamina provocada tras la administración de cocaína era dramáticamente superior comparado con animales WT (*Rouge-Pont, et al., 2002*). Estas dos vías, por lo tanto, pueden controlar la búsqueda y el aprendizaje relacionado con la recompensa, y tienen efectos opuestos en la actividad motora (*Durieux, et al., 2012*).

Estos antecedentes, junto a los resultados obtenidos con el receptor D_1 de dopamina, condujeron directamente a cuestionar el posible papel de la vía indirecta del estriado, donde se encuentra el receptor D_2 de dopamina en la adicción a cocaína.

En el trabajo ***Cocaine inhibits dopamine D_2 receptor signaling via sigma-1-D_2 receptor heteromer*** (*Navarro, et al., 2013*) ha sido confirmado que el receptor sigma-1 es capaz de modular el receptor D_2 de dopamina en presencia de cocaína, alterando el equilibrio establecido entre las vías directa e indirecta del estriado. Mediante técnicas de transferencia de energía y microscopía confocal ha sido determinado que el receptor sigma-1 forma heterómeros específicamente con el receptor D_2 a nivel de membrana plasmática, pero no con los otros miembros de la familia de receptores D_2-*like*, el D_3 y el D_4. En la literatura se describe la capacidad de los receptores D_2 de dopamina para formar homodímeros (*Guo, et al., 2008*), esto planteaba la cuestión de si el receptor sigma-1 era capaz de interaccionar con el homodímero, y cuál era la estequiometria del oligómero. Mediante la técnica de BRET, en primer lugar, ha sido demostrado que el receptor sigma-1 puede formar homodímeros; y mediante la combinación de las técnicas de BRET y doble complementación en un mismo ensayo ha sido determinado que estos heterómeros sigma-1-D_2 forman oligómeros de orden superior con una estructura mínima heterotetramérica formada por la interacción entre sigma-1-sigma-1-D_2-D_2. Estos cambios estructurales han sugerido un cambio en la funcionalidad y señalización del receptor D_2 en presencia de cocaína. Mediante la técnica de *label free* y el análisis de los niveles de AMPc ha sido observado que la cocaína es capaz de inhibir parcialmente la capacidad del receptor D_2 de señalizar a través de la proteína G_i. Este efecto se ve bloqueado cuando las células han sido transfectadas con un RNA de interferencia contra el receptor sigma-1, demostrando así que la capacidad de la cocaína para contrarrestar el efecto del agonista del receptor D_2, quinpirole, es mediado por el receptor sigma-1. Estos resultados han sido reproducidos utilizando el agonista del receptor sigma-1, PRE-084, confirmando la capacidad del receptor sigma-1 para disminuir la habilidad del receptor D_2 para señalizar a través de la proteína G_i. En el análisis de la vía de las MAPK ha sido observado que, tanto la activación del receptor sigma-1 como del D_2 en el heterómero sigma-1-D_2 inducen la fosforilación de ERK1/2, actuando como agonistas en la activación de esta vía a través del heterómero.

Una propiedad de algunos heterómeros es la habilidad del antagonista de uno de los receptores para bloquear la función del agonista del otro receptor; este fenómeno recibe el nombre de *cross-antagonismo*. En estas células ha sido descrito que la fosforilación de ERK1/2 mediada por la cocaína es contrarrestada no solo por el antagonista de sigma-1, PD-144418, sino también por el antagonista del receptor D_2, raclopride. Del mismo modo que la activación de la vía de las MAPK inducida por el agonista del receptor D_2, quinpirole, es bloqueada por raclopride pero también por PD-144418. Estos resultados sugieren que la unión del antagonista provoca cambios estructurales en las interacciones directas proteína-proteína del heterómero sigma-1-D_2, bloqueando la señalización a través del otro receptor del complejo; es decir, se observa un fenómeno de *cross-antagonismo*.

Como ha sido comentado anteriormente, la cocaína puede inhibir el transportador DAT incrementando la concentración de dopamina en el estriado, de modo que en base a los resultados obtenidos, en presencia de esta droga los dos receptores en el heterómero sigma-1-D_2 podrían estar activos. Esto ha hecho que nos cuestionemos qué sucede con la fosforilación de las ERK1/2 después de coactivar los dos receptores. Sorprendentemente ha sido observada una disminución en la fosforilación de las ERK1/2 comparado con la fosforilación inducida por el tratamiento de quinpirole únicamente; este fenómeno se conoce como *cross-talk* negativo.

Una vez definido el *fingerprint* bioquímico característico de este heterómero en células, nos planteamos resolver su existencia y funcionalidad en tejido estriatal de animales. En primer lugar, mediante la técnica co-inmunoprecipitación y ensayos de Ligación por proximidad (PLA) ha sido detectada la expresión del heterómero de receptores sigma-1-D_2 en el estriado de animales *wild type* (WT), pero no en animales *Knock-out* (KO) para sigma-1. La funcionalidad del heterómero en estriado ha sido determinada en base a la fosforilación de las ERK1/2. Tanto el quinpirole como

la cocaína inducen la activación de esta vía en animales WT; sin embargo, la co-activación con los dos ligandos induce un bloqueo en la fosforilación de las ERK1/2, de modo que el mismo *fingerprint* bioquímico observado en células ha sido reproducido en tejido estriatal, confirmando la existencia y funcionalidad del heterómero de receptores sigma-1-D_2 e indicando que algunos de los efectos producidos por la cocaína sobre el receptor D_2 son debidos a la formación de este complejo.

Los resultados obtenidos en este trabajo van en la misma dirección que los anteriormente citados por Durieux y colaboradores donde la cocaína limita los efectos locomotores y de refuerzo de las neuronas estriatales que expresan el receptor D_2 (*Durieux, et al., 2009*), además, ofrecen una explicación a las observaciones realizadas por Luo y colaboradores donde una administración aguda de cocaína induce una rápida activación de las neuronas estriatales que expresan el receptor D_1, a la vez que una inactivación progresiva de las neuronas que expresan el receptor D_2 en ratones (*Luo, et al., 2011*). Los efectos producidos por la cocaína sobre la señalización del heterómero sigma-1-D_2 son opuestos a los efectos descritos en el heterómero sigma-1-D_1 por Navarro y colaboradores (*Navarro, et al., 2010*). En una visión conjunta, se observa que la cocaína, a través del receptor sigma-1, desestabiliza el balance existente entre la vía directa e indirecta de los ganglios basales influenciando significativamente la neurotransmisión dopaminérgica. El equilibrio se rompe a favor de las neuronas que contienen el receptor D_1, implicadas en la motivación y activando la vía de la recompensa, facilitando la creación de un vínculo de adicción con la droga de abuso, así como distintas consecuencias a largo plazo.

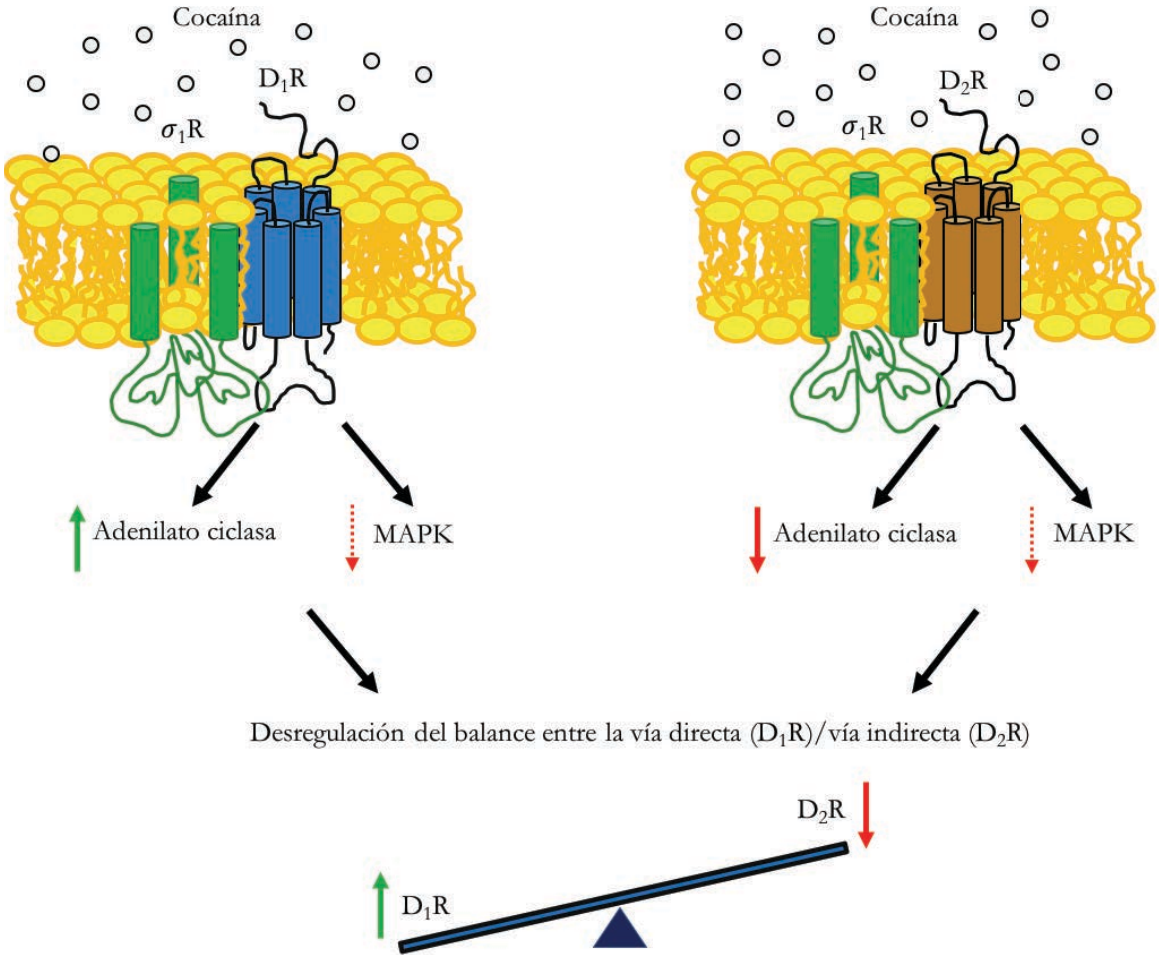

Figura 31. Representación esquemática del efecto modulador de la cocaína ejercido por el receptor sigma-1 sobre los receptores D_1 y D_2 de dopamina.

Entender los mecanismos a través de los que la cocaína es capaz de modular a su favor la señalización de estos receptores es de gran relevancia, pues significa la base a partir de la cual podrán ser diseñados fármacos que puedan evitar dichos efectos y el inicio de toda la cascada de eventos que acaban provocando la adicción a esta sustancia. En esta línea ya han empezado a hacerse algunos trabajos, como los elaborados por Xu y colaboradores en los que muestran como un ligando del receptor sigma-1 puede revertir los efectos de la cocaína en ratas (*Xu, et al., 2012*), sugiriendo que el bloqueo de la acción de la cocaína en el heterómero sigma-1-D_2 podría tenerse en cuenta como estrategia para mitigar los efectos de la cocaína.

No obstante, el receptor sigma-1 no es el único responsable de la unión de cocaína y la consiguiente modulación de receptores. En 1994 fue descrita la existencia del receptor sigma-2 por Hellewell y colaboradores (*Hellewell, et al., 1994*), y durante mucho tiempo, debido a la tardía secuenciación de este receptor, los ensayos de unión a radioligandos eran exclusivamente la vía a través de la que se estudiaba este receptor. Años más tarde, en 2011, Xu y colaboradores identificaron al *progesterone receptor membrane component-1* (PGRMC-1) como la entidad potencial del receptor sigma-2 (*Xu, et al., 2011)* abriendo la puerta a una revolución de nuevos estudios. Este receptor ha sido relacionado básicamente con el cáncer, llegando a ser considerado actualmente como un biomarcador del estatus proliferativo de las células tumorales (*Van Waarde, et al., 2015*). No obstante, también han sido realizados algunos estudios que relacionan el receptor sigma-2 con la adicción a cocaína. En 2007 fue descrito que el tratamiento con antagonistas del receptor sigma-2 atenuaba los efectos conductuales inducidos por esta droga en células (*Matsumoto, et al., 2007*) y en ratones (*Lever, et al., 2014*). En base a los resultados obtenidos acerca del papel modulador del receptor sigma-1 sobre los receptores dopaminérgicos, y a pesar de existir, aún, pocas referencias bibliográficas que relacionen el receptor sigma-2 con la adicción a cocaína, nos planteamos ver si este receptor se encuentra involucrado en los efectos producidos por la cocaína en la modulación de la neurotransmisión dopaminérgica, aportando nueva información respecto los mecanismos de acción de esta droga.

En el trabajo ***Sigma-2 receptors mediate cocaine effects on dopamine D_1 receptor signaling*** (*Aguinaga, et al., 2017;* manuscrito preparado para ser enviado a *Molecular Psychiatry*) ha sido determinado que el receptor sigma-2, igual que el receptor sigma-1, es capaz de modular la señalización dopaminérgica al formar complejos heteroméricos con el receptor D_1 de dopamina, pero no con el D_2R. Al analizar el efecto modulador del receptor sigma-2 sobre el receptor D_1 ha sido observada una inhibición a nivel de la acumulación de AMPc inducida por ligando y una potenciación a nivel de fosforilación de MAPK. Estos resultados han sido descritos en células HEK-293 pero también en cultivos primarios neuronales, donde ha sido bloqueada la expresión del receptor sigma-1 mediante el tratamiento con RNAi contra este receptor. Los resultados obtenidos muestran como, en presencia de cocaína, tiene lugar un comportamiento contrario del heterómero D_1-sigma-2 respecto al heterómero D_1-sigma-1 descrito por Navarro y colaboradores (*Navarro, et al., 2010*).

De manera interesante, ha sido demostrado que el receptor D_1 puede formar complejos heteroméricos de orden superior en los que pueden interaccionar, simultáneamente, los receptores sigma-1 y sigma-2, siendo el receptor sigma-1 capaz de desplazar al receptor sigma-2 del heterotrímero, pero no al contrario. Navarro y colaboradores observaron un incremento de la expresión del receptor sigma-1 a nivel de membrana celular tras la exposición aguda de células a cocaína (*Navarro, et al., 2010*). Al producirse este aumento de los niveles de sigma-1R en la membrana plasmática, el receptor sigma-2 podría ser desplazado de los complejos heteroméricos D_1-sigma-2 y D_1-sigma-1-sigma-2, incrementando así el número de heterómeros D_1-sigma-1. Estos resultados podrían inducir a pensar que es únicamente el receptor sigma-1 el responsable de

los efectos mediados por cocaína, debido a su mayor afinidad por esta droga y a la capacidad por desplazar al receptor sigma-2 en la interacción con D_1R.

La existencia de los complejos D_1-sigma-1-sigma-2 puede ser de gran importancia en los ganglios basales. Tal y como ha sido comentado anteriormente, el control motor en los ganglios basales se basa en un complejo circuito formado por neuronas GABAérgicas que contienen mayoritariamente el receptor D_1 de dopamina (vía directa) o neuronas GABAérgicas que contienen mayoritariamente el receptor D_2 de dopamina (vía indirecta). De modo que, un control motor fino depende del balance de estas señales dopaminérgicas, unas vía D_1R, el cual está acoplado a proteína G_s, y otras vía D_2R, el cual se encuentra acoplado a proteína G_i (*Heinsbroeck, et al., 2017; Grillner y Robertson, 2016*). El impedimento del control motor provocado por la cocaína es causado por un fuerte aumento de los niveles de dopamina en el espacio sináptico induciendo una sobreexcitación de los receptores dopaminérgicos y un desbalance de las vías directa/indirecta del estriado. Ha sido observado que la cocaína induce un aumento en los niveles de AMPc en las células que expresan el heterómero D_1-sigma-1, mientras que, en la vía indirecta, donde las células expresan el complejo D_2-sigma-1, la cocaína disminuye la señalización dopaminérgica (*Navarro, et al., 2013*). En relación al desequilibrio resultante de los efectos dependientes de sigma-1, la existencia de los trímeros D_1-sigma-1-sigma-2 en neuronas de la vía directa podría responder a una estrategia de control del organismo para mitigar los efectos negativos de la modulación ejercida por el complejo D_1-sigma-1. Por otro lado, a nivel de la señalización mediada por las MAPK, ha sido descrito que la cocaína modula negativamente la señalización dopaminérgica en células que expresan el heterómero D_1-sigma-1, mientras en células que expresan el heterómero D_1-sigma-2 se observa una potenciación. Las ERK1/2 están implicadas en los cambios plásticos inducidos por el consumo de drogas de abuso (*Radwanska, et al., 2005*). Ha sido demostrado que la activación de la vía de las ERK1/2 es necesaria para que se establezca la asociación entre lugar y consumo de droga de abuso en un ensayo de preferencia de lugar condicionada (*Valjent, et al., 2006; Du, et al., 2017*). Además, ha sido demostrado que una depleción de la quinasa ERK1 provoca un incremento de la activación de la ERK2 dependiente de estímulo, facilitando la sensibilización psicomotora inducida por cocaína y la preferencia de lugar motivada por la cocaína (*Ferguson, et al., 2006*). De forma interesante, Zhang y colaboradores han descrito que el receptor D_1 promueve en el núcleo accumbens la plasticidad neuronal a largo plazo inducida por cocaína (*Zhang, et al., 2016*), no obstante, no ha sido descrito el mecanismo subyacente a este fenómeno. En base a los resultados obtenidos en nuestro laboratorio, y acorde con los trabajos anteriormente citados, es posible sugerir que la potenciación de la señalización de la vía de las MAP quinasas mediada por el heterómero D_1-sigma-2 podría ser el mecanismo mediante el cual el receptor sigma-2 induce la plasticidad neuronal a largo plazo favoreciendo el establecimiento de la adicción. Los datos obtenidos sugieren un papel predominante del receptor sigma-1 en consumo agudo de cocaína y un papel más relevante del receptor sigma-2 en el establecimiento de la adicción a la droga de abuso.

Ambos receptores sigma se expresan de forma constitutiva y se encuentran ampliamente distribuidos por el SNC, aunque el receptor sigma-1 tiene una afinidad por cocaína superior al receptor sigma-2, 2 μM *versus* 19 μM (*Garcés-Ramírez, et al., 2011*), los niveles de cocaína en sangre en un adicto a cocaína son suficientes para activar al receptor sigma-2, de modo que, los efectos netos observados tras un tratamiento con cocaína dependerán de la expresión relativa de sigma-1 y sigma-2. Esto sugiere que, en una situación de consumo de cocaína, momento en que se produce un importante incremento de los niveles de dopamina en las regiones cerebrales motoras relacionadas con la recompensa, el receptor sigma-1 potenciaría los efectos de la droga de abuso mientras que el receptor sigma-2 los contrarrestaría. En dicho escenario los antagonistas de sigma-1 podrían tener potencial para contrarrestar los efectos agudos producidos por la cocaína. No obstante, en este trabajo ha sido observado que en cortes cerebrales de ratas con una

administración aguda de cocaína predominan los heterómeros entre los receptores D_1-sigma-1, mientras que en ratas tratadas de forma crónica predominan los heterómeros D_1-sigma-2. Además, en cultivos primarios de neuronas estriatales tratados con diferentes tiempos de administración de cocaína, ha sido analizada la acumulación de AMPc inducida por el agonista del receptor D_1, SKF-81297. De manera interesante, a tiempos cortos de tratamiento de cocaína ha sido observada una potenciación de la señal inducida por SKF-81297, fenómeno atribuido a la heteromerización entre los receptores D_1-sigma1, mientras a tiempos largos (de 3 a 7 días de tratamiento) ha sido observada una inhibición de la acumulación de AMPc inducida por SKF-81297, fenómeno asociado al heterómero D_1-sigma-2. Con estos resultados podemos concluir que en un consumo agudo de cocaína prevalece la señalización mediada por el heterómero D_1-sigma-1, pero en exposiciones a la cocaína más prolongadas en el tiempo, la señalización mediada por el receptor D_1 de dopamina corresponde a la determinada para el heterómero D_1-sigma-2. Estos resultados a nivel de cultivos primarios de neuronas estriatales concuerdan con el incremento en la expresión del heterómero de receptores D_1-sigma-1 a dosis agudas de cocaína y del heterómero D_1-sigma-2 a dosis crónicas observado en cortes de rata administrada con cocaína. Estos datos sugieren que la sobreexpresión inicial a nivel de membrana celular del receptor sigma-1 inducida por la cocaína es transitoria, una vez estos niveles disminuyen, sería sigma-2 el receptor predominante en los heterómeros con el receptor D_1 de dopamina, iniciando así cambios neuronales a largo plazo responsables del establecimiento de la adicción a la cocaína.

Recientemente, Singer y colaboradores han determinado que a partir de las 2 horas de la exposición a la droga se inician estos mecanismos de plasticidad neuronal (*Singer, et al., 2017*), resultados que concuerdan con las observaciones realizadas en este trabajo respecto al momento en que cambia la prevalencia de la señalización mediada por D_1-sigma-1 a la mediada por D_1-sigma-2. El mecanismo de acción descrito en este trabajo, sin embargo, no puede explicar los resultados obtenidos por Matsumoto y colaboradores (*Matsumoto, et al., 2007*) y Lever y colaboradores (*Lever, et al., 2014*) en los que antagonistas del receptor sigma-2 bloquean los efectos locomotores inducidos tras la administración de cocaína. Una posible explicación se debería a la inespecificidad de los ligandos utilizados por estos autores, que no son selectivos para el receptor sigma-2, existiendo la posibilidad de que la atenuación observada tras la administración de dichos antagonistas sea debida a la inhibición del receptor sigma-1. En este caso, Matsumoto y colaboradores coincidirían con nuestros resultados, donde la inhibición de la expresión del receptor sigma-1 en cultivos primarios de neuronas estraitales provoca la desaparición de los efectos de la cocaína sobre los receptores dopaminérgicos. Por otro lado, cabe destacar que los resultados presentados en los trabajos de Matsumoto y Lever corresponden a ensayos de comportamiento en ratones vivos a los que les han sido administrados los antagonistas de forma intraperitoneal, de modo que los efectos observados pueden ser la combinación de muchos factores, a diferencia de los resultados presentados en esta Tesis, que corresponden a ensayos bioquímicos realizados en cultivos primarios de neuronas estriatales o cortes estriatales de ratas administradas con cocaína.

En resumen, los datos obtenidos sugieren que los eventos relacionados con la adicción y las actividades motoras relacionadas con la cocaína mediadas por el sistema dopaminérgico resultan probablemente del equilibrio entre el impacto de la cocaína sobre el receptor sigma-1 y el receptor sigma-2 en los efectos derivados de la activación de los receptores D_1R, D_2R en el SNC.

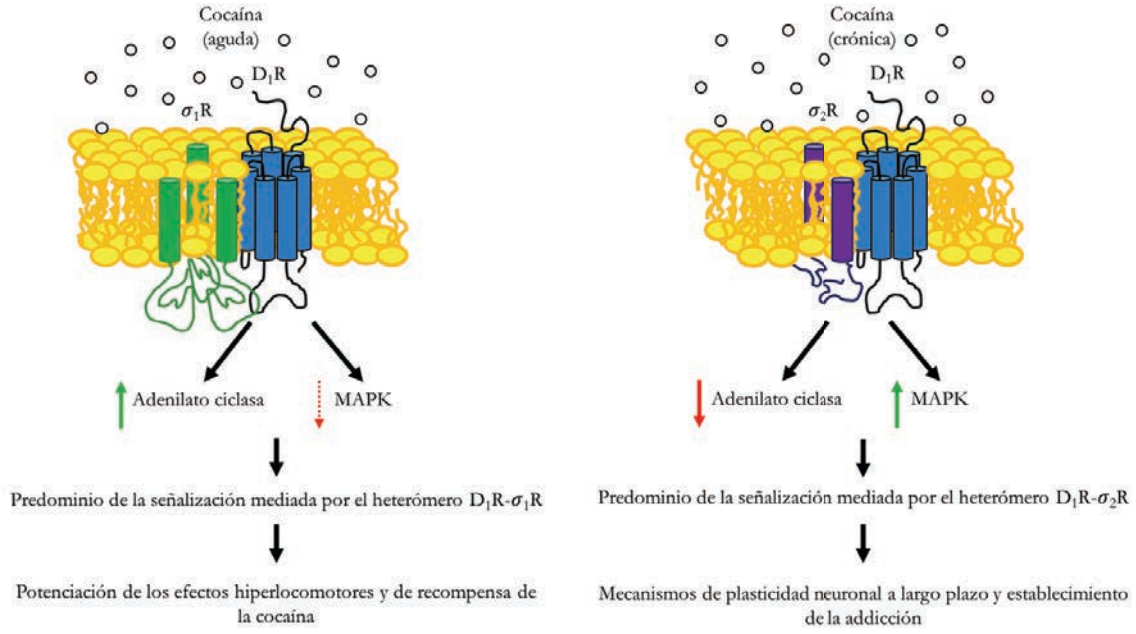

Figura 32. Representación esquemática del efecto modulador de la cocaína en tratamientos agudos y crónicos ejercido por el receptor sigma-1 sobre el receptor D_1 dopamina.

Es sabido que el estrés es un factor importante relacionado con los mecanismos de la drogadicción, ya que incrementa la vulnerabilidad de los humanos a caer en conductas adictivas (*Sinha, 2008; de Giovanni, et al., 2016*). Son muchas las evidencias que sugieren el solapamiento entre los sistemas cerebrales del estrés y el de la recompensa, y que las alteraciones en el sistema del estrés pueden contribuir al consumo de drogas de abuso, como la cocaína (*de Jong y de Kloet, 2004; Polter y Kauer, 2014*). Algunos autores hipotetizan que esta desregulación entre la vía de la recompensa y la vía del estrés lleva a la transición de una búsqueda recreativa a una búsqueda compulsiva de la droga, así como desregulaciones a largo plazo de estos sistemas conducen a la vulnerabilidad del individuo a recaer en la drogadicción (*Doura y Unterwald, 2016; Stelly, et al., 2016*). Estas hipótesis han sido confirmadas en distintos estudios donde ha sido observado qué agentes estresantes incrementan el comportamiento de búsqueda (*Polter, et al., 2017*) y auto-administración de drogas de abuso (*Miczek, et al., 2008; Mantsch, et al., 2008*). Mediante ensayos de comportamiento ha sido observado que las situaciones de estrés repetidas como la dependencia a psicoestimulantes están asociadas con alteraciones en la vía mesocorticolímbica y el circuito corticolímbico glutamatérgico de la corteza prefrontal y la señalización mediada por el *corticotropin-releasing factor* (CRF) en el área tegmental ventral (VTA) (*Holly, et al., 2016*). Es importante puntualizar que el CRF es una de las principales moléculas implicadas en estrés y recientemente ha sido demostrado que poblaciones de neuronas dopaminérgicas de la VTA expresan receptores para esta molécula (*Grieder, et al., 2014*), siendo el receptor CRF_1R el que está más implicado en los comportamientos de búsqueda de droga inducidos por estrés (*Blacktop, et al., 2013*). Otros investigadores también afirman que tanto el estrés (reproducido mediante el tratamiento con Corticotropin Related Factor) como las drogas de abuso sensibilizaban las neuronas dopaminérgicas de la VTA a los *inputs* excitadores aumentado la fuerza de esta señalización mediante modificaciones sinápticas (*Saal, et al., 2003; Ungless, et al., 2003*). Además, en la VTA de animales que han sido sometidos a contacto previo con la cocaína, pero no en animales *naive*, la liberación de CRF inducida por estrés incrementa los niveles extracelulares de glutamato y de dopamina a lo largo de toda la vía de la recompensa (*Holly, et al., 2015; Holly, et al., 2016*). En la misma línea, Vranjkovic y colaboradores han observado que un antagonista del receptor de CRF administrado en la VTA evita la recaída en esta búsqueda de

cocaína tras la exposición a un agente estresante en ratas previamente auto-administradas (*Vranjkovic, et al., 2014*). Sin embargo, los mecanismos moleculares que interrelacionan la vía del estrés y la adicción a drogas de abuso se desconocen. Con ello, uno de los objetivos de esta tesis ha sido determinar cómo se establece la conexión entre estas vías cerebrales.

Por otro lado, a las neuronas dopaminérgicas de la VTA también llegan inervaciones desde el hipotálamo de neuronas orexinérgicas. A parte del papel que tradicionalmente se le otorga a la orexina en la regulación del ciclo sueño-vigilia y el apetito, ha sido recientemente descrito que participa también en procesos de recompensa y adicción a sustancias de abuso (*Sakurai, 2014; Mahler, et al., 2014*), a través del receptor OX_1R (*Mahler, et al. 2014*). Diversos estudios han analizado la conexión entre el sistema orexinérgico y los mecanismos de recompensa y drogadicción determinado que las neuronas orexinérgicas del hipotálamo se activan por estímulos que predicen recompensa mediada tanto por comida como por drogas de abuso y pueden ser relevantes en la dependencia de drogas como morfina, heroína o cocaína (*Harris y Aston-Jones, 2006; Narita, et al., 2006; Cason, et al., 2010*). Wang y colaboradores afirmaron que la VTA es un área cerebral clave en la habilidad que tiene el sistema orexinérgico de promover la búsqueda de cocaína, debido a que la administración intra-VTA de orexina-A inducía la recaída en la auto-administración de cocaína, lo cual era asociado a la liberación de glutamato y dopamina en la VTA (*Wang, et al., 2009*). Y anteriormente, Boutrel y colaboradores habían observado que la administración de orexina-A inducía una recaída dosis-dependiente de la búsqueda de cocaína, y este comportamiento era prevenido al tratar con un antagonista no-selectivo de CRF, además, un antagonista selectivo de OX_1R bloqueaba la recaída inducida por estrés en animales en los que ya había sido extinguido el comportamiento de búsqueda de cocaína (*Boutrel, et al., 2005*). Estos resultados relacionan directamente los mecanismos de la adicción a cocaína y recaída con el estrés vía orexina y CRF, sin embargo, el papel de estos receptores en la VTA siempre ha sido estudiado de forma independiente. Además, nos planteamos cual es el sentido biológico de que el CRF o la orexina-A, moléculas implicadas en estrés, puedan activar la vía de la recompensa.

En el trabajo ***Orexin-corticotropin-releasing factor receptor heteromers in the ventral tegmental area as targets for cocaine*** (*Navarro, et al., 2015*) ha sido demostrada por primera vez la existencia funcional de heterómeros de receptores CRF_1R-Ox_1R en células transfectadas y en la VTA. Este trabajo representa el nexo de unión entre todos aquellos trabajos que mostraban la existencia de una relación tanto del CRF (*Vranjkovic, et al., 2014; Holly, et al., 2016*) por un lado como de la orexina (*Sakurai, 2014; Mahler, et al., 2014*) por el otro con la recaída en la búsqueda y consumo de cocaína asociados al estrés, mostrando que no se trataba de mecanismos independientes sino de un mismo complejo. En el presente manuscrito se describe que el antagonismo cruzado entre los receptores OX_1R y CRF_1R en el heterómero CRF_1R-OX_1R disminuye la liberación de dopamina en la VTA. Este efecto explica por qué una situación de estrés, que en ausencia de heterómeros induciría la liberación de dopamina en la VTA, con la consecuente activación de la vía de la recompensa y la creación de una sensación placentera para el individuo, induce efectos opuestos. Finalmente, en este trabajo ha sido descrita la interacción del receptor sigma-1 con el heterómero CRF_1R-OX_1R y la capacidad de los agonistas de sigma-1, incluida la cocaína, para modificar la estructura cuaternaria del heterómero bloqueando así las interacciones alostéricas que se establecen entre la orexina-A y CRF en el heterómero.

Las interacciones moleculares entre los receptores CRF_1R y OX_1R han sido demostradas en células HEK-293T mediante técnicas de BRET, complementación bimolecular y PLA. Mediante el uso de toxinas (CTX y PTX) ha sido observada la capacidad del heterómero CRF_1R-OX_1R para interaccionar simultáneamente con ambas proteínas G, las cuales muestran una interdependencia funcional. Además, ha sido caracterizada la funcionalidad del complejo CRF_1R-OX_1R con un fenómeno de *cross-talk* y *cross-antagonismo* en la coactivación de ambos receptores en las señales de

MAPK, AMPc y DMR. Estos efectos han desaparecido cuando las células han sido pre-tratadas con péptidos sintéticos con la secuencia aminoacídica correspondiente a dominios TM específicos del receptor OX_1R indicando la especificidad de los resultados obtenidos. Estas mismas herramientas han sido utilizadas *in situ* e *in vivo*, en *slices* de la VTA y en ensayos de microdiálisis, demostrando la presencia del heterómero CRF_1R-OX_1R en este núcleo cerebral.

Cuando células que expresan el complejo CRF_1R-OX_1R o *slices* de VTA han sido tratadas con cocaína, se han perdido las interacciones alostéricas existentes entre los ligandos que forman el heterómero, provocando la desestabilización de la función característica del complejo. El efecto inducido por la cocaína en el heterómero CRF_1R-OX_1R no es un fenómeno aislado de este caso, recientemente en nuestro laboratorio ha sido descrito un mecanismo parecido entre el heterómero de receptores sigma-1-D_1-H_3R (*Moreno, et al., 2014*), donde la cocaína produce una modificación del heterómero observable 24 horas después de una única administración sistémica, dando respuesta a algunos de los efectos neurotóxicos de la cocaína.

Los resultados obtenidos en este trabajo sugieren que los heterómeros CRF_1R-OX_1R controlan la funcionalidad de las células dopaminérgicas en la VTA, perdiendo este control en animales adictos a cocaína. La neutralización del *crosstalk* negativo entre la orexina-A y el CRF en la VTA por el tratamiento simultáneo con el agonista de sigma-1, PRE-084, o por la administración previa de cocaína, explica los resultados obtenidos por Wang y colaboradores en los que el CRF únicamente inducía la liberación de dopamina en la VTA en animales expuestos previamente a cocaína (*Wang, et al., 2005*). En esta situación, la señalización mediada por el CRF_1R no está inhibida por la activación tónica del receptor OX_1R a través de su ligando endógeno, orexina-A. En la misma línea, la neutralización de la interacción alostérica entre los agonistas en el heterómero CRF_1R-OX_1R puede explicar los resultados observados también por Wang y colaboradores en los que afirmaban que aparentemente la orexina-A, de forma independiente de CRF, era capaz de provocar la liberación de dopamina en la VTA e inducir así la aparición de comportamientos de búsqueda de droga (*Wang, et al., 2009*).

Ha sido demostrado que la exposición a cocaína incrementa los niveles del receptor sigma-1 en cerebro (*Robson, et al., 2012*), y esta sobreexpresión del receptor sigma-1 en el estriado ha sido relacionada con el incremento en membrana plasmática de la presencia de oligómeros entre los receptores sigma-1 y el canal de potasio dependiente de voltaje Kv1.2, el cual ha sido involucrado en la sensibilización a los efectos psicoestimulantes (*Kourrich, et al., 2013*). La sobreexpresión de sigma-1 en la VTA podría traducirse también en un incremento de los oligómeros sigma-1-CRF_1R-OX_1R, acentuando los cambios inducidos por la cocaína en el control de la liberación de dopamina por acción del CRF y la orexina-A en la VTA. Estos cambios pueden explicar el aumento en el comportamiento de búsqueda de cocaína dependiente del receptor CRF_1 en respuesta al estrés o a la administración de CRF en la VTA después de periodos largos de auto-aministración, como describió Blacktop y colaboradores (*Blacktop, et al., 2011*). Así, el estudio del complejo CRF_1R-OX_1R en modelos animales de adicción a psicoestimulantes debería proporcionar nueva información que apoyara el papel de este oligómero como una nueva diana terapéutica en la adicción a drogas de abuso.

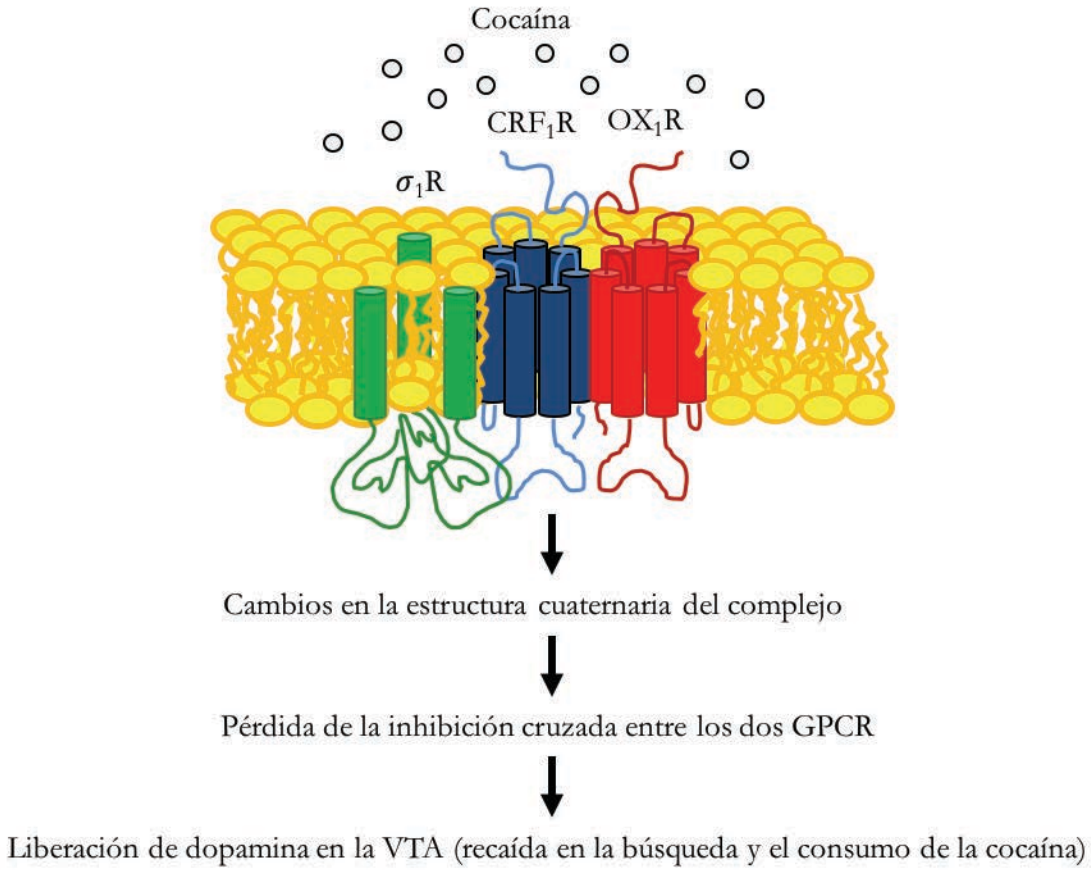

Figura 33. Representación esquemática del efecto modulador de la cocaína ejercido por el receptor sigma-1 sobre el heterómero de receptores CRF_1R-OX_1R.

A pesar de todos los resultados discutidos hasta el momento, es importante destacar que la cocaína no incide exclusivamente sobre el sistema dopaminérgico o en los mecanismos que controlan la liberación de este neurotransmisor. Desde hace siglos, los chamanes de las regiones andinas de centro y sud-américa han sabido que masticar la hoja de coca o la ingesta de infusiones realizadas con estas mismas hojas producía, entre otros efectos, la desaparición de la sensación de hambre. Esta característica, junto a la eliminación de la sensación de fatiga y dolor también provocada por el consumo de esta sustancia, ha sido explotada durante siglos por los habitantes de las zonas rurales andinas permitiendo la realización de largos viajes a través de los Andes o intensísimas jornadas de trabajo en el campo. Actualmente el consumo en Europa o Estados Unidos ya no es en forma de la hoja de coca, sino que es consumido el extracto de su principio activo, la cocaína, presentada en distintas composiciones. El consumo de cocaína sigue proporcionando este efecto de eliminación de la sensación de hambre. De hecho, es habitual asociar el concepto de individuo adicto a la cocaína con un individuo que presenta una extrema delgadez. Es sorprendente que, a pesar de ser un efecto ampliamente conocido, se desconozca el mecanismo a nivel molecular. En esta tesis se ha querido determinar la relación existente entre los mecanismos del hambre y la adicción a cocaína, definiendo cómo esta droga puede alterar dichos mecanismos.

El sistema del hambre está formado por la principal hormona orexinérgica: la grelina, inductora de la sensación de hambre (*Mason, et al., 2014*). Este péptido es producido en el estómago cuando distintos sensores del organismo detectan la necesidad de ingerir alimentos y liberado al torrente sanguíneo donde los niveles en plasma fluctúan, aumentando previamente a las comidas y disminuyendo después de la ingesta (*Cabral, et al., 2017*). La grelina es conducida hasta distintos

órganos periféricos y al cerebro, gracias a su capacidad para cruzar la barrera hematoencefálica. Una vez allí, la grelina ejerce su función mediante la unión al receptor acoplado a proteína G conocido como *growth-hormone secretatogue receptor 1a* (GHS-R1a). Las células que expresan el receptor GHS-R1a, también expresan el receptor GHS-R1b, una variante truncada de GHS-R1a a la que le faltan los dominios transmembrana TM 6 y 7. La grelina no puede unirse ni señalizar mediante este receptor truncado, GHS-R1b (*Mary, et al., 2013*). El papel de este receptor truncado en la señalización mediada por grelina es actualmente motivo de debate, han aparecido diferentes hipótesis sobre su posible rol después de haber sido considerado un vestigio de la evolución durante mucho tiempo. Ha sido demostrada la habilidad del receptor GHS-R1a para heteromerizar con el receptor GHS-R1b ejerciendo un efecto dominante negativo sobre la señalización de GHS-R1a, que podría ser debida a una retención intracelular de GHS-R1a por la incapacidad del receptor GHS-R1b para llegar a la membrana plasmática (*Leung, et al., 2007; Chow, et al., 2012*) o mediante un mecanismo alostérico que estabilizaría el receptor GHS-R1a en una conformación incapaz de señalizar (*Mary, et al., 2013*). En base a estos resultados, en nuestro laboratorio nos hemos propuesto investigar el papel de la variante truncada del receptor de grelina en un modelo de células neuronales, y dar explicación al mecanismo de la regulación ejercida por este receptor.

En el trabajo **A significant role of the truncated ghrelin receptor GHS-R1b in ghrelin-induced signaling in neurons** (*Navarro, et al., 2016*) ha sido revelado un nuevo papel modulador del receptor GHS-R1b en el tráfico y señalización del receptor GHS-R1a. En primer lugar, el receptor GHS-R1b facilita el tráfico hacia la membrana plasmática de GHS-R1a con una eficiencia que dependen de la ratio específica existente entre la expresión de ambos receptores, GHS-R1b/GHS-R1a. A medida que la ratio en la expresión GHS-R1b/GHS-R1a incrementa, la facilitación del tráfico hacia membrana disminuye y acaba desapareciendo. Estos resultados han servido para descartar la hipótesis de la retención intracelular mediada por el receptor truncado (*Leung, et al., 2007; Chow, et al., 2012*), ya que serían necesarios niveles de expresión del receptor GHS-R1b muy altos, probablemente no fisiológicos, para promover esta retención intracelular del GHS-R1a.

En segundo lugar, mediante la técnica de biotinilación y ensayos de señalización ha sido observado que el receptor GHS-R1b puede actuar como un modulador dual de la función de GHS-R1a: niveles de expresión de GHS-R1b relativamente bajos respecto los de GHS-R1a potenciarían la señalización inducida por grelina, mientras que niveles altos de expresión de GHS-R1b relativos inhibirían la función de GHS-R1a ejerciendo un efecto alostérico negativo en la señalización de GHS-R1a. Este efecto modulador ha sido observado a nivel de inhibición de la adenilato ciclasa, de reclutamiento de β-arrestina-2, de fosforilación de ERK1/2, y de incremento de calcio citosólico.

Ha sido demostrada la capacidad del receptor GHS-R1a para homodimerizar y formar estructuras de orden superior al interaccionar con una o varias moléculas del receptor GHS-R1b. Esta capacidad proporciona el marco necesario para que se produzca de manera precisa la modulación de la función del receptor GHS-R1a, dependiente de la estequiometria entre ambas proteínas. En base a nuestros resultados y de acuerdo con Damián y colaboradores, ha sido observado que el receptor GHS-R1a es la mínima unidad funcional (*Damian, et al., 2015*), en ausencia de GHS-R1b, GHS-R1a es capaz de señalizar, pero de manera mucho menos eficiente que en presencia de bajas concentraciones de GHS-R1b.

Cuando nos movemos a un modelo de cultivos primarios neuronales, los resultados indican, en primer lugar, que los niveles relativos de expresión endógena de los receptores GHS-R1a y GHS-R1b fluctúan dependiendo de la región del cerebro analizada, mostrando en neuronas de

hipocampo una mayor ratio de receptores GHS-R1b/GHS-R1a y una menor funcionalidad del receptor GHS-R1a respecto a cultivos estriatales.
En células GH de la glándula pituitaria ha sido descrito el acoplamiento del receptor GHS-R1a principalmente a la proteína G_q, activando así la fosfolipasa C, IP_3 y la movilización de calcio intracelular (*Mary, et al., 2013; Damian, et al., 2015*) e induciendo la liberación de la hormona de crecimiento. En cambio, en las células β de los islotes pancráticos, el receptor GHS-R1a se acopla a la proteína $G_{i/o}$ (*Bennett, et al., 2009*) donde su activación provoca la inhibición de la liberación de insulina (*Dezaki, 2013*). Ha sido también descrito que la grelina provoca señalización a través de la vía AMPc-PKA, aunque la activación de estas vías no se atribuye exclusivamente a la acción de la proteína G_s (*Cuellar y Isokawa, 2011; Sun, et al., 2014*).

En este trabajo, mediante el uso de toxinas e inhibidores, ha sido demostrado en células HEK-293T el acoplamiento preferencial del receptor GHS-R1a a proteína $G_{i/o}$ y, sorprendentemente, un acoplamiento a $G_{s/olf}$ tanto en los cultivos neuronales de estriado como hipocampo. Esta sorprendente promiscuidad del receptor GHS-R1a en el acoplamiento a proteína G puede explicarse mediante la formación de nuevos complejos heteroméricos. Ha sido demostrado que la oligomerización de GHS-R1a con GHS-R1b confiere al oligómero GHS-R1a-GHS-R1b la capacidad para heteromerizar con el receptor D_1 de dopamina, promoviendo el cambio de acoplamiento y produciendo así a la señalización de la grelina a través de la proteína $G_{s/olf}$. Estudios previos realizados en células HEK-293T habían sugerido la posible interacción del receptor GHS-R1a con el receptor D_1 de dopamina (*Jiang, et al., 2006*), pero sin describir la importante participación del receptor GHS-R1b. Este mismo grupo de investigación también ha descrito que la heteromerización de los receptores GHS-R1a-D_1R permite al receptor D_1R acoplarse y señalizar a través de la proteína G_q (*Kern, et al., 2015*). Sin embargo, no ha sido tenido en cuenta en ningún momento el rol de GHS-R1b. En células co-transfectadas con los receptores D_1 de dopamina, GHS-R1a y GHS-R1b, ha sido observado un fenómeno de *cross-antagonismo*, es decir, tanto el antagonista de D_1, SCH-23390, como el antagonista de GHS-R1a, YIL-781, han sido capaces de bloquear los incrementos de AMPc inducidos por el SKF-81297 y la grelina, una propiedad bioquímica característica de los heterómeros de receptores. Este fenómeno de *cross-antagonismo* ha sido reproducido en cultivos primarios estriatales; además, ha sido observado que el receptor GHS-R1a ha sufrido un cambio de acoplamiento a proteína G, donde la activación con grelina induce un incremento de los niveles de AMPc. Estos resultados demuestran la presencia de complejos D_1R-GHS-R1a-GHS-R1b en neuronas estriatales. En el hipocampo, a pesar de las recientes evidencias de la existencia de interacciones moleculares y funcionales entre los receptores GHS-R1a y D_1 (*Kern, et al., 2015*), debido a la baja expresión del receptor D_1 de dopamina, otras interacciones más abundantes deben ser los responsables del acoplamiento del complejo GHS-R1a-GHS-R1b a la proteína $G_{s/olf}$. Estos resultados explican la complejidad de las redes de GPCR donde distintos tipos de complejos que contienen el heterómero GHS-R1a-GHS-R1b pueden ser expresados en el cerebro.

En este trabajo por lo tanto ha sido demostrado que el receptor truncado GHS-R1b tiene un papel mucho más activo y más complejo en la señalización mediada por grelina de lo que tradicionalmente era asumido. Con estos resultados ha sido puesto de manifiesto que los niveles de expresión relativos del receptor GHS-R1b no solo determinan la eficacia de la señalización mediada por la grelina a través del GHS-R1a, sino que también determinan la habilidad de GHS-R1a para formar complejos oligoméricos con otros receptores, provocando así cambios muy relevantes en la señalización mediada por la grelina. En este punto, nos planteamos describir otras interacciones capaces de modular y explicar la señalización mediada por grelina. En nuestro laboratorio había sido demostrado que de la interacción de sigma-1 con los receptores D_1 y D_2 de dopamina o el heterómero CRF_1R-OX_1R resultaban mecanismos de acción importantes en la adicción a cocaína. Por todos es conocida la asociación de la adicción a cocaína con la disminución

del hambre, por lo que nos planteamos estudiar la posible interacción del receptor de grelina con sigma-1 en diferentes tratamientos de cocaína.
En el trabajo **Cocaine blocks ghrelin effects via interaction with sigma-1 receptors** (*Aguinaga, et al., 2017;* manuscrito enviado a *Neuropsychopharmacology*) ha sido demostrada la formación de complejos heteroméricos de receptores GHS-R1a-GHS-R1b-sigma-1. El nuevo heterómero descrito adquiere nuevas propiedades farmacológicas y es sensible a la unión de cocaína debido a la presencia del receptor sigma-1. Ha sido observado que la cocaína incrementa la expresión del heterómero a nivel de superficie celular. Este resultado va en la misma línea que resultados previos que describían un aumento del receptor sigma-1 a nivel de membrana plasmática debido al tratamiento con cocaína (*Navarro, et al., 2010*). Al analizar la señalización del receptor GHS-R1a en presencia de cocaína ha sido observado que a nivel de formación de AMPc, fosforilación de MAPK, movilización de calcio y dinámica de redistribución de masas (DMR) la cocaína produce una fuerte inhibición a nivel de todas las vías de señalización. Estos resultados son debidos a la interacción de la cocaína con sigma-1 en la formación del complejo GHS-R1a-sigma-1, debido a que la inhibición de la expresión del receptor sigma-1 mediante RNAi, hace desaparecer la inhibición de la señalización inducida por cocaína sobre el receptor GHS-R1a. Este bloqueo podría explicar la inhibición de la sensación de hambre característica tras el consumo de cocaína. En este estudio también han sido analizadas las regiones implicadas en la formación de la interfase del heterómero GHS-R1a-GHS-R1b-sigma-1. Mediante el uso de péptidos específicos para las regiones TM de los receptores de grelina ha sido descrito por primera vez que los receptores GHS-R1a y GHS-R1b interaccionan por la interfase TM5/TM6. Además, mediante el uso de la estructura cristalina del complejo homotrimérico de sigma-1 (*Schmidt, et al., 2016*) ha sido descrita la interfase de interacción entre sigma-1 y GHS-1a, los dominios TM1/TM2 del receptor de GHS-R1a. Con estos datos, mediante técnicas biofísicas se ha elaborado por primera vez el modelo estructural entre un GPCR y el receptor sigma-1. La combinación de estos resultados sugiere la existencia de complejos heteroméricos en los que los receptores de grelina GHS-R1a-GHS-R1b interaccionarían a través de los TM5/6, quedando libres los dominios TM1 y TM2 del receptor GHS-R1a para interaccionar con el receptor sigma-1R. Debido a la estructura homotrimérica del receptor sigma-1, se abre la posibilidad de la existencia de complejos de orden superior entre los receptores de grelina y sigma-1R mediante la combinación sucesiva de hetrómeros GHS-R1a-sigma-1. Pudiéndose formar así *clusters* especializados en la señalización mediada por grelina.

El núcleo accumbens, una de las estructuras que conforma el estriado, forma parte del sistema de la recompensa. Este sistema produce una sensación placentera frente a la comida y otras acciones vitales para la supervivencia del individuo (*Kim y Hikosaka, 2015*). La vía de la recompensa es activada por la expectativa de un estímulo placentero, que es reconocido mediante una sólida base de experiencias previas (*Richardson y Gratton, 1998*). En el estriado se expresan los receptores de grelina (*Engel, et al., 2015*). Así, la señal inducida por grelina puede activar la vía de la recompensa induciendo una sensación placentera al generar expectativas de ingesta de alimentos. Es importante destacar que en estas regiones mesolímbicas, el receptor de grelina es coexpresado con el receptor sigma-1. En este trabajo ha sido demostrada la existencia del heterómero GHS-R1a-sigma-1 en células HEK-293T, así como también en cultivos primarios de neuronas estriatales.

Ha sido descrito que el receptor sigma-1 es capaz de unir cocaína incluso a las dosis consideradas de uso recreativo, alterando la función locomotora (*Barr, et al., 2015*), la inducción de convulsiones (*Matsumoto, et al., 2001*), la sensibilidad (*Ujike, et al., 1996*) y los efectos de las drogas de abuso relacionados con la recompensa (*Romieu et al., 2002*). En base a los resultados obtenidos en este trabajo, ha sido descrito por primera vez que sigma-1, al heteromerizar con el receptor de grelina, puede estar implicado en la supresión del apetito inducida por cocaína, manteniéndose este efecto tanto en una exposición aguda como en tratamientos crónicos. Además, a través del heterómero

GHS-R1a-sigma-1, la cocaína bloqueará la activación de la vía de la recompensa mediada por grelina, disminuyendo la sensación placentera frente a estímulos de comida.

En este estudio ha sido observado que la interacción entre los receptores sigma-1 y GHS-R1a se traduce en un *cross-talk* entre receptores que altera la funcionalidad normal del receptor de grelina tanto en presencia de cocaína como de agonistas de sigma-1R, del mismo modo que sucede cuando el receptor sigma-1 interacciona con los receptores D_1 (*Navarro, et al., 2010*) o D_2 de dopamina (*Navarro, et al., 2013*). No obstante, hay que destacar que el mecanismo de acción mediante el cual sigma-1 modula los receptores no siempre es el mismo, ya que en el heterómero de receptores sigma-1-CRF_1R-OX_1R la interacción de sigma-1 con el receptor CRF provoca la disrupción del *cross-talk* negativo existente entre los receptores CRF_1R y OX_1R, inducido por cocaína (*Navarro et al., 2015*).

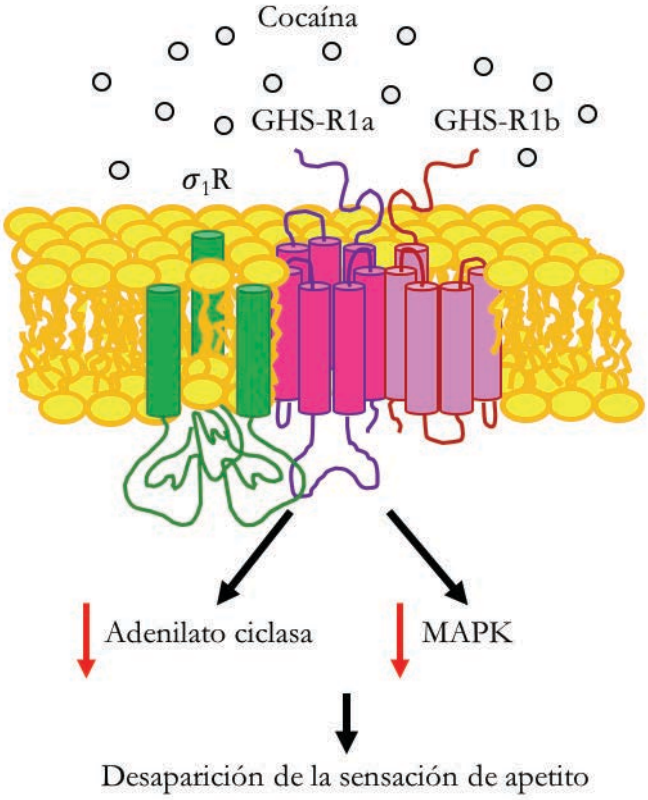

Figura 34. Representación esquemática del efecto modulador de la cocaína ejercido por el receptor sigma-1 sobre el receptor GHS-R1a.

Estos trabajos han demostrado como distintos GPCR ven modificada su funcionalidad al interaccionar con otras proteínas o con otros GPCR. Al producirse la interacción, el nuevo complejo formado puede ajustar su actividad a distintos ambientes o necesidades celulares que el receptor por sí solo no sería incapaz de detectar. En esta misma línea ha sido descrita la capacidad de las proteínas sensoras de calcio en la modulación de la actividad de algunos GPCR. El calcio es un mensajero imprescindible en las células. Las fluctuaciones en los niveles de este ion, que puede ir des de niveles submicromolares hasta milimolares (*Tsien y Tsien, 1990; Hu, et al., 2016; Ghosh, et al., 2017*), son uno de los mecanismos de regulación más importantes a nivel celular. Hay muchos estudios acerca del papel modulador que ejercen los niveles intracelulares del calcio sobre la actividad neuronal o directamente sobre los GPCR. Entre ellos, Navarro y colaboradores describieron la interacción y la modulación ejercida por la calmodulina, proteína sensora de calcio,

sobre el heterómero A_{2A}-D_2 (*Navarro, et al., 2009*). En estudios más recientes ha sido demostrado como las *neuronal calcium-binding proteins* (nCaBP), pueden interaccionar, y modular, también los receptores de adenosina A_{2A} (*Navarro, et al., 2012*) y de dopamina D_2 (*Pandalaneni, et al., 2015*).
El heterómero A_{2A}-D_2 fue uno de los primeros oligómeros de GPCR detectados en cerebro, concretamente en el estriado, donde tiene un papel fundamental en el control de la función y disfunción de los ganglios basales (*Ferré, et al., 1991; Borroto-Escuela, et al., 2016*). Los receptores A_{2A} y D_2 se acoplan preferentemente a proteínas $G_{s/olf}$ y G_i, respectivamente. Distintos estudios han determinado que entre ellos se establece una interacción antagónica recíproca en la que el receptor de adenosina A_{2A} provoca una disminución de la afinidad por la dopamina del receptor D_2 (*Ferré, et al., 1991*) y los ligandos del receptor D_2 inhiben la activación de la adenilato ciclasa mediada vía A_{2A} (*Kull, et al., 1999*). Aparte de modular la afinidad por los ligandos, la formación de oligómeros de GPCRs permite que los ligandos muestren una eficacia intrínseca distinta para la inducción de diferentes vías de señalización (*Ferré, et al., 2014*). Sin embargo, la modulación existente entre los receptores que forman el complejo heteromérico no recae exclusivamente en las interacciones que se producen entre estos mismos receptores, sino que ha sido demostrada la existencia de proteínas citosólicas capaces de interaccionar con ellos, participando así en esta modulación o regulación de la funcionalidad del heterómero.

En base a estos resultados previos, ha sido elaborado el trabajo **Intracellular calcium levels determine differential modulation of allosteric interactions within G protein-coupled receptor heteromers** (*Navarro, et al., 2014*) con el fin de estudiar si las proteínas sensoras de calcio pueden ejercer de moduladores alostéricos del heterómero A_{2A}-D_2. Los resultados obtenidos en este estudio han aportado datos de gran interés para el entendimiento de la modulación de la funcionalidad de los GPCR. En primer lugar, ha sido demostrado que, en neuronas, diferentes niveles de calcio pueden determinar la unión de distintas proteínas sensoras de calcio a los heterómeros de GPCR. En segundo lugar, ha sido demostrado que la unión a estas proteínas neuronales de unión a calcio puede promover o bloquear distintas modulaciones alostéricas en un complejo heteromérico de GPCRs. Y, por último, ha sido observado que estas uniones de distintos sensores de calcio permiten la modulación de manera selectiva de vías de señalización dependientes del heterómero de GPCR. Mediante la técnica de BRET ha sido determinado que las proteínas de unió a calcio NCS-1 y calneurona-1, pero no caldendrina, interaccionan con los receptores A_{2A} y D_2, viéndose afectados los niveles de BRET obtenidos cuando las células han sido tratadas con ionomicina, un ionóforo que induce la liberación de calcio intracelular y el consecuente cambio estructural de las proteínas sensoras de calcio debido a la unión de este ión. En el análisis de la señalización del heterómero A_{2A}-D_2 en función de los niveles de calcio ha sido observado a nivel de la vía de las MAPK que, en situaciones de altos niveles de calcio intracelular, la proteína calneurona-1 facilita una interacción alostérica negativa de forma recíproca entre el CGS-21680, agonista del receptor A_{2A}, y el quinpirole, agonista del receptor D_2 de dopamina. Por lo que respecta a la producción de AMPc, en células que expresan el heterómero de GPCR, pero no las proteínas de unión a calcio, el CGS-21680 induce un aumento en los niveles de AMPc, el quinpirole una reducción. Sin embargo, cuando las células son tratadas con ambos ligandos a la vez el quinpirole no es capaz de contrarrestar el aumento de AMPc inducido por el CGS-21680, indicando la existencia de una modulación alostérica negativa mediante la cual el CGS-21680 disminuye significativamente la eficacia intrínseca del quinpirole para inhibir la actividad de la adenilato ciclasa. En cambio, en una situación de altos niveles de calcio intracelular, en presencia de calneurona-1, ha sido observado que el quinpirole es capaz de reducir los niveles de AMPc producidos por el CGS-21680. Contrariamente, en una situación de bajos niveles de calcio, es la proteína NCS-1 quien deshace la interacción alostérica negativa a nivel de MAPK, aunque se mantiene a nivel de producción de AMPc. Estos resultados indican la existencia de una modulación diferencial dependiente de los niveles de calcio intracelulares sobre las interacciones alostéricas atribuidas al complejo heteromérico A_{2A}-D_2. Para poder determinar el papel de las proteínas NCS-

1 y calneurona-1 en la modulación de la función del heterómero se utilizaron cultivos primarios estriatales transfectados o no con un *small hairpin RNA* (shRNA) contra el RNAm del NCS-1 o calneurona-1 y se analizó la vía de las MAPK y la producción de AMPc. Los resultados obtenidos se corresponden perfectamente con los descritos en células HEK, indicando que, en neuronas estriatales los niveles de calcio intracelular determinan que proteína de unión a calcio se unirá al heterómero A_{2A}-D_2 siendo imprescindible para el correcto funcionamiento de dicho heterómero. Finalmente, mediante la técnica de PLA ha sido observado, en condiciones de bajos niveles de calcio, marcaje en muestras incubadas con anticuerpos contra A_{2A}-NCS-1 y D_2-NCS-1 pero no en las muestras incubadas contra A_{2A}-calneurona-1 o D_2-calneurona-1. Por el contrario, en presencia de ionomicina, ha sido observado marcaje en las muestras incubadas con anticuerpos contra A_{2A}-calneurona-1 y D_2-calneurona-1, pero no en las incubadas contra A_{2A}-NCS-1 ni D_2-NCS-1. De modo que, bajos niveles de calcio intracelular promueven la unión de NCS-1 al heterómero A_{2A}-D_2, y altos niveles de calcio, la unión de calneurona-1, transduciendo de manera diferencial las señales dependientes de calcio.

Aparte de la adenosina y la dopamina, la modulación dependiente de calcio de la función del heterómero A_{2A}-D_2 permite la integración de otros sistemas de neurotransmisores como el glutamato (a través de la activación del receptor NMDA) y acetilcolina (a través de receptores muscarínicos acoplados a G_q) (*Tozzi, et al., 2011*). Esto pone de manifiesto que los heterómeros de GPCR son dispositivos celulares que integran y modulan las señales de distintos neurotransmisores que en última instancia dependen de factores fisiológicos como los niveles de calcio.

Los resultados obtenidos a lo largo de esta tesis reafirman la existencia de los oligómeros de GPCR. Si bien es cierto que pocos autores hoy en día dudan de la existencia de estos complejos, sí que hay divergencia de opinión respecto a la unidad mínima funcional a considerar. Algunos investigadores mantienen la concepción tradicional afirmando que la unidad mínima funcional corresponde a un solo receptor de 7 dominios TM, siendo este capaz de funcionar por sí solo, aunque pueda desarrollar otras funciones o verse modulado al interaccionar con otro receptor. Por otro lado, una corriente de pensamiento más reciente defiende que la unidad mínima funcional de estos receptores correspondería a la formada por dos protómeros, es decir, un dímero de receptores de 7 dominios TM, pudiendo ser estos iguales (homodímeros) o diferentes (heterodímeros) (*Bouvier y Hébert, 2014; Vischer, et al., 2015*). Otra cuestión que divide aún a los expertos recae en la estequiometria entre receptores y proteínas G. La opinión mayoritaria acepta la estequiometria 2:1, dos protómeros del receptor por una proteína G (*Jastrzebska, et al., 2013*). Esta estructura encajaría con la relación de tamaños que se calcula para los receptores y la proteína G, siendo los receptores de un tamaño correspondiente aproximadamente a la mitad del tamaño de una proteína G (*Cordomí, et al., 2015*). Estas incógnitas tan básicas en el campo estructural demuestran que actualmente aún hay muchos vacíos de conocimiento por rellenar en el campo de los GPCR. En 2011, fue cristalizada por primera vez la unión del receptor β2 adrenérgico a su proteína Gαs, determinándose las regiones implicadas en esta interacción (*Rasmussen, et al., 2011*), sin embargo es de vital importancia seguir avanzando en el estudio de la estructura cuaternaria de las proteínas para entender cómo se producen físicamente las interacciones proteína-proteína en un complejo oligomérico, describiendo las interfases implicadas en las interacciones entre receptores u otras proteínas. No es descartable que el factor desencadenante de algunas enfermedades sea, en primera instancia, la incapacidad de un GPCR por formar heterómero con otras proteínas, no pudiendo así ejercer una función concreta. A la vez, el conocimiento estructural de los complejos oligoméricos será indispensable en el futuro para el diseño de nuevos fármacos más específicos que permitan, por ejemplo, la disrupción de un heterómero formado por dos GPCR concretos (receptor A-receptor B), y no los otros heterómeros que puedan formar estos mismos receptores con terceros receptores (receptor A-receptor C, receptor B-receptor D).

Con la finalidad de profundizar en la estructura de un complejo heteromérico dando respuesta a pequeñas y grandes incógnitas estructurales, ha sido escogido como modelo heteromérico de estudio el complejo formado por los receptores A_1-A_{2A} ya que constituye un paradigma en el campo de los oligómeros. Tal y como ha sido comentado anteriormente, el receptor A_1 de adenosina se acopla a la proteína G_i mientras que el receptor A_{2A} a la proteína G_s, de modo que transducen señales opuestas en las cascadas de señalización intracelulares dependientes de AMPc. Inicialmente este heterómero había sido descrito como un mecanismo de control de la liberación de glutamato dependiente de la concentración de adenosina en neuronas glutamaérgicas de estriado. La adenosina tiene mayor afinidad por el receptor A_1R que por el $A_{2A}R$, de modo que bajas concentraciones de adenosina (rango de 70 nM) se unen predominantemente al receptor A_1R, induciendo una señalización mediada por la proteína G_i, mientras que concentraciones más elevadas (150 nM) de adenosina permitirán que este nucleósido se una también al receptor $A_{2A}R$, promoviendo la señalización vía G_s y bloqueando la señalización vía A_1R (*Ciruela, et al., 2006*). Este mecanismo sensor de la concentración de adenosina es de gran importancia fisiológica ya que permite a este nucleósido modular de un modo muy preciso la liberación de neurotransmisores des de los terminales pre-sinápticos. No obstante, el mecanismo mediante el que el heterómero A_1R-$A_{2A}R$ integra la señalización dependiente de G_i y de G_s aún no ha sido entendido. En un principio, al no ser posible el acoplamiento de dos proteínas G en un heterodímero debido a enfrentamientos estéricos (*Cordomí, et al., 2015*), se creía que este fenómeno funcionaba mediante un mecanismo de cambio de acoplamiento de proteína G_s/G_i por el cual bajas o altas concentraciones de adenosina inhibían o estimulaban, respectivamente, la liberación de glutamato (*Ciruela, et al., 2006; Orru, et al., 2011*). También había sido descrito el fenómeno controlado por los receptores A_1 y A_{2A}, donde la proteína quinasa A (PKA) ejercía un papel regulador dependiente de AMPc sobre la liberación de serotonina en neuronas hipocampales (*Okada, et al., 2001*). Otro ejemplo es el mecanismo de control observado en el transporte de GABA en astrocitos, el cual era atribuido a la expresión de heterómeros de receptores A_1-A_{2A} (*Cristóvão-Ferrerira, et al., 2013*). No obstante, este fenómeno de cambio de proteína G dependiente de la concentración de adenosina no había sido explicado aún hasta la fecha, de modo que resultaba necesario investigar las bases estructurales de este heterómero para poder explicar su propia funcionalidad.

Así pues, en el trabajo ***Quaternary structure of a G-protein-coupled receptor heterotetramer in complex with G_i and G_s*** (*Navarro, et al., 2016*) han sido revelados nuevos datos que contribuirán al mejor entendimiento del fenómeno de la oligomerización. En este estudio se recurrió a la técnica de *single-particle tracking*, una de las pocas técnicas actuales capaces de detectar la estequiometria de complejos oligoméricos, para describir la estructura de GPCR que constituía el heterómero de receptores A_1-A_{2A}. En primer lugar, mediante el análisis de las dinámicas de los receptores de adenosina fusionados a proteínas fluorescentes, ha sido observado que la presencia del receptor A_{2A} afecta a la dinámica característica del receptor A_1 restringiendo los desplazamientos observados en el receptor A_1 cuando el receptor es expresado junto al receptor A_{2A}. Datos muy parecidos han sido obtenidos al analizar las dinámicas del receptor A_{2A} en presencia o ausencia del receptor A_1. Estos resultados, demuestran la existencia de heterómeros A_1-A_{2A}. Además, mediante el análisis de la intensidad de fluorescencia emitida, ha sido demostrado que la estequiometria predominante es 2:2, es decir, un homodímero de A_1R y un homodímero de $A_{2A}R$, formando una unidad tetramérica. Siendo estos los primeros datos de estequiometria obtenidos en células vivas. Estudios recientes sugieren que la unidad funcional más común es la formada por un homodímero de GPCR y una proteína G (*Ferré, et al., 2014*). Así se nos planteaba una incógnita por resolver, ¿qué proteína G se acoplaría al complejo A_1-A_{2A}? En este trabajo mediante el uso de las toxinas colérica (CTX) y pertusis (PTX), que bloquean de manera específica las proteínas Gs y Gi respectivamente, ha sido resuelta esta cuestión al determinar que el heterotetramero A_1-A_{2A} está constituido por dos proteínas G distintas, una Gs y una Gi, funcionando como una única unidad funcional. En último lugar, han sido definidos los dominios

TM involucrados en la interfase de receptores A_1-A_{2A}, siendo los TM4/5 los responsables de la homodimerización y los TM5/6 los responsables de la heteromerización conformando una estructura romboidal del heterómero. La orientación molecular del complejo queda resuelta de tal modo que le confiere la suficiente habilidad a uno de los subcomplejos, protómero-proteína G, para influenciar la señalización del otro subcomplejo. Esta disposición de los elementos del complejo sugiere que los efectos alostéricos que ocurren tanto entre hetero-receptores como entre las proteínas G_i y G_s son debidos a cambios conformacionales transmitidos a lo largo de las regiones que interactúan en el complejo. En este trabajo ha sido descrito por primera vez un complejo formado por un homodímero de receptores A_1, un homodímero de receptores A_{2A} y dos proteínas G: G_s y G_i que funciona como unidad estructural única con características propias. La capacidad de este macrocomplejo de inducir diferentes señalizaciones en función de la situación a la que se encuentra expuesta la célula implica la existencia de una comunicación a nivel de receptores, pero también a nivel de proteínas G. Estos resultados abren la puerta a una nueva dimensión en la heteromerización de receptores y establecen las bases para analizar otros complejos multiméricos en el futuro. Recientemente, una estructura tetramérica parecida ha sido propuesta para el complejo formado por los receptores A_{2A}-D_2 (*Bonaventura, et al., 2015*).

Una vez definida la estructura del heterómero A_1R-$A_{2A}R$, nos planteamos estudiar la funcionalidad característica de este nuevo complejo. Con este fin realizamos el trabajo titulado: ***Cross-communication between G_i and G_s in a G-protein-coupled receptor heterotetramer guided by a receptor C-terminal domain*** (*Navarro, et al., 2016*; manuscrito enviado a *Nature communications*). Los datos obtenidos indican que en el complejo tetramérico ambos receptores de adenosina, A_1 y A_{2A}, pueden ser activados individualmente. Sin embargo, la señalización mediada por la activación del receptor A_1 acoplado a proteína G_i está modulada por la proteína G_s, puesto que cuando ambos receptores del heterómero son activados solo tiene lugar la señalización mediada por el receptor $A_{2A}R$, mientras el receptor A_1R permanece bloqueado. Este resultado refuerza la idea cada vez más aceptada que la comunicación entre las proteínas G es una importante propiedad funcional de los heterómeros de GPCR, posibilitando a un mismo complejo señalizar por vías completamente opuestas en función de cada situación. Seguidamente, nos cuestionamos el mecanismo mediante el cual la activación del receptor A_{2A} bloqueaba al receptor A_1. Mediante el uso de los mutantes $A_{2A}{}^{\Delta 40}R$ y $A_{2A}{}^{\Delta CT}R$ del receptor A_{2A}, donde los últimos 40 aminoácidos o la cola entera del receptor han sido deleccionados, ha sido demostrado que es el dominio C-terminal del receptor A_{2A} el responsable de dicho bloqueo. La hipótesis planteada en este trabajo propone que la activación del receptor A_{2A} induce la apertura del dominio α_sAH, provocando un movimiento característico de la cola C-terminal y el consecuente bloqueo de la apertura del dominio α_iAH del receptor A_1. Esto explicaría el mecanismo por el que el heterómero A_1R-$A_{2A}R$ actúa como un sensor de concentración de adenosina que puede inducir incluso respuestas opuestas en función de la concentración extracelular de adenosina.

Los datos obtenidos en este estudio revelan la importancia de la comunicación que se establece entre las dos proteínas G en el complejo tetramérico A_1-A_{2A}, regulando la señalización del heterómero en función de los niveles extracelulares de adenosina. Ha sido observado que la interrelación entre G_i y G_s reside en las restricciones estructurales que rodean el mecanismo de intercambio de nucleótidos GDP/GTP, el cual implica la apertura del dominio αAH de la subunidad α de cualquier proteína G. La interrelación en el complejo heterotramérico A_1R-A_1R-$A_{2A}R$-$A_{2A}R$-G_s-G_i es una propiedad asociada a una estructura cuaternaria específica, la anteriormente citada estructura romboidal, en la que los dominios α_iAH y α_sAH quedan muy próximos provocando que solo uno de los dos dominios αAH pueda abrirse. Alteraciones de esta estructura cuaternaria del heterómero A_1-A_{2A} mediante la inserción de péptidos sintéticos entre los receptores A_1R y $A_{2A}R$ bloquean la interrelación existente sin romper el complejo heteromérico,

incrementando la distancia entre las proteínas G_i y G_s y permitiendo la consecuente apertura simultánea de los dominios α_iAH y α_sAH, posibilitando así la activación simultánea de ambos receptores A_1 y A_{2A}. En este trabajo ha sido también observado que el heterómero romboidal A_1-A_{2A} solo es capaz de reclutar una proteína β-arrestina con una estequiometría 2:2:1 (A_1R:A_{2A}R:β-arrestina), mientras que la alteración del heterómero mediante el uso de péptidos sintéticos posibilita la unión simultánea de dos moléculas de β-arrestina, una reclutada por el receptor A_1R y la otra por el receptor A_{2A}R.

Del mismo modo que sucede con la pintura, donde un solo trazo en un lienzo en blanco suele estar falto de mensaje, en la ciencia, un solo resultado examinado fuera de contexto de forma aislada tampoco suele ser suficientemente informativo. A la vez, este lienzo en blanco requiere de la combinación de distintos colores para convertirse en una obra de arte, así como la ciencia requiere de la combinación de distintas técnicas experimentales mediante las cuales elucidar un enigma. Y no es hasta que el cuadro, o los resultados obtenidos científicamente, son analizados desde cierta distancia, con suficiente perspectiva como para ver todos los trazos y los distintos colores combinados de un solo vistazo, que somos capaces de entender el mensaje final de la obra. Es así como, tras una infinidad de trazos y la combinación de múltiples colores, ha quedado constatado, en este trabajo, la gran importancia de las interacciones que tienen lugar entre los GPCR, tanto entre ellos, como con otros receptores no acoplados a proteína G o proteínas sensoras de calcio, siendo todas estas interacciones capaces de modificar el comportamiento de dichos receptores GPCR, o hacerlos sensibles a ligandos o cambios celulares que por sí solos no podrían percibir. Estas interacciones y su capacidad moduladora sobre la funcionalidad de los GPCR implicados es de gran interés pues conforman nuevas dianas terapéuticas para el diseño de fármacos frente a enfermedades que hasta la fecha siguen sin poder ser tratadas con efectividad.

CONCLUSIONES

1. Ha sido demostrado, mediante técnicas de transferencia de energía y microscopía confocal, que el receptor sigma-1 heteromeriza con el receptor D_2 de dopamina formando complejos oligoméricos en células vivas. Ha sido demostrado que la unión de la cocaína a sigma-1 modula negativamente la señalización del receptor D_2 vía proteína G_i, inhibiendo la disminución de los niveles de AMPc, y la señalización independiente de proteína G, disminuyendo la fosforilación de ERK 1/2 tanto en células transfectadas como en tejido estriatal. Con estos resultados ha sido descrito un nuevo modelo de acción en el que la cocaína, al interaccionar con sigma-1, disminuye la señalización mediada por los receptores D_2 a la vez que potencia la señalización mediada por los receptores D_1 de dopamina alterando el equilibrio entre estas dos vías de señalización, favoreciendo la activación de la vía de la recompensa y la generación de un vínculo de adicción a la cocaína.

2. Mediante técnicas de transferencia de energía y microscopía confocal ha sido demostrado que el receptor sigma-2 puede formar heterómeros con el receptor D_1, pero no con el D_2 de dopamina, tanto en células transfectadas como en neuronas estriatales. La cocaína, mediante su unión a sigma-2, induce una modulación negativa a nivel de AMPc y una potenciación a nivel de MAPK sobre la activación del receptor D_1 en células transfectadas y en neuronas estriatales. En secciones de estriado de ratas administradas con cocaína ha sido observado que a nivel de expresión y funcionalidad el heterómero D_1-sigma-1 prevalece en condiciones agudas mientras el heterómero D_1-sigma-2 predomina en condiciones crónicas. El receptor sigma-2 ejerce un papel modulador sobre el receptor D_1 contrario al descrito para el receptor sigma-1, siendo responsable de los efectos crónicos de la adicción a cocaína.

3. Ha sido demostrada, por primera vez, la existencia funcional de heterómeros entre los receptores CRF_1R y OX_1R en células transfectadas y en la VTA de rata, mediante técnicas de transferencia de energía y microscopía confocal. En el complejo heteromérico CRF_1R-OX_1R ha sido observado un fenómeno de *cross-talk* negativo y *cross*-antagonismo, de modo que los ligandos de un receptor inhiben la capacidad del otro para señalizar, evitando así la liberación de dopamina en la VTA frente a una situación de estrés. Además, ha sido observado que la unión de la cocaína al receptor sigma-1 es capaz de romper el *cross-talk* negativo y *cross*-antagonismo del heterómero CRF_1R-OX_1R mediante la inducción de cambios estructurales, explicando por primera vez el mecanismo molecular que relaciona el estrés con la recaída y aumento en el consumo de cocaína.

4. Ha sido puesto de manifiesto el papel modulador del receptor GHS-R1b en el tráfico y señalización del receptor GHS-R1a, con una eficiencia que depende de la ratio específica existente entre la expresión de las dos isoformas, GHS-R1b/GHS-R1a. Ha sido determinado cómo a ratios bajas de expresión del receptor GHS-R1b respecto el receptor GHS-R1a se potencia el tráfico y la señalización mediada por GHS-R1a mientras que, a ratios altas, el receptor GHS-R1b ejerce un efecto alostérico negativo sobre la señalización de la isoforma GHS-R1a. Además, ha sido demostrado que la isoforma GHS-R1b determina la capacidad del receptor GHS-R1a para formar heterómeros con otros receptores, como el D_1 de dopamina, lo que supone en este caso concreto un cambio en el acoplamiento a proteína G y por lo tanto una señalización mediada por la grelina radicalmente distinta.

5. Mediante técnicas de transferencia de energía y microscopía confocal ha sido demostrado que el receptor sigma-1 puede formar heterómeros con el receptor GHS-R1a en células transfectadas y en neuronas estriatales de rata. La unión de la cocaína al receptor sigma-1 bloquea la capacidad del receptor GHS-R1a para señalizar, impidiendo la disminución de los niveles de AMPc, la fosforilación de ERK 1/2, y la señalización por calcio inducida por la grelina tanto en células transfectadas como en neuronas estriatales. Además, han sido

determinadas por primera vez las regiones implicadas en la interacción entre el receptor sigma-1 y un GPCR, siendo los dominios TM 1 y TM2 de los receptores GHS-R1a o GHS-R1b los involucrados en la formación de la interfase con el complejo trimérico del receptor sigma-1.

6. Ha sido demostrado que las proteínas sensoras de calcio NCS-1 y calneurona, pero no la caldendrina, pueden interaccionar con el heterómero de receptores A_{2A} de adenosina – D_2 de dopamina de manera dependiente de los niveles de calcio intracelular, uniéndose NCS-1 en una situación de bajos niveles de calcio intracelular, y calneurona-1 cuando son altos. La unión de estas proteínas sensoras de calcio puede promover o bloquear distintas modulaciones alostéricas en un complejo heteromérico de GPCRs; en el heterómero A_{2A}-D_2, una situación de bajos niveles de calcio intracelular conduce a la señalización única a través de la vía de las MAPK, mientras que, en una situación de altos niveles de calcio, la coactivación de ambos receptores da lugar a una disminución de la señalización mediada por el heterómero. Ha sido puesto de manifiesto el mecanismo mediante el cual una sola población de receptores A_{2A} formando heterómeros con el receptor D_2 puede dar respuestas funcionales muy distintas en base a los niveles intracelulares de calcio.

7. Ha sido propuesto un nuevo modelo estructural tetramérico formado por un homodímero de receptores A_1 de adenosina y un homodímero de receptores A_{2A} de adenosina. En este complejo son las regiones transmembrana TM4/5 las responsables de la homodimerización y las regiones TM5/6 las responsables de la heteromerización, formando una estructura romboidal a la que se acoplan dos proteínas G, G_i y G_s. Esta nueva unidad funcional adquiere características propias permitiendo a la célula inducir diferentes señalizaciones en función de la situación a la que se encuentra expuesta, sugiriendo la existencia de una comunicación a nivel de receptores, pero también a nivel de proteínas G. Este modelo puede servir de referencia para explicar cómo se establecen las interacciones en un heterómero de GPCR y cómo se ensamblan los diferentes elementos que lo conforman.

8. Ha sido demostrada la importancia de la comunicación entre las proteínas G en un heterómero de GPCR. En el heterómero de receptores A_1-A_{2A}, la señalización mediada por la proteína G_i del receptor A_1R se encuentra modulada por la proteína G_s del receptor $A_{2A}R$ cuando este está activado. El bloqueo observado en la proteína G_i es debido al movimiento que sufre el dominio C-terminal del receptor $A_{2A}R$ al ser activado por ligando, imposibilitando la apertura del dominio α_iAH del receptor A_1 y su consecuente activación. Ha sido explicando, por primera vez, el mecanismo por el que el heterómero A_1R-$A_{2A}R$ actúa como sensor de la concentración de adenosina pudiendo dar respuestas opuestas, vía proteína G_i o G_s, en función de la concentración extracelular de adenosina.

BIBLIOGRAFÍA

Abbracchio, M.P., Brambilla, R., Ceruti, S., Kim, H.O., von Lubitz, D.K., Jacobson, K.A., and Cattabeni, F. (1995). G protein-dependent activation of phospholipase C by adenosine A3 receptors in rat brain. Mol. Pharmacol. *48*, 1038–1045.

AbdAlla, S., Lother, H., and Quitterer, U. (2000). AT1-receptor heterodimers show enhanced G-protein activation and altered receptor sequestration. Nature *407*, 94–98.

Abizaid, A., and Horvath, T.L. (2008). Brain circuits regulating energy homeostasis. Regul. Pept. *149*, 3–10.

Abizaid, A., Liu, Z.-W., Andrews, Z.B., Shanabrough, M., Borok, E., Elsworth, J.D., Roth, R.H., Sleeman, M.W., Picciotto, M.R., Tschöp, M.H., et al. (2006). Ghrelin modulates the activity and synaptic input organization of midbrain dopamine neurons while promoting appetite. J. Clin. Invest. *116*, 3229–3239.

Adamantidis, A.R., Tsai, H.-C., Boutrel, B., Zhang, F., Stuber, G.D., Budygin, E.A., Touriño, C., Bonci, A., Deisseroth, K., and de Lecea, L. (2011). Optogenetic interrogation of dopaminergic modulation of the multiple phases of reward-seeking behavior. J. Neurosci. *31*, 10829–10835.

Adell, A., and Artigas, F. (2004). The somatodendritic release of dopamine in the ventral tegmental area and its regulation by afferent transmitter systems. Neurosci Biobehav Rev *28*, 415–431.

Agnati, L.F., Ferré, S., Lluis, C., Franco, R., and Fuxe, K. (2003). Molecular mechanisms and therapeutical implications of intramembrane receptor/receptor interactions among heptahelical receptors with examples from the striatopallidal GABA neurons. Pharmacol. Rev. *55*, 509–550.

Ahmed, I.S., Rohe, H.J., Twist, K.E., and Craven, R.J. (2010). Pgrmc1 (progesterone receptor membrane component 1) associates with epidermal growth factor receptor and regulates erlotinib sensitivity. J. Biol. Chem. *285*, 24775–24782.

Ahmed, I.S.A., Chamberlain, C., and Craven, R.J. (2012). S2R(Pgrmc1): the cytochrome-related sigma-2 receptor that regulates lipid and drug metabolism and hormone signaling. Expert Opin Drug Metab Toxicol *8*, 361–370.

Ainscough, J.S., Gerberick, G.F., Kimber, I., and Dearman, R.J. (2015). Interleukin-1β Processing Is Dependent on a Calcium-mediated Interaction with Calmodulin. J. Biol. Chem. *290*, 31151–31161.

Alexander, G.E., and Crutcher, M.D. (1990). Functional architecture of basal ganglia circuits: neural substrates of parallel processing. Trends Neurosci. *13*, 266–271.

Alonso, G., Phan, V., Guillemain, I., Saunier, M., Legrand, A., Anoal, M., and Maurice, T. (2000). Immunocytochemical localization of the sigma(1) receptor in the adult rat central nervous system. Neuroscience *97*, 155–170.

Al-Saif, A., Al-Mohanna, F., and Bohlega, S. (2011). A mutation in sigma-1 receptor causes juvenile amyotrophic lateral sclerosis. Ann. Neurol. *70*, 913–919.

Angers, S., Salahpour, A., Joly, E., Hilairet, S., Chelsky, D., Dennis, M., and Bouvier, M. (2000). Detection of beta 2-adrenergic receptor dimerization in living cells using bioluminescence resonance energy transfer (BRET). Proc. Natl. Acad. Sci. U.S.A. *97*, 3684–3689.

Angulo, E., Casadó, V., Mallol, J., Canela, E.I., Viñals, F., Ferrer, I., Lluis, C., and Franco, R. (2003). A1 adenosine receptors accumulate in neurodegenerative structures in Alzheimer disease and mediate both amyloid precursor protein processing and tau phosphorylation and translocation. Brain Pathol. *13*, 440–451.

Areal, L.B., Rodrigues, L.C.M., Andrich, F., Moraes, L.S., Cicilini, M.A., Mendonça, J.B., Pelição, F.S., Nakamura-Palacios, E.M., Martins-Silva, C., and Pires, R.G.W. (2015). Behavioural, biochemical and molecular changes induced by chronic crack-cocaine inhalation in mice: The role of dopaminergic and endocannabinoid systems in the prefrontal cortex. Behav. Brain Res. *290*, 8–16.

Arenas, E., Denham, M., and Villaescusa, J.C. (2015). How to make a midbrain dopaminergic neuron. Development *142*, 1918–1936.

Bai, M., Trivedi, S., and Brown, E.M. (1998). Dimerization of the extracellular calcium-sensing receptor (CaR) on the cell surface of CaR-transfected HEK293 cells. J. Biol. Chem. *273*, 23605–23610.

Bale, T.L., and Vale, W.W. (2004). CRF and CRF receptors: role in stress responsivity and other behaviors. Annu. Rev. Pharmacol. Toxicol. *44*, 525–557.

Baltoumas, F.A., Theodoropoulou, M.C., and Hamodrakas, S.J. (2016). Molecular dynamics simulations and structure-based network analysis reveal structural and functional aspects of G-protein coupled receptor dimer interactions. J. Comput. Aided Mol. Des. *30*, 489–512.

Banères, J.-L., and Parello, J. (2003). Structure-based analysis of GPCR function: evidence for a novel pentameric assembly between the dimeric leukotriene B4 receptor BLT1 and the G-protein. J. Mol. Biol. *329*, 815–829.

Bardo, M.T. (1998). Neuropharmacological mechanisms of drug reward: beyond dopamine in the nucleus accumbens. Crit Rev Neurobiol *12*, 37–67.

Bariselli, S., Glangetas, C., Tzanoulinou, S., and Bellone, C. (2016). Ventral tegmental area subcircuits process rewarding and aversive experiences. J. Neurochem.

Barr, J.L., Deliu, E., Brailoiu, G.C., Zhao, P., Yan, G., Abood, M.E., Unterwald, E.M., and Brailoiu, E. (2015). Mechanisms of activation of nucleus accumbens neurons by cocaine via sigma-1 receptor-inositol 1,4,5-trisphosphate-transient receptor potential canonical channel pathways. Cell Calcium *58*, 196–207.

Basu, S., Barawkar, D.A., Thorat, S., Shejul, Y.D., Patel, M., Naykodi, M., Jain, V., Salve, Y., Prasad, V., Chaudhary, S., et al. (2017). Design, Synthesis of Novel, Potent, Selective, Orally Bio-available Adenosine A2A Receptor Antagonists and Their Biological Evaluation. J. Med. Chem.

Bayburt, T.H., Leitz, A.J., Xie, G., Oprian, D.D., and Sligar, S.G. (2007). Transducin activation by nanoscale lipid bilayers containing one and two rhodopsins. J. Biol. Chem. *282*, 14875–14881.

Bayburt, T.H., Vishnivetskiy, S.A., McLean, M.A., Morizumi, T., Huang, C.-C., Tesmer, J.J.G., Ernst, O.P., Sligar, S.G., and Gurevich, V.V. (2011). Monomeric rhodopsin is sufficient for normal rhodopsin kinase (GRK1) phosphorylation and arrestin-1 binding. J. Biol. Chem. *286*, 1420–1428.

Beaulieu, J.-M., and Gainetdinov, R.R. (2011). The Physiology, Signaling, and Pharmacology of Dopamine Receptors. Pharmacol Rev *63*, 182–217.

Belin, D., and Everitt, B.J. (2008). Cocaine seeking habits depend upon dopamine-dependent serial connectivity linking the ventral with the dorsal striatum. Neuron *57*, 432–441.

Benkirane, M., Jin, D.Y., Chun, R.F., Koup, R.A., and Jeang, K.T. (1997). Mechanism of transdominant inhibition of CCR5-mediated HIV-1 infection by ccr5delta32. J. Biol. Chem. *272*, 30603–30606.

Bennett, K.A., Langmead, C.J., Wise, A., and Milligan, G. (2009). Growth hormone secretagogues and growth hormone releasing peptides act as orthosteric super-agonists but not allosteric regulators for activation of the G protein Galpha(o1) by the Ghrelin receptor. Mol. Pharmacol. *76*, 802–811.

Berardi, F., Abate, C., Ferorelli, S., Uricchio, V., Colabufo, N.A., Niso, M., and Perrone, R. (2009). Exploring the importance of piperazine N-atoms for sigma(2) receptor affinity and activity in a series of analogs of 1-cyclohexyl-4-[3-(5-methoxy-1,2,3,4-tetrahydronaphthalen-1-yl)propyl]piperazine (PB28). J. Med. Chem. *52*, 7817–7828.

Berchtold, M.W., and Villalobo, A. (2014). The many faces of calmodulin in cell proliferation, programmed cell death, autophagy, and cancer. Biochim. Biophys. Acta *1843*, 398–435.

Bernardis, L.L., and Bellinger, L.L. (1996). The lateral hypothalamic area revisited: ingestive behavior. Neurosci Biobehav Rev *20*, 189–287.

Berne, R.M., Knabb, R.M., Ely, S.W., and Rubio, R. (1983). Adenosine in the local regulation of blood flow: a brief overview. Fed. Proc. *42*, 3136–3142.

Bernstein, H.-G., Seidenbecher, C.I., Smalla, K.-H., Gundelfinger, E.D., Bogerts, B., and Kreutz, M.R. (2003). Distribution and cellular localization of caldendrin immunoreactivity in adult human forebrain. J. Histochem. Cytochem. *51*, 1109–1112.

Berridge, M.J. (1998). Neuronal calcium signaling. Neuron *21*, 13–26.

Berthouze, M., Rivail, L., Lucas, A., Ayoub, M.A., Russo, O., Sicsic, S., Fischmeister, R., Berque-Bestel, I., Jockers, R., and Lezoualc'h, F. (2007). Two transmembrane Cys residues are involved in 5-HT4 receptor dimerization. Biochem. Biophys. Res. Commun. *356*, 642–647.

Bertolino, A., Fazio, L., Di Giorgio, A., Blasi, G., Romano, R., Taurisano, P., Caforio, G., Sinibaldi, L., Ursini, G., Popolizio, T., et al. (2009). Genetically determined interaction between the dopamine transporter and the D2 receptor on prefronto-striatal activity and volume in humans. J. Neurosci. *29*, 1224–1234.

Beuming, T., Kniazeff, J., Bergmann, M.L., Shi, L., Gracia, L., Raniszewska, K., Newman, A.H., Javitch, J.A., Weinstein, H., Gether, U., et al. (2008). The binding sites for cocaine and dopamine in the dopamine transporter overlap. Nat. Neurosci. *11*, 780–789.

Blacktop, J.M., Seubert, C., Baker, D.A., Ferda, N., Lee, G., Graf, E.N., and Mantsch, J.R. (2011). Augmented cocaine seeking in response to stress or CRF delivered into the ventral tegmental area following long-access self-administration is mediated by CRF receptor type 1 but not CRF receptor type 2. J. Neurosci. *31*, 11396–11403.

Blaess, S., and Ang, S.-L. (2015). Genetic control of midbrain dopaminergic neuron development. Wiley Interdiscip Rev Dev Biol *4*, 113–134.

Blasiole, B., Kabbani, N., Boehmler, W., Thisse, B., Thisse, C., Canfield, V., and Levenson, R. (2005). Neuronal calcium sensor-1 gene ncs-1a is essential for semicircular canal formation in zebrafish inner ear. J. Neurobiol. *64*, 285–297.

Bofill-Cardona, E., Kudlacek, O., Yang, Q., Ahorn, H., Freissmuth, M., and Nanoff, C. (2000). Binding of calmodulin to the D2-dopamine receptor reduces receptor signaling by arresting the G protein activation switch. J. Biol. Chem. *275*, 32672–32680.

Böhm, S.K., Grady, E.F., and Bunnett, N.W. (1997). Regulatory mechanisms that modulate signalling by G-protein-coupled receptors. Biochem. J. *322 (Pt 1)*, 1–18.

Bonaventura, J., Navarro, G., Casadó-Anguera, V., Azdad, K., Rea, W., Moreno, E., Brugarolas, M., Mallol, J., Canela, E.I., Lluís, C., et al. (2015). Allosteric interactions between agonists and antagonists within the adenosine A2A receptor-dopamine D2 receptor heterotetramer. Proc. Natl. Acad. Sci. U.S.A. *112*, E3609-3618.

Borea, P.A., Varani, K., Vincenzi, F., Baraldi, P.G., Tabrizi, M.A., Merighi, S., and Gessi, S. (2015). The A3 adenosine receptor: history and perspectives. Pharmacol. Rev. *67*, 74–102.

Borgland, S.L., Ungless, M.A., and Bonci, A. (2010). Convergent actions of orexin/hypocretin and CRF on dopamine neurons: Emerging players in addiction. Brain Res. *1314*, 139–144.

Borroto-Escuela, D.O., Wydra, K., Pintsuk, J., Narvaez, M., Corrales, F., Zaniewska, M., Agnati, L.F., Franco, R., Tanganelli, S., Ferraro, L., et al. (2016). Understanding the Functional Plasticity in Neural Networks of the Basal Ganglia in Cocaine Use Disorder: A Role for Allosteric Receptor-Receptor Interactions in A2A-D2 Heteroreceptor Complexes. Neural Plast. *2016*, 4827268.

Boulay, F., and Rabiet, M.-J. (2005). The chemoattractant receptors FPR and C5aR: same functions--different fates. Traffic *6*, 83–86.

Bourne, H.R., Sanders, D.A., and McCormick, F. (1991). The GTPase superfamily: conserved structure and molecular mechanism. Nature *349*, 117–127.

Bourne, Y., Dannenberg, J., Pollmann, V., Marchot, P., and Pongs, O. (2001). Immunocytochemical localization and crystal structure of human frequenin (neuronal calcium sensor 1). J. Biol. Chem. *276*, 11949–11955.

Boutrel, B., Kenny, P.J., Specio, S.E., Martin-Fardon, R., Markou, A., Koob, G.F., and de Lecea, L. (2005). Role for hypocretin in mediating stress-induced reinstatement of cocaine-seeking behavior. Proc. Natl. Acad. Sci. U.S.A. *102*, 19168–19173.

Bouvier, M. (2001). Oligomerization of G-protein-coupled transmitter receptors. Nat. Rev. Neurosci. *2*, 274–286.

Bouvier, M., and Hébert, T.E. (2014). CrossTalk proposal: Weighing the evidence for Class A GPCR dimers, the evidence favours dimers. J. Physiol. (Lond.) *592*, 2439–2441.

Bradberry, C.W. (2000). Acute and chronic dopamine dynamics in a nonhuman primate model of recreational cocaine use. J. Neurosci. *20*, 7109–7115.

Braunewell, K.-H. (2005). The darker side of Ca2+ signaling by neuronal Ca2+-sensor proteins: from Alzheimer's disease to cancer. Trends Pharmacol. Sci. *26*, 345–351.

Bridges, T.M., and Lindsley, C.W. (2008). G-protein-coupled receptors: from classical modes of modulation to allosteric mechanisms. ACS Chem. Biol. *3*, 530–541.

Brooks, D.J., Doder, M., Osman, S., Luthra, S.K., Hirani, E., Hume, S., Kase, H., Kilborn, J., Martindill, S., and Mori, A. (2008). Positron emission tomography analysis of [11C]KW-6002 binding to human and rat adenosine A2A receptors in the brain. Synapse *62*, 671–681.

Buchanan, J.D., Corbett, R.J., and Roche, R.S. (1986). The thermodynamics of calcium binding to thermolysin. Biophys. Chem. *23*, 183–199.

Bulenger, S., Marullo, S., and Bouvier, M. (2005). Emerging role of homo- and heterodimerization in G-protein-coupled receptor biosynthesis and maturation. Trends Pharmacol. Sci. *26*, 131–137.

Bunzow, J.R., Van Tol, H.H., Grandy, D.K., Albert, P., Salon, J., Christie, M., Machida, C.A., Neve, K.A., and Civelli, O. (1988). Cloning and expression of a rat D2 dopamine receptor cDNA. Nature *336*, 783–787.

Burgoyne, R.D. (2007). Neuronal calcium sensor proteins: generating diversity in neuronal Ca2+ signalling. Nat. Rev. Neurosci. *8*, 182–193.

Burgoyne, R.D., O'Callaghan, D.W., Hasdemir, B., Haynes, L.P., and Tepikin, A.V. (2004). Neuronal Ca2+-sensor proteins: multitalented regulators of neuronal function. Trends Neurosci. *27*, 203–209.

Bush, G., Vogt, B.A., Holmes, J., Dale, A.M., Greve, D., Jenike, M.A., and Rosen, B.R. (2002). Dorsal anterior cingulate cortex: a role in reward-based decision making. Proc. Natl. Acad. Sci. U.S.A. *99*, 523–528.

Cabral, A., López Soto, E.J., Epelbaum, J., and Perelló, M. (2017). Is Ghrelin Synthesized in the Central Nervous System? Int J Mol Sci *18*.

Cahill, M.A. (2007). Progesterone receptor membrane component 1: an integrative review. J. Steroid Biochem. Mol. Biol. *105*, 16–36.

Callén, L., Moreno, E., Barroso-Chinea, P., Moreno-Delgado, D., Cortés, A., Mallol, J., Casadó, V., Lanciego, J.L., Franco, R., Lluis, C., et al. (2012). Cannabinoid receptors CB1 and CB2 form functional heteromers in brain. J. Biol. Chem. *287*, 20851–20865.

Canals, M., Burgueño, J., Marcellino, D., Cabello, N., Canela, E.I., Mallol, J., Agnati, L., Ferré, S., Bouvier, M., Fuxe, K., et al. (2004). Homodimerization of adenosine A2A receptors: qualitative and quantitative assessment by fluorescence and bioluminescence energy transfer. J. Neurochem. *88*, 726–734.

Canals, M., Angulo, E., Casadó, V., Canela, E.I., Mallol, J., Viñals, F., Staines, W., Tinner, B., Hillion, J., Agnati, L., et al. (2005). Molecular mechanisms involved in the adenosine A and A receptor-induced neuronal differentiation in neuroblastoma cells and striatal primary cultures. J. Neurochem. *92*, 337–348.

Carafoli, E. (2002). Calcium signaling: a tale for all seasons. Proc. Natl. Acad. Sci. U.S.A. *99*, 1115–1122.

Carriba, P., Ortiz, O., Patkar, K., Justinova, Z., Stroik, J., Themann, A., Müller, C., Woods, A.S., Hope, B.T., Ciruela, F., et al. (2007). Striatal adenosine A2A and cannabinoid CB1 receptors form functional heteromeric complexes that mediate the motor effects of cannabinoids. Neuropsychopharmacology *32*, 2249–2259.

Carriba, P., Navarro, G., Ciruela, F., Ferré, S., Casadó, V., Agnati, L., Cortés, A., Mallol, J., Fuxe, K., Canela, E.I., et al. (2008). Detection of heteromerization of more than two proteins by sequential BRET-FRET. Nat. Methods *5*, 727–733.

Casadó-Anguera, V., Bonaventura, J., Moreno, E., Navarro, G., Cortés, A., Ferré, S., and Casadó, V. (2016). Evidence for the heterotetrameric structure of the adenosine A2A-dopamine D2 receptor complex. Biochem. Soc. Trans. *44*, 595–600.

Cason, A.M., Smith, R.J., Tahsili-Fahadan, P., Moorman, D.E., Sartor, G.C., and Aston-Jones, G. (2010). Role of orexin/hypocretin in reward-seeking and addiction: implications for obesity. Physiol. Behav. *100*, 419–428.

Catterall, W.A., and Few, A.P. (2008). Calcium channel regulation and presynaptic plasticity. Neuron *59*, 882–901.

Centonze, D., Grande, C., Saulle, E., Martin, A.B., Gubellini, P., Pavón, N., Pisani, A., Bernardi, G., Moratalla, R., and Calabresi, P. (2003). Distinct roles of D1 and D5 dopamine receptors in motor activity and striatal synaptic plasticity. J. Neurosci. *23*, 8506–8512.

Chen, X., Zheng, X., Ding, K., Zhou, Z., Zhan, C.-G., and Zheng, F. (2017). A quantitative LC-MS/MS method for simultaneous determination of cocaine and its metabolites in whole blood. J Pharm Biomed Anal *134*, 243–251.

Cherezov, V., Rosenbaum, D.M., Hanson, M.A., Rasmussen, S.G.F., Thian, F.S., Kobilka, T.S., Choi, H.-J., Kuhn, P., Weis, W.I., Kobilka, B.K., et al. (2007). High-resolution crystal structure of an engineered human beta2-adrenergic G protein-coupled receptor. Science *318*, 1258–1265.

Chiu, F.-L., Lin, J.-T., Chuang, C.-Y., Chien, T., Chen, C.-M., Chen, K.-H., Hsiao, H.-Y., Lin, Y.-S., Chern, Y., and Kuo, H.-C. (2015). Elucidating the role of the A2A adenosine receptor in neurodegeneration using neurons derived from Huntington's disease iPSCs. Hum. Mol. Genet. *24*, 6066–6079.

Chow, K.B.S., Sun, J., Chu, K.M., Tai Cheung, W., Cheng, C.H.K., and Wise, H. (2012). The truncated ghrelin receptor polypeptide (GHS-R1b) is localized in the endoplasmic reticulum where it forms heterodimers with ghrelin receptors (GHS-R1a) to attenuate their cell surface expression. Mol. Cell. Endocrinol. *348*, 247–254.

Christian, D.T., Wang, X., Chen, E.L., Sehgal, L.K., Ghassemlou, M.N., Miao, J.J., Estepanian, D., Araghi, C.H., Stutzmann, G.E., and Wolf, M.E. (2016). Dynamic Alterations of Rat Nucleus Accumbens Dendritic Spines over 2 Months of Abstinence from Extended-Access Cocaine Self-Administration. Neuropsychopharmacology.

Ciruela, F., Burgueño, J., Casadó, V., Canals, M., Marcellino, D., Goldberg, S.R., Bader, M., Fuxe, K., Agnati, L.F., Lluis, C., et al. (2004). Combining mass spectrometry and pull-down techniques for the study of receptor heteromerization. Direct epitope-epitope electrostatic interactions between adenosine A2A and dopamine D2 receptors. Anal. Chem. *76*, 5354–5363.

Ciruela, F., Canela, L., Burgueño, J., Soriguera, A., Cabello, N., Canela, E.I., Casadó, V., Cortés, A., Mallol, J., Woods, A.S., et al. (2005). Heptaspanning membrane receptors and cytoskeletal/scaffolding proteins: focus on adenosine, dopamine, and metabotropic glutamate receptor function. J. Mol. Neurosci. *26*, 277–292.

Ciruela, F., Casadó, V., Rodrigues, R.J., Luján, R., Burgueño, J., Canals, M., Borycz, J., Rebola, N., Goldberg, S.R., Mallol, J., et al. (2006). Presynaptic control of striatal glutamatergic neurotransmission by adenosine A1-A2A receptor heteromers. J. Neurosci. *26*, 2080–2087.

Civelli, O., Bunzow, J.R., and Grandy, D.K. (1993). Molecular diversity of the dopamine receptors. Annu. Rev. Pharmacol. Toxicol. *33*, 281–307.

Cobos, E.., Entrena, J.., Nieto, F.., Cendán, C.., and Del Pozo, E. (2008). Pharmacology and Therapeutic Potential of Sigma1 Receptor Ligands. Curr Neuropharmacol *6*, 344–366.

Colabufo, N.A., Berardi, F., Contino, M., Niso, M., Abate, C., Perrone, R., and Tortorella, V. (2004). Antiproliferative and cytotoxic effects of some sigma2 agonists and sigma1 antagonists in tumour cell lines. Naunyn Schmiedebergs Arch. Pharmacol. *370*, 106–113.

Cole, S., Mayer, H.S., and Petrovich, G.D. (2015). Orexin/Hypocretin-1 Receptor Antagonism Selectively Reduces Cue-Induced Feeding in Sated Rats and Recruits Medial Prefrontal Cortex and Thalamus. Sci Rep *5*, 16143.

Colpaert, F.C., Niemegeers, C.J., and Janssen, P.A. (1978). Discriminative stimulus properties of cocaine and d-amphetamine, and antagonism by haloperidol: a comparative study. Neuropharmacology *17*, 937–942.

Corbera, J., Vaño, D., Martínez, D., Vela, J.M., Zamanillo, D., Dordal, A., Andreu, F., Hernandez, E., Perez, R., Escriche, M., et al. (2006). A medicinal-chemistry-guided approach to selective and druglike sigma 1 ligands. ChemMedChem *1*, 140–154.

Cordomí, A., Navarro, G., Aymerich, M.S., and Franco, R. (2015). Structures for G-Protein-Coupled Receptor Tetramers in Complex with G Proteins. Trends Biochem. Sci. *40*, 548–551.

Costa, T., and Herz, A. (1989). Antagonists with negative intrinsic activity at delta opioid receptors coupled to GTP-binding proteins. Proc. Natl. Acad. Sci. U.S.A. *86*, 7321–7325.

Costa-Neto, C.M., Parreiras-E-Silva, L.T., and Bouvier, M. (2016). A Pluridimensional View of Biased Agonism. Mol. Pharmacol. *90*, 587–595.

Cowley, M.A., Smith, R.G., Diano, S., Tschöp, M., Pronchuk, N., Grove, K.L., Strasburger, C.J., Bidlingmaier, M., Esterman, M., Heiman, M.L., et al. (2003). The distribution and mechanism of action of ghrelin in the CNS demonstrates a novel hypothalamic circuit regulating energy homeostasis. Neuron *37*, 649–661.

Crawford, K.W., and Bowen, W.D. (2002). Sigma-2 receptor agonists activate a novel apoptotic pathway and potentiate antineoplastic drugs in breast tumor cell lines. Cancer Res. *62*, 313–322.

Creed, M., Kaufling, J., Fois, G.R., Jalabert, M., Yuan, T., Lüscher, C., Georges, F., and Bellone, C. (2016). Cocaine Exposure Enhances the Activity of Ventral Tegmental Area Dopamine Neurons via Calcium-Impermeable NMDARs. J. Neurosci. *36*, 10759–10768.

Cristalli, G., Costanzi, S., Lambertucci, C., Lupidi, G., Vittori, S., Volpini, R., and Camaioni, E. (2001). Adenosine deaminase: functional implications and different classes of inhibitors. Med Res Rev *21*, 105–128.

Cristóvão-Ferreira, S., Navarro, G., Brugarolas, M., Pérez-Capote, K., Vaz, S.H., Fattorini, G., Conti, F., Lluis, C., Ribeiro, J.A., McCormick, P.J., et al. (2013). A1R-A2AR heteromers coupled to Gs and G i/0 proteins modulate GABA transport into astrocytes. Purinergic Signal. *9*, 433–449.

Cuellar, J.N., and Isokawa, M. (2011). Ghrelin-induced activation of cAMP signal transduction and its negative regulation by endocannabinoids in the hippocampus. Neuropharmacology *60*, 842–851.

Cui, G., Meyer, A.C., Calin-Jageman, I., Neef, J., Haeseleer, F., Moser, T., and Lee, A. (2007). Ca2+-binding proteins tune Ca2+-feedback to Cav1.3 channels in mouse auditory hair cells. J. Physiol. (Lond.) *585*, 791–803.

Cunha, R.A. (2016). How does adenosine control neuronal dysfunction and neurodegeneration? J. Neurochem.

Cunha, R.A., and Ribeiro, J.A. (2000). Purinergic modulation of [(3)H]GABA release from rat hippocampal nerve terminals. Neuropharmacology *39*, 1156–1167.

Cunha, R.A., Ferré, S., Vaugeois, J.-M., and Chen, J.-F. (2008). Potential therapeutic interest of adenosine A2A receptors in psychiatric disorders. Curr. Pharm. Des. *14*, 1512–1524.

Cvejic, S., and Devi, L.A. (1997). Dimerization of the delta opioid receptor: implication for a role in receptor internalization. J. Biol. Chem. *272*, 26959–26964.

Daaka, Y., Luttrell, L.M., Ahn, S., Della Rocca, G.J., Ferguson, S.S., Caron, M.G., and Lefkowitz, R.J. (1998). Essential role for G protein-coupled receptor endocytosis in the activation of mitogen-activated protein kinase. J. Biol. Chem. *273*, 685–688.

Dal Toso, R., Sommer, B., Ewert, M., Herb, A., Pritchett, D.B., Bach, A., Shivers, B.D., and Seeburg, P.H. (1989). The dopamine D2 receptor: two molecular forms generated by alternative splicing. EMBO J. *8*, 4025–4034.

Dalley, J.W., and Everitt, B.J. (2009). Dopamine receptors in the learning, memory and drug reward circuitry. Semin. Cell Dev. Biol. *20*, 403–410.

Damian, M., Mary, S., Maingot, M., M'Kadmi, C., Gagne, D., Leyris, J.-P., Denoyelle, S., Gaibelet, G., Gavara, L., Garcia de Souza Costa, M., et al. (2015). Ghrelin receptor conformational dynamics regulate the transition from a preassembled to an active receptor: Gq complex. Proc. Natl. Acad. Sci. U.S.A. *112*, 1601–1606.

Davis, R.J. (1995). Transcriptional regulation by MAP kinases. Mol. Reprod. Dev. *42*, 459–467.

De Castro, E., Nef, S., Fiumelli, H., Lenz, S.E., Kawamura, S., and Nef, P. (1995). Regulation of rhodopsin phosphorylation by a family of neuronal calcium sensors. Biochem. Biophys. Res. Commun. *216*, 133–140.

De Giovanni, L.N., Guzman, A.S., Virgolini, M.B., and Cancela, L.M. (2016). NMDA antagonist MK 801 in nucleus accumbens core but not shell disrupts the restraint stress-induced reinstatement of extinguished cocaine-conditioned place preference in rats. Behav. Brain Res. *315*, 150–159.

De Mei, C., Ramos, M., Iitaka, C., and Borrelli, E. (2009). Getting specialized: presynaptic and postsynaptic dopamine D2 receptors. Curr Opin Pharmacol *9*, 53–58.

De Wit, H., and Wise, R.A. (1977). Blockade of cocaine reinforcement in rats with the dopamine receptor blocker pimozide, but not with the noradrenergic blockers phentolamine or phenoxybenzamine. Can J Psychol *31*, 195–203.

Dearry, A., Gingrich, J.A., Falardeau, P., Fremeau, R.T., Bates, M.D., and Caron, M.G. (1990). Molecular cloning and expression of the gene for a human D1 dopamine receptor. Nature *347*, 72–76.

DeFea, K.A., Zalevsky, J., Thoma, M.S., Déry, O., Mullins, R.D., and Bunnett, N.W. (2000). beta-arrestin-dependent endocytosis of proteinase-activated receptor 2 is required for intracellular targeting of activated ERK1/2. J. Cell Biol. *148*, 1267–1281.

DeLong, M.R., and Wichmann, T. (2007). Circuits and circuit disorders of the basal ganglia. Arch. Neurol. *64*, 20–24.

DeWire, S.M., Ahn, S., Lefkowitz, R.J., and Shenoy, S.K. (2007). Beta-arrestins and cell signaling. Annu. Rev. Physiol. *69*, 483–510.

Dezaki, K. (2013). Ghrelin function in insulin release and glucose metabolism. Endocr Dev *25*, 135–143.

Di Chiara, G., and Bassareo, V. (2007). Reward system and addiction: what dopamine does and doesn't do. Curr Opin Pharmacol *7*, 69–76.

Di Chiara, G., and Imperato, A. (1988). Drugs abused by humans preferentially increase synaptic dopamine concentrations in the mesolimbic system of freely moving rats. Proc. Natl. Acad. Sci. U.S.A. *85*, 5274–5278.

Di Ciano, P., Cardinal, R.N., Cowell, R.A., Little, S.J., and Everitt, B.J. (2001). Differential involvement of NMDA, AMPA/kainate, and dopamine receptors in the nucleus accumbens core in the acquisition and performance of pavlovian approach behavior. J. Neurosci. *21*, 9471–9477.

Di Donato, V., Auer, T.O., Duroure, K., and Del Bene, F. (2013). Characterization of the calcium binding protein family in zebrafish. PLoS ONE *8*, e53299.

Dickinson, S.D., Sabeti, J., Larson, G.A., Giardina, K., Rubinstein, M., Kelly, M.A., Grandy, D.K., Low, M.J., Gerhardt, G.A., and Zahniser, N.R. (1999). Dopamine D2 receptor-deficient mice exhibit decreased dopamine transporter function but no changes in dopamine release in dorsal striatum. J. Neurochem. *72*, 148–156.

DiLeone, R.J., Taylor, J.R., and Picciotto, M.R. (2012). The drive to eat: comparisons and distinctions between mechanisms of food reward and drug addiction. Nat. Neurosci. *15*, 1330–1335.

Dohlman, H.G., Caron, M.G., and Lefkowitz, R.J. (1987). A family of receptors coupled to guanine nucleotide regulatory proteins. Biochemistry *26*, 2657–2664.

Doura, M.B., and Unterwald, E.M. (2016). MicroRNAs Modulate Interactions between Stress and Risk for Cocaine Addiction. Front Cell Neurosci *10*, 125.

Du, Y., Du, L., Cao, J., Hölscher, C., Feng, Y., Su, H., Wang, Y., and Yun, K.-M. (2017). Levo-tetrahydropalmatine inhibits the acquisition of ketamine-induced conditioned place preference by regulating the expression of ERK and CREB phosphorylation in rats. Behav. Brain Res. *317*, 367–373.

Duarte, J.M.N., Cunha, R.A., and Carvalho, R.A. (2016). Adenosine A_1 receptors control the metabolic recovery after hypoxia in rat hippocampal slices. J. Neurochem. *136*, 947–957.

Dunwiddie, T.V., and Masino, S.A. (2001). The role and regulation of adenosine in the central nervous system. Annu. Rev. Neurosci. *24*, 31–55.

Durieux, P.F., Bearzatto, B., Guiducci, S., Buch, T., Waisman, A., Zoli, M., Schiffmann, S.N., and de Kerchove d'Exaerde, A. (2009). D2R striatopallidal neurons inhibit both locomotor and drug reward processes. Nat. Neurosci. *12*, 393–395.

Durieux, P.F., Schiffmann, S.N., and de Kerchove d'Exaerde, A. (2012). Differential regulation of motor control and response to dopaminergic drugs by D1R and D2R neurons in distinct dorsal striatum subregions. EMBO J. *31*, 640–653.

Egecioglu, E., Jerlhag, E., Salomé, N., Skibicka, K.P., Haage, D., Bohlooly-Y, M., Andersson, D., Bjursell, M., Perrissoud, D., Engel, J.A., et al. (2010). Ghrelin increases intake of rewarding food in rodents. Addict Biol *15*, 304–311.

El Far, O., Bofill-Cardona, E., Airas, J.M., O'Connor, V., Boehm, S., Freissmuth, M., Nanoff, C., and Betz, H. (2001). Mapping of calmodulin and Gbetagamma binding domains within the C-terminal region of the metabotropic glutamate receptor 7A. J. Biol. Chem. *276*, 30662–30669.

El Moustaine, D., Granier, S., Doumazane, E., Scholler, P., Rahmeh, R., Bron, P., Mouillac, B., Banères, J.-L., Rondard, P., and Pin, J.-P. (2012). Distinct roles of metabotropic glutamate receptor dimerization in agonist activation and G-protein coupling. Proc. Natl. Acad. Sci. U.S.A. *109*, 16342–16347.

Elsworth, J.D., and Roth, R.H. (1997). Dopamine synthesis, uptake, metabolism, and receptors: relevance to gene therapy of Parkinson's disease. Exp. Neurol. *144*, 4–9.

Engel, J.A., Nylander, I., and Jerlhag, E. (2015). A ghrelin receptor (GHS-R1A) antagonist attenuates the rewarding properties of morphine and increases opioid peptide levels in reward areas in mice. Eur Neuropsychopharmacol *25*, 2364–2371.

Etori, K., Saito, Y.C., Tsujino, N., and Sakurai, T. (2014). Effects of a newly developed potent orexin-2 receptor-selective antagonist, compound 1 m, on sleep/wakefulness states in mice. Front Neurosci *8*, 8.

Faure, M., Voyno-Yasenetskaya, T.A., and Bourne, H.R. (1994). cAMP and beta gamma subunits of heterotrimeric G proteins stimulate the mitogen-activated protein kinase pathway in COS-7 cells. J. Biol. Chem. *269*, 7851–7854.

Favrod-Coune, T., and Broers, B. (2010). The Health Effect of Psychostimulants: A Literature Review. Pharmaceuticals (Basel) *3*, 2333–2361.

Feoktistov, I., and Biaggioni, I. (1995). Adenosine A2b receptors evoke interleukin-8 secretion in human mast cells. An enprofylline-sensitive mechanism with implications for asthma. J. Clin. Invest. *96*, 1979–1986.

Ferguson, S.S. (2001). Evolving concepts in G protein-coupled receptor endocytosis: the role in receptor desensitization and signaling. Pharmacol. Rev. *53*, 1–24.

Ferguson, S.M., Fasano, S., Yang, P., Brambilla, R., and Robinson, T.E. (2006). Knockout of ERK1 enhances cocaine-evoked immediate early gene expression and behavioral plasticity. Neuropsychopharmacology *31*, 2660–2668.

Ferré, S. (2008). [Caffeine in Parkinson's disease]. Med Clin (Barc) *131*, 710–715.

Ferré, S. (2010). Role of the central ascending neurotransmitter systems in the psychostimulant effects of caffeine. J. Alzheimers Dis. *20 Suppl 1*, S35-49.

Ferre, S., von Euler, G., Johansson, B., Fredholm, B.B., and Fuxe, K. (1991). Stimulation of high-affinity adenosine A2 receptors decreases the affinity of dopamine D2 receptors in rat striatal membranes. Proc. Natl. Acad. Sci. U.S.A. *88*, 7238–7241.

Ferré, S., Karcz-Kubicha, M., Hope, B.T., Popoli, P., Burgueño, J., Gutiérrez, M.A., Casadó, V., Fuxe, K., Goldberg, S.R., Lluis, C., et al. (2002). Synergistic interaction between adenosine A2A and glutamate mGlu5 receptors: implications for striatal neuronal function. Proc. Natl. Acad. Sci. U.S.A. *99*, 11940–11945.

Ferré, S., Ciruela, F., Woods, A.S., Lluis, C., and Franco, R. (2007). Functional relevance of neurotransmitter receptor heteromers in the central nervous system. Trends Neurosci. *30*, 440–446.

Ferré, S., Quiroz, C., Woods, A.S., Cunha, R., Popoli, P., Ciruela, F., Lluis, C., Franco, R., Azdad, K., and Schiffmann, S.N. (2008). An update on adenosine A2A-dopamine D2 receptor interactions: implications for the function of G protein-coupled receptors. Curr. Pharm. Des. *14*, 1468–1474.

Ferré, S., Baler, R., Bouvier, M., Caron, M.G., Devi, L.A., Durroux, T., Fuxe, K., George, S.R., Javitch, J.A., Lohse, M.J., et al. (2009). Building a new conceptual framework for receptor heteromers. Nat. Chem. Biol. *5*, 131–134.

Ferré, S., Navarro, G., Casadó, V., Cortés, A., Mallol, J., Canela, E.I., Lluís, C., and Franco, R. (2010a). G protein-coupled receptor heteromers as new targets for drug development. Prog Mol Biol Transl Sci *91*, 41–52.

Ferré, S., Woods, A.S., Navarro, G., Aymerich, M., Lluís, C., and Franco, R. (2010b). Calcium-mediated modulation of the quaternary structure and function of adenosine A2A-dopamine D2 receptor heteromers. Curr Opin Pharmacol *10*, 67–72.

Ferré, S., Casadó, V., Devi, L.A., Filizola, M., Jockers, R., Lohse, M.J., Milligan, G., Pin, J.-P., and Guitart, X. (2014). G protein-coupled receptor oligomerization revisited: functional and pharmacological perspectives. Pharmacol. Rev. *66*, 413–434.

Ferreira, S.G., Gonçalves, F.Q., Marques, J.M., Tomé, Â.R., Rodrigues, R.J., Nunes-Correia, I., Ledent, C., Harkany, T., Venance, L., Cunha, R.A., et al. (2015). Presynaptic adenosine A2A receptors dampen cannabinoid CB1 receptor-mediated inhibition of corticostriatal glutamatergic transmission. Br. J. Pharmacol. *172*, 1074–1086.

Filipek, S., Krzysko, K.A., Fotiadis, D., Liang, Y., Saperstein, D.A., Engel, A., and Palczewski, K. (2004). A concept for G protein activation by G protein-coupled receptor dimers: the transducin/rhodopsin interface. Photochem. Photobiol. Sci. *3*, 628–638.

Florian, C., Vecsey, C.G., Halassa, M.M., Haydon, P.G., and Abel, T. (2011). Astrocyte-derived adenosine and A1 receptor activity contribute to sleep loss-induced deficits in hippocampal synaptic plasticity and memory in mice. J. Neurosci. *31*, 6956–6962.

Flower, D.R. (1999). Modelling G-protein-coupled receptors for drug design. Biochim. Biophys. Acta *1422*, 207–234.

Fotiadis, D., Liang, Y., Filipek, S., Saperstein, D.A., Engel, A., and Palczewski, K. (2003). Atomic-force microscopy: Rhodopsin dimers in native disc membranes. Nature *421*, 127–128.

Fotiadis, D., Liang, Y., Filipek, S., Saperstein, D.A., Engel, A., and Palczewski, K. (2004). The G protein-coupled receptor rhodopsin in the native membrane. FEBS Lett. *564*, 281–288.

Franco, R., Casadó, V., Ciruela, F., Mallol, J., Lluis, C., and Canela, E.I. (1996). The cluster-arranged cooperative model: a model that accounts for the kinetics of binding to A1 adenosine receptors. Biochemistry *35*, 3007–3015.

Franco, R., Canals, M., Marcellino, D., Ferré, S., Agnati, L., Mallol, J., Casadó, V., Ciruela, F., Fuxe, K., Lluis, C., et al. (2003). Regulation of heptaspanning-membrane-receptor function by dimerization and clustering. Trends Biochem. Sci. *28*, 238–243.

Franco, R., Ciruela, F., Casadó, V., Cortes, A., Canela, E.I., Mallol, J., Agnati, L.F., Ferré, S., Fuxe, K., and Lluis, C. (2005). Partners for adenosine A1 receptors. J. Mol. Neurosci. *26*, 221–232.

Franco, R., Lluis, C., Canela, E.I., Mallol, J., Agnati, L., Casadó, V., Ciruela, F., Ferré, S., and Fuxe, K. (2007). Receptor-receptor interactions involving adenosine A1 or dopamine D1 receptors and accessory proteins. J Neural Transm (Vienna) *114*, 93–104.

Franco, R., Casadó, V., Cortés, A., Mallol, J., Ciruela, F., Ferré, S., Lluis, C., and Canela, E.I. (2008a). G-protein-coupled receptor heteromers: function and ligand pharmacology. Br. J. Pharmacol. *153 Suppl 1*, S90-98.

Franco, R., Casadó, V., Cortés, A., Pérez-Capote, K., Mallol, J., Canela, E., Ferré, S., and Lluis, C. (2008b). Novel pharmacological targets based on receptor heteromers. Brain Res Rev *58*, 475–482.

Franco, R., Martínez-Pinilla, E., Ricobaraza, A., and McCormick, P.J. (2013). Challenges in the development of heteromer-GPCR-based drugs. Prog Mol Biol Transl Sci *117*, 143–162.

Franco, R., Martínez-Pinilla, E., Lanciego, J.L., and Navarro, G. (2016). Basic Pharmacological and Structural Evidence for Class A G-Protein-Coupled Receptor Heteromerization. Front Pharmacol *7*, 76.

Fraser, C.M., Chung, F.Z., Wang, C.D., and Venter, J.C. (1988). Site-directed mutagenesis of human beta-adrenergic receptors: substitution of aspartic acid-130 by asparagine produces a receptor with high-affinity agonist binding that is uncoupled from adenylate cyclase. Proc. Natl. Acad. Sci. U.S.A. *85*, 5478–5482.

Fredholm, B.B., IJzerman, A.P., Jacobson, K.A., Klotz, K.N., and Linden, J. (2001a). International Union of Pharmacology. XXV. Nomenclature and classification of adenosine receptors. Pharmacol. Rev. *53*, 527–552.

Fredholm, B.B., Irenius, E., Kull, B., and Schulte, G. (2001b). Comparison of the potency of adenosine as an agonist at human adenosine receptors expressed in Chinese hamster ovary cells. Biochem. Pharmacol. *61*, 443–448.

Fredholm, B.B., Chen, J.-F., Cunha, R.A., Svenningsson, P., and Vaugeois, J.-M. (2005). Adenosine and brain function. Int. Rev. Neurobiol. *63*, 191–270.

Fredholm, B.B., IJzerman, A.P., Jacobson, K.A., Linden, J., and Müller, C.E. (2011). International Union of Basic and Clinical Pharmacology. LXXXI. Nomenclature and classification of adenosine receptors--an update. Pharmacol. Rev. *63*, 1–34.

Fredriksson, R., Lagerström, M.C., Lundin, L.-G., and Schiöth, H.B. (2003). The G-protein-coupled receptors in the human genome form five main families. Phylogenetic analysis, paralogon groups, and fingerprints. Mol. Pharmacol. *63*, 1256–1272.

Fredriksson, S., Gullberg, M., Jarvius, J., Olsson, C., Pietras, K., Gústafsdóttir, S.M., Ostman, A., and Landegren, U. (2002). Protein detection using proximity-dependent DNA ligation assays. Nat. Biotechnol. *20*, 473–477.

Friedberg, F., and Rhoads, A.R. (2001). Evolutionary aspects of calmodulin. IUBMB Life *51*, 215–221.

Fuenzalida, J., Galaz, P., Araya, K.A., Slater, P.G., Blanco, E.H., Campusano, J.M., Ciruela, F., and Gysling, K. (2014). Dopamine D1 and corticotrophin-releasing hormone type-2α receptors assemble into functionally interacting complexes in living cells. Br. J. Pharmacol. *171*, 5650–5664.

Fung, J.J., Deupi, X., Pardo, L., Yao, X.J., Velez-Ruiz, G.A., Devree, B.T., Sunahara, R.K., and Kobilka, B.K. (2009). Ligand-regulated oligomerization of beta(2)-adrenoceptors in a model lipid bilayer. EMBO J. *28*, 3315–3328.

Furlong, T.M., Supit, A.S.A., Corbit, L.H., Killcross, S., and Balleine, B.W. (2015). Pulling habits out of rats: adenosine 2A receptor antagonism in dorsomedial striatum rescues meth-amphetamine-induced deficits in goal-directed action. Addict Biol.

Fuxe, K., and Ungerstedt, U. (1974). Action of caffeine and theophyllamine on supersensitive dopamine receptors: considerable enhancement of receptor response to treatment with DOPA and dopamine receptor agonists. Med. Biol. *52*, 48–54.

Fuxe, K., Canals, M., Torvinen, M., Marcellino, D., Terasmaa, A., Genedani, S., Leo, G., Guidolin, D., Diaz-Cabiale, Z., Rivera, A., et al. (2007a). Intramembrane receptor-receptor interactions: a novel principle in molecular medicine. J Neural Transm (Vienna) *114*, 49–75.

Fuxe, K., Ferré, S., Genedani, S., Franco, R., and Agnati, L.F. (2007b). Adenosine receptor-dopamine receptor interactions in the basal ganglia and their relevance for brain function. Physiol. Behav. *92*, 210–217.

Gahbauer, S., and Böckmann, R.A. (2016). Membrane-Mediated Oligomerization of G Protein Coupled Receptors and Its Implications for GPCR Function. Front Physiol *7*, 494.

Galvan, A., Hu, X., Rommelfanger, K.S., Pare, J.-F., Khan, Z.U., Smith, Y., and Wichmann, T. (2014). Localization and function of dopamine receptors in the subthalamic nucleus of normal and parkinsonian monkeys. J. Neurophysiol. *112*, 467–479.

Gandía, J., Lluís, C., Ferré, S., Franco, R., and Ciruela, F. (2008). Light resonance energy transfer-based methods in the study of G protein-coupled receptor oligomerization. Bioessays *30*, 82–89.

Garcés-Ramírez, L., Green, J.L., Hiranita, T., Kopajtic, T.A., Mereu, M., Thomas, A.M., Mesangeau, C., Narayanan, S., McCurdy, C.R., Katz, J.L., et al. (2011). Sigma receptor agonists: receptor binding and effects on mesolimbic dopamine neurotransmission assessed by microdialysis. Biol. Psychiatry *69*, 208–217.

Gehl, C., Waadt, R., Kudla, J., Mendel, R.-R., and Hänsch, R. (2009). New GATEWAY vectors for high throughput analyses of protein-protein interactions by bimolecular fluorescence complementation. Mol Plant *2*, 1051–1058.

George, S.R., O'Dowd, B.F., and Lee, S.P. (2002). G-protein-coupled receptor oligomerization and its potential for drug discovery. Nat Rev Drug Discov *1*, 808–820.

Gerdes, D., Wehling, M., Leube, B., and Falkenstein, E. (1998). Cloning and tissue expression of two putative steroid membrane receptors. Biol. Chem. *379*, 907–911.

Gerfen, C.R., Engber, T.M., Mahan, L.C., Susel, Z., Chase, T.N., Monsma, F.J., and Sibley, D.R. (1990). D1 and D2 dopamine receptor-regulated gene expression of striatonigral and striatopallidal neurons. Science *250*, 1429–1432.

German, D.C., and Manaye, K.F. (1993). Midbrain dopaminergic neurons (nuclei A8, A9, and A10): three-dimensional reconstruction in the rat. J. Comp. Neurol. *331*, 297–309.

Gerwins, P., and Fredholm, B.B. (1992). Stimulation of adenosine A1 receptors and bradykinin receptors, which act via different G proteins, synergistically raises inositol 1,4,5-trisphosphate and intracellular free calcium in DDT1 MF-2 smooth muscle cells. Proc. Natl. Acad. Sci. U.S.A. *89*, 7330–7334.

Gessi, S., Merighi, S., Sacchetto, V., Simioni, C., and Borea, P.A. (2011). Adenosine receptors and cancer. Biochim. Biophys. Acta *1808*, 1400–1412.

Gether, U. (2000). Uncovering molecular mechanisms involved in activation of G protein-coupled receptors. Endocr. Rev. *21*, 90–113.

Ghosh, A., and Greenberg, M.E. (1995). Calcium signaling in neurons: molecular mechanisms and cellular consequences. Science *268*, 239–247.

Ghosh, D., Syed, A.U., Prada, M.P., Nystoriak, M.A., Santana, L.F., Nieves-Cintrón, M., and Navedo, M.F. (2017). Calcium Channels in Vascular Smooth Muscle. Adv. Pharmacol. *78*, 49–87.

Ginés, S., Hillion, J., Torvinen, M., Le Crom, S., Casadó, V., Canela, E.I., Rondin, S., Lew, J.Y., Watson, S., Zoli, M., et al. (2000). Dopamine D1 and adenosine A1 receptors form functionally interacting heteromeric complexes. Proc. Natl. Acad. Sci. U.S.A. *97*, 8606–8611.

Gingrich, J.A., and Caron, M.G. (1993). Recent advances in the molecular biology of dopamine receptors. Annu. Rev. Neurosci. *16*, 299–321.

Giros, B., Jaber, M., Jones, S.R., Wightman, R.M., and Caron, M.G. (1996). Hyperlocomotion and indifference to cocaine and amphetamine in mice lacking the dopamine transporter. Nature *379*, 606–612.

Goeders, N.E., and Smith, J.E. (1983). Cortical dopaminergic involvement in cocaine reinforcement. Science *221*, 773–775.

Golan, M., Schreiber, G., and Avissar, S. (2009). Antidepressants, beta-arrestins and GRKs: from regulation of signal desensitization to intracellular multifunctional adaptor functions. Curr. Pharm. Des. *15*, 1699–1708.

Gomes, I., Jordan, B.A., Gupta, A., Trapaidze, N., Nagy, V., and Devi, L.A. (2000). Heterodimerization of mu and delta opioid receptors: A role in opiate synergy. J. Neurosci. *20*, RC110.

Gomez, M., De Castro, E., Guarin, E., Sasakura, H., Kuhara, A., Mori, I., Bartfai, T., Bargmann, C.I., and Nef, P. (2001). Ca2+ signaling via the neuronal calcium sensor-1 regulates associative learning and memory in C. elegans. Neuron *30*, 241–248.

Gonzalez, A., Cordomí, A., Matsoukas, M., Zachmann, J., and Pardo, L. (2014). Modeling of G protein-coupled receptors using crystal structures: from monomers to signaling complexes. Adv. Exp. Med. Biol. *796*, 15–33.

González-Maeso, J., Ang, R.L., Yuen, T., Chan, P., Weisstaub, N.V., López-Giménez, J.F., Zhou, M., Okawa, Y., Callado, L.F., Milligan, G., et al. (2008). Identification of a serotonin/glutamate receptor complex implicated in psychosis. Nature *452*, 93–97.

Gotter, A.L., Webber, A.L., Coleman, P.J., Renger, J.J., and Winrow, C.J. (2012). International Union of Basic and Clinical Pharmacology. LXXXVI. Orexin receptor function, nomenclature and pharmacology. Pharmacol. Rev. *64*, 389–420.

Goudet, C., Kniazeff, J., Hlavackova, V., Malhaire, F., Maurel, D., Acher, F., Blahos, J., Prézeau, L., and Pin, J.-P. (2005). Asymmetric functioning of dimeric metabotropic glutamate receptors disclosed by positive allosteric modulators. J. Biol. Chem. *280*, 24380–24385.

Gouldson, P.R., Higgs, C., Smith, R.E., Dean, M.K., Gkoutos, G.V., and Reynolds, C.A. (2000). Dimerization and domain swapping in G-protein-coupled receptors: a computational study. Neuropsychopharmacology *23*, S60-77.

Gracia, E., Cortés, A., Meana, J.J., García-Sevilla, J., Herhsfield, M.S., Canela, E.I., Mallol, J., Lluís, C., Franco, R., and Casadó, V. (2008). Human adenosine deaminase as an allosteric modulator of human A(1) adenosine receptor: abolishment of negative cooperativity for [H](R)-pia binding to the caudate nucleus. J. Neurochem. *107*, 161–170.

Greer, P.L., and Greenberg, M.E. (2008). From synapse to nucleus: calcium-dependent gene transcription in the control of synapse development and function. Neuron *59*, 846–860.

Grieder, T.E., Herman, M.A., Contet, C., Tan, L.A., Vargas-Perez, H., Cohen, A., Chwalek, M., Maal-Bared, G., Freiling, J., Schlosburg, J.E., et al. (2014). VTA CRF neurons mediate the aversive effects of nicotine withdrawal and promote intake escalation. Nat. Neurosci. *17*, 1751–1758.

Grillner, S., and Robertson, B. (2016). The Basal Ganglia Over 500 Million Years. Curr. Biol. *26*, R1088–R1100.

Gudermann, T., Schöneberg, T., and Schultz, G. (1997). Functional and structural complexity of signal transduction via G-protein-coupled receptors. Annu. Rev. Neurosci. *20*, 399–427.

Guegan, T., Cebrià, J.P., Maldonado, R., and Martin, M. (2016). Morphine-induced locomotor sensitization produces structural plasticity in the mesocorticolimbic system dependent on CB1-R activity. Addict Biol *21*, 1113–1126.

Guitart, X., Codony, X., and Monroy, X. (2004). Sigma receptors: biology and therapeutic potential. Psychopharmacology (Berl.) *174*, 301–319.

Guitart, X., Navarro, G., Moreno, E., Yano, H., Cai, N.-S., Sánchez-Soto, M., Kumar-Barodia, S., Naidu, Y.T., Mallol, J., Cortés, A., et al. (2014). Functional selectivity of allosteric interactions within G protein-coupled receptor oligomers: the dopamine D1-D3 receptor heterotetramer. Mol. Pharmacol. *86*, 417–429.

Guo, L., and Zhen, X. (2015). Sigma-2 receptor ligands: neurobiological effects. Curr. Med. Chem. *22*, 989–1003.

Guo, W., Urizar, E., Kralikova, M., Mobarec, J.C., Shi, L., Filizola, M., and Javitch, J.A. (2008). Dopamine D2 receptors form higher order oligomers at physiological expression levels. EMBO J. *27*, 2293–2304.

Haeseleer, F., Imanishi, Y., Sokal, I., Filipek, S., and Palczewski, K. (2002). Calcium-binding proteins: intracellular sensors from the calmodulin superfamily. Biochem. Biophys. Res. Commun. *290*, 615–623.

Hage, S.R., and Jürgens, U. (2006). Localization of a vocal pattern generator in the pontine brainstem of the squirrel monkey. Eur. J. Neurosci. *23*, 840–844.

Hamm, H.E. (1998). The many faces of G protein signaling. J. Biol. Chem. *273*, 669–672.

Hanner, M., Moebius, F.F., Flandorfer, A., Knaus, H.G., Striessnig, J., Kempner, E., and Glossmann, H. (1996). Purification, molecular cloning, and expression of the mammalian sigma1-binding site. Proc. Natl. Acad. Sci. U.S.A. *93*, 8072–8077.

Harris, G.C., and Aston-Jones, G. (2006). Arousal and reward: a dichotomy in orexin function. Trends Neurosci. *29*, 571–577.

Hasbi, A., Perreault, M.L., Shen, M.Y.F., Zhang, L., To, R., Fan, T., Nguyen, T., Ji, X., O'Dowd, B.F., and George, S.R. (2014). A peptide targeting an interaction interface disrupts the dopamine D1-D2 receptor heteromer to block signaling and function in vitro and in vivo: effective selective antagonism. FASEB J. *28*, 4806–4820.

Hashimoto, K., and Kudla, J. (2011). Calcium decoding mechanisms in plants. Biochimie *93*, 2054–2059.

Hausdorff, W.P., Bouvier, M., O'Dowd, B.F., Irons, G.P., Caron, M.G., and Lefkowitz, R.J. (1989). Phosphorylation sites on two domains of the beta 2-adrenergic receptor are involved in distinct pathways of receptor desensitization. J. Biol. Chem. *264*, 12657–12665.

Hauser, R.A., Hubble, J.P., Truong, D.D., and Istradefylline US-001 Study Group (2003). Randomized trial of the adenosine A(2A) receptor antagonist istradefylline in advanced PD. Neurology *61*, 297–303.

Hayashi, T., and Su, T. (2005). The sigma receptor: evolution of the concept in neuropsychopharmacology. Curr Neuropharmacol *3*, 267–280.

Hayashi, T., and Su, T.-P. (2007). Sigma-1 receptor chaperones at the ER-mitochondrion interface regulate Ca(2+) signaling and cell survival. Cell *131*, 596–610.

Haynes, A.C., Jackson, B., Overend, P., Buckingham, R.E., Wilson, S., Tadayyon, M., and Arch, J.R. (1999). Effects of single and chronic intracerebroventricular administration of the orexins on feeding in the rat. Peptides *20*, 1099–1105.

Haynes, L.P., Thomas, G.M.H., and Burgoyne, R.D. (2005). Interaction of neuronal calcium sensor-1 and ADP-ribosylation factor 1 allows bidirectional control of phosphatidylinositol 4-kinase beta and trans-Golgi network-plasma membrane traffic. J. Biol. Chem. *280*, 6047–6054.

Hebert, T.E., Moffett, S., Morello, J.P., Loisel, T.P., Bichet, D.G., Barret, C., and Bouvier, M. (1996). A peptide derived from a beta2-adrenergic receptor transmembrane domain inhibits both receptor dimerization and activation. J. Biol. Chem. *271*, 16384–16392.

Heikkila, R.E., Cabbat, F.S., and Duvoisin, R.C. (1979). Motor activity and rotational behavior after analogs of cocaine: correlation with dopamine uptake blockade. Commun Psychopharmacol *3*, 285–290.

Heinsbroek, J.A., Neuhofer, D.N., Griffin, W.C., Siegel, G.S., Bobadilla, A.-C., Kupchik, Y.M., and Kalivas, P.W. (2017). Loss of Plasticity in the D2-Accumbens Pallidal Pathway Promotes Cocaine Seeking. J. Neurosci. *37*, 757–767.

Hellewell, S.B., Bruce, A., Feinstein, G., Orringer, J., Williams, W., and Bowen, W.D. (1994). Rat liver and kidney contain high densities of sigma 1 and sigma 2 receptors: characterization by ligand binding and photoaffinity labeling. Eur. J. Pharmacol. *268*, 9–18.

Hermans, E., Vanisberg, M.A., Geurts, M., and Maloteaux, J.M. (1997). Down-regulation of neurotensin receptors after ligand-induced internalization in rat primary cultured neurons. Neurochem. Int. *31*, 291–299.

Herrick-Davis, K., Grinde, E., and Mazurkiewicz, J.E. (2004). Biochemical and biophysical characterization of serotonin 5-HT2C receptor homodimers on the plasma membrane of living cells. Biochemistry *43*, 13963–13971.

Herrick-Davis, K., Weaver, B.A., Grinde, E., and Mazurkiewicz, J.E. (2006). Serotonin 5-HT2C receptor homodimer biogenesis in the endoplasmic reticulum: real-time visualization with confocal fluorescence resonance energy transfer. J. Biol. Chem. *281*, 27109–27116.

Herrick-Davis, K., Grinde, E., Lindsley, T., Teitler, M., Mancia, F., Cowan, A., and Mazurkiewicz, J.E. (2015). Native serotonin 5-HT2C receptors are expressed as homodimers on the apical surface of choroid plexus epithelial cells. Mol. Pharmacol. *87*, 660–673.

Hikida, T., Kimura, K., Wada, N., Funabiki, K., and Nakanishi, S. (2010). Distinct roles of synaptic transmission in direct and indirect striatal pathways to reward and aversive behavior. Neuron *66*, 896–907.

Hikosaka, O. (2007). GABAergic output of the basal ganglia. Prog. Brain Res. *160*, 209–226.

Hill, C.A., Fox, A.N., Pitts, R.J., Kent, L.B., Tan, P.L., Chrystal, M.A., Cravchik, A., Collins, F.H., Robertson, H.M., and Zwiebel, L.J. (2002). G protein-coupled receptors in Anopheles gambiae. Science *298*, 176–178.

Hiranita, T., Soto, P.L., Kohut, S.J., Kopajtic, T., Cao, J., Newman, A.H., Tanda, G., and Katz, J.L. (2011). Decreases in cocaine self-administration with dual inhibition of the dopamine transporter and σ receptors. J. Pharmacol. Exp. Ther. *339*, 662–677.

Hirschberg, B.T., and Schimerlik, M.I. (1994). A kinetic model for oxotremorine M binding to recombinant porcine m2 muscarinic receptors expressed in Chinese hamster ovary cells. J. Biol. Chem. *269*, 26127–26135.

Hlavackova, V., Goudet, C., Kniazeff, J., Zikova, A., Maurel, D., Vol, C., Trojanova, J., Prézeau, L., Pin, J.-P., and Blahos, J. (2005). Evidence for a single heptahelical domain being turned on upon activation of a dimeric GPCR. EMBO J. *24*, 499–509.

Hnasko, T.S., Sotak, B.N., and Palmiter, R.D. (2007). Cocaine-conditioned place preference by dopamine-deficient mice is mediated by serotonin. J. Neurosci. *27*, 12484–12488.

Hollenstein, K., Kean, J., Bortolato, A., Cheng, R.K.Y., Doré, A.S., Jazayeri, A., Cooke, R.M., Weir, M., and Marshall, F.H. (2013). Structure of class B GPCR corticotropin-releasing factor receptor 1. Nature *499*, 438–443.

Holly, E.N., DeBold, J.F., and Miczek, K.A. (2015). Increased mesocorticolimbic dopamine during acute and repeated social defeat stress: modulation by corticotropin releasing factor receptors in the ventral tegmental area. Psychopharmacology (Berl.) *232*, 4469–4479.

Holly, E.N., Boyson, C.O., Montagud-Romero, S., Stein, D.J., Gobrogge, K.L., DeBold, J.F., and Miczek, K.A. (2016). Episodic Social Stress-Escalated Cocaine Self-Administration: Role of Phasic and Tonic Corticotropin Releasing Factor in the Anterior and Posterior Ventral Tegmental Area. J. Neurosci. *36*, 4093–4105.

Howard, A.D., McAllister, G., Feighner, S.D., Liu, Q., Nargund, R.P., Van der Ploeg, L.H., and Patchett, A.A. (2001). Orphan G-protein-coupled receptors and natural ligand discovery. Trends Pharmacol. Sci. *22*, 132–140.

Hradsky, J., Bernstein, H.-G., Marunde, M., Mikhaylova, M., and Kreutz, M.R. (2015). Alternative splicing, expression and cellular localization of Calneuron-1 in the rat and human brain. J. Histochem. Cytochem. *63*, 793–804.

Hu, C.-D., Chinenov, Y., and Kerppola, T.K. (2002). Visualization of interactions among bZIP and Rel family proteins in living cells using bimolecular fluorescence complementation. Mol. Cell *9*, 789–798.

Hu, E.Y., Bouteiller, J.-M.C., Dong Song, null, and Berger, T.W. (2016). Development of a detailed model of calcium dynamics at the postsynaptic spine of an excitatory synapse. Conf Proc IEEE Eng Med Biol Soc *2016*, 6102–6105.

Hu, J., Thor, D., Zhou, Y., Liu, T., Wang, Y., McMillin, S.M., Mistry, R., Challiss, R.A.J., Costanzi, S., and Wess, J. (2012). Structural aspects of M_3 muscarinic acetylcholine receptor dimer formation and activation. FASEB J. *26*, 604–616.

Huang, J., Chen, S., Zhang, J.J., and Huang, X.-Y. (2013). Crystal structure of oligomeric β1-adrenergic G protein-coupled receptors in ligand-free basal state. Nat. Struct. Mol. Biol. *20*, 419–425.

Hughes, A.L., Powell, D.W., Bard, M., Eckstein, J., Barbuch, R., Link, A.J., and Espenshade, P.J. (2007). Dap1/PGRMC1 binds and regulates cytochrome P450 enzymes. Cell Metab. *5*, 143–149.

Hui, H., McHugh, D., Hannan, M., Zeng, F., Xu, S.-Z., Khan, S.-U.-H., Levenson, R., Beech, D.J., and Weiss, J.L. (2006). Calcium-sensing mechanism in TRPC5 channels contributing to retardation of neurite outgrowth. J. Physiol. (Lond.) *572*, 165–172.

Ikura, M., and Ames, J.B. (2006). Genetic polymorphism and protein conformational plasticity in the calmodulin superfamily: two ways to promote multifunctionality. Proc. Natl. Acad. Sci. U.S.A. *103*, 1159–1164.

Isoda, M., and Hikosaka, O. (2008). Role for subthalamic nucleus neurons in switching from automatic to controlled eye movement. J. Neurosci. *28*, 7209–7218.

J Gingell, J., Simms, J., Barwell, J., Poyner, D.R., Watkins, H.A., Pioszak, A.A., Sexton, P.M., and Hay, D.L. (2016). An allosteric role for receptor activity-modifying proteins in defining GPCR pharmacology. Cell Discov *2*, 16012.

Jaakola, V.-P., Griffith, M.T., Hanson, M.A., Cherezov, V., Chien, E.Y.T., Lane, J.R., Ijzerman, A.P., and Stevens, R.C. (2008). The 2.6 angstrom crystal structure of a human A2A adenosine receptor bound to an antagonist. Science *322*, 1211–1217.

Jacobson, K.A. (2015). New paradigms in GPCR drug discovery. Biochem. Pharmacol. *98*, 541–555.

Jacobson, K.A., and Costanzi, S. (2012). New insights for drug design from the X-ray crystallographic structures of G-protein-coupled receptors. Mol. Pharmacol. *82*, 361–371.

Jacoby, E., Bouhelal, R., Gerspacher, M., and Seuwen, K. (2006). The 7 TM G-protein-coupled receptor target family. ChemMedChem *1*, 761–782.

Jastrzebska, B., Orban, T., Golczak, M., Engel, A., and Palczewski, K. (2013). Asymmetry of the rhodopsin dimer in complex with transducin. FASEB J. *27*, 1572–1584.

Jastrzebska, B., Chen, Y., Orban, T., Jin, H., Hofmann, L., and Palczewski, K. (2015). Disruption of Rhodopsin Dimerization with Synthetic Peptides Targeting an Interaction Interface. J. Biol. Chem. *290*, 25728–25744.

Jay, T.M. (2003). Dopamine: a potential substrate for synaptic plasticity and memory mechanisms. Prog. Neurobiol. *69*, 375–390.

Jenner, P., Mori, A., Hauser, R., Morelli, M., Fredholm, B.B., and Chen, J.F. (2009). Adenosine, adenosine A 2A antagonists, and Parkinson's disease. Parkinsonism Relat. Disord. *15*, 406–413.

Jerlhag, E., Egecioglu, E., Dickson, S.L., Andersson, M., Svensson, L., and Engel, J.A. (2006). Ghrelin stimulates locomotor activity and accumbal dopamine-overflow via central cholinergic systems in mice: implications for its involvement in brain reward. Addict Biol *11*, 45–54.

Jiang, H., Betancourt, L., and Smith, R.G. (2006). Ghrelin amplifies dopamine signaling by cross talk involving formation of growth hormone secretagogue receptor/dopamine receptor subtype 1 heterodimers. Mol. Endocrinol. *20*, 1772–1785.

Jockers, R., Angers, S., Da Silva, A., Benaroch, P., Strosberg, A.D., Bouvier, M., and Marullo, S. (1999). Beta(2)-adrenergic receptor down-regulation. Evidence for a pathway that does not require endocytosis. J. Biol. Chem. *274*, 28900–28908.

Joffe, M.E., Grueter, C.A., and Grueter, B.A. (2014). Biological substrates of addiction. Wiley Interdiscip Rev Cogn Sci *5*, 151–171.

Johansson, B., Halldner, L., Dunwiddie, T.V., Masino, S.A., Poelchen, W., Giménez-Llort, L., Escorihuela, R.M., Fernández-Teruel, A., Wiesenfeld-Hallin, Z., Xu, X.J., et al. (2001). Hyperalgesia, anxiety, and decreased hypoxic neuroprotection in mice lacking the adenosine A1 receptor. Proc. Natl. Acad. Sci. U.S.A. *98*, 9407–9412.

Johansson, S.M., Lindgren, E., Yang, J.-N., Herling, A.W., and Fredholm, B.B. (2008). Adenosine A1 receptors regulate lipolysis and lipogenesis in mouse adipose tissue-interactions with insulin. Eur. J. Pharmacol. *597*, 92–101.

Johnston, J.M., Aburi, M., Provasi, D., Bortolato, A., Urizar, E., Lambert, N.A., Javitch, J.A., and Filizola, M. (2011). Making structural sense of dimerization interfaces of delta opioid receptor homodimers. Biochemistry *50*, 1682–1690.

Jones, K.A., Borowsky, B., Tamm, J.A., Craig, D.A., Durkin, M.M., Dai, M., Yao, W.J., Johnson, M., Gunwaldsen, C., Huang, L.Y., et al. (1998). GABA(B) receptors function as a heteromeric assembly of the subunits GABA(B)R1 and GABA(B)R2. Nature *396*, 674–679.

de Jong, I.E.M., and de Kloet, E.R. (2004). Glucocorticoids and vulnerability to psychostimulant drugs: toward substrate and mechanism. Ann. N. Y. Acad. Sci. *1018*, 192–198.

Jonhede, S., Petersen, A., Zetterberg, M., and Karlsson, J.-O. (2010). Acute effects of the sigma-2 receptor agonist siramesine on lysosomal and extra-lysosomal proteolytic systems in lens epithelial cells. Mol. Vis. *16*, 819–827.

Jordan, B.A., and Devi, L.A. (1999). G-protein-coupled receptor heterodimerization modulates receptor function. Nature *399*, 697–700.

Josefsson, L.G. (1999). Evidence for kinship between diverse G-protein coupled receptors. Gene *239*, 333–340.

Kabbani, N., Negyessy, L., Lin, R., Goldman-Rakic, P., and Levenson, R. (2002). Interaction with neuronal calcium sensor NCS-1 mediates desensitization of the D2 dopamine receptor. J. Neurosci. *22*, 8476–8486.

Kabe, Y., Nakane, T., Koike, I., Yamamoto, T., Sugiura, Y., Harada, E., Sugase, K., Shimamura, T., Ohmura, M., Muraoka, K., et al. (2016). Haem-dependent dimerization of PGRMC1/Sigma-2 receptor facilitates cancer proliferation and chemoresistance. Nat Commun *7*, 11030.

Kalivas, P.W. (2004). Choose to study choice in addiction. Am J Psychiatry *161*, 193–194.

Kanda, T., Jackson, M.J., Smith, L.A., Pearce, R.K., Nakamura, J., Kase, H., Kuwana, Y., and Jenner, P. (2000). Combined use of the adenosine A(2A) antagonist KW-6002 with L-DOPA or with selective D1 or D2 dopamine agonists increases antiparkinsonian activity but not dyskinesia in MPTP-treated monkeys. Exp. Neurol. *162*, 321–327.

Kang, D.S., Tian, X., and Benovic, J.L. (2014). Role of β-arrestins and arrestin domain-containing proteins in G protein-coupled receptor trafficking. Curr. Opin. Cell Biol. *27*, 63–71.

Kang, Y., Zhou, X.E., Gao, X., He, Y., Liu, W., Ishchenko, A., Barty, A., White, T.A., Yefanov, O., Han, G.W., et al. (2015). Crystal structure of rhodopsin bound to arrestin by femtosecond X-ray laser. Nature *523*, 561–567.

Kapp-Barnea, Y., Melnikov, S., Shefler, I., Jeromin, A., and Sagi-Eisenberg, R. (2003). Neuronal calcium sensor-1 and phosphatidylinositol 4-kinase beta regulate IgE receptor-triggered exocytosis in cultured mast cells. J. Immunol. *171*, 5320–5327.

Kasai, R.S., and Kusumi, A. (2014). Single-molecule imaging revealed dynamic GPCR dimerization. Curr. Opin. Cell Biol. *27*, 78–86.

Kaupmann, K., Malitschek, B., Schuler, V., Heid, J., Froestl, W., Beck, P., Mosbacher, J., Bischoff, S., Kulik, A., Shigemoto, R., et al. (1998). GABA(B)-receptor subtypes assemble into functional heteromeric complexes. Nature *396*, 683–687.

Kawasaki, H., Nakayama, S., and Kretsinger, R.H. (1998). Classification and evolution of EF-hand proteins. Biometals *11*, 277–295.

Kearn, C.S., Blake-Palmer, K., Daniel, E., Mackie, K., and Glass, M. (2005). Concurrent stimulation of cannabinoid CB1 and dopamine D2 receptors enhances heterodimer formation: a mechanism for receptor cross-talk? Mol. Pharmacol. *67*, 1697–1704.

Kelly, E., Bailey, C.P., and Henderson, G. (2008). Agonist-selective mechanisms of GPCR desensitization. Br. J. Pharmacol. *153 Suppl 1*, S379-388.

Kenakin, T. (2014). What is pharmacological "affinity"? Relevance to biased agonism and antagonism. Trends Pharmacol. Sci. *35*, 434–441.

Kenakin, T., and Christopoulos, A. (2013). Signalling bias in new drug discovery: detection, quantification and therapeutic impact. Nat Rev Drug Discov *12*, 205–216.

Kenakin, T., and Miller, L.J. (2010). Seven transmembrane receptors as shapeshifting proteins: the impact of allosteric modulation and functional selectivity on new drug discovery. Pharmacol. Rev. *62*, 265–304.

Kern, A., Mavrikaki, M., Ullrich, C., Albarran-Zeckler, R., Brantley, A.F., and Smith, R.G. (2015). Hippocampal Dopamine/DRD1 Signaling Dependent on the Ghrelin Receptor. Cell *163*, 1176–1190.

Kim, H.F., and Hikosaka, O. (2015). Parallel basal ganglia circuits for voluntary and automatic behaviour to reach rewards. Brain *138*, 1776–1800.

Kim, F.J., Kovalyshyn, I., Burgman, M., Neilan, C., Chien, C.-C., and Pasternak, G.W. (2010). Sigma 1 receptor modulation of G-protein-coupled receptor signaling: potentiation of opioid transduction independent from receptor binding. Mol. Pharmacol. *77*, 695–703.

Kim, H., Lee, B.-K., Naider, F., and Becker, J.M. (2009). Identification of specific transmembrane residues and ligand-induced interface changes involved in homo-dimer formation of a yeast G protein-coupled receptor. Biochemistry *48*, 10976–10987.

Kinoshita, M., Matsui, R., Kato, S., Hasegawa, T., Kasahara, H., Isa, K., Watakabe, A., Yamamori, T., Nishimura, Y., Alstermark, B., et al. (2012). Genetic dissection of the circuit for hand dexterity in primates. Nature *487*, 235–238.

Klein Herenbrink, C., Sykes, D.A., Donthamsetti, P., Canals, M., Coudrat, T., Shonberg, J., Scammells, P.J., Capuano, B., Sexton, P.M., Charlton, S.J., et al. (2016). The role of kinetic context in apparent biased agonism at GPCRs. Nat Commun *7*, 10842.

Klotz, K.N., and Lohse, M.J. (1986). The glycoprotein nature of A1 adenosine receptors. Biochem. Biophys. Res. Commun. *140*, 406–413.

Kniazeff, J., Prézeau, L., Rondard, P., Pin, J.-P., and Goudet, C. (2011). Dimers and beyond: The functional puzzles of class C GPCRs. Pharmacol. Ther. *130*, 9–25.

Koch, W.J., Hawes, B.E., Allen, L.F., and Lefkowitz, R.J. (1994). Direct evidence that Gi-coupled receptor stimulation of mitogen-activated protein kinase is mediated by G beta gamma activation of p21ras. Proc. Natl. Acad. Sci. U.S.A. *91*, 12706–12710.

Koeltzow, T.E., Xu, M., Cooper, D.C., Hu, X.T., Tonegawa, S., Wolf, M.E., and White, F.J. (1998). Alterations in dopamine release but not dopamine autoreceptor function in dopamine D3 receptor mutant mice. J. Neurosci. *18*, 2231–2238.

Koh, P.O., Undie, A.S., Kabbani, N., Levenson, R., Goldman-Rakic, P.S., and Lidow, M.S. (2003). Up-regulation of neuronal calcium sensor-1 (NCS-1) in the prefrontal cortex of schizophrenic and bipolar patients. Proc. Natl. Acad. Sci. U.S.A. *100*, 313–317.

Kojima, M., Hosoda, H., Date, Y., Nakazato, M., Matsuo, H., and Kangawa, K. (1999). Ghrelin is a growth-hormone-releasing acylated peptide from stomach. Nature *402*, 656–660.

Kolakowski, L.F. (1994). GCRDb: a G-protein-coupled receptor database. Recept. Channels *2*, 1–7.

Kong, M.M.C., Hasbi, A., Mattocks, M., Fan, T., O'Dowd, B.F., and George, S.R. (2007). Regulation of D1 dopamine receptor trafficking and signaling by caveolin-1. Mol. Pharmacol. *72*, 1157–1170.

Koob, G.F., and Volkow, N.D. (2016). Neurobiology of addiction: a neurocircuitry analysis. Lancet Psychiatry *3*, 760–773.

Korosi, A., Veening, J.G., Kozicz, T., Henckens, M., Dederen, J., Groenink, L., van der Gugten, J., Olivier, B., and Roubos, E.W. (2006). Distribution and expression of CRF receptor 1 and 2 mRNAs in the CRF over-expressing mouse brain. Brain Res. *1072*, 46–54.

Kosten, T.R., and Domingo, C.B. (2013). Can you vaccinate against substance abuse? Expert Opin Biol Ther *13*, 1093–1097.

Kourrich, S., Hayashi, T., Chuang, J.-Y., Tsai, S.-Y., Su, T.-P., and Bonci, A. (2013). Dynamic interaction between sigma-1 receptor and Kv1.2 shapes neuronal and behavioral responses to cocaine. Cell *152*, 236–247.

Krebs, C.J., Jarvis, E.D., Chan, J., Lydon, J.P., Ogawa, S., and Pfaff, D.W. (2000). A membrane-associated progesterone-binding protein, 25-Dx, is regulated by progesterone in brain regions involved in female reproductive behaviors. Proc. Natl. Acad. Sci. U.S.A. *97*, 12816–12821.

Kreitzer, A.C., and Malenka, R.C. (2008). Striatal plasticity and basal ganglia circuit function. Neuron *60*, 543–554.

Kretsinger, R.H., and Nockolds, C.E. (1973). Carp muscle calcium-binding protein. II. Structure determination and general description. J. Biol. Chem. *248*, 3313–3326.

Krueger, K.M., Daaka, Y., Pitcher, J.A., and Lefkowitz, R.J. (1997). The role of sequestration in G protein-coupled receptor resensitization. Regulation of beta2-adrenergic receptor dephosphorylation by vesicular acidification. J. Biol. Chem. *272*, 5–8.

Kull, B., Ferré, S., Arslan, G., Svenningsson, P., Fuxe, K., Owman, C., and Fredholm, B.B. (1999). Reciprocal interactions between adenosine A2A and dopamine D2 receptors in Chinese hamster ovary cells co-transfected with the two receptors. Biochem. Pharmacol. *58*, 1035–1045.

Kuszak, A.J., Pitchiaya, S., Anand, J.P., Mosberg, H.I., Walter, N.G., and Sunahara, R.K. (2009). Purification and functional reconstitution of monomeric mu-opioid receptors: allosteric modulation of agonist binding by Gi2. J. Biol. Chem. *284*, 26732–26741.

Lanfranco, F., Motta, G., Baldi, M., Gasco, V., Grottoli, S., Benso, A., Broglio, F., and Ghigo, E. (2010). Ghrelin and anterior pituitary function. Front Horm Res *38*, 206–211.

Leach, K., and Gregory, K.J. (2016). Molecular insights into allosteric modulation of Class C G protein-coupled receptors. Pharmacol. Res.

de Lecea, L., Kilduff, T.S., Peyron, C., Gao, X., Foye, P.E., Danielson, P.E., Fukuhara, C., Battenberg, E.L., Gautvik, V.T., Bartlett, F.S., et al. (1998). The hypocretins: hypothalamus-specific peptides with neuroexcitatory activity. Proc. Natl. Acad. Sci. U.S.A. *95*, 322–327.

Lee, S.P., So, C.H., Rashid, A.J., Varghese, G., Cheng, R., Lança, A.J., O'Dowd, B.F., and George, S.R. (2004). Dopamine D1 and D2 receptor Co-activation generates a novel phospholipase C-mediated calcium signal. J. Biol. Chem. *279*, 35671–35678.

Lefkowitz, R.J. (1998). G protein-coupled receptors. III. New roles for receptor kinases and beta-arrestins in receptor signaling and desensitization. J. Biol. Chem. *273*, 18677–18680.

Leung, P.-K., Chow, K.B.S., Lau, P.-N., Chu, K.-M., Chan, C.-B., Cheng, C.H.K., and Wise, H. (2007). The truncated ghrelin receptor polypeptide (GHS-R1b) acts as a dominant-negative mutant of the ghrelin receptor. Cell. Signal. *19*, 1011–1022.

Lever, J.R., Miller, D.K., Green, C.L., Fergason-Cantrell, E.A., Watkinson, L.D., Carmack, T.L., Fan, K.-H., and Lever, S.Z. (2014). A selective sigma-2 receptor ligand antagonizes cocaine-induced hyperlocomotion in mice. Synapse *68*, 73–84.

Limbäck-Stokin, K., Korzus, E., Nagaoka-Yasuda, R., and Mayford, M. (2004). Nuclear calcium/calmodulin regulates memory consolidation. J. Neurosci. *24*, 10858–10867.

Limbird, L.E., Meyts, P.D., and Lefkowitz, R.J. (1975). Beta-adrenergic receptors: evidence for negative cooperativity. Biochem. Biophys. Res. Commun. *64*, 1160–1168.

Liu, H., and Xia, Y. (2015). Beneficial and detrimental role of adenosine signaling in diseases and therapy. J. Appl. Physiol. *119*, 1173–1182.

Liu, X., Hashimoto-Torii, K., Torii, M., Haydar, T.F., and Rakic, P. (2008). The role of ATP signaling in the migration of intermediate neuronal progenitors to the neocortical subventricular zone. Proc. Natl. Acad. Sci. U.S.A. *105*, 11802–11807.

Liu, Y., Buck, D.C., Macey, T.A., Lan, H., and Neve, K.A. (2007). Evidence that calmodulin binding to the dopamine D2 receptor enhances receptor signaling. J. Recept. Signal Transduct. Res. *27*, 47–65.

Lohse, M.J., Benovic, J.L., Caron, M.G., and Lefkowitz, R.J. (1990). Multiple pathways of rapid beta 2-adrenergic receptor desensitization. Delineation with specific inhibitors. J. Biol. Chem. *265*, 3202–3211.

Londos, C., Cooper, D.M., and Wolff, J. (1980). Subclasses of external adenosine receptors. Proc. Natl. Acad. Sci. U.S.A. *77*, 2551–2554.

Lönnroth, P., Jansson, P.A., Fredholm, B.B., and Smith, U. (1989). Microdialysis of intercellular adenosine concentration in subcutaneous tissue in humans. Am. J. Physiol. *256*, E250-255.

Lovinger, D.M., and Alvarez, V.A. (2017). Alcohol and basal ganglia circuitry: Animal models. Neuropharmacology.

Lu, M., and Wu, B. (2016). Structural studies of G protein-coupled receptors. IUBMB Life *68*, 894–903.

Lu, L., Liu, Z., Huang, M., and Zhang, Z. (2003). Dopamine-dependent responses to cocaine depend on corticotropin-releasing factor receptor subtypes. J. Neurochem. *84*, 1378–1386.

Luo, Z., Volkow, N.D., Heintz, N., Pan, Y., and Du, C. (2011). Acute cocaine induces fast activation of D1 receptor and progressive deactivation of D2 receptor striatal neurons: in vivo optical microprobe [Ca2+]i imaging. J. Neurosci. *31*, 13180–13190.

Lüscher, C. (2016). The Emergence of a Circuit Model for Addiction. Annu. Rev. Neurosci. *39*, 257–276.

Luttrell, L.M. (2005). Composition and function of g protein-coupled receptor signalsomes controlling mitogen-activated protein kinase activity. J. Mol. Neurosci. *26*, 253–264.

Luttrell, L.M., and Lefkowitz, R.J. (2002). The role of beta-arrestins in the termination and transduction of G-protein-coupled receptor signals. J. Cell. Sci. *115*, 455–465.

Luttrell, L.M., Ferguson, S.S., Daaka, Y., Miller, W.E., Maudsley, S., Della Rocca, G.J., Lin, F., Kawakatsu, H., Owada, K., Luttrell, D.K., et al. (1999). Beta-arrestin-dependent formation of beta2 adrenergic receptor-Src protein kinase complexes. Science *283*, 655–661.

MacDonald, R.L., Skerritt, J.H., and Werz, M.A. (1986). Adenosine agonists reduce voltage-dependent calcium conductance of mouse sensory neurones in cell culture. J. Physiol. (Lond.) *370*, 75–90.

Mach, R.H., Zeng, C., and Hawkins, W.G. (2013). The σ2 receptor: a novel protein for the imaging and treatment of cancer. J. Med. Chem. *56*, 7137–7160.

Magalhaes, A.C., Dunn, H., and Ferguson, S.S.G. (2012). Regulation of GPCR activity, trafficking and localization by GPCR-interacting proteins. Br. J. Pharmacol. *165*, 1717–1736.

Maggio, R., Vogel, Z., and Wess, J. (1993). Coexpression studies with mutant muscarinic/adrenergic receptors provide evidence for intermolecular "cross-talk" between G-protein-linked receptors. Proc. Natl. Acad. Sci. U.S.A. *90*, 3103–3107.

Mahler, S.V., Moorman, D.E., Smith, R.J., James, M.H., and Aston-Jones, G. (2014). Motivational activation: a unifying hypothesis of orexin/hypocretin function. Nat. Neurosci. *17*, 1298–1303.

Maillot, C., Million, M., Wei, J.Y., Gauthier, A., and Taché, Y. (2000). Peripheral corticotropin-releasing factor and stress-stimulated colonic motor activity involve type 1 receptor in rats. Gastroenterology *119*, 1569–1579.

Manglik, A., Kruse, A.C., Kobilka, T.S., Thian, F.S., Mathiesen, J.M., Sunahara, R.K., Pardo, L., Weis, W.I., Kobilka, B.K., and Granier, S. (2012). Crystal structure of the μ-opioid receptor bound to a morphinan antagonist. Nature *485*, 321–326.

Mantsch, J.R., Baker, D.A., Francis, D.M., Katz, E.S., Hoks, M.A., and Serge, J.P. (2008). Stressor- and corticotropin releasing factor-induced reinstatement and active stress-related behavioral responses are augmented following long-access cocaine self-administration by rats. Psychopharmacology (Berl.) *195*, 591–603.

Marcellino, D., Ferré, S., Casadó, V., Cortés, A., Le Foll, B., Mazzola, C., Drago, F., Saur, O., Stark, H., Soriano, A., et al. (2008). Identification of dopamine D1-D3 receptor heteromers. Indications for a role of synergistic D1-D3 receptor interactions in the striatum. J. Biol. Chem. *283*, 26016–26025.

Marcelo, K.L., Means, A.R., and York, B. (2016). The Ca(2+)/Calmodulin/CaMKK2 Axis: Nature's Metabolic CaMshaft. Trends Endocrinol. Metab. *27*, 706–718.

Margeta-Mitrovic, M., Jan, Y.N., and Jan, L.Y. (2000). A trafficking checkpoint controls GABA(B) receptor heterodimerization. Neuron *27*, 97–106.

Marinissen, M.J., and Gutkind, J.S. (2001). G-protein-coupled receptors and signaling networks: emerging paradigms. Trends Pharmacol. Sci. *22*, 368–376.

Martin, W.R., Eades, C.G., Thompson, J.A., Huppler, R.E., and Gilbert, P.E. (1976). The effects of morphine- and nalorphine- like drugs in the nondependent and morphine-dependent chronic spinal dog. J. Pharmacol. Exp. Ther. *197*, 517–532.

Martinelli, A., and Ortore, G. (2013). Molecular modeling of adenosine receptors. Meth. Enzymol. *522*, 37–59.

Martínez-Pinilla, E., Reyes-Resina, I., Oñatibia-Astibia, A., Zamarbide, M., Ricobaraza, A., Navarro, G., Moreno, E., Dopeso-Reyes, I.G., Sierra, S., Rico, A.J., et al. (2014). CB1 and GPR55 receptors are co-expressed and form heteromers in rat and monkey striatum. Exp. Neurol. *261*, 44–52.

Mary, S., Fehrentz, J.-A., Damian, M., Gaibelet, G., Orcel, H., Verdié, P., Mouillac, B., Martinez, J., Marie, J., and Banères, J.-L. (2013). Heterodimerization with Its splice variant blocks the ghrelin receptor 1a in a non-signaling conformation: a study with a purified heterodimer assembled into lipid discs. J. Biol. Chem. *288*, 24656–24665.

Mason, B.L., Wang, Q., and Zigman, J.M. (2014). The central nervous system sites mediating the orexigenic actions of ghrelin. Annu. Rev. Physiol. *76*, 519–533.

Matsukawa, N., Maki, M., Yasuhara, T., Hara, K., Yu, G., Xu, L., Kim, K.M., Morgan, J.C., Sethi, K.D., and Borlongan, C.V. (2007). Overexpression of D2/D3 receptors increases efficacy of ropinirole in chronically 6-OHDA-lesioned Parkinsonian rats. Brain Res. *1160*, 113–123.

Matsumoto, R.R., Hewett, K.L., Pouw, B., Bowen, W.D., Husbands, S.M., Cao, J.J., and Newman, A.H. (2001a). Rimcazole analogs attenuate the convulsive effects of cocaine: correlation with binding to sigma receptors rather than dopamine transporters. Neuropharmacology *41*, 878–886.

Matsumoto, R.R., McCracken, K.A., Friedman, M.J., Pouw, B., De Costa, B.R., and Bowen, W.D. (2001b). Conformationally restricted analogs of BD1008 and an antisense oligodeoxynucleotide targeting sigma1 receptors produce anti-cocaine effects in mice. Eur. J. Pharmacol. *419*, 163–174.

Matsumoto, R.R., McCracken, K.A., Pouw, B., Zhang, Y., and Bowen, W.D. (2002). Involvement of sigma receptors in the behavioral effects of cocaine: evidence from novel ligands and antisense oligodeoxynucleotides. Neuropharmacology *42*, 1043–1055.

Matsumoto, R.R., Liu, Y., Lerner, M., Howard, E.W., and Brackett, D.J. (2003). Sigma receptors: potential medications development target for anti-cocaine agents. Eur. J. Pharmacol. *469*, 1–12.

Matsumoto, R.R., Gilmore, D.L., Pouw, B., Bowen, W.D., Williams, W., Kausar, A., and Coop, A. (2004). Novel analogs of the sigma receptor ligand BD1008 attenuate cocaine-induced toxicity in mice. Eur. J. Pharmacol. *492*, 21–26.

Matsumoto, R.R., Pouw, B., Mack, A.L., Daniels, A., and Coop, A. (2007). Effects of UMB24 and (+/-)-SM 21, putative sigma2-preferring antagonists, on behavioral toxic and stimulant effects of cocaine in mice. Pharmacol. Biochem. Behav. *86*, 86–91.

Mattera, R., Pitts, B.J., Entman, M.L., and Birnbaumer, L. (1985). Guanine nucleotide regulation of a mammalian myocardial muscarinic receptor system. Evidence for homo- and heterotropic cooperativity in ligand binding analyzed by computer-assisted curve fitting. J. Biol. Chem. *260*, 7410–7421.

Mavlyutov, T.A., Epstein, M.L., Verbny, Y.I., Huerta, M.S., Zaitoun, I., Ziskind-Conhaim, L., and Ruoho, A.E. (2013). Lack of sigma-1 receptor exacerbates ALS progression in mice. Neuroscience *240*, 129–134.

May, L.T., Leach, K., Sexton, P.M., and Christopoulos, A. (2007). Allosteric modulation of G protein-coupled receptors. Annu. Rev. Pharmacol. Toxicol. *47*, 1–51.

McClure, S.M., Daw, N.D., and Montague, P.R. (2003). A computational substrate for incentive salience. Trends Neurosci. *26*, 423–428.

McCue, H.V., Haynes, L.P., and Burgoyne, R.D. (2010a). Bioinformatic analysis of CaBP/calneuron proteins reveals a family of highly conserved vertebrate Ca2+-binding proteins. BMC Res Notes *3*, 118.

McCue, H.V., Haynes, L.P., and Burgoyne, R.D. (2010b). The diversity of calcium sensor proteins in the regulation of neuronal function. Cold Spring Harb Perspect Biol *2*, a004085.

McFerran, B.W., Graham, M.E., and Burgoyne, R.D. (1998). Neuronal Ca2+ sensor 1, the mammalian homologue of frequenin, is expressed in chromaffin and PC12 cells and regulates neurosecretion from dense-core granules. J. Biol. Chem. *273*, 22768–22772.

McKay, M.M., and Morrison, D.K. (2007). Integrating signals from RTKs to ERK/MAPK. Oncogene *26*, 3113–3121.

McLellan, T.M., Caldwell, J.A., and Lieberman, H.R. (2016). A review of caffeine's effects on cognitive, physical and occupational performance. Neurosci Biobehav Rev *71*, 294–312.

McVey, M., Ramsay, D., Kellett, E., Rees, S., Wilson, S., Pope, A.J., and Milligan, G. (2001). Monitoring receptor oligomerization using time-resolved fluorescence resonance energy transfer and bioluminescence resonance energy transfer. The human delta -opioid receptor displays constitutive oligomerization at the cell surface, which is not regulated by receptor occupancy. J. Biol. Chem. *276*, 14092–14099.

Mediavilla, C., and Risco, S. (2014). [Orexin: clinical and therapeutic implications]. Rev Neurol *58*, 117–124.

Meiergerd, S.M., Patterson, T.A., and Schenk, J.O. (1993). D2 receptors may modulate the function of the striatal transporter for dopamine: kinetic evidence from studies in vitro and in vivo. J. Neurochem. *61*, 764–767.

Menkel, M., Terry, P., Pontecorvo, M., Katz, J.L., and Witkin, J.M. (1991). Selective sigma ligands block stimulant effects of cocaine. Eur. J. Pharmacol. *201*, 251–252.

Mercuri, N.B., Saiardi, A., Bonci, A., Picetti, R., Calabresi, P., Bernardi, G., and Borrelli, E. (1997). Loss of autoreceptor function in dopaminergic neurons from dopamine D2 receptor deficient mice. Neuroscience *79*, 323–327.

Mésangeau, C., Narayanan, S., Green, A.M., Shaikh, J., Kaushal, N., Viard, E., Xu, Y.-T., Fishback, J.A., Poupaert, J.H., Matsumoto, R.R., et al. (2008). Conversion of a highly selective sigma-1 receptor-ligand to sigma-2 receptor preferring ligands with anticocaine activity. J. Med. Chem. *51*, 1482–1486.

Messina, A., De Fusco, C., Monda, V., Esposito, M., Moscatelli, F., Valenzano, A., Carotenuto, M., Viggiano, E., Chieffi, S., De Luca, V., et al. (2016). Role of the Orexin System on the Hypothalamus-Pituitary-Thyroid Axis. Front Neural Circuits *10*, 66.

Métayé, T., Gibelin, H., Perdrisot, R., and Kraimps, J.-L. (2005). Pathophysiological roles of G-protein-coupled receptor kinases. Cell. Signal. *17*, 917–928.

Meyer, C., Schmid, R., Scriba, P.C., and Wehling, M. (1996). Purification and partial sequencing of high-affinity progesterone-binding site(s) from porcine liver membranes. Eur. J. Biochem. *239*, 726–731.

Miczek, K.A., and Yoshimura, H. (1982). Disruption of primate social behavior by d-amphetamine and cocaine: differential antagonism by antipsychotics. Psychopharmacology (Berl.) *76*, 163–171.

Miczek, K.A., Yap, J.J., and Covington, H.E. (2008). Social stress, therapeutics and drug abuse: preclinical models of escalated and depressed intake. Pharmacol. Ther. *120*, 102–128.

Mifsud, W., and Bateman, A. (2002). Membrane-bound progesterone receptors contain a cytochrome b5-like ligand-binding domain. Genome Biol. *3*, RESEARCH0068.

Mikhaylova, M., Sharma, Y., Reissner, C., Nagel, F., Aravind, P., Rajini, B., Smalla, K.-H., Gundelfinger, E.D., and Kreutz, M.R. (2006). Neuronal Ca2+ signaling via caldendrin and calneurons. Biochim. Biophys. Acta *1763*, 1229–1237.

Mikhaylova, M., Reddy, P.P., Munsch, T., Landgraf, P., Suman, S.K., Smalla, K.-H., Gundelfinger, E.D., Sharma, Y., and Kreutz, M.R. (2009). Calneurons provide a calcium threshold for trans-Golgi network to plasma membrane trafficking. Proc. Natl. Acad. Sci. U.S.A. *106*, 9093–9098.

Mikhaylova, M., Hradsky, J., and Kreutz, M.R. (2011). Between promiscuity and specificity: novel roles of EF-hand calcium sensors in neuronal Ca2+ signalling. J. Neurochem. *118*, 695–713.

Miller, E.K., Freedman, D.J., and Wallis, J.D. (2002). The prefrontal cortex: categories, concepts and cognition. Philos. Trans. R. Soc. Lond., B, Biol. Sci. *357*, 1123–1136.

Milligan, G., and Bouvier, M. (2005). Methods to monitor the quaternary structure of G protein-coupled receptors. FEBS J. *272*, 2914–2925.

Milligan, G., and Kostenis, E. (2006). Heterotrimeric G-proteins: a short history. Br. J. Pharmacol. *147 Suppl 1*, S46-55.

Min, L., Strushkevich, N.V., Harnastai, I.N., Iwamoto, H., Gilep, A.A., Takemori, H., Usanov, S.A., Nonaka, Y., Hori, H., Vinson, G.P., et al. (2005). Molecular identification of adrenal inner zone antigen as a heme-binding protein. FEBS J. *272*, 5832–5843.

Missale, C., Nash, S.R., Robinson, S.W., Jaber, M., and Caron, M.G. (1998). Dopamine receptors: from structure to function. Physiol. Rev. *78*, 189–225.

Miura, S.-I., Karnik, S.S., and Saku, K. (2005). Constitutively active homo-oligomeric angiotensin II type 2 receptor induces cell signaling independent of receptor conformation and ligand stimulation. J. Biol. Chem. *280*, 18237–18244.

Mizuno, Y., Kondo, T., and Japanese Istradefylline Study Group (2013). Adenosine A2A receptor antagonist istradefylline reduces daily OFF time in Parkinson's disease. Mov. Disord. *28*, 1138–1141.

Mochida, S., Few, A.P., Scheuer, T., and Catterall, W.A. (2008). Regulation of presynaptic Ca(V)2.1 channels by Ca2+ sensor proteins mediates short-term synaptic plasticity. Neuron *57*, 210–216.

Montinaro, A., Iannone, R., Pinto, A., and Morello, S. (2013). Adenosine receptors as potential targets in melanoma. Pharmacol. Res. *76*, 34–40.

Moore, K.E., and Gudelsky, G.A. (1977). Drug actions on dopamine turnover in the median eminence. Adv. Biochem. Psychopharmacol. *16*, 227–235.

Moore, C.A.C., Milano, S.K., and Benovic, J.L. (2007). Regulation of receptor trafficking by GRKs and arrestins. Annu. Rev. Physiol. *69*, 451–482.

Morales, M., and Margolis, E.B. (2017). Ventral tegmental area: cellular heterogeneity, connectivity and behaviour. Nat. Rev. Neurosci.

Moreno, E., Hoffmann, H., Gonzalez-Sepúlveda, M., Navarro, G., Casadó, V., Cortés, A., Mallol, J., Vignes, M., McCormick, P.J., Canela, E.I., et al. (2011). Dopamine D1-histamine H3 receptor heteromers provide a selective link to MAPK signaling in GABAergic neurons of the direct striatal pathway. J. Biol. Chem. *286*, 5846–5854.

Moreno, E., Moreno-Delgado, D., Navarro, G., Hoffmann, H.M., Fuentes, S., Rosell-Vilar, S., Gasperini, P., Rodríguez-Ruiz, M., Medrano, M., Mallol, J., et al. (2014). Cocaine disrupts histamine H3 receptor modulation of dopamine D1 receptor signaling: σ1-D1-H3 receptor complexes as key targets for reducing cocaine's effects. J. Neurosci. *34*, 3545–3558.

Moreno, E., Quiroz, C., Rea, W., Cai, N.-S., Mallol, J., Cortés, A., Lluís, C., Canela, E.I., Casadó, V., and Ferré, S. (2016). Functional μ-opioid-galanin receptor heteromers in the ventral tegmental area. J. Neurosci.

Mortensen, O.V., and Amara, S.G. (2003). Dynamic regulation of the dopamine transporter. Eur. J. Pharmacol. *479*, 159–170.

Nakamura, T.Y., Jeromin, A., Smith, G., Kurushima, H., Koga, H., Nakabeppu, Y., Wakabayashi, S., and Nabekura, J. (2006). Novel role of neuronal Ca2+ sensor-1 as a survival factor up-regulated in injured neurons. J. Cell Biol. *172*, 1081–1091.

Nambu, A., Tokuno, H., and Takada, M. (2002). Functional significance of the cortico-subthalamo-pallidal "hyperdirect" pathway. Neurosci. Res. *43*, 111–117.

Narita, M., Nagumo, Y., Hashimoto, S., Narita, M., Khotib, J., Miyatake, M., Sakurai, T., Yanagisawa, M., Nakamachi, T., Shioda, S., et al. (2006). Direct involvement of orexinergic systems in the activation of the mesolimbic dopamine pathway and related behaviors induced by morphine. J. Neurosci. *26*, 398–405.

Nauta, H.J., and Cole, M. (1978). Efferent projections of the subthalamic nucleus: an autoradiographic study in monkey and cat. J. Comp. Neurol. *180*, 1–16.

Navarro, G., Carriba, P., Gandía, J., Ciruela, F., Casadó, V., Cortés, A., Mallol, J., Canela, E.I., Lluis, C., and Franco, R. (2008). Detection of heteromers formed by cannabinoid CB1, dopamine D2, and adenosine A2A G-protein-coupled receptors by combining bimolecular fluorescence complementation and bioluminescence energy transfer. ScientificWorldJournal *8*, 1088–1097.

Navarro, G., Aymerich, M.S., Marcellino, D., Cortés, A., Casadó, V., Mallol, J., Canela, E.I., Agnati, L., Woods, A.S., Fuxe, K., et al. (2009). Interactions between calmodulin, adenosine A2A, and dopamine D2 receptors. J. Biol. Chem. *284*, 28058–28068.

Navarro, G., Moreno, E., Aymerich, M., Marcellino, D., McCormick, P.J., Mallol, J., Cortés, A., Casadó, V., Canela, E.I., Ortiz, J., et al. (2010). Direct involvement of sigma-1 receptors in the dopamine D1 receptor-mediated effects of cocaine. Proc. Natl. Acad. Sci. U.S.A. *107*, 18676–18681.

Navarro, G., Hradsky, J., Lluís, C., Casadó, V., McCormick, P.J., Kreutz, M.R., and Mikhaylova, M. (2012). NCS-1 associates with adenosine A(2A) receptors and modulates receptor function. Front Mol Neurosci *5*, 53.

Navarro, G., McCormick, P.J., Mallol, J., Lluís, C., Franco, R., Cortés, A., Casadó, V., Canela, E.I., and Ferré, S. (2013a). Detection of receptor heteromers involving dopamine receptors by the sequential BRET-FRET technology. Methods Mol. Biol. *964*, 95–105.

Navarro, G., Moreno, E., Bonaventura, J., Brugarolas, M., Farré, D., Aguinaga, D., Mallol, J., Cortés, A., Casadó, V., Lluís, C., et al. (2013b). Cocaine inhibits dopamine D2 receptor signaling via sigma-1-D2 receptor heteromers. PLoS ONE *8*, e61245.

Navarro, G., Aguinaga, D., Moreno, E., Hradsky, J., Reddy, P.P., Cortés, A., Mallol, J., Casadó, V., Mikhaylova, M., Kreutz, M.R., et al. (2014a). Intracellular calcium levels determine differential modulation of allosteric interactions within G protein-coupled receptor heteromers. Chem. Biol. *21*, 1546–1556.

Navarro, G., Borroto-Escuela, D.O., Fuxe, K., and Franco, R. (2014b). Potential of caveolae in the therapy of cardiovascular and neurological diseases. Front Physiol *5*, 370.

Navarro, G., Quiroz, C., Moreno-Delgado, D., Sierakowiak, A., McDowell, K., Moreno, E., Rea, W., Cai, N.-S., Aguinaga, D., Howell, L.A., et al. (2015). Orexin-corticotropin-releasing factor receptor heteromers in the ventral tegmental area as targets for cocaine. J. Neurosci. *35*, 6639–6653.

Navarro, G., Aguinaga, D., Angelats, E., Medrano, M., Moreno, E., Mallol, J., Cortés, A., Canela, E.I., Casadó, V., McCormick, P.J., et al. (2016a). A Significant Role of the Truncated Ghrelin Receptor GHS-R1b in Ghrelin-induced Signaling in Neurons. J. Biol. Chem. *291*, 13048–13062.

Navarro, G., Cordomí, A., Zelman-Femiak, M., Brugarolas, M., Moreno, E., Aguinaga, D., Perez-Benito, L., Cortés, A., Casadó, V., Mallol, J., et al. (2016b). Quaternary structure of a G-protein-coupled receptor heterotetramer in complex with Gi and Gs. BMC Biol. *14*, 26.

Nayak, P.K., Misra, A.L., and Mulé, S.J. (1976). Physiological disposition and biotransformation of (3H) cocaine in acutely and chronically treated rats. J. Pharmacol. Exp. Ther. *196*, 556–569.

Nef, S., Fiumelli, H., de Castro, E., Raes, M.B., and Nef, P. (1995). Identification of neuronal calcium sensor (NCS-1) possibly involved in the regulation of receptor phosphorylation. J. Recept. Signal Transduct. Res. *15*, 365–378.

Neubig, R.R., Spedding, M., Kenakin, T., Christopoulos, A., and International Union of Pharmacology Committee on Receptor Nomenclature and Drug Classification (2003). International Union of Pharmacology Committee on Receptor Nomenclature and Drug Classification. XXXVIII. Update on terms and symbols in quantitative pharmacology. Pharmacol. Rev. *55*, 597–606.

Ng, G.Y., O'Dowd, B.F., Lee, S.P., Chung, H.T., Brann, M.R., Seeman, P., and George, S.R. (1996). Dopamine D2 receptor dimers and receptor-blocking peptides. Biochem. Biophys. Res. Commun. *227*, 200–204.

Nutt, J.G. (1990). Levodopa-induced dyskinesia: review, observations, and speculations. Neurology *40*, 340–345.

Oades, R.D., and Halliday, G.M. (1987). Ventral tegmental (A10) system: neurobiology. 1. Anatomy and connectivity. Brain Res. *434*, 117–165.

Obeso, J.A., Rodríguez-Oroz, M.C., Benitez-Temino, B., Blesa, F.J., Guridi, J., Marin, C., and Rodriguez, M. (2008). Functional organization of the basal ganglia: therapeutic implications for Parkinson's disease. Mov. Disord. *23 Suppl 3*, S548-559.

Okada, T., and Palczewski, K. (2001). Crystal structure of rhodopsin: implications for vision and beyond. Curr. Opin. Struct. Biol. *11*, 420–426.

Okada, M., Nutt, D.J., Murakami, T., Zhu, G., Kamata, A., Kawata, Y., and Kaneko, S. (2001). Adenosine receptor subtypes modulate two major functional pathways for hippocampal serotonin release. J. Neurosci. *21*, 628–640.

Okosi, A., Brar, B.K., Chan, M., D'Souza, L., Smith, E., Stephanou, A., Latchman, D.S., Chowdrey, H.S., and Knight, R.A. (1998). Expression and protective effects of urocortin in cardiac myocytes. Neuropeptides *32*, 167–171.

Oldham, W.M., and Hamm, H.E. (2008). Heterotrimeric G protein activation by G-protein-coupled receptors. Nat. Rev. Mol. Cell Biol. *9*, 60–71.

Orrenius, S., Zhivotovsky, B., and Nicotera, P. (2003). Regulation of cell death: the calcium-apoptosis link. Nat. Rev. Mol. Cell Biol. *4*, 552–565.

Orru, M., Bakešová, J., Brugarolas, M., Quiroz, C., Beaumont, V., Goldberg, S.R., Lluís, C., Cortés, A., Franco, R., Casadó, V., et al. (2011). Striatal pre- and postsynaptic profile of adenosine A(2A) receptor antagonists. PLoS ONE *6*, e16088.

Ostrom, R.S., and Insel, P.A. (2004). The evolving role of lipid rafts and caveolae in G protein-coupled receptor signaling: implications for molecular pharmacology. Br. J. Pharmacol. *143*, 235–245.

Ozcan, L., and Tabas, I. (2010). Pivotal role of calcium/calmodulin-dependent protein kinase II in ER stress-induced apoptosis. Cell Cycle *9*, 223–224.

Pagnussat, N., Almeida, A.S., Marques, D.M., Nunes, F., Chenet, G.C., Botton, P.H.S., Mioranzza, S., Loss, C.M., Cunha, R.A., and Porciúncula, L.O. (2015). Adenosine A(2A) receptors are necessary and sufficient to trigger memory impairment in adult mice. Br. J. Pharmacol. *172*, 3831–3845.

Pak, Y., O'Dowd, B.F., Wang, J.B., and George, S.R. (1999). Agonist-induced, G protein-dependent and -independent down-regulation of the mu opioid receptor. The receptor is a direct substrate for protein-tyrosine kinase. J. Biol. Chem. *274*, 27610–27616.

Palczewski, K., Kumasaka, T., Hori, T., Behnke, C.A., Motoshima, H., Fox, B.A., Le Trong, I., Teller, D.C., Okada, T., Stenkamp, R.E., et al. (2000). Crystal structure of rhodopsin: A G protein-coupled receptor. Science *289*, 739–745.

Palmer, T.M., Gettys, T.W., and Stiles, G.L. (1995). Differential interaction with and regulation of multiple G-proteins by the rat A3 adenosine receptor. J. Biol. Chem. *270*, 16895–16902.

Pandalaneni, S., Karuppiah, V., Saleem, M., Haynes, L.P., Burgoyne, R.D., Mayans, O., Derrick, J.P., and Lian, L.-Y. (2015). Neuronal Calcium Sensor-1 Binds the D2 Dopamine Receptor and G-protein-coupled Receptor Kinase 1 (GRK1) Peptides Using Different Modes of Interactions. J. Biol. Chem. *290*, 18744–18756.

Pandey, P., Mersha, M.D., and Dhillon, H.S. (2013). A synergistic approach towards understanding the functional significance of dopamine receptor interactions. J Mol Signal *8*, 13.

Paradis, J.S., Ly, S., Blondel-Tepaz, É., Galan, J.A., Beautrait, A., Scott, M.G.H., Enslen, H., Marullo, S., Roux, P.P., and Bouvier, M. (2015). Receptor sequestration in response to β-arrestin-2 phosphorylation by ERK1/2 governs steady-state levels of GPCR cell-surface expression. Proc. Natl. Acad. Sci. U.S.A. *112*, E5160-5168.

Park, P.S.-H., Lodowski, D.T., and Palczewski, K. (2008). Activation of G protein-coupled receptors: beyond two-state models and tertiary conformational changes. Annu. Rev. Pharmacol. Toxicol. *48*, 107–141.

Parmar, V.K., Grinde, E., Mazurkiewicz, J.E., and Herrick-Davis, K. (2016). Beta2-adrenergic receptor homodimers: Role of transmembrane domain 1 and helix 8 in dimerization and cell surface expression. Biochim. Biophys. Acta.

Parton, R.G., and del Pozo, M.A. (2013). Caveolae as plasma membrane sensors, protectors and organizers. Nat. Rev. Mol. Cell Biol. *14*, 98–112.

Pascoli, V., Terrier, J., Hiver, A., and Lüscher, C. (2015). Sufficiency of Mesolimbic Dopamine Neuron Stimulation for the Progression to Addiction. Neuron *88*, 1054–1066.

Paspalas, C.D., Wang, M., and Arnsten, A.F.T. (2013). Constellation of HCN channels and cAMP regulating proteins in dendritic spines of the primate prefrontal cortex: potential substrate for working memory deficits in schizophrenia. Cereb. Cortex *23*, 1643–1654.

Paulmurugan, R., and Gambhir, S.S. (2003). Monitoring protein-protein interactions using split synthetic renilla luciferase protein-fragment-assisted complementation. Anal. Chem. *75*, 1584–1589.

Pavlos, N.J., and Friedman, P.A. (2016). GPCR Signaling and Trafficking: The Long and Short of It. Trends Endocrinol. Metab.

Pei, L., Li, S., Wang, M., Diwan, M., Anisman, H., Fletcher, P.J., Nobrega, J.N., and Liu, F. (2010). Uncoupling the dopamine D1-D2 receptor complex exerts antidepressant-like effects. Nat. Med. *16*, 1393–1395.

Peluso, J.J., Pappalardo, A., Losel, R., and Wehling, M. (2005). Expression and function of PAIRBP1 within gonadotropin-primed immature rat ovaries: PAIRBP1 regulation of granulosa and luteal cell viability. Biol. Reprod. *73*, 261–270.

Peluso, J.J., Lodde, V., and Liu, X. (2012). Progesterone regulation of progesterone receptor membrane component 1 (PGRMC1) sumoylation and transcriptional activity in spontaneously immortalized granulosa cells. Endocrinology *153*, 3929–3939.

Perello, M., Sakata, I., Birnbaum, S., Chuang, J.-C., Osborne-Lawrence, S., Rovinsky, S.A., Woloszyn, J., Yanagisawa, M., Lutter, M., and Zigman, J.M. (2010). Ghrelin increases the rewarding value of high-fat diet in an orexin-dependent manner. Biol. Psychiatry *67*, 880–886.

Perreault, M.L., Hasbi, A., Shen, M.Y.F., Fan, T., Navarro, G., Fletcher, P.J., Franco, R., Lanciego, J.L., and George, S.R. (2016). Disruption of a dopamine receptor complex amplifies the actions of cocaine. Eur Neuropsychopharmacol *26*, 1366–1377.

Pettit, H.O., and Justice, J.B. (1991). Effect of dose on cocaine self-administration behavior and dopamine levels in the nucleus accumbens. Brain Res. *539*, 94–102.

Peyron, C., Tighe, D.K., van den Pol, A.N., de Lecea, L., Heller, H.C., Sutcliffe, J.G., and Kilduff, T.S. (1998). Neurons containing hypocretin (orexin) project to multiple neuronal systems. J. Neurosci. *18*, 9996–10015.

Pfleger, K.D.G., and Eidne, K.A. (2005). Monitoring the formation of dynamic G-protein-coupled receptor-protein complexes in living cells. Biochem. J. *385*, 625–637.

Phatarpekar, P.V., Wen, J., and Xia, Y. (2010). Role of adenosine signaling in penile erection and erectile disorders. J Sex Med *7*, 3553–3564.

Phillipson, O.T. (1979). The cytoarchitecture of the interfascicular nucleus and ventral tegmental area of Tsai in the rat. J. Comp. Neurol. *187*, 85–98.

Pierce, K.L., and Lefkowitz, R.J. (2001). Classical and new roles of beta-arrestins in the regulation of G-protein-coupled receptors. Nat. Rev. Neurosci. *2*, 727–733.

Pierce, K.D., Furlong, T.J., Selbie, L.A., and Shine, J. (1992). Molecular cloning and expression of an adenosine A2b receptor from human brain. Biochem. Biophys. Res. Commun. *187*, 86–93.

Pin, J.-P., Galvez, T., and Prézeau, L. (2003). Evolution, structure, and activation mechanism of family 3/C G-protein-coupled receptors. Pharmacol. Ther. *98*, 325–354.

Pintsuk, J., Borroto-Escuela, D.O., Pomierny, B., Wydra, K., Zaniewska, M., Filip, M., and Fuxe, K. (2016). Cocaine self-administration differentially affects allosteric A2A-D2 receptor-receptor interactions in the striatum. Relevance for cocaine use disorder. Pharmacol. Biochem. Behav. *144*, 85–91.

Polter, A.M., and Kauer, J.A. (2014). Stress and VTA synapses: implications for addiction and depression. Eur. J. Neurosci. *39*, 1179–1188.

Polter, A.M., Barcomb, K., Chen, R.W., Dingess, P.M., Graziane, N.M., Brown, T.E., and Kauer, J.A. (2017). Constitutive activation of kappa opioid receptors at ventral tegmental area inhibitory synapses following acute stress. Elife *6*.

Pongs, O., Lindemeier, J., Zhu, X.R., Theil, T., Engelkamp, D., Krah-Jentgens, I., Lambrecht, H.G., Koch, K.W., Schwemer, J., and Rivosecchi, R. (1993). Frequenin--a novel calcium-binding protein that modulates synaptic efficacy in the Drosophila nervous system. Neuron *11*, 15–28.

Probst, W.C., Snyder, L.A., Schuster, D.I., Brosius, J., and Sealfon, S.C. (1992). Sequence alignment of the G-protein coupled receptor superfamily. DNA Cell Biol. *11*, 1–20.

Racioppi, L., and Means, A.R. (2008). Calcium/calmodulin-dependent kinase IV in immune and inflammatory responses: novel routes for an ancient traveller. Trends Immunol. *29*, 600–607.

Radwanska, K., Caboche, J., and Kaczmarek, L. (2005). Extracellular signal-regulated kinases (ERKs) modulate cocaine-induced gene expression in the mouse amygdala. Eur. J. Neurosci. *22*, 939–948.

Ramlackhansingh, A.F., Bose, S.K., Ahmed, I., Turkheimer, F.E., Pavese, N., and Brooks, D.J. (2011). Adenosine 2A receptor availability in dyskinetic and nondyskinetic patients with Parkinson disease. Neurology *76*, 1811–1816.

Rana, B.K., Shiina, T., and Insel, P.A. (2001). Genetic variations and polymorphisms of G protein-coupled receptors: functional and therapeutic implications. Annu. Rev. Pharmacol. Toxicol. *41*, 593–624.

Ranjan, R., Gupta, P., and Shukla, A.K. (2016). GPCR Signaling: β-arrestins Kiss and Remember. Curr. Biol. *26*, R285-288.

Rasmussen, S.G.F., DeVree, B.T., Zou, Y., Kruse, A.C., Chung, K.Y., Kobilka, T.S., Thian, F.S., Chae, P.S., Pardon, E., Calinski, D., et al. (2011). Crystal structure of the β2 adrenergic receptor-Gs protein complex. Nature *477*, 549–555.

Reeves, S., Brown, R., Howard, R., and Grasby, P. (2009). Increased striatal dopamine (D2/D3) receptor availability and delusions in Alzheimer disease. Neurology *72*, 528–534.

Ribeiro, J.A., Sebastião, A.M., and de Mendonça, A. (2002). Adenosine receptors in the nervous system: pathophysiological implications. Prog. Neurobiol. *68*, 377–392.

Ribeiro, J.A., Sebastiao, A.M., and de Mendonca, A. (2003). Participation of adenosine receptors in neuroprotection. Drug News Perspect. *16*, 80–86.

Richardson, N.R., and Gratton, A. (1998). Changes in medial prefrontal cortical dopamine levels associated with response-contingent food reward: an electrochemical study in rat. J. Neurosci. *18*, 9130–9138.

Ritz, M.C., Lamb, R.J., Goldberg, S.R., and Kuhar, M.J. (1987). Cocaine receptors on dopamine transporters are related to self-administration of cocaine. Science *237*, 1219–1223.

Rivkees, S.A., Barbhaiya, H., and IJzerman, A.P. (1999). Identification of the adenine binding site of the human A1 adenosine receptor. J. Biol. Chem. *274*, 3617–3621.

Roberts, D.C., Corcoran, M.E., and Fibiger, H.C. (1977). On the role of ascending catecholaminergic systems in intravenous self-administration of cocaine. Pharmacol. Biochem. Behav. *6*, 615–620.

Robinson, T.E., and Kolb, B. (1999). Alterations in the morphology of dendrites and dendritic spines in the nucleus accumbens and prefrontal cortex following repeated treatment with amphetamine or cocaine. Eur. J. Neurosci. *11*, 1598–1604.

Robinson, T.E., Gorny, G., Mitton, E., and Kolb, B. (2001). Cocaine self-administration alters the morphology of dendrites and dendritic spines in the nucleus accumbens and neocortex. Synapse *39*, 257–266.

Robson, M.J., Noorbakhsh, B., Seminerio, M.J., and Matsumoto, R.R. (2012). Sigma-1 receptors: potential targets for the treatment of substance abuse. Curr. Pharm. Des. *18*, 902–919.

Rocha, B.A. (2003). Stimulant and reinforcing effects of cocaine in monoamine transporter knockout mice. Eur. J. Pharmacol. *479*, 107–115.

Rocheville, M., Lange, D.C., Kumar, U., Patel, S.C., Patel, R.C., and Patel, Y.C. (2000a). Receptors for dopamine and somatostatin: formation of hetero-oligomers with enhanced functional activity. Science *288*, 154–157.

Rocheville, M., Lange, D.C., Kumar, U., Sasi, R., Patel, R.C., and Patel, Y.C. (2000b). Subtypes of the somatostatin receptor assemble as functional homo- and heterodimers. J. Biol. Chem. *275*, 7862–7869.

Rodaros, D., Caruana, D.A., Amir, S., and Stewart, J. (2007). Corticotropin-releasing factor projections from limbic forebrain and paraventricular nucleus of the hypothalamus to the region of the ventral tegmental area. Neuroscience *150*, 8–13.

Rohe, H.J., Ahmed, I.S., Twist, K.E., and Craven, R.J. (2009). PGRMC1 (progesterone receptor membrane component 1): a targetable protein with multiple functions in steroid signaling, P450 activation and drug binding. Pharmacol. Ther. *121*, 14–19.

Romano, C., Yang, W.L., and O'Malley, K.L. (1996). Metabotropic glutamate receptor 5 is a disulfide-linked dimer. J. Biol. Chem. *271*, 28612–28616.

Romano, C., Miller, J.K., Hyrc, K., Dikranian, S., Mennerick, S., Takeuchi, Y., Goldberg, M.P., and O'Malley, K.L. (2001). Covalent and noncovalent interactions mediate metabotropic glutamate receptor mGlu5 dimerization. Mol. Pharmacol. *59*, 46–53.

Romieu, P., Martin-Fardon, R., and Maurice, T. (2000). Involvement of the sigma1 receptor in the cocaine-induced conditioned place preference. Neuroreport *11*, 2885–2888.

Romieu, P., Phan, V.L., Martin-Fardon, R., and Maurice, T. (2002). Involvement of the sigma(1) receptor in cocaine-induced conditioned place preference: possible dependence on dopamine uptake blockade. Neuropsychopharmacology *26*, 444–455.

Root, D.H., Mejias-Aponte, C.A., Zhang, S., Wang, H.-L., Hoffman, A.F., Lupica, C.R., and Morales, M. (2014). Single rodent mesohabenular axons release glutamate and GABA. Nat. Neurosci. *17*, 1543–1551.

Rosenbaum, D.M., Rasmussen, S.G.F., and Kobilka, B.K. (2009). The structure and function of G-protein-coupled receptors. Nature *459*, 356–363.

Ross, S.B., and Renyi, A.L. (1967). Inhibition of the uptake of tritiated catecholamines by antidepressant and related agents. Eur. J. Pharmacol. *2*, 181–186.

Ross, G.A., Mihok, M.L., and Murrant, C.L. (2013). Extracellular adenosine initiates rapid arteriolar vasodilation induced by a single skeletal muscle contraction in hamster cremaster muscle. Acta Physiol (Oxf) *208*, 74–87.

Rouge-Pont, F., Usiello, A., Benoit-Marand, M., Gonon, F., Piazza, P.V., and Borrelli, E. (2002). Changes in extracellular dopamine induced by morphine and cocaine: crucial control by D2 receptors. J. Neurosci. *22*, 3293–3301.

Russell, S.H., Small, C.J., Sunter, D., Morgan, I., Dakin, C.L., Cohen, M.A., and Bloom, S.R. (2002). Chronic intraparaventricular nuclear administration of orexin A in male rats does not alter thyroid axis or uncoupling protein-1 in brown adipose tissue. Regul. Pept. *104*, 61–68.

Saal, D., Dong, Y., Bonci, A., and Malenka, R.C. (2003). Drugs of abuse and stress trigger a common synaptic adaptation in dopamine neurons. Neuron *37*, 577–582.

Sakmar, T.P. (1998). Rhodopsin: a prototypical G protein-coupled receptor. Prog. Nucleic Acid Res. Mol. Biol. *59*, 1–34.

Sakurai, T. (2007). The neural circuit of orexin (hypocretin): maintaining sleep and wakefulness. Nat. Rev. Neurosci. *8*, 171–181.

Sakurai, T. (2014). The role of orexin in motivated behaviours. Nat. Rev. Neurosci. *15*, 719–731.

Sakurai, T., Amemiya, A., Ishii, M., Matsuzaki, I., Chemelli, R.M., Tanaka, H., Williams, S.C., Richardson, J.A., Kozlowski, G.P., Wilson, S., et al. (1998). Orexins and orexin receptors: a family of hypothalamic neuropeptides and G protein-coupled receptors that regulate feeding behavior. Cell *92*, 573–585.

Salahpour, A., Angers, S., Mercier, J.-F., Lagacé, M., Marullo, S., and Bouvier, M. (2004). Homodimerization of the beta2-adrenergic receptor as a prerequisite for cell surface targeting. J. Biol. Chem. *279*, 33390–33397.

Sarnyai, Z., Shaham, Y., and Heinrichs, S.C. (2001). The role of corticotropin-releasing factor in drug addiction. Pharmacol. Rev. *53*, 209–243.

Saura, C.A., Mallol, J., Canela, E.I., Lluis, C., and Franco, R. (1998). Adenosine deaminase and A1 adenosine receptors internalize together following agonist-induced receptor desensitization. J. Biol. Chem. *273*, 17610–17617.

Scammell, T.E., and Winrow, C.J. (2011). Orexin receptors: pharmacology and therapeutic opportunities. Annu. Rev. Pharmacol. Toxicol. *51*, 243–266.

Scarselli, M., Armogida, M., Chiacchio, S., DeMontis, M.G., Colzi, A., Corsini, G.U., and Maggio, R. (2000). Reconstitution of functional dopamine D(2s) receptor by co-expression of amino- and carboxyl-terminal receptor fragments. Eur. J. Pharmacol. *397*, 291–296.

Schapira, A.H.V., Bezard, E., Brotchie, J., Calon, F., Collingridge, G.L., Ferger, B., Hengerer, B., Hirsch, E., Jenner, P., Le Novère, N., et al. (2006). Novel pharmacological targets for the treatment of Parkinson's disease. Nat Rev Drug Discov *5*, 845–854.

Scheerer, P., Park, J.H., Hildebrand, P.W., Kim, Y.J., Krauss, N., Choe, H.-W., Hofmann, K.P., and Ernst, O.P. (2008). Crystal structure of opsin in its G-protein-interacting conformation. Nature *455*, 497–502.

Schiffmann, S.N., Fisone, G., Moresco, R., Cunha, R.A., and Ferré, S. (2007). Adenosine A2A receptors and basal ganglia physiology. Prog. Neurobiol. *83*, 277–292.

Schindler, C.W., and Goldberg, S.R. (2012). Accelerating cocaine metabolism as an approach to the treatment of cocaine abuse and toxicity. Future Med Chem *4*, 163–175.

Schlötzer-Schrehardt, U., Zenkel, M., Decking, U., Haubs, D., Kruse, F.E., Jünemann, A., Coca-Prados, M., and Naumann, G.O.H. (2005). Selective upregulation of the A3 adenosine receptor in eyes with pseudoexfoliation syndrome and glaucoma. Invest. Ophthalmol. Vis. Sci. *46*, 2023–2034.

Schmidt, H.R., Zheng, S., Gurpinar, E., Koehl, A., Manglik, A., and Kruse, A.C. (2016). Crystal structure of the human σ1 receptor. Nature *532*, 527–530.

Schröder, B., Schlumbohm, C., Kaune, R., and Breves, G. (1996). Role of calbindin-D9k in buffering cytosolic free Ca2+ ions in pig duodenal enterocytes. J. Physiol. (Lond.) *492 (Pt 3)*, 715–722.

Schulte, G., and Fredholm, B.B. (2003). Signalling from adenosine receptors to mitogen-activated protein kinases. Cell. Signal. *15*, 813–827.

Schultz, W., Dayan, P., and Montague, P.R. (1997). A neural substrate of prediction and reward. Science *275*, 1593–1599.

Schwaller, B. (2009). The continuing disappearance of "pure" Ca2+ buffers. Cell. Mol. Life Sci. *66*, 275–300.

Sebastião, A.M., de Mendonca, A., Moreira, T., and Ribeiro, J.A. (2001). Activation of synaptic NMDA receptors by action potential-dependent release of transmitter during hypoxia impairs recovery of synaptic transmission on reoxygenation. J. Neurosci. *21*, 8564–8571.

Seidenbecher, C.I., Langnaese, K., Sanmartí-Vila, L., Boeckers, T.M., Smalla, K.H., Sabel, B.A., Garner, C.C., Gundelfinger, E.D., and Kreutz, M.R. (1998). Caldendrin, a novel neuronal calcium-binding protein confined to the somato-dendritic compartment. J. Biol. Chem. *273*, 21324–21331.

Seifert, R., and Wenzel-Seifert, K. (2002). Constitutive activity of G-protein-coupled receptors: cause of disease and common property of wild-type receptors. Naunyn Schmiedebergs Arch. Pharmacol. *366*, 381–416.

Sellings, L.H.L., and Clarke, P.B.S. (2003). Segregation of amphetamine reward and locomotor stimulation between nucleus accumbens medial shell and core. J. Neurosci. *23*, 6295–6303.

Sexton, P.M., Poyner, D.R., Simms, J., Christopoulos, A., and Hay, D.L. (2009). Modulating receptor function through RAMPs: can they represent drug targets in themselves? Drug Discov. Today *14*, 413–419.

Shen, M., Zhang, N., Zheng, S., Zhang, W.-B., Zhang, H.-M., Lu, Z., Su, Q.P., Sun, Y., Ye, K., and Li, X.-D. (2016). Calmodulin in complex with the first IQ motif of myosin-5a functions as an intact calcium sensor. Proc. Natl. Acad. Sci. U.S.A. *113*, E5812–E5820.

Sheng, M., and Hoogenraad, C.C. (2007). The postsynaptic architecture of excitatory synapses: a more quantitative view. Annu. Rev. Biochem. *76*, 823–847.

Shonberg, J., Kling, R.C., Gmeiner, P., and Löber, S. (2015). GPCR crystal structures: Medicinal chemistry in the pocket. Bioorg. Med. Chem. *23*, 3880–3906.

Shorter, D., Nielsen, D.A., Huang, W., Harding, M.J., Hamon, S.C., and Kosten, T.R. (2013). Pharmacogenetic randomized trial for cocaine abuse: disulfiram and α1A-adrenoceptor gene variation. Eur Neuropsychopharmacol *23*, 1401–1407.

Shukla, A.K., Westfield, G.H., Xiao, K., Reis, R.I., Huang, L.-Y., Tripathi-Shukla, P., Qian, J., Li, S., Blanc, A., Oleskie, A.N., et al. (2014). Visualization of arrestin recruitment by a G-protein-coupled receptor. Nature *512*, 218–222.

Silver, R., and Balsam, P. (2010). Oscillators entrained by food and the emergence of anticipatory timing behaviors. Sleep Biol Rhythms *8*, 120–136.

Singer, B.F., Bryan, M.A., Popov, P., Robinson, T.E., and Aragona, B.J. (2017). Rapid induction of dopamine sensitization in the nucleus accumbens shell induced by a single injection of cocaine. Behav. Brain Res. *324*, 66–70.

Sinha, R. (2008). Chronic stress, drug use, and vulnerability to addiction. Ann. N. Y. Acad. Sci. *1141*, 105–130.

Sippy, T., Cruz-Martín, A., Jeromin, A., and Schweizer, F.E. (2003). Acute changes in short-term plasticity at synapses with elevated levels of neuronal calcium sensor-1. Nat. Neurosci. *6*, 1031–1038.

Skibicka, K.P., Hansson, C., Alvarez-Crespo, M., Friberg, P.A., and Dickson, S.L. (2011). Ghrelin directly targets the ventral tegmental area to increase food motivation. Neuroscience *180*, 129–137.

Soares-Cunha, C., Coimbra, B., Sousa, N., and Rodrigues, A.J. (2016). Reappraising striatal D1- and D2-neurons in reward and aversion. Neurosci Biobehav Rev *68*, 370–386.

Söderberg, O., Gullberg, M., Jarvius, M., Ridderstråle, K., Leuchowius, K.-J., Jarvius, J., Wester, K., Hydbring, P., Bahram, F., Larsson, L.-G., et al. (2006). Direct observation of individual endogenous protein complexes in situ by proximity ligation. Nat. Methods *3*, 995–1000.

Sonntag, K.C., Brenhouse, H.C., Freund, N., Thompson, B.S., Puhl, M., and Andersen, S.L. (2014). Viral over-expression of D1 dopamine receptors in the prefrontal cortex increase high-risk behaviors in adults: comparison with adolescents. Psychopharmacology (Berl.) *231*, 1615–1626.

Sorensen, A.B., Søndergaard, M.T., and Overgaard, M.T. (2013). Calmodulin in a heartbeat. FEBS J. *280*, 5511–5532.

Sotnikova, T.D., Beaulieu, J.-M., Gainetdinov, R.R., and Caron, M.G. (2006). Molecular biology, pharmacology and functional role of the plasma membrane dopamine transporter. CNS Neurol Disord Drug Targets *5*, 45–56.

Spano, P.F., Govoni, S., and Trabucchi, M. (1978). Studies on the pharmacological properties of dopamine receptors in various areas of the central nervous system. Adv. Biochem. Psychopharmacol. *19*, 155–165.

Spina, M., Merlo-Pich, E., Chan, R.K., Basso, A.M., Rivier, J., Vale, W., and Koob, G.F. (1996). Appetite-suppressing effects of urocortin, a CRF-related neuropeptide. Science *273*, 1561–1564.

Stanley, S., Wynne, K., McGowan, B., and Bloom, S. (2005). Hormonal regulation of food intake. Physiol. Rev. *85*, 1131–1158.

Steketee, J.D., and Kalivas, P.W. (2011). Drug wanting: behavioral sensitization and relapse to drug-seeking behavior. Pharmacol. Rev. *63*, 348–365.

Stelly, C.E., Pomrenze, M.B., Cook, J.B., and Morikawa, H. (2016). Repeated social defeat stress enhances glutamatergic synaptic plasticity in the VTA and cocaine place conditioning. Elife *5*.

Stone, J.M., Arstad, E., Erlandsson, K., Waterhouse, R.N., Ell, P.J., and Pilowsky, L.S. (2006). [123I]TPCNE--a novel SPET tracer for the sigma-1 receptor: first human studies and in vivo haloperidol challenge. Synapse *60*, 109–117.

Stryer, L. (1978). Fluorescence energy transfer as a spectroscopic ruler. Annu. Rev. Biochem. *47*, 819–846.

Stuber, G.D., Hnasko, T.S., Britt, J.P., Edwards, R.H., and Bonci, A. (2010). Dopaminergic terminals in the nucleus accumbens but not the dorsal striatum corelease glutamate. J. Neurosci. *30*, 8229–8233.

Su, T.-P., Hayashi, T., Maurice, T., Buch, S., and Ruoho, A.E. (2010). The sigma-1 receptor chaperone as an inter-organelle signaling modulator. Trends Pharmacol. Sci. *31*, 557–566.

Sun, H., Shi, M., Zhang, W., Zheng, Y.-M., Xu, Y.-Z., Shi, J.-J., Liu, T., Gunosewoyo, H., Pang, T., Gao, Z.-B., et al. (2016). Development of Novel Alkoxyisoxazoles as Sigma-1 Receptor Antagonists with Antinociceptive Efficacy. J. Med. Chem. *59*, 6329–6343.

Sun, Y., Shi, N., Li, H., Liu, K., Zhang, Y., Chen, W., and Sun, X. (2014). Ghrelin suppresses Purkinje neuron P-type Ca(2+) channels via growth hormone secretagogue type 1a receptor, the βγ subunits of Go-protein, and protein kinase a pathway. Cell. Signal. *26*, 2530–2538.

Syrovatkina, V., Alegre, K.O., Dey, R., and Huang, X.-Y. (2016). Regulation, Signaling, and Physiological Functions of G-Proteins. J. Mol. Biol. *428*, 3850–3868.

Tadross, M.R., Dick, I.E., and Yue, D.T. (2008). Mechanism of local and global Ca2+ sensing by calmodulin in complex with a Ca2+ channel. Cell *133*, 1228–1240.

Takakusaki, K., Saitoh, K., Harada, H., and Kashiwayanagi, M. (2004). Role of basal ganglia-brainstem pathways in the control of motor behaviors. Neurosci. Res. *50*, 137–151.

Tecuapetla, F., Patel, J.C., Xenias, H., English, D., Tadros, I., Shah, F., Berlin, J., Deisseroth, K., Rice, M.E., Tepper, J.M., et al. (2010). Glutamatergic signaling by mesolimbic dopamine neurons in the nucleus accumbens. J. Neurosci. *30*, 7105–7110.

Terrillon, S., and Bouvier, M. (2004). Roles of G-protein-coupled receptor dimerization. EMBO Rep. *5*, 30–34.

Terui, K., Higashiyama, A., Horiba, N., Furukawa, K.I., Motomura, S., and Suda, T. (2001). Coronary vasodilation and positive inotropism by urocortin in the isolated rat heart. J. Endocrinol. *169*, 177–183.

Thomsen, A.R.B., Plouffe, B., Cahill, T.J., Shukla, A.K., Tarrasch, J.T., Dosey, A.M., Kahsai, A.W., Strachan, R.T., Pani, B., Mahoney, J.P., et al. (2016). GPCR-G Protein-β-Arrestin Super-Complex Mediates Sustained G Protein Signaling. Cell *166*, 907–919.

Tozzi, A., de Iure, A., Di Filippo, M., Tantucci, M., Costa, C., Borsini, F., Ghiglieri, V., Giampà, C., Fusco, F.R., Picconi, B., et al. (2011). The distinct role of medium spiny neurons and cholinergic interneurons in the D_2/A_2A receptor interaction in the striatum: implications for Parkinson's disease. J. Neurosci. *31*, 1850–1862.

Trejo, J., Hammes, S.R., and Coughlin, S.R. (1998). Termination of signaling by protease-activated receptor-1 is linked to lysosomal sorting. Proc. Natl. Acad. Sci. U.S.A. *95*, 13698–13702.

Trifilieff, P., Rives, M.-L., Urizar, E., Piskorowski, R.A., Vishwasrao, H.D., Castrillon, J., Schmauss, C., Slättman, M., Gullberg, M., and Javitch, J.A. (2011). Detection of antigen interactions ex vivo by proximity ligation assay: endogenous dopamine D2-adenosine A2A receptor complexes in the striatum. BioTechniques *51*, 111–118.

Trillo, L., Das, D., Hsieh, W., Medina, B., Moghadam, S., Lin, B., Dang, V., Sanchez, M.M., De Miguel, Z., Ashford, J.W., et al. (2013). Ascending monoaminergic systems alterations in Alzheimer's disease. translating basic science into clinical care. Neurosci Biobehav Rev *37*, 1363–1379.

Tritsch, N.X., Oh, W.-J., Gu, C., and Sabatini, B.L. (2014). Midbrain dopamine neurons sustain inhibitory transmission using plasma membrane uptake of GABA, not synthesis. Elife *3*, e01936.

Trussell, L.O., and Jackson, M.B. (1985). Adenosine-activated potassium conductance in cultured striatal neurons. Proc. Natl. Acad. Sci. U.S.A. *82*, 4857–4861.

Tsien, R.W., and Tsien, R.Y. (1990). Calcium channels, stores, and oscillations. Annu. Rev. Cell Biol. *6*, 715–760.

Tunstall, B.J., and Carmack, S.A. (2016). Social Stress-Induced Alterations in CRF Signaling in the VTA Facilitate the Emergence of Addiction-like Behavior. J. Neurosci. *36*, 8780–8782.

Turčin, A., Dolžan, V., Porcelli, S., Serretti, A., and Plesničar, B.K. (2016). Adenosine Hypothesis of Antipsychotic Drugs Revisited: Pharmacogenomics Variation in Nonacute Schizophrenia. OMICS *20*, 283–289.

Turner, J.H., Gelasco, A.K., and Raymond, J.R. (2004). Calmodulin interacts with the third intracellular loop of the serotonin 5-hydroxytryptamine1A receptor at two distinct sites: putative role in receptor phosphorylation by protein kinase C. J. Biol. Chem. *279*, 17027–17037.

Uchida, S., Soshiroda, K., Okita, E., Kawai-Uchida, M., Mori, A., Jenner, P., and Kanda, T. (2015). The adenosine A2A receptor antagonist, istradefylline enhances anti-parkinsonian activity induced by combined treatment with low doses of L-DOPA and dopamine agonists in MPTP-treated common marmosets. Eur. J. Pharmacol. *766*, 25–30.

Ujike, H., Kuroda, S., and Otsuki, S. (1996). sigma Receptor antagonists block the development of sensitization to cocaine. Eur. J. Pharmacol. *296*, 123–128.

Ulrich, C.D., Holtmann, M., and Miller, L.J. (1998). Secretin and vasoactive intestinal peptide receptors: members of a unique family of G protein-coupled receptors. Gastroenterology *114*, 382–397.

Ungless, M.A., Singh, V., Crowder, T.L., Yaka, R., Ron, D., and Bonci, A. (2003). Corticotropin-releasing factor requires CRF binding protein to potentiate NMDA receptors via CRF receptor 2 in dopamine neurons. Neuron *39*, 401–407.

Urry, E., and Landolt, H.-P. (2015). Adenosine, caffeine, and performance: from cognitive neuroscience of sleep to sleep pharmacogenetics. Curr Top Behav Neurosci *25*, 331–366.

Vale, W., Spiess, J., Rivier, C., and Rivier, J. (1981). Characterization of a 41-residue ovine hypothalamic peptide that stimulates secretion of corticotropin and beta-endorphin. Science *213*, 1394–1397.

Valjent, E., Corbillé, A.-G., Bertran-Gonzalez, J., Hervé, D., and Girault, J.-A. (2006). Inhibition of ERK pathway or protein synthesis during reexposure to drugs of abuse erases previously learned place preference. Proc. Natl. Acad. Sci. U.S.A. *103*, 2932–2937.

Vallone, D., Picetti, R., and Borrelli, E. (2000). Structure and function of dopamine receptors. Neurosci Biobehav Rev *24*, 125–132.

Van Craenenbroeck, K., Borroto-Escuela, D.O., Skieterska, K., Duchou, J., Romero-Fernandez, W., and Fuxe, K. (2014). Role of dimerization in dopamine D(4) receptor biogenesis. Curr. Protein Pept. Sci. *15*, 659–665.

Varani, K., Vincenzi, F., Targa, M., Paradiso, B., Parrilli, A., Fini, M., Lanza, G., and Borea, P.A. (2013). The stimulation of A(3) adenosine receptors reduces bone-residing breast cancer in a rat preclinical model. Eur. J. Cancer *49*, 482–491.

Vassilatis, D.K., Hohmann, J.G., Zeng, H., Li, F., Ranchalis, J.E., Mortrud, M.T., Brown, A., Rodriguez, S.S., Weller, J.R., Wright, A.C., et al. (2003). The G protein-coupled receptor repertoires of human and mouse. Proc. Natl. Acad. Sci. U.S.A. *100*, 4903–4908.

Vaupel, D.B. (1983). Naltrexone fails to antagonize the sigma effects of PCP and SKF 10,047 in the dog. Eur. J. Pharmacol. *92*, 269–274.

Vilardaga, J.-P., Nikolaev, V.O., Lorenz, K., Ferrandon, S., Zhuang, Z., and Lohse, M.J. (2008). Conformational cross-talk between alpha2A-adrenergic and mu-opioid receptors controls cell signaling. Nat. Chem. Biol. *4*, 126–131.

Villar, V.A.M., Cuevas, S., Zheng, X., and Jose, P.A. (2016). Localization and signaling of GPCRs in lipid rafts. Methods Cell Biol. *132*, 3–23.

Vischer, H.F., Castro, M., and Pin, J.-P. (2015). G Protein-Coupled Receptor Multimers: A Question Still Open Despite the Use of Novel Approaches. Mol. Pharmacol. *88*, 561–571.

Volkow, N.D., Wang, G.J., Fowler, J.S., Fischman, M., Foltin, R., Abumrad, N.N., Gatley, S.J., Logan, J., Wong, C., Gifford, A., et al. (1999). Methylphenidate and cocaine have a similar in vivo potency to block dopamine transporters in the human brain. Life Sci. *65*, PL7-12.

Volkow, N.D., Fowler, J.S., Wang, G.J., Baler, R., and Telang, F. (2009). Imaging dopamine's role in drug abuse and addiction. Neuropharmacology *56 Suppl 1*, 3–8.

Vranjkovic, O., Gasser, P.J., Gerndt, C.H., Baker, D.A., and Mantsch, J.R. (2014). Stress-induced cocaine seeking requires a beta-2 adrenergic receptor-regulated pathway from the ventral bed nucleus of the stria terminalis that regulates CRF actions in the ventral tegmental area. J. Neurosci. *34*, 12504–12514.

van Waarde, A., Rybczynska, A.A., Ramakrishnan, N., Ishiwata, K., Elsinga, P.H., and Dierckx, R.A.J.O. (2010). Sigma receptors in oncology: therapeutic and diagnostic applications of sigma ligands. Curr. Pharm. Des. *16*, 3519–3537.

van Waarde, A., Rybczynska, A.A., Ramakrishnan, N.K., Ishiwata, K., Elsinga, P.H., and Dierckx, R.A.J.O. (2015). Potential applications for sigma receptor ligands in cancer diagnosis and therapy. Biochim. Biophys. Acta *1848*, 2703–2714.

Walther, C., and Ferguson, S.S.G. (2015). Minireview: Role of intracellular scaffolding proteins in the regulation of endocrine G protein-coupled receptor signaling. Mol. Endocrinol. *29*, 814–830.

Wang, B., You, Z.-B., Rice, K.C., and Wise, R.A. (2007). Stress-induced relapse to cocaine seeking: roles for the CRF(2) receptor and CRF-binding protein in the ventral tegmental area of the rat. Psychopharmacology (Berl.) *193*, 283–294.

Wang, B., You, Z.-B., and Wise, R.A. (2009). Reinstatement of cocaine seeking by hypocretin (orexin) in the ventral tegmental area: independence from the local corticotropin-releasing factor network. Biol. Psychiatry *65*, 857–862.

Wang, D., Sadée, W., and Quillan, J.M. (1999). Calmodulin binding to G protein-coupling domain of opioid receptors. J. Biol. Chem. *274*, 22081–22088.

Wardas, J. (2008). Potential role of adenosine A2A receptors in the treatment of schizophrenia. Front. Biosci. *13*, 4071–4096.

Wehbi, V.L., Stevenson, H.P., Feinstein, T.N., Calero, G., Romero, G., and Vilardaga, J.-P. (2013). Noncanonical GPCR signaling arising from a PTH receptor-arrestin-Gβγ complex. Proc. Natl. Acad. Sci. U.S.A. *110*, 1530–1535.

Weis, W.I., and Kobilka, B.K. (2008). Structural insights into G-protein-coupled receptor activation. Curr. Opin. Struct. Biol. *18*, 734–740.

Weiss, J.L., Archer, D.A., and Burgoyne, R.D. (2000). Neuronal Ca2+ sensor-1/frequenin functions in an autocrine pathway regulating Ca2+ channels in bovine adrenal chromaffin cells. J. Biol. Chem. *275*, 40082–40087.

Wells, T. (2009). Ghrelin - Defender of fat. Prog. Lipid Res. *48*, 257–274.

van der Westhuizen, E.T., Breton, B., Christopoulos, A., and Bouvier, M. (2014). Quantification of ligand bias for clinically relevant β2-adrenergic receptor ligands: implications for drug taxonomy. Mol. Pharmacol. *85*, 492–509.

Weston, C., Lu, J., Li, N., Barkan, K., Richards, G.O., Roberts, D.J., Skerry, T.M., Poyner, D., Pardamwar, M., Reynolds, C.A., et al. (2015). Modulation of Glucagon Receptor Pharmacology by Receptor Activity-modifying Protein-2 (RAMP2). J. Biol. Chem. *290*, 23009–23022.

Whalen, E.J., Rajagopal, S., and Lefkowitz, R.J. (2011). Therapeutic potential of β-arrestin- and G protein-biased agonists. Trends Mol Med *17*, 126–139.

Whorton, M.R., Bokoch, M.P., Rasmussen, S.G.F., Huang, B., Zare, R.N., Kobilka, B., and Sunahara, R.K. (2007). A monomeric G protein-coupled receptor isolated in a high-density lipoprotein particle efficiently activates its G protein. Proc. Natl. Acad. Sci. U.S.A. *104*, 7682–7687.

Wichmann, T., and DeLong, M.R. (1996). Functional and pathophysiological models of the basal ganglia. Curr. Opin. Neurobiol. *6*, 751–758.

Will, R.G., Martz, J.R., and Dominguez, J.M. (2016). The medial preoptic area modulates cocaine-induced locomotion in male rats. Behav. Brain Res. *305*, 218–222.

Wingard, J.N., Chan, J., Bosanac, I., Haeseleer, F., Palczewski, K., Ikura, M., and Ames, J.B. (2005). Structural analysis of Mg2+ and Ca2+ binding to CaBP1, a neuron-specific regulator of calcium channels. J. Biol. Chem. *280*, 37461–37470.

Wise, R.A. (2002). Brain reward circuitry: insights from unsensed incentives. Neuron *36*, 229–240.

Wolf, M.E. (2016). Synaptic mechanisms underlying persistent cocaine craving. Nat. Rev. Neurosci. *17*, 351–365.

Wong, A.C., Shetreat, M.E., Clarke, J.O., and Rayport, S. (1999). D1- and D2-like dopamine receptors are co-localized on the presynaptic varicosities of striatal and nucleus accumbens neurons in vitro. Neuroscience *89*, 221–233.

Wong, K.K.Y., Ng, S.Y.L., Lee, L.T.O., Ng, H.K.H., and Chow, B.K.C. (2011). Orexins and their receptors from fish to mammals: a comparative approach. Gen. Comp. Endocrinol. *171*, 124–130.

Woods, A.S. (2004). The mighty arginine, the stable quaternary amines, the powerful aromatics, and the aggressive phosphate: their role in the noncovalent minuet. J. Proteome Res. *3*, 478–484.

Woods, A.S., and Huestis, M.A. (2001). A study of peptide--peptide interaction by matrix-assisted laser desorption/ionization. J. Am. Soc. Mass Spectrom. *12*, 88–96.

Woods, A.S., Marcellino, D., Jackson, S.N., Franco, R., Ferré, S., Agnati, L.F., and Fuxe, K. (2008). How calmodulin interacts with the adenosine A(2A) and the dopamine D(2) receptors. J. Proteome Res. *7*, 3428–3434.

Wootten, D., Lindmark, H., Kadmiel, M., Willcockson, H., Caron, K.M., Barwell, J., Drmota, T., and Poyner, D.R. (2013). Receptor activity modifying proteins (RAMPs) interact with the VPAC2 receptor and CRF1 receptors and modulate their function. Br. J. Pharmacol. *168*, 822–834.

Wreggett, K.A., and Wells, J.W. (1995). Cooperativity manifest in the binding properties of purified cardiac muscarinic receptors. J. Biol. Chem. *270*, 22488–22499.

Wu, Z., and Bowen, W.D. (2008). Role of sigma-1 receptor C-terminal segment in inositol 1,4,5-trisphosphate receptor activation: constitutive enhancement of calcium signaling in MCF-7 tumor cells. J. Biol. Chem. *283*, 28198–28215.

Wu, D.-F., Yang, L.-Q., Goschke, A., Stumm, R., Brandenburg, L.-O., Liang, Y.-J., Höllt, V., and Koch, T. (2008). Role of receptor internalization in the agonist-induced desensitization of cannabinoid type 1 receptors. J. Neurochem. *104*, 1132–1143.

Wu, H., Wacker, D., Mileni, M., Katritch, V., Han, G.W., Vardy, E., Liu, W., Thompson, A.A., Huang, X.-P., Carroll, F.I., et al. (2012). Structure of the human κ-opioid receptor in complex with JDTic. Nature *485*, 327–332.

Xu, J., Zeng, C., Chu, W., Pan, F., Rothfuss, J.M., Zhang, F., Tu, Z., Zhou, D., Zeng, D., Vangveravong, S., et al. (2011). Identification of the PGRMC1 protein complex as the putative sigma-2 receptor binding site. Nat Commun *2*, 380.

Xu, M., Hu, X.T., Cooper, D.C., Moratalla, R., Graybiel, A.M., White, F.J., and Tonegawa, S. (1994). Elimination of cocaine-induced hyperactivity and dopamine-mediated neurophysiological effects in dopamine D1 receptor mutant mice. Cell *79*, 945–955.

Xu, Y.-T., Robson, M.J., Szeszel-Fedorowicz, W., Patel, D., Rooney, R., McCurdy, C.R., and Matsumoto, R.R. (2012). CM156, a sigma receptor ligand, reverses cocaine-induced place conditioning and transcriptional responses in the brain. Pharmacol. Biochem. Behav. *101*, 174–180.

Yamada, K., Kobayashi, M., and Kanda, T. (2014). Involvement of adenosine A2A receptors in depression and anxiety. Int. Rev. Neurobiol. *119*, 373–393.

Yamamoto, K., Mirabeau, O., Bureau, C., Blin, M., Michon-Coudouel, S., Demarque, M., and Vernier, P. (2013). Evolution of dopamine receptor genes of the D1 class in vertebrates. Mol. Biol. Evol. *30*, 833–843.

Yan, R., Hu, Z.-Y., Zhou, W.-X., Wang, Q., and Zhang, Y.-X. (2014). [Roles of adenosine receptors in Alzheimer's disease]. Yao Xue Xue Bao *49*, 751–756.

Yang, Y., and Raine, A. (2009). Prefrontal structural and functional brain imaging findings in antisocial, violent, and psychopathic individuals: a meta-analysis. Psychiatry Res *174*, 81–88.

Yang, J., Brown, M.S., Liang, G., Grishin, N.V., and Goldstein, J.L. (2008). Identification of the acyltransferase that octanoylates ghrelin, an appetite-stimulating peptide hormone. Cell *132*, 387–396.

Yin, J., Mobarec, J.C., Kolb, P., and Rosenbaum, D.M. (2015). Crystal structure of the human OX2 orexin receptor bound to the insomnia drug suvorexant. Nature *519*, 247–250.

Yin, J., Babaoglu, K., Brautigam, C.A., Clark, L., Shao, Z., Scheuermann, T.H., Harrell, C.M., Gotter, A.L., Roecker, A.J., Winrow, C.J., et al. (2016). Structure and ligand-binding mechanism of the human OX1 and OX2 orexin receptors. Nat. Struct. Mol. Biol. *23*, 293–299.

Young, J.J., Mehdi, A., Stohl, L.L., Levin, L.R., Buck, J., Wagner, J.A., and Stessin, A.M. (2008). "Soluble" adenylyl cyclase-generated cyclic adenosine monophosphate promotes fast migration in PC12 cells. J. Neurosci. Res. *86*, 118–124.

Yuan, M., Cross, S.J., Loughlin, S.E., and Leslie, F.M. (2015). Nicotine and the adolescent brain. J. Physiol. (Lond.) *593*, 3397–3412.

Zack, M., and Poulos, C.X. (2009). Parallel roles for dopamine in pathological gambling and psychostimulant addiction. Curr Drug Abuse Rev *2*, 11–25.

Zampese, E., and Pizzo, P. (2012). Intracellular organelles in the saga of Ca2+ homeostasis: different molecules for different purposes? Cell. Mol. Life Sci. *69*, 1077–1104.

Zeng, C., Vangveravong, S., Xu, J., Chang, K.C., Hotchkiss, R.S., Wheeler, K.T., Shen, D., Zhuang, Z.-P., Kung, H.F., and Mach, R.H. (2007). Subcellular localization of sigma-2 receptors in breast cancer cells using two-photon and confocal microscopy. Cancer Res. *67*, 6708–6716.

Zeng, C., Rothfuss, J.M., Zhang, J., Vangveravong, S., Chu, W., Li, S., Tu, Z., Xu, J., and Mach, R.H. (2014). Functional assays to define agonists and antagonists of the sigma-2 receptor. Anal. Biochem. *448*, 68–74.

Zhang, D., Zhang, L., Tang, Y., Zhang, Q., Lou, D., Sharp, F.R., Zhang, J., and Xu, M. (2005a). Repeated cocaine administration induces gene expression changes through the dopamine D1 receptors. Neuropsychopharmacology *30*, 1443–1454.

Zhang, L., Huang, L., Lu, K., Liu, Y., Tu, G., Zhu, M., Ying, L., Zhao, J., Liu, N., Guo, F., et al. (2016a). Cocaine-induced synaptic structural modification is differentially regulated by dopamine D1 and D3 receptors-mediated signaling pathways. Addict Biol.

Zhang, R., Dzhura, I., Grueter, C.E., Thiel, W., Colbran, R.J., and Anderson, M.E. (2005b). A dynamic alpha-beta inter-subunit agonist signaling complex is a novel feedback mechanism for regulating L-type Ca2+ channel opening. FASEB J. *19*, 1573–1575.

Zhang, X., Sun, N., Zheng, M., and Kim, K.-M. (2016b). Clathrin-mediated endocytosis is responsible for the lysosomal degradation of dopamine D3 receptor. Biochem. Biophys. Res. Commun. *476*, 245–251.

Zhang, X., Wu, Y., Hao, J., Zhu, J., Tang, N., Qi, J., Wang, S., Wang, H., Peng, S., Liu, J., et al. (2016c). Intraperitoneal injection urocortin-3 reduces the food intake of Siberian sturgeon (Acipenser baerii). Peptides *85*, 80–88.

Zhang, X.C., Liu, J., and Jiang, D. (2014). Why is dimerization essential for class-C GPCR function? New insights from mGluR1 crystal structure analysis. Protein Cell *5*, 492–495.

Zhou, H., Kim, S.-A., Kirk, E.A., Tippens, A.L., Sun, H., Haeseleer, F., and Lee, A. (2004). Ca2+-binding protein-1 facilitates and forms a postsynaptic complex with Cav1.2 (L-type) Ca2+ channels. J. Neurosci. *24*, 4698–4708.

Zhou, Q.Y., Li, C., Olah, M.E., Johnson, R.A., Stiles, G.L., and Civelli, O. (1992). Molecular cloning and characterization of an adenosine receptor: the A3 adenosine receptor. Proc. Natl. Acad. Sci. U.S.A. *89*, 7432–7436.

Zhu, X., and Wess, J. (1998). Truncated V2 vasopressin receptors as negative regulators of wild-type V2 receptor function. Biochemistry *37*, 15773–15784.

Zhu, W., Mao, Z., Zhu, C., Li, M., Cao, C., Guan, Y., Yuan, J., Xie, G., and Guan, X. (2016). Adolescent exposure to cocaine increases anxiety-like behavior and induces morphologic and neurochemical changes in the hippocampus of adult rats. Neuroscience *313*, 174–183.

Zigman, J.M., Jones, J.E., Lee, C.E., Saper, C.B., and Elmquist, J.K. (2006). Expression of ghrelin receptor mRNA in the rat and the mouse brain. J. Comp. Neurol. *494*, 528–548.

Zorrilla, E.P., Logrip, M.L., and Koob, G.F. (2014). Corticotropin releasing factor: a key role in the neurobiology of addiction. Front Neuroendocrinol *35*, 234–244.

van Zundert, G.C.P., Rodrigues, J.P.G.L.M., Trellet, M., Schmitz, C., Kastritis, P.L., Karaca, E., Melquiond, A.S.J., van Dijk, M., de Vries, S.J., and Bonvin, A.M.J.J. (2016). The HADDOCK2.2 Web Server: User-Friendly Integrative Modeling of Biomolecular Complexes. J. Mol. Biol. *428*, 720–725.

ANEXOS

7.1. COLABORACIONES

En el transcurso de la elaboración de la presente Tesis doctoral se ha colaborado en el siguiente manuscrito:

- 7.1.1. E. Martínez-Pinilla, A.I. Rodríguez-Pérez, Gemma Navarro, **David Aguinaga**, Estefanía Moreno, J.L. Lanciego, J.L. Labandeira-García y Rafael Franco. **Dopamine D_2 and angiotensin II type 1 receptors form functional heteromers in rat striatum.**

  Manuscrito publicado en *Biochemical Pharmacology*.

- 7.1.2. Mireia Medrano, **David Aguinaga**, Irene Reyes-Resina, Enric I. Canela, Josefa Mallol, Gemma Navarro[*] y Rafael Franco[*]. **Orexin A modulates leptin receptor-mediated signaling by an allosteric modulation mediated by the ghrelin GHS-R1a receptor in hypothalamic neurons.**

  [*]Coautores del manuscrito

  Manuscrito enviado a *Molecular Neurobiology*.

- 7.1.3. Gemma Navarro[*], Mireia Medrano[*], **David Aguinaga**, Ignacio Vega-Quiroga, Enric I. Canela, Josefa Mallol Katia Gysling y Rafael Franco. **Differential effect of amphetamine over corticotropin-releasing factor receptor CRF_2, orexin receptor OX_1 and CRF_2-OX_1 heteroreceptor complex.**

  [*]Coautores del manuscrito

  Manuscrito en preparación para ser enviado *Neuropharmacology*.

Para abrir nuevos caminos,
hay que ser capaz de perderse.

David Aguinaga Andrés

Universitat de Barcelona
Departament de Bioquímica i Biomedicina molecular
Grup de NeuroBiologia Molecular

Barcelona, 2017